PRINCIPLES OF ENERGY CONVERSION

Second Edition

Archie W. Culp, Jr., Ph.D.

Professor of Mechanical and Basic Engineering
University of Missouri-Rolla

McGraw-Hill, Inc.

New York St. Louis San Francisco Auckland
Bogotá Caracas Hamburg Lisbon London Madrid
Mexico Milan Montreal New Delhi Paris San Juan
São Paulo Singapore Sydney Tokyo Toronto

PRINCIPLES OF ENERGY CONVERSION

Copyright © 1991, 1979 by McGraw-Hill, Inc. All rights reserved.
Printed in the United States of America. Except as permitted under the United States Copyright Act of 1976, no part of this publication may be reproduced or distributed in any form or by any means, or stored in a data base or retrieval system, without the prior written permission of the publisher.

1 2 3 4 5 6 7 8 9 0 HAL HAL 9 5 4 3 2 1 0

ISBN 0-07-014902-X

This book was set in Times Roman.
The editors were John J. Corrigan and James W. Bradley;
the production supervisor was Denise L. Puryear.
The cover was designed by Rafael Hernandez.
Arcata Graphics/Halliday was printer and binder.

Library of Congress Cataloging-in-Publication Data

Culp, Archie W.
Principles of energy conversion / Archie W. Culp. Jr.—2nd ed.
p. cm.—(McGraw-Hill series in mechanical engineering)
Includes bibliographical references and index.
ISBN 0-07-014902-X
1. Power (Mechanics) 2. Power resources. 3. Energy conservation.
I. Title. II. Series.
TJ163.9.C84 1991
621.042—dc20 90-6323

CONTENTS

Preface xiii

1 Energy Classification, Sources, Utilization, Economics, and Terminology 1

1.1 Introduction 1
1.2 Mass-Energy Dependence 3
1.3 Energy, Mass, and Power Units 4
1.4 Energy Types and Classifications 4
1.5 Energy Sources 7
1.6 Energy Reserves 13
1.7 Energy Utilization 14
1.8 Electrical Power Generation and Consumption 17
1.9 Growth Rates 19
1.10 Energy Economics 20
1.11 Power Generation Terminology 30
1.12 Energy-Conversion Matrix 34
List of Symbols 36
Problems 37
References 42

2 Principal Fuels for Energy Conversion 43

2.1 Introduction 43
2.2 Biomass Fuels 43
2.3 Fossil Fuels 47
2.3.1 Background 47
2.3.2 Hydrocarbon Chemistry 47
2.3.3 Standard Fuels 50
2.3.4 Coal 51
2.3.5 Petroleum 58
2.3.6 Gaseous Fuels 61

2.4 Nuclear Fuels 66
2.4.1 Source of Nuclear Energy 66
2.4.2 Radioactive Decay 69
2.4.3 Nuclear Fission 79
2.4.4 Nuclear Fusion 89
2.5 Solar Energy 97
2.5.1 Introduction 97
2.5.2 Solar-Energy Calculations 98
2.5.3 Solar Collection Systems 108
List of Symbols 113
Problems 115
References 120

3 Production of Thermal Energy 122
3.1 Introduction 122
3.2 Conversion of Mechanical Energy 122
3.3 Conversion of Electrical Energy 123
3.4 Conversion of Electromagnetic Energy 123
3.5 Conversion of Chemical Energy 124
3.5.1 Introduction 124
3.5.2 Combustion Reactions 124
3.5.3 Theoretical Air-Fuel Ratio 126
3.5.4 Actual Combustion Process 129
3.5.5 Combustion Mechanics 140
3.6 Conversion of Nuclear Energy 141
3.6.1 Introduction 141
3.6.2 Nuclear Reactor Terminology 142
3.6.3 Neutron Reaction Rates 144
3.6.4 Neutron Reactions and Cross Sections 147
3.6.5 Classification of Nuclear Reactors 154
3.6.6 Reactor Physics 165
3.6.7 Composition of a Nuclear Power Reactor 170
List of Symbols 183
Problems 184
References 187

4 Fossil-Fuel Systems 189
4.1 Introduction 189
4.2 Fluid-Moving Systems 189
4.2.1 Introduction 189
4.2.2 Boiler Feed Pumps 190
4.2.3 Combustion Air Systems 193
4.2.4 Draft Systems 195
4.3 Combustion Methods and Systems 203
4.3.1 Gas-Fired Systems 203
4.3.2 Oil-Fired Systems 204
4.3.3 Coal-Combustion Systems 206

4.4 Steam Generators 219
4.4.1 General 219
4.4.2 Boiler Types and Classifications 221
4.4.3 Primary Boiler Heat-Transfer Surfaces 226
4.4.4 Secondary Boiler Heat-Transfer Surfaces 228
4.4.5 Boiler Ratings and Performance 234
List of Symbols 243
Problems 244
References 247

5 Nuclear Reactor Design and Operation 249

5.1 Introduction 249
5.2 Power Reactor Systems 251
5.2.1 Light-Water Reactors 251
5.2.2 Gas-Cooled Reactors 262
5.2.3 Liquid-Metal, Fast-Breeder Reactors 264
5.3 Reactor Thermal Design 267
5.3.1 Reactor In-Core Power Distributions 267
5.3.2 Fuel Element Temperatures and Heat Fluxes 275
5.4 Reactor Operations 284
5.4.1 Reactor Kinetics 284
5.4.2 Reactivity Coefficients 293
5.4.3 Fission-Product Poisoning 295
5.4.4 Fuel Requirements for a Nuclear Reactor 304
List of Symbols 311
Problems 313
References 316

6 Environmental Impact of Power Plant Operation 317

6.1 Introduction 317
6.2 Particulate Emissions 321
6.3 Gaseous Pollutants 329
6.4 Thermal Pollution 333
6.5 Solid-Waste Pollution 337
List of Symbols 341
Problems 342
References 343

7 Production of Mechanical Energy 345

7.1 Introduction 345
7.2 Conversion of Thermal Energy 346
7.2.1 Thermodynamic Power Cycles 346
7.2.2 Reversible Heat-Engine Cycles 347
7.2.3 Internal-Combustion Engine Cycles 353
7.2.4 Internal-Combustion Engines 358
7.2.5 Engine Performance 361
7.2.6 External-Combustion Systems 366

7.2.7 Vapor Power Cycles 374
7.2.8 Combined Cycles 388
7.3 Turbines 392
7.3.1 Steam Turbines 392
7.3.2 Hydraulic Turbines 399
7.3.3 Wind Turbines 405
7.4 Electromechanical Conversion 409
7.4.1 General 409
7.4.2 Electric Motors 410
7.4.3 Types of Motors 411
7.4.4 Electromagnetic Pump 416
List of Symbols 417
Problems 419
References 427

8 Production of Electrical Energy 428
8.1 Introduction 428
8.2 Conversion of Thermal Energy into Electricity 429
8.2.1 Thermoelectric Converters 429
8.2.2 Thermoelectric Refrigerators 434
8.2.3 Thermoelectric Systems 438
8.2.4 Thermionic Converters 440
8.2.5 Other Thermal-Electric Conversion Systems 446
8.3 Conversion of Chemical Energy into Electricity 447
8.3.1 General Systems 447
8.3.2 Fuel-Cell Performance 448
8.3.3 Types of Fuel Cells 453
8.4 Conversion of Electromagnetic Energy into Electricity 456
8.4.1 Operational Characteristics of Solar Cells 456
8.4.2 Solar-Cell Performance 461
8.5 Conversion of Nuclear Energy into Electricity 463
8.6 Conversion of Mechanical Energy into Electricity 463
8.6.1 Electric Generators and Alternators 463
8.6.2 Fluiddynamic Converters 466
List of Symbols 475
Problems 478
References 479

9 Energy Storage 481
9.1 Introduction 481
9.2 Storage of Mechanical Energy 482
9.2.1 Kinetic Energy Storage 482
9.2.2 Elastic-Strain Energy Storage 484
9.2.3 Gravitational Energy Storage 486
9.2.4 Compressed-Fluid Energy Storage 487
9.2.5 Magnetic-Field Energy Storage 488

9.3 Storage of Electrical Energy 488
9.3.1 Introduction 488
9.3.2 Electrostatic-Field Energy Storage 488
9.3.3 Inductive-Field Energy Storage 489
9.3.4 Batteries 489
9.4 Storage of Chemical Energy 490
9.5 Storage of Nuclear Energy 492
9.6 Storage of Thermal Energy 493
List of Symbols 495
References 496

List of Appendixes 497

A Physical Constants 498
B Conversion Factors and Standards 500
C Ultimate Analysis of Biomass Fuels 506
D ASTM Coal Classification System (Summary of ASTM D388) 509
E Typical Coal Analyses 511
F Converting Proximate to Ultimate Analyses 514
G Liquid Fuels 517
H Fuel-Gas Analyses 519
I Reactant Properties 522
J List of Chemical Elements 523
K Partial List of Isotopes 525
L Radioisotope Fuels 542
M Solar Constants (for Northern Latitudes) 544
N Solar Position and Irradiation Values 546
O Variation of Solar Radiation with Latitude (for Northern Latitudes) 549

Index 551

PREFACE

The field of energy conversion is so broad and covers so many disciplines that it is a difficult course to teach. Moreover, so much research is being carried out in this area that the field is constantly changing. The area is further clouded by political decisions and regulations as well as by media bias. Writing a textbook on energy conversion is like trying to write an objective political or religious treatise on any highly controversial subject. Each "expert" involved in the energy program has a pet energy source and/or conversion system that he or she feels should be exploited.

Although the author also has definite opinions as to which energy sources should be exploited, he has tried to be relatively objective in presenting the basic theory associated with almost all of the proposed energy-conversion systems. A relatively detailed description is presented for those systems that produce the bulk of humanity's fuel energy at this time. The presentation may generate some controversy because more of the solar and other exotic systems are not extensively covered in this text, although the basic principles and some of the systems are covered. The author does not intend to imply that solar energy and some of these other systems are not important energy sources; it just means that, at this time in history, they produce very little of our fuel energy, and more attention and detail are given to those systems that do produce the bulk of our fuel energy. It is felt that such an approach better prepares the student for a possible career in the energy area.

One can find several excellent textbooks on nuclear engineering and reactor systems and also good books on fossil-fuel systems and direct energy conversion. Unfortunately, there are very few textbooks that try to cover all aspects of energy conversion, including systems and theory. This book attempts to bridge that gap.

Most of the material in the following chapters has been presented in a mechanical-engineering (ME) course on energy conversion developed by the author during the last 19 years. That course is required for all ME students at the University of Missouri-Rolla and replaced an established course in

steam-power systems along with a modern physics course in the old ME curriculum.

This book is intended for use by senior-level or early graduate-level students in the various engineering disciplines associated with the conversion, utilization, and transfer of energy. These disciplines include the conventional fields of chemical, electrical, mechanical, and nuclear engineering. It is expected that any student using this text will have a working knowledge of basic classical thermodynamics.

Because of the wide scope of the material presented, it is difficult to cover this book in one three-semester-hour course. If it is used for such a course, the instructor must be somewhat selective about what is to be covered. Some of the material may duplicate the subject matter of other courses, depending on the background of the students. If so, that material can be reviewed very quickly or omitted altogether, at the discretion of the instructor.

Chapters 1 and 2 should be covered rather thoroughly, as they discuss basic background, terminology, and fundamental conversion principles. Chapters 3, 7, and 8 deal with the production of thermal, mechanical, and electrical energy, respectively, and should have the next order of priority. Chapter 4 presents a more-detailed description of the conventional fossil-fuel combustion systems and their components. Chapter 5 should be covered by those people who want to go into some of the details of nuclear reactor design and operation. Chapter 6 is very important as it deals with the environmental impact of power-plant operation. Chapter 9 presents a general background information on energy-storage units, even though, strictly speaking, they are not energy-conversion systems.

It has been suggested by some reviewers that this book should be reorganized to emphasize the exploitation of each of the fuel sources discussed, i.e., the utilization of fossil fuels, the utilization of nuclear fuels, the utilization of renewable energy sources, etc. Some thought was given to such a presentation but it was decided to employ the original format because it forces the student to review the basic theory each time the particular fuel is discussed in subsequent chapters. It is felt that these reviews are very important in the learning process. Thus, the properties of fossil fuels are discussed in Chap. 2; their combustion requirements and theory are presented in Chap. 3; their various combustion systems are discussed in Chap. 4; and the environmental problems associated with operation of the systems are given in Chap. 6.

A reviewer has also suggested that the presentation on fission reactors should be deemphasized because there have been no new systems ordered since 1978. While this is true, nuclear power currently produces around 20 percent of our electricity and the total capital investment in the more than 100 plants in operation in the United States is more than $400 billion. Many of these plants will be in operation during the next 30 years. Most energy experts also believe that more nuclear reactors will be ordered as soon as the public (and particularly the news media which shape public opinion) realize that nuclear energy is probably the safest, most economical, most dependable, and most environmentally benign large energy source for the production of electricity. Although the nuclear-power

industry is at a standstill in the United States in 1990, the rest of the world is proceeding with the development of new reactor systems. Consequently, the author feels that the intensive coverage of nuclear power should be retained in the revised edition of this textbook.

A number of example problems are included in the text, and many of them can be worked by simply using dimensional analysis. Students should be urged to write down the dimensions associated with each of the variables along with those of the appropriate conversion factors. The dimensions should be canceled just like numbers when working the problems. This procedure has been employed in most of the example problems and in the solution manual except that none of the dimensions are actually canceled.

A number of new problems have been added to this second edition of the book and in most problems two of the variables have five different values. This means that there are 25 different answers for most of the problems. The solution manual contains the detailed solution for the midpoint values and a matrix of other answers. The use of different values in the problems means that the instructor can assign one pair of values one semester and a different pair the next, thereby minimizing the value of a homework file. Moreover, the five values of the problem parameters have been selected so that students can be asked to develop a computer program which will generate all 25 answers.

McGraw-Hill and the author would like to thank the following reviewers for their many helpful comments and suggestions for this edition: Richard B. Cole, Stephen Institute of Technology; Lawrence W. Evers, Michigan Technical University; Frank C. Hooper, University of Toronto; Edward R. Lady, University of Michigan; James W. Leach, North Carolina State University; Edward H. Perry, Memphis State University; and Samuel Shelton, Georgia Institute of Technology.

The author woulld like to express his appreciation to his family and friends for their moral support during preparation of the manuscript. He would also like to thank Dr. John Sheffield and Dr. Virgil Flanigan for their assistance with the energy-conversion course and to Dr. Ronald Fannin for his support in the preparation of the second edition.

Archie W. Culp, Jr.

PRINCIPLES OF ENERGY CONVERSION

CHAPTER 1

ENERGY CLASSIFICATION, SOURCES, UTILIZATION, ECONOMICS, AND TERMINOLOGY

1.1. INTRODUCTION

Throughout the history of the human race, major advances in civilization have been accompanied by increases in the rate of energy consumption. Today, energy consumption appears to be directly related to the level of living of the populace and the degree of industrialization of the country. Those countries that have had abundant supplies of energy available to them have realized substantially higher rates of industrial growth and a corresponding increase in the gross national product.

In many instances, the availability of low-cost energy has led to the inefficient utilization of the energy and, in some instances, to disastrous ecological effects. However, it is obvious that in order to raise the level of living of the majority of the world's population, the present rate of energy consumption must be greatly expanded. Figure 1.1 shows the relationship between the per capita energy consumption and the level of living as measured by the value of the per capita gross national product for the various countries of the world. During the past two decades, there has been a concerted effort to use energy more efficiently with the development of more efficient automobiles, etc. This is reflected in the data tabulated for the United States, as shown in Fig. 1.1.

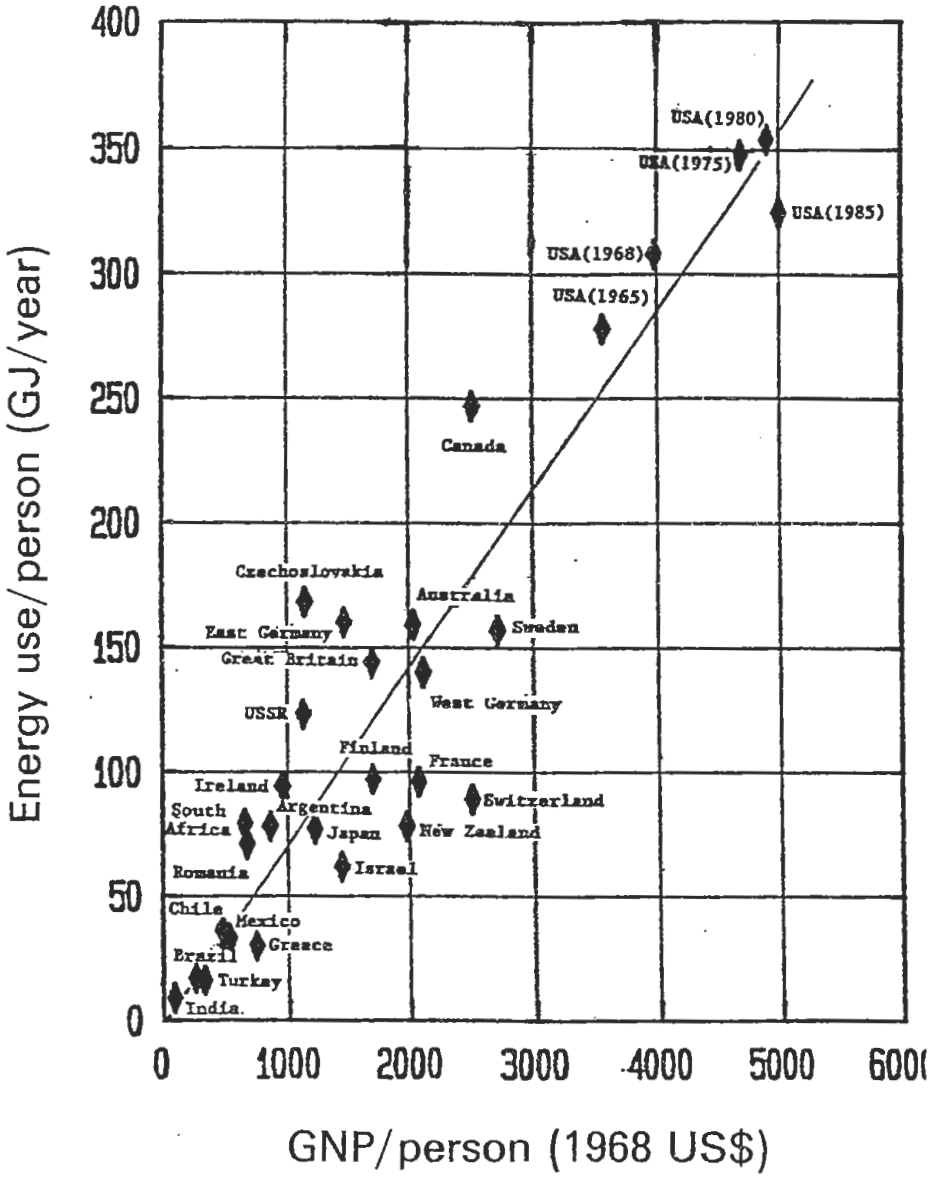


FIGURE 1.1
Dependence of the gross national product (in 1968 U.S. dollars) on energy consumption for various countries of the world.

Recently, some of the countries that have large supplies of low-cost energy are using those supplies as a potential political and economic weapon to achieve political ends that could not be realized through normal diplomatic channels. Because of this "energy blackmail," the people of the energy-dependent countries of the world are becoming increasingly aware of the importance of the conversion and conservation of energy along with the development of new energy sources.

It is the responsibility of the scientist, the engineer, and the power technician to locate, develop and exploit these new sources for the benefit of the human race. In order to accomplish this, it is imperative that these people have an intimate knowledge of the various energy forms, sources, conversion techniques, and conservation methods, along with their advantages, limitations, and inherent problems.

In the first half of the twentieth century, energy sources were exploited with the primary consideration given to economics—low cost. In the third quarter of the century, the power engineer had to be concerned with the three "E's" of energy conversion—energy, economy, and ecology. Proper balancing of these three "E's" was (and still is) a major technological challenge. During the final quarter of this century, the power engineer is further burdened and must be concerned with the six "P's" of energy conversion—power, pennies, pollution, politics, prejudice, and public relations.

Trying to satisfy all these conditions can be quite demoralizing and frustrating at times. Moreover, conversion systems which appear to be the best possible choice today may not be economical or acceptable to the general public when they actually go into operation. When it takes eight to twelve years to put a large power plant on line, it is difficult to predict what the demand will be at that time and just what bureaucratic rules and new laws that the new plant will have to satisfy.

1.2. MASS-ENERGY DEPENDENCE

An early statement of the first law of thermodynamics stated, in effect, that energy must be conserved in any process. A related postulate stated that mass can be neither created nor destroyed. In 1922, however, Albert Einstein hypothesized that energy and mass are actually related according to the following relationship:

$$E = mc^2 \tag{1.1}$$

where E is the energy release, in joules, m is the actual mass converted into energy, in kilograms, and c is the velocity of light (3×10^8 m/s). This equation actually represents a reversible process but the primary result is that the sum of mass and energy must be conserved in any energy-conversion process.

When Eq. (1.1) is used, it becomes evident that a small amount of mass, completely annihilated, produces huge amounts of energy. A 600,000-kW_e power plant (the subscript "e" indicates that this is electrical power), operating continuously, consumes about 220 tons of coal per hour or about 2,000,000 tons of coal per year. A 600,000-kW_e nuclear power plant, operating continuously,

consumes about one ton of uranium fuel per year. The actual fuel mass that is converted into energy in either of these systems is around 640 g or about $1\frac{1}{2}$ lb of matter per year.

Any time stored energy is converted into transitional energy, as in a nuclear reaction, there must be a corresponding decrease in mass accompanying the process. In this text, no distinction is made between the actual energy or the mass converted into energy. When reference is made to any stored energy form, it actually refers to that portion of the total mass of reactants which can be converted into other energy forms in some type of conversion process. There may be some debate whether Eq. (1.1) applies to all stored energy forms or only nuclear energy but it really does not matter since nuclear reactions are the only reactions in which the decrease in mass can be measured when stored energy is released.

1.3 ENERGY, MASS, AND POWER UNITS

Care must be exercised when performing energy calculations not to confuse energy units with power units. Power is an energy rate ($P = dE/dt$) and energy is equal to the integral of power over a given time interval. Standard International (SI) units are commonly used throughout the text, although other units are also employed. Conversion factors for the various units are given in App. B at the end of the book.

The SI unit of energy is the joule (J), but some of the other energy units used in this text are electron volts (eV), million electron volts (MeV), calories (cal), British thermal units (Btu), and foot-pound force (ft · lbf). In addition, energy is commonly expressed in terms of power and time units, such as the watthour (Wh), kilowatthour (kWh), horsepowerhour (hph), etc. Subscripts such as "e," "em," "m," "c," "n," and "th" are used throughout the text to identify the type of energy (or power) terms such as electrical, electromagnetic, mechanical, chemical, nuclear, and thermal, respectively.

The SI unit of power is the watt (W). This unit, along with multiples of it such as kilowatts (kW), megawatts (MW), gigawatts (GW), and terawatts (TW), are commonly used in this text.) Occasionally, the English power unit of horsepower (hp) is used. Power units can also be expressed in terms of energy rates such as joules per second (J/s), British thermal units per hour (Btu/h), etc.

The SI unit of mass is the kilogram (kg). Other mass units employed in this text are the pound mass (lbm), the atomic mass unit (amu), short tons (tons), metric tons (tonnes), grams (g), and multiples of grams.

1.4 ENERGY TYPES AND CLASSIFICATIONS

There are two basic types of energy—transitional and stored. Transitional energy is energy in motion and, as such, can move across system boundaries. Stored-energy forms, as implied, are energy forms that can exist as mass, position of a substance in a force field, etc. These stored energy forms can usually be easily converted into some form of transitional energy.

While there is no generally accepted method or system of energy classification, this text will divide the different energy forms into six major groups or classifications—mechanical energy, electrical energy, electromagnetic energy, chemical energy, nuclear energy, and thermal energy.

In the study of thermodynamics, mechanical energy is defined as energy which can be used to raise a weight. The common system of units for mechanical energy in the United States is the foot-pound force (ft · lbf) for energy and horsepower (hp) for the unit of power. In this text, Standard International (SI) units of J and kW are also used for mechanical energy and power units. Mechanical energy is a very useful form of energy and can be easily and efficiently converted into other energy forms.

The transitional form of mechanical energy is called *work*. Stored mechanical energy may be lumped under a general energy term called *potential energy*. In this text, potential energy is defined, very broadly, as the energy associated with a substance's position in a force field. Using this very general definition, there are five subgroups of potential energy, including: the energy associated with the position of a substance in a gravitational force field (the classical thermodynamic definition of potential energy); the energy of a substance due to its position in an inertial force field (the classical thermodynamic definition of kinetic energy); the energy associated with a compressed fluid; the energy associated with a substance's position in an elastic-strain field; and finally, the energy associated with a ferromagnetic material's position in a magnetic field. Thus, stored mechanical energy can exist in the form of elevated weights, flywheels, compressed gases, springs and torsion bars, and the magnetic attraction of iron bodies.

Electrical energy is that class of energy associated with the flow or accumulation of electrons. This form of energy is commonly reported in units of power and time, such as Wh or kWh. The transitional form of electrical energy is the flow of electrons through a conductor. Large quantities of electrical energy are transferred over long distances with the use of high-voltage transmission lines.

Electrical energy may be stored as either electrostatic-field energy or as inductive-field energy. Electrostatic-field energy is the energy associated with the accumulation of charge (electrons) on the plates of a capacitor. Inductive-field energy, which is sometimes called electromagnetic-field energy, is the energy associated with the magnetic field established by the flow of electrons through an induction coil. Electrical energy, like mechanical energy, is a very useful energy form because it can be easily and efficiently converted into other energy forms.

Electromagnetic energy is that form of energy associated with electromagnetic radiation. Radiation energy is usually reported in terms of very small energy units called electron volts (eV) or million electron volts (MeV). This energy unit is also employed extensively in the study of nuclear energy.

Electromagnetic radiation is a form of pure energy because there is no mass associated with it. Electromagnetic energy is the only major energy classification that cannot exist as a stored energy form as it is pure transitional energy traveling at the speed of light, c. The velocity of an electromagnetic wave, c, is equal to

the product of the wavelength, λ, of the wave, in meters, and the frequency of the wave, ν, in hertz, and the wave energy is given by Eq. (1.2),

$$E = h\nu = \frac{hc}{\lambda} \tag{1.2}$$

where E is the energy, in joules, and h is Planck's constant (6.626×10^{-32} J · s). Planck's constant, along with other basic physical constants, is listed in App. A at the end of the book. The more energetic electromagnetic waves have short wavelengths and high frequencies.

There are several different classes of electromagnetic radiation, depending on the wavelength (energy) or the source of the radiation. Gamma radiation is the most energetic form of electromagnetic energy and most of it emanates from the atomic nucleus. The next most energetic form of radiation is x-rays, which are produced as the result of excitation of orbiting electrons. Thermal radiation is electromagnetic radiation that is produced as the result of atomic vibration. This band of radiation is very broad and includes the high-temperature or ultraviolet radiation, the narrow band of visible radiation, and the band of low-temperature or infrared radiation. Microwave and millimeter waves are the next most energetic form of radiation and are used in radar and microwave ovens. These waves, along with radio waves, which are the least energetic form of radiation, are produced as the result of electrical discharges. The electromagnetic-radiation spectrum is shown in Fig. 1.2.

Chemical energy is energy that is released as the result of electron interactions in which two or more atoms and/or molecules combine to produce a more stable chemical compound. Chemical energy exists as only a stored-energy form. If energy is released in a chemical reaction, the reaction is called an *exothermic*

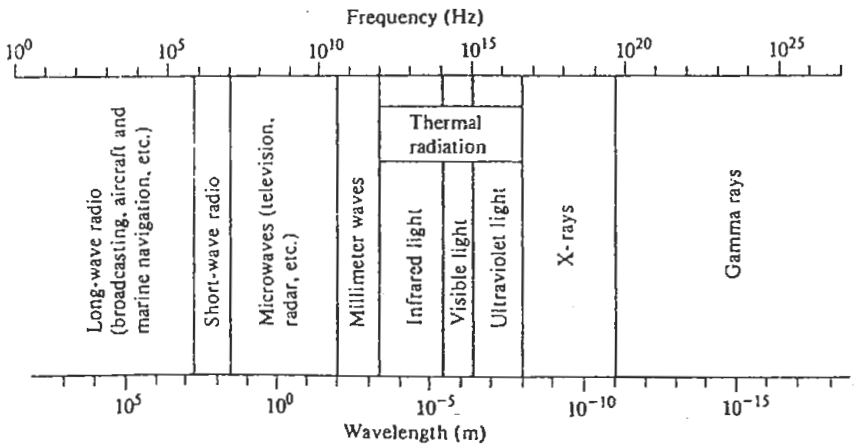


FIGURE 1.2
The electromagnetic energy spectrum.

reaction. This energy is commonly reported in the units of energy per unit mass or "mole" of fuel reactant. If chemical energy is produced from another energy form, the reaction is called an *endothermic* reaction. The most important source of fuel energy for the human race at this time is the exothermic chemical reaction called *combustion.* In this reaction, chemical energy is released which was produced in the endothermic heliochemical reaction called *photosynthesis.*

Nuclear energy is another major energy classification that exists only in the form of stored energy. It is energy which is released as the result of particle interactions with or within the atomic nucleus. This energy is released as the result of the product particles assuming a more stable configuration, and it is usually reported in units of MeV per reaction.

There are three general types of nuclear reactions, including radioactive decay, fission, and fusion. The radioactive-decay process is one in which only one unstable nucleus, a radioisotope, randomly decays to a more stable configuration, with the release of particles and energy. The fission reaction, which is the principal process in the nuclear reactor, occurs when a heavy-mass nucleus absorbs a neutron and the resulting excited compound nucleus splits into two or more light-mass nuclei with the release of energy. In the fusion reaction, two light-mass nuclei combine to produce a more stable configuration with the release of energy.

The annihilation reaction is commonly considered to be a nuclear reaction, but it is actually a separate reaction that is not associated with the atomic nucleus. Instead, this reaction involves the "building blocks" of the nucleus. This reaction is the ultimate energy-conversion reaction in that all reactant mass is converted into energy. In the annihilation reaction, matter and antimatter combine and are completely converted into electromagnetic energy. This reaction is the only reaction in which particles are completely destroyed, but the only known naturally occurring reaction of this type involves subatomic particles and is not an important source of energy.

The last major energy classification is thermal energy, which is the energy associated with atomic and molecular vibration. Thermal energy is a basic energy form in that all other energy forms can be completely converted into thermal energy but the conversion of thermal energy into other energy forms is severely limited by the second law of thermodynamics. The transitional form of thermal energy is heat, which is commonly expressed in units of joules, calories, or Btus. Thermal energy can be stored in almost any media in the form of either sensible heat or latent heat. Sensible-heat storage is accompanied by an increase in temperature while latent-heat storage is an isothermal process associated with a change of phase in the storage medium.

1.5 ENERGY SOURCES

All sources of energy may be grouped into two general categories—income energy, which is the energy reaching the earth from outer space, and capital energy, which is the energy that already exists on or within the earth. Income energy

includes solar and lunar energy while capital energy sources include fossil fuels, geothermal energy, and nuclear energy.

Income energy sources actually include all possible sources that provide energy to the earth from outer space. This includes electromagnetic, gravitational, and particle energy from stars, planets, and the moon as well as the potential energy of meteorities entering the earth's atmosphere. The only useful income energy sources are the electromagnetic energy from the earth's sun, called *direct solar energy*, and the gravitational energy of the earth's moon which produces tidal flows. The utilization of income energy sources is very attractive because they are continuing or nondepletable sources of energy and because they are relatively pollution-free—a very important consideration.

Direct solar energy also generates a number of indirect nondepletable sources of energy. The direct solar heating, combined with the earth's rotation, produces some large convection currents in the form of wind in the atmosphere and ocean currents in the seas. The absorption of solar energy also generates significant thermal gradients in the ocean that have the potential of producing power. In addition, the evaporation of surface water generates clouds, which, when condensed into rain at higher altitudes, provides the source for hydroelectric or water power. The wind also generates large ocean waves that have the potential of generating energy.

Another indirect form of direct solar energy is all the living material produced as the result of the photosynthesis process. This source is given the general name of *biomass* and includes trees, animals, plants, organic wastes, and other products that can be derived from them. Some of these materials, like wood, can be used as a fuel directly or can be used to generate other fuels, such as charcoal, alcohols, methane, and other fuel gases. Different forms of biomass have found widespread application in the underdeveloped countries of the world and their utilization is being studied as a potential alternative source of fuel energy in the United States.

The utilization of the temperature gradients in the ocean by some sort of OTEC (ocean thermal energy conversion) system has received a lot of study and discussion in recent years. Actually, the first operational OTEC system was a 40-kW_e power plant built in Cuba in 1926. This system uses the warm surface waters of the ocean to boil a working fluid in a Rankine-cycle power plant and then uses the cooler deep water to condense the vapor leaving the turbine. A small, 50-kW_e power plant has been operating off the coast of Hawaii in recent years.

One of the major problems with these systems is that the 16 to 20°C temperature difference yields a very low thermal efficiency for the system. This means that these systems must be extremely large in order to produce reasonable amounts of power. The large size of the plants means that the capital investment charges are very high, which is also the case for many of the solar energy conversion systems. A diagram of a proposed OTEC system is shown in Fig. 1.3.

The other major source of income energy is lunar energy, which is essentially the gravitational energy from the moon. This gravitational energy produces tidal

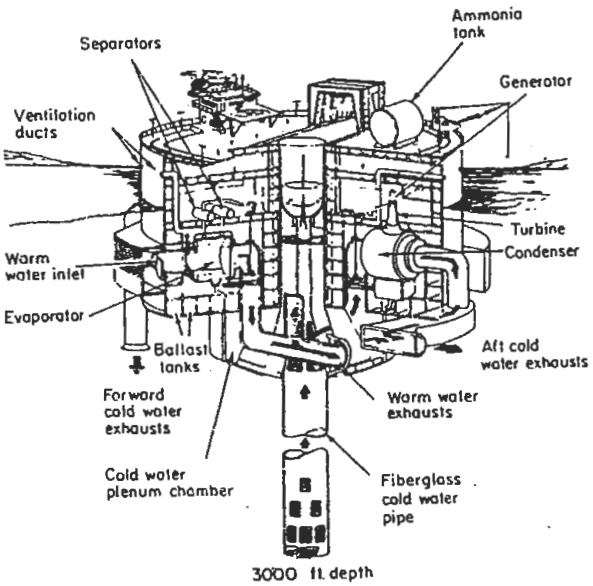


FIGURE 1.3
Concept of a 100-ME_e cylindrical-surface-vessel baseline OTEC plant developed by TRW Systems Group/Global Marine Development Corp/United Engineers and Construction team.

flows that range from a few inches in some tidal basins to 25 to 30 ft (7.5 to 9 m) in the Passamaquoddy Bay, which is a part of the Bay of Fundy, located between Maine, United States, and New Brunswick, Canada.

There have been several proposals to harness tidal power to produce electricity, including one to build an 800- to 14,000-MW_e tidal-electric system in the Passamaquoddy Bay. Such a system involves the construction of a number of dams across the entrances to the tidal basin. The water then flows back and forth through a number of reversible water turbines in the dams.

Three tidal-electric systems have been constructed in the world. They include a very small (2-MW_e) tidal-electric plant at Kislaya Guba, Russia, a relatively new 20-MW_e system off the Bay of Fundy on the Annapolis River in Nova Scotia, Canada, and a 240-MW_e tital system on the Rance River Estuary on the channel island coast of France. A diagram of one of the twenty-four 10-MW_e reversible hydraulic turbines used in the Rance installation is shown in Fig. 1.4. This plant is currently being used as a pumped-storage system. During times of low power demand, the generator-motor units are reversed and they pump seawater into the estuary. The water is subsequently released through the same generator during times of peak power demand.

The Canadian tidal system was completed in 1984 and is considered to be a prototype of other systems that might be installed along the Bay of Fundy, in Canada. The Annapolis tidal installation employs a single-effect water turbine,

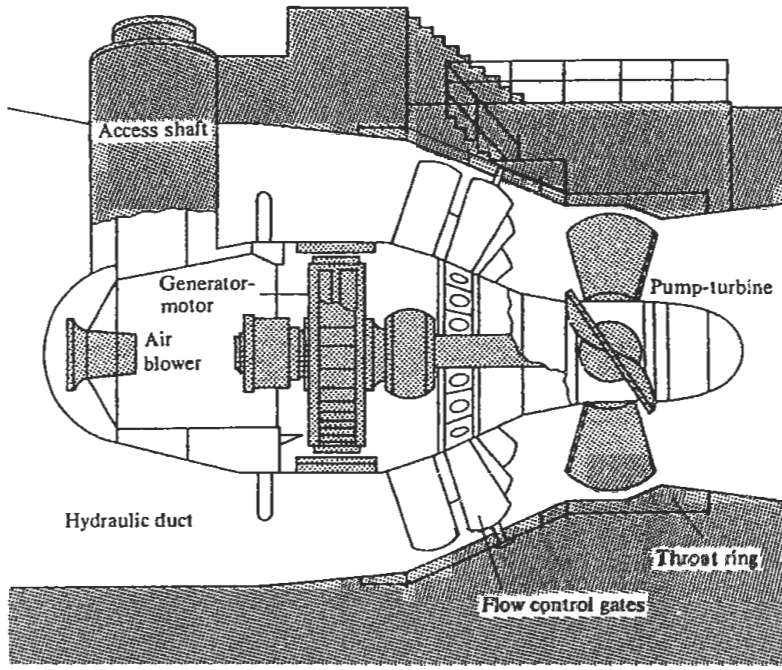


FIGURE 1.4
A pump-turbine unit of the La Rance tidal-electric station. The system is composed of 24 of these 10-MW_e units. (*Courtesy of the Editors of Power, the McGraw-Hill Magazine of Energy Systems Engineering.*)

which is one that produces power only when the tide is going out, whereas the Rance tidal plant employs double-effect water turbines. The tidal range on the Annapolis averages 21 ft. The next installation on the Bay of Fundy is likely to be at the entrance to Cobequid Bay on the Minas Basin where the average tidal range is 39 ft—the highest in the world. In fact, a tidal-electric station with a total power of 5000 MW_e has been proposed for this site.

The total potential of all the tidal-power systems of the world has been estimated to be some 64,000 MW_e. While this is a very large block of power, it is less than 10 percent of the total generation capacity of the world. Although the utilization of tidal power does not provide a solution to the world's energy requirements, this source is nondepletable and relatively pollution-free. There is, however, some concern that major utilization of tidal energy could effect the tides in surrounding tidal basins, causing flooding of some areas.

Since the tide has a cycle of about 12.5 h, tidal power systems have a low capacity factor, particularly if they employ single-effect water turbines (capacity factor $\approx$35 percent with no service outages). Since the high tide is approximately 30 min later every day, there will be some times each month when the time of peak power generation will also occur during the time of minimum power demand.

Presently, the major source of the world's fuel energy is a capital energy source called *fossil fuel.* This source supplies about 90 percent of the total fuel energy in the United States. The other 10 percent is primarily hydroelectric power and nuclear power. The conversion processes for these energy sources are presented in later chapters.

The final major source of fuel energy available to the human race is geothermal energy. This is thermal energy trapped beneath and within the solid crust of the earth. This energy exists in the form of steam, hot water, and/or hot and molten rock. It is released naturally as geysers, hot springs, and volcanic eruptions. Geothermal energy comes from two sources. It includes the primordial thermal energy which was present when the earth was formed as well as the thermal energy produced from the decay of heavy radioisotopes.

Geothermal energy sources are normally put into one of two categories. *Hydrothermal* geothermal sources are those associated with steam and hot water. The geothermal energy sources that are associated with hot rock are called *petrothermal* energy sources.

There are tremendous reserves of thermal energy trapped beneath the earth's crust. However, to date, it has not been possible to drill through the earth's crust, despite several attempts. Consequently, the only recoverable geothermal reserves are those pockets that are trapped within the earth's crust. These pockets are normally found near active geological fault lines.

The utilization of geothermal energy is not a new technology, as the first geothermal steam well was drilled at Larderello, Italy, in 1904. The present electrical capacity of that plant is now around 400 MW_e. There are several geothermal power plants in the United States (California and Utah) and there are also plants in Mexico, Iceland, New Zealand, Japan, and Russia. All these are located on or near major geological faults. A schematic diagram of a typical power system is shown in Fig. 1.5.

Many people have been promoting geothermal energy as a major source of pollution-free energy. Upon closer examination, however, geothermal energy may not be as pollution-free as is promoted. Air pollution at a geothermal installation may be a significant problem because of the emission of radioactive radon gas and hydrogen sulfide (H_2S) gas. Hydrogen sulfide is a poisonous gas.

Because of the relatively poor steam conditions at most sites, a geothermal power plant usually pumps over 3 times more thermal energy into the environment for each unit of electricity produced than does a conventional fossil power plant. This is called *thermal pollution* and is discussed in greater detail in Chap. 6.

Hot-water geothermal (hydrothermal) energy sources normally have very high mineral content. This produces several problems. First, the minerals will plate out on the heat-transfer surfaces as the hot water is cooled. Second, the disposal of the saturated cold water may be a problem. Another problem with hot-water sources is possible land subsidence.

In most of the geothermal steam systems, the waste steam is sometimes vented directly to the atmosphere with an accompanying noise pollution. Another possible problem is increased seismic activity that might be caused by the

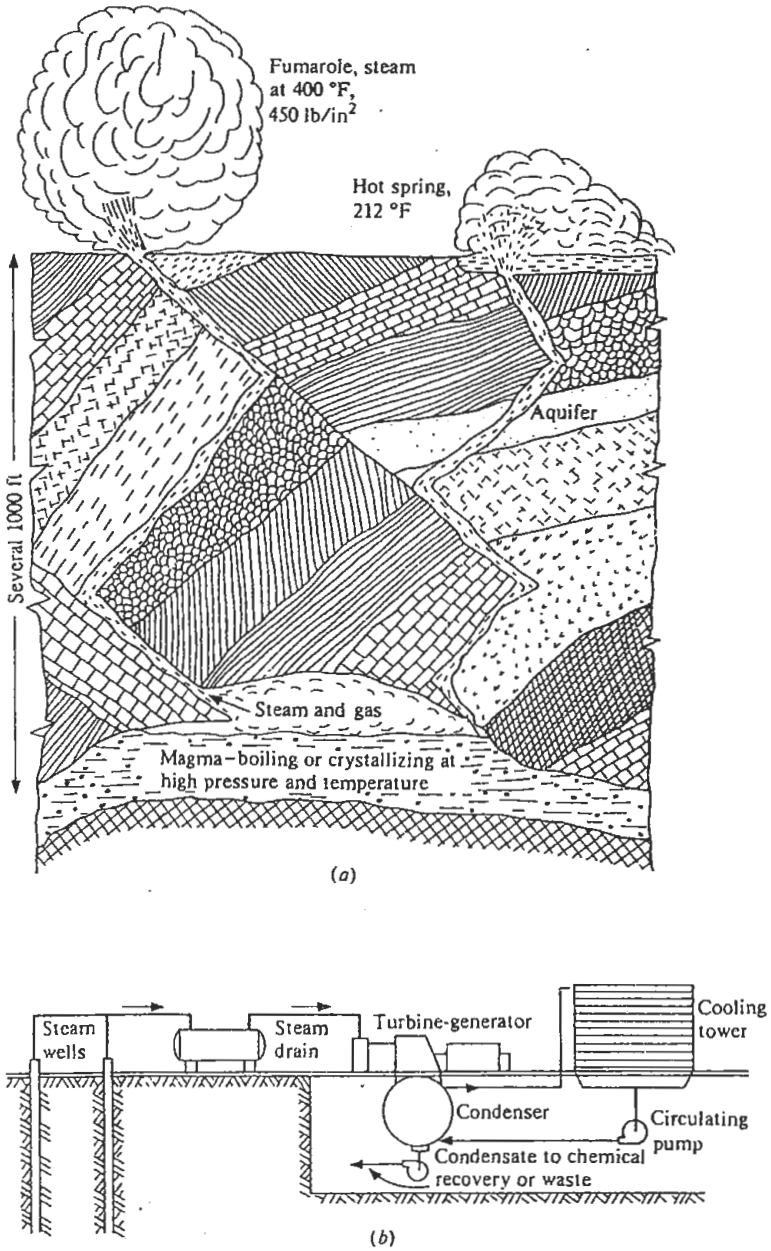


FIGURE 1.5
Schematic diagram of a typical geothermal deposit and geothermal power plant. (*Summers, 1971.*)

ıtilization of the energy source. This is particularly true if water is injected into ractured hot rock to remove the heat. The water can lubricate the fault and hereby increase the seismic activity.

While there are vast quantities of geothermal energy trapped beneath the :arth's crust in the hot mantle and the molten core, the recoverable geothermal :nergy trapped within the earth's crust is fairly limited. Moreover, these pockets, ike fossil fuels, are normally depleted when the thermal energy is removed. The otal estimated recoverable energy from the world's major geothermal areas is ıbout 3,000,000 MW_{th} · years.

1.6 ENERGY RESERVES

The energy reserves of the earth can be divided into four general categories. These include renewable or nondepletable sources, fossil fuels, fissionable and 'ertile materials, and fusionable isotopes. In some instances, the amount of energy ·eserves is strongly dependent on the current market price of raw energy. This s particularly true for nonrenewable energy reserves such as shale oil, oil, and ıranium. As the cost of energy increases, it becomes profitable to mine the .ow-grade ores and resort to secondary and tertiary recovery methods for the production of petroleum. This effectively increases the usable reserves.

A good example of just how price effects the recoverable reserves is shown by the price of natural uranium. The useful fuel in this material is uranium-235 (U-235), the only naturally occurring fissionable isotope. In Table 1.1, the U-235 reserves are listed as 13.7×10^{21} J, which corresponds to the present price of $30 per pound of U_3O_8. If the uranium price is increased by a factor of 4 ($120 per lbm), the available reserves would rise to 22.0×10^{21} J. If the price is further increased to $1800 per pound, the available reserves would increase to $30{,}880 \times 10^{21}$ J, a two-thousand-fold increase. While a sixty-fold increase in the price of uranium feedstock would certainly increase the cost of nuclear power, it is estimated that the total increase in the cost of nuclear power would be less than a factor of 4 since the present ore cost is such a small part of the current overall cost of electrical energy from nuclear power.

A partial list of the world's energy reserves is given in Table 1.1. The values in this table came from a number of different references, but in each case, the highest or most optimistic values are listed. These values change constantly as new discoveries are made, as the world consumes some sources, and as the price of energy changes.

Care must be taken when comparing the energy reserves from different sources in Table 1.1. The values in the table are pure energy or power values and most of them are utilized by first converting them to thermal energy. If the final desired energy form is either mechanical or electrical energy, some of the sources, such as tidal, water, and wind power, can be converted to these energy forms with a much higher conversion efficiency than the other sources.

Figure 1.6 depicts several logarithmic energy scales along with some of the more important energy terms. The energy scale ranges from very small values

TABLE 1.1
Estimated energy reserves of the world

Source	Amount	Type
Total available tidal power[a,b]	6.7×10^{10} W	Mechanical
Total available water power[a,b]	300.0×10^{10} W	Mechanical
Wind power in the United States[a,b]	970.0×10^{10} W	Mechanical
Recoverable geothermal energy	0.4×10^{21} J	Thermal
Shale-oil reserves[c,d]	1.2×10^{21} J	Chemical
Tar-sand oil reserves[c,d]	1.8×10^{21} J	Chemical
Natural gas reserves[c]	9.5×10^{21} J	Chemical
Petroleum reserves[c]	11.7×10^{21} J	Chemical
Uranium-235 reserves[d,e]	13.7×10^{21} J	Nuclear
Solar power in the United States[a]	$187{,}000.0 \times 10^{10}$ W	Electromagnetic
Thorium ($^{233}_{92}$U)[f]	71.7×10^{21} J	Nuclear
Coal and lignite[c]	200.0×10^{21} J	Chemical
Uranium-238 ($^{239}_{94}$Pu)[f]	$1{,}800.0 \times 10^{21}$ J	Nuclear
Deuterium ($^{2}_{1}$H)-tritium ($^{3}_{1}$H)[g]	$6{,}100.0 \times 10^{21}$ J	Nuclear
Deuterium ($^{2}_{1}$H)-deuterium ($^{2}_{1}$H)[g]	$6{,}000{,}000.0 \times 10^{21}$ J	Nuclear

[a] These reserves are nondepletable reserves and are actually power sources.

[b] These reserves can be converted directly to mechanical energy while most of the rest of the reserves must normally be converted into thermal energy.

[c] These reserves are classed as fossil fuels.

[d] These reserves are strongly dependent on the price of energy.

[e] This is the only naturally occurring fissionable fuel isotope.

[f] Utilization of these reserves depends on the development of the breeder fission reactor and subsequent fissioning of the isotope shown in parentheses.

[g] Utilization of these reserves depends on the development of the fusion reactor.

such as the kinetic energy of atoms through 56 orders of magnitude to the daily output of the sun. A mass-to-energy scale is also included.

1.7 ENERGY UTILIZATION

Since the dawn of history, the human race has used more and more energy as new energy sources have been discovered and new and better conversion methods and techniques have been developed. The earliest source of energy was muscle power—first that of humans and later that of animals. Sometime early in social evolution, people learned to produce energy from the combustion of carbohydrates (plants and wood). Around 3000 B.C. they began to utilize the wind to drive ships, and during the Dark Ages wind was harnessed to drive windmills. Water power was first utilized around the time of the birth of Christ, but it was not until the late eighteenth century that thermal energy was utilized to produce large quantities of mechanical energy.

It is interesting to examine the primary sources of fuel energy in the United States during the last 130 years or so to see how the primary sources of fuel energy have changed. In 1850, over 90 percent of the fuel energy came from the

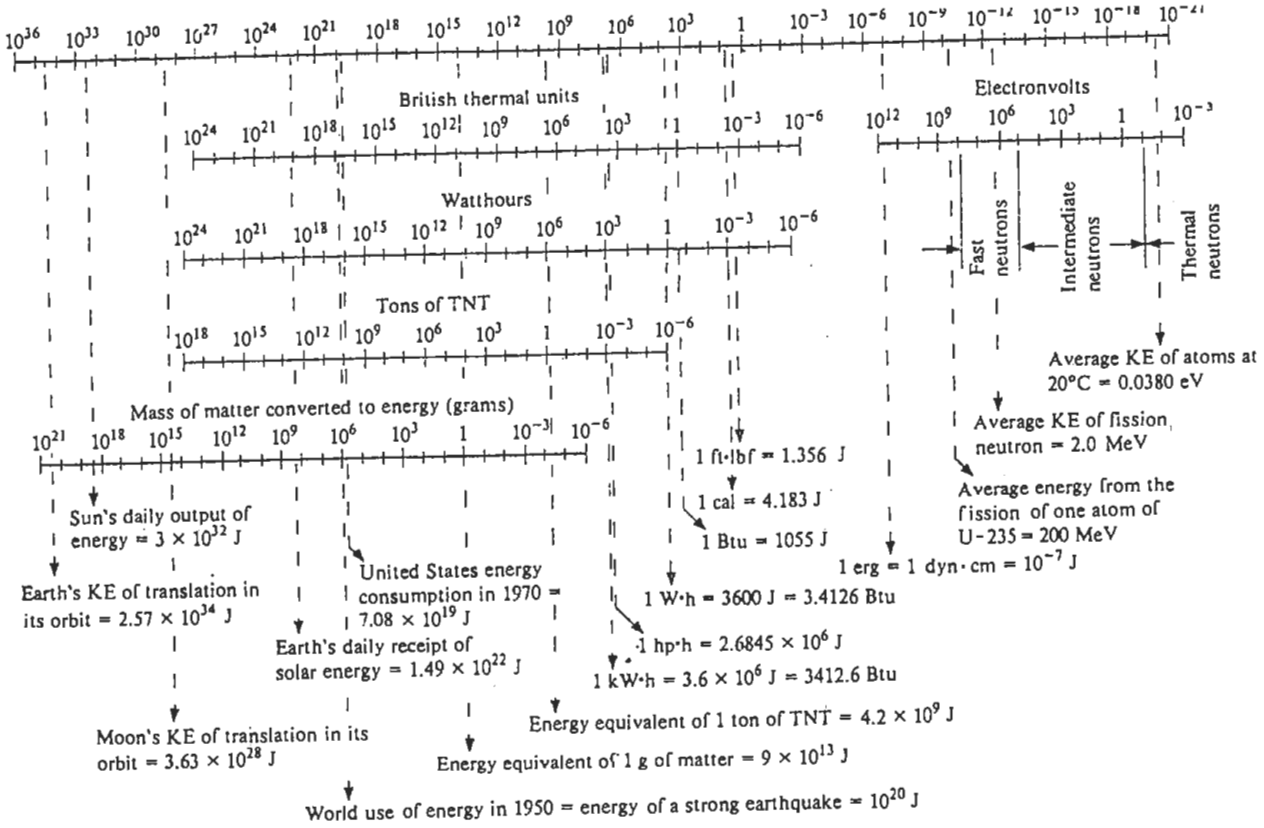


FIGURE 1.6
Energy scales.

combustion of wood and wood products. Sixty-five years later, in 1915, coal provided about 80 percent of the fuel energy and wood's contribution had dropped to 10 percent. Sixty-five years later again, in 1980, 75 percent of the fuel energy came from the combustion of petroleum and natural gas and 20 percent was provided by coal.

In 1980, the United States consumed approximately 80.1×10^{18} J (75.9×10^{15} Btu). The energy sources and utilization for the United States are presented in Table 1.2 and these data are shown graphically for the last 50 years or so in Fig. 1.7. The energy flow through the United States economy during the 1970–1990 time period is shown in Fig. 1.8.

Realizing how the principal source of fuel energy has changed over the years, it is interesting to speculate as to just what the primary source of fuel energy will be in the year 2050, another 60 years or so from now. Will it be solar energy, fossil fuels, fission reactors, fusion reactors, or some other power source?

TABLE 1.2
The production and consumption of energy in the United States

		Production by type of fuel,‡ %						Consumption by economic sector, § %				
Year	Total Usage, quads†	P	C	G	H	N	O	R	I	T	E	O
1950	34.0	39.7	38.0	18.1	4.2	0.0	0.0	22.3	36.2	25.3	14.7	1.5
1955	39.7	44.1	29.1	23.3	3.5	0.0	0.0	21.6	35.2	24.8	16.6	1.8
1960	44.1	45.0	22.8	28.5	3.7	<0.1	0.0	22.8	32.9	24.3	18.5	1.5
1965	53.3	43.6	22.3	30.2	3.8	0.1	0.0	22.2	32.2	23.8	20.8	1.0
1970	67.1	44.0	18.9	32.8	4.0	0.3	0.0	20.8	30.1	24.2	24.2	0.7
1971	68.7	44.5	17.5	33.2	4.2	0.6	0.0	20.7	29.1	24.8	25.1	0.3
1972	71.9	45.8	17.3	32.0	4.1	0.8	0.0	20.3	28.5	25.1	25.8	0.3
1973	74.7	46.6	17.8	30.4	4.0	1.2	0.0	19.1	28.6	25.3	26.6	0.4
1974	73.0	45.8	17.9	30.2	4.5	1.6	0.0	19.1	27.9	25.3	27.4	0.3
1975	70.6	46.2	18.2	28.4	4.6	2.6	0.0	19.2	25.4	26.3	28.7	0.4
1976	74.2	47.3	18.4	27.4	4.1	2.8	0.0	19.3	26.2	25.6	28.9	0.0
1977	76.3	48.7	18.2	26.1	4.1	2.9	0.0	18.3	26.0	25.8	29.9	0.0
1978	78.2	47.1	19.1	26.1	4.4	3.3	0.0	18.1	25.5	26.3	30.1	0.0
1979	78.9	47.5	19.6	25.4	4.0	3.5	0.0	16.6	27.5	25.2	30.7	0.0
1980	76.0	45.1	20.3	26.8	4.0	3.7	0.1	16.0	27.0	24.4	32.6	0.0
1981	74.0	43.2	21.5	26.9	4.0	4.3	0.1	15.6	25.6	25.3	33.5	0.0
1982	70.8	42.7	21.6	26.1	4.9	4.6	0.1	16.2	23.6	25.9	34.3	0.0
1983	70.5	42.6	22.6	24.6	5.2	4.8	0.2	15.8	22.7	26.1	35.4	0.0
1984	74.1	42.0	23.0	25.0	4.5	5.2	0.3	15.6	23.5	25.8	35.1	0.0
1985	74.0	41.9	23.6	24.1	4.1	6.0	0.3	15.2	22.7	26.2	35.9	0.0
1986	73.9	43.1	23.4	22.4	4.3	6.5	0.3	15.1	21.6	27.0	36.3	0.0

† A quad is a unit of heat energy equal to 10^{15} Btu (in the United States).

‡ Type of fuel for production: P—petroleum; C—coal; G—gas; H—hydroelectric; N—nuclear; O—other.

§ Sector for consumption: R—residential; I—industrial; T—transportation; E—electricity production.

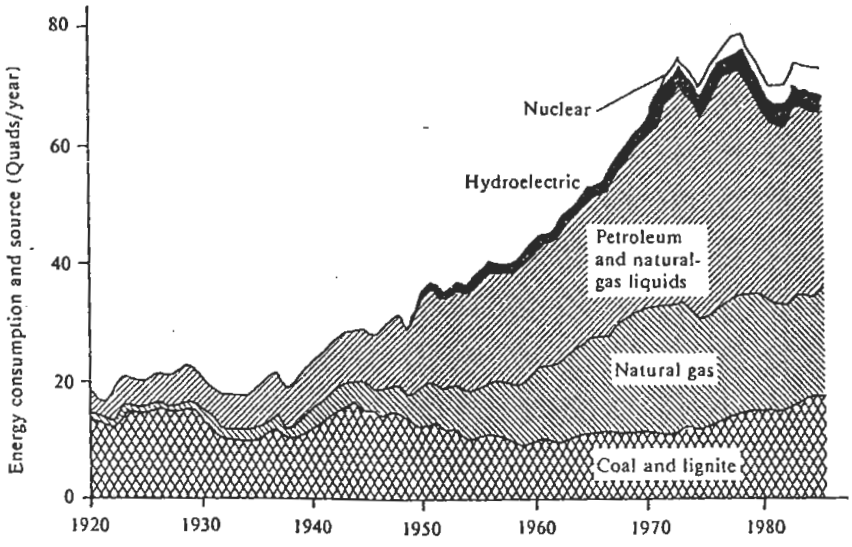


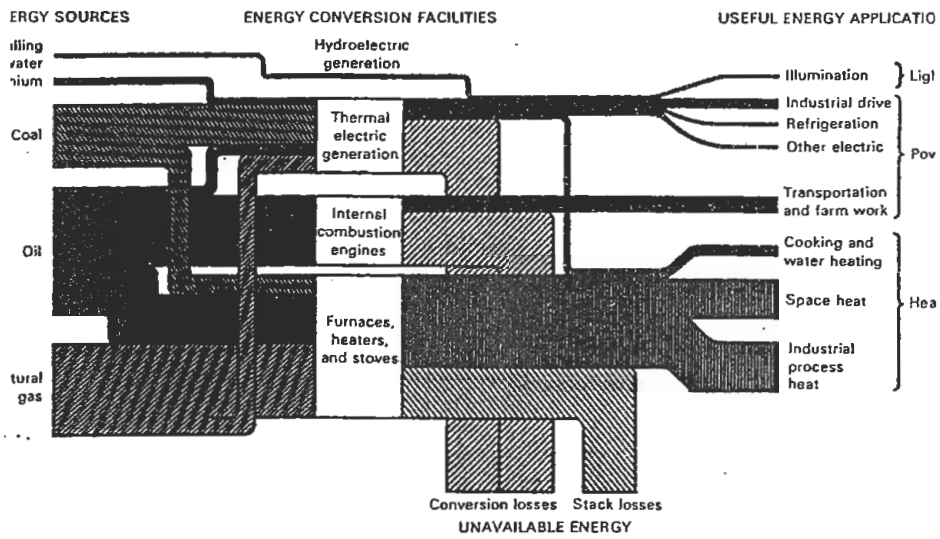
FIGURE 1.7
U.S. energy supply and consumption, 1920-1986.

One can find any number of "energy experts" who will predict that any of these four sources, plus some others, will become the primary source of fuel energy by then.

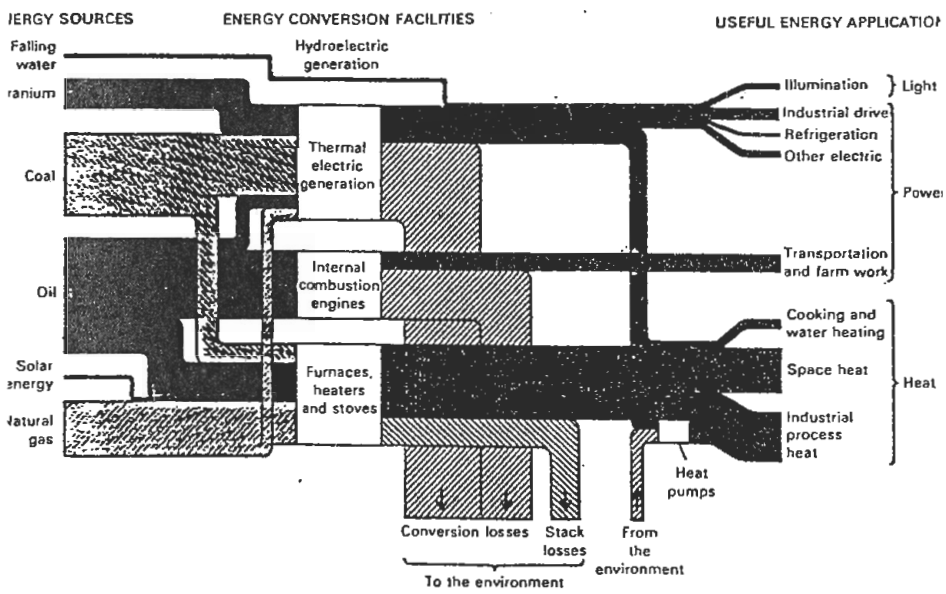
1.8 ELECTRICAL POWER GENERATION AND CONSUMPTION

The electrical power generation in the Uuited States for the year 1970 totaled 1.62×10^{12} kWh (5.5×10^{15} Btu). The total installed capacity was 356,000 MW_e. This means that the average capacity factor for the electrical grid was about 50 percent. The prime sources for the production of electricity were as follows: 6.3 percent from oil, 22.0 percent from natural gas, 52.5 percent from coal and lignite, 18.2 percent from hydroelectric plants, and 1.0 percent from nuclear power.

By 1975, the installed nuclear capacity had risen to almost 8 percent and over half of the new electrical generation ordered in 1975 was nuclear. After the Three Mile Island (TMI) Nuclear Station suffered a severe accident in 1978, no new nuclear plants have been ordered in the United States and a number of nuclear units already ordered and some well under construction or even completed have been canceled. Despite this, a total of 100 nuclear power plants were in operation in the United States by 1986 and nuclear power supplied about 15 percent of the electrical energy. In 1984, nuclear power had displaced hydroelectric power as the second largest source of electrical energy.



(a)



(b)

FIGURE 1.8
Energy sources and consumption in the United States. (*a*) Typical flow of energy through the United States economy in the mid-1970s. (*b*) Predicted flow of energy through the United States economy in the 1990s.

It is difficult to predict just what the future of nuclear power will be in the United States. Economic problems associated with high interest rates, inflation, extended construction periods, and backfitting required by the Nuclear Regulatory Commission (NRC) as a result of TMI along with the poor public relations caused by the TMI and Chernobyl accidents have clouded the once promising future of nuclear power in the United States. The rest of the world, however, including the USSR, seems to believe that nuclear energy is the best source of energy for the production of electricity.

Barring any significant technical breakthroughs in the utilization of other energy sources or politically motivated moratoriums, the primary sources of fuel energy for the production of electricity during the balance of the twentieth century are expected to be coal and lignite, nuclear fission reactors, and hydroelectric systems.

1.9 GROWTH RATES

It is interesting to examine the consequences of a quantity that is continuously increasing, whether it is energy consumption, population, gross national product, personal income, or any other variable that might be chosen. If a quantity, such as the rate of energy consumption (power) P, increases at the same annual fractional rate i, the rate of change of the quantity per unit time becomes:

$$\frac{dP}{dt} = i(P) \qquad \text{or} \qquad \frac{dP}{P} = i\,dt \tag{1.3}$$

Setting the initial power to be P_0 at some arbitrary time $t = 0$, Eq. (1.3) can be integrated to yield:

$$\ln\left[\frac{P}{P_0}\right] = it \qquad \text{or} \qquad P = P_0\, e^{it} \tag{1.4}$$

In these equations, i is the constant growth rate on an annual basis.

A graph of power versus time is shown in Fig. 1.9. To make this a general plot, dimensionless parameters P/P_0 and t/t_D are used, where t_D is the doubling time or the time required for the power to increase by a factor of 2. Thus, when $t = t_D$, $P = 2P_0$, and substituting into Eq. (1.4) gives:

$$it_D = \ln 2 \qquad \text{or} \qquad t_D = \frac{[\ln 2]}{i} = \frac{0.693}{i} \tag{1.5}$$

From 1920 to 1975, the electrical energy consumption in the United States historically averaged around 7 percent per year. This means that the electrical generating capacity doubled every 0.693/0.07 or 9.9 years in order to keep up with the demand. Since 1975, the consumption of electricity has not increased nearly as rapidly.

The total energy consumed during a given period of time can be found by integrating Eq. (1.4) over the time interval. It is convenient to assume that the

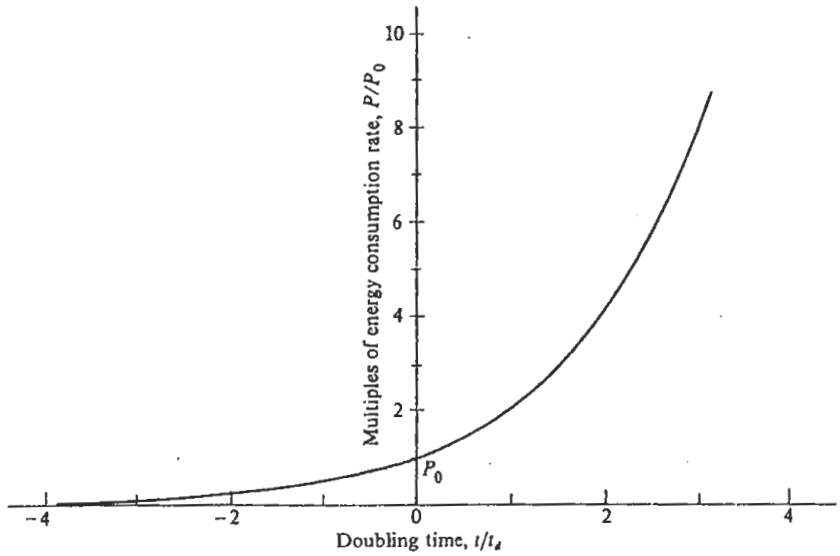


FIGURE 1.9
Variation of energy-consumption rate for a constant rate of growth.

exponential growth rate has occurred from time $t = -\infty$. The total energy consumed, E_0, from time $t = -\infty$ to time $t = t_1$ is obtained as follows:

$$E_0 = \int_{-\infty}^{t_1} P(t)\, dt = \int_{-\infty}^{t_1} P_0\, e^{it}\, dt = \frac{P_0}{i}\, e^{it_1} \tag{1.6}$$

Let E_1 be equal to the total energy consumed between $t = t_1$ and $t = t_2$. Then,

$$E_1 = \int_{t_1}^{t_2} P_0\, e^{it}\, dt = \frac{P_0}{i}[e^{it_2} - e^{it_1}]$$

$$= \frac{P_0}{i}\, e^{it_1}[e^{i(t_2 - t_1)} - 1] = E_0[e^{i(t_2 - t_1)} - 1] \tag{1.7}$$

If the time interval $(t_2 - t_1)$ in Eq. (1.7) is set equal to the doubling time t_D, the exponential term in Eq. (1.7) becomes numerically equal to 2.0 and this means that $(E_1 = E_0)$. Thus, in any given doubling period, the total energy consumed in that period is equal to the total energy consumption in all the time prior to the doubling period.

This result leads to some sobering if not frightening prospects and conclusions. If new fuel discoveries extend our present known fuel reserves by an order of magnitude of say, 10 times as much, the new fuel reserves will last only 3.32 doubling times unless the annual growth rate is reduced. Thus, in Example 1.2, the U.S. coal reserves are expected to last 93 years based on a 4 per cent/year growth rate (a doubling time of 17.3 years). If 10 times our current coal reserves

are found, they will not last another 930 years but only another (3.32) (17.3) = 59 years, unless the growth rate is reduced.

Example 1.1. Using the 1970 value of U.S. energy consumption rate of 70.8×10^{18} J/year, and assuming a 4 percent growth rate per year, find the doubling time and the energy consumption rate in the year 2000.

Solution. Given: $i = 0.04$ per year, $P_0 = 70.8 \times 10^{18}$ J/year, $t = 0$ @ 1970, $t = 30$ years @ 2000. Then

$$\text{Doubling time} = t_D = \frac{\ln 2}{i} = \frac{0.693}{0.04} = 17.33 \text{ years}$$

$$\text{Power at year 2000} = P_{30} = P_0 e^{it} = 70.8 \times 10^{18} e^{(0.04)(30)}$$

$$= 235.1 \times 10^{18} \text{ J/year}$$

Example 1.2. Using the energy consumption rate and growth rate of Example 1.1 along with the U.S. coal reserves of 70×10^{21} J, estimate how long the coal will last as an energy source if it supplies all the fuel energy.

Solution. Given: $i = 0.04$ per year, $P_0 = 70.8 \times 10^{18}$ J/year, $t_1 = 0$, $E_1 = 70.0 \times 10^{21}$ J. Then

$$E_1 = 70 \times 10^{21} = \frac{P_0}{i} e^{it_1}[e^{i(t_2 - t_1)} - 1]$$

$$t_2 = \frac{1}{i} \ln \left[\frac{E_1 i}{P_0} + 1 \right] = \frac{1}{0.04} \ln \left\{ \frac{70 \times 10^{21}(0.04)}{70.8 \times 10^{18}} + 1 \right\}$$

$$= 92.56 \text{ years}$$

1.10 ENERGY ECONOMICS

GENERAL. One of the most important considerations of any proposed engineering system, particularly energy-conversion systems, is its cost. While the general public is generally supportive of systems that protect the environment, the support generally lasts only as long as a system does not have significant costs associated with it. Consequently, it is imperative that today's power engineer know how to estimate the costs associated with any new system.

Energy costs from a given power plant can be divided into two general categories—capital and operational. The capital costs are those parts of the overall power costs which are constant and must be paid regardless of whether the plant operates or not, unless the company declares bankruptcy. Consequently, while the total annual value of the capital cost is constant, the capital costs per energy unit output (cost/kWh) decrease as the plant output increases (an increase in the capacity factor). The capital costs include the land cost, construction costs, equipment costs, investment charges, and some taxes and some insurance. Out of this list, the larger costs are usually those relating to construction, equipment, and investment charges.

The operational power costs include all the expenses associated with the operation of the plant. They consist of the wages and fringe benefits of the operating personnel, the raw material (fuel) costs, maintenance costs, certain taxes, and some insurance. Since these costs are essentially directly proportional to the energy output or capacity factor for the plant, the unit power costs, in cents/kWh, associated with operation are essentially constant and independent of the energy output of the plant. Moreover, since these costs are incurred as the system is operated and the company is promptly reimbursed for the energy, there is normally no interest cost associated with these expenses. The principal operating cost for a power plant is usually for fuel, and this can normally be easily estimated.

CAPITAL COSTS. The capital costs associated with the initial plant cost (land, equipment, and construction) and the associated interest charges can be determined from basic economic equations. If the original cost or present value of an energy-conversion system is (Pr) dollars, the value of this investment, including the interest earned over the life of the system, can be evaluated from the compound-interest formula. When an investment of (Pr) dollars is made at an annual interest rate of i percent/year, which is compounded n times a year, the total future or final worth, F_{nt}, of the investment at the end of t years is:

$$F_{nt} = \Pr\left[1+\frac{i}{n}\right]^{nt} \tag{1.8}$$

F_{nt} is sometimes called the *future value* of the investment. As n approaches infinity, the principal, Pr, grows at a constant rate and Eq. (1.8) becomes the same as Eq. (1.4), or:

$$F_t = \Pr e^{it} \tag{1.9}$$

If the power payments are made to the company in equal increments of A dollars m times a year for t' years, these funds can be invested and subsequently used to pay off the original investment plus accrued interest at the end of the operating period. The total value at the end of t' years, including compounded interest, of equal payments of A dollars made m times a year can be found from the general "annuity equation" for the case where the payments are made at the end of each time interval, or:

$$F_{mt'} = \frac{Am}{j}\left[\left(1+\frac{j}{m}\right)^{mt'} - 1\right] \tag{1.10}$$

In Eq. (1.10), j is the effective short-term interest rate when it is compounded m times a year. If the actual interest rate is j' and is compounded m' times a year, and m' is not equal to m, the effective short-term rate j, based on m compounding periods per year, must be evaluated from the following equation:

$$j = m\left[\left(1+\frac{j'}{m'}\right)^{m'/m} - 1\right] \tag{1.11}$$

Occasionally, it is desirable to determine the future value of periodic payments where the payments are increased or escalated at a constant annual

rate of e, based on m payments per year, and also where the payments are escalated at a fixed dollar amount E, when each payment is made. The final or future value F_{mt} of periodic payments which are escalated at an annual percentage rate of e per year is given by the following formulas:

$$F_{mt} = \frac{mA_1}{j-e}\left[\left(1+\frac{j}{m}\right)^{mt} - \left(1+\frac{e}{m}\right)^{mt}\right] \qquad \text{for } j \neq e \qquad (1.12)$$

$$F_{mt} = mtA_0\left[1+\frac{j}{m}\right]^{mt} = mtA_1\left[1+\frac{j}{m}\right]^{mt-1} \qquad \text{for } j = e \qquad (1.13)$$

In these equations, A_1 is the value of the first payment. The value of the mt payment, A_{mt}, is given by the following equation:

$$A_{mt} = A_0\left[1+\frac{e}{m}\right]^{mt} = A_1\left[1+\frac{e}{m}\right]^{mt-1} \qquad (1.14)$$

The total amount of money paid into the account can be determined by simply setting j equal to zero over the investment period and applying Eq. (1.12).

If each payment is escalated by a fixed dollar amount E, the final or future value F_{mt} of the payments, including interest, is given by the following equation:

$$F_{mt} = \left\{\left(A_1+\frac{mE}{j}\right)\left[\left(1+\frac{j}{m}\right)^{mt}-1\right] - mtE\right\} \quad (m/j) \qquad (1.15)$$

The total amount of money paid into the account can be determined from the following equation:

$$\text{Sum of payments} = mt\left[A_1+\left(\frac{E}{2}\right)(mt-1)\right] \qquad (1.16)$$

If e and E are zero, the equations for F_{mt} all reduce to Eq. (1.10). Using Eq. (1.8) and (1.12) or (1.13) or (1.15) along with the salvage value of the system at the end of life, one can determine either the principal Pr, given the value of the first payment, A_1, or the value of the first payment, A_1, given the principal Pr, in order for the system to break even over t'' years; t'' is the true "payback period." Combining these equations gives:

At breakeven ($t = t''$),

Future value ($t = t''$) of initial investment ($F_{nt''}$)

= future value ($t = t''$) of the periodic savings ($F_{mt''}$)

+ salvage value (SV)

or

$$F_{nt''} = F_{mt''} + \text{SV}$$

or

$$\text{Pr}\left(1+\frac{i}{n}\right)^{nt''} = \frac{mA_1}{j-e}\left[\left(1+\frac{j}{m}\right)^{mt''} - \left(1+\frac{e}{m}\right)^{mt''}\right] + \text{SV} \qquad (1.17)$$

Large electrical generating stations typically have a construction period of 3 to 15 years. Since money is spent during the entire construction period and prices and wages will probably escalate due to inflation, the effective value of the plant before it goes into operation, Pr, is considerably larger than the actual cash outlay during the construction period. If p construction payments of R_1 dollars are made each year, and assuming that these payments could earn an annual interest rate of i percent/year compounded p times a year, the value of the investment at plant startup is:

$$\text{Pr} = \frac{pR_1}{i-e}\left[\left(1+\frac{i}{p}\right)^{pt_c} - \left(1+\frac{e}{p}\right)^{pt_c}\right] \qquad \text{for } i \neq e \tag{1.18}$$

or

$$\text{Pr} = pR_1 t_c \left[1+\frac{i}{p}\right]^{pt_c-1} \qquad \text{for } i = e \tag{1.19}$$

where t_c is the construction time in years. The values of a given individual payment can be determined from Eq. (1.15). The value of the first payment, R_1, can be determined from the following equation:

$$R_1 = \frac{(\text{nominal cost, \$/kW})(\text{rated capacity, kW})}{pt_c}\left[1+\frac{e}{p}\right] \tag{1.20}$$

It will be noted in the economic equations that two interest rates, i and j, are employed. The interest rate i is a long-term interest rate while j is a short-term interest rate. If one has a large sum of money and is willing to invest it, untouched, for a long time, a higher (long-term) interest rate can normally be obtained. Thus, the long-term rate i is applied to the equations involving Pr while the short-term rate j is used in those equations involving the periodic payments A. The number of compounding periods for i is always n while m and p are used for both j and e. Normally, i is always larger than j—if not, Pr should be invested in a series of short-term investments.

OPERATING COSTS. As indicated earlier, the operating costs include the maintenance costs, labor costs, fuel costs, and some insurance and taxes. These are directly associated with the operation of the plant and the annual operating costs are, essentially, directly proportional to the plant output. Of these costs, the labor and fuel costs can be estimated and probably the insurance and taxes can also be estimated. Maintenance costs, on the other hand, cannot be estimated accurately unless the maintenance history of a similar system is known.

Most utilities will negotiate with fuel suppliers to provide the fuel at a certain price per unit of energy, usually cost per million Btu. If the fuel cost is f cents per MBtu, the average unit power cost associated with the fuel is:

$$\text{Unit fuel cost} = \frac{f(\text{HR})}{10^6} = \frac{0.003413f}{\eta_{\text{th}}} \qquad \text{¢/kWh} \tag{1.21}$$

In this equation, η_{th} is the overall thermal efficiency of the power system and

HR is overall heat rate of the plant, in Btu/kWh. The heat rate is defined in the next section of this chapter.

The operational cost associated with labor is somewhat dependent on the power output of the plant if the system produces any energy at all. The unit labor cost, in ¢/kWh, can be evaluated from the following equation:

$$\text{Unit labor cost} = (1.14 \times 10^{-5}) \frac{(\text{AS})(N)}{(P_{\max})(\text{CF})} \quad ¢/\text{kWh} \tag{1.22}$$

In this equation, N is the number of workers at the plant, AS is the average annual salary, in dollars per year, including fringe benefits, $P_{\max}$ is the rated power output of the plant, in MW_e, and CF is the capacity factor of the plant for the period of operation. The capacity factor is the ratio of average-to-rated power output of the plant.

SYSTEM POWER COSTS. The power costs for various energy-conversion systems can be determined with the use of the basic economic equations, although the examples presented here are very simple compared to the actual calculations. An economic analysis for a solar heating system is presented in Example 1.3. This example shows the use of Eq. (1.17) in determining the system costs.

Various electrical generation systems have different distributions between the capital and operating costs, and the distribution of these costs often dictate how the system is employed in the power grid. Systems with high capital costs but low operating costs are used where long continuous operation is desired. Systems with low capital costs and high operating costs are used where intermittent operation is desired such as to meet peak power demands.

Combustion-turbine power plants are characterized by relatively low capital costs but have high fuel and maintenance costs. These systems are used as peaking units, which means they are employed only at times of peak power demand. Oil and gas-fired systems have intermediate capital and operating costs. Nuclear and coal-fired power plants are characterized by relatively high capital costs and low fuel costs. Thus, these plants are best suited for operation as "base-loaded" power plants where they operate as close to rated capacity as possible to reduce the unit capital power cost.

Example 1.3. Assume that a solar-powered home heating system can be built which will supply all the heating requirements of a house for 20 years. If the original investment could earn 10 percent/year, compounded daily, and annual fuel savings could earn 8 percent/year, compounded daily, calculate the annual heating bill at this time (a year before the solar system is installed, $t = 0$) which will make the system "break even" at the end of 20 years. Assume that the initial cost of the system is $8000 and that the salvage value of the plant is $5000. Also assume that the annual fuel costs escalate at a rate of 6 percent/year due to inflation, and based on this calculate the expected annual fuel cost during the eighteenth year if the solar system is not installed.

Solution. Given: Pr = \$8000; $i = 0.1$/year; $n = 360$ compounding periods/year; $t_c = 0$; $t_{op} = 20$ years; $e = 0.06$/year; $j' = 0.08$/year; $m' = 360$/times/year; $m = 1$ time/year; SV = \$5000. Effective short-term interest rate, compounded annually = j.

$$j = m\left[\left(1+\frac{j'}{m'}\right)^{m'/m} - 1\right] = 1\left[\left(1+\frac{0.08}{360}\right)^{360/1} - 1\right] = 0.08328/\text{year}$$

Final value of the investment if it is put in the bank = $F_{20(360)}$.

$$F_{20(360)} = \text{Pr}\left[1+\frac{i}{n}\right]^{nt_{op}} = 8000\left[1+\frac{0.1}{360}\right]^{360(20)} = \$59{,}096$$

In order to break even, the final value of the annual savings plus the salvage value must equal F_{7200} or \$59,096.

$$F_{7200} = \frac{mA_1}{j-e}\left[\left(1+\frac{j}{m}\right)^{mt_{op}} - \left(1+\frac{e}{m}\right)^{mt_{op}}\right] + \text{SV}$$

$$= \frac{1(A_1)}{0.08328-0.06}[1.08328^{20} - 1.06^{20}] + 5000$$

$$= 74.957A_1 + 5000 = \$59{,}096$$

A_1 = required annual heating bill at end of the first year

$$= \frac{59{,}096}{74.957} = \$721.70/\text{year}$$

The required present heating bill (before solar system is installed) is A_0.

$$A_0 = \frac{A_1}{1+e/m} = \frac{721.70}{1+0.06/1} = \$680.80/\text{year}$$

Expected fuel cost during year 18 = $A_{18} = A_0(1+e/m)^{mt}$.

$$A_{18} = A_1\left(1+\frac{e}{m}\right)^{mt-1} = 721.70(1.06)^{17} = \$1{,}943.40/\text{year}$$

Example 1.4 gives an insight into the amount of capital required to build a modern power plant. Although the interest rates change constantly, this example is fairly representative of today's systems. It is interesting to note that if the construction period could be reduced from 12 to 6 years (which is about the time required to build a nuclear power plant in France), the total capital cost of the plant is reduced from \$633 billion to \$359 billion and the unit capital costs will be reduced from 9.11 to 5.14 cents/kWh. This example also shows the effect of charging or not charging for *construction work in progress* (CWIP). Some estimated power costs for large power stations that went on line in 1986 are presented in Table 1.3.

Example 1.4. Estimate the unit capital, fuel, and labor costs (in cents/kWh) associated with a 1200-MW_e nuclear reactor power plant if the nominal cost is \$1500 per kW_e. The annual interest rate is 12 percent/year, compounded quarterly. Assume that the plant requires a support staff of 400 people at an average annual salary of

TABLE 1.3
Estimated power costs for a 1000-MW_e power system (for operation in 1986)

Capital cost estimates, $/kW$_e$			
Capital costs	Nuclear (LWR)	Coal-fired with SO_2 scrubbers	Oil-fired
Plant cost (no escalation) in 1977 dollars	580	480	315
Escalation at 7% per year	260	260	175
Interest during construction (at 9%)	260	170	110
Total cost on completion ($/$kW_e$)	1100	910	600

Power generation costs						
	Nuclear (LWR)		Coal-fired with SO_2 scrubbers		Oil-fired	
Costs	$/$kW_e$	cents/kWh	$/$kW_e$	cents/kWh	$/$kW_e$	cents/kWh
Capital costs	1100	2.69	910	2.23	600	1.46
Fuel costs		1.33		2.12		4.96
Operation and maintenance		0.33		0.44		0.19
Total costs		4.35		4.79		6.61

Note: Fixed charge rate of 15 percent and plant capacity factor of 70 percent (from Bechtel).

$50,000 per year (including fringe benefits). The overall heat rate of the plant is 10,500 $Btu_{th}/kW_e h$, the capacity factor is 70 percent, the construction time is 12 years (a 6-year construction time will also be investigated) with an annual escalation of 7 percent/year on construction costs. The plant lifetime is 40 years, the fuel cost is 75 cents/MBtu and a construction payment is made each quarter during the construction period. The company will collect equal monthly payments (no escalation) from its customers once the plant goes into operation, and it is assumed that it will cost an estimated $200,000,000 to decommission the plant 52 years from now (a salvage value of −$200,000,000). The 6-year construction values are shown in parentheses.

Solution. Given: $N = 400$ workers; AS = $50,000/per year; $P_{max} = 1200$ MW_e; CF = 70 percent; $f = 75$ cents/MBtu; HR = 10,500 Btu/kWh; nominal cost = $1500 per kW_e; salvage value = SV = −$200,000,000.

During construction:

$t_c = 12$ years (6 years) $\quad i = j = 0.12$/year $\quad n = p = 4$ times/year $\quad e = 0.07$/year

During operation:

$i = j' = 0.12$/year $\quad n = m' = 4$/year $\quad m = .12$/year $\quad t_{op} = 40$ years $\quad e = 0$

Capital costs: During the construction, the initial value ($t = 0$) of all payments is

$$R_0 = P_{max}(\text{nominal cost})/pt_c = \frac{(1500)(1200)(1000)}{(4)(12)}$$

$$= \$37.5 \times 10^6/\text{quarter} \qquad (\$75 \times 10^6/\text{quarter})$$

First construction payment is

$$R_1 = R_0\left(1+\frac{e}{p}\right) = 3.75 \times 10^7\left(1+\frac{0.07}{4}\right)$$

$$= \$38.16 \times 10^6/\text{quarter}(\$76.31 \times 10^6/\text{quarter})$$

Total investment in the plant at reactor startup $= F_{12y} = F_{48}$

$$F_{48} = \frac{R_1 p}{j-e}\left[\left(1+\frac{j}{p}\right)^{nt_{op}} - \left(1+\frac{e}{p}\right)^{nt_{op}}\right]$$

$$= \frac{38.16 \times 10^6(4)}{0.12-0.070}\left[\left(1+\frac{0.12}{4}\right)^{48} - \left(1+\frac{0.07}{4}\right)^{48}\right]$$

$$= \$5594 \times 10^6 \qquad (\$3152 \times 10^6)$$

Value of the investment at the end of the operating period

$$F_{52y} = F_{48}\left[1+\frac{i}{n}\right]^{nt_{op}} = (5.594 \times 10^9)\left[1+\frac{0.12}{4}\right]^{4(40)}$$

$$= \$633.4 \times 10^9 \qquad (\$356.9 \times 10^9)$$

Effective annual interest rate based on monthly compounding is

$$j = m\left[\left(1+\frac{j'}{m'}\right)^{m'/m} - 1\right] = 12\left[\left(1+\frac{0.12}{4}\right)^{4/12} - 1\right] = 0.11882/\text{year}$$

Final value of power payments + earned interest + salvage value is

$$F_{52y} = \frac{mA_1}{j-e}\left[\left(1+\frac{j}{m}\right)^{mt_{op}} - \left(1+\frac{e}{m}\right)^{mt_{op}}\right] + \text{SV}$$

Since $e = 0$ during the operating period, $A_1 = A_0 = A_{mt} = A$. Thus

$$F_{52y} = \frac{12A}{0.11882-0}\left[\left(1+\frac{0.1188}{12}\right)^{480} - 1\right] + (-2 \times 10^8)$$

$$= 11{,}334A - 200{,}000{,}000 = 633.4 \times 10^9 \qquad (356.7 \times 10^9)$$

Required monthly charges to customers is

$$A = \$55.90 \times 10^6 \qquad (\$31.51 \times 10^6)$$

Average electrical energy output per month is

$$P_m = 1000(P_{max})(\text{CF})\frac{8766}{12}$$

$$= 1000(1200)(0.7)\frac{8766}{12} = 6.1362 \times 10^8 \text{ kWh/month}$$

$$\text{Unit capital cost} = \frac{(55.9 \times 10^6)(100)}{6.1362 \times 10^8}$$

$$= 9.11 \text{ cents/kWh} \qquad (5.14 \text{ cents/kWh})$$

Total capital costs charged to customers is

$$480A = \$26.83 \times 10^9 \qquad (\$15.12 \times 10^9)$$

Operating costs:

$$\text{Unit fuel costs} = (\text{HR})(f) \times 10^{-6} = (10{,}500)(75)(10^{-6})$$

$$= 0.79 \text{ cents/kWh}$$

$$\text{Unit labor costs} = \frac{(1.14 \times 10^{-5})(N)(\text{AS})}{(P_{\max})(\text{CF})}$$

$$= \frac{(1.14 \times 10^{-5})(400)(50{,}000)}{(1200)(0.7)}$$

$$= 0.27 \text{ cents/kWh}$$

Effect of CWIP and Construction Time on Power Costs
(All values except unit power costs are in millions of dollars)

	Construction time = 12 years		Construction time = 6 years	
	No CWIP	With CWIP	No CWIP	With CWIP
Utility charges				
During construction				
Construction cost ($e = 7\%$)	2,834	2,834	2,252	2,252
Interest charges ($i = 12\%$)	2,761	0	900	0
Total investment value	5,594	2,834	3,152	2,252
Value of investment at plant shutdown	633,430	320,848	356,939	255,001
Charges to customers				
During construction	0	1,803	0	789
During operation	26,833	13,586	15,124	10,798
Total bill to customer	26,833	15,389	15,124	11,587
Unit capital cost, cents/kWh	9.11	4.61	5.14	3.67

Occasionally, it is useful to make a rough estimate of either the allowable cost of a system knowing the return, or an estimate of the needed return knowing the initial cost of the system. A quick approximation of either of these quantities can be determined using the capital recovery factor (CRF). The CRF is then multiplied by the principal Pr to obtain the required annual rate of return A. The CRF is obtained from Eq. (1.17) after a number of simplifying assumptions have been made. These assumptions include: SV = 0, $e = 0$, $i = j$, and $m = n$. This leads

to

$$\text{CRF} = \frac{A}{\text{Pr}} = \frac{(i/n)[(1+i/n^{nt'}]}{(1+i/n)^{nt'}-1}$$

$$= \frac{(i/n)}{1-(1+i/n)^{-nt'}} \tag{1.23}$$

The CRF is commonly used to establish monthly mortgage payments for both automobile and home loans. Thus, if one borrows \$10,000 at an annual interest rate of 8 percent/year for 4 years, the monthly payment can be evaluated from the CRF. For these conditions, $t' = 4$ years, $i = 0.08$ per year, $n = 12$ per year, Pr = \$10,000, and the CRF is:

$$\text{CRF} = \frac{(0.08/12)}{1-(1+0.08/12)^{-48}} = 0.024413$$

The monthly payments will be

$$A = (\text{Pr})(\text{CRF}) = 10{,}000(0.024413)$$

$$= \$244.13 \text{ per month}$$

1.11 POWER GENERATION TERMINOLOGY

GENERAL. There are two common terms applied to energy conversion systems—"*power density*" and "*specific power.*" The *power density* is the power per unit volume (kW/m^3). The *specific power* is the power per unit mass of fuel (kW/kg fuel).

In his 1977 message to Congress, President Carter introduced a new term to the electric-power industry—"cogeneration." Cogeneration was formerly called "in-plant generation" or "byproduct power." Broadly, cogeneration was defined as the production of electricity along with other useful energy forms, such as process heat or steam, at the same location. Theoretically, if the latent heat of condensation of the turbine exhaust (which is normally lost) could be utilized in an industrial process, the overall system efficiency would increase from around 35 to 40 percent to around 75 to 80 percent. The Public Utility Regulatory and Policies Act (PURPA) of 1978 gave a boost to cogeneration as it dictated that a utility would have to credit any industry involved in cogeneration at the kilowatt hour cost equal to the production cost of the most expensive piece of electric generating equipment in use by the utility at that time.

The terminology associated with electric-power generation can be divided into three basic categories. These categories are: power system performance factors, types of power generation systems, and economic factors. It is important that the novice power engineer have some understanding of the general terminology.

POWER SYSTEMS PERFORMANCE FACTORS. Almost all engineers who have had a basic thermodynamics course probably know the definition of thermal

efficiency, η_{th}, of a power system. Normally this term is considered dimensionless, but it really has units of output energy or power (usually electricity) divided by the input energy or power (usually chemical or nuclear energy which has been converted into thermal energy).

Most engineers at an operating power plant usually do not talk about thermal efficiency. Instead, they worry about a closely related term called the *heat rate.* The heat rate gives the number of thermal Btus required to produce 1 kWh of electric energy. The heat rate can be calculated from the thermal efficiency using the following equation:

$$\text{Heat rate} = 3412/\eta_{th} \qquad \text{Btu}_{th}(\text{kW}_e\text{h}) \tag{1.24}$$

"Capacity factor" is one of the common terms applied to plant performance. It is defined as the ratio of the average power of a generating system to the rated power over a given time interval. Another performance factor is the *load factor,* which is the ratio of the average power to the maximum power for a given system over the time interval. The load factor is commonly applied to power users or consumers while the capacity factor is applied to power generating systems. The *availability factor* for a power system is the fraction of a particular time interval that the system is available for power generation.

A power system term that is commonly used in power plants is "spinning reserve." In the operation of a power system, there should be excess capacity that is running and synchronized with the system. This excess capacity is called the *spinning reserve* and it should be at least equal to the power of the largest unit in the system. Thus, if the largest unit "trips" (is lost to the system), the spinning reserve can quickly pick up the load.

Another power system term in common use is the "reserve capacity." The *reserve capacity* of a power grid is the difference between the total rated capacity of all the units in the grid and the expected peak load or demand on the system. There should be some excess capacity or reserve in any system because at any given time there are normally some units that cannot be operated because of a plant failure or scheduled maintenance. Most systems try to have a minimum of 20 percent excess capacity.

TYPES OF POWER SYSTEMS. Electric-power generating systems can normally be categorized as one of three different types—base-load power plants, intermediate-load plants, and peaking units. Those systems that average more than 5000 full-power hours per year (capacity factor > 57 percent) are called *base-loaded* plants. They typically have high rated output, high capital costs, and low operating costs. As indicated earlier, coal-fired power plants and nuclear units are commonly used as base-loaded power plants.

Power plants that average more than 2000 but fewer than 5,000 full-power hours per year (23 percent < capacity factor < 57 percent) are called *intermediate-load* power systems. Older, less-efficient power plants are used for this service, along with oil-fired units and the new combined-cycle power systems. The combined-cycle units are discussed in Chap. 7.

Peaking power systems are units that are operated only to meet the power demands at time of maximum demand—usually during the summer in the South and during the winter in the North. Since the units have low utilization, usually less than 2000 full-power hours per year (capacity factor < 23 percent), systems with low capital costs are often employed. Unfortunately, these systems usually have high operating costs, which make the overall unit power costs high. Combustion turbines, diesel engines, and pumped-storage units are commonly employed as peaking units.

POWER ECONOMIC TERMINOLOGY. When discussing power plant operation, there are a few economic terms and acronyms that the power engineer should recognize. The *depreciation* of a power plant or any capital investment was not discussed in the economics section but represents a return of investment which is realized in lower taxes. The depreciation of a plant is the amount of plant investment that can be written off as part of the annual operating costs. There are a number of books that discuss how to determine the annual depreciation based on "straight-line" depreciation, "sum-of-years-digits" depreciation, and "accelerated" depreciation. It is usually an advantage to the utility to depreciate a power system as rapidly as possible.

The *rate base* of a utility is the sum value of all the capital and operating assets of that utility—from the largest power plant to the smallest roll of wire. The rate base is used by state commissions supervising utility rates to assure that the utility earns a fair return on the investment or rate base. These commissions require that only the items needed in the operation of the utility be included in the rate base.

Recent economic developments in the power industry have introduced two new terms or acronyms to the print media. These acronyms are CWIP and AFUDC. CWIP is an acronym for "Construction Work in Progress" and pertains to interest paid on the money borrowed to build the power plant. As noted in Example 1.4, the utility pays a considerable amount of interest on the money borrowed for construction because of the large amounts of money involved and the long construction times. Some states permit the utilities to pass the interest charges on to the customers in the form of rate hikes even before the plant is producing electricity. Allowing the utility to pass on CWIP significantly reduces the overall power costs over the life of the plant, as indicated in Example 1.4. However, it does allow the utility to increase rates during construction of the new plant to pay the interest as it comes due.

Many customers maintain that the interest costs should not be passed on to the consumer until the plant produces useful power. If a utility cannot increase its rates for CWIP, it must borrow additional money to pay the interest and this adds significantly to total plant cost. When the new plant goes into operation, the utility will then ask the state regulating commission for AFUDC. AFUDC is an acronym for: "Allowance for Funds Used during Construction." AFUDC typically requires the utility to seek rate increases of 30 to 60 percent. When these increases go into effect, it commonly produces an effect called *rate shock*.

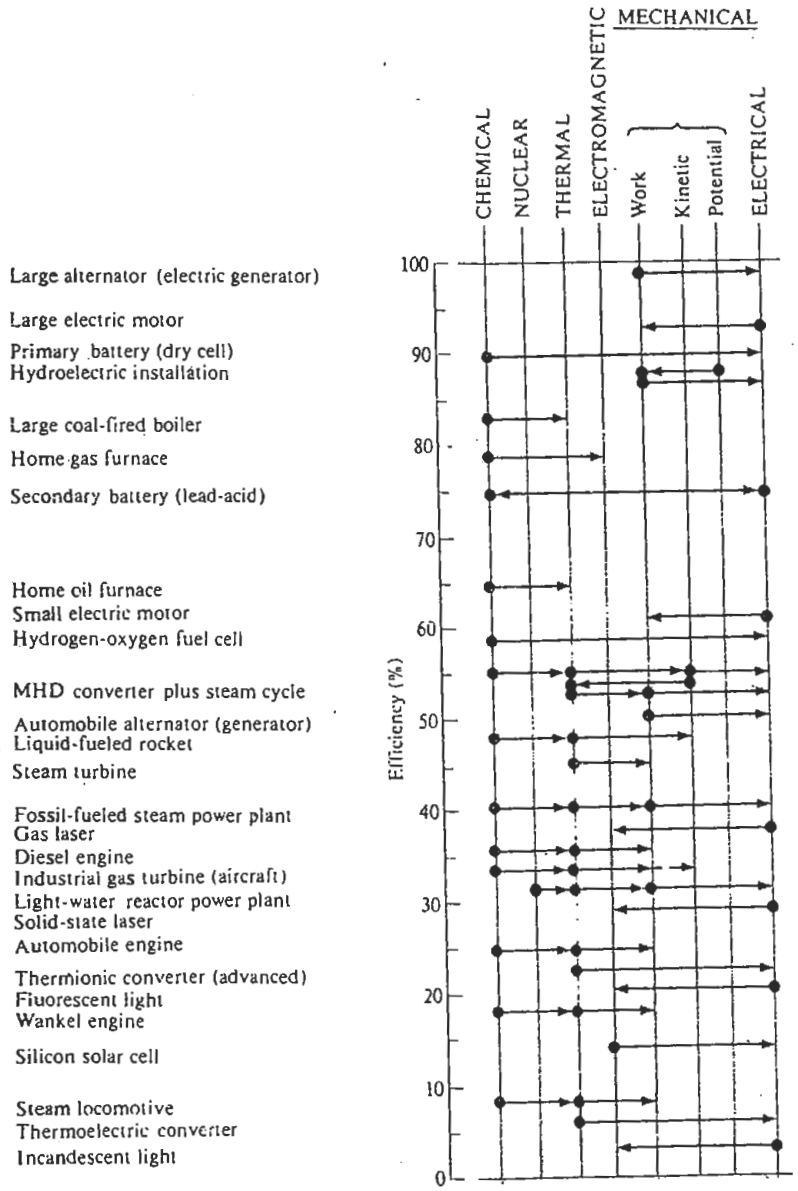


FIGURE 1.10
Some typical operational efficiencies of energy-conversion systems.

1.12 ENERGY-CONVERSION MATRIX

The energy-conversion matrix, presented in Fig. 1.11, lists the various processes, reactions, and systems used in the conversion of one form or classification of

FROM→ / TO↓			Mechanical energy				
				Potential energy			
			Work	Inertial field (kinetic) energy	Gravitational field energy	Elastic-strain energy	Compressed fluid energy
Mechanical energy	Work		——	Impulse and momentum changes (turbine blades)† Wind turbines	Falling weight Hydraulic turbines†	Springs	Bellows Air motors Turbines†
	Potential energy	Inertial field (kinetic) energy	Flywheel† Linear acceleration	——	Dropping weight	Catapault	Nozzle
		Gravitational field energy	Raise weight	Pitot tube and manometer Rockets	——	Spring-weight systems	Upward nozzle Hydraulic lifts & jacks
		Elastic-strain energy	Spring compression and extension Elastic deformation	Pitot tube and pressure gauge	Spring-weight systems	——	Bourdon-tube gauge Strain gauge
		Compressed-fluid energy	Mechanical pump or compressor	Diffuser	Piston in cylinder	????	——
		Magnetic field energy	Pull ferromagnetic materials from magnetic poles	????	????	????	????
Electrical energy			DC generator† Alternator†	Magnetohydrodynamic generator (MHD)† Electrogasdynamic generator (EDG)† Electrokinetic Gen.	Ferroelectric generator Rayleigh generator†	Piezo-electricity	Electrogas-dynamic (EGD) generator†
Electromagnetic energy			????	Phosphorescence Bremstrahlung Cerenkov radiation		????	????
Chemical energy			????	Dissociation by radiolysis		????	????
Nuclear energy			????	Threshold reactions Charged-particle reactions		????	????
Thermal energy	Heat		Friction	Friction Inelastic impact	Friction	Plastic flow	Unrestrained expansion
	Internal energy		Compression Friction	Diffuser	Friction	Plastic flow	Friction

† These systems are discussed in the text.

FIGURE 1.11
Energy-conversion matrix.

energy to another. Those processes, reactions, and systems which are discussed at length in this text, are indicated with a dagger in the matrix.

The conversion efficiencies of various systems, along with the different energy conversion processes, are shown in Fig. 1.10.

					Thermal energy	
Magnetic field energy	Electrical energy	Electromagnetic energy	Chemical energy	Nuclear energy	Heat	Internal energy
Attraction of ferromagnetic materials with magnets	Electric motors† Electromagnets Electrostriction	????	Muscles	????	Heat-engine cycles†	Expansion processes
Linear acceleration of ferromagnetic materials	Particle accelerator Electromagnetic pump†	Compton scattering Radiometer	Firearms Rockets	Particle emission	Pulse jet Turbo jet†	Nozzle
Lifting of ferromagnetic materials with magnets	Electromagnets	????	????	????	Hot-air balloons Evaporation (clouds)	????
Solenoid valve actuators	Electromagnetic spring compression	????	????	????	Thermal stress Bimetallic strips	????
????	Electromagnetic pump†	????	????	????	Fluid heating	????
—	Electron flow through an inductor	????	????	????	????	????
Use of magnets in small motors and generators	—	Photoelectricity Solar cells† Radio antennae	Fuel cells† Batteries†	Nuclear battery†	Thermoelectrics† Thermionics† Thermomagnetism Ferroelectricity Nernst effect	????
????	Lasers and Masers Radio transmitter Electroluminescense	—	Chemiluminescence (fireflies)	Phosphors X-ray emission Gamma emission Annihilation	Thermal radiation	Thermal radiation
????	Electrolysis Battery charging	Photosynthesis Photochemistry	—	Ionization Radiation catalysis	Endothermic reactions	????
????	????	Gamma-ray reactions	Phosphors	—	????	????
Hysteresis	Joule heating	Absorption reactions	Exothermic reactions Combustion†	Radioactive decay† Fission† Fusion†	—	Conduction Convection
Hysteresis	Resistance heating	????	????	Radiation damage	Sensible heat† Latent heat†	—

LIST OF SYMBOLS

A	Value of periodic payments with no escalation, \$
A_0	Initial (@ $t=0$) value of all escalated periodic payments, \$
A_1	Value of the first escalated payment, \$
A_{mt}	Value of the mt-th periodic payment, \$
AS	Average annual salary of power-plant personnel, \$/year
c	Velocity of light, 3×10^8 m/s
CF	Capacity factor of a power system = average power/rated power
CRF	Capital recovery factor = A/Pr
e	Annual escalation rate of periodic payments, \$/\$ · year
e	Base of natural logarithms, 2.718.
E	Energy, J
E	Fixed-dollar escalation amount of periodic payments, \$
E_0	Energy consumed from $t=-\infty$ to $t=0$, J
f	Fuel cost in cents/MBtu
F_t	Future value of an investment at the end of t years, \$
F_{mt}	Future value of periodic payments when the mt-th payment is made, \$
F_{nt}	Future value of a lump-sum investment at the end of nt compounding periods, \$
h	Plancks constant, 6.626×10^{-32} J · s
HR	Heat rate of a power plant, Btu/kWh
i	Annual constant growth rate, 1/year
i	Annual long-term interest rate which is compounded n times a year, \$/\$ · year
j	Effective annual short-term interest rate, compounded m times a year, \$/\$ · year
j'	Actual annual short-term interest rate, compounded m' times a year, \$/\$ · year
m	Mass, kg
m	Number of periodic payments made per year, 1/year
m'	Number of times a year that the short-term interest rate j' is compounded, 1/year
n	Number of times a year that the long-term interest rate i is compounded, 1/year
N	Number of operating personnel, persons
p	Number of construction payments made per year, 1/year
P	Power, W
P_0	Initial power (at $t=0$), W
P_{max}	Maximum rated power output, MW_e
Pr	Present value or principal of an investment (value at $t=0$), \$
R_0	Initial worth (at $t=0$) of all the periodic construction payments, \$
R_1	Value of the first periodic construction payment, \$
R_{pt}	Value of the pt-th periodic construction payment, \$
SV	Salvage value of an investment in a system at the end of life, \$

t	Time, s or years
t'	Time at the end of the investment period, years
t''	True payback period or time to breakeven on an investment, years
t_D	Doubling time of a quantity that grows at a constant rate, years
t_c	Construction time, years
η_{th}	Thermal efficiency of a power system, MW_e/MW_{th}
λ	Wavelength of electromagnetic radiation, m
ν	Frequency of electromagnetic radiation, Hz

PROBLEMS

1.1. A 2400-MW_e power plant has the following power demand for a given day:

12–5 a.m.:	850 MW	9–12 a.m.:	2150 MW	5–6 p.m.:	2250 MW
5–7 a.m.:	1250 MW	12–1 p.m.:	2040 MW	6–8 p.m.:	1850 MW
7–8 a.m.:	1840 MW	1–4 p.m.:	2350 MW	8–10 p.m.:	1500 MW
8–9 a.m.:	1960 MW	4–5 p.m.:	XXXX MW	10–12 p.m.:	1150 MW

If the power between 4:00 and 5:00 p.m. is [2,250; 2,350; 2,450; 2,550; 2,650] MW_e, find the total power output in (*a*) $MW_e \cdot$ days/day, (*b*) $kW_e \cdot h$/day, (*c*) MeV_e/day, (*d*) J_e/day, and (*e*) Btu_e/day. Assume that the plant burns coal with a heating value (energy content) of 26,400 kJ/kg with an overall thermal efficiency of [32; 34; 36; 38; 40] percent. Determine: (*f*) the total mass of coal, in short tons consumed during the day's operation, and find (*g*) the maximum design coal rate, in short tons per hour, required for proper operation of the plant. Also, evaluate (*h*) the heat rate of the unit in Btu/kWh, (*i*) the capacity factor of the unit for one day's operation, and (*j*) the load factor for the same period of operation.

1.2. A 1-GW_e power plant with a heat rate of [8600; 9000; 9400; 9800; 10,200] Btu/kWh operates at full power for a period of 1 day. Find (*a*) the mass of coal, in short tons per day, and (*b*) the volume of oil, in barrels per day, required for operation at full power. Assume that the energy content (heating value) of the coal is [25,000; 26,400; 27,800; 29,200; 30,600] kJ/kg, and that of the oil is [138,000; 139,500; 141,000; 142,500; 144,000] kJ/gal. There are 42 gal of petroleum per barrel. Also, determine (*c*) the actual mass of fuel, in grams of matter, that is actually converted into energy for each day of full-power operation.

1.3. A 2400-MW_e power plant has a coal pile containing 2,500,000 short tons of coal with a heating value of [25,000; 26,400; 27,800; 29,200; 30,600] kJ/kg. The plant operates at a heat rate of 9200 Btu/kWh. If the capacity factor is [0.6; 0.65; 0.7; 0.75; 0.8], determine the number of days that the coal will last and the mass of coal, in lbm, that is actually converted into energy.

1.4. If the world's supply of fossil fuels (from Table 1.1) is uniformly consumed over a [5; 7.5; 10; 12.5; 15]-year period, find the ratio of the fossil-fuel energy release to the amount of solar energy absorbed by the earth for the same time period. In the determination of the amount of solar energy received by the earth, use the "solar constant" of 1395 W_{em}/m^2 as the incident energy flux at the earth's orbital position. Assume that the earth receives solar energy as a disk and that [27; 28; 29; 30; 31] percent of the incident energy is reflected. The diameter of the earth is 12,756,000 m and the distance from the sun to the earth is 1.49×10^{11} m. Using these values, also determine the rate at which the sun is converting mass into energy.

1.5. A common form of residential electrical rate of billing is as follows:

1. First 10 kWh/month or less at a flat $3.50
2. Next 40 kWh/month at 9 cents/kWh
3. Next 50 kWh/month at 7.5 cents/kWh
4. Next 100 kWh/month at 5.5 cents/kWh
5. All kWh consumption in excess of 200 kWh/month at 5 cents/kWh

Calculate the monthly bills for the following electrical consumption per month:

(*a*) [3; 5; 7; 9; 11; 15; 20; 25; 30; 35; 40] kWh
(*b*) [45; 50; 55; 60; 70; 80; 90; 100; 125; 150] kWh
(*c*) [200; 250; 500; 1000; 1500; 2000; 2500; 3000; 4000; 5000] kWh

1.6. Many industrial firms commonly buy electrical energy under the so-called demand rate. The rate encourages the customer to reduce the peak demand and increase the load factor. Under this rate, the customer is billed as if all the energy consumed during the month was received at the maximum demand rate in the period. A typical demand-rate price schedule is as follows:

1. First 30 h at the maximum demand, cost 10 cents/kWh
2. Next 100 h at the maximum demand, cost 5 cents/kWh
3. Next 200 h at the maximum demand, cost 3 cents/kWh
4. All energy in excess of the foregoing blocks at 1.5 cents/kWh

(*a*) Calculate the monthly bill and the load factor for a total electrical energy consumption of [300,000; 350,000; 400,000; 450,000; 500,000] kWh with a maximum demand of [1000; 1500; 2000; 2500; 3000] kW for a 30-day month.
(*b*) Calculate the minimum monthly bill for the same total energy consumption as in part (*a*) for a 30-day month.

1.7. The Nuclear Regulatory Commission (NRC) limits the maximum thermal power of any commercial power reactor to 3800 MW_{th} plus the thermal power required to drive the plant auxilliaries, such as pumps, etc. The GE BWR-6 power reactor has a maximum thermal power of 3833 MW_{th}. Find the equivalent energy release rate, in tons of TNT per second. For this sytem, also evaluate the total electric generation, in kWh/year, if the plant operates with a capacity factor of [0.6; 0.65; 0.7; 0.75; 0.8] and a thermal efficiency of [30; 31; 32; 33; 34] percent.

1.8. The nuclear arsenal of the superpowers of the world has been estimated to be 13,000 megatons of TNT. Determine the minutes of equivalent sunshine that would yield the same amount of energy to the earth. Also, evaluate the length of time this stockpile could supply one hundred 1000-MW_e power reactors with a thermal efficiency of [30; 32; 34; 36; 38] percent and a capacity factor of [55; 60; 65; 70; 75] percent.

1.9. A 1-GW_e power plant with an overall thermal efficiency of [32; 34; 36; 38; 40] percent has a capacity factor of 80 percent for an operating period of 345 days with an additional 20 days/year allotted for scheduled maintenance. Find the annual fuel cost and the annual income for the plant. The cost of coal is [70; 90; 110; 130; 150] cents/million Btu and the power sells for [3; 5; 7; 9; 11] cents/kWh. Also, find the effective mass of coal that is actually converted into energy, in kg/year.

1.10. Determine the short tons of coal that could be saved per year if all the world's water and tidal power (from Table 1.1) could be utilized. Assume that [76; 78; 80; 82; 84] percent of this energy could be converted into electricity but that only

[30; 32; 34; 36; 38] percent of the coal's energy can be transformed into electricity. Assume that the higher heating value (HHV) of the coal is 28,000 kJ/kg.

1.11. Determine the amount of "antimatter," in kg/year, required to fuel a 10,000-MW_e matter-antimatter power system that operates with a conversion efficiency of [35; 40; 45; 50; 55] percent and a capacity factor of [60; 65; 70; 75; 80] percent.

1.12. A 600-MW_e power plant with a heat rate of [8700; 8900; 9100; 9300; 9500] Btu/kWh is operated at a capacity factor of [55; 60; 65; 70; 75] percent for an operating period of 335 days. If 30 days/year are allotted for scheduled outages, find (*a*) the annual fuel cost, dollars/year, (*b*) the area of coal field that must be mined, in acres/year, and (*c*) the total annual income from the sale of electricity produced by the plant. Assume the fuel cost is 120 cents/million Btu and that the company receives 4.5 cents/kWh of electrical output. The density of coal is 1200 kg/m^3, the HHV equals 10,800 Btu/lbm and the coal seam is 6 ft thick. Also, find (*d*) the effective mass of coal that is actually converted into energy, in lbm/year.

1.13. A reservoir has a water surface of 1200 acres and an available storage of 4000 million gal. The watershed contributing to and including the reservoir covers 35 mi^2. The dam of the reservoir contains a hydroelectric turbine with an available head of [40; 80; 120; 160; 200] ft and a mechanical efficiency of 83 percent. If the runoff of rainwater is [20; 28; 36; 44; 52] in/year and the evaporation from the surface is 8 in/year, compute the average electrical output of the generator, in kW_e assuming that all the overflow goes through the turbine.

1.14. A proposed solution for the supply of electrical energy to a house involves the use of a windmill to pump water from a depth of [30; 48; 66; 84; 102] m with a reversible water pump-turbine. The pumped water is then stored in a tank for use when there is no wind. The windmill shaft is not only connected to the water pump-turbine but it is also directly connected to an electrical generator. If the average household consumes [80; 95; 110; 125; 140] kWh/day, determine (*a*) the size of storage tank, in gal, required to store water for a 3-day period of no wind. Assume that the mechanical-electrical conversion efficiency of the water turbine and generator unit is 60 percent. Also, determine (*b*) the dimensions of the cylindrical storage tank if the tank diameter is equal to the height.

1.15. The cost of mining and transporting coal are roughly independent of the heating value of the coal. Consider that the coal in the ground is valued at 50 cents/million kJ, that mining costs are [6; 7; 8; 9; 10] dollars/ton and that transportation costs are 8 cents/ton-mile. If the price of other delivered coals are [120; 140; 160; 180; 200] cents/million kJ, find:

(*a*) The radius from the mine, in miles, that a coal of 32,560 kJ/kg can be delivered and sold for zero profit or loss

(*b*) The same radius for a coal with a heating value of 23,200 kJ/kg

(*c*) The minimum heating value of a coal that could be used locally

1.16. The fuel cost for an 800-MW_e steam power plant is [80; 100; 120; 140; 160] cents/million kJ. Find the annual fuel cost for the plant if the overall thermal efficiency is [32; 34; 36; 38; 40] percent and the capacity factor is 75 percent. Also, determine the savings in the annual fuel cost if the overall thermal efficiency of the unit can be increased by one percentage point.

1.17. The fuel cost for a 2400-MW_e steam power plant is 100 cents/million Btu. Find the annual fuel cost for the plant if it has an overall heat rate of [8500; 9000; 9500; 10,000; 10,500] Btu/kWh and a capacity factor of [60; 65; 70; 75; 80] percent.

Also, determine the savings in the annual fuel bill if the heat rate could be decreased by 100 Btu/kWh.

1.18. It is proposed to power an automobile with a hybrid mechanical-electrical drive system. The prime mover is a 50-hp, external-combustion steam engine with a thermal efficiency of 30 percent. The steam engine drives an alternator with an overall thermal efficiency of [68; 70; 72; 74; 76] percent. Power from the alternator is either stored in a lead-acid battery system or fed directly to electric traction motors with an electromechanical efficiency of [60; 65; 70; 75; 80] percent. The storage-battery efficiency, including charging, discharging, and storage losses, is around 65 percent. Find the power delivered to the drive wheels, in kW, and the overall conversion efficiency of the system, when:
(*a*) The storage batteries are bypassed.
(*b*) The storage batteries are not bypassed.

1.19. Determine the area of solar cells required to drive a commuter electric car if the overall conversion efficiency of the propulsion system, including the electromagnetic-electric-mechanical conversion is [5; 7; 9; 11; 13] percent. Assume that the car requires [8; 12; 16; 20; 24] hp and that the average gross solar input is 650 W/m^2. If the system can store energy while sitting in the parking lot, etc., and is storing energy at the rate of 4 h for each hour of operation, find the required area of the solar-cell array. Assume the storage efficiency of the batteries is 60 percent.

1.20. It has been estimated that the electrical energy consumption for the United States in the year 2000 will be 10^{10} MWh/year. Determine (*a*) the size, in miles, and (*b*) the cost of a square array of solar cells that will produce all the electrical energy. Assume the cells have a conversion efficiency of [7; 9; 11; 13; 15] percent and that the location chosen for the installation receives an average solar energy flux of 700 W/m^2 for 10 h/day and [260; 280; 300; 320; 340] days/year. Assume that the cost of the array, including support and storage material, is \$90 per m^2. Also, determine (*c*) the length of a dual-lane highway (four 12-ft lanes), in miles, that could be constructed from the same area as the solar-cell array.

1.21. Using the data in Table 1.2, determine the average rate of increase for the total annual energy consumption in the United States, from [1955; 1960; 1965; 1970; 1973] to [1973; 1976; 1979; 1982; 1985].

1.22. Repeat Prob. 1.21 except determine the rate of increase of annual energy consumption for the use of electrical energy in the United States.

1.23. The total amount of solar energy falling on the United States is estimated to be 1.87×10^{15} W. A typical solar cell has a conversion efficiency of [8; 10; 13; 14; 16] percent. Using the 1970 consumption rate of 5.5 quads of electricity per year, determine how long it would be before the entire surface of the United States were covered with solar cells if all of the electricity were produced this way. Assume that the electrical consumption rate grows at a constant rate of [2; 3; 4; 5; 6] percent/year.

1.24. Estimate the power required in the United States during the year 2050, in GW$_e$, and the energy consumed, in GJ, from the year [1990; 2000; 2010; 2020; 2030] to 2050 if the average consumption rate increases at an average rate of [2.4; 2.8; 3.2; 3.6; 4.0] percent/year. Start with the 1980 annual consumption.

1.25. The world's estimated energy reserves of uranium (with utilization of the breeder reactor and low-grade ore deposits) are 4.1×10^{27} J. The total annual energy consump-

tion rate of the earth in 1980 was estimated to be 2.1×10^{17} Btu/year. Assuming a constant growth rate with a doubling time of [10; 20; 30; 40; 50] years, determine how long the uranium could supply the entire energy requirements of the earth. Also, determine the total energy consumption, in Btu, between the year 1990 and [2000; 2010; 2020; 2030; 2040], assuming the growth rate is constant.

1.26. An engineering graduate, starting work in 1984, accepts a starting salary of $2000 per month. Assuming that this salary is constantly increased at an annual rate of [5; 7; 9; 11; 13] percent/year, determine her monthly salary exactly [10; 20; 30; 40; 50] years from the starting date. Also, determine the total amount of money earned during the last 10 years of the time interval.

1.27. Repeat Prob. 1.26, but instead of a constant growth rate of salary, assume that the graduate gets a salary increase every 6 months during the work period. Calculate the salary after the final increase was obtained (the graduate received an increase on the last day of the time interval). For calculational purposes, assume that the graduate gets paid at the end of each 6-month period. *Hint*: take a compounding and payment period of 6 months, a zero interest rate, and an annual escalation rate equal to the annual rate of increase of the salary.

1.28. The current heating bill for a large house is $1000 per year. Determine the maximum price that could be paid for a solar heating system which will pay for itself in 20 years. Assume that the system supplies 80 percent of the space heating requirement and the final salvage value of the system is 50 percent of the initial investment. Assume that the available interest for the initial investment and energy payments is [7; 9; 11; 13; 15] percent, compounded daily, and that the annual heating costs escalate because of inflation at an annual rate of [2; 4; 6; 8; 10] percent/year. Also, evaluate the total annual heating costs during the tenth year if the solar system is not installed.

1.29. A person pays $8000 for a solar heating system instead of investing the money in money-market certificates that pay an average rate of [6; 8; 10; 12; 14] percent/year, compounded semianually. The system is designed to operate for 20 years with an estimated salvage value of $3000 at that time. Determine the annual fuel savings during the first year and also during the tenth and twentieth years that must be achieved in order for the system to break even over the life of the system. Assume that the annual savings increase because of inflation at an annual rate of [2; 4; 6; 8; 10] percent/year. Also, assume that these annual savings can be invested at an annual rate of 7 percent, compounded daily.

1.30. A person puts $2000 into an IRA account on his birthday at age [21; 25; 35; 46; 50] and continues to put $2000 into the account every birthday until he reaches sixty-five, when he makes the last payment. At age 65, the person retires and receives monthly payments from the IRA account that are equal to the interest paid to the account so that the value of the IRA is unchanged. Determine the amount of the monthly checks if the account earns an interest rate of [6; 7; 8; 9; 10] percent/year, compounded daily.

1.31. A certain power plant has a nominal cost of $1000 per kW_e and requires a construction time of [5; 7; 9; 11; 13] years with construction payments made once a month. The system has a capacity factor of 70 percent. Assume that the construction costs escalate at an annual rate of 6 percent/year and that the power payments have no escalation. Assume that the construction money and the power payments earn a constant annual interest rate of [9; 11; 13; 15; 16] percent, compounded daily. If

the operating life is 40 years and the salvage value is negligible, determine the unit capital cost associated with the investment, in cents/kWh.

1.32. If the capital cost of a 70-MW_e combustion-turbine power system is \$200 kW_e, find the cost of energy (unit capital and fuel costs). The plant has a capacity factor of [20; 25; 30; 35; 40] percent and a plant life of 15 years with a salvage value of 35 percent of the original cost. Also, assume that the annual interest rate for investment and the payments is [8; 10; 12; 14; 16] percent/year, compounded daily. The plant efficiency is 35percent and the fuel costs are \$5.50 per million kJ.

1.33. A person puts a certain amount of money in the bank each month for 10 years. The first payment is \$100 and each subsequent payment is increased by [2; 4; 6; 8; 10] dollars. The bank pays an annual interest rate of [6; 8; 10; 12; 14] percent, compounded daily. Determine the value of the account at the end of 20 years and calculate the amount of interest paid to the account by the bank.

1.34. A person puts a given amount of money into the bank where it earns an annual interest rate of [7; 8; 9; 10; 11] percent, compounded daily. The initial payment is \$100 and each payment is escalated at the rate of 1 percent/month. At the end of 5 years (after 60 payments), no additional payments are made to the account but the money is left in the bank for another [5; 10; 15; 20; 25] years. Determine:

(*a*) The amount of the final payment

(*b*) The total amount of money put into the account by the individual

(*c*) The total value of the accoount at the end of the total time period

REFERENCES

Britton, Peter: "Tapping the Tides for Power," *Popular Science*, vol. 227, no. 1, January 1985.

Bureau of Census, *Statistical Abstract of the United States*, 108th ed. U.S. Dept. of Commerce, Washington, D.C., 1988.

Considine, Douglas M. (editor in chief): *Energy Technology Handbook*, McGraw-Hill, New York, 1977.

Douglas, Robert H.: "Systems Aspects of Ocean Thermal Energy Conversion," *AIAA/AAS Solar Energy for Earth Conference*, Los Angeles, Apr. 21–24, 1975.

Hammond, A. L.: "Energy Options: Challenge for the Future," *Science*, vol. 177, pp. 875–876, 1972.

———: "Geothermal Energy: An Emerging Major Resource," *Science*, vol. 177, pp. 978–980, 1972.

———: "Solar Energy: The Largest Resource," *Science*, vol. 177, pp. 1088–1090, 1972.

Hollander, J. M., and M. K. Simmons (eds.): *Annual Review of Energy*, vol. 1, Annual Reviews, Palo Alto, Calif., 1976.

Hubbert, M. K.: *Scientific American*, vol. 224, no. 3, p. 61, 1971.

Koenig, J. B.: "Worldwide Status of Geothermal Resources Development," in P. Kruger and C. Otto (eds.), *Geothermal Energy*, Stanford University Press, Stanford, Calif., 1973.

Krenz, J. H.: *Energy Conversion and Utilization*, Allyn and Bacon, Boston, 1976.

Lapedes, Daniel N. (editor in chief): *Encyclopedia of Energy*, McGraw-Hill, New York, 1976.

Roberts, R.: "Energy Sources and Conversion Techniques," *American Scientist*, vol. 61, pp. 66–75, 1973.

Shepard, M. L., F. H. Cocks, J. B. Chaddock, and C. M. Harmon: *Introduction to Energy Technology*, Ann Arbor Science Publishers, Ann Arbor, Mich., 1976.

Skrotzki, B. G. A., and W. A. Vopat: *Power Station Engineering and Economy*, McGraw-Hill, New York, 1963.

Summers, C. M.: *Scientific American*, vol. 224, no. 3, p. 151, 1971.

CHAPTER 2

PRINCIPAL FUELS FOR ENERGY CONVERSION

2.1 INTRODUCTION

This chapter reviews the properties and conversion principles for those sources of energy currently used as fuel energy. Specifically, four general categories of fuels are studied—biomass, fossil, nuclear, and solar. The energy conversion processes for the biomass fuels, the radioactive-decay process, the fusion process, and solar systems are also presented in this chapter, but the fossil-fuel and nuclear-fission-reactor conversion systems are discussed in detail in later chapters.

2.2 BIOMASS FUELS

The term "biomass fuel" is a general name applied to matter which has recently been produced directly or indirectly from the photosynthesis process. This includes wood and plants which are produced directly but it also includes animals that consume the plants and organic wastes such as garbage, sewage sludge, etc. Actually, biomass fuels are an indirect form of solar energy.

The energy associated with various types of woods and solid wastes is listed in App. C at the end of this book. Most of the conversion processes for biomass fuels involve the direct combustion of the fuel although some of the processes involve the production of fuel gases and liquids from the biomass material. Most of the combustion equipment discussed in Chap. 4 can usually be easily adapted

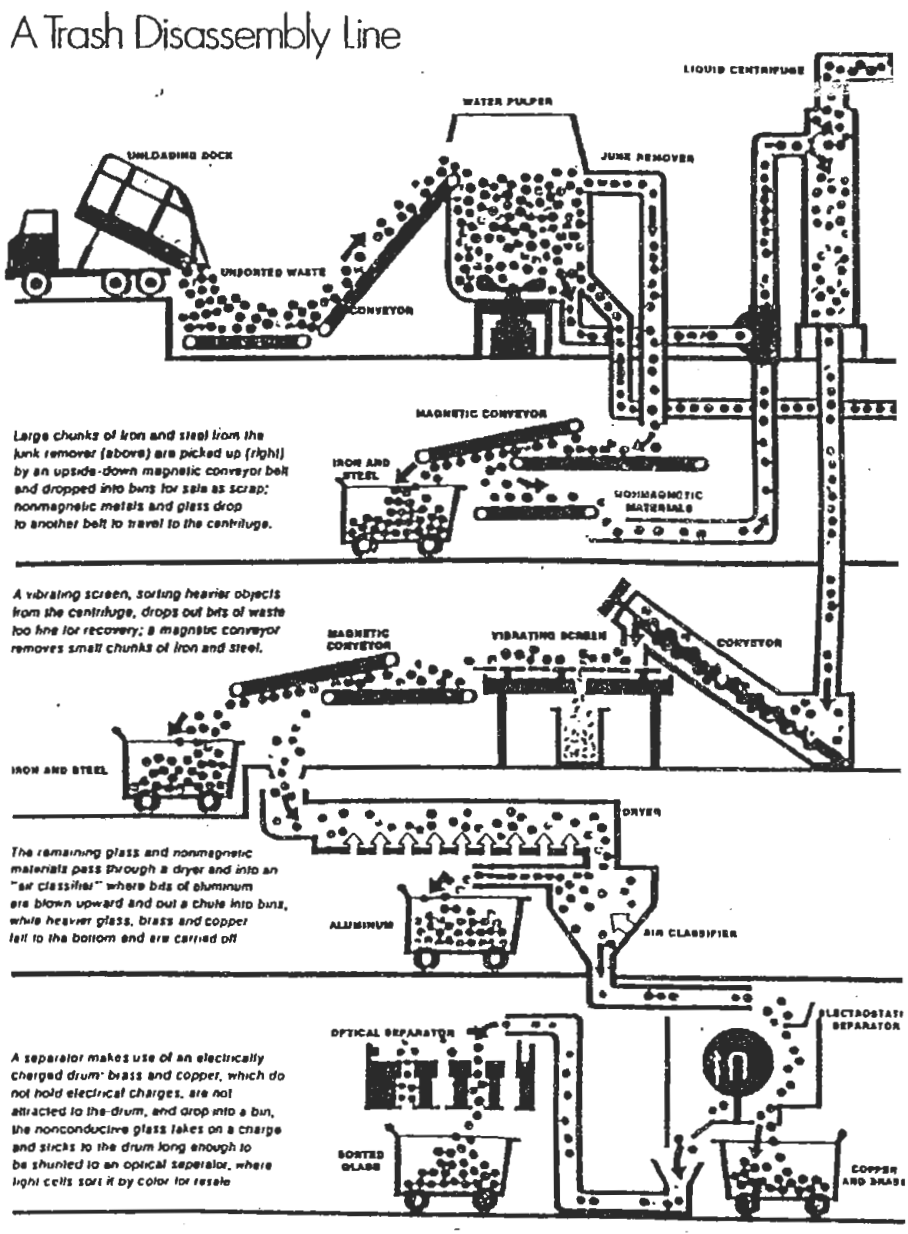
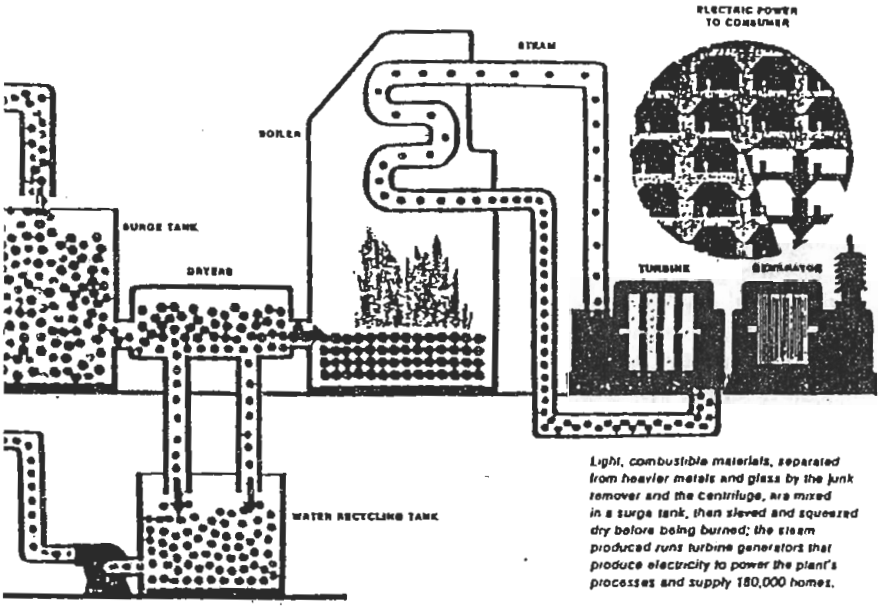
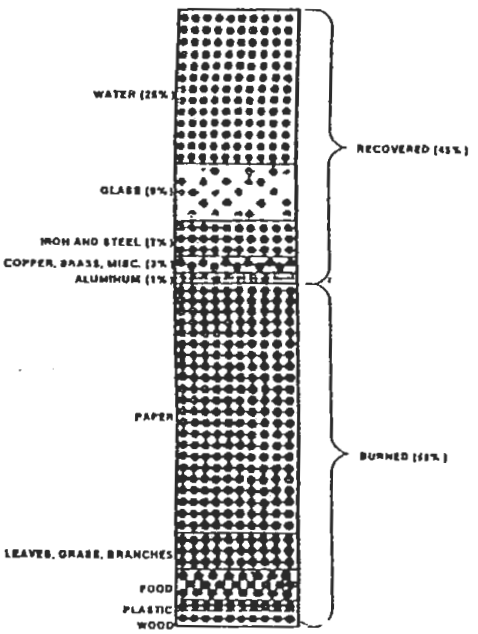


FIGURE 2.1
A proposed solid-waste recovery system.



Light, combustible materials, separated from heavier metals and glass by the junk remover and the centrifuge, are mixed in a surge tank, then sieved and squeezed dry before being burned; the steam produced runs turbine generators that produce electricity to power the plant's processes and supply 180,000 homes.

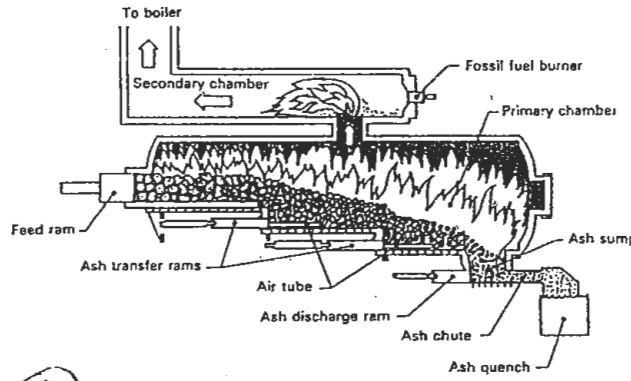
A solid-waste recovery plant that has been proposed for Hempstead, Long Island—borrowing machinery from the paper, scrap-metals, mining and wine-making industries—would convert 2,000 tons of refuse a day into one million kilowatts of electricity, 140 tons of iron and steel, 80 tons of glass, 20 tons of aluminum and smaller quantities of copper and brass. Unsorted garbage is dumped onto conveyor belts *(top, left)* that take it to a water pulper, where rotary blades reduce it to a mush, or "slurry". Large pieces of metal are spun to the surface and tumble out through a "junk remover" slot onto a series of moving belts. These remove the iron and steel and send the glass and nonmagnetic metals to rejoin the stream of slurry entering a liquid centrifuge. Here heavier bits of glass and metals are spun off and taken to another section for further sorting, as shown in the three steps at left. Meanwhile, lighter paper, plastics and food scraps are pumped to a surge tank *(above, center)* where they are held and mixed, then sent through a two-stage drying process and finally fed into the boiler furnace to produce steam for electricity-generating turbines. Water recovered from the drying process is returned for re-use in the initial pulping tank. The percentages of materials burned and recovered by weight, are indicated in the chart at right.

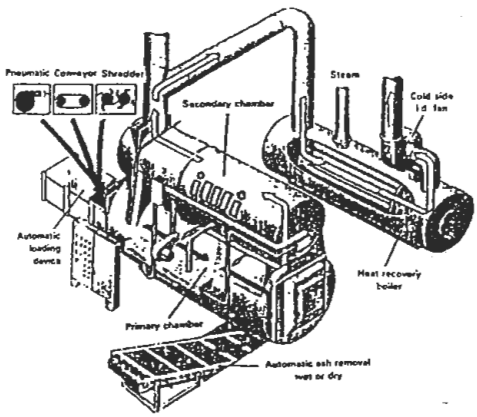


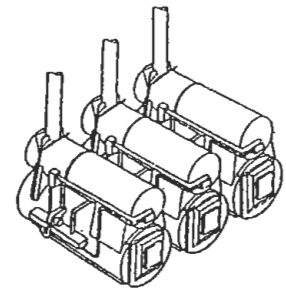
to burn biomass. Some special biomass combustion systems are discussed in this section.

Wood is probably the principal fuel source of the biomass energy sources. The combustion of wood was major source of fuel energy for the human race until the middle of the nineteenth century, when it was displaced by coal. It is still a primary source of fuel energy in many of the underdeveloped areas of the world and has also become very popular as a fuel for space heating of homes in the United States. In fact, in some areas of the country, wood smoke has become a major atmospheric pollutant.

More and more interest is being shown in the utilization of solid waste (garbage), because legal disposal of it is becoming increasingly difficult and because it represents a potential energy source. At the present time, a large fraction of the solid waste generated in the United States is being buried in sanitary landfills, where it decomposes. Because of the environmental concerns associated with this disposal method and because it is becoming increasingly difficult to find acceptable locations for landfills, more and more interest is being







Multiple packaged low profile units available for large quantities of waste disposal

FIGURE 2.2
Diagram of a small "starved air" refuse combustion system.

shown in other disposal methods, including combustion of the waste combined with the recovery of some of the noncombustibles such as metals and glass.

The recovery of the noncombustibles is normally accomplished before burning the waste. Recovery of ferrous materials is easily accomplished with magnets but nonferrous metals and glass are much harder to separate from the general refuse. In fact, unless there is a large amount of refuse, it is difficult to justify the installation of such a recovery system from an economical standpoint. The diagram of a large refuse recovery system is shown in Fig. 2.1.

A number of small systems have been developed for the combustion of general solid waste or garbage. In most of them the waste is fed into a lower combustion chamber where it is burned with insufficient air. This process, called *thermal pyrolysis*, produces a fuel gas which is subsequently burned in an upper chamber with more air. The thermal energy produced from this two-stage combustion process is then transferred to water in a small boiler. The relatively low-pressure, low-temperature steam produced in the boiler is then sold to local industry as process steam. It is imperative that an industrial customer be found for the steam or it is very difficult to justify the combustion system from an economical standpoint. A diagram of a small refuse combustion system is shown in Fig. 2.2.

While biomass represents a significant source of continuing fuel energy, it cannot meet the world's fuel energy demand. Moreover, the unregulated use of some of these sources, as in the case of wood, is creating a number of environmental problems.

2.3 FOSSIL FUELS

2.3.1 Background

The three general classes of fossil fuels are coal, oil, and natural gas. Other fuels, such as shale oil, tar-sand oil, and other fossil-fuel derivatives are somewhat different, but they are still considered to be fossil fuels and are commonly lumped under one of the three common fossil-fuel categories.

All of the fossil fuels were produced from the fossilization of carbohydrate compounds. These compounds, with a general chemical formula of $C_x(H_2O)_y$, were produced by living plants in the photosynthesis process as the plants converted direct solar energy into chemical energy. Most of the fossil fuels were produced during the Carboniferous Period of the Paleozoic Era—some 325 million years ago. After the plants died, the carbohydrates were converted, by pressure and heat, in the absence of oxygen, into hydrocarbon compounds with a general chemical formula of C_nH_m. Since all fossil fuels are composed of hydrocarbon compounds, a brief, general review of hydrocarbon chemistry would appear to be warranted.

2.3.2 Hydrocarbon Chemistry

Although hydrocarbon compounds are composed of only carbon and hydrogen atoms, in some of the more complex molecules the same number of carbon and

hydrogen atoms can be arranged in different structures to produce compounds with strikingly different chemical and physical properties. The hydrogen atom has only one electron and therefore needs to share an additional electron to fill the inner or K shell. This means that hydrogen has a chemical valence of ± 1 and that it will share one bond with another atom in an organic molecule. Carbon atoms have six electrons, with two in the K shell and four in the L shell. Since eight electrons are needed to fill the L shell, carbon has a chemical valence of ± 4 and will share four electrons or bonds with the other atoms in an organic molecule.

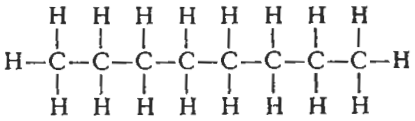
There are three major groups of hydrocarbon compounds—the aliphatic hydrocarbons, the alicyclic hydrocarbons, and the aromatic hydrocarbons. The aliphatic hydrocarbons are compounds which are composed of carbon-atom "chains," and most of the fossil-fuel compounds fall into this major group. The other two major hydrocarbon groups are "ring" hydrocarbons. The adjectives "saturated" and "unsaturated" are sometimes applied to hydrocarbon compounds. Saturated hydrocarbons are those compounds in which there are only single bonds between any two carbon atoms. Unsaturated hydrocarbons have at least two carbon atoms that share multiple bonds.

The aliphatic or chain hydrocarbons are further divided into three subgroups—the alkane, the alkene, and the alkyne hydrocarbons. The alkane hydrocarbons, also called the *paraffin series*, are the saturated group of chain hydrocarbons. The general chemical formula for this group is C_nH_{2n+2}. Many of the common fuel compounds fall into this subgroup and some of the typical compounds are listed below with their chemical formulas:

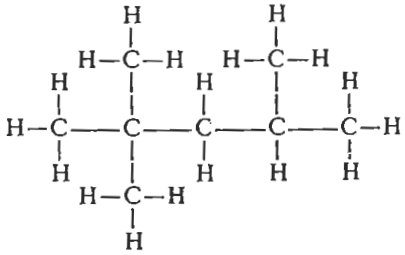
Methane, CH_4	Pentane, C_5H_{12}	Nonane, C_9H_{20}
Ethane, C_2H_6	Hexane, C_6H_{14}	Decane, $C_{10}H_{22}$
Propane, C_3H_8	Heptane, C_7H_{16}	⋮
Butane, C_4H_{10}	Octane, C_8H_{18}	Hexadecane, $C_{16}H_{34}$

Some of the compounds listed above are readily recognizable as the prime components of some of the common fossil fuels. Methane and ethane comprise most of the natural gases. Propane and butane make up liquified petroleum gas (LPG), and octane is a common compound used in gasolines. As the number of atoms in the alkane molecules increase, the hydrogen fraction decreases and the hydrocarbons become less volatile. The first four compounds are gases at room temperature and atmospheric pressure, while the balance of those listed are liquids at those conditions. The very long-chained molecules are solids.

As indicated earlier, the exact structure of the hydrocarbon molecule strongly influences its chemical and physical properties. If the prefix *n*-, which stands for "normal," appears in front of the hydrocarbon name, it means that all of the carbon atoms are connected in one long chain. The prefix *iso* in front of the name means that there are carbon-atom branches, usually methyl groups (CH_3^-) connected to the main chain. The *n*-octane and isooctane molecules are:



n-Octane

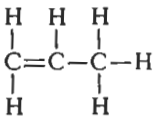


Isooctane

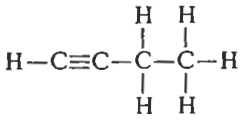
The isooctane shown here is called 2,2,4-trimethylpentane because there are three methyl groups (trimethyl) attached to the basic pentane (five-atom) chain at the second (first "2"), second (second "2"), and fourth ("4") carbon-atom positions in the pentane chain. Both of these molecules have the same chemical formula, C_8H_{18}, but they have very different chemical and physical properties.

If one of the hydrogen atoms in an alkane hydrocarbon is replaced with an OH^- radical, the compound is an alcohol. These compounds are also used as fuels. Some of the more common alcohols are methyl alcohol or methanol (CH_3OH), ethyl alcohol or ethanol (C_2H_5OH), and propyl alcohol or propanol (C_3H_7OH).

The alkene and alkyne subgroups of aliphatic hydrocarbons are unsaturated hydrocarbon compounds. The alkene hydrocarbons, also called the *olefin series*, have one double bond between two of the carbon atoms in the chain. The general formula for this group is C_nH_{2n}, and some of the typical compounds are ethylene (C_2H_4), propylene (C_3H_6), butene (C_4H_8), pentene (C_5H_{10}), and hexene (C_6H_{12}). The alkyne hydrocarbons, also called the *acetylene series*, have one triple carbon-atom bond in the hydrocarbon chain. The general formula for this series is $C_nH_{2(n-1)}$, and some typical compounds are acetylene (C_2H_2) and ethylacetylene (C_4H_6). Two unsaturated aliphatic hydrocarbons are as follows:



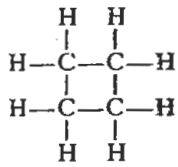
Propylene



Ethylacetylene

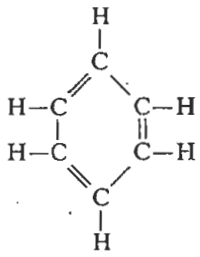
The other two major hydrocarbon groups, the alicyclic and the aromatic compounds, are "ring" hydrocarbons because the molecules are composed of

carbon-atom rings. The alicyclic hydrocarbons are composed of saturated carbon-atom rings and have a general formula that is identical to that of the alkene subgroup of aliphatic hydrocarbons, i.e., C_nH_{2n}. The names of the alicyclic compounds are simply the names of the alkane group preceded by the prefix "cyclo." Thus, there is cyclopropane (C_3H_6), cyclobutane (C_4H_8), cyclopentane (C_5H_{10}), etc. A typical alicyclic compound is shown, as follows:

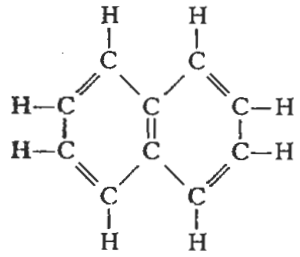


Cyclobutane

The aromatic hydrocarbons are composed of the basic benzene ring or rings. This ring is a six-atom carbon ring with double bonds between every other carbon atom (three double bonds in the simple ring). The general chemical formula for single-ring molecules is C_nH_{2n-6} and for double-ring molecules is C_nH_{2n-12}. Some of the typical aromatic compounds are benzene (C_6H_6), toluene (C_7H_8), xylene (C_8H_{10}), and naphthalene ($C_{10}H_8$). These compounds are made by adding methyl groups to the basic ring or rings. The two basic rings are shown as follows:



Benzene



Naphthalene

2.3.3 Standard Fuels

There are a number of basic hydrocarbon compounds that are used as standards for internal-combustion-engine fuels. Spark-ignition, internal-combustion-engine fuels are rated according to the *octane number.* Compression-ignition, internal-combustion-engine fuels are rated according to the *cetane number.*

The 100-octane fuel standard is 2,2,4-trimethylpentane, C_8H_{18} (the isooctane pictured previously), while the 0-octane fuel standard is *n*-heptane, C_7H_{16}. The octane number of an unknown fuel is determined in a cooperative fuels research engine (CFR engine). This engine is a single-cylinder engine with a compression ratio that can be adjusted from about 4:1 to about 14:1. The unknown fuel is burned in the engine and the compression ratio is slowly increased until a certain

"knock" or detonation reading is obtained from a vibration detector. Blends of the standard fuels are then burned at the same compression ratio until approximately the same "knock" reading is obtained. The percent by volume of 2,2,4-trimethylpentane in a blend of 2,2,4-trimethylpentane and *n*-heptane is the octane number of the unknown fuel. The octane ratings of most "regular" gasolines range from 85 to 95.

Some premium gasolines have octane numbers greater than 100. Octane numbers in excess of 100 can be achieved by using lighter hydrocarbons and alcohols and/or by putting additives, such as tetraethyl lead (TEL), in the basic fuel. These fuels are sometimes rated according to the *performance number* instead of the octane number. A fuel with a performance number of 5 has the same combustion characteristics as a mixture of 5 cm^3 of tetraethyl lead in 1 gal of 100-octane fuel.

The 100-cetane fuel standard for compression-ignition or diesel fuels is *n*-hexadecane ($C_{16}H_{34}$), which is sometimes called *n-cetane*. The 0-cetane fuel standard is alpha-methylnaphthalene ($C_{11}H_{10}$), which is similar to the naphthalene molecule just shown except that one of the hydrogen atoms in the alpha position (one of the four carbon atoms closest to the two carbon atoms shared by both rings) is replaced by a methyl group. The cetane rating of an unknown diesel fuel is equal to the percent by volume of *n*-hexadecane in a mixture of the standard fuels that has the same combustion characteristics in a CFR diesel engine as that of the unknown fuel. The cetane ratings of most diesel fuels range between 30 and 60.

2.3.4 Coal

COAL COMPOSITION AND RANK. Coal, the most abundant fossil fuel, is thought to be fossilized vegetation. It is estimated that at least 20 ft of compacted vegetation was necessary to produce a 1-ft-thick seam of coal. This compacted vegetation, in the absence of air and under the influence of pressure and temperature, is subsequently converted into peat, a low-grade fuel, then into brown coal, then into lignite, then into subbituminous coal, then into bituminous coal, and finally into anthracitic coal. As the aging process progresses, the coal becomes harder, the hydrogen and oxygen fractions decrease, the moisture content usually decreases, and the carbon fraction increases, as indicated in Fig. 2.3.

Coal is normally found in seams in the earth's crust. The average seam thickness in the United States is around 1.7 m (5.6 ft), although there is a 36-m (118-ft) seam in Lincoln County, Wyoming. The thickest known seam of coal is a 130-m (426-ft) seam of coal found in Manchuria.

There are several different systems used for classifying coal, but the American Society for Testing Materials (ASTM) has developed a method that ranks coal into four major classifications with subdivisions in each major class. According to this system, the four major divisions are, starting with the oldest: anthracitic coals (class I coals), bituminous coals (class II coals), subbituminous coals (class III coals), and lignitic coals (class IV coals). Under this classification

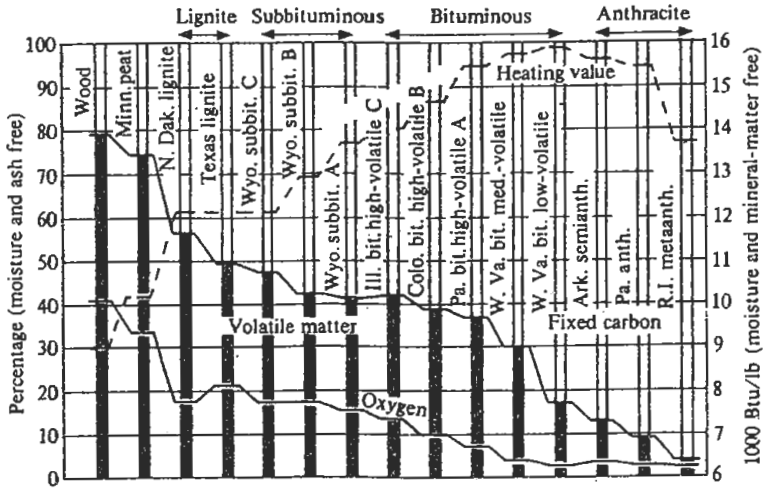


FIGURE 2.3
Variation of coal composition and properties with age. (*De Lorenzi, 1952.*)

system, the coals are ranked according to certain properties. The ASTM classification system and the classification parameters are presented in App. D of this book.

COAL ANALYSES. The two common coal analyses are the "proximate" analysis and the "ultimate" analysis. Both of these analyses give mass or gravimetric fractions of the components in coal and either analysis can be reported several different ways. In any coal seam, there are two components that can have significant variation throughout the seam. These are moisture and ash. The ash fraction varies because ash is essentially the inorganic matter deposited with the organic material during the compaction process. The moisture content of the coal varies significantly, depending on the exposure to groundwater before mining and upon exposure to the weather during transportation and storage before it is burned.

Since the moisture and ash fractions can vary widely for a given coal, it is common practice to report coal analyses (both proximate and ultimate) on a moisture-free (dry), ash-free basis. However, for ranking, handling, and burning the coal, these dry, ash-free analyses must be converted to an as-mined ("bed-moisture basis"), an as-received, and an as-burned basis, respectively. These latter analyses include both the existing moisture and the existing ash fractions of the coal.

The proximate analysis is the simplest coal analysis and gives the mass fractions of fixed carbon (FC), volatile matter (VM), ash (A), and moisture (M) in the coal. This analysis can be determined by simply weighing, heating, and burning a small sample of powdered coal. The coal sample is carefully weighed

and then heated to 110°C (230°F) for 20 min. The sample is then weighed again and the mass loss is divided by the original mass to obtain the moisture fraction. The remaining sample is heated to 954°C (1750°F) in a closed container for 7 min. The sample is then reweighed and the resulting mass loss in this heating process is divided by the original mass to obtain the fraction of the volatile matter in the sample. The sample is then heated to 732°C (1350°F) in an open crucible until it is completely burned. The residue is then weighed and the final weight is divided by the original weight to obtain the ash fraction. The mass fraction of fixed carbon is obtained by subtracting the moisture, volatile matter, and ash fractions from unity. In addition to the FC, VM, M, and A, most proximate analyses list separately the sulfur mass fraction (S) and the higher heating value (HHV) of the coal.

The ultimate coal analysis is a laboratory analysis that lists the mass fractions of carbon (C), hydrogen (H_2), oxygen (O_2), nitrogen (N_2), and sulfur (S) in the coal along with the higher heating value. Most ultimate analyses include the moisture and ash separately, but some analyses include the moisture as part of the hydrogen and oxygen mass fractions. The ultimate analysis is required to determine the combustion-air requirements for a given combustion system and this, in turn, is used to size the draft system for the furnace. These calculations should be based on the as-burned, ultimate coal analysis, if possible.

Coal analyses for some typical American coals are presented in App. E at the end of this book, along with the higher heating values. All of these analyses are reported on a dry, ash-free basis along with the expected range of moisture and ash fractions of the as-mined coal. Once the moisture and ash fractions are known, the other mass fractions and the higher heating value of the coal can be determined from the following equations:

$$\text{As-burned mass fraction} = [\text{dry, ash-free mass fraction}][1 - M - A] \quad (2.1)$$

$$\text{As-burned higher heating value} = [\text{dry, ash-free HHV}][1 - M - A] \quad (2.2)$$

As was discussed earlier, the ASTM coal classification system depends on the coal properties—specifically the dry, mineral-matter-(Mm-) free fixed carbon (or volatile matter) and/or the moist, mineral-matter-free higher heating value, in Btu/lbm. The appropriate formulas for calculating these values are given in App. D along with the classification parameters.

The ultimate coal analysis is much harder to obtain than the proximate analysis. Since the ultimate analysis is normally of greater interest to the power engineer and may not be available, it is sometimes necessary to estimate the ultimate analysis from an experimentally determined proximate analysis. A method of estimating such an analysis is presented in a *Power*'s "Data Sheet" (*Power* is a McGraw-Hill periodical). This procedure is given in App. F at the end of this book.

COAL PROPERTIES. There are a number of properties that should be considered when selecting a coal for a given application. Among these are its sulfur content,

its burning characteristics, its weatherability, its ash-softening temperature, its grindability index, and its energy content.

One very important consideration in the selection of a coal is its sulfur content. While sulfur is one of the combustile elements in the coal and generates energy, the primary product of that combustion is sulfur dioxide, SO_2, which is a major atmospheric pollutant. Sulfur dioxide and accompanying sulfur trioxide both react with atmospheric water vapor to produce sulfurous and sulfuric acids—both of which contribute to "acid rain." In 1984, the EPA required all new power plants to remove at least 70 percent of the sulfur in the coal they used. It is difficult and expensive either to remove the sulfur before the coal is burned or to remove the sulfur oxides from the combustion products. Consequently, it is desirable to use a coal with a low sulfur content.

When choosing a coal for a particular combustion system, one must be concerned as to how the coal burns. If the coal is burned in a stationary bed with little agitation (e.g., in a chain grate stoker), the coal should be a free-burning coal, not a caking coal. A free-burning coal tends to break apart as it burns, thereby exposing the unburned portion to combustion air. This facilitates the complete combustion of the coal. A caking coal produces a fused coal mass as it burns, so that much of the fixed carbon appears in the refuse pit as unburned carbon. Caking coals (which used to be in demand for the production of coke used in the steel industry) must be mechanically agitated when they are burned to break up the fused-coal masses. A high value of the "free-swelling index" for a given coal normally indicates that the coal is a free-burning coal.

The "weatherability" of a coal is a measure of its ability to withstand exposure to atmospheric conditions without excessive crumbling. All large coal-fired power stations normally keep a 90- to 180-day supply of coal in a large pile near the power plant. As the coal is delivered by unit train or barge, it is spread in thin layers and packed down with large earth-moving machines to get as much air out of the pile as possible. This reduces the risk of spontaneous combustion. A typical large coal pile is shown in Fig. 2.4. If the coal crumbles severely during storage, the small particles will be washed away during rainstorms, producing a monetary and energy loss as well as polluting the watershed.

The "grindability index" is another important property that should be considered when selecting a coal. This is particularly true for the common pulverized-coal power system where the coal is ground up finer than face powder. The grindability index is inversely proportional to the power required to grind the coal to a certain texture. Thus, if coal A has a grindability index of 100 while coal B has an index of 50, coal B will require twice the grinding power of coal A. An index of 100 has been arbitrarily assigned to a low-volatile bituminous (class II, group 1) coal. The anthracitic coals, because of their hardness, and the lignitic coals, because of their plasticity, have low grindability indices.

The ash-softening temperature is an important consideration in the choice of coals for a particular power plant. The ash-softening temperature is the temperature where the ash becomes very plastic, somewhat below the melting point of the ash. This temperature is determined by heating ash cones similar to

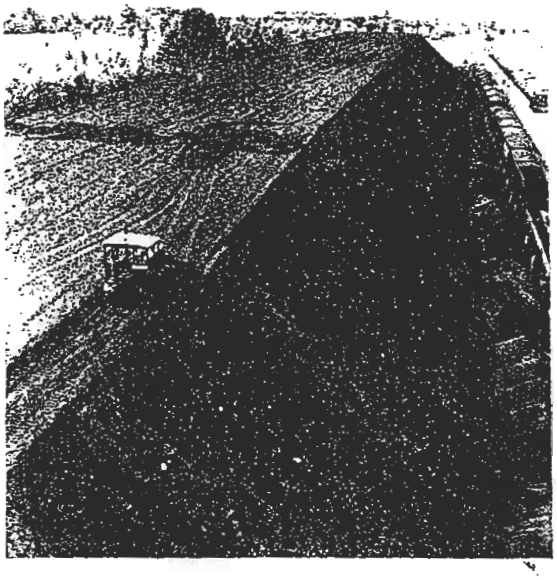
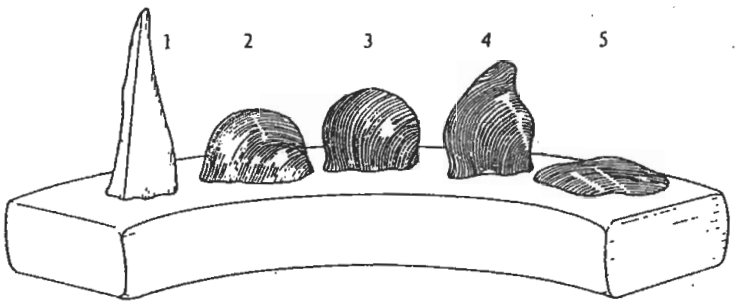


FIGURE 2.4
A typical coal pile containing about 200,000 tons of coal.

those shown in Fig. 2.5. Some furnaces discharge the ash from the firebox in the form of a molten slag, and a coal with a low ash-softening temperature is desirable for these systems. A coal with a high ash-softening temperature is desirable for those systems that handle the ash in solid form. If a coal with a low ash-softening temperature is used in a stoker furnace, large troublesome fused-ash masses, called *clinkers*, may be produced. In other systems, "slagging" occurs as ash deposits build up on the heat-transfer surfaces.



Cone 1, initial deformation temperature
Cones 2 and 3, softening temperature
Cone 4 has almost reached softening temperature
Cone 5, fluid temperature

FIGURE 2.5
Fusibility of ash cones in determining the ash-softening temperature. (*De Lorenzi, 1952.*)

The energy content or heating value of a coal is a very important property. The heating value represents the amount of chemical energy in a given mass or volume of fuel. In most American textbooks and periodicals, it has been common practice to report the heating values of coal in units of British thermal units per pound-mass (Btu/lbm) but this text uses the units of kilojoules per kilogram (kJ/kg). The conversion factor for going from kJ/kg to Btu/lbm is 0.43 Btu · kg/kJ · lbm.

Reference has been made in the previous paragraphs to the higher heating value or HHV. There are actually two heating values—a higher or gross heating value and a lower or net heating value (LHV). The difference between these values is essentially the latent heat of vaporization of the water vapor present in the exhaust products when the fuel is burned with dry air. In an actual combustion system, this includes the water present in the as-burned fuel (the moisture) and the water produced from the combustion of hydrogen. It does not include any moisture that is introduced with the combustion air. Since the latent heat of vaporization of the water at 7 kPa (the approximate partial pressure of the water vapor in the exhaust) is around 2400 kJ/kg, the difference between the higher and lower heating values is approximated by the following equation which is applicable to any fuel on a mass basis:

$$\text{HHV} - \text{LHV} = 2400(M + 9\text{H}_2) \quad \text{kJ/kg} \tag{2.3}$$

In Eq. (2.3), M and H_2 are the as-burned moisture and hydrogen mass fractions of the fuel.

Most combustion tables always list the higher heating values for coal because the moisture content varies so widely. There is a different lower heating value for each moisture value of the coal. The higher heating values, on a "dry, ash-free basis" are listed in App. E at the end of this book. These values should be converted to an as-burned basis, as given by Eq. (2.2), when determining the fuel rate for a given power plant. If an experimental value of the higher heating value is unavailable, the higher heating value, in kJ/kg, for the better grades of coal can be estimated from the ultimate analysis and the use of Dulong's formula, which is:

$$\text{HHV} = 33{,}950\text{C} + 144{,}200\left(\text{H}_2 - \frac{\text{O}_2}{8}\right) + 9400\text{S} \tag{2.4}$$

All values in the above equation are mass fractions and the resulting higher heating value is for the same basis (as-collected, as-mined, etc.) as the values from the ultimate analysis that is used in the equation.

Example 2.1. Determine the as-received proximate and ultimate analyses, the estimated lower heating value from the listed higher heating value, the higher heating value as determined by Dulong's formula, and the ASTM classification (class and group) of Stark County, N.D., coal, with $A = 8$ percent and $M = 39$ percent.

Solution. Given: Stark County coal with $A = 0.08$ and $M = 0.39$. From App. E, the dry, ash-free proximate coal analysis gives:

$$\text{VM} = 54.0\% \qquad \text{FC} = 46.0\% \qquad \text{S} = 2.8\% \qquad \text{HHV} = 28{,}922 \text{ kJ/kg}$$

The dry, ash-free ultimate coal analysis gives:

$$C = 72.4\%, \quad H_2 = 4.7\%, \quad O_2 = 18.6\%, \quad N_2 = 1.5\%, \quad S = 2.8\%$$

To convert to an as-received coal basis, the correction factor or multiplier is $[1 - M - A] = [1.00 - 0.39 - 0.08] = 0.53$. The as-received proximate analysis becomes:

$VM = 0.53 \times 54.0 =$	28.6%	$S = 0.53 \times 2.8 = 1.5\%$	
$FC = 0.53 \times 46.0 =$	24.4%		
$M =$	39.0%	HHV $= 0.53 \times 28{,}922 = 15{,}329$ kJ/kg	
$A =$	8.0%	$= 0.43 \times 15{,}329 = 6591$ Btu/lbm	
	100.0%		

The as-received ultimate analysis becomes:

$C = 0.53 \times 72.4 =$	38.4%		
$H_2 = 0.53 \times 4.7 =$	2.5%	HHV $= 15{,}329$ kJ/kg	
$O_2 = 0.53 \times 18.6 =$	9.9%	$= 6591$ Btu/lbm	
$N_2 = 0.53 \times 1.5 =$	0.8%		
$S = 0.53 \times 2.8 =$	1.5%		
$M =$	39.0%		
$A =$	8.0%		
	100.1%	(0.1% roundoff error)	

Lower heating value (*must* use as-received values):

$$\text{LHV} = \text{HHV} - 2400[M + 9H_2] = 15{,}329 - 2400[0.39 + 9(0.025)]$$

$$= 13{,}853 \text{ kJ/kg} = 5957 \text{ Btu/lbm}$$

Estimated HHV, using Dulong's formula:

$$\text{HHV} = 33{,}950C + 144{,}200\left[H_2 - \frac{O_2}{8}\right] + 9400S$$

$$= 33{,}950(0.384) + 144{,}200\left[0.025 - \frac{0.099}{8}\right] + 9400(0.015)$$

$$= 14{,}998 \text{ kJ/kg} = 6449 \text{ Btu/lbm}$$

Classification of the coal according to the ASTM method (*must* use the as-mined or bed-moisture values):

$$\text{Dry, Mm-free FC} = \frac{\text{FC} - 0.15\text{S}}{1 - M - 1.08A - 0.55\text{S}}$$

$$= \frac{0.244 - 0.15(0.015)}{1 - 0.39 - 1.08(0.08) - 0.55(0.015)}$$

$$= 0.469 = 46.9\%$$

Since this value is less than 69 percent, the coal cannot be classified according to the dry, mineral-matter-free value of fixed carbon. Thus:

$$\text{Moist Mm-free Btu} = \frac{\text{Btu} - 5000S}{1 - 1.08A - 0.55S}$$

$$= \frac{6591 - 5000(0.015)}{1 - 1.08(0.08) - 0.55(0.015)}$$

$$= 7197 \text{ Btu/lbm}$$

Since the moist, mineral-matter-free value of the higher heating value is between 6300 and 8300 Btu/lbm, this coal is ranked as a class IV, group 1 coal → lignite A.

2.3.5 Petroleum

FORMATION AND CLASSIFICATION. While coal is thought to be fossilized vegetation, petroleum is thought to be partially decomposed marine life. Petroleum or crude oil is normally found in large domes of porous rock. Crude oils are normally ranked into one of three categories, depending on the type of residue left after the lighter fractions have been distilled from the crude. Based on this method, any crude oil is classified as either paraffin-based crudes (a waxy residue), asphalt-based crudes (an asphalt-type residue), or mixed-based crudes (a combination asphalt-wax residue).

Although crude oil is a composition of many organic compounds, the ultimate analyses of all crude oils are fairly constant. The carbon mass fraction ranges from 84 to 87 percent, the hydrogen mass fraction ranges from 11 to 16 percent, the sum of the oxygen and nitrogen mass fractions range from 0 to 7 percent, and the sulfur mass fraction ranges from 0 to 4 percent.

Shale oil is a fuel that is different from petroleum, but it can be used to produce the same products that can be obtained from crude oil. Shale oil is composed of an organic compound called *kerogen*, and tremendous energy reserves of shale oil are found in the mountains of Colorado and Wyoming. One ton of high-grade oil shale produces about 26 gal of shale oil.

The main problem associated with shale oil involves the development of a shale-oil recovery process that is both economical and environmentally acceptable. One of the most popular methods of oil recovery involves retorting the oil from crushed ore. Unfortunately, this requires a lot of cooling water and the resulting solid waste expands so that it cannot be deposited in the original excavation. Some companies are working on an in situ process in which the oil can be recovered from the ore without mining it. Development of this huge energy source presents a major technological challenge.

There are six grades of commercial fuel oil; however, fuel oil No. 3 is no longer commercially available. Fuel oil No. 1 is a distillate oil and is the lightest and least viscous of the fuel oils. It is essentially the same as kerosene and is used in vaporizing burners. Fuel oil No. 2 is a distillate oil and is the general-purpose domestic heating oil. Fuel oil No. 4 is a relatively light, residual,

commercial-grade heating oil that can be pumped without heating at moderate temperatures. Fuel oil No. 5 is a heavy, viscous, residual, commercial-grade fuel oil, and fuel oil No. 6, or "bunker-C" oil, is the heaviest and most viscous of the residual fuel oils. Both Nos. 5 and 6 fuel oils require heating before they can be pumped. Some of the average properties of these fuel oils and other liquid fuels are given in App. G at the end of the book.

PROPERTIES OF PETROLEUM DERIVATIVES. The important properties of petroleum and petroleum products are the heating value, the specific gravity, the flash point, and the pour point. The heating value, usually the higher heating value, is commonly reported in units of kJ/kg or Btu/lbm or in units of kJ/L or Btu/gal. In Fig. 2.6, the approximate HHV of petroleum derivatives is plotted as a function of the specific gravity in units of °API (API is an acronym for American Petroleum Institute). The gravimetric HHV of these fuels increases with increasing values of °API and °Bé (degrees Baumé).

The specific gravity s of any liquid is the density of that liquid divided by the density of water at 60°F (15.6°C), which is 62.4 lbm/ft^3 (1000 kg/m^3). The

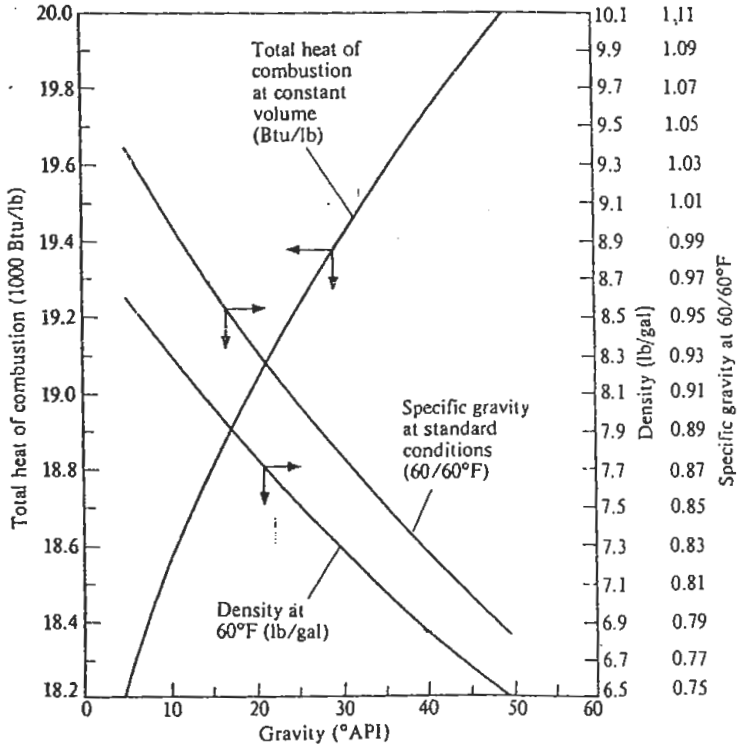


FIGURE 2.6
Properties of petroleum derivatives. (*From Steam: Its Generation and Use, 1972.*)

specific gravity of petroleum and petroleum products is usually expressed in units of °Bé or °API. The relationship between the specific gravity s and these units are as follows:

$$\text{Specific gravity} = s = \frac{140}{130 + °\text{Bé}} \tag{2.5}$$

$$\text{Specific gravity} = s = \frac{141.5}{131.5 + °\text{API}} \tag{2.6}$$

It will be noted in both of these equations that water at 60°F (15.6°C) has a specific gravity of 10° and the specific gravity decreases as the °Bé or °API increases.

The *flash point* of a liquid fuel is the minimum fluid temperature at which the vapors coming from a free surface of the liquid will just ignite, producing a flash. At a slightly higher temperature, called the *flame point*, the vapors will support combustion and the surface ignites. When handling a liquid fuel, care should be taken to assure that the maximum liquid fuel temperature does not exceed the flash point.

The *pour point* of a liquid fuel is the lowest fluid temperature at which an oil or oil product will flow under "standard conditions." It is experimentally determined by finding the maximum temperature at which the surface of a liquid sample in a half-filled standard test tube does not move for 5 s when the test tube is rotated to the horizontal position. The pour point is equal to this temperature plus 5F° (2.78C°). Consequently, the liquid is very viscous at the pour point.

The combustion of crude-oil products has a number of advantages over coal. Oil is cleaner and easier to handle, store, and transport. It is easier to burn than coal and produces little ash. There are some problems encountered in the combustion of fuel oil, however. Although there is little ash produced, the ash is quite adhesive and difficult to remove. Some crudes have a significant sulfur fraction, and although it can be removed from the oil before it is burned, it is an expensive process. Another problem element found in some crudes is vanadium. Vanadium oxidizes during combustion to vanadium pentaoxide (V_2O_5), and this compound causes rapid corrosion of the ferrous materials found in most boilers.

Finely pulverized coal, called *micronized coal*, has recently been mixed with heavy fuel oil and the coal-oil mixture (COM) has been used as fuel. This was done to use COM in oil-fired installations, thereby reducing the nation's dependence on fuel oil. The principal problem with this fuel is the coal ash and the abrasiveness of the coal particles. The fuel and ash particles cause rapid erosion and wear in the fuel nozzles and in the burners themselves.

Example 2.2. Find the volumetric heating values (HHV_v) of liquid propane and No. 6 fuel oil, in Btu/gal. Also, determine the cost of No. 6 fuel oil, in cents/gal and in dollars/million Btu (MBtu), if the price of liquid propane is 80 cents/gal.

Solution. Given: liquid propane at 80 cents/gal. From App. G,

Propane:

$s = 112.5°\text{API}$ HHV = 50,400 kJ/kg Rel. cost/unit of energy = 122

No. 6 fuel oil:

$s = 14.5°\text{API}$ HHV = 42,330 kJ/kg Rel. cost/unit of energy = 51

Let $X \equiv \text{HHV}_v$, Btu/gal; $Y \equiv$ cost, dollars/MBtu; and $Z \equiv$ cost, cents/gal. Then

$$X = \frac{[0.43(\text{HHV})\ \text{Btu/lbm}][62.4\ \text{lbm/ft}^3]}{[(131.5+°\text{API})/141.5][7.48\ \text{gal/ft}^3]} = \frac{507.6(\text{HHV})}{131.5+°\text{API}}$$

For propane, $Z = \text{cost} = 80$ cents/gal. Thus

$$X = \text{HHV}_v = \frac{507.6(50{,}400)}{131.5+112.5}$$

$$= 104{,}850\ \text{Btu/gal}$$

$$Y = \text{cost} = \frac{(0.80\ \$/\text{gal})(10^6\ \text{Btu/MBtu})}{104{,}850\ \text{Btu/gal}}$$

$$= \$7.63/\text{MBtu}$$

For No. 6 fuel oil,

$$Y = \frac{7.93(51)}{122} = \$3.19/\text{MBtu}$$

$$X = \text{HHV}_v = \frac{507.6(42{,}330)}{131.5+14.5}$$

$$= 147{,}160\ \text{Btu/gal}$$

$$Z = \frac{(319\ \text{cents/MBtu})(147{,}160\ \text{Btu/gal})}{(10^6\ \text{Btu/MBtu})}$$

$$= 47\ \text{cents/gal}$$

2.3.6 Gaseous Fuels

GENERAL. Almost all gaseous fuels are either fossil fuels or byproducts of fossil fuels. These fuels can be divided into three general groups including natural gases, manufactured fuel gases, and byproduct fuel gases. Some of the fuel gas compositions and other properties are presented in App. H at the end of the book.

The composition of a fuel gas is commonly expressed in terms of the mole or volume fractions of the chemical compounds found in it. The analysis can also be expressed in terms of the elemental mass fractions—an ultimate analysis. For mixtures of ideal gases, the mole and volume fractions are the same. The heating value of any fuel gas is commonly expressed in units of energy per unit volume (kJ/L, kJ/m^3, or Btu/ft^3) but this value is directly proportional to the gas density, which in turn is directly proportional to the absolute pressure and

inversely proportional to the absolute temperature. The heating value can also be expressed in terms of energy per unit mass (kJ/kg or Btu/lbm) and this quantity is independent of the gas pressure and temperature.

The volumetric heating value of a mixture of fuel gases is equal to the sum of the products of the individual component volumetric or molar fraction and the corresponding volumetric heating value of the component. If the volumetric heating values of the gas components at some reference pressure p_r and reference temperature T_r are known, the volumetric heating value of the gas mixture, HHV_v is obtained from the following equation:

$$(\text{HHV}_v \text{ of mixture})_{p_r,T_r} = \sum_{i=1}^{i=n} (\text{HHV}_v)_{i,p_r,T_r}(V_i) \tag{2.7}$$

where $(\text{HHV}_v)_i$ and V_i are the volumetric higher heating value and the volumetric fraction of the ith gaseous component, respectively. The higher heating values of a number of combustible compounds are tabulated in App. I. The following equation can be used to convert the volumetric higher heating value at the reference pressure and temperature to some other pressure and temperature:

$$(\text{HHV}_v)_{p,T} = (\text{HHV}_v)_{p_r,T_r}\left(\frac{p}{p_r}\right)\left(\frac{T_r}{T}\right) \tag{2.8}$$

The pressures and temperatures in Eq. (2.8) must be absolute values.

A volumetric heating value HHV_v at some temperature T and pressure p can be converted into a gravimetric heating value HHV_m, by multiplying the volumetric value by the specific volume v of the gas at the same pressure and temperature:

$$\text{HHV}_m = (\text{HHV}_v)_{p,T}(v)_{p,T} \tag{2.9}$$

The specific volume of a gas mixture can be determined from the molecular weight (MW) of the gas and the ideal-gas equation of state, as follows:

$$v = \frac{V}{m} = \frac{RT}{p} = \frac{R_u T}{p(\text{MW})} \tag{2.10}$$

where R_u is the universal gas constant.

Example 2.3. Calculate the higher heating value, in kJ/m^3 and kJ/kg, at 10°C and 3 atm for a gas mixture with the following composition: 94.3% CH_4, 4.2% C_2H_6, and 1.5% CO_2.

Solution. Given: volumetric or molar fractions of the gas components.
At 20°C and 1 atm (from App. I):

$$\text{HHV}_v \text{ for } CH_4 = 37{,}030 \text{ kJ/m}^3$$

$$\text{HHV}_v \text{ for } C_2H_6 = 64{,}910 \text{ kJ/m}^3$$

$$\text{HHV}_v \text{ for } CO_2 = 0 \text{ kJ/m}^3$$

$$\text{MW} = 0.943(16.043) + 0.042(30.071) + 0.015(44.01)$$

$$= 17.052 \text{ kg/kg} \cdot \text{mol}$$

At 20°C and 1 atm:

$$(HHV_v)_{mixture} = 0.943(37{,}030) + 0.042(64{,}910) + 0.015(0)$$

$$= 37{,}645 \text{ kJ/m}^3$$

$$v = \frac{R_u T}{p(MW)} = \frac{(0.008314 \text{ MPa} \cdot \text{m}^3/\text{kg} \cdot \text{mol} \cdot \text{K})(293.16 \text{ K})}{(1 \text{ atm})(0.1013 \text{ MPa/atm})(17.05 \text{ kg/kg} \cdot \text{mol})}$$

$$= 1.411 \text{ m}^3/\text{kg}$$

$$HHV_m = (v)(HHV_v) = 1.411(37{,}645) = 53{,}120 \text{ kJ/kg}$$

$$= 22{,}840 \text{ Btu/lbm}$$

At 10°C and 3 atm:

$$(HHV_v)_{mixture} = (HHV_v)_{P_r, T_r}\left(\frac{p}{p_r}\right)\left(\frac{T_r}{T}\right)$$

$$= (37645)\left(\frac{3 \text{ atm}}{1 \text{ atm}}\right)\left(\frac{293.16 \text{ K}}{283.16 \text{ K}}\right)$$

$$= 116{,}920 \text{ kJ/m}^3$$

$$v = \frac{R_u T}{p} = \frac{(0.008314 \text{ MPa} \cdot \text{m}^3/\text{kg} \cdot \text{mol} \cdot \text{K})(283.16 \text{ K})}{(3 \text{ atm})(0.1013 \text{ MPa/atm})(17.05 \text{ kg/kg} \cdot \text{mol})}$$

$$= 0.4543 \text{ m}^3/\text{kg}$$

$$HHV_m = (v)(HHV_v) = 0.4543(116{,}920) = 53{,}120 \text{ kJ/kg}$$

Alternative calculation of HHV_m using mass fractions:
From App. I:

$$HHV_m \text{ for } CH_4 = 55{,}530 \text{ kJ/kg}$$

$$HHV_m \text{ for } C_2H_6 = 51{,}920 \text{ kJ/kg}$$

$$\text{Mass fraction of } CH_4 = \frac{0.943(16.043)}{17.052} = 0.887$$

$$\text{Mass fraction of } C_2H_6 = \frac{0.042(30.071)}{17.052} = 0.074$$

$$(HHV_m)_{mixture} = 0.887(55{,}530) + 0.074(51{,}920)$$

$$= 53{,}110 \text{ kJ/kg}$$

TYPICAL FUEL GASES. Natural gas is the only true fossil-fuel gas and is usually trapped beneath limestone casings above petroleum reserves. Actually, there are two types of natural gas—that produced from the decay of organic matter and that which has been trapped deep in the earth's crust since the earth was formed. These latter gas sources are called *primordial* natural-gas sources. Typical gas reservoir pressures may run as high as 35 to 70 MPa (5000 to 10,000 lb/in^2). Natural gas is composed of methane plus smaller fractions of other gases. The composition of some typical natural gases is presented in App. H.

Natural gas has the highest gravimetric heating value of all fossil fuels, about 55,000 kJ/kg or 24,000 Btu/lbm. The volumetric heating value of natural gas is about 37,000 kJ/m^3 or 1000 Btu/ft^3 at 1 atm and 20°C (68°F). Natural gas is commonly sold in units of *therms*, where 1 therm is equal to 100,000 Btu. Of the three principal types of fossil fuels, natural gas has the lowest known fuel reserves.

Natural gas is the easiest of the three fossil fuels to burn; it mixes well with air and burns cleanly with little ash. Natural gas can be easily and cheaply transported in pipelines, and overseas gas is sometimes converted to liquified natural gas (LNG) at −127°C (−197°F) and shipped in cryogenic tankers to the energy-consuming nations. If there is any disadvantage associated with the use of natural gas as a source of fuel energy, it would be that it is difficult to store large quantities of energy in the form of natural gas. Some gas companies are injecting high-pressure gas into large underground cavities, including domed, sealed aquifers. When the gas is pumped into the aquifier, it displaces the groundwater.

Manufactured fuel gases include liquified petroleum gas (LPG), water gas, carbureted water gas, synthetic or substitute natural gas (SNG), and producer gas. A number of other fuel gases are produced as byproducts of some other process. These include coke-oven gas, sewage gas, and blast-furnace gas. The composition and properties of some of these gases are presented in App. H.

Liquified petroleum gas, sometimes called *refinery gas*, is composed of the light distillates of petroleum—primarily propane and butane. Because of the higher molecular weight and resulting higher gas density, it has a higher volumetric heating value than natural gas. Actually, LPG is heavier than air, which makes it more dangerous to handle than natural gas. This fuel gas is usually stored and transported as a liquid under pressures ranging from 0.4 to 2.0 MPa (60 to 290 psia), depending on the atmospheric temperature.

Water gas is a manufactured fuel gas that is produced by alternately passing steam and air through a bed of incandescent coke. The steam reacts with the hot coke in the "water-gas reaction" to produce hydrogen and carbon monoxide—gases with very low volumetric heating values. Oil vapors are sometimes added to the water gas to improve the heating value of the gas. When this is done, the resulting gas is called *carbureted water gas.*

There are many proposed processes for producing "high-Btu" and "medium-Btu" fuel gases from coal. The high-Btu gas is commonly called *synthetic natural gas* or simply *SNG.* Many of these processes are designed to permit the utilization of high-sulfur coal by converting it into a cheap, clean, fuel gas. Solid hydrocarbon compounds, such as those found in coal, have a low hydrogen-to-carbon atom ratio compared to the gaseous hydrocarbons. Thus, any scheme for converting coal into fuel gas requires the addition of hydrogen to the coal compounds.

In the hydrogenation process, pressurized hydrogen at 900°C (1650°F) is combined with coal to produce a number of light hydrocarbon compounds, particularly methane. This process, as is the case with all the SNG processes, is

TABLE 2.1
Characteristics of coal-to-SNG processes

Process	Type of process†	Chemical reactor parameters: Temp, °C	Chemical reactor parameters: Pressure, bars abs	Status
Koppers-Totzek	G	1480–1820	1+	Commercial
Wellman-Galusha	G	540–650	1+	Commercial
Winkler	G	820–1010	1+	Commercial
Texaco	G	1480–1820	70	Pilot plant
Ash agglomerating	G	870–980	16	Pilot plant
COGAS	G	870–930	1+	Pilot plant
Lurgi	G/HD	620–870	30	Commercial
Hygas	G/H	650–980	75	Pilot plant
CO_2 acceptor	G/HD	860–1040	10	Pilot plant
BI-GAS	G/HD	1650–930	70	Pilot plant
Synthane	G/H	980	70	Pilot plant

† G—gasification process; H—hydrogasification process; HD—hydrodevolatilization process. In the gasification process, the coal is reacted with steam to produce a gas that can subsequently be converted to methane. In the hydrogasification process, high-pressure hydrogen is added to the coal for the direct production of methane gas.

not economically competitive with the other fuel gases at this time. Some of the SNG processes under development, along with some low-Btu fuel gas processes, are listed in Table 2.1.

There are several fuel gases that are called *producer gas.* However, the name is normally applied to a fuel gas that is produced by burning low-grade coal seams in the ground (in situ) with insufficient air for complete combustion. Only enough air is added to the bed to maintain the bed at a high enough temperature to drive off some of the hydrogen and the volatile matter and to oxidize some of the carbon to carbon monoxide. While the resulting fuel gas is a low-quality fuel gas, this method does permit the utilization of thin-seam, low-grade coal deposits that cannot be recovered economically. Producer gas has been extensively used in the U.S.S.R. and has been tried on an experimental basis in the United States.

Coke-oven gas is an excellent fuel gas with a high heating value. The gas is essentially composed of the volatile matter of a caking coal. The gas is a byproduct of the industry that supplies coke to the steel industry. The only problem with coke-oven gas is its limited availability.

Blast-furnace gas was a low-quality fuel gas resulting from the steel industry. It was produced by burning natural gas or other fuel with insufficient air. The resulting exhaust gas was then used to provide a reducing atmosphere over the molten metal to inhibit its oxidation. Although the gas had a heating value which was only one-tenth that of natural gas, so much of it was generated in the operation of a blast furnace that it was economically feasible to recover and burn it in large

internal-combustion engines. Blast-furnace gas consisted primarily of nitrogen, carbon dioxide, and carbon monoxide. The carbon monoxide was the only combustible gas in this mixture.

Sewage gas has been used as a heating fuel in several cities in the eastern United States since colonial times. Currently, most of the interest in sewage gas involves the utilization of animal and vegetable wastes (biomass), particularly the waste from large cattle feed lots, to generate the gas. Sewage gas is almost pure methane, which is produced in the decay process.

2.4 NUCLEAR FUELS

2.4.1 Source of Nuclear Energy

If mass is indeed converted into energy in an exothermic chemical reaction, it is too small to be detected. In nuclear reactions, however, the energy release per reaction is high enough that the mass conversion can actually be detected. Consequently, it is possible to calculate the energy release per nuclear reaction from a mass balance of the reactants and products without having to rely on an experimental determination of the energy release.

In any nuclear energy conversion reaction, there are four rules or laws that must be satisfied, and these are useful in defining the reaction, determining the energy released in the reaction, and also determining the distribution of this energy among the products. These rules are as follows:

1. The *sum* of mass and energy must be conserved.
2. Total charge (atomic number Z) must be conserved.
3. Total number of nucleons (atomic mass number A) must be conserved.
4. Total momentum must be conserved.

The atomic number Z is equal to the number of protons (positively charged particles) in the nucleus of an atom. In a nonionized atom, the atomic number if also equal to the number of electrons (much smaller, negatively charged particles) that orbit the nucleus. All atoms with the same atomic number are members of the same chemical element, and these atoms exhibit essentially the same chemical behavior.

The nucleus of an atom is composed of protons and neutrons. The neutron is a neutrally charged particle with approximately the same mass as a proton. Outside the nucleus, a neutron is radioactive and decays to a proton and an electron (a hydrogen atom). Both the protons and the neutrons are called *nucleons*, and the total number of nucleons in a given atom is called the *atomic mass number A*.

As discussed earlier, all atoms with the same atomic number Z are members of the same chemical element. If some of these atoms have a different atomic mass number A, they are said to be *isotopes* of the element. The different isotopes of an element differ only in the number of neutrons in the nucleus. These ato-

exhibit essentially identical chemical behavior but vastly different nuclear behavior.

It is common practice to identify a given atom or nucleus with the chemical symbol preceded or followed by a superscript of the atomic mass number and preceded by a subscript of the atomic number. Thus, ${}_{1}^{2}\mathrm{H}$ represents a hydrogen atom or nucleus with 1 proton and 1 neutron for a total of 2 nucleons. ${}_{92}^{235}\mathrm{U}$, on the other hand, is an uranium isotope with 92 protons and 143 neutrons for a total of 235 nucleons. Since the atomic number and chemical symbol are redundant, these isotopes are sometimes written as hydrogen-2 and uranium-235 or H-2 and U-235.

The mass of an atomic nucleus is less than the mass of the individual particles or nucleons that compose it. This mass difference is called the *mass defect* and it is this mass difference ("negative mass glue") that prevents the coulomb forces associated with the protons in the nucleus from tearing it apart. In order to break a nucleus into its individual nucleons, a minimum amount of energy equivalent to the mass defect has to be added to the nucleus. The mass defect of a given nucleus can be calculated from the following equation:

$$\text{Mass defect} = Zm_p + (A-Z)m_n - \text{nuclear mass} \tag{2.11}$$

where m_p and m_n are the mass of a proton and neutron, respectively. Unfortunately, it is very difficult to measure nuclear masses directly, but atomic masses (the nuclear mass plus the mass of the orbiting electrons) can be accurately measured. Consequently, the mass defect is usually determined from the following equation:

$$\text{Mass defect} = Zm_{H-1} + (A-Z)m_n - \text{atomic mass} \tag{2.12a}$$

m_{H-1} is the mass of the light-hydrogen (${}_{1}^{1}\mathrm{H}$) atom. This atom contains one proton and one electron.

Atomic masses are very small and they are usually reported in units called *atomic mass units* or simply *amu*, where one of these units is one-twelfth the mass of the C-12 atom. This means that an amu is about the mass of a neutron or proton. The actual mass of 1 amu is equal to the reciprocal of Avagadro's number (AV), in kg, or 1.66×10^{-27} kg. The energy equivalent ($E = mc^2$) of 1 amu is 931.5 MeV.

A partial list of isotopes, along with their atomic masses, is presented in App. K at the end of this book. The masses in App. K have been normalized so that the carbon-12 isotope has an atomic mass of exactly 12.00000 amu. Some of the older atomic-mass compilations of atomic masses were normalized so that the oxygen-16 isotope had an atomic mass of 16.00000 amu. Care should be exercised when using the atomic masses from more than one table to be sure that they are normalized to the same value.

The atomic mass of the hydrogen-1 isotope is 1.007825 amu and the mass of a neutron is 1.008665 amu. Using these values, Eq. (2.12*a*) reduces to:

$$\text{Mass defect} = 1.007825Z + 1.008665(A-Z) - (\text{atomic mass, amu}) \tag{2.12b}$$

The mass defect increases as the atomic mass number increases because there are more particles in the nucleus. The energy equivalent of the mass defect is called the *total binding energy* (total BE) and this energy, in MeV, can be found from the following relationship:

$$\text{Total binding energy, MeV} = 931.5(\text{mass defect, amu}) \qquad (2.13)$$

The total binding energy is the absolute minimum amount of energy required to break up a nucleus into Z protons and $(A-Z)$ neutrons or A nucleons.

While the mass defect or binding energy increases with the atomic mass, the average mass defect or binding energy per nucleon rapidly increases and then slowly decreases as the atomic mass is increased. A plot of the average binding energy per nucleon, which is obtained by dividing the total binding energy from Eq. (2.13) by the atomic mass number A, is shown in Fig. 2.7.

It will be noted in Fig. 2.7 that the average binding energy per nucleon is a maximum of 8 to 9 MeV for intermediate-mass nuclei. This indicates that these intermediate-mass nuclei are the most stable nuclei. Consequently, excess binding energy is released in any nuclear reaction in which a heavy-mass nucleus is broken into two intermediate-mass nuclei, as in the fission process. Also, excess binding energy is released in any nuclear reaction in which two light-mass nuclei are combined to form a heavier nucleus, as in the fusion reaction. The energy

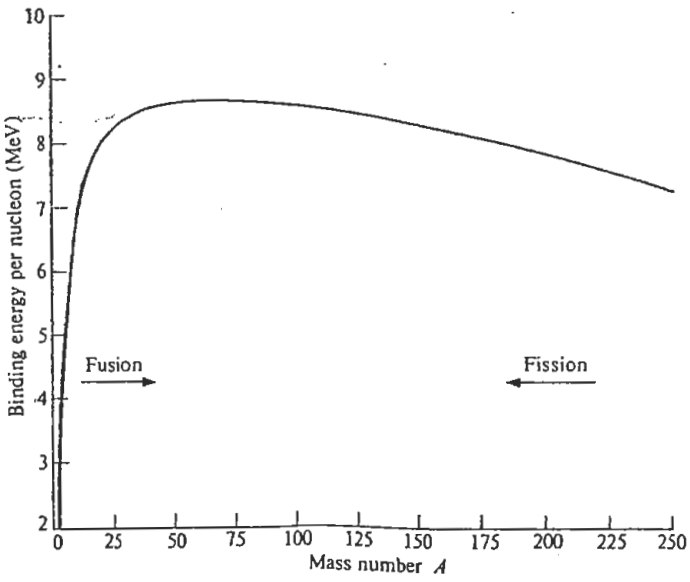


FIGURE 2.7
Variation of the binding energy per nucleon with the atomic mass. (*From Steam: Its Generation and Use, 1972.*)

eleased in any radioactive-decay process is also excess binding energy as the ucleus decays to a more stable configuration.

.4.2 Radioactive Decay

1ECHANICS OF THE DECAY PROCESS. In the radioactive-decay process, the adioisotope spontaneously assumes a more stable configuration with the release of excess binding energy, usually with the release of a lighter particle. There are our basic types of naturally occurring radioactive decay—including alpha decay, eta decay, positron decay, and K-capture decay. These processes may or may ıot be accompanied with the release of gamma radiation. Usually, most of the lecay energy is released in the form of the kinetic energy of the product particles, vith the balance carried away by the gamma radiation.

Example 2.4. Calculate the average binding energy per nucleon for the following isotopes: (*a*) heavy hydrogen ($^{2}_{1}$H), (*b*) a nickel isotope ($^{59}_{28}$Ni), and (*c*) a uranium isotope ($^{235}_{92}$U).

Solution. (*a*) For hydrogen-2, the atomic mass is 2.0141 amu (from App. K). Thus

$$\text{Mass defect} = 1.007825(1) + 1.008665(2-1) - 2.0141$$

$$= 0.00239 \text{ amu}$$

$$\text{Total binding energy} = 931.5 \text{ (mass defect)}$$

$$= 931.5(0.00239) = 2.226 \text{ MeV}$$

$$\text{Average BE per nucleon} = \frac{\text{total binding energy}}{A}$$

$$= \frac{2.226}{2} = 1.113 \text{ MeV per nucleon}$$

(*b*) For nickel-59, the atomic mass is 58.9342 amu (from App. K). Thus

$$\text{Mass defect} = 1.007825(28) + 1.008665(59-28) - 58.9342$$

$$= 0.5535 \text{ amu}$$

$$\text{Total binding energy} = 931.5(0.5535) = 515.60 \text{ MeV}$$

$$\text{Average BE per nucleon} = \frac{515.60}{59} = 8.739 \text{ MeV per nucleon}$$

(*c*) For uranium-235, the atomic mass is 235.0439 amu (from App. K). Thus

$$\text{Mass defect} = 1.007825(92) + 1.008665(235-92) - 235.0439$$

$$= 1.91510 \text{ amu}$$

$$\text{Total binding energy} = 931.5(1.9151) = 1783.9 \text{ MeV}$$

$$\text{Average BE per nucleon} = \frac{1783.9}{235} = 7.591 \text{ MeV per nucleon}$$

In any radioactive-decay reaction, the sum of mass and energy must be conserved and the energy distribution among the product particles can be determined from the conservation of momentum. Suppose that a given radioactive-decay process produces a heavy-mass nucleus with mass M and a light-mass particle of mass m, and that the two products have respective velocities of U and u. The total energy E_T released in a radioactive-decay process can be determined from the following equation:

$$E_T = 931.5\ [(\text{parent nuclear mass, amu}) - (\text{particle mass, amu}) - (\text{daughter nuclear mass, amu})] \quad (2.14)$$

where the "daughter nucleus" is the residual nucleus produced in the reaction. The total kinetic energy of the product particles, E_{KE}, is obtained by subtracting the total emitted gamma ray energy, E_γ, from the total emitted energy. The total emitted decay-gamma energy is an experimentally determined quantity:

$$\text{Total product KE} = E_{KE} = E_T - E_\gamma = \frac{mu^2}{2} + \frac{MU^2}{2} \quad (2.15)$$

If the momentum of the gamma radiation is neglected, and the initial momentum of the parent nucleus is assumed to be zero, the product of MU must equal the product of mu in order to conserve momentum. Substituting this relationship into Eq. (2.15) gives:

$$E_{KE} = \left[\frac{MU^2}{2}\right]\left[1 + \frac{M}{m}\right] = \left[\frac{mu^2}{2}\right]\left[1 + \frac{m}{M}\right] \quad (2.16)$$

Solving for the kinetic energy of the individual particles gives:

$$\text{KE of the heavy-mass product} = \frac{MU^2}{2} = \frac{E_{KE}}{1 + M/m} \quad (2.17)$$

$$\text{KE of the light-mass product} = \frac{mu^2}{2} = \frac{E_{KE}}{1 + m/M} \quad (2.18)$$

Since the mass of the light particle, m, is usually very small compared to that of the heavy particle, M, Eqs. (2.17) and (2.18) indicate that the light-mass particle carries off most of the kinetic energy in order to conserve momentum.

Example 2.5. Uranium-235 atoms undergo alpha (a helium-4 nucleus) decay with the emission of a 0.17-MeV gamma ray. Find the kinetic energy of the product nucleus and the alpha particle.

Solution. Decay reaction:

$$^{235}_{92}\text{U} \rightarrow {}^{231}_{90}\text{Th} + {}^{4}_{2}\text{He} + 0.17\ \text{MeV gamma ray}$$

From App. K, the atomic masses are:

$$m_{\text{U-235}} = 235.0439\ \text{amu}$$

$$m_{\text{He-4}} = 4.0026\ \text{amu}$$

$$m_{\text{Th-231}} = 231.0347\ \text{amu}$$

$$\text{Total KE} = 931.5[(m_U - 92m_e) - (m_{Th} - 90m_e) - (m_{He} - 2m_e)] - E_\gamma$$

$$= 931.5(0.0066) - 0.17 = 5.978 \text{ MeV}$$

$$\text{KE of Th-231 nucleus} = \frac{E_{KE}}{1 + M/m} = \frac{5.978}{1 + 231/4}$$

$$= 0.102 \text{ MeV}$$

$$\text{KE of alpha particle} = \frac{E_{KE}}{1 + m/M} = \frac{5.978}{1 + 4/231}$$

$$= 5.876 \text{ MeV}$$

TYPES OF RADIOACTIVE DECAY. One of the important radioactive-decay processes with respect to power production is the alpha-decay process, with or without the production of gamma radiation. There are about 150 radioisotopes that emit alpha particles. A typical alpha-decay process is given below:

$$^{238}_{92}U \rightarrow {}^{234}_{90}Th + {}^{4}_{2}\alpha + \gamma_d \qquad (t_{1/2} = 4.51 \times 10^9 \text{ years})$$

The alpha particle ${}^{4}_{2}\alpha$ is actually a helium-4 nucleus and γ_d is gamma radiation produced in the decay process (a decay-gamma ray or rays). In any alpha-decay process, the product or daughter nucleus (Th-231 in the preceding reaction) has a mass number which is 4 less than the parent nucleus (U-238) in the preceding reaction) and the atomic number of the parent nucleus is decreased by 2. The *half*-life, designated by $t_{1/2}$, is the time required for half of the radioactive atoms to decay and is constant for a particular radioisotope. Thus, 1 kg of U-238 will decay to 0.5 kg 4,510,000,000 years later. The resulting product nucleus may be stable or it may be radioactive.

The alpha-decay process is normally limited to heavy-mass radioisotopes and a few very light-mass radioisotopes. The alpha particles from a particular radioisotope are essentially monoenergetic (constant KE) and have a very high kinetic energy (4 to 6 MeV). Alpha particles have very low penetrating power and do not present a biological hazard unless they are ingested.

The most common type of radioactive decay is the beta-decay process, with or without decay-gamma radiation. There are approximately 450 beta-emitting radioisotopes. A typical beta-decay process, commonly used in medical radiation therapy ("cobalt treatments") is shown below:

$$^{60}_{27}Co \rightarrow {}^{60}_{28}Ni + {}^{0}_{-1}\beta + \gamma_d + \upsilon \qquad (t_{1/2} = 5.3 \text{ years})$$

The beta particle, ${}^{0}_{-1}\beta$, is essentially an electron and the υ is a strange particle called a *neutrino* that is produced in the beta-decay process. The average kinetic energy of the beta particle is about one-third the total kinetic energy, with the balance of the energy being carried away by the neutrino. The neutrino has no mass but it does have spin, and the energy of this particle cannot be recovered. In any beta-decay reaction, the atomic number of the product nucleus is increased by one more than that of the parent nucleus and the atomic mass number is unchanged because the electron mass is very small (1/1847 times the proton

mass). The beta-decay process is another reaction that is useful in the production of thermal energy.

One radioactive-decay process that is not useful in the production of radioisotope power is the positron-decay process. Approximately 150 radioisotopes emit a positron, ${}^{0}_{+1}\beta$. An example of a positron-decay process is shown below:

$$ {}^{55}_{27}\mathrm{Co} \rightarrow {}^{55}_{26}\mathrm{Fe} + {}^{0}_{+1}\beta + \gamma_d + \upsilon \qquad (t_{1/2} = 18 \text{ days}) $$

The atomic mass number of the product is always unchanged with respect to the parent nucleus while the atomic number decreases by 1 in a positron reaction.

The positron is an antielectron and, as such, it rapidly reacts with an ordinary electron and both particles are destroyed in an annihilation reaction. The products of this reaction are two annihilation gamma rays, γ_a, each having a rest-mass energy of an electron [931.5(0.000549) = 0.51 MeV]. Both of the rays go in opposite directions to conserve momentum. This is the only naturally occurring reaction in which mass is completely converted into energy. The annihilation reaction is shown in Fig. 2.8. This particular reaction happens to be reversible because if a high-energy gamma ray ($E_\gamma > 1.02$ MeV) passes near a nucleus, it can be converted into an electron and a positron in a gamma ray reaction called *pair production.*

The fourth common type of radioactive decay is the *K*-capture process. Approximately 350 radioisotopes decay by means of the *K*-capture process. In it, the nucleus absorbs one of the two nearest orbiting electrons from the inner or *K* shell as a proton in the nucleus is converted into a neutron. An example of the *K*-capture reaction is given below:

$$ {}^{57}_{27}\mathrm{Co} + {}^{0}_{-1}e \rightarrow {}^{57}_{26}\mathrm{Fe} + \gamma_d + \text{x-rays} \qquad (t_{1/2} = 270 \text{ days}) $$

In this reaction, the resulting product nucleus (Fe-57) has the same atomic mass number as the parent nucleus (Co-57) but the atomic number is decreased by 1. Some of the remaining orbiting electrons fall into the vacated positions, thereby producing a series of x-rays when the electrons assume lower potential energies.

SOURCES OF RADIOISOTOPES. The two basic sources of radioisotopes are the naturally occuring isotopes and the manufactured radioisotopes. The naturally occurring radioisotopes include those produced by cosmic radiation and the

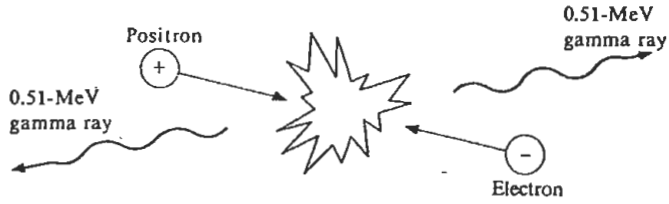


FIGURE 2.8
The annihilation of an electron and a positron.

long-lived radioisotopes with their products. The manufactured radioisotopes are the activation products and the radioactive isotopes from the fission reactions (fission products).

The long-lived radioisotopes and their products have been around since the formation of the earth. There are many of these, including K-40, U-235, etc. Actually, most of them are produced from the decay of three parent isotopes—Th-232, U-235, and U-238. These three eventually decay to the three stable lead isotopes—Pb-208, Pb-207, and Pb-206, respectively. The results of these decay processes are:

$$^{232}_{90}\text{Th} \rightarrow {}^{208}_{82}\text{Pb} + 6^{4}_{2}\alpha + 4^{0}_{-1}\beta$$

$$^{235}_{92}\text{U} \rightarrow {}^{207}_{82}\text{Pb} + 7^{4}_{2}\alpha + 4^{0}_{-1}\beta$$

$$^{238}_{92}\text{U} \rightarrow {}^{206}_{82}\text{Pb} + 8^{4}_{2}\alpha + 6^{0}_{-1}\beta$$

Thus, U-238 undergoes 14 stages of radioactive decay before it reaches a stable nucleus. Included in the U-238 decay chain are radium-226 ($t_{1/2} = 1690$ years), which was the radioisotope isolated by M. Curie in 1902 and radon-222 ($t_{1/2} = 3.82$ days), which is a noble radioactive gas that accumulates in some unventilated houses and is also released from some geothermal wells.

Cosmic radiation is actually high-energy neutrons, protons, and heavier nuclei, and it produces radioisotopes as the result of reactions with the atoms in the atmosphere. Two examples of such radioisotopes are radiocarbon (C-14) and tritium (H-3).

Manufactured radioisotopes can be produced by either splitting nuclei with high-energy ions or by adding additional nucleons, usually neutrons, to the nuclei of stable atoms. Radioisotopes produced in this manner are called *activation products.* These can be generated in either a high-energy accelerator, a neutron generator, or a nuclear fission reactor. Activation products can be either alpha emitters or beta emitters, depending on the target nuclei and the incident particle.

An example of an activation product produced in this manner is cobalt-60, the radioisotope used in cancer therapy. This reaction is shown below and the intermediate compound nucleus (Co-60*) is designated with an asterisk to indicate that it is in an excited state because of the binding energy of the absorbed neutron. This reaction is called a *radiative-capture* reaction because the target nucleus captures a neutron and the excess binding energy of the absorbed neutron is given off in the form of a "capture-gamma" ray (γ_c).

$$^{59}_{27}\text{Co} + {}^{1}_{0}n \rightarrow {}^{60*}_{27}\text{Co} \rightarrow {}^{60}_{27}\text{Co} + \gamma_c$$

The other major group of manufactured radioisotopes is fission products. These atoms are the undesirable byproducts or intermediate-mass nuclei formed from the fission reaction. All the fission products are highly radioactive and, on the average, undergo three stages of beta-particle decay before they form a stable isotope.

RADIOACTIVE-DECAY RATES. The radioactive-decay process is a random process and the radioactive-decay rate is directly proportional to the number of

radioactive atoms present at any instant. The constant of proportionality, called the *decay constant* λ, is inversely proportional to the half-life $t_{1/2}$ of the radioisotope. The decay rate is equal to $(-dN/dt)$, where N is the total number of nuclei present at the time t. The negative sign indicates that the number of nuclei is decreasing with increasing time.

$$\text{Activity} = \text{decay rate} = -\frac{dN}{dt} = N\lambda \tag{2.19}$$

Separating the variables in Eq. (2.19), integrating, and applying the boundary condition that $N = N_0$ at some arbitrary time $t = 0$ gives:

$$N = N_0\, e^{-\lambda t} \qquad \text{or} \qquad \lambda t = \ln \frac{N_0}{N} \tag{2.20}$$

According to Eq. (2.19), the activity A is directly proportional to the number of atoms N. Therefore, activity A has the same time dependence as that of N in Eq. (2.20), or:

$$\text{Activity} = A = A_0\, e^{-\lambda t} \tag{2.21}$$

The activity or number of radioactive atoms present at any time, t, is plotted as a function of time in Fig. 2.9. It will be noted that the exponential relationship is a straight line when plotted on semilog graph paper.

The half-life $t_{1/2}$ of a given radioisotope has been defined as the time required for the number of radioactive atoms to be reduced by a factor of 2. Thus, using Eq. (2.20) and the fact that $N = N_0/2$ at $t = t_{1/2}$, the following relationship is obtained:

$$t_{1/2}\lambda = \ln (2) = 0.693 \tag{2.22}$$

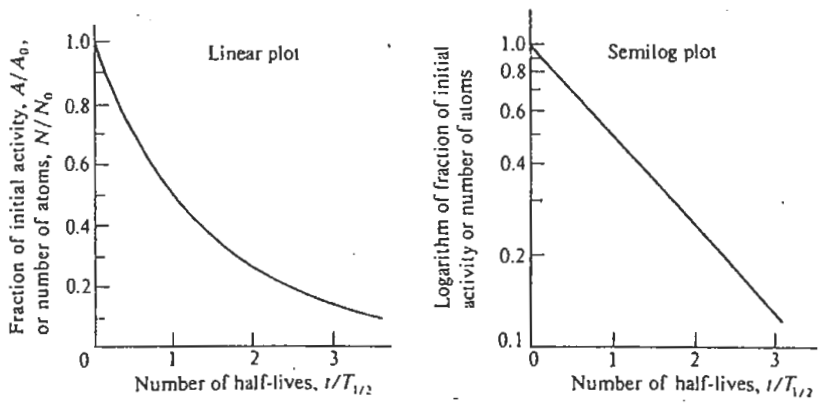


FIGURE 2.9
Variation of activity (A) or number of radioactive atoms (N) with time.

Most of the tables of radioisotopes list the half-life $t_{1/2}$ rather than the decay constant λ (see Apps. K and L at the end of this book) so that Eq. (2.22) must be used to evaluate the decay constant.

A quantity that will prove useful in a later section on nuclear reactor kinetics is the average lifetime of a radioisotope, t_{ave}. This quantity can be found by averaging the time t over the number of atoms, N, from $N = N_0$ to $N = 0$:

$$t_{ave} = \frac{\int_{N_0}^{0} t\, dN}{\int_{N_0}^{0} dN} = \frac{1}{\lambda} = \frac{t_{1/2}}{\ln(2)} = \frac{t_{1/2}}{0.693} \tag{2.23}$$

In order to evaluate the activity of a radioisotope, one needs to determine the number of radioactive atoms present. This can be done if either the mass of the radioisotope or the mass of the material containing the radioisotope is known. If the mass of the material containing the radioisotope, m_C, is known, the number of radioactive atoms, N, is:

$$N = \frac{m_C(\mathrm{AV})nf}{\mathrm{MW}} \tag{2.24a}$$

where m_C is the mass of the radioactive material in kg, (AV) is Avogadro's number (6.022×10^{26} atoms or molecules/kg · mol), n is the number of atoms of the element of interest per molecule, f is the isotopic abundance or the fraction of the atoms of the element that is the isotope of interest, and MW is the molecular weight or atomic weight of the material containing the radioisotope.

If the actual mass m_R of the radioisotope is known, the number of radioactive atoms is:

$$N = \frac{m_R(\mathrm{AV})}{\mathrm{AW}} \tag{2.24b}$$

where AW is the actual atomic weight of the radioisotope.

There are three units of radioactivity—the SI unit of radioactivity is the becquerel (Bq) where 1 Bq is equal to one disintegration per second; the curie (Ci) is commonly used when dealing with large quantities of radioactivity and is equal to the decay rate of 1 g of pure radium-226 or 3.7×10^{10} disintegrations/s; the rutherford is a much smaller unit of radioactivity and is equal to 10^6 Bq.

Example 2.6. Determine the activity, in curies, of the three uranium isotopes in 100 kg of uranium nitride (U_3N_4) when natural uranium is used.

Solution. From App. K,

U-234:	$f = 0.00006$	$t_{1/2} = 2.47 \times 10^5$ years
U-235:	$f = 0.00720$	$t_{1/2} = 7.10 \times 10^8$ years
U-238:	$f = 0.99274$	$t_{1/2} = 4.51 \times 10^9$ years
	$m_C = 100$ kg U_3N_4	n for U = 3 atoms of U/molecule

$$\text{Molecular weight of compound} = 3(238)+4(14)=770\ \text{kg/kg}\cdot\text{mol}$$

$$N=\frac{100(6.022\times10^{26})(3)f}{770}=2.346\times10^{26}f$$

$$\text{Decay constant}=\frac{\lambda=\ln(2)}{\text{half-life}}=\frac{\ln(2)}{t_{1/2}}$$

$$\text{Activity}=\frac{N\ln(2)}{t_{1/2}}=\frac{2.346\times10^{26}\ln(2)}{8766(3600)}(f/t_{1/2})$$

$$=5.153\times10^{18}(f/t_{1/2})$$

$$\text{Activity of U-234}=5.153\times10^{18}\left(\frac{0.00006}{2.47\times10^{5}}\right)$$

$$=1.252\times10^{9}\ \text{Bq}$$

$$\text{Activity of U-235}=5.153\times10^{18}\left(\frac{0.00720}{7.10\times10^{8}}\right)$$

$$=0.052\times10^{9}\ \text{Bq}$$

$$\text{Activity of U-238}=5.153\times10^{18}\left(\frac{0.99274}{4.51\times10^{9}}\right)$$

$$=1.134\times10^{9}\ \text{Bq}$$

Since the only reason U-234 appears in nature is that it appears in the U-238 decay chain, the activity of U-234 is identical to that of U-238. The f_{234} does not have enough significant digits. Thus, it will be assumed that the activity of U-234 is 1.134×10^{9} Bq.

$$\text{Total activity}=[2(1.134)+0.052]\times10^{9}=2.321\times10^{9}\ \text{Bq}$$

$$=0.0627\ \text{Ci}=62.7\ \text{mCi}$$

POWER FROM RADIOISOTOPES. The power produced by a radioisotope heat source is equal to the activity of the radioisotope times the energy released per disintegration. Since the power P is proportional to the activity, the dependence of the power on time is essentially the same as that given in Eq. (2.21), or,

$$P=P_0\,e^{-\lambda t} \tag{2.25}$$

If the radioisotope of interest is actually a daughter product, or if the radioisotope decays to another short-lived radioisotope, the power output may be different from that given by Eq. (2.25) because the two radioisotopes are being produced and lost at two different rates. In most of the work involving radioisotopes, Eq. (2.25) is commonly used to determine the variation of power with time.

The energy released in a radioactive decay process is in the form of decay-gamma energy and the kinetic energy of the emitted particles. Since the gamma rays are very penetrating, the energy may or may not be deposited in the

radioisotope power source. It is recommended that the source designer be conservative and neglect the gamma energy. Since most of the radioisotopes, picked as power sources, emit very little gamma radiation, this is not a major loss. The decay energy per disintegration should also include the decay energy of any product isotopes if they are radioactive with short half-lives.

When choosing a radioisotope for use as a power source, there are a number of criteria that must be considered. First, the fuel isotope should have a reasonable half-life. If the half-life is too short, the source will have very limited use, and if the half-life is too long, the activity is too low to achieve a reasonable value of specific power (power per unit mass). A reasonable half-life would appear to be between 100 days and 100 years. Second, the material used to contain the radioisotope should have a reasonable value of specific power, probably greater than 1 kW/kg. Third, the radioisotope and its daughter products should not emit large quantities of gamma radiation because of the biological hazard it presents. Fourth, the material containing the radioisotope should be a solid and have a high melting point and high thermal conductivity and should be chemically stable or inert. Finally, the availability of the source material should be such that the material and fabrication costs are not excessive.

Out of a total of around 1100 radioisotopes, only 100 or so have half-lives between 100 days and 100 years. Applying the second and third criteria to the remaining isotopes narrows the list to about 30 isotopes. When the final two criteria are imposed, eight radioisotopes remain. Four of these isotopes are alpha-emitting activation products while the other four are beta-emitting fission products. These eight radioisotopes along with the base material used, the important properties, the specific power, and the power densities are listed in App. L at the end of the book.

PROBLEMS WITH RADIOISOTOPE POWER SOURCES. There are a number of problems associated with the design and use of radioisotope power systems that limit their use to small, low-power applications. The lack of availability of these materials is such that they are still very expensive. Plutonium-238, which is commonly used in radioisotope power sources, costs over $1000 per gram. Since plutonium metal is very dense (about 19 g/cm^3), a cubic centimeter of Pu-238 would cost more than $20,000. Decay-gamma radiation is a problem common to almost all radioisotope sources, and since some of the materials are also radiologically toxic, it is very important that the source containment system be leaktight.

From a design standpoint, a major problem arises because the power is not constant. As indicated by Eq. (2.25), the power of a radioisotope power system varies exponentially with time, assuming there are no radioactive daughters. This means that the source must be designed for the desired power output at the end of service life. Consequently, the source will produce more power than is needed at startup, and some provision must be incorporated in the source design to "dump" this excess power to prevent the source from overheating.

A similar problem arises from the fact that there is no way to control the power output of the source. Since the system cannot be shut down, some provision

must be incorporated in the source design to "dump" all the power if it is not needed.

Finally, a problem that is peculiar to only alpha sources arises because of the buildup of helium gas in the source. The alpha particle is a helium-4 nucleus, and once it slows down it picks up two electrons to become a helium atom. The accumulation of helium gas in the source can develop very high pressures unless a proper expansion volume is incorporated into the source.

APPLICATIONS OF RADIOISOTOPE POWER SOURCES. Radioisotope power sources are not applicable where large quantities of power are required but they have found use in specialized applications where small, compact, reliable sources of energy are desired. These sources have been used to power heart pacemakers and have also been proposed as the power source for some of the mechanical, self-contained artificial heart systems under development.

Radioisotope power systems have been widely used in TEG systems. TEG is an acronym for thermoelectric generators. These generators have been widely used in the United States for the SNAP systems. SNAP is an acronym for systems for nuclear auxiliary power. All the even-numbered SNAP units are powered by nuclear reactors while all the odd-numbered SNAP units are powered by radioisotope power systems. A typical radioisotope-powered SNAP system is shown in Fig. 2.10. These units have been used to power remote, automated weather stations, the Apollo lunar laboratories, Coast Guard buoys, orbiting and deep-space satellites, etc.

Example 2.7. Find the initial mass of plutonium-238 metal (80 percent Pu-238) that must be used to supply a minimum thermal power of 0.1 kW_{th} for a period of 30 years. Also the calculate initial excess power that must be "dumped" and the helium-expansion volume which will limit the helium-gas pressure to 5 MPa at 400°C.

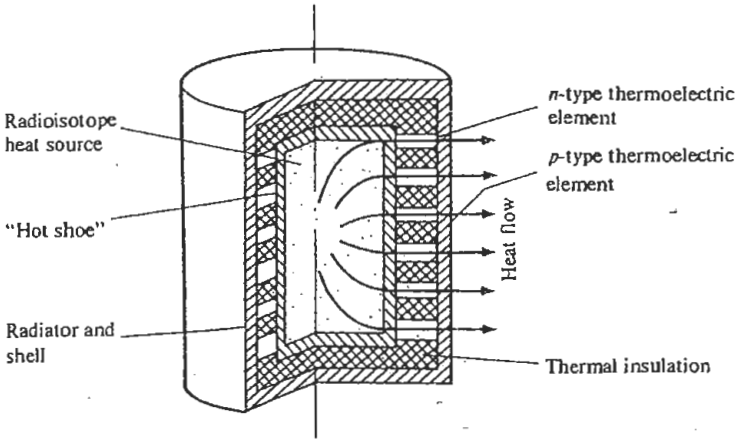


FIGURE 2.10
A radioisotope-powered, SNAP, thermoelectric generator.

Solution. From App. L:

$$\text{Specific power} = \text{SP} = 0.45\ \text{kW/kg}$$

$$\text{Half-life of Pu-238} = 86.0\ \text{years}$$

$$\text{Initial thermal power of source} = P_0 = P \exp \frac{t \ln (2)}{t_{1/2}}$$

$$P_0 = (0.1) \exp \left[\frac{(30)(0.693)}{86.0} \right]$$

$$= 0.1274\ \text{kW}$$

$$\text{Initial mass of Pu-238} = \frac{P_0}{\text{SP}} = \frac{0.1274}{0.45} = 0.2830\ \text{kg}$$

$$\text{Initial power that must be dumped} = P_0 - 0.1\ \text{kW} = 0.1274 - 0.1$$

$$= 0.0274\ \text{kW}$$

Pu-238 eventually decays to stable Pb-206 according to:

$$^{238}_{94}\text{Pu} \rightarrow {}^{206}_{82}\text{Pb} + 8^4_2\alpha + 4_^0_{-1}\beta$$

Thus, each Pu atom eventually produces eight He atoms.

$$\text{Mass of helium} = \frac{N_{\text{He}}(4)}{\text{AV}} = \frac{8N_{\text{Pu}}(4)}{\text{AV}}$$

$$= \frac{8(m_{\text{Pu}})(\text{AV})(4)}{(\text{AV})(238)} = \frac{32(0.283)}{238}$$

$$= 0.0381\ \text{kg of He}$$

$$\text{Helium volume} = \frac{mRT}{p} = \frac{(0.0381)(0.008314/4)(400+273)}{5}$$

$$= 0.01065\ \text{m}^3 = 10{,}650\ \text{cm}^3$$

2.4.3 Nuclear Fission

THE FISSION PROCESS. The fission process is very different from the radioactive-decay process because a particle (the neutron) must react with the nucleus to initiate the reaction. Consequently, fission is a controllable reaction or process when compared to radioactive decay. In the fission process, the heavy, fissionable isotope absorbs a low-energy neutron and forms an excited compound nucleus. The compound nucleus (designated by the asterisk after the atomic mass number) is in an excited state because of the binding energy of the absorbed neutron (7 to 8 MeV). Within 10^{-14} s, the excited compound nucleus either decays to the ground state with the emission of capture-gamma radiation in the "radiative-capture" reaction or else the excited, compound nucleus fissions:

$$^{235}_{92}\text{U} + {}^1_0n \rightarrow {}^{236*}_{92}\text{U} \begin{cases} \rightarrow {}^{236}_{92}\text{U} + \gamma_c & \text{(Radiative-capture process)} \\ \rightarrow \text{FP \#1} + \text{FP \#2} + (2 \text{ to } 3)_0n^1 + \gamma_f & \text{(Fission process)} \end{cases}$$

The radiative-capture process occurs for all isotopes, but it produces only 6 to 8 MeV of energy and, when it occurs to a fissionable nucleus, it converts a fuel atom (U-235) into a nonfuel atom (U-236), which is undesirable. This neutron reaction is desirable with the "fertile" nuclei which are subsequently converted into fuel nuclei. The reaction is also desirable in control-rod material which is inserted into the reactor specifically to absorb neutrons. These processes and materials are discussed in greater detail in a later section.

In the fission reaction, the excited compound nucleus splits into two lower mass nuclei, called *fission products* (FP#1 and FP#2 in the above reaction). These products are accompanied by two or three neutrons and fission-gamma radiation, (γ_f). The fission process releases a total energy of about 200 MeV/fission (including the decay-beta and decay-gamma energy from the fission products). This is the largest amount of energy released from any nuclear reaction, including fusion and radioactive decay. The product neutrons from fission are very important because they can be used to react with other fuel nuclei in a "chain reaction," and since there is more than one neutron produced in the reaction, some of the extra neutrons can be used to produce new fuel atoms.

The average energy release from fission depends to some extent on the velocity of the incident neutron, the type of fuel nucleus, and the other kinds of material used in the reactor. In this text, it will be assumed that the average energy release from fission is a constant 200 MeV. This corresponds to 3.225×10^{-11} J/fission, or, taking the reciprocal, 3.1×10^{10} fissions/W · s. This means that a 3800-MW_{th} reactor, which is the highest net thermal power permitted by the NRC in the United States, has a fission rate equal to $(3800 \times 10^6)(3.1 \times 10^{10})$ or 1.178×10^{20} fissions/s.

The distribution of fission energy is given in Table 2.2. It will be noted in the table that the neutrinos carry away 10 MeV or 5 percent of the energy, which makes it unavailable. The loss of neutrino energy is compensated by the capture-gamma-ray energy and the radioactive decay-beta and -gamma energy resulting from the absorption of neutrons by nonfuel nuclei. This is the reason the average energy from fission is somewhat dependent on the type of nonfuel material used in the reactor.

Almost all of the fission energy is deposited in the reactor core and, in fact, most of the energy is converted into thermal energy at the point where the fission occurs in the fuel. The fission products travel a very short distance, and consequently their kinetic energy (over 80 percent of the fission energy) is deposited directly in the fuel. The fission neutron energy (about 5 percent of the fission energy) is deposited in light-mass material (called *moderating material*), which is inserted into the reactor specifically to slow down the neutrons. The fission-gamma and decay-gamma energies are also deposited in the reactor but some of this energy is deposited in the shielding around the reactor.

Most of the binding energy from fission is released within a millisecond following the fission reaction. This includes the kinetic energy of the fission products and the neutrons and the fission-gamma and capture-gamma radiation. The balance of the energy, which is associated with the radioactive decay of the

TABLE 2.2
Distribution of fission energy

Products of fission	Type of energy	Amount, MeV	Percentage of total	Where deposited	When deposited
Fission products	Kinetic	165	82.5	Fuel	Immediately
Fission neutrons	Kinetic	5	2.5	Moderator	Immediately
Fission gammas	Electromagnetic	7	3.5	Diffuse	Immediately
FP decay betas	Kinetic	7	3.5	Fuel	Later
Decay gammas	Electromagnetic	6	3.0	Diffuse	Later
Neutrinos†	Kinetic	10	...	Nowhere	
Capture gammas‡	Electromagnetic	7	3.5	Diffuse	Immediately
Decay energy‡	Electromagnetic and kinetic	3	1.5	Diffuse and fuel	Later
Total usable energy		200	100.0		

† The neutrino energy is not available as usable energy.

‡ This energy is not produced directly from fission but is produced as the result of nonfission neutron absorption by the fuel and other in-core materials.

fission products, is delayed. This portion of the fission energy, therefore, does not go to zero immediately after reactor shutdown.

The shutdown power production creates a severe problem in most modern high-power reactors in the event of a loss of coolant accident (LOCA). Without proper cooling, the fuel could conceivably melt, producing the so-called China Syndrome. In the Three-Mile Island (TMI) accident, the fuel rods failed and the fuel pellets were spilled to the bottom of the reactor vessel, where there was partial melting. All this happened after the reactor operator turned off all cooling to the reactor core. All power reactors normally have two independent emergency core cooling systems (ECCS) to provide for the removal of the decay heat following LOCA. Each ECCS has its own separate water and separate power supplies.

The shutdown power P_S of a reactor that has operated at a constant power P_O for t_O seconds is given by the following empirical equation:

$$\frac{P_S}{P_O} = 0.1[t_S + 10)^{-0.2} - (t_S + t_O + 10)^{-0.2}] - 0.087[(t_S + 2\times 10^7)^{-0.2} - (t_S + t_O + 2\times 10^7)^{-0.2}] \qquad (2.26)$$

where t_S is the time following reactor shutdown in seconds and the shutdown power P_S has the same power units as that of the operating power.

FISSIONABLE ISOTOPES. As indicated earlier, there are a number of different heavy-mass nuclei that will undergo fission, but the availability of most of these isotopes is such that only three isotopes are commonly listed as fissionable fuel material. They are uranium-235, uranium-233, and plutonium-239. All of these

fuel isotopes have even atomic numbers and odd atomic mass numbers. Evidentally, the even-even atomic and atomic mass number combination formed by neutron absorption is so unstable that the binding energy of the absorbed neutron is sufficient to cause fission.

Some of the other fissionable isotopes are Pu-241, Pu-243, Cf-243, Cf-245, etc. The availability of these isotopes is so poor that they are not used as the initial reactor fuel. Some of these fissionable isotopes appear in irradiated fission fuels. Some even-even (A and Z) heavy mass isotopes such as U-238 and Th-232 will also fission if the incident neutron has a high kinetic energy so that the binding plus the kinetic energy of the absorbed neutron will cause the excited compound nucleus to fission. However, since the binding energy of the absorbed neutron, by itself, is insufficient to cause fission, these isotopes are not considered to be fissionable isotopes.

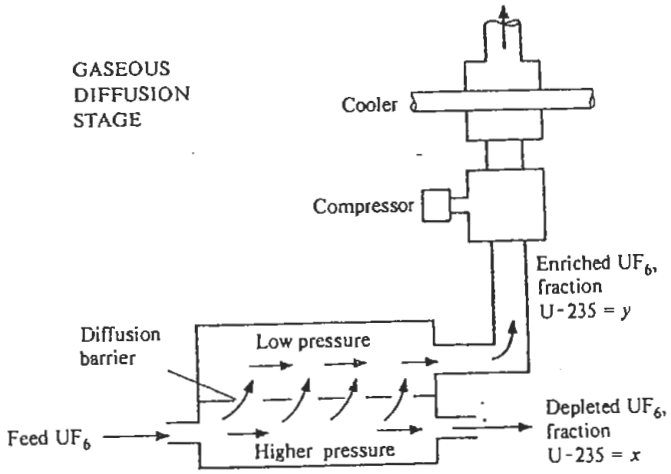
Of the three common fissionable isotopes, only uranium-235 occurs in nature. The atomic composition of natural uranium is 99.274% U-238, 0.72% U-235, and 0.006% U-234. Thus, the U-235 isotope comprises less than 1 percent of the natural uranium atoms. In fact, the isotopic abundance of U-235 is so low that many reactors cannot operate using natural-uranium fuel. This means that the U-235 concentration in the uranium must be increased. The reactor fuel is then said to be *enriched uranium.* An enrichment of X percent means that the fuel has a U-235 *mass* fraction of X percent. Any uranium that has less than the natural isotopic concentration of U-235 (0.72%) is called *depleted uranium.*

In order to produce enriched or depleted uranium, it is necessary to be able to separate the uranium isotopes. This is not easily done because all the isotopes have the same chemical behavior. Thus, most of the separation techniques must depend upon the actual physical differences between the uranium isotopes.

The electromagnetic separation process was the first process employed to separate the uranium isotopes. In this process, the uranium atoms are ionized and accelerated through a linear electric field, and then the ions are passed through a perpendicular magnetic field. All the uranium ions are acted upon by the Lorentz force and traverse a circular path through the magnetic field. The lighter U-235 ions have a smaller radius of curvature and can be collected on a separate electrode. This method was carried out at the Y-12 plant at Oak Ridge, Tennessee, during the early 1940s. It has now been supplemented by more economical and more efficient separation processes.

Most of the current uranium-separation methods employ a gaseous compound of uranium. This compound is chosen such that the total molecular weight difference is due solely to the uranium isotopes. Uranium hexafluoride (UF_6) gas is employed as the feed material in these processes because the element fluorine consists of only one stable isotope—fluorine-19.

The process that is currently employed to separate most of the uranium isotopes in the United States is the gaseous-diffusion process. Since the average velocities of the gas molecules at a given temperature depend on their molecular weights, the different isotopes will diffuse through a porous barrier at different rates, as is shown in Fig. 2.11.



Separation factor

$$\alpha \equiv \frac{y(1-x)}{x(1-y)} = \sqrt{\frac{M_{^{238}UF_6}}{M_{^{235}UF_6}}} = \sqrt{\frac{352}{349}} = 1.00429$$

Minimum theoretical energy input for unit separative work

$$\frac{4RT_0}{(\alpha-1)^2} = 634 \text{ kW·h/kg separative work unit}$$

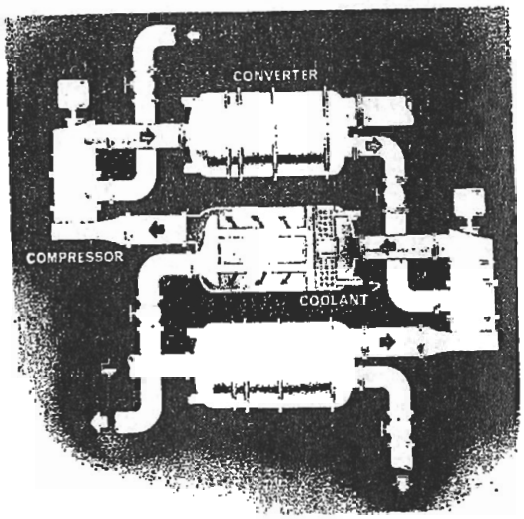


FIGURE 2.11
The basic gaseous-diffusion isotope separator. (*Benedict, 1976.*)

The degree of separation obtained in a single barrier is equal to the square root of the ratio of the molecular weights of the gasses, or $(352/349)^{1/2} = 1.000429$. In a single diffusion stage, the uranium hexafluoride gas is pumped into a porous metallic tube and the gas diffuses through the wall. To obtain 3%-enriched uranium from natural uranium, the diffusion-process gas must be cycled and recycled through hundreds of stages.

Enriched uranium is priced according to the amount of energy (called *separative work units* or *SWU*) required to produce the desired enrichment. The relationship between uranium-235 enrichment and SWU is presented in Table 2.3.

TABLE 2.3
Table of uranium-enriching services

	Standard table of enriching services†	
Assay, wt% U-235	Feed component (normal), kg U feed/kg U product	Separative work component, kg SWU/kg product
0.40	0.391	−0.198
0.50	0.587	−0.173
0.60	0.783	−0.107
0.70	0.978	−0.012
0.711 (normal)	1.000	0.000
0.80	1.174	0.104
0.90	1.370	0.236
1.00	1.566	0.380
1.20	1.957	0.698
1.40	2.348	1.045
1.60	2.740	1.413
1.80	3.131	1.797
2.00	3.523	2.194
2.20	3.914	2.602
2.40	4.305	3.018
2.60	4.697	3.441
2.80	5.088	3.871
3.00	5.479	4.306
3.40	6.262	5.191
3.80	7.045	6.090
4.00	7.436	6.544
5.00	9.393	8.851
10.00	19.178	20.863
90.00	175.734	227.341
98.00	191.389	269.982

† The kilograms of feed and separative work components for assays not shown can be determined by linear interpolation between the nearest assays listed.

There are three government-owned gaseous-diffusion plants in the United States. They are located at Paducah, Kentucky, in Portsmouth, Ohio, and in Oak Ridge, Tennessee. These plants require large quantities of electricity. In 1962, they used a total of 47×10^9 kWh or approximately 5 percent of the total electrical generation in the United States for that year.

A typical reactor fuel pellet is about 0.25 in(10 cm) in diameter and 0.5 in (20 cm) long and enriched to 2 to 3 percent. This pellet has the energy equivalent of about three barrels of oil and is capable of producing about 30 times the electricity required to produce the pellet.

Large quantities of depleted uranium have been generated from these gaseous-diffusion plants. This material, which is primarily uranium-238, is currently stored. The energy equivalent of this material, which is already mined, refined, and stored, exceeds all the known coal reserves in the United States. However, utilization of this fuel material depends on the development and deployment of the "breeder reactor" which converts the U-238 atoms into Pu-239 atoms—a fissionable fuel isotope. In 1984, the U.S. Congress terminated all funding for the development of a breeder reactor.

Another uranium isotopic separation system that is finding increasing use is the gas-centrifuge separation process. This method also employs uranium hexafluoride gas and depends on the centrifugal force acting on the gas molecules to separate them. This system is shown schematically in Fig. 2.12. The gas-centrifuge process appears to be more efficient than the gaseous-diffusion process for moderate enrichments. There are two large gas-centrifuge plants in western Europe—one in the United Kingdom and one in Belgium.

There are two other uranium separation processes that also use UF_6 gas as the feed material. One of these is the *Becker nozzle* process and the other is the so-called *South African* process which is thought to utilize a vortex tube. Neither of these last two processes has found widespread application in the free world.

A relatively new and promising separation system is the atomic vapor laser isotope separation (AVLIS) system. It is currently under development and deployment. This system uses a two-stage laser to preferentially ionize the U-235 atoms in a cloud of uranium vapor. The ionized atoms can then be collected on a charge plate or electrode, as is shown in Fig. 2.13. This process has the potential of separating the uranium isotopes at a fraction of the cost of the other methods. It also has the potential of recovering a much higher fraction of the U-235 atoms in the feed material. This method was undergoing pilot-plant evaluation in the United States during the late 1980s.

The other two fissionable isotopes, uranium-233 and plutonium-239, are manufactured nuclei and are produced as the result of neutron absorption by nonfuel isotopes, called *fertile material.* Following neutron absorption by fertile nuclei in the radiative-capture reaction, the resulting compound nuclei undergo two stages of beta decay to produce fuel nuclei. The common fertile isotopes are thorium-232 and uranium-238 which are respectively converted to uranium-233 and plutonium-239. Since the fuel and fertile isotopes are different chemical elements, they can be separated by chemical means.

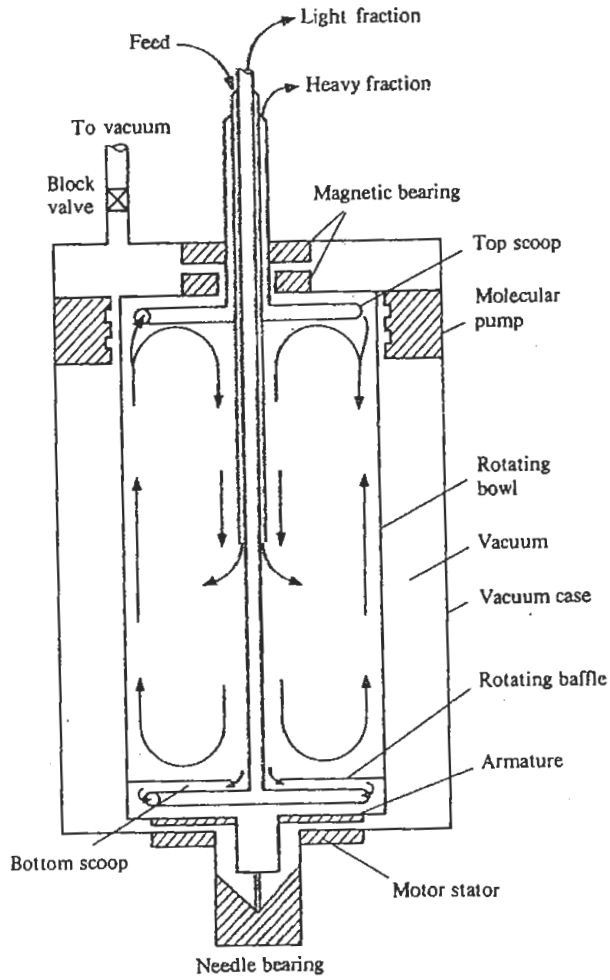


FIGURE 2.12
The gas-centrifuge isotope separation system. (*Benedict, 1976.*)

The neutron activation and subsequent beta-decay processes for the production of U-233 are as follows:

$$^{232}_{90}\mathrm{Th} + {}^{1}_{0}n \rightarrow {}^{233*}_{90}\mathrm{Th} \rightarrow {}^{233}_{90}\mathrm{Th} + \gamma_c \qquad \text{(Radiative-capture reaction)}$$

$$^{233}_{90}\mathrm{Th} \rightarrow {}^{233}_{91}\mathrm{Pa} + {}^{0}_{-1}\beta + \gamma_d + \upsilon \qquad (t_{1/2} = 22.4 \text{ min})$$

$$^{233}_{91}\mathrm{Pa} \rightarrow {}^{233}_{92}\mathrm{U} + {}^{0}_{-1}\beta + \gamma_d + \upsilon \qquad (t_{1/2} = 27.4 \text{ days})$$

$$^{233}_{92}\mathrm{U} \rightarrow {}^{229}_{90}\mathrm{Th} + {}^{4}_{2}\alpha + \gamma_d \qquad (t_{1/2} = 162{,}000 \text{ years})$$

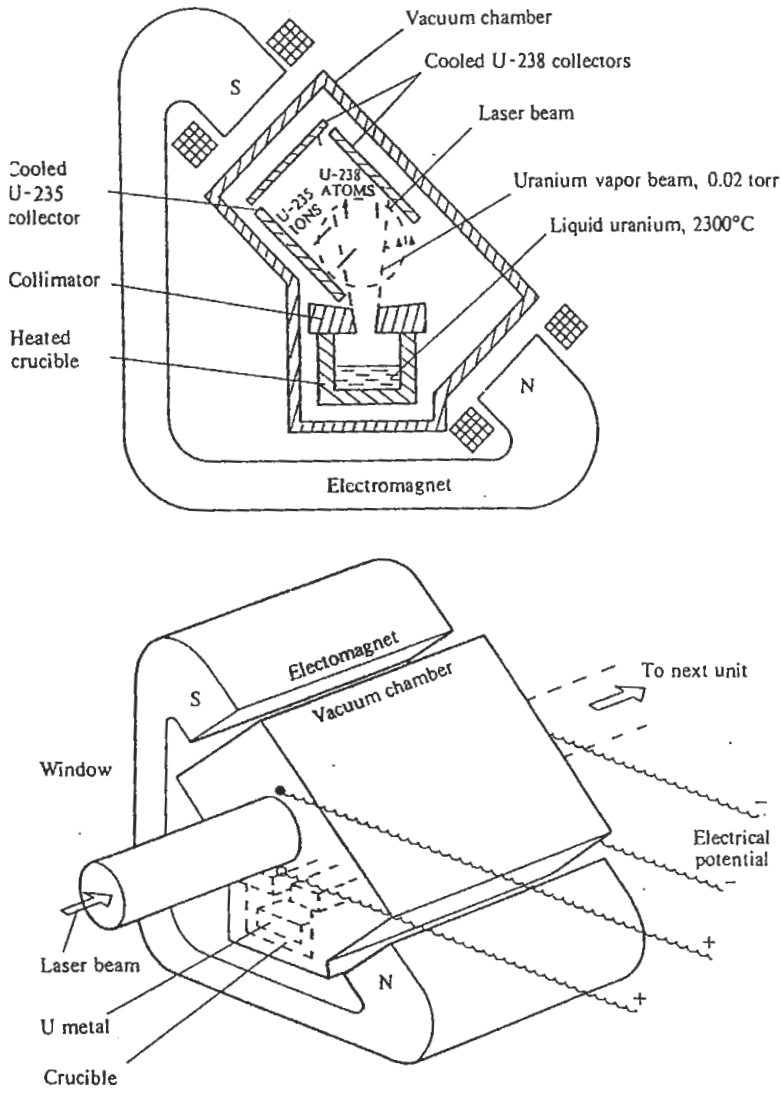


FIGURE 2.13
The Avco-Exxon laser isotope separation system. (*Benedict, 1976.*)

Unfortunately, another neutron reaction occurs during the thorium activation-decay sequence that produces uranium-232 and this isotope comes out with U-233 in the chemical separation process that recovers uranium from the fertile material. The U-232 isotope has a much shorter half-life (73.4 years) and consequently a much higher activity than the U-233 isotope. The radiation from the

U-232 and its daughter products is so high that it presents a biological hazard to personnel handling the uranium fuel material. Thus, any fuel elements fabricated from U-233 must be manufactured using remote manipulators and biological shielding. This significantly increases the fabrication and handling costs.

The neutron activation and subsequent beta-decay reactions for the production of plutonium-239 are as follows:

$$^{238}_{92}\mathrm{U} + ^{1}_{0}n \rightarrow ^{239*}_{92}\mathrm{U} \rightarrow ^{239}_{92}\mathrm{U} + \gamma_c \qquad \text{(Radiative-capture reaction)}$$

$$^{239}_{92}\mathrm{U} \rightarrow ^{239}_{93}\mathrm{Np} + ^{0}_{-1}\beta + \gamma_d + \upsilon \qquad (t_{1/2} = 23.4 \text{ min})$$

$$^{239}_{93}\mathrm{Np} \rightarrow ^{239}_{94}\mathrm{Pu} + ^{0}_{-1}\beta + \gamma_d + \upsilon \qquad (t_{1/2} = 2.35 \text{ days})$$

$$^{239}_{94}\mathrm{Pu} \rightarrow ^{235}_{92}\mathrm{U} + ^{4}_{2}\alpha + \gamma_d \qquad (t_{1/2} = 24{,}000 \text{ years})$$

The feed material for this process is the U-238 isotope, which comprises over 99 percent of the natural uranium atoms. Utilization of this nonfuel isotope as a fissionable fuel increases the naturally occuring fissionable fuel reserves (now only U-235) by a factor of almost 140. The element, plutonium, is a radiological poison and consequently fuel elements fabricated from Pu-239 must be fabricated in glove boxes. This makes the fabrication of Pu-239 fuel elements easier than the manufacture of U-233 fuel but not as easy as the manufacture of U-235 fuel.

CONVERSION OF FERTILE MATERIAL. The production of the manufactured fuels is initiated with the absorption of a neutron by the fertile material. The uranium-235 fission process, on the average, produces about 2.5 neutrons per fission and only one of these neutrons is required to sustain the chain reaction. It would seem logical to use the excess fission neutrons to produce new fuel atoms in the reactor by activating the fertile isotopes. An important reactor parameter, designated here by symbol r, is defined as the ratio of the number of fertile atoms consumed (the number of new fuel atoms produced) to the number of original fuel atoms consumed in both the fission and radiative-capture processes. If the parameter r is equal to or greater than unity, it is called the *breeding ratio* and the reactor is called a *breeder reactor.* If the value of r is nonzero but less than unity, it is called the *conversion ratio* and the reactor is called a *converter reactor.*

The breeder reactor produces energy plus more fuel than it consumes. These reactors actually consume or "burn" fertile material. The important operating parameter for breeder reactors is the *doubling time*, defined as the time required for a breeder reactor to double its initial fuel inventory. Thus, at the end of one doubling time, the reactor has produced enough extra fuel that an identical system could be fueled with the excess. A good breeder reactor will have a short doubling time and this can be achieved by having a high value of breeding ratio, a high power, and a low initial fuel loading. Most of the proposed breeder reactors have a doubling time of 7 to 15 years.

While the converter reactor does not produce as much fuel as it consumes, it does convert some fertile material into fuel as long as the conversion ratio is

nonzero. When the reactor is operated an infinite period of time, a certain number of fertile atoms will be converted into fuel and burned over the life of the reactor. For an infinite operating time, this number is called the *maximum possible conversion of fertile material.*

Assume that N_O is the original number of fuel atoms consumed in the reactor. These N_O original fuel atoms produce $N_O r$ new fuel atoms in the first generation. The first-generation fuel atoms will produce $N_O r^2$ fuel atoms during the next generation. When these second generation fuel atoms are consumed, they will produce $N_O r^3$ new fuel atoms during the third generation and so on. Thus, during the nth generation, $N_O r^n$ new fuel atoms are produced. The total number of fertile atoms converted into fuel and burned during n generations is:

$$N_O r + N_O r^2 + N_O r^3 + \cdots + N_O r^n = N_O(r + r^2 + r^3 + \cdots + r^n)$$
$$= rN_O(1 + r + r^2 + \cdots + r^{n-1})$$

The maximum possible conversion of fertile material occurs as the number of cycles or generations approaches infinity. As long as r is less than unity, which it is for a converter reactor, the infinite series has a finite limit:

$$\lim_{n\to\infty}(r + r^2 + r^3 + \cdots + r^n) = r \lim_{n\to\infty}(1 + r + r^2 + \cdots + r^{n-1})$$
$$= \frac{r}{1-r}$$

Substituting this limit into the definition for the maximum conversion of fertile material yields:

$$\text{Maximum possible conversion of fertile material} = \frac{N_O r/(1-r)}{N_O}$$
$$= \frac{r}{(1-r)} \qquad (2.27)$$

If $r = 0.8$, $r/(1-r)$ is 4. This means that the reactor could eventually consume four atoms of fertile material for each atom of fuel material originally consumed. It might appear that this reactor produces more fuel than it consumes (4 to 1) and hence is actually a breeder reactor. The breeder reactor, however, produces extra fuel at the end of each fuel cycle so that not all of the new fuel is burned in this reactor. If the breeding ratio is exactly unity, an unlikely situation, all of the fertile material in the world could be theoretically converted into fuel material and burned in this system. However, there would never be any extra fuel to build another reactor. Thus, the doubling time is infinity.

2.4.4 Nuclear Fusion

FUSION REACTIONS. The fusion process is essentially the antithesis of the fission process. In the fission process, heavy-mass nuclei are split into lighter-mass nuclei, releasing excess binding energy. In the fusion reaction, light-mass nuclei are

combined in order to release excess binding energy. The fusion reaction is the general reaction that "fuels" the sun and it has been used on earth to release large quantities of uncontrolled fusion energy in the thermonuclear or "hydrogen" bomb. Unfortunately, the technical problems leading to the controlled release of fusion energy have not been solved despite an extensive research effort over the past three decades.

The five most probable, high-temperature (thermonuclear), fusion reactions, along with the energy released in the reaction and the ignition energy or corresponding temperature, are given in Table 2.4. It will be noted that those fusion reactions that produce an alpha particle ($^4_2$He) are accompanied by a very high energy release. The combination of two neutrons and two protons that comprise the alpha particle produces an extremely stable configuration with a high value of binding energy per nucleon. This probably accounts for the fact that one of the common particles emitted in radioactive decay is the alpha particle. It will also be noted that each of these reactions have two product particles. This is necessary in order to conserve momentum in a thermonuclear reaction.

In the list of reactions, the one with the lowest ignition energy or temperature is the reaction involving hydrogen-2 (commonly called *deuterium* or simply D) and hydrogen-3 (commonly called *tritium* or simply T). This reaction has an ignition energy of around 10 keV and releases about 17.6 MeV. Because of the low ignition energy, the "D–T" reaction is probably the one that will be used in the first thermonuclear fusion reactor.

Another nuclear fusion reaction has been proposed as a possible source of nuclear energy. This reaction is called the *thermonuclear fission* reaction and involves a reaction between the hydrogen-1 and boron-11 isotopes. The reaction is shown below:

$$^1_1\text{H} + ^{11}_5\text{B} \rightarrow ^{12*}_6\text{C} \rightarrow 3[^4_2\text{He}] + 8.68\ \text{MeV}$$

This reaction has several attractions. First, boron is one of the more common elements in the earth's crust and 80 percent of the boron atoms are boron-11 atoms. Boron is also much easier to isolate than the heavy-hydrogen isotopes. Second, and most important, the products of this reaction are three alpha particles and these particles are not radioactive. This reaction produces only energy and

TABLE 2.4
Thermonuclear fusion reactions

	Ignition	
Reaction	**Energy, keV**	**Temperature, K**
$^2_1\text{H} + ^3_1\text{H} \rightarrow ^4_2\text{He} + ^1_0n + 17.6\ \text{MeV}$	10	1.2×10^8
$^2_1\text{H} + ^2_1\text{H} \rightarrow ^3_2\text{He} + ^1_0n + 3.25\ \text{MeV}$	50	5.8×10^8
$^2_1\text{H} + ^2_1\text{H} \rightarrow ^3_1\text{H} + ^1_1\text{H} + 4.03\ \text{MeV}$	50	5.8×10^8
$^3_2\text{He} + ^2_1\text{H} \rightarrow ^4_2\text{He} + ^1_1\text{H} + 18.4\ \text{MeV}$	100	1.2×10^9
$^6_3\text{Li} + ^1_1\text{H} \rightarrow ^3_2\text{He} + ^4_2\text{He} + 4.02\ \text{MeV}$	200	2.3×10^9

helium. It is sometimes called a "super-clean" reaction. Unfortunately, it has a much higher ignition energy (because of the large disparity in the masses) than any of the other reactions listed in Table 2.4.

ADVANTAGES AND DISADVANTAGES OF FUSION. The fusion reaction offers several advantages over the fission reaction when it comes to the conversion of nuclear energy. One major advantage of fusion is that there are much greater known reserves of fusionable isotopes. In fact, there is essentially an unlimited supply of fuel. The common fuel isotope for most fusion reactions is deuterium, H-2, which exists in nature a ratio of about one part in 6700 parts of ordinary hydrogen. Considering the amount of hydrogen available in the waters of the world, it means there is a tremendous supply of fuel.

Another advantage of the fusion reaction is that its products are not as highly radioactive as the products of the fission reaction. Of the products produced by the six fusion reactions listed earlier, only the hydrogen-3 and the neutrons are radioactive and the neutrons soon decay to hydrogen atoms if they are not absorbed by the reactor materials. In those reactions that release neutrons, the radioactivity produced as the result of neutron activation of the containment structure is more of a problem than are the fusion products.

The last major advantage of fusion over fission is associated with the safety of the process. This inherent safety factor arises because of two things. First, there is so little fuel material in the reactor at a given time that there is no danger of a power excursion. Second, the reaction is so hard to achieve and maintain that any perturbation in the operating system will probably shut down the reaction. This last "advantage" could be considered a disadvantage when it comes to the continuity of system operation.

The primary problem associated with the development of fusion power arises from the fact that the reacting particles are both positively charged nuclei. This means that the reacting particles must have sufficient kinetic energy (the ignition energy) to overcome the coulomb repulsion forces. For minimum ignition energy, the two reacting particles should have approximately equal masses and they should have high mass-to-charge (A/Z) ratios. The D–T reaction has the highest mass-to-charge ratio (A/Z), 5/2, and it has the lowest ignition energy.

The neutrons produced in the deuterium-tritium reaction can cause severe problems in the reactor containment. These neutrons have an average kinetic energy of 14 MeV, and at this energy a neutron can cause major radiation damage by knocking metal atoms out of their lattice positions in the containment vessel material. Not only can the neutrons displace the metallic atoms but they can be absorbed by the atoms and produce radioactive activation products.

A fusion reactor operating at the same thermal power as a fission reactor produces at least 5 times as many neutrons as the fission reactor. Consequently, the neutron damage and activation problems will be very severe for those fusion systems producing neutrons. This problem can be circumvented by employing a fusion reaction that does not produce a neutron even though it does require a higher ignition temperature.

FUSION RESEARCH. Three things are required to achieve a controlled fusion reaction—a high kinetic energy (above the ignition energy), a high ion density (N/V), and a long containment time (t). It has been estimated that an exothermic fusion reaction can be achieved if the ignition energy can be attained along with a product of Nt/V equal to 10^{21} ions/s · m^3. This Nt/V product is called a *Lawson's criterion.* Actually, the magnitude of this product can be reduced at higher energies and this envelope of conditions is called *Lawson's criteria.*

As discussed earlier, the only significant release of fusion energy has been in the thermonuclear bomb where the reaction is "triggered" by detonating a fission bomb to develop the necessary pressures and temperatures. The fusion reaction is the basic reaction powering the sun and other stars. In the sun, gravitational forces are so great that they produce extremely high temperatures near the core and these temperatures are sufficient to initiate and maintain a continuous fusion reaction. If the fusion rate gets too high, the hot plasma expands, reducing N/V, thereby reducing the reaction rate.

Several methods and systems have been proposed for the production of controlled fusion power on earth. The major problem is associated with the containment of the plasma. Two basic containment systems are currently under development. These are the magnetic-containment systems and the inertial-containment systems.

A charged particle, such as an electron or a nucleus, spirals around a magnetic line of force as the particle travels along the line. Consequently, it has been proposed to contain the high-energy plasma in an intense magnetic field. As the magnetic field lines are compressed, the amplitude of the spiral gets smaller and smaller.

There are two basic types of magnetic-containment systems under development—mirror machines and tokamaks. In the common mirror machine, the magnetic field density is shaped like a football, as is shown in Fig. 2.14. It will be noted that the magnetic field is "pinched" at each end of the reactor. As the charged particle moves to one end of the machine, the increasing density of the magnetic lines of force compresses the amplitude of the spiraling particle until it actually turns around and spirals out again. Thus, the particles are essentially trapped in the magnetic field as if there were a mirror at each end of the machine.

This basic containment process is the same one that produces a phenomenon called the *Van Allen radiation belts* above the earth. In effect, the earth's magnetic field has trapped solar protons and electrons as they spiral back and forth along magnetic lines of force from the north magnetic pole to the south magnetic pole. At times of high solar activity, these particles "spill over" into the atmosphere causing the aurora australis and aurora borealis ("southern" and "northern lights").

The theta-pinch fusion device or thetatron is composed of a linear mirror machine to contain the plasma and this plasma is compressed to an extremely high temperature by the sudden imposition of an intense magnetic field on the system. This is accomplished by discharging a high capacitor bank through a conductor surrounding the plasma, as is shown in Fig. 2.14.

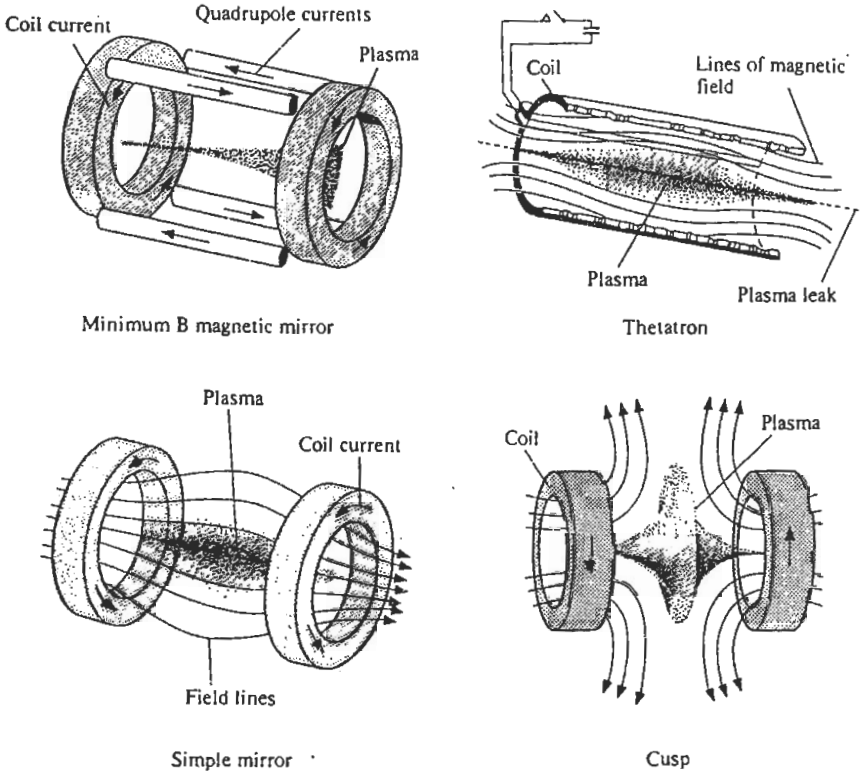


FIGURE 2.14
Schematic diagrams of some of the mirror fusion machines for the magnetic containment of plasma. (*Reprinted with permission of the American Nuclear Society.*)

The tokamak fusion device has a magnetic field contained in a toroidal vacuum chamber. The toroidal magnetic field is used because there is no end to the magnetic force lines. The magnetic field is also twisted so that each of the magnetic field lines is approximately the same length in order to reduce plasma leakage. The external surface of the tokamak chamber is wrapped with superconducting magnetic windings to achieve the desired magnetic field strength and configuration. Of all the magnetic containment systems, the tokamak is one of the most promising and successful. A schematic diagram of a tokamak fusion reactor is shown in Fig. 2.15.

Superconducting magnets are commonly used in all magnetic-containment systems. In a superconducting magnet, the windings must be maintained at a temperature around 10 K using liquid helium as a coolant. This means that the magnetic-containment fusion devices essentially run the gamut of temperatures—from near absolute zero for the windings to millions of degrees for the plasma.

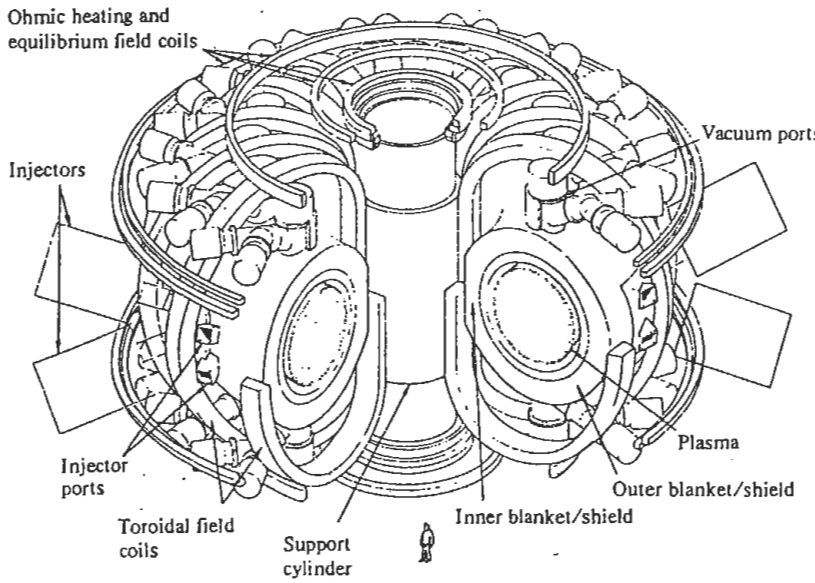


FIGURE 2.15
A schematic diagram of the Argonne tokamak experimental power reactor (TEPR). (*Reprinted with permission of the American Nuclear Society.*)

Inertial-containment fusion systems are relatively late entries in the search for a system for controlled fusion. In this system, small, solid-fuel pellets are suddenly exposed on all sides to a burst of high-energy, pulsed laser and/or ion beams. The sudden deposition of energy on the external surface of the pellet causes the surface to ablate which, in turn, causes the pellet to "implode." This produces extremely high pressures and temperatures at the center of the pellet—hopefully, above the ignition point of the fusion reactants. The small fuel pellets will probably be fabricated from either a heavy-water-tritium ice mixture or a plastic fabricated from the same reactants. A diagram of a proposed pulsed-laser fusion reactor and its associated power cycle is shown in Fig. 2.16.

One of the major problems facing this type of fusion reactor is that it requires the exact positioning of the fuel pellets so that they are hit simultaneously on all sides by the laser/ion beams. Moreover, in order to produce 3800 MW_{th}, the system must produce more than 180 "bangs" per second assuming the yield from each pellet is equivalent to 10 lbm (4.5 kg) of TNT.

In the system shown in Fig. 2.16, the neutrons produced in the D–T reaction are used to react with the lithium coolant to produce tritium and additional energy in the following reaction:

$$ {}^{1}_{0}n + {}^{6}_{3}\mathrm{Li} \rightarrow {}^{4}_{2}\mathrm{He} + {}^{3}_{1}\mathrm{H} + 4.8\ \mathrm{MeV} $$

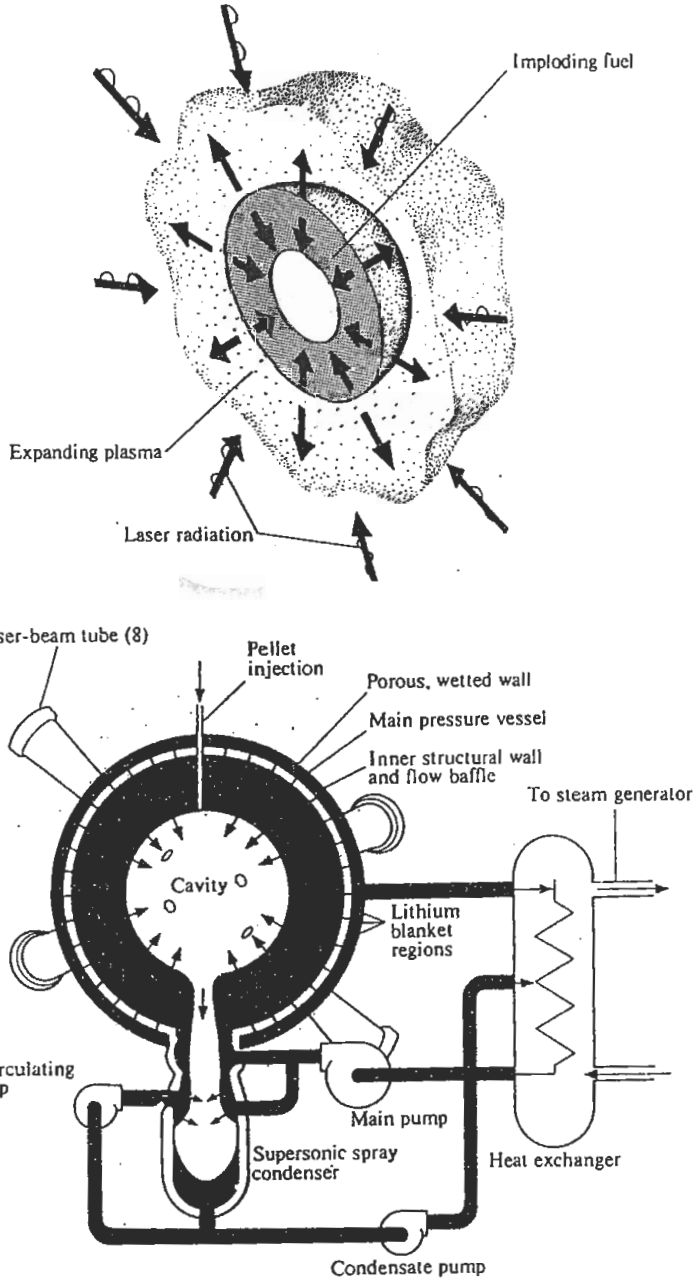


FIGURE 2.16
The inertial containment system with laser implosion and a possible power reactor. (*From Popular Science, vol. 209, no. 6, p. 69, December 1976.*)

Another scheme, called the *fusion-fission hybrid reactor*, calls for the utilization of the fusion neutrons to react with fertile material, U-238 and Th-232, to convert it into fission fuel, Pu-239 and U-233, for consumption in fission reactors. This hybrid system effectively increases the net energy from fusion by an order of magnitude but care must be taken to make sure that very few fissions take place in the fusion system. Because of public relations, many people do not want to link the fusion reactor to the fission reaction.

"COLD FUSION." In recent years, interest has been kindled in the possibility of achieving controlled fusion at low ("cold") temperatures. Two possibilities have been proposed—muon fusion and fusion in palladium electrodes.

A real "dark horse" in the development of controlled fusion is *muon fusion* sometimes called "cold fusion." This system uses molecules of deuterium and tritium. A muon is a negatively charged strange particle with a mass about 200 times that of an electron. The muon replaces one of the electrons in the D–T molecule and the heavy muon mass forces the two nuclei so close that they actually fuse together. When the fusion occurs, the muon is released to repeat the reaction.

Unfortunately, the muon has a relatively short lifetime and the question is whether it can produce more energy from fusion than is required to produce the muon. Initial theoretical studies indicated that the muons could not produce enough fusions to "pay" for themselves but a subsequent experimental study indicated that the muon may actually produce more fusions than required to produce the muon. The outlook for muon fusion depends upon the results of further research on the process.

In the spring of 1989, Fleischmann and Pons, two electrochemists at the University of Utah, shocked the world with the announcement that they had produced an exothermic "cold" fusion reaction in a "test tube." The process involved the use a palladium electrode in a solution of heavy water. Palladium has the property of absorbing hydrogen, forming a metal hydride. In fact, the hydrogen density is greater than that in liquid hydrogen and consequently this material has been promoted as a possible medium for the storage of hydrogen. Supposedly, the palladium incorporated the deuterium atoms (H-2) in the lattice and when an electric current was passed through the lattice some of the deuterium atoms were forced together and subsequently fused.

Because the energy release was much greater than that caused by the typical D–D reactions discussed earlier, it was proposed that the following reaction could be occurring which would have an energy release about an order of magnitude greater than that from the D–D reactions discussed earlier:

$$^{2}_{1}\mathrm{H} + {}^{2}_{1}\mathrm{H} \rightarrow {}^{4}_{2}\mathrm{He} + 23.85\ \mathrm{MeV}$$

In the other proposed fusion reactions, a lighter particle had to be emitted in order to conserve momentum. Since this reaction is a low-energy reaction, the initial momentum is very small. Thus, the two deuterium atoms could fuse to helium-4 but the energy release would have to be essentially all electromagnetic

energy. Unless this radiation is composed of many, many rays, it would be very difficult to recover and would present a major biological hazard.

The big question is whether this reaction actually occurs and if it does whether it is a fusion or chemical reaction. Scientists throughout the world have been attempting to duplicate the experiment with mixed results. In general, most of the major research institutions have been unable to duplicate the reaction and have expressed doubts that it occurs. If the reaction is indeed valid, it would rank as one of the major discoveries in the history of the human race because it provides a simple key for the unlocking of fusion energy.

The future of controlled fusion energy is still uncertain. In spite of a long and costly research effort, none of the current plasma-containment systems have reached Lawson's criteria. Even if the Utah experiments prove valid, current estimates are that large-scale usable controlled fusion power systems will not be a reality until the middle of the twenty-first century, at the earliest. There are still formidable technical problems to overcome.

2.5 SOLAR ENERGY

2.5.1. Introduction

The most abundant continuing source of energy available to the human race is solar energy—specifically the electromagnetic energy emitted by the sum. While solar energy is not being used as a primary source of fuel energy at the present time, a large research and development effort is underway to develop economical systems to harness solar energy and make it a major source of fuel energy, particularly for the heating and cooling of buildings.

Solar energy is very attractive because it is nonpolluting, nondepletable, reliable, and free. The two principal disadvantages are associated with the fact that it is very dilute and that it is not constant for terrestrial applications. The low solar energy flux dictates the use of large surface area collectors and systems to collect and concentrate the energy, and these systems are usually quite expensive.

The other problem with solar energy is associated with the fact that the supply is not continuous for terrestrial collectors. This means that some sort of energy-storage system or another standby energy conversion system is required to supply energy at night and during prolonged cloudy weather. The storage system or alternative conversion system adds significantly to the expense of the overall solar unit.

Solar energy can be converted directly into other forms in three separate conversion processes—the heliochemical process, the heliothermal process, and the helioelectrical process. The principal heliochemical process is the photosynthesis reaction. As was discussed earlier, this reaction is the source of all biomass and fossil fuels. The principal helioelectrical process is the production of electricity by photovoltaic or solar cells. These systems are discussed in a later section. The heliothermal process is the absorption of solar radiation and the

conversion of this energy into thermal energy. This is the only solar conversion process that has a theoretical conversion efficiency of 100 percent. The balance of this chapter is devoted to the heliothermal process.

The total amount of solar energy falling on a unit area is called the *solar insolation.* The total solar insolation on a given surface is composed of a direct (beam) component, a diffuse-scattered component, and the reflected short-wave length (solar) radiation from the surrounding terrestrial surfaces.

The direct solar insolation on a surface normal to the sun's rays depends on the time of day, the time of year, and the local latitude as well as the amount of cloud cover, the amount of atmospheric pollution, etc. The latitude of a location on the earth is measured from the center of the earth and is the angle between the equatorial plane and a radial line to the location of interest. The latitude angle L ranges from 0° at a point on the equator to +90° (or simply 90° N. Lat.) at the North Pole and −90° (or 90° S. Lat.) at the South Pole.

The calculational method for determining the solar insolation on a surface presented in this chapter is applicable for a normal day with few clouds and no atmospheric pollution. This method closely parallels the procedure outlined in the ASHRAE *Handbook of Fundamentals.*

2.5.2 Solar-Energy Calculations

SOLAR TIMES. The earth travels around the sun on an eliptical orbit that is almost circular. At the nearest point, in December, the earth is approximately 1.45×10^{11} m (89.9 million miles) from the sun, while in July the earth is about 1.54×10^{11} m (95.9 million miles) from the sun. The "mean sun time" would equal the local sun time if the earth moved around the sun at a constant velocity. But because of the eliptical orbit of the earth, it does not move at a constant velocity and at certain times of the year, the sun appears to be earlier or later than the mean sun time. The difference between the true sun time, called the *apparent sun time,* or *AST,* and the mean sun time is called the *equation of time.*

The equation of time is not an actual equation, although it can be approximated by an equation. The equation of time is simply a correction factor that is dependent on the time of year. These correction factors range from +16.3 min in November to −14.4 min in February. Values of the equation of time for various days of the year are tabulated in App. M at the end of this book.

The mean sun time can be calculated directly from the local longitude. The local longitude is the angle measured east or west along the equatorial plane from an imaginary line (called the *prime meridian*) that runs from the North Pole to the South Pole through Greenwich, England. The prime meridian is designated to be 0° Long. Since the earth revolves 360° in 24 h, 1° of earth rotation (1 Long. degree) corresponds to [24(60)/360] or four min. There is an imaginary longitude line running from the North Pole to the South Pole through the approximate center of each time zone. These lines (on 15° increments) are called the *standard meridians* for the time zones. The location of the standard meridian for a given

local longitude can usually be determined from the following relationship:

$$\text{Longitude of standard meridian} = 15 \cdot \left(\frac{\text{local longitude}}{15}\right)_{\text{round to integer}} \tag{2.28}$$

Care must be taken when using the above relationship because not all time zones are exactly 15° wide and not all boundaries are ±7.5° from the standard meridian, which is the assumption made in Eq. (2.28).

At the location of the standard meridian for the time zone, the local standard time is identical to the mean sun time. East or west of the standard meridian, the mean sun time is respectively later or earlier (4 min/degree of rotation) than the local standard time. If this correction is greater than 30 min, one must be sure that the location is in the proper time zone. The mean sun time can be determined from the following equations:

$$\text{Mean sun time} = \text{local } \textit{standard} \text{ time} \pm 0{:}04[\text{degrees east } (+) \text{ or west } (-) \text{ of the standard meridian}] \tag{2.29a}$$

$$\text{Mean sun time} = \text{local } \textit{standard} \text{ time} + 0{:}04[\text{longitude of standard meridian} - \text{local longitude}] \tag{2.29b}$$

Equation (2.29*b*) is somewhat better suited for computer applications.

The standard meridians for the time zones in the United States are located at the following longitudes: 60° W. Long. (Atlantic ST), 75° W. Long. (Eastern ST), 90° W. Long. (Central ST), 105° W. Long. (Mountain ST), 120° W. Long. (Pacific ST), 135° W. Long. (Yukon ST), and 150° W. Long. (Alaska-Hawaii ST).

Since many time zones operate on daylight savings time part of the year, the standard time can be obtained from the following equation.

$$\text{Local standard time} = (\text{local daylight savings time}) - 1 \text{ hour} \tag{2.30}$$

Once the mean sun time has been determined, the apparent solar time can be determined by simply adding the equation of time to the mean sun time, or:

$$\text{Apparent solar time} = \text{mean sun time} + \text{equation of time} \tag{2.31}$$

The apparent solar time is needed to calculate the "hour angle," an important solar angle in the solar calculations.

SOLAR ANGLES. The center of the earth travels around the sun on a plane called the *ecliptic plane*. The axis of the earth's rotation (the polar axis) is always inclined at an angle of 23.45° from a normal to the eliptic plane. The polar axis of the earth is essentially unidirectional with respect to Polaris (the "North Star"). This inclination of the polar axis causes the earth to appear to "wobble" with respect to the sun as it moves around the sun. This phenomenon is depicted in Fig. 2.17. This "wobble" produces the seasonal variations and produces an important solar angle called the *angle of declination*, δ.

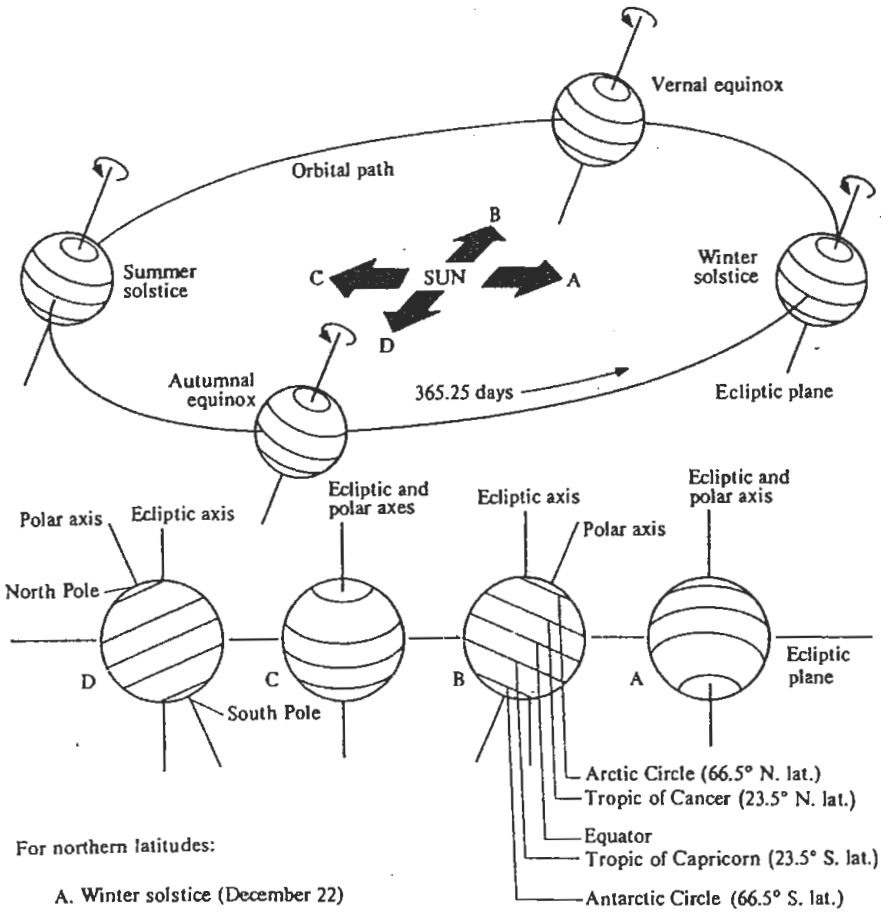
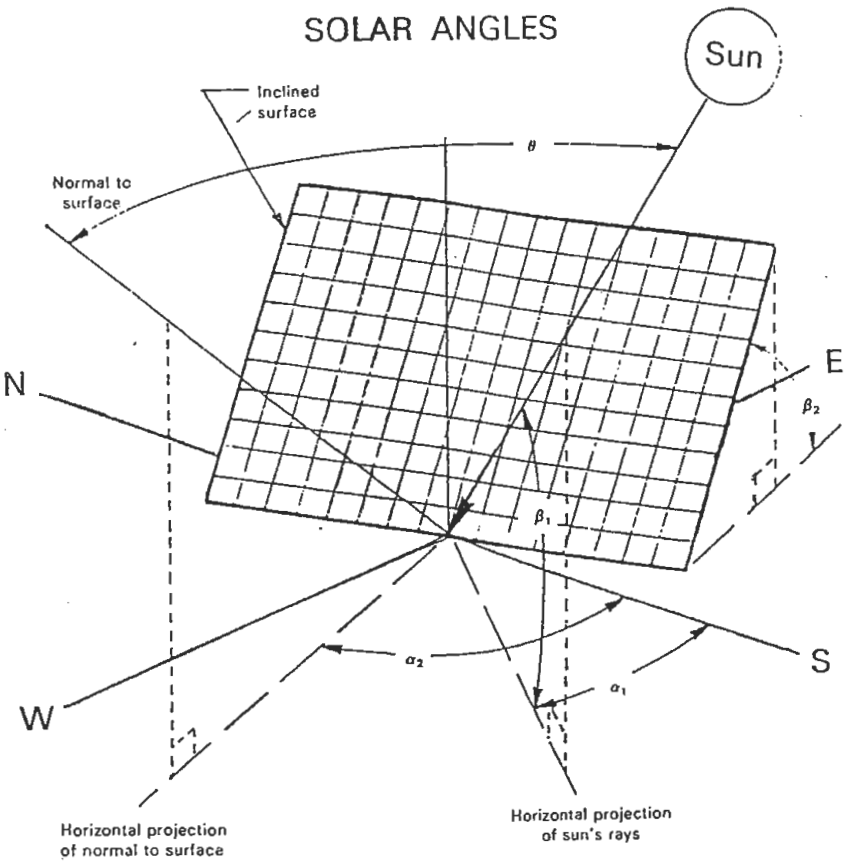


FIGURE 2.17
Orientation of the earth with respect to the sun's rays.

The angle of delination δ is defined as the angle between the sun's rays and the earth's equatorial plane. It is also equal to that latitude on the earth at 12 noon (apparent sun time) when the sun's rays are perpendicular to a horizontal surface. For northern latitudes, the angle of declination ranges from 0° at the vernal equinox (March 21) to +23.45° at the summer solstice (June 22), to 0° at the autumnal equinox (September 22), to −23.45° at the winter solstice (December 22). The values of the angle of declination are presented in App. M at the end of the book.

Several other angles are essential for the solar energy calculations. A diagram showing the orientation of the various angles discussed in this section is given in Fig. 2.18. At a given latitude L, the sun's position can be defined in terms of the altitude angle, β_1, and the azimuth angle, α_1, of the sun. The altitude angle β_1 is the angle between the sun's rays and the horizontal surface at that location.



α_1 = Azimuth angle of sun's rays.
α_2 = Azimuth angle of normal to the surface.
β_1 = Altitude angle of sun's rays.
β_2 = Tilt angle of the surface.
θ = Angle between the normal to the surface and the sun's rays.

$$\cos\theta = (\sin\beta_1)(\cos\beta_2) + (\cos\beta_1)(\sin\beta_2)[\cos(\alpha_1 - \alpha_2)]$$

FIGURE 2.18
Solar angles.

The azimuth angle α_1 is the angle between the horizontal projection of the sun's rays and the local longitude (north-south) line.

For northern latitudes, α_1 is normally measured from the due south line going in a clockwise (+) direction or in a counterclockwise (−) direction. At low northern latitudes ($L < 23.45°$), the angle of declination may exceed the local latitude during the summer months, in which case the sun always appears to be in the northern hemisphere and the absolute value of α_1 is greater than 90°. At higher latitudes, $|\alpha_1|$ can also exceed 90° early in the morning or late in the afternoon. This condition will be discussed later.

The altitude angle of the sun's rays, β_1, can be calculated using the latitude angle L, the angle of declination δ, and the hour angle H, as follows:

$$\sin \beta_1 = (\cos L)(\cos \delta)(\cos H) + (\sin L)(\sin \delta) \tag{2.32}$$

The hour angle H, like the azimuth angle of the sun's rays, is positive after noon, AST, and negative before noon, AST. The hour angle can be determined from either of the following equations:

$$H = \frac{\text{number of minutes before } (-) \text{ or after } (+) \text{ noon, AST}}{4} \tag{2.33a}$$

$$H = \frac{\text{number of minutes past 12 midnight, AST} - 720}{4} \tag{2.33b}$$

If the altitude angle β_1, as determined from Eq. (2.32), is negative, it means that the sun is below the horizon and the calculation should be terminated because the sun is not shining on the surface.

If the altitude angle is positive, the calculated value of the solar azimuth angle, $\alpha_{1,c}$, can be obtained from the following equation:

$$\sin \alpha_{1,c} = \frac{(\cos \delta)(\sin H)}{\cos \beta_1} \tag{2.34}$$

Values of $|\alpha_1|$ and β_1 are tabulated in App. N at the end of this book, along with solar insolation values for 40° N. Lat.

A problem occurs in the summer (any time $\delta > 0°$) when solving for the azimuth angle of the sun's rays from Eq. (2.32). This equation always gives value from −90° to +90° even though the absolute value of α_1 may exceed 90°. This happens when the sun is north of a latitude (east-west) line which occurs early in the morning or late in the evening when $L > \delta$. If $L \leq \delta$, the sun is always north of a latitude line and $|\alpha_1|$ is always greater than 90°.

If the angle of declination is greater than zero, one should calculate the time that the sun is due east, t_E, or the time that the sun is due west, t_W, for the given location. These equations are as follows:

$$t_E = \frac{180 - \arccos[(\tan \delta)/(\tan L)]}{15} \quad \text{a.m., AST} \tag{2.35}$$

$$t_W = \frac{\arccos[(\tan \delta)/(\tan L)]}{15} \quad \text{p.m., AST} \tag{2.36}$$

If the apparent sun time is earlier than t_E or later than t_W, the sun is north of an east-west (constant latitude) line and the absolute value of α_1 is greater than 90°. The proper value of α_1 can be obtained from Eq. (2.37):

$$|\alpha_1| = 180° - |\alpha_{1,c}| \tag{2.37}$$

The angle of interest in the solar insolation calculations is the angle between the sun's rays and the normal to the surface, θ. The surface is normal to the sun's rays when θ is zero and $A_S(\cos\theta)$ is the projected area of the surface normal to the sun's rays. The angle θ can be evaluated from the azimuth, and altitude angles of the sun's rays, α_1 and β_1, are known along with the orientation of the collecting surface.

The orientation of the collecting surface is expressed in terms of the tilt angle β_2 and the azimuth angle α_2 of the surface. These angles are depicted in Fig. 2.18, along with the other solar angles. The angles α_2 and β_2 give the orientation of the surface with respect to a horizontal surface at the location. The azimuth angle of the surface of interest is the angle between the horizontal projection of the normal to the surface and the due south line measured positive in the clockwise direction and negative in the counterclockwise direction. Thus, α_2 is measured just like α_1. The tilt angle of the surface, β_2, is the angle between the surface and the horizontal plane. Thus, β_2 is measured just like β_1. If the surface is horizontal ($\beta_2 = 0°$), α_2 is undefined but it is not needed.

Once $\alpha_1, \beta_1, \alpha_2$, and β_2 have been evaluated, the value of $\cos\theta$ can be calculated from the following equation:

$$\cos\theta = (\sin\beta_1)(\cos\beta_2) + (\cos\beta_1)(\sin\beta_2)[\cos(\alpha_1 - \alpha_2)] \tag{2.38}$$

For a horizontal surface, β_2 is zero and Eq. (2.38) reduces to $\cos\theta = \sin\beta_1$, or $\theta = 90° - \beta_1$. For a vertical wall ($\beta_2 = 90°$) that "faces" the sun ($\alpha_2 = \alpha_1$), Eq. (2.38) reduces to $\cos\theta = \cos\beta_1$, or $\theta = \beta_1$.

If $\cos\theta$ is negative, it means that the sun does not shine directly on the surface (the direct solar component is zero). Under this condition, this calculational method cannot be used to evaluate the solar insolation.

SOLAR INSOLATION VALUES. The total solar energy flux on a surface, I_{tot}, on a terrestrial surface of any orientation is equal to the sum of the direct solar component, I_D, the diffuse-scattered component, I_{DS}, and the reflected solar radiation from the surroundings, I_R. The calculational method presented in this section permits an estimation of the first two components—I_D and I_{DS}. This does not mean that the reflected component is negligible or unimportant. In fact, in some systems, like the "solar power tower," the reflected solar component may be the predominate component. The solar reflection from the surrounding surfaces must be evaluated on an individual basis.

The amount of direct solar energy flux or insolation falling on a given surface is equal to the product of the direct radiation falling on a surface normal to the sun's rays, I_{DN}, and $\cos\theta$, or:

$$I_D = I_{DN}(\cos\theta) \tag{2.39}$$

The value of the direct normal insolation is a function of the thickness of the atmosphere traversed by the radiation as well as the amount of water vapor in the air and the amount of atmospheric pollution present.

The atmospheric path length is commonly expressed in units of air mass, am. The parameter am is defined as the ratio of the atmospheric mass or path length traversed by the sun's rays to the path length traversed if the sun were directly overhead, $\beta_1 = 90°$, at sea level. Outside the earth's atmosphere, am = 0. At other locations on the surface of the earth, the atmospheric path length can be estimated as $\text{am} = 1/(\sin \beta_1)$.

Many people have investigated the effect of atmospheric transmittance, particularly with respect to the effect of moisture, ozone, and dust particles. The intensity of the direct-normal irradiation, I_{DN}, in W/m^2, at the earth's surface on a clear day may be estimated from the following equation:

$$I_{DN} = A_S \exp \frac{-B_S}{\sin \beta_1} \tag{2.40}$$

In Eq. (2.39), A_S is the apparent extraterrestrial insolation (at am = 0) and B_S is the atmospheric extinction coefficient. The value of B_S depends on the time of year and the amount of water vapor present in the average atmosphere. Values of A_S and B_S are listed in App. M.

The local value of atmospheric moisture and the local elevation may be markedly different from that of the average atmosphere at sea level. The ratio of the clear-day direct insolation at a particular location to the value for the standard atmosphere at the same location and date is called the *clearness number.* The clearness numbers for various locations in the United States are shown in Fig. 2.19 along with the average daily solar insolation. The lines of equal insolation are called *isopleths.*

The diffuse-scattered solar component, I_{DS}, is difficult to calculate because of the nondirectional nature of the component, but for those surfaces that are exposed to direct solar radiation, it appears to be a linear function of the direct solar component. The diffuse-scattered solar insolation can be estimated from the following expression:

$$I_{DS} = C_S I_{DN} F_{SS} \tag{2.41}$$

where C_S is the ratio of the diffuse-scattered to direct solar radiation falling on a horizontal surface and F_{SS} is the radiation shape factor for radiation leaving the surface that "hits" the sky. The value of C_S is tabulated along with A_S and B_S in App. M and the shape factor F_{SS} can be approximated by:

$$F_{SS} = \frac{1 + \cos \beta_2}{2} \tag{2.42}$$

The reflected component of the solar insolation, I_R, depends on the geometry and the reflection characteristics of the surrounding surfaces. The amount of reflected radiation can be calculated using conventional radiation calculational

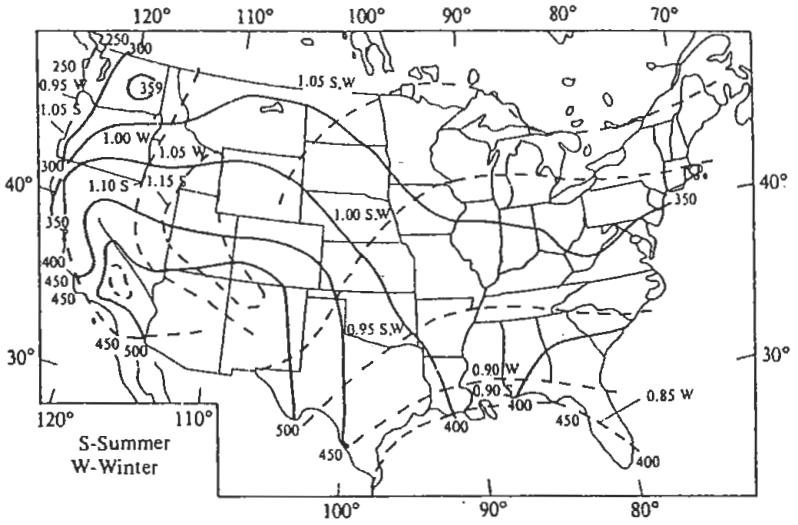


FIGURE 2.19
Clearness numbers for winter and summer in the United States (dashed lines) and the approximate average annual insolation (solid lines) in langleys per day. (*Reprinted with permission from the 1974 Applications Volume, ASHRAE, Handbook and Product Directory.*)

techniques. Except for special applications, I_R is not normally a major component in most solar-energy calculations.

The direct-normal insolation, I_{DN}, can be estimated from Eq. (2.40) or from the solar tables presented in App. O at the end of the book, as a function of the latitude, the time of year, and the apparent solar time.

The amount of solar energy absorbed by a given surface is equal to the product of the incident solar irradiation, I_{tot}, and the absorptivity or emissivity of the surface for the short wavelength solar radiation, ε_{SU}. The emissivity of a surface may be considerably different for solar radiation when compared to that for ordinary infrared thermal radiation because of the higher energy of the solar radiation. The emissivities for the high-energy solar radiation of some common surfaces are listed in Table 2.5 along with the emissivity values for ordinary infrared radiation.

An example of a significant difference between the values is given by flat, white paint. For ordinary radiation, the emissivity of flat, white paint ranges from 0.95 to 0.99 while the value for solar radiation ranges from 0.12 to 0.25. Thus, if one wants to reduce the solar heat load on a surface, paint it white.

Example 2.8. The southeast roof of a building is made of dirty galvanized iron and is inclined at an angle of 70° from the vertical. It is located at 38° N. Lat. and 67° W. Long. Evaluate the combined absorbed direct and diffuse-scattered solar energy flux at 9:00 a.m., local daylight savings time, on July 21.

TABLE 2.5
Solar emissivities

Materials	Infrared (low-temp.) radiation	Solar radiation
Building materials:		
Red brick, tile, concrete	0.85–0.95	0.65–0.77
Yellow and buff brick	0.85–0.95	0.50–0.70
Plaster	0.90–0.95	0.50–0.70
Asphalt pavement	0.90–0.95	0.82–0.88
Roofing materials:		
Asphalt	0.90–0.95	0.86–0.90
Galvanized iron, dirty	0.25–0.35	0.87–0.91
Galvanized iron, new	0.20–0.30	0.64–0.68
Roofing paper	0.85–0.95	0.85–0.90
Slate	0.90–0.98	0.85–0.95
Paints:		
Aluminum (bright), gilt	0.25–0.65	0.30–0.50
Black, flat	0.95–0.98	0.85–0.95
Dark (red, brown, green, etc.)	0.75–0.95	0.65–0.83
White, flat	0.95–0.99	0.12–0.25
Metals:		
Aluminum, nickel, chromium (polished)	0.02–0.10	0.10–0.40
Copper, brass, monel metal (polished)	0.02–0.15	0.30–0.50
Dull aluminum, brass, copper, and polished iron	0.20–0.50	0.40–0.65
Iron oxide	0.60–0.65	0.70–0.80

Solution. Given: $\beta_2 = 20°$; $\alpha_2 = -45°$; local time = 9:00 a.m., DST; $L = 38°$. From App. M: $A_S = 1085\ \text{W/m}^2$; $B_S = 0.206$; $C_S = 0.135$; $\delta = 23.1 + (7/10)(22.1 - 23.1) = 22.4°$ (by interpolation); equation of time $= -3.4 + (7/10)[-5.6 - (-3.4)] = -0{:}04.9$. From Table 2.5.: $\varepsilon_{SU} = 0.89$.

$$\text{Longitude of standard meridian} = \left(\frac{67}{15}\right)_{\text{round}} \cdot 15 = 4 \times 15 = 60°$$

Mean sun time = MST = 9:00 − 1:00 + 0:04(60 − 67) = 7:32 a.m.

$$\text{Apparent sun time} = \text{MST} + \text{equation of time} = 7{:}32 + (-0{:}04.9)$$

$$= 7{:}27.1 \text{ a.m.}$$

$$\text{Time sun is due east} = t_E = \frac{180 - \cos^{-1}(\tan 22.4/\tan 38)}{15}$$

$$= 8{:}07.3 \text{ a.m., AST}$$

Since t_E is later than the apparent sun time, $|\alpha_1| = 180 - |\alpha_{1,c}|$.

$$\text{Hour angle} = \text{H} = 0.25[7(60) + 27.1 - 720] = -68.23°$$

$$\sin \beta_1 = (\cos L)(\cos \delta)(\cos \text{H}) + (\sin L)(\sin \delta)$$

$$= (\cos 38)(\cos 22.4)(\cos -68.23) + (\sin 38)(\sin 22.4)$$

$$= 0.5049$$

$$\beta_1 = \sin^{-1} 0.5049 = 30.32°$$

$$\alpha_{1,c} = \sin^{-1} \frac{(\cos \delta)(\sin H)}{\cos \beta_1)}$$

$$= \sin^{-1} \frac{(\cos 22.4)(\sin -68.23)}{\cos 30.32} = -84.07°$$

$$|\alpha_1| = 180 - |\alpha_{1,c}| = 180 - 84.07 = 95.93°$$

$$\alpha_1 = -95.93°$$

$$\cos \theta = (\sin \beta_1)(\cos \beta_2) + (\cos \beta_1)(\sin \beta_2)[\cos (\alpha_1 - \alpha_2)]$$

$$= (\sin 30.32)(\cos 20) + (\cos 30.32)(\sin 20)[\cos (-95.93 + 45)]$$

$$= 0.6605$$

$$I_{\text{DN}} = A_S \exp \frac{-B_S}{\sin \beta_1} = 1085 \exp \frac{-0.206}{\sin 30.32}$$

$$= 721.5 \text{ W/m}^2$$

$$F_{\text{SS}} = \frac{1 + \cos \beta_2}{2} = \frac{1 + \cos 20}{2} = 0.9698$$

$$I_{\text{tot}} = I_{\text{DN}}(\cos \theta + C_S F_{\text{SS}}) = 721.5[0.6605 + 0.135(0.9698)]$$

$$= 571.02 \text{ W/m}^2$$

$$\text{Absorbed solar energy flux} = \varepsilon_{\text{SU}} I_{\text{tot}} = 0.89(571.02) = 508.2 \text{ W/m}^2$$

$$= (508.2)(0.3173) = 161.25 \text{ Btu/h} \cdot \text{ft}^2$$

The calculational method presented in this section permits the estimation of the incident solar radiation on a surface on a clear day at any time of the year. To obtain the amount of solar energy falling on a surface for a day, in kJ/m^2, kWh/m^2, or Btu/ft^2, the equations presented earlier would have to be programmed on a digital computer for a given time interval and summed over the period of interest.

The number of clear days available at a given location can be estimated from data compiled by the U.S. Weather Bureau, now titled the National Oceanographic and Atmospheric Administration (NOAA). Maps of the average monthly and average annual percentage of possible sunshine along with other atmospheric and weather data are presented in the *Climatic Atlas of the United States.*

2.5.3 Solar Collection Systems

GENERAL. Solar-energy collection systems can normally be divided into three general categories: the solar-cell conversion systems that produce dc electricity directly from the electromagnetic energy of the sun, those systems that produce low-temperature (less than 150°F) thermal energy for the heating and cooling of buildings; and, finally concentrating solar collection systems that produce high-temperature thermal energy for the generation of electrical energy.

For temperatures above 150°F (65°C), some form of solar concentration must be attained. The degree of concentration required to obtain a given temperature can be estimated from Fig. 2.20. The solar energy can be concentrated with the use of either parabolic mirrors, with an array of focused mirrors, or with the use of concentrating lens such as the Fresnel lens. One of the earliest concentrating mirror systems in the world was the large solar furnace constructed at Odeillo, France. This system uses a system of large parabolic mirrors to obtain temperatures in the thousands of degrees Celcius at the focal point of the mirrors.

SOLAR SYSTEMS FOR SPACE AND WATER HEATING. The low-temperature solar heating-cooling systems normally employ a glass or plastic covered flat-plate collector. The glass or plastic layer or layers effectively "trap" the solar radiation by letting the short-wavelength solar radiation into the collector but not letting the long-wavelength reradiated energy from the absorber to escape. The thermal

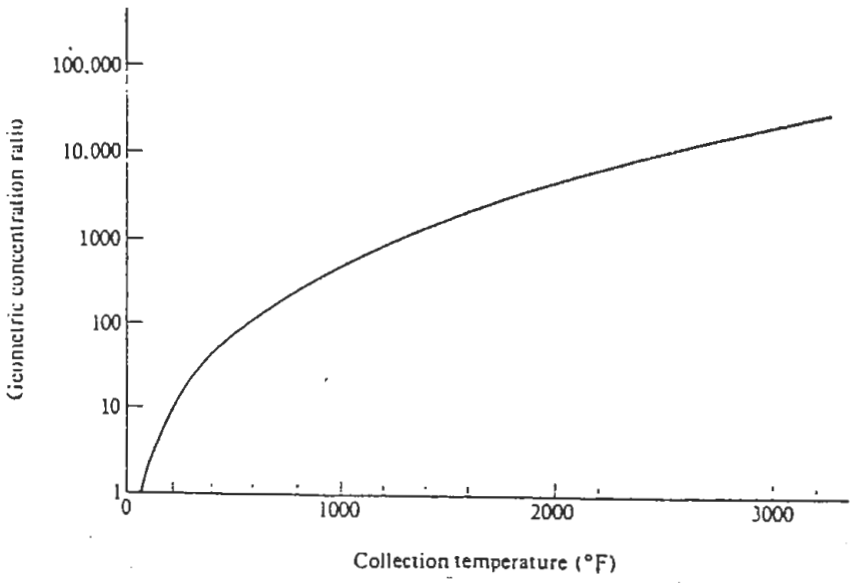


FIGURE 2.20
The approximate geometric concentration required for a desired temperature from a high-performance solar collector.

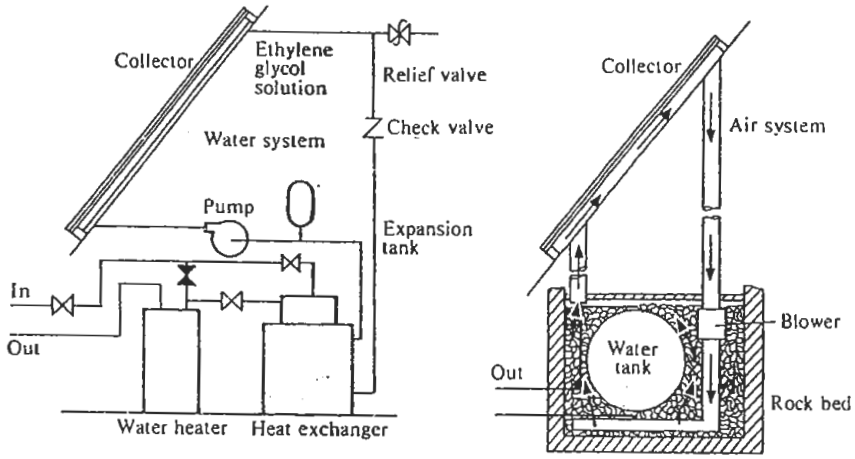


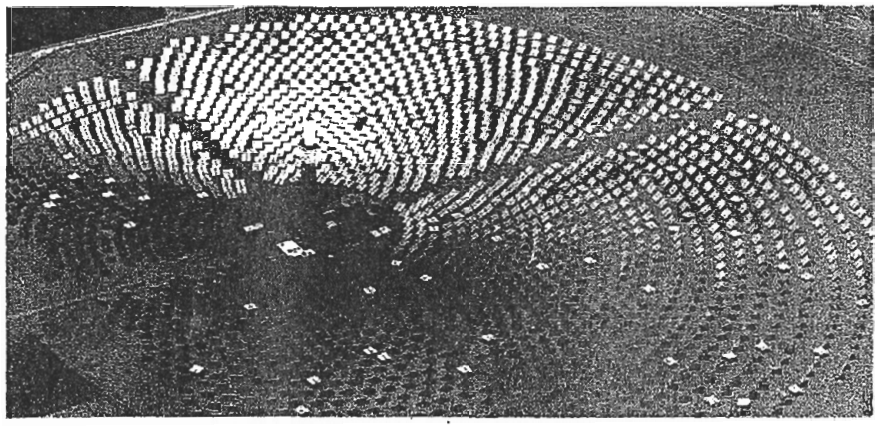
FIGURE 2.21
Typical flat-plate solar collection systems.

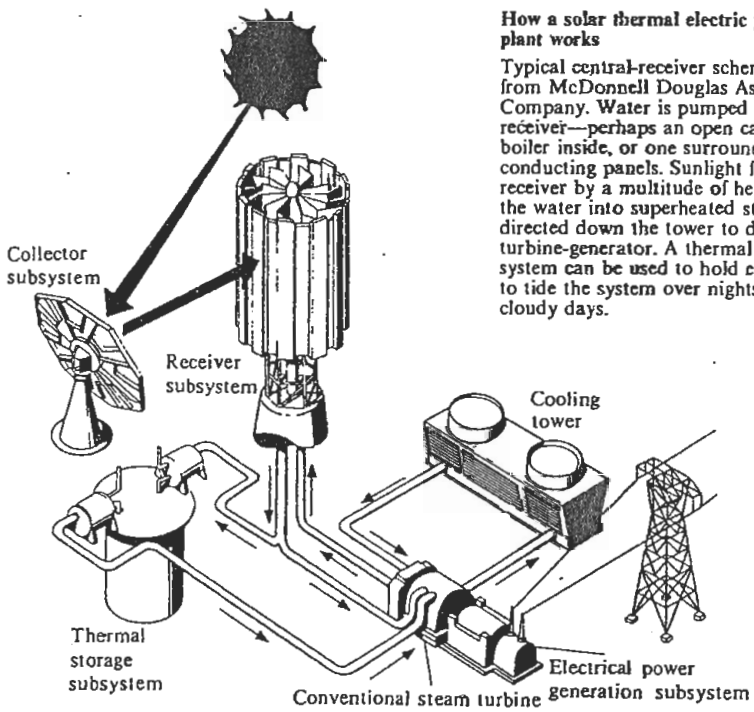
energy generated in the collector is usually removed by either air or an ethylene glycol-water solution. Most flat-plate collectors are similar in appearance and also similar in operation to the two schematics shown in Fig. 2.21.

SOLAR SYSTEMS FOR THE PRODUCTION OF ELECTRICITY. One of the larger solar systems for the production of electricity is Solar I, a 10-mW_e solar power station operating near Barstow, California. This is a "solar-power-tower" plant. It consists of a large array of mirrors called *heliostats* that track the sun and focus the solar radiation on a water-cooled receiver mounted on top of a 300-ft (91-m) tower. The system also employs an oil-sand storage reservoir to provide electrical power for 3 to 4 h after sunset. The total cost of Solar I was $140,000,000 or $14,000 per installed kW. A picture and schematic of the solar-power-tower system is shown in Fig. 2.22.

It is hoped that the capital cost can be significantly reduced in the next unit. In fact, the operating utility, Southern California Edison, is planning to build a 100-kW_e solar power tower with a minimum of government support. However, even if the capital costs can be reduced by a factor of 5 so that they are equivalent to those of a nuclear plant, the costs per kWh will still be higher because of the lower capacity factor. This is partially offset by a zero fuel cost.

A relatively new concept for the conversion of solar energy into electricity is the *solar salt pond.* This concept is sort of a small-scale, inverse OTEC system. In this system, a shallow (1- to 2-m-deep) pond saturated with a salt is used as the primary solar collector. As the surface waters of the pond are heated by the solar radiation, the solubility of this warm water increases and the solution becomes heavier as it absorbs more salt. This causes the hot water to sink to the bottom of the pond. Consequently, the bottom of the pond becomes very hot,





How a solar thermal electric power plant works

Typical central-receiver scheme is this one from McDonnell Douglas Astronautics Company. Water is pumped up into the receiver—perhaps an open cavity with a boiler inside, or one surrounded by heat-conducting panels. Sunlight focused on the receiver by a multitude of heliostats turns the water into superheated steam, which is directed down the tower to drive a steam turbine-generator. A thermal storage system can be used to hold enough heat to tide the system over nights and cloudy days.

FIGURE 2.22
The "Solar Power Tower," a proposed solar-electrical generation system.

from 150 to 180°F, (65 to 82°C) while the surface remains at something below 100°F (38°C).

The hot water from the bottom of the pond is then pumped through a boiler, where it boils a low boiling point working fluid in a Rankine power cycle. The cooler water from the surface of the pond is then used to cool the turbine exhaust vapor in the condenser. This is the same concept that is employed in the OTEC system, except that in the OTEC system the surface waters are warmer.

The principal advantage of this solar system is that the pond serves as both a relatively inexpensive collector and a storage medium. The main problems with this conversion system are the mixing of pond water by the wind, the relatively low value of thermal efficiency, the difficulty of finding suitable locations for the plant, and the problem of fouling of the boiler heat-transfer surfaces when the saturated salt solution is cooled. The mixing problem can be alleviated with the installation of horizontal curtains in the pond to keep the water segregated.

There have been two small (less than 100-kW_e) solar-salt-pond power systems built in the vicinity of the dead sea in Israel. A schematic diagram of this system is shown in Fig. 2.23.

One of the more ambitious solar energy projects has been proposed by Dr. Peter Glaser and involves the use of a large earth satellite in geosynchronous orbit of 35,890 km (22,300 mi) to intercept and convert the solar energy. The satellite (see Fig. 2.24) is composed of a large array of solar cells which converts the electromagnetic energy of the sun into electricity. This energy is then converted

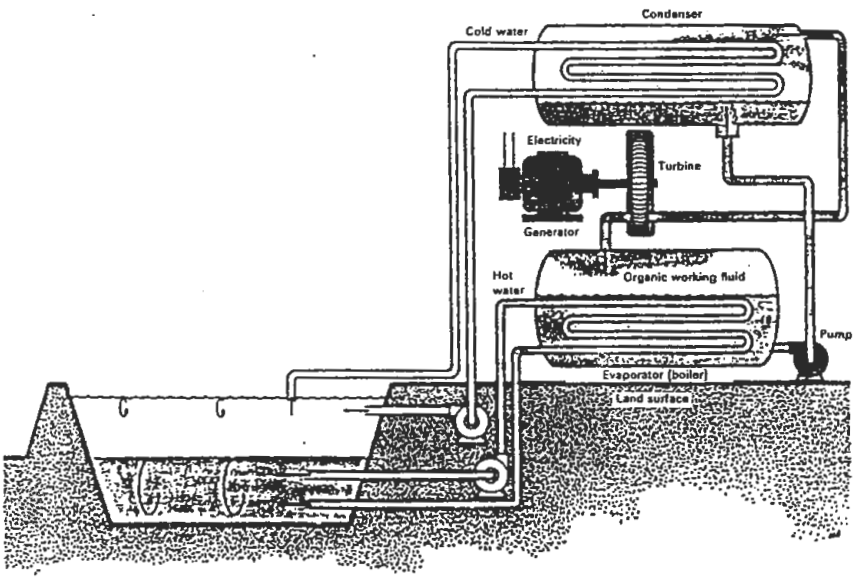


FIGURE 2.23
The solar-salt-pond electrical power system.

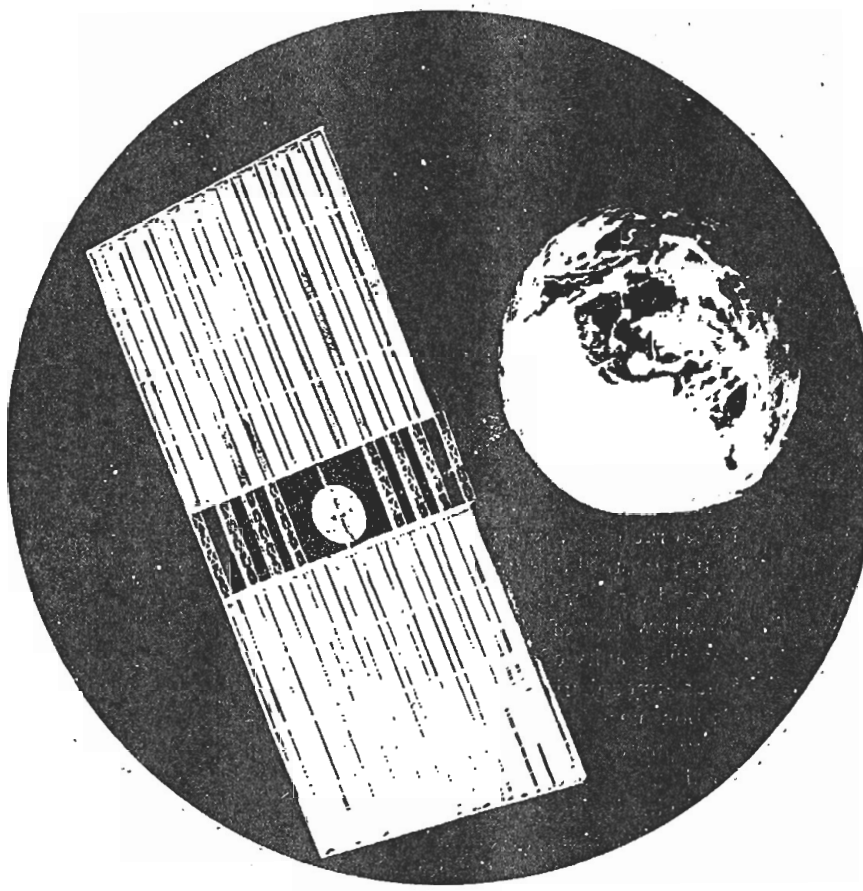


FIGURE 2.24
The proposed solar satellite power system (SSPS) for the generation of electricity. (*From Mechanical Engineering, vol. 100, no. 1, January 1978.*)

into microwave energy so that it can be beamed to an earth receiving station where it is transformed back into dc electricity.

One of the major advantages of this solar-powered satellite system (SPSS) is that it receives an almost constant supply of solar energy except for a few hours on several days around the equinox when the satellite passes through the earth's shadow for a few hours each day. It also receives a significantly higher energy flux than a comparable terrestrial system since there is no atmospheric attenuation.

In a proposed 5000-mW_e SPSS, a satellite with a solar-cell surface area of about 50 km^2 (about 7 mi by 4 mi) would transmit the microwave radiation through a 1-km (0.62-mi) transmitting antenna to a terrestrial receiving antenna 7 km (4.3 mi) in diameter. After an initial solar-electrical conversion efficiency

of 15 to 20 percent in the solar cells, the transmission efficiency and subsequent electrical conversion would be 55 to 70 percent. The microwave energy received at the earth station would be converted into 40,000 V dc, and fed into a conventional transmission system.

The satellite power plant (SPSS) does not appear to be a viable contender for the near-term production of electrical energy because of high cost (in the tens of billions of dollars) and because of the many technical and political problems associated with it. However, as the cost of electricity continues to rise and as the cost of putting materials into orbit decreases, the SPSS may become a reality.

LIST OF SYMBOLS

am	Standard atmospheric air mass
A	Activity of a radioisotope, Bq
A	Ash mass fraction in a coal, kg ash/kg coal
A	Atomic mass number = number of nucleons in the nucleus
°API	Specific gravity of a liquid in degrees API (American Petroleum Institute)
A_0	Initial radioactivity (at $t = 0$), Bq
A_S	Extraterrestrial direct normal solar insolation, W/m^2
AV	Avogadro's number, 6.022×10^{26} molecules/kg · mol
AW	Atomic weight of an element, kg/kg · mol
°Bé	Specific gravity of a liquid in degrees Baumé
B_S	Solar atmospheric attenuation coefficient, am
C	Carbon mass fraction in a fuel, kg carbon/kg fuel
C_S	Fraction of direct solar energy that is diffuse-scattered radiation
E	Total energy, J or MeV
E_{KE}	Total kinetic energy, J or MeV
E_γ	Gamma ray energy, J or MeV
f	Isotopic abundance = fraction of atoms of an element that are atoms of the isotope of interest (less than or equal to unity)
F_{SS}	Radiation shape factor from the surface to the sky
FC	Mass fraction of fixed carbon in the coal
FP	Fission product
H	Hour angle for solar calculations, degrees
H_2	Hydrogen mass fraction in a fuel, kg hydrogen/kg fuel
HHV	Higher heating value of a fuel, kJ/kg or kJ/m^3
HHV_m	Gravimetric higher heating value of a fuel, kJ/kg
HHV_v	Volumetric higher heating value of a fuel, kJ/m^3
I	Solar insolation on a surface, W/m^2
I_D	Direct solar insolation on a surface, W/m^2
I_{DN}	Direct-normal insolation on a surface = direct solar insolation on a surface normal to the sun's rays, W/m^2
I_{DS}	Diffuse-scattered component of the total solar insolation, W/m^2

I_R	Reflected component of the total solar insolation, W/m^2
I_{tot}	Total direct and diffuse-scattered solar insolation, W/m^2
KE	Kinetic energy, J
L	Latitude angle for solar calculations = local latitude in degrees
LHV	Lower heating value of a fuel, kJ/kg
m	Mass of light-mass product from radioactive decay process, kg
m_C	Mass of compound containing the radioisotope, kg
m_e	Mass of an electron = 0.000549 amu = 9.115×10^{-31} kg
$m_{H\text{-}1}$	Mass of a hydrogen-1 atom = 1.007825 amu = 1.673×10^{-27} kg
m_n	Mass of a neutron = 1.008665 amu = 1.675×10^{-27} kg
m_p	Mass of a proton = 1.007276 amu = 1.672×10^{-27} kg
m_R	Mass of a certain radioisotope, kg
M	Mass of heavy-mass product from radioactive decay process, kg
M	Mass fraction of water in the fuel, kg water/kg fuel
Mm	Mass fraction of mineral matter in a coal, kg mineral matter/kg coal
MW	Molecular or atomic weight of a compound or element, kg/kg · mol
n	Number of atoms of an element per molecule
n	Number of carbon atoms in a hydrocarbon compound
N	Total number of atoms of a particular isotope in a material
N_0	Initial number of atoms present at $t = 0$
N_O	Number of original fuel atoms "burned" in a fission reactor
N_2	Mass fraction of nitrogen in a fuel, kg nitrogen/kg fuel
O_2	Mass fraction of oxygen in a fuel, kg oxygen/kg fuel
p	Absolute pressure, kPa
p_r	Reference pressure (usually 1 atm) = 101.325 kPa
P	Power, W
P_0	Initial power of a system at $t = 0$, W
P_O	Constant operating power of a nuclear reactor, W
P_S	Shutdown power in a nuclear reactor, W
r	Conversion or breeding ratio for a nuclear reactor
s	Specific gravity of a liquid, (liquid density)/(density of water at 60°F)
S	Mass fraction of sulfur in a fuel, kg sulfur/kg fuel
SP	Specific power in a certain fuel, W/kg
t	Time, s
t_{ave}	Average lifetime of a radioisotope, s
t_O	Time of constant power operation for a nuclear reactor, s
t_S	Time following reactor shutdown, s
$t_{1/2}$	Half-life of a radioisotope, s
T	Temperature, °C or K
T_r	Reference temperature (usually 20°C or 293.15 K), K
u	Velocity of light-mass product from radioactive decay, m/s
U	Velocity of heavy-mass product from radioactive decay, m/s
v	Specific volume of a gas, m^3/kg
V	Total volume, m^3
Z_i	Moles of the ith element per mole of fuel

α	Alpha particle = helium-4 nucleus = ${}_2^4\alpha$
α_1	Azimuth angle of the sun's rays, degrees
α_2	Azimuth angle of the normal to the surface, degrees
β	Beta particle = electron = ${}_{-1}^{0}\beta$
β_1	Altitude angle of the sun's rays, degrees
β_2	Tilt angle of the surface, degrees
γ	Gamma radiation
γ_a	Gamma radiation from the annihilation reaction
γ_c	Gamma radiation from the radiative-capture neutron reaction
γ_d	Gamma radiation from the radioactive decay process
γ_f	Gamma radiation from the fission neutron reaction
δ	Angle of declination, degrees
ε_{SU}	Emissivity (absorptivity) of surface for solar radiation
λ	Decay constant, s^{-1}
ν	Neutrino
θ	Angle between the sun's rays and the normal to the surface, degrees

PROBLEMS

2.1. Estimate the as-burned ultimate analysis for the following coals, evaluate the percentage error incurred in estimating the higher heating value (HHV) with Dulong's formula, find the lower heating value (LHV), and rank the coals according to the ASTM classification system.

(*a*) Luzerne County, Pennsylvania, coal with $M = [2; 4; 6]$ percent and $A = [6; 11; 16]$ percent

(*b*) Coal County, Oklahoma, coal with $M = [5; 6; 7]$ percent and $A = [9; 10.5; 12]$ percent

(*c*) Custer County, Montana, coal with $M = [27; 28.5; 30]$ percent and $A = [3; 9; 15]$ percent

(*d*) Stark County, North Dakota, coal with $M = [35; 39; 43]$ percent and $A = [5; 8.5; 12]$ percent

(*e*) Wyoming County, West Virginia, coal with $M = [2; 3; 4]$ percent and $A = [3; 4.5; 6]$ percent

(*f*) Logan County, Arkansas, coal with $M = [2; 3; 4]$ percent and $A = [6; 9; 12]$ percent

2.2. A sample of coal weighs 25 kg at the time it is collected. When the sample is tested, it is found that the weight has dropped to [24.6; 24.2; 23.8; 23.4; 23.0] kg as the result of moisture loss. A proximate coal analysis is then made with the following result: VM = 35.7 percent, FC = 41.5 percent, $M = 11.6$ percent, $A = 11.2$ percent, S = 4.0 percent, and the HHV = [25,700; 25,800; 25,900; 26,000; 26,100] kJ/kg. Compute the as-collected proximate coal analysis. Determine the ASTM classification of the coal. Make an empirical calculation of the ultimate coal analysis using the method presented in App. F.

2.3. A 14-kg coal sample, as received, weighs [13.6; 13.4; 13.2; 13.0; 12.8] kg after air drying. When oven-dried, a 5-g sample of the air-dried coal is reduced to a weight of [4.94; 4.90; 4.86; 4.82; 4.78] g. Find the total moisture percentage in the as-received coal.

2.4. A [1.0; 1.1; 1.2; 1.3; 1.4]-g sample of coal is burned in an oxygen-bomb calorimeter. The temperature rise of 2000 g of water and the calorimeter metal is [3.54; 3.58; 3.62; 3.66; 3.70]°C, of which 0.20°C is due to the fuse wire and acid formation. The water equivalent of the metal parts of the calorimeter is 450 g. Determine the higher heating value of the coal in kJ/kg and in Btu/lbm.

2.5. A fuel oil has an API gravity of [24; 28; 32; 36; 40] °API at 20°C. Compute the energy, in Btu/gal of fuel oil, and the higher heating value, in kJ/kg. Calculate the same quantities at [40; 50; 60; 70; 80]°C, if $\rho_T = \rho_{20}[1 - 0.00073(T - 20)]$, where T is in °C and ρ is the liquid density.

2.6. A certain No. 2 fuel oil has a API gravity of [32; 33; 34; 35; 36]°API, while a certain No. 5 fuel oil has a specific gravity of [16; 17; 18; 19; 20] °API. Calculate the gravimetric (in Btu/lbm) and the volumetric higher heating value, in kJ/m^3, of the fuel oils.

2.7. If the price of a 42-gal barrel of [Texas No. 1; Texas No. 2; California] crude oil is [14; 20; 26; 32; 38; 44] dollars a barrel, find the cost of energy in dollars/million Btu. Also, estimate the cost of 70°API gasoline and the cost of Nos. 2 and 6 fuel oils, in dollars/million Btu and in cents/gal, assuming that the cost of the crude oil, in dollars/million Btu, is the same as that for No. 4 fuel oil.

2.8. If the price of 70°API gasoline is [90; 100; 110; 120; 130] cents/gal, find the cost of Nos. 1 and 5 fuel oils, propane, and butane, in dollars/million Btu and in cents/gal.

2.9. A gas storage tank of 25,000 ft^3 contains gas at a pressure of [0.1; 0.15; 0.2; 0.25; 0.3] MPa at a temperature of [10; 15; 20; 25; 30] °C. The higher heating value of the gas is 22,100 kJ/m^3 at 20°C and 1 atm. Find the number of therms of energy in the tank.

2.10. For [Missouri; Arkansas; Illinois; Kansas; West Virginia] natural gas, find the theoretical volumetric heating value of the gas, in kJ/m^3 at 20°C and 1 atm. Using this calculated value, find the HHV in kJ/kg and in Btu/ft^3 if the gas is supplied at 0.3 MPa and [10; 15; 20; 25; 30] °C. Determine the volume of the gas at this condition needed to supply 1000 therms of energy. Also, evaluate the mass fraction of each of the chemical elements in the fuel gas (an ultimate analysis of the fuel).

2.11. Repeat Prob. 2.10 for a producer gas with the following composition: 3.8 percent CH_4, 0.1 percent C_2H_6, 4.8 percent CO_2, 11.7 percent H_2, 0.6 percent O_2, and [23.2; 23.6; 24.0; 24.4; 24.8; 25.2] percent CO, with the balance being nitrogen.

2.12. Repeat Prob. 2.10 for a carbureted water gas with the following composition: 35.0 percent H_2, 2.0 percent N_2, 1.0 percent CO_2, 15.0 percent CH_4, and [9; 11; 13; 15; 17] percent C_2H_4 with the balance being carbon monoxide.

2.13. Repeat Prob. 2.10 for a liquified petroleum gas composed of [30; 40; 50; 60; 70] percent propane and the balance butane.

2.14. Find the maximum kinetic energy of emitted particle and that of the residual nucleus from the radioactive decay of [scandium-46 (0.889 MeV); scandium-47 (0.159 MeV); scandium-48 (1.312 MeV); arsenic-76 (0.559 MeV); arsenic-77 (0.239 MeV); arsenic-78 (0.614 MeV); yttrium-90 (1.761 MeV); yttrium-91 (1.205 MeV); yttrium-92 (0.936 MeV)]. The energy quantities in parentheses are the amounts of gamma ray energy (γ_d) emitted in each of the decay processes. If 1 tonne of the isotope was present when the earth was formed 4.5 billion years ago, either determine the number of atoms existing at this time (if greater than 10^{10} atoms) or determine how many years it took for the number of atoms to drop to 10^{10}.

2.15. Repeat Prob. 2.14 for the following alpha-emitting radioisotopes: [uranium-233 (0.043 MeV); uranium-234 (0.053 MeV); uranium-235 (0.186 MeV) uranium-236 (0.049 MeV); plutonium-239 (0.052 MeV); plutonium-240 (0.045 MeV); plutonium-242 (0.044 MeV); plutonium-244 (0.085 MeV); californium-245 (0.0174 MeV); californium-246 (0.089 MeV)]. As in the previous problem, the energy quantities in parentheses are the amount of gamma ray energy emitted in each of the decay processes.

2.16. Radioactive carbon-14 (radiocarbon) is used to estimate the age of materials composed of organic carbon. It is formed by an (n, p) reaction between the nitrogen atoms in the upper atmosphere and high-energy neutrons (part of the cosmic radiation) that bombard the earth. Living organic material absorbs and uses carbon dioxide from the atmosphere which contains about 1 percent $^{14}CO_2$. When the organism dies, the ratio of C-14 to C-12 decreases with time as the radiocarbon decays. If the proportion of C-14 to stable carbon in an old manuscript is found to be [0.6; 0.65; 0.7; 0.75; 0.8; 0.85; 0.9; 0.95] percent, determine the age of the manuscript, assuming the atmospheric bombardment of high-energy neutrons is constant.

2.17. Rutherford proposed that when the earth was first formed, it contained equal amounts of U-235 and U-238. There are now 137.88 atoms of U-238 for each atom of U-235. Estimate the age of the earth using Rutherford's hypothesis. Also, determine the ratio of U-238 atoms to U-235 atoms at [10^7 B.C.; 5×10^7 B.C.; 10^8 B.C.; 5×10^8 B.C.; 10^9 B.C.; 2×10^9 B.C.; 3×10^9 B.C.; 4×10^9 B.C.; 4.5×10^9 B.C.; 5.0×10^9 B.C.; 5.5×10^9 B.C.].

2.18. A rock returned from the surface of the moon has a ratio of Rb-87 to Sr-87 atoms of 14.45. The Sr-87 is produced as the result of beta decay of the Rb-87. Assuming that all of the Sr-87 was Rb-87 when the solar system was formed, estimate the age of the solar system. Also, determine the value of the Rb-87/Sr-87 ratio at [10^8 B.C.; 5×10^8 B.C.; 10^9 B.C.; 2×10^9 B.C.; 3×10^9 B.C.; 4×10^9 B.C.; 4.5×10^9 B.C.].

2.19. The uranium-234 isotope appears in nature only because it is in the uranium-238 decay chain as U-238 decays to Pb-206. There are a total of 14 radioisotopes in the U-238 decay chain. Find the ratio of [Pa-234; U-234; Th-230; Ra-226; Rn-222; Po-218] to U-238. Assume that all the intermediate radioisotopes are in "secular equilibrium," which means that the number of atoms of each of the products is constant. For the U-234 isotope, this means that $d(\text{U-234})/dt = 0$, and is also equal to $d(\text{U-238})/dt$.

2.20. A sample of radioactive material is composed of two independent radioisotopes—a long-lived radioisotope and a short-lived radioisotope. A geiger counter, whose output is directly proportional to the total activity of the sample, gave the following results:

Time, h	0	10	20	30	40	60	90	120	180	240	360
Activity, Bq:											
Sample A	5500	3883	2778	2020	1500	892	510	364	255	199	125
Sample B	4850	2877	1761	1113	734	380	210	152	95	61	26
Sample C	9000	3818	1703	837	472	231	139	95	47	23	5

Plot the data for a particular sample on semilog graph paper and determine the half-life of each of the two radioisotopes. Assume that the half-life of one of the isotopes is much longer than the other. If the total initial activity of the mixture is 1 Ci, calculate the number of radioactive atoms of the short and the long-lived radioisotopes at $t = 0$ and at the end of [20; 30; 40; 60; 90; 120] h.

Hint: Assume that all of the activity at long times is due to the long-lived radioisotope and establish the activity of that isotope by drawing a straight line through the last two or three data points. Subtract the short-time activities from this line from the total activity at the corresponding times and plot this difference. This difference should be a straight line and should correspond to the activity of the short-lived radioisotope.

2.21. It is desired to produce a Pu-238-fueled radioisotope power source which will supply a minimum of 100 W_e for a [10; 15; 20; 25; 30]-year period from a thermoelectric generator with a thermal efficiency of 8 percent. Find the initial mass of PuN (74.6 percent Pu-238) required and the volume, in cm^3, required to limit the maximum helium gas pressure to [5; 10; 15; 20; 25] MPa at 300°C. Assume that all the Pu-238 decays to Pb-206.

2.22. A certain radioisotope-powered generator is fueled with Cm_2O_3 (Cm-244 fuel) and is designed to provide a thermal power of [5; 10; 15; 20; 25] kW_{th} for [8; 10; 12; 14; 16] years. Find the minimum mass of Cm_2O_3 required and the maximum mass of helium gas generated in the source.

2.23. It is desired to build a radioisotope-powered thermoelectric generator with a thermal efficiency of 7 percent which will provide at least 50 W_e for a period of [8; 11; 14; 17; 20] years and a minimum of 300 W_e for a period of [100; 120; 140; 160; 180] days. The source will utilize PuC (74.6 percent Pu-238) for the long-term power requirement and GdPo-Ta (98 percent) for the short-term power requirement. Determine the minimum mass of each fuel material that should be loaded into the generator to meet the power criteria. Also, determine the amount of thermal power that must be "dumped" initially and calculate the volume, in cm^3, required to limit the maximum helium gas pressure to 20 MPa at 300°C. Both Pu-238 and Po-210 eventually decay to Pb-206.

2.24. Calculate the energy equivalent, in MW · days, from the U-235 that can be recovered from 1 tonne of natural uranium ore. The ore contains [0.3; 0.4; 0.5; 0.6; 0.7]% U_3O_8 by weight and 80 percent of this compound can be extracted from the ore in the refining process. Assume that [30; 40; 50; 60; 70] percent of the U-235 atoms can be fissioned to produce thermal energy.

2.25. In the gaseous diffusion process, the separation factor for each stage of diffusion is equal to the square root of the ratio of the molecular weights of the UF_6 molecule. Using the equations in Fig. 2.11, determine the number of stages required to produce [1; 2; 3; 4; 5; 10; 20; 40; 60; 80; 93.8]% enriched uranium and assume that the balance is U-238.

2.26. Find the energy release, in thermal MW · days, resulting from the complete fissioning of all the atoms in 1 g of [U-233; U-235; Pu-239]. Assume that 200 MeV of energy is released in each fission reaction. Also calculate the electrical energy, in kWh, resulting from the complete fissioning of 1 g of U-235 if the conversion efficiency is [32; 35; 38] percent and [20; 30; 40] percent of the U-235 atoms undergo fission.

2.27. Determine the percent of U-235 atoms fissioned in 1 tonne of UO_2 if the thermal-energy burnup is [10,000; 20,000; 40,000; 60,000; 80,000] MW · days/tonne if the uranium is fully enriched.

2.28. A [U-233; U-235; Pu-239] nucleus absorbs a neutron and forms an excited compound nucleus. If the excited compound nucleus fissions and eventually produces [Ba-135; La-139; Sm-149], [2; 3] neutrons, another stable fission product, and several beta particles, determine the energy released if the excited compound nucleus goes to the ground state with the emission of one or more capture-gamma rays (γ_c) in the radiative-capture reaction. Also, calculate the average binding energy per nucleon for the ground state of the compound nucleus.

2.29. A given power reactor operates at a power level of 2000 MW_{th} for 100 days when the power is increased to 3800 MW_{th} for a period of [100; 150; 200; 250; 300] days when the reactor is shut down for refueling. Calculate the thermal power of the reactor for shutdown times of [30 s; 1 min; 30 min; 1 h; 1 day; 1 week; 2 weeks; 30 days; 1 year; 2 years].

2.30. A power reactor operates for 180 days at a constant power of 3800 MW_{th}. During the next 90 days, the power is lowered to [1000; 1400; 1800; 2200; 2600] MW_{th}. At the end of this time, the power is increased to 3800 MW_{th} and held constant for the next 30 days. Find the reactor shutdown power at the end of [30 s; 1 min; 30 min; 1 h; 1 day; 1 week; 2 weeks; 30 days; 1 year; 2 years].

2.31. A 1200-MW_e reactor operates with a thermal efficiency of [32; 34; 36; 38; 40] percent and a capacity factor of [60; 65; 70; 75; 80] percent for 1 year. During this time, find:
   (*a*) The mass of U-235 consumed in the fission process
   (*b*) The mass of fission products produced if 2.5 neutrons and 200 MeV of energy are produced in the fission process
   (*c*) The mass of deuterium and tritium consumed in the D-T reaction if the reactor is a fusion reactor
   (*d*) The mass of boron-11 and hydrogen-1 consumed in the "thermonuclear fusion" reaction.

2.32. Find the energy release, in MW_e · years, that can be produced from the atoms of deuterium in 1 mi^3 of water if [20; 40; 60; 80; 100] percent of the atoms can be consumed in the D-T fusion reactor which has a heat rate of [8400; 8800; 9200; 9600; 10,000] Btu/kWh.

2.33. If the price of raw fuel energy is \$1/million Btu, find the value of the following fuels, in dollars/lbm:
   (*a*) Vermillion County, Indiana, coal with M = [10; 12; 14] percent and A = [6; 9; 12] percent.
   (*b*) Natural uranium oxide (U_3O_8) assuming that [80; 70; 60; 50; 40; 30; 20] percent of the U-235 atoms and [3; 6; 9] percent of the U-238 atoms can be utilized in fission.
   (*c*) Number 2 fuel oil with a hydrogen mass fraction of 12.5 percent, assuming that [90; 80; 70; 60; 50; 40; 30; 20] percent of all the deuterium atoms can be "burned" in the four fusion reactions involving deuterium. Assume that all of the D reactions (a total of four reactions involving six D atoms) "go" with equal probability.
   (*d*) Borax ($Na_2B_4O_7$) assuming that [80; 70; 60; 50; 40; 30; 20] percent of the B-11 atoms in the borax can be utilized in the "thermonuclear fission" reaction.

2.34. Find the apparent solar times and the hour angles for the tenth day of [June; August; October; December] at [8 a.m.; 10 a.m.; 12 noon; 2 p.m.; 4 p.m.] for the following locations:
(*a*) 72 degrees [East; West] longitude
(*b*) 88 degrees [East; West] longitude
(*c*) 102 degrees [East; West] longitude
(*d*) 124 degrees [East; West] longitude
(*e*) 155 degrees [East; West] longitude
All times in June, August, and October are daylight savings time.

2.35. Calculate the sun's altitude and azimuth angles at [10; 20; 30; 40; 50] degrees [North; South] latitude at [7; 8; 9; 10; 11] a.m., apparent sun time, on July 21.

2.36. For the location and time designated in Prob. 2.35, find the angle of incidence, θ, for a surface that "faces" east-southeast and is inclined at:
(*a*) 0° (horizontal surface)
(*b*) angles of [20; 40; 60; 80]° from the horizontal
(*c*) 90° (vertical surface)

2.37. The southeast roof of a building is covered with roofing paper and is inclined at an angle of [0; 10; 20; 30; 40]° from the horizontal. It is located at [30; 34; 38; 42; 46] degrees North Latitude and 82 degrees West longitude. Calculate the absorbed direct and diffuse-scattered solar energy flux, in W/m^2, at 9:00 a.m. local standard time on February 10, if the sky is clear.

2.38. Repeat Prob. 2.37, for 82 degrees East longitude.

2.39. Repeat Prob. 2.37, for the same latitudes in the Southern Hemisphere. Use values of B_S and C_S 6 months earlier or later than indicated in the problem.

2.40. Repeat Prob. 2.37 for the east longitude of 2.38 and the southern latitudes of 2.39.

2.41. The west wall of a red-brick building is located at 35 degrees North latitude and [120; 117; 114; 111; 108] degrees West longitude. Evaluate the combined absorbed direct and diffuse-scattered solar energy flux at 6:00 p.m. daylight savings time on [May; June; August; September; October] 15, if the sky is clear.

2.42. Repeat Prob. 2.41. for eastern longitudes.

2.43. Repeat Prob. 2.41, for 35 degrees South latitude. Use values of B_S and C_S 6 months earlier or later than indicated in the problem. Take the time to be 4:00 p.m., local standard time.

2.44. A certain solar collector "tracks" the sun so that the collector surface is always perpendicular to the sun's rays. The collector is located at [10; 20; 30; 40; 50] degrees North latitude and [73; 78; 83; 88; 93] degrees West longitude. Find the tilt and azimuth angles of the surface and determine the combined direct and diffuse-scattered solar insolation at 9:00 a.m., local standard time on May 10, if the sky is clear.

2.45. Repeat Prob. 2.44. for eastern longitudes.

2.46. Repeat Prob. 2.44. for southern latitudes. Use values of B_S and C_S 6 months earlier or later than indicated in the problem.

REFERENCES

ASHRAE: *Handbook of Fundamentals*, American Society of Heating, Refrigeration, and Air Conditioning Engineers, New York, 1974.

Also Available from McGraw-Hill

Schaum's Outline Series in Mechanical Engineering

Most outlines include basic theory, definitions, and hundreds of solved problems and supplementary problems with answers.

Titles on the Current List Include:

Acoustics
Basic Equations of Engineering
Continuum Mechanics
Engineering Economics
Engineering Mechanics, 4th edition
Fluid Dynamics
Fluid Mechanics & Hydraulics, 2d edition
Heat Transfer
Introduction to Engineering Calculations
Lagrangian Dynamics
Machine Design
Mathematical Handbook of Formulas & Tables
Mechanical Vibrations
Operations Research
Strength of Materials, 2d edition
Theoretical Mechanics
Thermodynamics 2d edition

Schaum's Solved Problems Books

Each title in this series is a complete and expert source of solved problems containing thousands of problems with worked out solutions.

Related Titles on the Current List Include:

3000 Solved Problems in Calculus
2500 Solved Problems in Differential Equations
2500 Solved Problems in Fluid Mechanics and Hydraulics
1000 Solved Problems in Heat Transfer
3000 Solved Problems in Linear Algebra
2000 Solved Problems in Mechanical Engineering Thermodynamics
2000 Solved Problems in Numerical Analysis
700 Solved Problems in Vector Mechanics for Engineers: Dynamics
800 Solved Problems in Vector Mechanics for Engineers: Statics

Available at your College Bookstore. A complete list of Schaum titles may be obtained by writing to: Schaum Division
McGraw-Hill, Inc.
Princeton Road, S-1
Hightstown, NJ 08520

CHAPTER 3

PRODUCTION OF THERMAL ENERGY

3.1 INTRODUCTION

Thermal energy is a basic form of energy in that all other energy forms can be completely converted into thermal energy. In fact, unless the energy is stored as some other form, it will eventually be degraded into thermal energy. The verb "degraded" is used here because the conversion of thermal energy into the other energy forms is limited to something less than 100 percent.

3.2 CONVERSION OF MECHANICAL ENERGY

Mechanical energy can be converted into thermal energy in both reversible and irreversible processes. A good example of a reversible conversion is in the operation of an ideal heat pump. In this device the mechanical energy is used to pump heat from a low-temperature to a high-temperature reservoir but the mechanical energy is also converted into thermal energy and dumped into the high-temperature reservoir. If the process is completely reversible, this mechanical energy equivalent can be recovered only if the rejected thermal energy can be put into an externally reversible heat engine.

The conversion of mechanical energy into thermal energy occurs in any irreversible process and can be summarized in essentially one word—friction. In many processes, friction is considered to be an undesirable phenomenon and every effort is made to reduce or eliminate it. This is particularly true in most

Benedict, Manson: "Enrichment: A Critical Status Report," *Trans. Amer. Nucl. Soc.*, vol. 25, pp. 44–56, 1976.

Bolon, Paul: "Power from the Dead Sea via Solar Ponds," *Popular Science*, vol. 218, no. 4, pp. 84–86, April 1981.

Boltz, R. E., and G. L. Tuve (eds.): *Handbook of Tables for Applied Engineering Science*, The Chemical Rubber Company, Cleveland, Ohio, 1970, pp. 348–349.

Bond, R. G., and C. P. Straub: *Handbook of Environmental Control*, vol. II, *Solid Waste*, The Chemical Rubber Company, Cleveland, Ohio, 1974.

Climatic Atlas of the United States, U.S. Government Printing Office, Washington, D.C., June 1968.

De Lorenzi, Otto (ed.): *Combustion Engineering*, Combustion Engineering-Superheater, New York, 1952.

Dillio, C. C., and E. P. Nye: *Thermal Engineering*, International Textbook Company, Scranton, Pa, 1963.

El-Wakil, M. M.: *Nuclear Heat Transport*, International Textbook Company, Scranton, Pa., 1971.

Fisher, A.: "Solar Power Tower," *Popular Science*, vol. 207, no. 4, pp. 88–90, October 1975.

Foster, A. R., and R. L. Wright: *Basic Nuclear Engineering*, Allyn and Bacon, Boston, in J. M. Hollander and M. K. Simmons (eds.), *Annual Review of Energy*, vol. I, Annual Reviews, Palo Alto, Calif., 1976.

Soucie, G. A.: "Turning Garbage into Gold," in *Noture/Science Annual*, Time-Life Books, New York, 1974, pp. 58–69.

Steam: Its Generation and Use, 38th ed., Babcock and Wilcox Company, New York, 1972.

thermodynamic or lubrication process. In any irreversible thermodynamic process, friction converts some of the mechanical energy into thermal energy, which makes the process irreversible.

Friction is not always bad, however. If it were not for the friction between the soles of your shoes and the floor, it would be impossible to walk. If it were not for the friction between the brake shoes or disks and the drums of the automobile wheel, it would not be possible to convert the kinetic energy of the automobile into thermal energy and stop the car.

3.3 CONVERSION OF ELECTRICAL ENERGY

Electrical energy can be converted into thermal energy in several processes but the principal energy-conversion process is the *joule-heating process.* This is the iv or i^2R loss encountered when an electrical current of i amperes is passed through a resistance of R ohms as the result of a potential difference of v volts. The resulting power loss or thermal energy production rate is in watts.

In most electrical circuits, the joule-heating loss is an undesirable power loss, but it occurs in every conductor except the superconductors that have absolutely zero resistance. In some systems, such as electric ranges and furnaces, this process is useful in the production of thermal energy. There is no theoretical upper temperature limit for this conversion process as long as the conductor remains intact. In this conversion process, the thermal energy is deposited in the volume of the conductor.

Another electrical power loss associated with alternating-current systems is the *power-factor loss.* When electrical energy is passed through a capacitor or an induction coil, part of this energy is stored in the electrostatic and magnetic field associated with each impedance. When the current reverses, the established electrostatic and magnetic fields collapse, producing a pulse of electrical energy. If the capacitive and inductive impedances are matched, the energy stored in the electrostatic field is sufficient to charge the magnetic field when the current reverses, and, conversely, so there is no net power loss. If the impedances are not matched, however, the excess electrical energy is converted into thermal energy, which means that the electrical utility must supply more energy to the customer than is actually metered in order to overcome the power-factor loss.

3.4 CONVERSION OF ELECTROMAGNETIC ENERGY

The conversion of electromagnetic energy into thermal energy is accomplished in some sort of absorption process. For high-energy electromagnetic radiation, such as gamma radiation and x-rays, the absorption process is a volumetric phenomenon. For lower-energy radiation, the absorption process is ususally a surface phenomenon. Many materials are transparent to some wavelengths of radiation and opaque to other wavelengths. Glass is transparent to the ultraviolet

and visible portions of the thermal radiation spectrum but is opaque to the infrared radiation emitted by most surfaces. This leads to the so-called greenhouse effect and is useful in trapping solar energy.

3.5 CONVERSION OF CHEMICAL ENERGY

3.5.1 Introduction

At this instant in the history of the human race, the primary source of fuel energy is the production of thermal energy from chemical energy. The most important exothermic chemical reaction in the production of this energy is the combustion of fossil fuels. This reaction is an oxidation reaction in which the three combustible elements found in most of the fossil fuels, i.e., carbon, hydrogen, and sulfur, are respectively converted into carbon dioxide (CO_2), water (H_2O), and sulfur dioxide (SO_2).

This section on the conversion of chemical energy deals primarily with the mechanics of the combustion reaction as well as some of the principal systems and components needed to accomplish the process. A more detailed description of the actual combustion systems is presented in Chap. 4, and the environmental problems associated with the conversion processes are discussed in Chap. 6.

3.5.2 Combustion Reactions

Hydrogen has the highest ignition temperature (582°C or 1080°F) of the three combustible elements. Since elemental hydrogen is a gas, however, the combustion kinetics are such that it burns very rapidly. Consequently, if there is sufficient oxygen, it will be assumed that all the hydrogen burns completely to water before any of the carbon or sulfur burns:

$$2H_2 + O_2 \rightarrow 2H_2O + Q_H \qquad Q_H = 286{,}470 \text{ kJ/kg} \cdot \text{mol } H_2$$

In this reaction, 2 mol of hydrogen (4.032 kg) react with 1 mol of oxygen (32 kg) to produce 2 mol of water (36.032 kg). Thus, the mass of oxygen required to completely burn a unit mass of hydrogen is 32/4.032 or 7.94:

$$\boxed{7.94 \text{ kg } O_2/\text{kg } H_2 = 7.94 \text{ lbm } O_2/\text{lbm } H_2}$$

or

$$\boxed{0.5 \text{ mol } O_2/\text{mol } H_2}$$

The higher heating value of hydrogen (equivalent to Q_H) is 142,097 kJ/kg or 61,095 Btu/lbm and the lower heating value is 120,067 kJ/kg or 51,623 Btu/lbm.

Sulfur has an ignition temperature of 243°C or 470°F, which is the lowest ignition temperature of any of the three combustible elements. While the oxidation of sulfur does release chemical energy in the following reaction, the product of combustion, the sulfur dioxide (SO_2), is considered to be a major atmospheric pollutant:

$$S + O_2 \rightarrow SO_2 + Q_S \qquad Q_S = 296{,}774 \text{ kJ/kg} \cdot \text{mol S}$$

One mol of sulfur (32.06 kg) plus 1 mol of oxygen (32 kg) produces 1 mol of sulfur dioxide (64.06 kg). Thus, 32/32.06 or 0.998 kg of oxygen is required to burn 1 kg of sulfur:

$$\boxed{0.998 \text{ kg } O_2/\text{kg S} = 0.998 \text{ lbm } O_2/\text{lbm S}}$$

or

$$\boxed{1.0 \text{ mol } O_2/\text{mol S}}$$

The higher and lower heating value of sulfur are the same and equal to 9257 kJ/kg or 3980 Btu/lbm. Because of the low ignition temperature, it will be assumed for combustion with incomplete air that all the sulfur burns after the hydrogen burns and before any carbon burns.

Carbon is one of the most important combustible elements and is an essential part of any hydrocarbon compound. The oxidation of carbon is slower and more difficult than that of either hydrogen or sulfur. Although carbon has a lower ignition temperature (407°C or 765°F) than hydrogen, carbon is a high-temperature solid and as such burns relatively slowly. This is the reason that it will be assumed that both the hydrogen and the sulfur burn completely before any of the carbon burns. Furthermore, it will be assumed that all the carbon will be oxidized to carbon monoxide (CO) before any carbon is converted into carbon dioxide. This chemical reaction is

$$2C + O_2 \rightarrow 2CO + Q_{CO} \qquad Q_{CO} = 110{,}380 \text{ kJ/kg} \cdot \text{mol C}$$

In this reaction, 2 mol of carbon (24.02 kg) react with 1 mol of oxygen (32 kg) to produce 2 mol of carbon monoxide (56.02 kg).

If there is sufficient oxygen available, the carbon monoxide will then be oxidized to carbon dioxide with the release of additional energy:

$$2CO + O_2 \rightarrow CO_2 + Q_{CO_2} \qquad Q_{CO_2} = 283{,}180 \text{ kJ/kg} \cdot \text{mol CO}$$

Thus, 2 mol of carbon monoxide (56.02 kg) react with 1 mol of oxygen (32 kg) to produce 2 mol of carbon dioxide (88.02 kg). Combining the two combustion equations for carbon gives

$$C + O_2 \rightarrow CO_2 + Q_C \qquad Q_C = 393{,}560 \text{ kJ/kg} \cdot \text{mol C}$$

Thus, for complete combustion of carbon, 1 mol of carbon (12.01 kg) reacts with

1 mol of oxygen (32 kg) to produce 1 mol of carbon dioxide (44.01 kg). Therefore, (32/12.01) or 2.66 kg of oxygen are required to completely burn 1 kg of carbon. This ratio is quite useful in evaluating the oxygen requirements for hydrocarbon fuels.

$$2.66 \text{ kg } O_2/\text{kg C} = 2.66 \text{ lbm } O_2/\text{lbm C}$$

or

$$1.0 \text{ mol } O_2/\text{mol C}$$

The higher and lower heating values of carbon are the same and equal to 32,778 kJ/kg or 14,093 Btu/lbm.

While this completes the combustion chemistry for the three combustible elements, a brief discussion of the source of oxygen is warranted. Almost all combustion processes rely on air as the source of oxygen. Air is composed of approximately 21 percent oxygen, by volume or mole, and the remaining 79 percent consists of nitrogen with small amounts of argon, carbon dioxide, and other gases. As far as combustion calculations are concerned, it will be assumed that air consists of 21 percent oxygen and 79 percent nitrogen on a volumetric or molar basis. These values translate to 23.2 percent oxygen and 76.8 percent nitrogen on a gravimetric or mass basis. The molecular weight of air is 28.97 kg/kg · mol or 28.97 lbm/lbm · mol.

If the combustion temperature is very high, some endothermic reactions, called *dissociation reactions*, take place. Some of these reactions are shown below:

$$O_2 + E \rightarrow 2O$$

$$N_2 + E \rightarrow 2N$$

$$N_2 + O_2 + E \rightarrow 2NO$$

$$N_2 + 2O_2 + E \rightarrow 2NO_2$$

$$2CO_2 + E \rightarrow 2CO + O_2$$

All of these dissociation reactions are undesirable because of the loss of energy associated with them. However, those reactions that produce oxides of nitrogen (NO_x) and CO are particularly undesirable because the products are major atmospheric pollutants. In most of the combustion processes, therefore, it is desirable to keep the combustion temperature as low as possible. In most of the combustion processes considered in this text, the temperatures are assumed to be low enough that the loss due to dissociation is negligible.

3.5.3 Theoretical Air–Fuel Ratio

The theoretical or stoichiometric air–fuel ratio gives the minimum air requirements for complete combustion of a fuel. It may be expressed in terms of mass of dry

air per unit mass of fuel, in terms of moles of dry air per mole of fuel, or in terms of volume of air per unit volume of fuel. All values should normally be reported on the basis of the "as-burned" fuel analysis.

The theoretical, gravimetric (mass), dry (no water vapor), air-fuel ratio, $(A/F)_{T,G,D}$, is determined from the as-burned ultimate fuel analysis. This ratio is evaluated by performing an oxygen mass balance on the combustible reactants, as follows:

(C mass fraction)(2.66) = _____ kg of O_2 to burn C in 1 kg fuel
(H_2 mass fraction)(7.94) = _____ kg of O_2 to burn H_2 in 1 kg fuel
(S mass fraction)(0.998) = _____ kg of O_2 to burn S in 1 kg fuel

Total = _____ kg of O_2 to burn the combustible elements in 1 kg of fuel
(O_2 mass fraction)(1.0) = _____ kg of O_2 in the fuel per kg of fuel

Difference = _____ kg of O_2 required from the air per kg of fuel

Theoretical, gravimetric, dry, air–fuel ratio = $(A/F)_{T,G,D}$:

$$\left(\frac{A}{F}\right)_{T,G,D} = \frac{\text{kg } O_2 \text{ needed from the air per kg fuel}}{0.232} \tag{3.1}$$

All the mass fractions in the above accounting system are from the as-burned ultimate fuel analysis. The factor of 0.232 in the denominator of Eq. (3.1) is the mass fraction of oxygen in the air, and the air-fuel ratio obtained from Eq. (3.1) can be expressed in units of kg of air/kg of fuel or in units of lbm of air/lbm of fuel. The theoretical gravimetric air–fuel ratios for most coals range between 8 and 12.

The rather complex accounting calculational procedure for determining the theoretical air–fuel ratio can be condensed into one simple equation, as follows:

$$\boxed{\left(\frac{A}{F}\right)_{T,G,D} = \frac{2.66C + 7.94H_2 + 0.998S - O_2}{0.232}} \tag{3.1a}$$

The values in Eq. (3.1*a*) are as-burned mass fractions. Since most coal analyses are listed as dry, ash-free values, it is often easier and faster to use the following equation for coals:

$$\boxed{\left(\frac{A}{F}\right)_{T,G,D} = \frac{(2.66C + 7.94H_2 + 0.998S - O_2)(1 - M - A)}{0.232}} \tag{3.1b}$$

where the moisture and ash values are as-burned values and all other values are dry, ash-free values.

Example 3.1. Calculate the theoretical, gravimetric, dry air-fuel ratio for Campbell County, Tennessee, coal if the as-burned moisture and ash fractions are 4 and 5 percent, respectively.

Solution. From App. E, the dry, ash-free, ultimate analysis is: 83.1% C, 5.5% H_2, 7.4% O_2, 2.1% N_2, 1.9% S, and HHV = 34,608 kJ/kg. Thus

$$\left(\frac{A}{F}\right)_{T,G,D} = \frac{[2.66(0.831) + 7.94(0.055) + 0.998(0.019) - 0.074][1 - 0.04 - 0.05]}{0.232}$$

$$= 10.17 \text{ kg air/kg fuel}$$

In determining the theoretical air-fuel ratios for gaseous and liquid fuels, it is simpler to work with molar quantities than with the mass fractions of the fuel elements. Let the quantity Z_i be defined as the number of moles of the ith element per mole of fuel. Z_i is actually the summation of the products of the mole fraction of the fuel compound containing the ith element and the number of atoms of the ith element in the compound. The subscripts C, H, S, O, and N will be used with Z to designate the moles of elemental carbon, hydrogen, sulfur, oxygen, and nitrogen, respectively, per mole of fuel.

Thus, for the liquid fuel, n-octane, C_8H_{18}, $Z_C = 8$ and $Z_H = 18$. For a fuel gas composed of 50% C_2H_6, 30% CO, 10% NH_3, and 10% H_2S, $Z_C = (0.5)(2) + (0.3)(1) = 1.3$; $Z_H = (0.5)(6) + (0.1)(3) + (0.1)(2) = 3.5$; $Z_O = (0.3)(1) = 0.3$; $Z_N = (0.1)(1) = 0.1$; and $Z_S = (0.1)(1) = 0.1$. This mixture of gases has an effective chemical formula of: $C_{1.3}H_{3.5}O_{0.3}N_{0.1}S_{0.1}$.

Once the Z values for the fuel have been determined, the oxygen mole balance, similar to the mass balance presented earlier, can be carried out:

$Z_C(1) =$ _____ moles of O_2 needed to burn C in 1 mol of fuel
$Z_H(\frac{1}{4}) =$ _____ moles of O_2 needed to burn H_2 in 1 mol of fuel
$Z_S(1) =$ _____ moles of O_2 needed to burn S in 1 mol of fuel

---

Total = _____ moles of O_2 needed to burn all the combustible elements in 1 mol of fuel
$Z_O(\frac{1}{2}) =$ _____ moles of O_2 in the fuel per mole of fuel

---

Difference = _____ moles of O_2 needed from the air to burn all the combustible elements in 1 mol of fuel

Theoretical, molar, dry air-fuel ratio = $(A/F)_{T,M,D}$:

$$\left(\frac{A}{F}\right)_{T,M,D} = \frac{\text{moles of } O_2 \text{ from air per mol of fuel}}{0.21} \tag{3.2a}$$

As before, this rather complicated calculational procedure can be condensed into one simple equation:

$$\boxed{\left(\frac{A}{F}\right)_{T,M,D} = \frac{Z_C + \frac{Z_H}{4} + Z_S - \frac{Z_O}{2}}{0.21}} \tag{3.2b}$$

For gaseous fuels, the molar and volumetric air–fuel ratios are the same and may be expressed in units of moles of air per mole of fuel or in units of cubic feet of air per cubic foot of fuel if the air and the fuel gas are at the same pressure and temperature.

The theoretical, molar, dry air–fuel ratio obtained from Eq. (3.2*b*) can be converted into a theoretical, gravimetric, dry air–fuel ratio by multiplying by the ratio of the molecular weight of air to that of the fuel:

$$\left(\frac{A}{F}\right)_{T,G,D} = \frac{28.97\left(\frac{A}{F}\right)_{T,M,D}}{\text{mol wt of fuel}} \tag{3.3}$$

Example 3.2. Calculate the theoretical, gravimetric, dry air–fuel ratio when burning a LPG composed of 40% propane and 60% butane, in lbm air/lbm gas.

Solution. Given: 40% C_3H_8 and 60% C_4H_{10}.

$$Z_C = 0.4(3) + 0.6(4) = 3.6 \text{ mol C/mol of gas}$$

$$Z_H = 0.4(8) + 0.6(10) = 9.2 \text{ mol H/mol of gas}$$

$$Z_O = Z_S = 0.0;$$

Theoretical, molar, dry air–fuel ratio = $(A/F)_{T,M,D}$:

$$\left(\frac{A}{F}\right)_{T,M,D} = \frac{3.6 + 9.2/4 + 0 - 0/2}{0.21}$$

$$= 28.10 \text{ mol of air/mol gas}$$

$$\text{Mol wt of gas} = 0.4(44.094) + 0.6(58.12) = 52.51 \text{ kg/kg} \cdot \text{mol}$$

Theoretical, gravimetric, dry air–fuel ratio = $(A/F)_{T,G,D}$:

$$\left(\frac{A}{F}\right)_{T,G,D} = \frac{(28.97)(28.10)}{(52.51)} = 15.50 \text{ lbm air/lbm gas}$$

3.5.4 Actual Combustion Process

The five requisites for good combustion are *MATTp*. *MATTp* stands for proper mixing (M) of the reactants; sufficient air (A); a temperature (T) above the ignition temperature; sufficient time (T) for the reaction to occur, and a reactant density (ρ) sufficient to propagate the flame. Since perfect mixing is never attained in the actual combustion process, good combustion can only be assured by supplying excess air for the process. Care must be exercised to keep the amount of excess air to a minimum because too much excess air increases the losses in the combustion process and increases NO_x emissions.

Depending on the amount of excess air supplied and the degree of mixing, the exhaust or flue gas includes the products of complete combustion, i.e., carbon dioxide, water, and sulfur dioxide. It also includes some products of incomplete combustion, including some unburned fuel, carbon monoxide, hydroxyls, and

aldehydes, along with nitrogen, unused oxygen, ash particles, and nitrogen oxides. All of these products except water, oxygen, and nitrogen are considered to be atmospheric pollutants.

There are two ways of expressing the amount of air supplied for a given combustion process—the *dilution coefficient* and the *percent excess air.* The dilution coefficient is defined as the ratio of the actual to the theoretical air-fuel ratios, or:

$$\text{Dilution coefficient} = \text{DC} = \frac{(A/F)_{act}}{(A/F)_{theo}} \tag{3.4}$$

The percent excess air is defined by the following equations:

$$\text{Percent excess air} = 100\frac{(A/F)_{act} - (A/F)_{theo}}{(A/F)_{theo}}$$

$$= 100\ (\text{dilution coefficient} - 1) \tag{3.5}$$

The actual air-fuel ratio for a given combustion process is normally estimated from an experimental measurement of the gaseous components of the exhaust gas. There are several ways of experimentally determining the concentration of the various gas compounds in a mixture of gases. These systems include the gas chromatograph and the orsat apparatus, among others. The gas chromatograph is a very sensitive device that can be used to detect trace amounts of gases in a mixture of gases but these units are complicated and difficult to use. The orsat apparatus, on the other hand, is a relatively simple and compact portable gas analyzer that is specifically designed to measure the concentration of three of the gas compounds found in the combustion products.

A typical orsat gas analyzer is shown in Fig. 3.1, and is used to determine the volumetric or molar fractions of carbon dioxide, oxygen, and carbon monoxide in the dry exhaust gas. A 100-cm^3 sample of exhaust gas is taken at room temperature in the burette by using the leveling water bottle to collect and transfer the gas sample. Since the gas is collected at room temperature over water, it is usually assumed that any water vapor in the exhaust gas will have condensed and that any sulfur dioxide in the exhaust gas will have reacted with the water in the exhaust gas and in the collecting bottle. Consequently, it is assumed that the resulting "dry" gas sample is composed of carbon dioxide, oxygen, carbon monoxide, and nitrogen.

Once the gas sample has been obtained, it is then sequentially passed through three chemical reactors in the device. The first chemical reactor contains an aqueous solution of potassium hydroxide (KOH) that preferentially removes any carbon dioxide in the gas sample. The second chemical reactor contains a solution of pyrogalic acid in potassium hydroxide and water, and this solution preferentially removes any oxygen in the sample. The final chemical reactor contains a solution of cuprous chloride in ammonia, and this solution absorbs any carbon monoxide present in the gas. By carefully measuring the decrease in sample volume as the gas is passed through each chemical reactor, in series, and dividing each decrease by the original gas volume (100 cm^3), the volume or mole

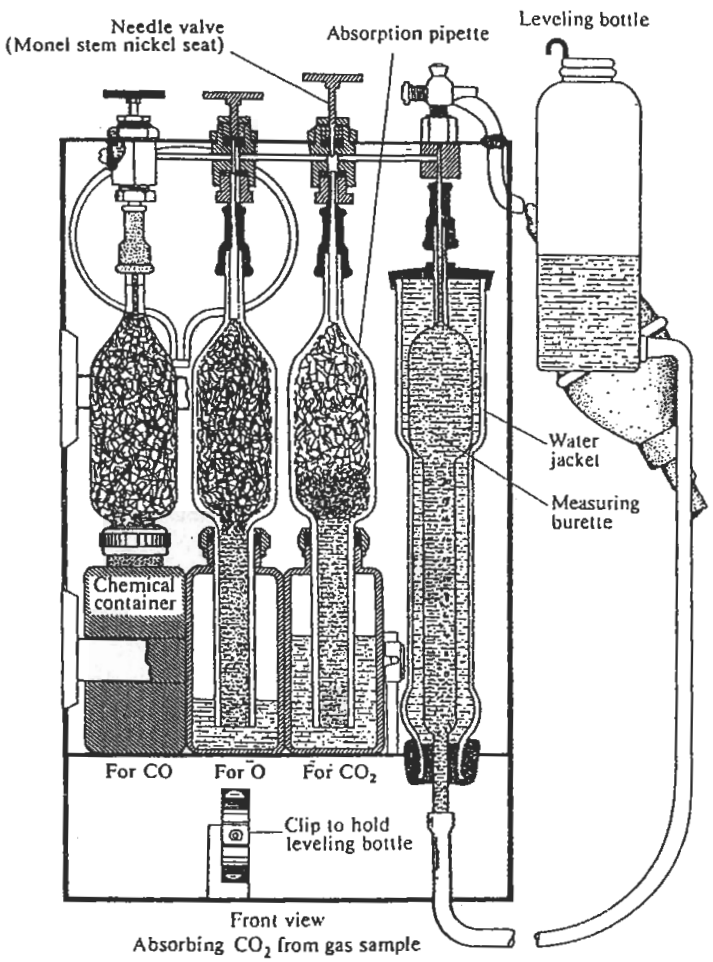


FIGURE 3.1
The orsat flue-gas analyzer.

fractions of carbon dioxide, oxygen and carbon monoxide in the dry exhaust gas are obtained. Any gas remaining after the sample has been passed through all three reactors (usually around 80 percent) is assumed to be nitrogen.

An orsat analysis is required and is usually sufficient to determine the actual air-fuel ratio when burning a gaseous fuel or a liquid fuel. One important additional analysis is needed to evaluate the actual air-fuel ratio when burning a solid fuel such as coal. This is the *refuse analysis*. The refuse analysis is simply an experimental determination of the higher heating value, HHV, of the refuse. This analysis can be reported in units of the amount of energy per unit mass of

refuse (kJ/kg or Btu/lbm) or as the mass fraction of unburned carbon or *percent combustible* in the refuse. If the refuse analysis is given in terms of the higher heating value of the refuse, the percent combustible can be found by dividing the refuse heating value by the heating value of pure carbon:

$$\text{Percent combustible} = 100\frac{(\text{HHV})_{\text{refuse}}}{(\text{HHV})_{\text{carbon}}}$$

$$= 100\frac{\text{HHV, kJ/kg} \cdot \text{refuse}}{32{,}778}$$

$$= 100\frac{\text{HHV, Btu/lbm} \cdot \text{refuse}}{14{,}093} \tag{3.6}$$

Unless additional information is available, it is normally assumed that all the ash in the coal appears in the refuse pit and further that the refuse is composed of only ash and unburned carbon. If C_r is the fuel mass fraction of unburned carbon in the refuse, then R, the mass of refuse collected per unit mass of coal burned, is equal to the sum of C_r and A, where A is the ash mass fraction from the ultimate analysis. The percent combustible is equal to the ratio of C_r/R times 100. Since $R = C_r + A$, $(1 - C_r/R)$ is equal to $(A/R)_r$, the mass fraction of ash in the refuse. If most of the ash in the coal appears in the refuse, the refuse mass fraction, R, can be obtained from the following equation:

$$R = \frac{\text{mass of refuse}}{\text{mass of coal}}$$

$$= \frac{\text{Mass fraction of ash in the coal, } A}{(A/R)_r} \tag{3.7}$$

Once the refuse fraction, R, has been determined, the mass of unburned carbon in the refuse per mass of fuel consumed, C_r, can be found from either of the following equations:

$$C_r = R\frac{\text{percent combustible}}{100} = R\frac{C_r}{R} \tag{3.8a}$$

or

$$C_r = R - A \tag{3.8b}$$

The balance of the carbon in the fuel is assumed to be burned and therefore produces either carbon monoxide or carbon dioxide. C_b is defined as the mass of carbon actually burned per unit mass of fuel and is obtained from the following equation:

$$C_b = C_{ult} - C_r \tag{3.9}$$

where C_{ult} is the carbon mass fraction from the as-burned ultimate fuel analysis.

Once the refuse analysis, the orsat analysis of the flue gas, and the ultimate analysis of the coal are known, the actual air-fuel ratio can be evaluated. Of all

the elements in the fuel and air, C, H_2, S, O_2, and N_2, only the carbon and nitrogen can be totally accounted for in the refuse and orsat analyses. The number of moles of carbon monoxide plus the moles of carbon dioxide in the exhaust gas per unit mass of coal is equal to $C_b/12.01$, and the number of moles of nitrogen in the exhaust gas per unit mass of coal is equal to $[N_F + N_A]/28.016$, where N_F is the as-burned nitrogen mass fraction of the fuel (from the ultimate analysis) and N_A is the mass of nitrogen from the air per unit mass of coal. The ratio of the percentage of nitrogen to the sum of the carbon monoxide and carbon dioxide in the orsat analysis is the ratio of the moles of nitrogen from the fuel and air to the moles of carbon burned in the combustion process. Using this ratio:

$$\text{Actual, gravimetric, dry air-fuel ratio} = \left(\frac{A}{F}\right)_{A,G,D} = \frac{N_A}{0.768}$$

$$\left(\frac{A}{F}\right)_{A,G,D} = \left\{\left[\frac{(\%N_2)(28.016)C_b}{(\%CO + \%CO_2)(12.01)}\right] - N_F\right\}\frac{1}{0.768} \tag{3.10}$$

where the percentages of carbon monoxide, carbon dioxide, and nitrogen are obtained from the orsat analysis; C_b is obtained from the refuse and ultimate analyses; and N_F is obtained from the as-burned ultimate analysis of the coal.

A similar equation can be developed for those fuels in which the analysis is given in terms of mole fractions, again using a carbon-nitrogen balance. The calculational procedure is actually simpler because, in the combustion of a gaseous or liquid fuel, all the carbon in the fuel is normally converted into a gaseous product—either CO or CO_2. For these fuels, the actual, molar, dry air-fuel ratio can be obtained from the following equation:

$$\text{Actual, molar, dry air-fuel ratio} = \left(\frac{A}{F}\right)_{A,M,D}$$

$$\left(\frac{A}{F}\right)_{A,M,D} = \left[\frac{(\%N_2)(Z_C)}{(\%CO + \%CO_2)} - \frac{Z_N}{2}\right]\frac{1}{0.79} \tag{3.11}$$

where Z_C is the moles of carbon per mole of fuel and Z_N is the moles of elemental nitrogen per mole of fuel. The actual, gravimetric, dry air-fuel ratio can be obtained from the molar ratio by multiplying the molar ratio by the ratio of molecular weights as given in Eq. (3.3).

In all of the equations for the air-fuel ratios, the ratio is given for dry air only. In reality, atmospheric air is not normally dry. To include the water vapor contained in atmospheric air, the "wet" air-fuel ratios can be obtained by multiplying the "dry" gravimetric ratios by $1+\omega$, or by multiplying the "dry" molar values by $(1+\omega/0.622)$ where ω is the humidity ratio or mass of water

vapor per unit mass of dry air. Thus, the ratios become:

$$\left(\frac{A}{F}\right)_{T,G,W} = (1+\omega)\left(\frac{A}{F}\right)_{T,G,D} \tag{3.12a}$$

$$\left(\frac{A}{F}\right)_{T,M,W} = \left(1+\frac{\omega}{0.622}\right)\left(\frac{A}{F}\right)_{T,M,D} \tag{3.12b}$$

$$\left(\frac{A}{F}\right)_{A,G,W} = (1+\omega)\left(\frac{A}{F}\right)_{A,G,D} \tag{3.12c}$$

$$\left(\frac{A}{F}\right)_{A,M,W} = \left(1+\frac{\omega}{0.622}\right)\left(\frac{A}{F}\right)_{A,M,D} \tag{3.12d}$$

Theoretically, oxygen and carbon monoxide cannot appear simultaneously in the exhaust gas but they commonly both appear in the exhaust gas because of poor mixing. A common rule of thumb states that the approximate percent excess air is 5 times the oxygen percentage in the orsat analysis, if the %CO is small and the $\%O_2$ is less than 5. For O_2 concentrations greater than 5%, the rule of thumb significantly underestimates the percent excess air.

There are some circumstances in which incomplete combustion of a fuel is desired. Incomplete combustion was commonly practiced in steel mills and the resulting exhaust gas, called *blast-furnace gas*, was used as a cover gas over the molten steel and then burned in large internal combustion engines. Burning a fuel with insufficient air gives the maximum power from a limited volume as in the internal combustion engine and also produces higher specific power from rockets. Reducing the combustion air also reduces the formation of nitrogen oxide pollutants, although it does increase the pollution associated with the emission of carbon monoxide and unburned fuel.

Example 3.3. A certain power plant burns Clay County, Missouri, coal with $M = 12$ percent and $A = 10$ percent, and an analysis of the refuse pit shows that the higher heating value of the refuse is 4581 kJ/kg. An orsat analysis of the flue gas gives 14.57% CO_2, 3.93% O_2, and 0.15% CO. Find the dilution coefficient and the percent excess air.

Solution. Ultimate coal analysis from App. E: 79.2% C, 5.5% H_2, 8.4% O_2, 1.3% N_2, 5.6% S, and HHV = 33,422 kJ/kg.

$$\text{Multiplier for as-burned analysis} = 1 - M - A = 1 - 0.12 - 0.10 = 0.78$$

$$\%\ N_2 \text{ in exhaust gas} = 100 - \%CO_2 - \%O_2 - \%CO$$

$$= 100 - 14.57 - 3.93 - 0.15 = 81.35\%$$

From the refuse analysis,

$$\frac{C_r}{R} = \frac{4581}{32{,}778} = 0.1398 \text{ kg C in refuse/kg refuse}$$

$$= 13.98\% \text{ combustible in the refuse}$$

$$\left(\frac{A}{R}\right)_r = 1.0 - \frac{C_r}{R} = 1.0 - 0.1398 = 0.8602 \text{ kg ash/kg refuse}$$

$$R = \frac{A}{(A/R)_r} = 0.10/0.8602 = 0.1163 \text{ kg refuse/kg coal}$$

$$C_r = R - A = 0.1163 - 0.10 = 0.0163 \text{ kg unburned C/kg coal}$$

$$C_b = C - C_r = 0.78(0.792) - 0.0163 = 0.6015 \text{ kg burned C/kg coal}$$

Theoretical air-fuel ratio:

$$\left(\frac{A}{F}\right)_{T,G,D} = 0.78\,\frac{2.66(0.792) + 7.94(0.055) + 0.998(0.056) - 0.084}{0.232}$$

$$= 8.457 \text{ kg air/kg coal}$$

Actual air-fuel ratio:

$$\left(\frac{A}{F}\right)_{A,G,D} = \frac{[(2.332)(\%N_2)(C_b)/(\%CO_2 + \%CO)] - N_F}{0.768}$$

$$= \frac{2.332(81.35)(0.6015)/(14.57 + 0.15) - 0.78(0.013)}{0.768}$$

$$= 10.081 \text{ kg air/kg coal}$$

$$\text{Dilution coefficient} = DC = \frac{(A/F)_{A,G,D}}{(A/F)_{T,G,D}} = \frac{10.081}{8.457}$$

$$= 1.192$$

$$\text{Percent excess air} = 100\,(DC - 1) = 19.2\%$$

Using the rule of thumb for percent excess air:

$$5(3.93) = 19.7\%$$

Example 3.4. If Linn County, Missouri, coal with $M = 13$ percent and $A = 11$ percent is burned with 12 percent excess air and 0.5% CO appears in the orsat analysis, calculate the balance of the orsat analysis. Assume that the HHV of the refuse is 2500 kJ/kg.

Solution. Ultimate coal analysis from App. E: 78.6% C, 5.6% H_2, 9.3% O_2, 1.3% N_2, 5.2% S, and HHV = 33,318 kJ/kg.

$$\text{Multiplier for as-burned analysis} = 1 - M - A = 1 - 0.13 - 0.11 = 0.76$$

$$\left(\frac{A}{F}\right)_{T,G,D} = \frac{[2.66(0.786) + 7.94(0.056) + 0.998(0.052) - 0.093](0.76)}{0.232}$$

$$= 8.171 \text{ kg air/kg coal}$$

$$\left(\frac{A}{F}\right)_{A,G,D} = (DC)\left(\frac{A}{F}\right)_{T,G,D} = 1.12(8.171) = 9.151 \text{ kg air/kg coal}$$

$$\frac{C_r}{R}=\frac{2500}{32{,}778}=0.0763 \qquad \left(\frac{A}{R}\right)_r=1-0.0763=0.9237$$

$$R=\frac{A}{(A/R)_r}=\frac{0.11}{0.9237}=0.1191 \text{ kg refuse/kg coal}$$

$$C_r=R-A=0.1191-0.11=0.0091 \text{ kg unburned C/kg coal}$$

$$C_b=C-C_r=0.76(0.786)-0.0091=0.5883 \text{ kg burned C/kg coal}$$

Moles of exhaust products per kilogram of coal burned:

$$\text{Moles CO/kg coal}=X, \qquad \text{Mol (CO}+\text{CO}_2\text{)/kg coal}=C_b/12.01$$

$$\text{Moles CO}_2\text{/kg coal}=C_b/12.01-X=0.5883/12.01-X$$

$$=0.04898-X$$

$$\text{Moles O}_2\text{/kg coal}=\frac{(DC-1)(0.232)(A/F)_{T,G,D}}{32}+\frac{C_R}{12.01}+\frac{X}{2}$$

$$=\frac{0.12(0.232)(8.171)}{32}+\frac{0.0091}{12.01}+\frac{X}{2}$$

$$=0.00787+\frac{X}{2}$$

$$\text{Moles N}_2\text{/kg coal}=\frac{(A/F)_{A,G,D}(0.768)+N_F}{28.016}$$

$$=\frac{9.151(0.768)+0.76(0.013)}{28.016}$$

$$=0.25122$$

$$\text{Moles dry exhaust/kg coal}=\text{summation}=0.30807+\frac{X}{2}$$

From orsat analysis of CO:

$$\text{Moles CO/mole dry exhaust}=0.5\%=0.005=\frac{X}{0.30807+X/2}$$

$$0.9975X=0.005(0.30807)$$

$$X=0.00154 \text{ mol CO/kg coal}$$

$$\text{Moles dry exhaust/kg coal}=0.30807+0.00077=0.30884$$

Orsat analysis:

$$\%\ \text{CO}=\frac{100(0.00154)}{0.30884}=0.50\%$$

$$\%\ \text{CO}_2=\frac{100(0.04898-0.00154)}{0.30884}=15.36\% \quad \text{Orsat readings}$$

$$\%\ O_2 = \frac{100(0.00787 + 0.00077)}{0.30884} = 2.80\%$$

$$\%\ N_2 = \frac{100(0.25126)}{0.30884} = 81.34\%$$

$$\text{Total} = 100.00\%$$

Check: Calculate the actual air-fuel ratio using these orsat readings:

$$\left(\frac{A}{F}\right)_{A,G,D} = \frac{2.332(81.34)(0.5883)/(15.36 + 0.50) - 0.76(0.013)}{0.768}$$

$$= 9.149 \text{ kg air/kg fuel} \qquad \text{(close enough to 9.151)}$$

Example 3.5. A natural gas with the following molar analysis is burned in a furnace: $CO_2 = 0.5$ percent, $CO = 5.0$ percent, $CH_4 = 87.0$ percent, $C_2H_4 = 3.0$ percent, and $N_2 = 4.5$ percent. An orsat analysis gives the following results: 9.39% CO_2, 3.88% O_2, and 0.83% CO. Calculate the percent excess air and the actual air-fuel ratio in kilograms of air per kilogram of fuel gas.

Solution. From the gas analysis,

$$Z_C = 0.005(1) + 0.05(1) + 0.87(1) + 0.03(2) = 0.985$$

$$Z_H = 0.87(4) + 0.03(4) = 3.6$$

$$Z_O = 0.005(2) + 0.05(1) = 0.06$$

$$Z_N = 0.045(2) = 0.09$$

$$\left(\frac{A}{F}\right)_{T,M,D} = \frac{Z_C + Z_H/4 + Z_S - Z_O/2}{0.21}$$

$$= \frac{0.985 + 3.6/4 + 0 - 0.06/2}{0.21}$$

$$= 8.833 \text{ mol air/mol gas} = 8.833 \text{ ft}^3 \text{ air/ft}^3 \text{ gas}$$

$$\text{Molecular weight (MW) of gas} = 0.005(44.01) + 0.05(28.01) + 0.87(16.04) + 0.03(28.05) + 0.045(28.016)$$

$$= 17.678 \text{ kg/kg} \cdot \text{mol of gas}$$

From orsat analysis:

$$\%\ N_2 = 100 - (\%CO_2 + \%O_2 + \%CO) = 100 - (9.39 + 3.88 + 0.83)$$

$$= 85.9\%$$

$$\left(\frac{A}{F}\right)_{A,M,D} = \frac{Z_C(\%N_2)/\%CO_2 + \%CO) - Z_N/2}{0.79}$$

$$= \frac{0.985(85.9)/(9.39 + 0.83) - 0.09/2}{0.79}$$

$$= 10.423 \text{ moles air/mole gas}$$

$$\text{Dilution coefficient} = \text{DC} = \frac{(A/F)_{A,M,D}}{(A/F)_{T,M,D}} = \frac{10.423}{8.833}$$

$$= 1.180$$

$$\text{Percent excess air} = 100\,(\text{DC} - 1) = 100\,(1.180 - 1) = 18.0\%$$

Actual, gravimetric, dry air-fuel ratio $= (A/F)_{A,G,D}$:

$$\left(\frac{A}{F}\right)_{A,G,D} = \frac{28.97(A/F)_{A,M,D}}{\text{MW}} = \frac{28.97(10.423)}{17.678}$$

$$= 17.08 \text{ kg air/kg gas}$$

Example 3.6. A certain LPG has a composition of 70% C_3H_8 and 30% C_4H_{10}. Calculate the theoretical orsat analysis and the energy released per kilogram of fuel gas when it is burned with (*a*) a dilution coefficient of 0.9 and (*b*) a dilution coefficient of 0.6.

Solution. From the gas analysis,

$$Z_C = 0.7(3) + 0.3(4) = 3.3$$

$$Z_H = 0.7(8) + 0.3(10) = 8.6$$

$$\text{Mol wt of fuel gas} = 0.7(44.099) + 0.3(58.126) = 30.869 + 17.438$$

$$= 48.307 \text{ kg/kg} \cdot \text{mol}$$

$$\text{HHV}_m = [(30.869/48.307)(50{,}399) + (17.438/48.307)(49{,}589)]$$

$$= 50{,}107 \text{ kJ/kg gas}$$

$$\left(\frac{A}{F}\right)_{T,M,D} = \frac{Z_C + Z_H/4}{0.21} = \frac{3.3 + 8.6/4}{0.21}$$

$$= 25.952 \text{ mol air/mol gas}$$

When burning a fuel with less than theoretical air, it is advisable to set up a table to establish the order of combustion. This table is as follows:

Z_O needed to burn H_2 to $H_2O = Z_H/2 = 4.3$ → 4.3

Z_O needed to burn S to $SO_2 = 2Z_S = 0.0$ → 4.3

Z_O needed to burn C to $CO = Z_C = 3.3$ → 7.6

Z_O needed to burn CO to $CO_2 = Z_C = 3.3$ → 10.9

Therefore:

$$Z_O \text{ needed from the air for complete combustion} = 10.9 - Z_{O,\text{Fuel}}$$

$$= 10.9$$

(*a*) Dilution coefficient = 0.9. Thus

$$Z_O \text{ Available} = 0.9(10.9) + Z_{O,\text{Fuel}} = 9.81 + 0 = 9.81$$

Since $7.6 < 9.81 < 10.9$, there is enough oxygen to burn all the hydrogen and sulfur and enough to burn all the carbon to CO but not completely to CO_2. Dry exhaust will contain CO, CO_2, and N_2.

$$\text{Moles CO/mole gas} = 10.9 - 9.81 = 1.09$$
$$\text{Moles } CO_2\text{/mole gas} = 9.81 - 7.6 = 2.21$$
$$\text{Moles } N_2\text{/mole gas} = 9.81(0.79/0.21)/2 + Z_N/2 = 18.45 + 0 = 18.45$$
$$\text{Moles dry exhaust/mole gas} = 21.75$$

Orsat analysis:

$$\left.\begin{aligned} \%\ CO_2 &= \frac{2.21(100)}{21.75} = 10.16\% \\ \%\ O_2 &= \frac{0.00(100)}{21.75} = 0.00\% \\ \%\ CO &= \frac{1.09(100)}{21.75} = 5.01\% \end{aligned}\right\} \text{Orsat readings}$$
$$\%\ N_2 = \frac{18.45(100)}{21.75} = 84.83\%$$
$$\text{Total} = 100.00\%$$

Check of dilution coefficient using the ideal orsat readings:

$$DC = \frac{(Z_C)(\%N_2)/(\%CO_2 + \%CO) - Z_N/2}{(0.79)(A/F)_{T,M,D}}$$
$$= \frac{(3.3)(84.83)/(10.16 + 5.01) - 0/2}{(0.79)(25.952)}$$
$$= 0.9001 \qquad \text{(close enough)}$$

$$\text{Energy release} = HHV_m - \frac{(\text{moles CO/mol gas})(28.01)(HHV_m)_{CO}}{MW}$$
$$= 50{,}107 - \frac{(1.09)(28.01)(10{,}110)}{48.307}$$
$$= 43{,}717 \text{ kJ/kg of fuel gas}$$

(*b*) Dilution coefficient = 0.6. Thus

$$Z_O \text{ available} = 0.6(10.9) + Z_{O,\text{Fuel}} = 6.54 + 0.0 = 6.54$$

Since $7.6 > 6.54 > 4.3$, there is enough oxygen to burn the hydrogen and sulfur but not enough to burn all the carbon to carbon monoxide. Products will include CO and unburned carbon, called *soot*. The dry exhaust gas will consist of CO and N_2, and the unburned carbon is a solid.

$$\text{Moles C/mole gas} = 7.6 - 6.54 = 1.06$$
$$\text{Moles CO/mole of gas} = 6.54 - 4.3 = 2.24$$
$$\text{Moles } N_2\text{/mole gas} = 6.54(0.79)/0.42 + 0 = 12.30$$
$$\text{Moles dry exhaust gas/mole fuel gas} = 14.54$$

Orsat analysis:

$$\left.\begin{aligned} \%\ CO_2 &= \frac{100(0.00)}{14.54} = 0.00\% \\ \%\ O_2 &= \frac{100(0.00)}{14.54} = 0.00\% \\ \%\ CO &= \frac{100(2.24)}{14.54} = 15.41\% \end{aligned}\right\} \text{Orsat readings}$$

$$\%N_2 = \frac{100(12.30)}{14.54} = 84.59\%$$

$$\text{Total} = 100.00\%$$

Check of dilution coefficient using the ideal orsat readings: When calculating the actual air-fuel ratio, Z_C should be the actual moles of carbon burned, 2.24 in this example. Then

$$DC = \frac{(2.24)(84.59)/(0.00+15.41)}{(0.79)(25.952)}$$

$$= 0.5997 \qquad \text{(close enough)}$$

$$\text{Energy release} = HHV_m - \frac{(\text{moles CO/mole gas})(HHV_m)_{CO}(28.01)}{MW} - \frac{(\text{moles C/mole gas})(HHV_{m,C}(12.01)}{MW}$$

$$= 50{,}107 - \frac{(2.24)(10{,}110)(28.01)}{(48.307)} - \frac{(1.06)(32{,}778)(12.01)}{(48.307)}$$

$$= 28{,}338 \text{ kJ/kg of fuel gas}$$

3.5.5 Combustion Mechanics

The actual combustion process for fossil fuels proceeds in one of two ways. If gaseous hydrocarbon fuels (including vaporized liquids) are mixed with some air (primary air) and heated before the actual combustion takes place, the oxygen in the air has a chance to react with the hydrocarbon molecules in a process called *hydroxylation*. The compounds formed by this interaction are called *hydroxylated compounds*, and are commonly aldehydes. The flame resulting from the combustion of these compounds is a "blue" or "nonluminous" flame. This type of combustion is normally used in the Bunsen burner in the laboratory and in the conventional gas stove where localized heating and a hot flame is desired.

The other basic mode of combustion involves the introduction of fuel and air at the burner with no premixing and heating of the reactants. This results in

a very short mixing time and in very rapid heating of the fuel and the air. Because of this rapid heating, the hydrocarbon compounds are "cracked" into lighter compounds and eventually into the basic elements—carbon and hydrogen. As the result of this thermal decomposition, most of the combustion occurs between elemental carbon and hydrogen. While elemental hydrogen burns with an invisible flame, elemental carbon burns with a characteristic yellow flame. Consequently, this mode of combustion produces a luminous flame. This is called *yellow-flame combustion.* This type of combustion also commonly occurs during the combustion of solid and many liquid hydrocarbon fuels. Actually, contrary to popular opinion, yellow-flame combustion is usually desired in a large power boiler because it increases the radiative heat-transfer rate from the flame to the boiler tubes, reducing the combustion temperature.

Three basic physical methods are utilized for the combustion of fossil fuels. These methods are: the burning bed, the traveling-flame-front, and the gaseous torch. The burning-bed system is commonly employed in the combustion of solid fuels, particularly coal and solid refuse. The burning bed is used in the stoker furnace where the coal is burned in a stationary bed and is also employed in the fluidized-bed combustion system where the coal particles are burned in a floating bed suspended by the combustion air.

The traveling-flame-front combustion system or mode is applicable where the reactants (fuel and oxidant) are completely mixed before combustion occurs. When ignition takes place, the flame front progressively moves through the mixture. This process can occur very rapidly as in a spark-ignition, internal-combustion engine, or more slowly as in a solid-fueled rocket.

The gaseous-torch combustion system is commonly used in large power installations and, in essence, the fuel and air are mixed and burned at the burner. The fuel-air mixture is burned like a gas at the burner and, as such, is applicable for finely atomized liquid fuels and finely powdered solids. When heavy fuel oil is burned in this type of burner, it must be heated and atomized at the burner. Before a coal can be burned in this system, it must be pulverized to a texture finer than face powder. This coal is called *pulverized coal* and the furnace is a *pulverized-coal furnace.*

One other combustion system is actually a combination of several of the combustion modes. This is the *cyclone furnace.* The cyclone furnace burns crushed coal in a flaming vortex. All of these combustion systems are discussed in greater detail in Chap. 4, along with the associated auxiliary equipment—fans, pumps, steam generators, scrubbers, etc.

3.6 CONVERSION OF NUCLEAR ENERGY

3.6.1 Introduction

As was discussed in Chaps. 1 and 2, there are three general nuclear reactions that convert stored nuclear energy into some other energy form—usually thermal energy. These three reactions are: radioactive decay, fission, and fusion. All of these reactions are discussed at length in Chap. 2. At the present time, the only

nuclear reaction that produces sizable amounts of thermal energy is the fission process, and the device in which this is carried out is the nuclear fission reactor.

Radioisotope power systems are normally low-power systems and the controlled fusion reactor has yet to be developed. Consequently, the balance of this chapter is solely concerned with the nuclear fission reactor, its terminology, its principles of operation, and its makeup. The detailed description, design, and kinetics of reactor operation are presented in Chap. 5.

3.6.2 Nuclear Reactor Terminology

The terminology associated with the nuclear reactor and the nuclear industry is, to say the least, unusual and, in some instances, extremely unfortunate. Some of the terminology, which in the early stages of reactor development seemed colorful, catchy, and cute, has subsequently returned to haunt the industry because it sounds so ominous to the average layperson who is unfamiliar with the true meaning.

The nuclear reactor is a device in which a controlled fission chain reaction is maintained in order to produce neutrons and/or energy. While there are other products from nuclear fission, e.g., the two intermediate-mass fission products and beta particles, the neutrons and energy are the most important products and the reason why nuclear reactors are constructed and operated.

Every operating fission reactor has a *critical mass* (one of the ominous-sounding terms). The critical mass is simply the minimum mass of fissionable material that will just sustain a fission chain reaction. Values of critical mass range from 200 g to more than 10,000 kg. The actual fuel loading for any reactor must exceed the critical mass to compensate for fuel burnup and other effects encountered during operation of the reactor.

The *multiplication factor*, designated k, for a reactor is defined as the ratio of the number of neutrons produced in one generation divided by the number of neutrons produced in the preceding generation. Since the fission process is initiated by neutrons, the fission rate or power is directly proportional to the neutron level in the reactor. Thus, if the multiplication factor is greater than unity, the neutron population is increasing with time, the reactor power is increasing with time, and the reactor is said to be *supercritical*. If k is exactly unity, the neutron population and the reactor power are constant and nonzero and the reactor is said to be *critical*. If k is less than unity, the neutron population and fission power are decreasing with time or zero and the reactor is said to be *subscritical*.

Another term which is closely related to the multiplication factor is the *reactivity* of the reactor system, which is designated by the symbol ρ. In fact, the reactivity is actually defined in terms of the multiplication factor k, as follows:

$$\rho \equiv \frac{k-1}{k} \tag{3.13}$$

Thus, for a supercritical reactor, ρ is positive; for a critical reactor, ρ is zero;

and for a subcritical reactor, ρ is negative. The system reactivity is a useful concept in the analysis of reactor kinetics and is used extensively in Chap. 5.

A term that is also used in reactor kinetics is the *reactor period*, or t_r. The reactor period is defined as the time required for the reactor power to increase by a factor of e, the base of natural logarithms. For a supercritical reactor, t_r is positive; for a critical reactor, t_r is infinite; and for a subcritical reactor, t_r is negative.

Since the neutron population and the fission reaction rate is directly proportional to the thermal power of the reactor, it is important to have some quantity or term that designates the neutron level in the reactor. That term is the *neutron flux*, or ϕ. The neutron flux is the number of neutrons passing through a unit area in a unit time and has the units of neutrons per square meter per second (neutrons/$m^2 \cdot s$). The neutron flux is a scalar quantity and ranges from 10^{15} neutrons/$m^2 \cdot s$ for some low-powered reactors to something less than 10^{20} neutrons/$m^2 \cdot s$ for some high-powered research reactors. The neutron flux is equal to the dot-vector product of the neutron density, $\bar{n}$ (neutrons/m^3), and the neutron velocity, $\bar{V}$(m/s):

$$\phi = \bar{n}\bar{V} \tag{3.14}$$

In Eq. (3.14), the neutron density and velocity are, respectively, functions of the spatial location (core volume V) and the kinetic energy (E) of the neutrons. Consequently, an average neutron flux Φ represents an average over the volume of interest as well as over the energy range of interest. If E_L and E_H are, respectively, the lower and higher energy boundaries of the neutron group under consideration, the average neutron flux is obtained from the following equation:

$$\Phi = \frac{\int_{E_L}^{E_H} \int_{\text{Vol}} \phi(E, V)\, dE\, dV}{\int_{E_L}^{E_H} \int_{\text{Vol}} dE\, dV} \tag{3.15}$$

It is common practice to divide the total range of neutron kinetic energy into a finite number of energy groups. The more energetic fission neutrons can have a kinetic energy as high as 10 MeV, while in most nuclear reactors many of the neutrons have kinetic energies less than 0.038 eV, which is the approximate neutron energy when it is in thermal equilibrium with the surrounding material at 20°C or 68°F. For most purposes, the reactor neutrons can be divided into three general energy groups—fast neutrons, intermediate neutrons, and thermal neutrons.

Fast neutrons are neutrons which have a kinetic energy in excess of 0.1 MeV, intermediate neutrons have a kinetic energy less than 0.1 MeV but greater than 0.1 eV, while thermal neutrons have a kinetic energy less than 0.1 eV. Thermal neutrons at 20°C have a most probable velocity of 2200 m/s, while the average velocity of neutrons produced from fission is about 2×10^7 m/s, which corresponds to a kinetic energy of about 2 MeV. All nuclear fission reactors have a fast flux and most of the reactors currently in operation also have intermediate and thermal neutron fluxes.

In detailed reactor-physics calculations, it is common practice to use many energy groups—perhaps more than 1000 groups. These calculations are performed on high-speed digital computers and there is an average neutron flux for each energy group. Only three groups of neutrons will be used in this text.

3.6.3 Neutron Reaction Rates

Since the reactor thermal power is directly proportional to the fission rate in the reactor, the power design engineer must know how to evaluate the total and the local fission rates in the reactor. Although the fission reaction is not the only neutron-induced reaction that takes place in the reactor core, it is the reaction that is of primary interest in the conversion of nuclear fission energy into thermal energy.

The reaction rate for a particular process in the reactor core is equal to the product of the average neutron flux Φ, in the core, the total number of nuclei, N, reacting with the neutrons to produce the reaction, and the average microscopic neutron cross section $\bar{\sigma}$, for the given reaction:

$$\text{Neutron reaction rate} = N\Phi\bar{\sigma} \tag{3.16}$$

The microscopic neutron cross section σ is essentially a target area associated with each nucleus for producing a given reaction with a neutron. The use of the microscopic cross section is not limited to just neutron reactions as it can be applied to other particles (such as protons and deuterons) that are used to bombard nuclei in cyclotrons and accelerators. The microscopic cross section has units of (reaction · m^2/nucleus · incident particle).

Since only neutron-induced reactions are of primary interest in the fission reactor, this book will be concerned only with microscopic cross sections where the incident particle is a neutron—neutron microscopic cross sections (reaction · m^2/nucleus · incident neutron). A subscript on the microscopic neutron cross section will be used to designate the type of neutron reaction that is caused by the incident neutron. Thus, σ_c is the microscopic capture (radiative-capture) cross section for a particular isotope and has units of (captures · m^2/nucleus · neutron). The neutron capture rate for a particular isotope in the reactor is equal to $N\Phi\bar{\sigma}_c$. The microscopic fission cross section σ_f has units of (fissions · m^2/fuel nucleus · neutron), and the fission rate in the reactor core is equal to the product of $N\Phi\bar{\sigma}_f$.

The microscopic neutron cross section σ is a function of the type of reaction, the type of target nucleus, and the kinetic energy of the incident neutron. The microscopic neutron cross sections are determined experimentally and are normally reported in units of *barns* or (reaction · barns/nucleus · neutron). One barn is equivalent to 10^{-28} m^2. A typical plot of the neutron cross section as a function of neutron energy is shown in Fig. 3.2. A comprehensive tabulation of cross-section data is reported in a Brookhaven National Laboratory Report BNL 325 and its supplements.

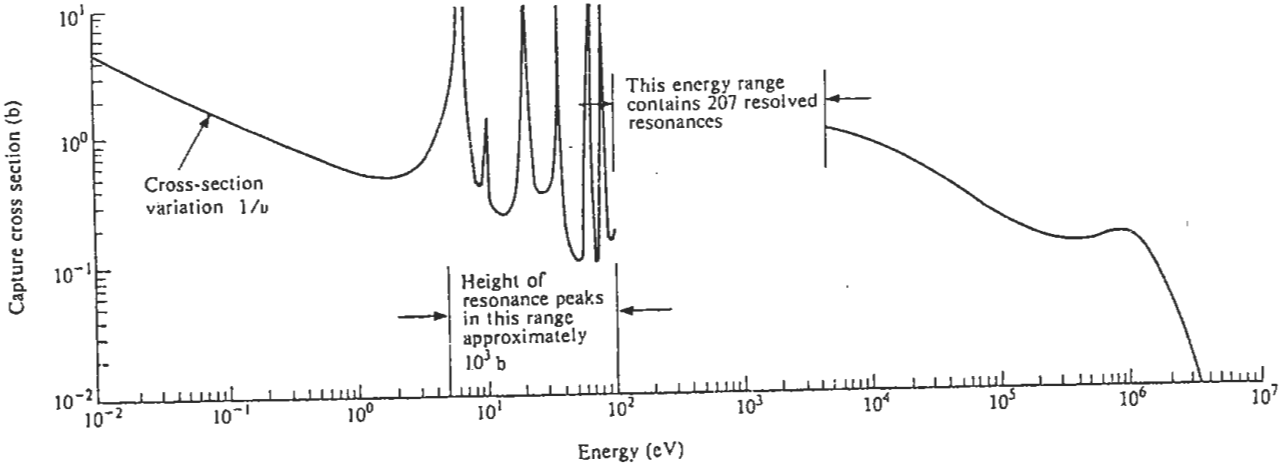


FIGURE 3.2
The microscopic neutron-absorption cross section for U-238. (*From Steam: Its Generation and Use, 1972.*)

Sometimes, it is convenient to use a neutron cross section for a given material, such as water or uranium dioxide, instead of for a particular isotope. The material cross section is called the *macroscopic neutron cross section*, with symbol Σ, and has units of (reactions/neutron · m). For a given isotope, this quantity is equal to the product of the microscopic cross section σ and the isotopic density N/V, or:

$$\Sigma = \frac{\sigma N}{V} \tag{3.17}$$

To get the macroscopic cross section for the material, the individual isotopic or elemental macroscopic cross sections for the atoms in the material are added together.

The macroscopic cross section Σ employs the same subscript as that on the microscopic cross section to identify the type of neutron-induced reaction. The reciprocal of the macroscopic neutron cross section is called the *neutron mean free path*, or λ, where λ is equal to the average distance that a neutron travels before it undergoes a given type of reaction (as designated by the subscript on the cross section):

$$\lambda = \frac{1}{\Sigma} = \frac{V}{N\sigma} \tag{3.18}$$

Substituting Eq. (3.17) into Eq. (3.16) gives the following equation for the neutron reaction rate:

$$\text{Neutron reaction rate} = \Phi N\bar{\sigma} = \Phi V\bar{\Sigma} \tag{3.19}$$

Since there are 3.1×10^{16} fissions/MW_{th} · s, the fission rate in a given reactor, operating at a power level of P MW_{th}, is:

$$\text{Fission rate, fissions/s} = 3.1 \times 10^{16} P = \Phi N_{\text{fuel}}\bar{\sigma}_f = \Phi V\bar{\Sigma}_f \tag{3.20}$$

where $\bar{\sigma}_f$ and $\bar{\Sigma}_f$ are the average microscopic and macroscopic fission cross sections for the neutrons causing fission, Φ is the average neutron flux of the neutrons causing fission, and N_{fuel} is the number of fuel atoms in the volume of the reactor core V_c. Equation (3.20) is valuable in determining the number of fuel atoms, and hence the fuel loading for a given reactor power and fuel loading.

Example 3.7. (*a*) Determine the reactor fuel loading, in kilograms of U-235, in a 1200-MW_e power reactor operating at a thermal efficiency of 33 percent, an average thermal-neutron flux of 6×10^{17} neutrons/m^2 · s in the core, and an average fission cross section of 365 barns. (*b*) If the reactor is fueled with 2.3% enriched UO_2, find the fuel loading of UO_2 in this system.

Solution

(*a*)

$$\text{Reactor power} = P_{\text{th}} = \frac{P_e}{\eta_{\text{th}}} = \frac{1200\ \text{MW}_e}{0.33\ \text{MW}_e/\text{MW}_{\text{th}}}$$

$$= 3636.36\ \text{MW}_{\text{th}}$$

$$\text{Fission rate} = (3.1 \times 10^{16} \text{ fissions/MW}_{th} \cdot \text{s})(3636.36 \text{ MW}_{th})$$

$$= 1.127 \times 10^{20} \text{ fissions/s} = \bar{\sigma}_f N_{fuel} \Phi$$

$$= (365 \text{ fissions} \cdot \text{barn/fuel atom} \cdot \text{neutron})(10^{-28} \text{ m}^2/\text{barn})$$

$$\times (N_{fuel} \text{ fuel atoms})(6 \times 10^{17} \text{ neutrons/m}^2 \cdot \text{s})$$

Number of fuel atoms in the core $= N_{fuel}$. Thus

$$N_{fuel} = \frac{1.127 \times 10^{20}}{(365 \times 10^{-28})(6 \times 10^{17})}$$

$$= 5.147 \times 10^{27} \text{ atoms U-235}$$

$$\text{Mass of U-235} = \frac{(5.147 \times 10^{27} \text{ atoms})(235 \text{ kg/kg} \cdot \text{mol})}{(6.022 \times 10^{26} \text{ atoms/kg} \cdot \text{mol})}$$

$$= 2008.7 \text{ kg U-235} = 2.0087 \text{ tonnes U-235}$$

(*b*) Molecular weight of $UO_2 = 238 + 2(16) = 270$ kg/kg · mol. The U-238 atomic weight is used here because most of the uranium is still U-238.

$$\text{Total mass of uranium} = \frac{2.0087 \text{ tonnes of U-235}}{0.023 \text{ tonnes of U-235/tonne U}}$$

$$= 87.33 \text{ tonnes U}$$

$$\text{Total mass of } UO_2 = \frac{87.33 \text{ tonne U}}{238 \text{ tonnes U}/270 \text{ tonne } UO_2}$$

$$= 99.08 \text{ tonnes of } UO_2$$

$$= 109.19 \text{ tons of } UO_2$$

3.6.4 Neutron Reactions and Cross Sections

Neutron reactions and cross sections can be divided into two general categories. These two classes are the absorption reactions and cross sections and the scattering reactions and cross sections. An absorption reaction (with cross sections of σ_a and Σ_a) is any neutron-induced reaction in which the target nucleus is converted into a different isotope or isotopes. Thus, the target nucleus is destroyed in any absorption reaction. Examples of absorption reactions are the radiative-capture reaction (σ_c and Σ_c), the fission reaction (σ_f and Σ_f), the $(n, 2n)$ reaction (σ_{2n} and Σ_{2n}), the (n, α) reaction (σ_α and Σ_α), and the (n, p) reaction (σ_p and Σ_p). The total absorption cross section is the sum of all five of these cross sections, or:

$$\sigma_a = \sigma_c + \sigma_f + \sigma_{2n} + \sigma_\alpha + \sigma_p$$

or

$$\Sigma_a = \Sigma_c + \Sigma_f + \Sigma_{2n} + \Sigma_\alpha + \Sigma_p \qquad (3.21)$$

It should be pointed out that some or most of the cross sections in Eq. (3.21) may be zero, depending on the material and the neutron energy. However, σ_a or Σ_a is never zero.

A scattering reaction is a neutron-induced reaction in which the target nucleus is not destroyed. Scattering reactions are designated σ_s and Σ_s. There are two types of scattering reactions—elastic scattering reactions (σ_{es} and Σ_{es}) and inelastic scattering reactions (σ_{is} and Σ_{is}). The inelastic scattering cross section may be zero but the total scattering cross section is the sum of the two scattering cross sections, or:

$$\sigma_s = \sigma_{es} + \sigma_{is}$$

or

$$\Sigma_s = \Sigma_{es} + \Sigma_{is} \tag{3.22}$$

The sum of the absorption and scattering cross section for a given material is called the *total cross section* and the subscript t is used on either the microscopic or the macroscopic total neutron cross section. Thus,

$$\sigma_t = \sigma_a + \sigma_s$$

or

$$\Sigma_t = \Sigma_a + \Sigma_s \tag{3.23}$$

As mentioned earlier, some of these cross sections may be zero—particularly for low-energy or thermal neutrons. Some of the cross sections are zero unless the incident neutrons have some minimum kinetic energy (called the *threshold energy*). These reactions are called *threshold reactions.* The $(n, 2n)$ and inelastic scattering reactions must be threshold reactions while the elastic scattering and radiative-capture reactions occur with neutrons of all energy. Only the fissionable isotopes have low-energy fission cross sections but the fission reaction is a threshold reaction for the fertile isotopes. The (n, p) and (n, α) reactions are usually threshold reactions for most materials but the (n, α) reaction occurs for neutrons of all energies for some light-mass isotopes such as lithium and boron.

The low-energy or thermal neutrons in a reactor achieve thermal equilibrium with the material in the reactor core. As such, these neutrons achieve an energy spectrum that can be approximated by a Maxwell-Boltzmann distribution. A plot of a Maxwell-Boltzmann distribution is shown in Fig. 3.3. At 20°C or 68°F, the most probable velocity of thermal neutrons, $\bar{V}_{mp}$, is 2200 m/s and this corresponds to a kinetic energy of 0.0253 eV. The average neutron velocity, $\bar{V}_{ave}$, is 1.128 times the most probable neutron velocity. Most thermal-neutron cross-section data are listed at 2200 m/s or 0.0253 eV.

When evaluating the average neutron cross sections $\bar{\sigma}$ and $\bar{\Sigma}$ for thermal neutrons, the following approximate rules can be applied. The scattering cross section σ_s, which, for low-energy neutrons, is composed of only the elastic scattering cross section, is essentially independent of the kinetic energy of the thermal neutrons. Thus, the average scattering cross section for thermal neutrons becomes

$$\bar{\sigma}_{s,th} = \sigma_{s,2200\ m/s} \tag{3.24}$$

where $\sigma_{s,2200\ m/s}$ is the microscopic neutron cross section for neutrons with a kinetic energy of 0.0253 eV or a velocity of 2200 m/s.

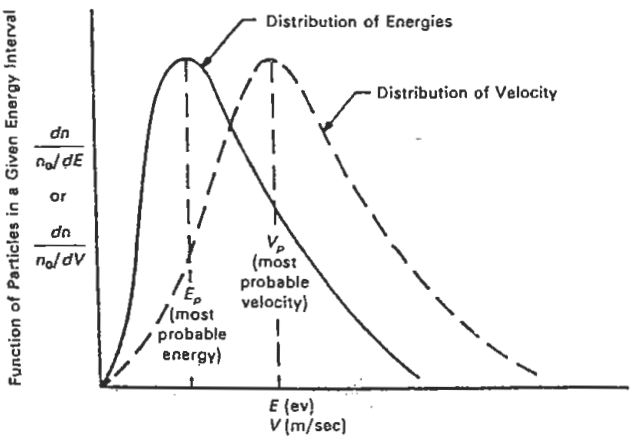


FIGURE 3.3
Velocity and kinetic energy distributions of thermal neutrons at temperature T.

The low-energy absorption cross section (usually only the radiative-capture cross section for most materials) usually varies as the reciprocal of the velocity of the thermal neutrons ($\sigma = K_1/\bar{V} = K_2/E^{1/2} = K_3/T^{1/2}$); see Fig. 3.2. Integrating this $1/\bar{V}$ cross-section dependence over a Maxwell-Boltzmann, thermal-neutron distribution gives the following relationships for the average absorption cross section:

$$\bar{\sigma}_{a,\text{th}} = \frac{\sigma_{a,2200\ \text{m/s}}(2200/\bar{V}_{\text{mp}})}{1.128} \tag{3.25a}$$

$$\bar{\sigma}_{a,\text{th}} = \frac{\sigma_{a,2200\ \text{m/s}}(0.0253/E_{\text{th}})^{1/2}}{1.128} \tag{3.25b}$$

$$\bar{\sigma}_{a,\text{th}} = \frac{\sigma_{a,2200\ \text{m/s}}(528/T_{M,R})^{1/2}}{1.128} \tag{3.25c}$$

$$\bar{\sigma}_{a,\text{th}} = \frac{\sigma_{a,2200\ \text{m/s}}(293/T_{M,K})^{1/2}}{1.128} \tag{3.25d}$$

The temperatures $T_{M,R}$ and $T_{M,K}$ are the absolute temperatures of the moderating material in the reactor core, in degrees Rankine or Kelvin. The moderating material is light-mass material which is put into the reactor core to slow down the neutrons. The factor of 1.128 in Eq. (3.25) comes from the integration of the $1/\bar{V}$ cross section over the thermal Maxwell-Boltzmann distribution.

In the intermediate-energy range, some neuclei exhibit very high cross-section peaks which are called *resonances* because they are similar to the amplitude-frequency plots obtained at the critical speeds of rotating machinery. The uranium-238 microscopic cross section, presented in Fig. 3.2, exhibits a strong

resonance structure. These resonance peaks may correspond to different scattering and absorption reactions and are associated with nuclear energy levels within the target nucleus. Thus, heavy-mass nuclei normally exhibit strong resonance cross-section behavior with energy because of the many energy levels in the nucleus.

The presence of resonance cross sections in the intermediate neutron energy range makes it very difficult to determine the average neutron cross sections in this energy range. These resonances also present an operational problem in some reactors because of a phenomenon called *doppler broadening*. Doppler broadening causes an increased neutron reaction rate with increasing temperature. This can produce a positive reactivity feedback with increasing temperature if the resonance is a fission resonance. This effect complicates reactor control and is discussed in greater detail in Chap. 5.

Example 3.8. Using the 2200-m/s cross-section values for U-235 from Table 3.1, find the average microscopic fission, capture, absorption, scattering, and total neutron cross sections for thermal neutrons when the temperature of the material used to slow down the neutrons (moderating material) is 580°F.

Solution. From Table 3.1, for 2200-m/s neutrons,

$$\sigma_f = 584 \text{ barns} \qquad \sigma_c = 98 \text{ barns} \qquad \sigma_s = 10 \text{ barns}$$

$$T_{M,R} = 460 + 580 = 1040°\text{R}$$

Since the radiative capture and fission cross sections are absorption cross sections,

$$\text{Absorption cross section correction factor} = \frac{(528/T_{M,R})^{1/2}}{1.128}$$

$$= \frac{(528/1040)^{1/2}}{1.128} = 0.6317$$

$$\bar{\sigma}_{f,\text{th}} = \sigma_{f,2200\ \text{m/s}}\,(0.6317) = 584(0.6317) = 368.9 \text{ barns}$$

$$\bar{\sigma}_{c,\text{th}} = \sigma_{c,2200\ \text{m/s}}\,(0.6317) = 98(0.6317) = 61.9 \text{ barns}$$

$$\bar{\sigma}_{a,\text{th}} = \bar{\sigma}_{f,\text{th}} + \bar{\sigma}_{c,\text{th}} = 368.9 + 61.9 = 430.8 \text{ barns}$$

$$\bar{\sigma}_{s,\text{th}} = \sigma_{s,2200\ \text{m/s}} = 10 \text{ barns}$$

$$\bar{\sigma}_{t,\text{th}} = \sigma_{a,\text{th}} + \sigma_{s,\text{th}} = 430.8 + 10 = 440.8 \text{ barns}$$

Example 3.9. Heavy water has a density of 1100 kg/m^3. Calculate the average lifetime of thermal neutrons at 60°C, the average absorption mean free path, and the average distance that a thermal neutron travels before some type of reaction occurs. From Table 3.1, for 2,200 m/s neutrons:

	σ_a, barns	σ_s, barns
Deuterium (H-2)	0.00053	7.0
Oxygen	0.00027	4.2

TABLE 3.1
Neutron cross sections for common reactor materials (for 2200-m/s neutrons)

Element or isotope	σ_f, barns	σ_c, barns	σ_a, barns	σ_s, barns	ν†	η‡	Purpose§
H-1	0.0	0.333	0.333	38.0	0.0	0.0	M, C
H-2	0.0	0.00053	0.00053	7.0	0.0	0.0	M, C
He	0.0	0.007	0.007	1.4	0.0	0.0	C
Be	0.0	0.008	0.008	7.0	0.0	0.0	M
B	0.0	760.0	760.0	4.0	0.0	0.0	A
B-10	0.0	3837	3837	4.0	0.0	0.0	A
C	0.0	0.0036	0.0036	4.8	0.0	0.0	M
N	0.0	1.9	1.9	10.0	0.0	0.0	C
O	0.0	0.00027	0.00027	4.2	0.0	0.0	C
Na	0.0	0.530	0.530	4.0	0.0	0.0	C
Mg	0.0	0.063	0.063	3.6	0.0	0.0	Cd
Al	0.0	0.233	0.233	1.7	0.0	0.0	Cd
Cr	0.0	3.10	3.10	3.0	0.0	0.0	Cd
Fe	0.0	2.55	2.55	11.0	0.0	0.0	Cd
Ni	0.0	4.40	4.40	17.5	0.0	0.0	Cd
Zr	0.0	0.184	0.184	8.0	0.0	0.0	Cd
Sm	0.0	5900	5900	5.0	0.0	0.0	A
Eu	0.0	4600	4600	8.0	0.0	0.0	A
Gd	0.0	4900	4900	?	0.0	0.0	A
Th	0.0	7.4	7.4	12.6	0.0	0.0	Fr
U	4.2	3.4	7.6	8.3	0.017	0.006	F
U-233	529	46	575	?	2.51	2.31	F
U-234	0.0	105	105	9.0	0.0	0.0	Fr
U-235	584	98	682	10.0	2.47	2.12	F
U-238	0.0	2.71	2.71	8.3	0.0	0.0	Fr
Pu-239	742	270	1012	9.6	2.89	2.12	F
Pu-240	0.0	290	290	?	0.0	0.0	Fr
			For 1.5-MeV neutrons				
U-233	1.85	0.034	1.884	4.5	2.65	2.60	F
U-235	1.28	0.078	1.358	4.5	2.65	2.48	F
Pu-239	1.95	0.040	1.990	4.6	3.10	3.04	F

† ν is the average number of neutrons produced per fission.

‡ η is the average number of neutrons produced per neutron absorbed by the fuel = $\nu\sigma_F/\sigma_A = \nu\sigma_F/(\sigma_C + \sigma_F)$.

§ Legend for Purpose column: A—absorber materials; C—coolant material; Cd—cladding materials; F—fuel material; Fr—fertile materials; M—moderating material.

Solution

$$\text{Multiplier for absorption cross sections} = \frac{(293/T_{M,K})^{1/2}}{1.128}$$

$$= \frac{[293/(273+60)]^{1/2}}{1.128} = 0.8316$$

The macroscopic cross section for heavy water $= \Sigma_{D_2O} = \Sigma_{2D} + \Sigma_O$. Then

$$\Sigma_{D_2O} = (\rho/\text{MW})(\text{AV})[2\bar{\sigma}_D + \bar{\sigma}_O] = \Sigma_{HW}$$

Average macroscopic absorption cross section for heavy water $= \Sigma_{a,HW}$.

$$\Sigma_{a,HW} = \frac{(1{,}100)(6.022 \times 10^{26})(0.8316)[2(0.00053) + 0.00027]}{[2(2.014) + 16] \times 10^{28}}$$

$$= 0.00366 \text{ absorptions/neutron} \cdot \text{m}$$

Average macroscopic scattering cross section for heavy water $= \Sigma_{s,HW}$.

$$\Sigma_{s,HW} = \frac{(1{,}100)(6.022 \times 10^{26})[2(7.0) + 4.2]}{20.028 \times 10^{28}}$$

$$= 60.196 \text{ scatterings/neutron} \cdot \text{m}$$

Average total macroscopic cross section for heavy water $= \Sigma_{t,HW}$.

$$\Sigma_{t,HW} = \Sigma_{a,HW} + \Sigma_{s,HW} = 0.004 + 60.196$$

$$= 60.200 \text{ reactions/neutron} \cdot \text{m}$$

$$\text{Absorption mean free path} = \frac{1}{\Sigma_{a,HW}} = \frac{1}{0.00366} = 273.22 \text{ m}$$

$$\text{Scattering mean free path} = \frac{1}{\Sigma_{s,HW}} = \frac{1}{60.196} = 0.0166 \text{ m}$$

$$= 16.6 \text{ cm}$$

$$\text{Average distance before some type of reaction occurs} = \frac{1}{\Sigma_{t,HW}}$$

$$= \frac{1}{60.200} = 0.0166 \text{ m}$$

$$\text{Average velocity of thermal neutrons} = \bar{V}_{ave,th} = 1.128\,\bar{V}_{mp,th}$$

$$= 1.128(2{,}200)[(273+60)/293]^{1/2}$$

$$= 2{,}645.6 \text{ m/s}$$

Average lifetime of thermal neutrons in an infinite heavy water medium $= l_{th}$. Thus

$$l_{th} = \frac{\text{average distance traveled by a thermal neutron}}{\text{average neutron velocity}}$$

$$= \frac{\text{absorption mean free path}}{\text{average thermal-neutron velocity}} = \frac{273.22}{2645.6} = 0.1033 \text{ s}$$

In the high-energy or fast-neutron energy range, the microscopic cross sections are relatively small and constant. The total microscopic cross section σ_t, which is the sum of the absorption and scattering cross sections, normally varies from 2 to 6 barns.

The microscopic neutron cross-section data and fission parameters for the common fuel, fertile, and other reactor materials are listed in Table 3.1. These data are listed for both thermal (0.0253-eV) neutrons and for fast (1.5-MeV) neutrons. The fission parameter, ν, in this table is the average number of neutrons produced per fission. The other fission parameter, η, listed in this table is the average number of neutrons produced per neutron absorbed by a fuel nucleus. In order to sustain a fission chain reaction, η must exceed unity. In order to "breed" in a reactor, η must exceed 2—one neutron is needed to continue the chain reaction and one neutron is needed to convert a fertile atom into a fuel atom.

The cross-section values and fission parameters listed in Table 3.1 point out the primary advantages of operating fission reactors with either fissions induced by low-energy neutrons (thermal reactors) or fissions induced by high-energy neutrons (fast reactors). Although the value of η exceeds 2.0 for all the fuels and for neutrons of all energy, the thermal-neutron values for uranium-235 and plutonium-239 are so close to 2.0 that it is improbable that these fuels could be used in a breeder reactor. This is due to the fact that some of the fission neutrons are absorbed by nonfuel and nonfertile material and some of the neutrons leak from the reactor core.

From the standpoint of breeding, uranium-233 is the best thermal-reactor fuel and it is possible to build a thermal breeder reactor operating on the thorium-uranium fuel cycle. Before decommissioning, the Shippingport Power Reactor in Shippingport, Pa., was converted into a thermal breeder using U-233 fuel although the doubling time was very long. The value of η for fast neutrons is much greater than 2.0 for all three of the fuel isotopes, although plutonium-239 is the best fuel for this application. The principal advantage of fission induced by high-energy neutrons is that high breeding ratios can be achieved with any fuel isotope. Consequently, when people talk of breeder reactors, they usually are talking about fast reactors.

Table 3.1 also underscores the principal advantage of thermal-neutron-induced fissions. The microscopic fission cross sections for thermal neutrons are at least a factor of 280 times larger than those for fast neutrons. The fission rate in any reactor is $\sigma_f N_{\text{fuel}} \Phi$, where Φ is either the average fast flux Φ_f in a fast reactor or the average thermal flux Φ_{th} in a thermal reactor. If a fast and a thermal power reactor are operated at the same thermal power level, the fission rates in both reactors are essentially the same. If the average fast and thermal-neutron fluxes are the same, the total fuel loadings (N_{fuel}) are directly proportional to the average microscopic neutron cross sections. Even if the average fast flux exceeds the thermal-neutron flux by an order of magnitude, the U-235-fueled fast reactor will have a fuel loading equal to 365/(1.28)(10) or 28.5 times the fuel loading of the thermal-reactor system. The thermal fission cross section of 365 barns has been corrected for a Maxwell-Boltzmann distribution and 600°F

(375°C). The lower fuel requirements are the principal advantage of thermal reactors over fast reactors.

3.6.5 Classification of Nuclear Reactors

There are many ways to classify nuclear reactor systems. Some of the common classification systems include classification with respect to the average kinetic energy of the neutrons causing fission, classification with respect to the purpose of the reactor, classification with respect to core composition and geometry, and classification with respect to the type of coolant used to transfer the thermal energy from the reactor core.

CLASSIFICATION WITH RESPECT TO KINETIC ENERGY OF NEUTRONS CAUSING FISSION. There was some discussion in the previous section about thermal and fast reactors, but when classifying reactors according to the average kinetic energy of the neutrons causing fission, there are actually three categories of reactors, including thermal, intermediate, and fast. In a fast reactor, the fission process is induced by fast neutrons with an average kinetic energy of a few tenths of an MeV. In the intermediate reactor, the average fission is initiated by neutrons with a kinetic energy between 0.1 eV and 0.1 MeV, although most intermediate reactors operate just above the thermal energy in the "epithermal" energy range. In the thermal reactor, the average fission process is induced by neutrons with an average kinetic energy below 0.1 eV.

The main advantage of fast reactors is that the fast-fission process produces a higher number of neutrons per neutron absorbed by the fuel. This is true for any of the three fuel isotopes and, as a result, yields very high values of breeding ratio. Consequently, it is possible to build a breeder reactor with any reactor fuel. Another advantage of these systems is that they can employ any structural material because all materials have low neutron absorption cross sections for high-energy neutrons. Only light-mass materials cannot be employed in fast reactors unless they are in the gaseous state as they tend to slow down the neutrons. Fast reactors are also usually small and compact, which makes them easier to "shield," but the small size increases the power density (thermal power to core volume ratio, kW/m^3) in the core and this complicates the transfer of thermal energy in the core. A typical fast reactor is shown in Fig. 3.4.

The principal disadvantage of fast-reactor system is the required high fuel loading, but there are some other disadvantages of fast reactors when they are compared to thermal-reactor systems. Fast reactors must employ enriched-uranium fuel as they cannot "go critical" with natural-uranium fuel. Another problem associated with fast neutrons is that associated with radiation damage of the structural material in the reactor core. The high-energy neutrons "knock" the metallic atoms out of their normal lattice positions, causing embrittlement and swelling of the structural material in the core. Fast neutrons also have much shorter "neutron lifetimes" than thermal neutrons, and this causes some control

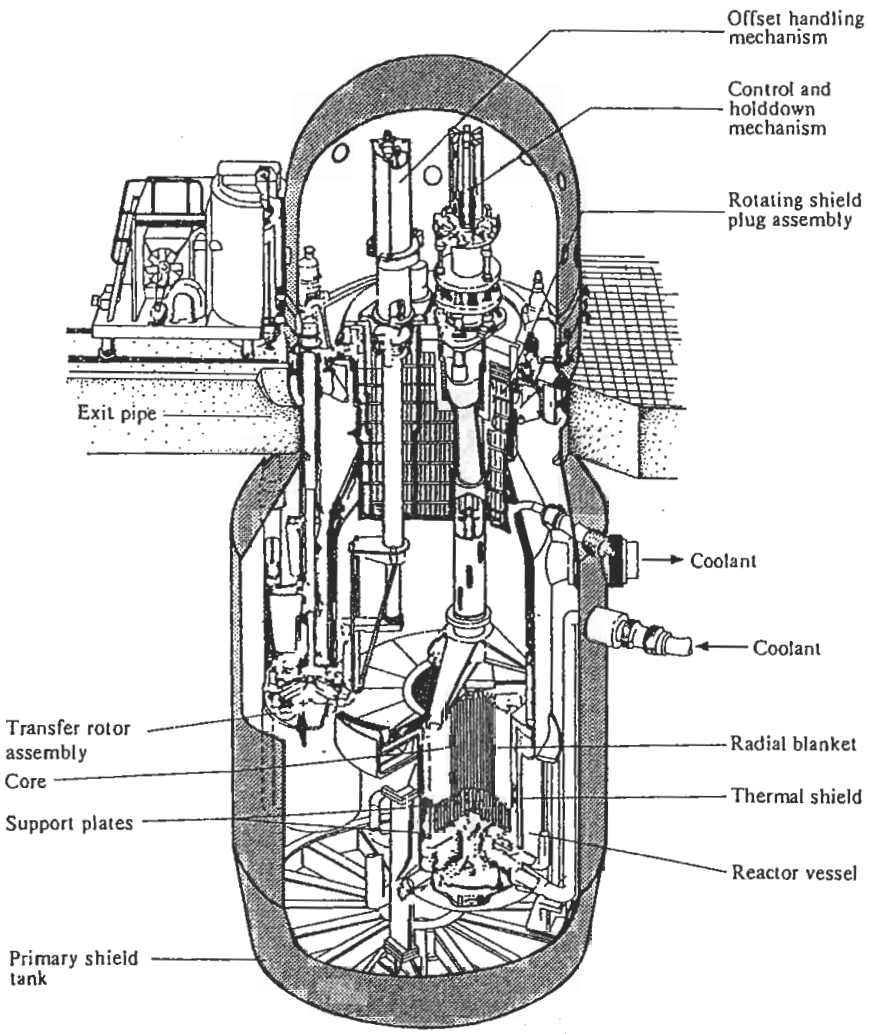


FIGURE 3.4
The Enrico Fermi fast-breeder reactor. (*Skrotzki and Vopat, 1960.*)

problems under certain conditions. This problem is discussed in greater detail in Chap. 5.

The advantages of thermal-reactor systems include the fact that they require a relatively low fuel loading; some thermal reactors can utilize natural-uranium fuel; thermal neutrons have the longest neutron lifetimes, which makes these systems somewhat easier to control; and thermal reactors have relatively low power density because a material, called *moderating material*, must be incorpor-

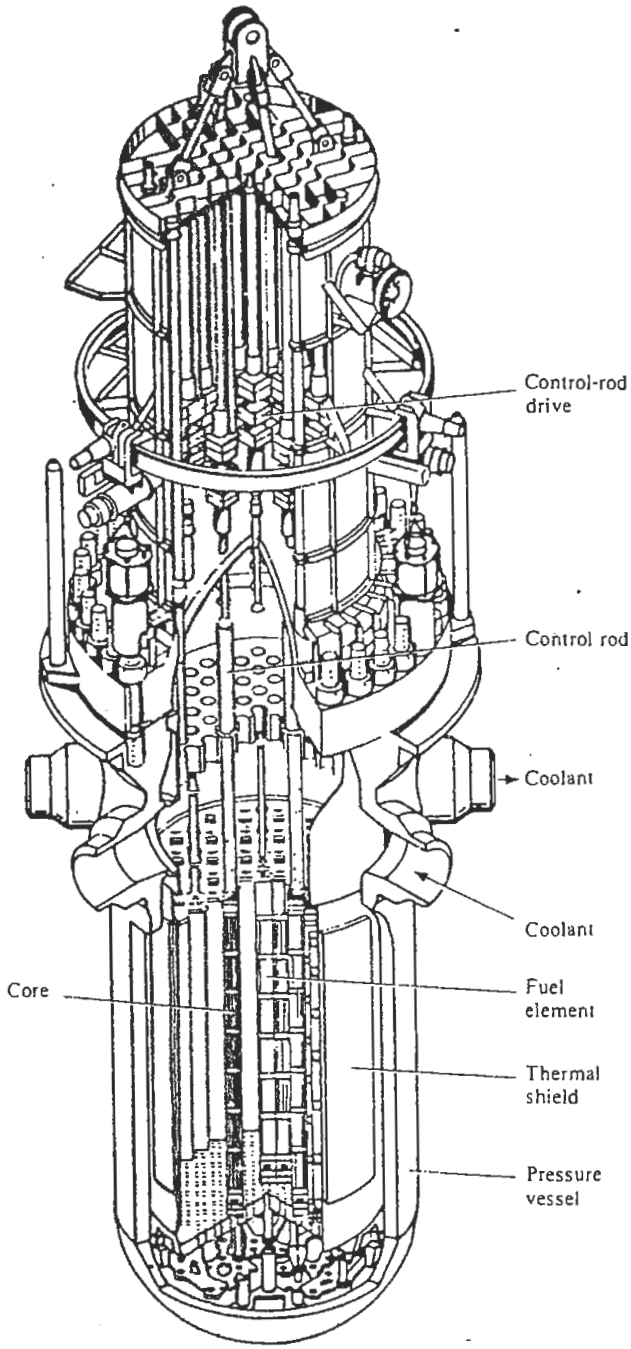


FIGURE 3.5
A typical pressurized-water power reactor. (*From Proceedings of the American Power Conference, 1974.*)

ated into the core to slow down the neutrons. Almost all of the existing reactors in the world are thermal reactors, and a typical thermal power reactor is shown in Fig. 3.5.

There are a number of disadvantages associated with thermal reactors. A principal disadvantage is the fact that it is essentially impossible to breed with any fuel except uranium-233. The choice of structural materials is limited to only those metals and alloys with very small thermal-neutron absorption cross sections. Some of the thermal-reactor systems have very large volumes, which makes them difficult to shield.

Intermediate reactors have some of the advantages and disadvantages of fast and thermal reactors. It is very difficult to design an intermediate-reactor system because of the resonance cross-section structure of the fuel materials in the intermediate energy range. Only two sodium-cooled intermediate submarine reactors have been built, but these are now decommissioned. Several other intermediate reactors have been proposed but have not been built.

CLASSIFICATION WITH RESPECT TO THE PURPOSE OF THE REACTOR. There are two important products from any nuclear reactor—neutrons and energy. The utilization of these products leads to another reactor classification system that classifies the reactors according to their purpose. Under this system, there are five groups of reactors. These include research reactors, experimental reactors, production reactors, compact-power reactors, and commercial-power reactors.

Almost every large university and private and government-operated laboratory has a research reactor of some kind. These systems each operate at a power ranging from a few microwatts to hundreds of megawatts. These reactors are used essentially as sources of neutrons, and the thermal energy generated in these systems is commonly dissipated to the environment.

Experimental reactors are relatively low-powered (up to 10 MW_{th}) reactor prototypes that are constructed to check the feasibility and delineate operating problems of the proposed systems. This is the one reactor system that normally uses neither the neutrons nor the energy generated in the fission process other than that required to meet the test goals for the system. The proposed reactor concept tested in the experiment may utilize one or both of the basic reactor products.

Production reactors are the high-powered reactors in operation at Hanford, Washington, and at Savannah River, South Carolina. These systems were originally designed to produce plutonium-239 fuel for the nation's weapons program. They are currently being used to produce Pu-239 as well as other transuranic elements and isotopes for radioisotope heat sources. Although there are a few exceptions, most of the thermal energy generated by these reactors is simply dissipated to the environment.

The compact-power reactors are sometimes called "burner uppers" because they are fueled with fully enriched uranium to keep their size and weight to a minimum. These systems are designed to produce only thermal energy and are widely used in the naval (submarine and surface ship) reactor program and for

the army power-package reactor program. The nuclear-powered carrier *Enterprise*, for instance, is powered by eight nuclear reactors.

The commercial power reactors utilize both of the basic products from fission. The excess neutrons are used to produce new fuel in a converter or breeder reactor and the thermal energy is used to generate electricity. Most of the power reactors in operation in this country are called *light-water reactors* or LWRs because they are cooled and moderated with ordinary water.

CLASSIFICATION WITH RESPECT TO THE NATURE OF THE REACTOR CORE. Sometimes nuclear reactors are classified as either "homogeneous" or "heterogeneous," depending on their core composition. Homogeneous reactors are those systems in which the fuel is in fluid form, including gases, liquids, and slurries. In this type of reactor, the fluid fuel is normally circulated from the reactor to an external heat exchanger, then to a pump, and back to the reactor. In the heterogeneous reactor systems, the fuel is in solid form and the fission energy is transferred from the solid fuel assemblies (called *fuel elements*) to a coolant circulated through the reactor core. Most of the reactors presently in operation are heterogeneous reactors.

Homogeneous reactors offer some very attractive advantages when compared to the heterogeneous assemblies. First, they have excellent in-core heat transfer because the fission energy is generated directly in the fuel-coolant solution. Next, they have excellent control characteristics because the system tries to maintain the same average core temperature as long as the fuel concentration in the core is a constant. An increase increase in the fuel concentration does not increase the reactor power but simply increases the mean operating temperature in the core. The reactor power is essentially controlled by the rate at which energy is removed from the fuel solution in the external heat exchanger. If the power demand in the external heat exchanger suddenly goes to zero, the hot fuel solution entering the reactor raises the average core temperature, which causes the fuel to be removed from the core due to expansion. As the fuel is removed, the reactor goes subcritical and remains subcritical until the average core temperature reaches the original operating value. Because of the inherent load-following characteristics of this system, some homogeneous reactors have no control rods. Rapid shutdown (SCRAM) of these systems is commonly achieved by dumping the fuel solution into a geometrically safe, noncritical tank where it is cooled.

Another major advantage of homogeneous reactors is associated with the fact that the reactor fuel can be added, removed, and reprocessed during reactor operation. This means that the reactor does not have to be shut down for refueling and that some of the fission products, particularly the high-cross-section gaseous fission products, like xenon-135, can be continuously removed during operation. As a result of this capability, the reactor fuel loading is less than that for a heterogeneous reactor because the heterogeneous system requires extra fuel to compensate for fuel burnup and fission-product poisoning. This means that the

homogeneous reactors are safer than the heterogeneous reactors because there is no excess fuel for a power excursion.

Despite all of the advantages offered by homogeneous reactors, there is one major disadvantage that has prevented their widespread application. This disadvantage arises from the fact that the fuel solution also contains the highly radioactive fission products. Any leaks or component failures in the primary reactor coolant system are extremely difficult to repair because of the presence of these fission products. Despite the problems due to maintenance and repair, some repair has been accomplished with the use of remote-handling tools in an experimental reactor system.

In some of the homogeneous reactors, either the fuel solution proved to be chemically unstable in the presence of a high-radiation environment or it proved to be highly corrosive. While the actual fuel loading in the homogeneous core is relatively small, there is a considerable portion of the total fuel inventory tied up in the external piping, heat exchanger, and pump.

Because of the problem associated with leakage from and repair of the highly radioactive primary loop, very few homogeneous reactors have been built. There are a few in operation which are fueled with aqueous solutions of uranyl nitrate and uranyl sulfate. The Oak Ridge National Laboratory has constructed and tested an experimental homogeneous power reactor fueled with a molten solution of uranium and beryllium fluoride salts. It was hoped that this system could permit breeding in a thermal reactor. Because of expensive developmental costs there are no plans to proceed with construction of a full-scale version of this molten-salt reactor (MSR).

The reactor fuel in a heterogeneous reactor is normally a solid and is encapsulated in a structural material, called *cladding*. The cladding is designed to contain all the fission products within the fuel element. This greatly facilitates maintenance and repair of the reactor system. All of the fuel material in this reactor is located in the reactor core as none is contained in the external cooling circuit, as in the homogeneous reactor.

There are a few heterogeneous reactors that have the capability of being refueled while in operation, but this requires a complicated and expensive refueling machine. This machine must be able to shield and cool the old fuel element before, during, and after extraction and it must also provide cooling to the new fuel element during insertion.

Most reactors are shut down during refueling and fuel is loaded in batches. This means that extra fuel must be added at every reloading to compensate for fuel burnup, fission-product poisoning, etc. This excess fuel complicates the reactor control, operation, and design. The shutdown of a power reactor at periodic intervals (usually every 12 to 18 months) for refueling does not cause serious problems, however. All larger power systems, fossil as well as nuclear, normally require annual shutdowns for turbine inspection and maintenance.

The heat transfer and thermal energy transport in the heterogeneous reactor core is much more difficult than in a homogeneous reactor. The thermal energy produced in the fission process must be transferred through the fuel material by

conduction, by conduction-convection through the fuel-clad interface, by conduction through the cladding material, and by convection from the external surface of the cladding to the coolant.

In many of the current water-cooled power reactors, it is not uncommon to find maximum fuel temperatures of 2200 to 2800°C (4000 to 5000°F) because of the low thermal conductivity of the ceramic fuel material. While the fuel temperature is very high, the cladding material normally operates at something less than 500°C (900°F). The heterogeneous fuel elements are more difficult to reprocess compared to the homogeneous reactor fuel because the cladding must be removed before the fuel can be reprocessed.

CLASSIFICATION WITH RESPECT TO THE TYPE OF COOLANT EMPLOYED. Classifying nuclear reactors with respect to the type of coolant used is applicable only to heterogeneous reactors. Using this system, there are five general types of reactor coolants—ordinary or "light-water" coolant, deuterium oxide or "heavy-water" coolant, organic coolants, gas coolants, and liquid-metal coolants.

Light-water reactors (LWRs) find widespread use as both power and research reactors in the United States and other countries. This coolant has good thermal properties and is inexpensive, and water technology is well developed. Since water has a high hydrogen concentration, the water also commonly serves as the moderating material in a thermal reactor to slow down the neutrons. In fact, water cannot be used as a coolant in a fast reactor unless it is in the form of steam.

Unfortunately, hot water is quite corrosive and it must be highly pressurized in order to operate at moderate temperatures. Another problem arises from the fact that the absorption cross section of ordinary hydrogen is high enough that these systems must employ enriched-uranium fuel (normally 2 to 3 percent in most power reactors) in order to achieve criticality. If water is used as a coolant but not as a moderator, a very reliable reactor control system must be employed because boiling of the water coolant effectively removes neutron absorber (the hydrogen) from the core, which could produce a power excursion. The Russian reactor that burned at Chernobyl was cooled with water but moderated with graphite. This effect undoubtedly contributed to the reactor accident.

There are two basic types of light-water power reactors in use in the United States—the pressurized-water reactor (PWR) and the boiling-water reactor (BWR). In the pressurized-water reactor, the core coolant (the primary coolant) is highly pressurized and no bulk boiling is permitted in the reactor core during normal operation. The turbine steam is generated at lower pressure in a secondary water loop. This prevents contamination of the steam turbine with radioactive material from the primary coolant. A schematic diagram of a typical PWR primary and secondary cooling system is shown in Fig. 3.6. A more detailed description of the PWR is presented in Chap. 5 along with some of the operating parameters.

The newer boiling-water reactors have a primary cooling system in which all the turbine steam is generated directly in the reactor core. This system is

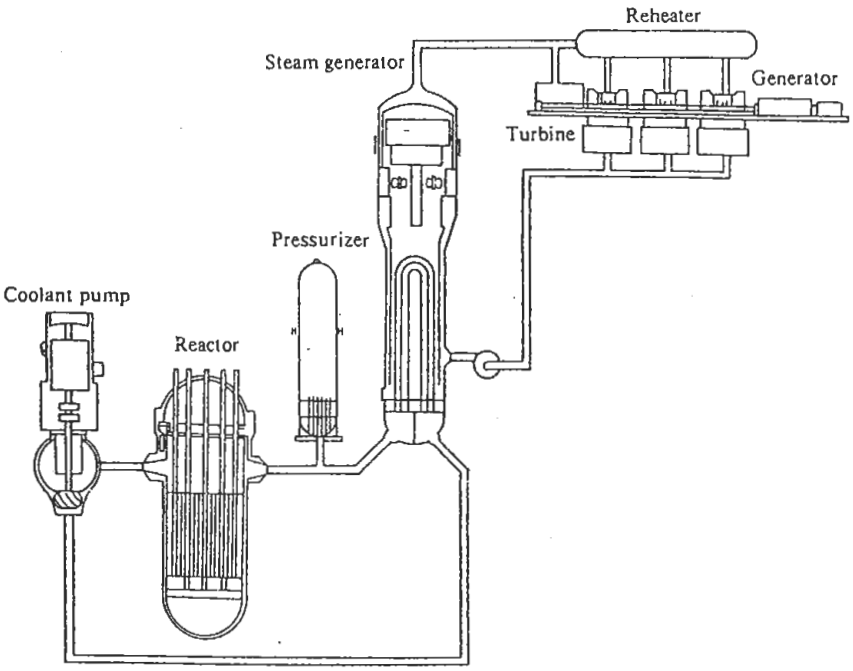


FIGURE 3.6
The primary and secondary cooling systems for a typical pressurized-water reactor power system. (*Courtesy of Westinghouse Electric Corporation.*)

somewhat less complicated than the PWR primary system because it does not require the large and expensive secondary steam generators. Reactor control is accomplished with the use of jet pumps that vary the water recirculation rate in the reactor core. A schematic diagram of a typical BWR system is given in Fig. 3.7. A more detailed description of the BWR is presented in Chap. 5 along with some of the operating parameters.

Heavy water, which is water composed of the heavy hydrogen isotope H-2, is used to moderate and cool some power and research reactors. Heavy-water power reactors commonly use heavy water as the moderation and primary coolant and light water in the secondary system to minimize the heavy-water inventory. The Canadians have exported a number of reactors of this type in the CANDU series. A flow diagram for a CANDU reactor system is shown in Fig. 3.8.

Heavy water has many of the desirable and undesirable characteristics of light water, with one marked difference. While ordinary hydrogen has a high enough absorption cross section (0.333 barns) that light water water cannot be used to moderate a natural-uranium reactor, the heavy hydrogen has a microscopic absorption cross section of only 0.00053 barns, and heavy water *can* be used to

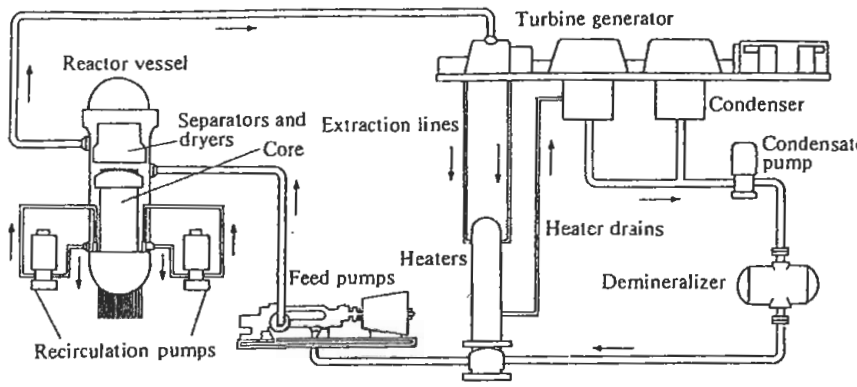


FIGURE 3.7
The schematic diagram of a typical boiling-water reactor power system. (*Courtesy of the General Electric Company.*)

moderate a natural-uranium-fueled reactor. This makes heavy-water reactor systems popular for those countries that do not have uranium isotopic separation facilities.

Heavy hydrogen exists in nature to the extent of one part of heavy hydrogen in 6700 parts of ordinary hydrogen. Consequently, heavy water is difficult and expensive to separate from ordinary water, although it is much easier to separate than the uranium isotopes. The 1990 price of heavy water was about $140 a pound, or about $1140 a gallon. The major drawback of heavy-water-moderated reactors is that they are physically large compared to the light-water reactors and they require a sizable inventory of heavy water. In this country, the production reactors at the Savannah River National Laboratory, along with several research reactors, including those at MIT and Georgia Tech, are cooled and moderated with heavy water.

Organic coolants, such as Dowtherm® and Sanowax®, have been proposed for use as reactor coolants. Their high hydrogen concentration also makes them acceptable as moderating materials to slow down the fission neutrons. These liquid organics can be operated at relatively high temperatures with only moderate pressurization and are much less corrosive than water.

The principal problem associated with the use of organic liquid coolants is the radiation damage caused by high-energy neutrons and gamma radiation. The combined radiation breaks molecular bonds, causing the fragments to recombine into longer and shorter organic molecules. The long-chained molecules usually have high melting points and therefore tend to plate out on the heat-transfer surfaces in the reactor core. Several small experimental organic reactors have been built and operated, including a small power reactor at Piqua, Ohio, but they have been shut down and dismantled.

Gaseous coolants are probably the poorest heat-transport media because they have a low thermal conductivity, a low density, and a low volumetric heat

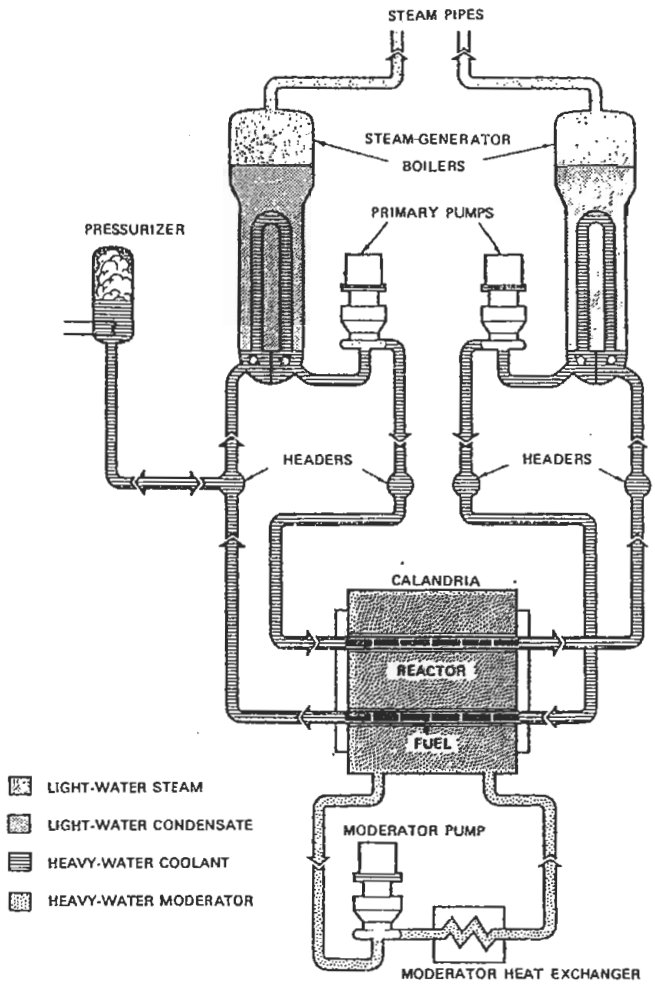


FIGURE 3.8
A schematic diagram of the CANDU power reactor system. (*Courtesy of Atomic Energy of Canada, Ltd.*)

capacity. This means that the gaseous coolants must be highly pressurized to be effective. For this reason, it is difficult to remove the fission-product decay power if the system undergoes a sudden depressurization. Because of their low nuclear density (N/V), gases cannot be used to moderate the neutrons in a thermal reactor.

Gases have some advantages over liquid coolants. For example, there is no concern about phase change at high temperature, and almost any gaseous coolant can be employed without much regard to the microscopic neutron absorption

cross section because the low nuclear density produces a low macroscopic neutron absorption cross section. It also may be possible to use gaseous coolants as the working fluid in the Brayton (gas turbine) power cycle, which takes advantage of the high-temperature capability of gases to achieve a high thermal efficiency. Of all the gaseous coolants, the low-atomic-mass gases, such as helium, have the best thermal properties.

Air has been used to cool the X-10 research reactor at the Oak Ridge National Laboratory, as well as some experimental test reactors in the early aircraft nuclear propulsion (ANP) program. Nitrogen has been used in a small Army test reactor to supply heat for a Brayton-cycle power system. Great Britain has built and exported a number of thermal power reactors cooled with carbon dioxide and moderated with graphite. These reactors are called the *Calder-Hall series* of power reactors.

Of all the gaseous reactor coolants, helium is probably the best. It has the best thermal properties of all the gases except hydrogen, and since helium is a "noble" gas, it is noncorrosive although it may be somewhat difficult to contain. Great Britain has built and is building a number of *advanced gas-cooled reactors* (AGRs) which are cooled with helium and moderated with graphite. In the United States, Gulf General Atomics, a division of the Gulf Oil Corporation, designed a series of large power reactors which are cooled with helium and moderated with graphite. These reactors are called the *high-temperature, gas-cooled reactors* (HTGRs). A schematic diagram of an HTGR is shown in Fig. 3.9, and this reactor

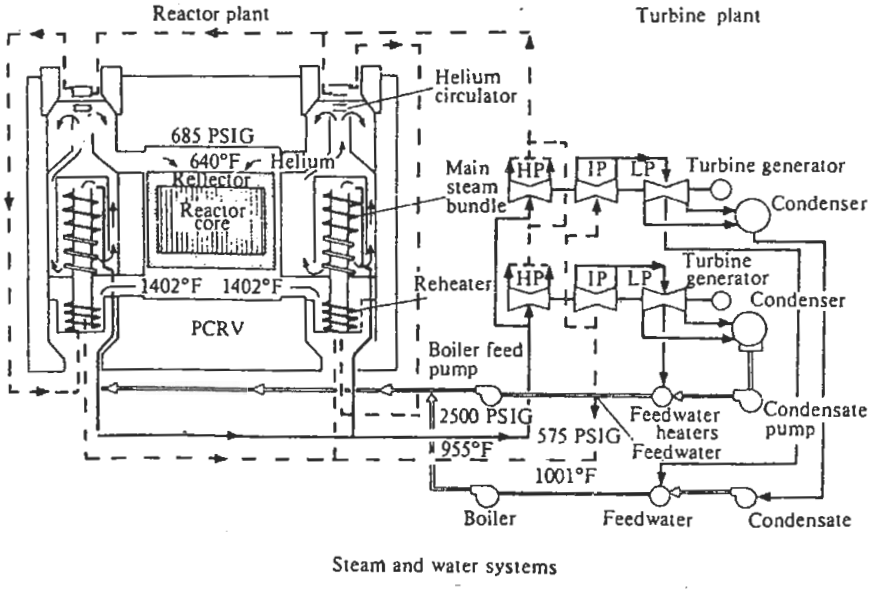


FIGURE 3.9
The schematic diagram for the high-temperature, gas-cooled reactor (HTGR) power system. (*Bonilla, 1957.*)

type is discussed in greater detail in Chap. 5. Gulf General Atomics is also promoting the use of helium coolant in a fast reactor.

Liquid metals have the best heat-transfer properties of all the proposed reactor coolants. They have very high thermal conductivities, low viscosities, and relatively high heat capacities. In addition, most liquid metals can operate at high temperatures with low system pressures. Some of the problems associated with these coolants include high radioactivity resulting from neutron activation of the coolant, high melting points, compatibility of the containment and surrounding materials, a flammability hazard, and the fact that most of these coolants are opaque to visible radiation, which complicates system refueling.

Sodium is the most widely used liquid-metal coolant. It is inexpensive, it has excellent thermal properties, and it boils at high temperature and low pressure (870°C or 1600°F at 1 atm.). Some of the disadvantages associated with liquid sodium include a relatively high melting point (97°C or 206°F), its rapid oxidation (combustion) when exposed to air, and its rapid oxidation in water, which generates large quantities of hydrogen. Although sodium has a low absorption cross section, it does become highly radioactive with a 15-h half-life. Because of this last problem, sodium-cooled power reactors employ a secondary sodium loop between the radioactive primary sodium and the water in the event of a leak in the steam generator.

Liquid sodium has been used to cool a number of thermal reactors moderated with graphite including an experimental thermal power system at Hallam, Nebraska, which has since been decommissioned. Sodium has been the coolant in most of the fast reactors in operation in the world, including the now decommissioned Enrico Fermi fast-breeder reactor, shown in Fig. 3.4. Sodium is the proposed coolant in a number of *liquid-metal, fast-breeder reactors* (LMFBRs) being built or already in operation in France, Great Britain, Japan, and Russia. It was the proposed coolant for the Clinch River Breeder Reactor which was canceled by the U.S. Congress in 1985. The "Superphoenix" LMFBR in France is a full-scale, sodium-cooled power reactor which went into operation in 1986. This reactor system is discussed in greater detail in Chap. 5.

A list of the number of different types of power reactors in operation or under construction as of June 1987 are listed in Table 3.2.

3.6.6 Reactor Physics

A detailed study of reactor physics and multigroup criticality calculations is beyond the scope of this text. However, the nonnuclear engineer can obtain a basic understanding of what takes place in the core of a reactor by examining an elementary neutron balance in a nuclear reactor. This can be done from qualitative considerations without delving deeply into the field of reactor physics.

There are three ways in which neutrons are "lost" in a nuclear fission reactor. These include neutron-absorption processes or reactions, neutron leakage from the reactor core, and, finally, radioactive decay since the neutrons are unstable outside the nucleus. The absorption reactions for the fuel and nonfuel

TABLE 3.2
Number of commercial nuclear power plants in the world of size 30 MW_e and above (as of June 30, 1987)

Type of reactor	Number ordered/number completed		
	Non-U.S.	U.S.	Total
Pressurized water reactors	242/143	84/66	326/209
Boiling water reactors	61/46	40/33	101/79
Pressurized, heavy-water reactor (CANDU)	44/26	0/0	44/26
Gas-cooled reactor (Calder-Hall)	33/33	0/0	33/33
Light-water, graphite reactor (U.S.S.R.)	28/21	1/1	29/22
Advanced, gas-cooled reactor (U.K.)	14/10	0/0	14/10
Liquid-metal, fast breeder reactor	8/4	0/0	8/4
Light-water-cooled, heavy-water reactor	2/0	0/0	2/0
Gas-cooled, heavy-water reactor	1/1	0/0	1/1
High-temperature reactor	1/0	0/0	1/0
High-temperature, gas-cooled reactor	0/0	1/1	1/1
Heavy-water, boiling light-water reactor	1/1	0/0	1/1
Totals	435/285	126/101	561/388
Total rated output, MW_e	317,415	116,939	434,354

materials in the core include: fission, radiative capture, and particle reactions, where applicable. In general, there are three materials in the reactor core that should have high neutron absorption cross sections. These are the fuel, fertile material, and absorber-control-rod materials. All other materials in the core should have low macroscopic neutron absorption cross sections so they do not compete with these materials for the neutrons.

The neutron-leakage rate from the reactor core is a function of the size of the core and the properties of the slowing-down or moderating media. Fast reactors are generally small, compact systems because the fission neutrons travel a very short distance before they are absorbed. Thermal reactors, on the other hand, are normally much larger. The actual leakage rate in the thermal reactor depends on the type of moderating material employed as well as the reactor size. Light-water reactors are usually considerably smaller than the heavy-water and graphite moderated systems simply because fewer scattering collisions are required to slow the neutrons to thermal energy.

The neutron leakage rate from a given reactor can be reduced by increasing the reactor size, and it can also be decreased by surrounding the core with a material that scatters leakage neutrons back to the core. Such material is called a *neutron reflector*, and, for a thermal reactor, is usually composed of a moderating material. In a fast reactor, the reflector, sometimes called a *tamper*, is composed of a heavy-mass material.

Outside the atomic nucleus, all neutrons are radioactive with a half life of 11.7 min. Since the maximum lifetime of the average neutron in any reactor is

around 1 ms, the loss due to radioactive decay is very small. The actual fraction of neutrons lost in 0.001 s is equal to $\{\exp[(0.001)(\ln 2)/11.7]-1\}$ or 0.00006 percent. Consequently, all neutron balances assume that the neutron loss rate due to radioactive decay is negligible.

A possible neutron balance (not necessarily typical of any particular reactor) is given in Table 3.3. In this balance, it is assumed that 1000 fission neutrons with an energy distribution, as given in Fig. 3.10, are introduced into the reactor assembly.

Several conclusions can be made from the neutron balance presented in Table 3.3. First, the reactor would be classified as a thermal reactor as most of the fissions are caused by low-energy neutrons. Second, the reactor would be classified as a converter reactor because $(28+446=474)$ U-235 and Pu-239 atoms (fuel) are destroyed while only $(120+196=316)$ new fuel (Pu-239) atoms are produced. This means that the conversion ratio for this reactor is (316/474) or 0.667. It should be noted that the new fuel atoms are all plutonium-239 atoms. In a typical light-water reactor, at the end of core life, about half the fissions are produced by plutonium-239.

Another conclusion that can be made from the neutron balance is that the reactor is just critical. The fast and intermediate neutrons react with fuel to produce 60 neutrons for the next generation, the fast neutrons react with the fertile material to produce 5 new fission neutrons, and the thermal neutrons react with the fuel to produce 935 neutrons. Thus, $(60+5+935=1000)$ new fissions neutrons are produced in the next generation from the 1000 fission neutrons in this generation, or $k=1000/1000=1.000$.

This reactor can be made supercritical by simply moving the control rods. If the rods are withdrawn from the core, the number of neutrons absorbed by the rods will be reduced. This means that the leakage rate and the neutron absorption rate by the other materials, including the fuel, will be slightly increased. If the absorption rate in the fuel is increased, the number of fission neutrons produced in the next generation will be slightly increased, k will exceed unity, the reactor will be supercritical, and the power will increase with time. On the other hand, if the rods are inserted into the core, they absorb more of the neutrons, proportionally reducing the number of absorptions by the fuel. This means that there will be fewer fission neutrons produced, k will be less than unity, the reactor will be subcritical, and the fission power will decrease with time.

The control of nuclear reactors is markedly different from the control of internal-combustion engines or other prime movers. If an increase in power is desired from an internal-combustion engine, the throttle is simply opened until the desired power is reached and then the throttle is left in that new position. In a nuclear reactor, however, the rods are withdrawn to increase the system reactivity and make the system supercritical. This condition is maintained until the desired power level is attained. When the new desired power level is reached, the control rods are reinserted to make the reactor just critical again. Barring temperature and other minor reactivity effects, the initial and final control rod positions will be the same, although the reactor power level may be much higher.

TABLE 3.3
Possible neutron balance for a reactor

Start with 1000 fission neutrons.

I. The slowing-down process.
  A. Assume that 130 of the fast and intermediate neutrons "leak" from the core during the slowing-down process.
  B. Assume that 160 of the fast and intermediate neutrons are absorbed by the core materials.
    1. Assume that 28 neutrons are absorbed by U-235 and Pu-239 (burned fuel atoms).
      a. 4 of these neutrons are lost in the radiative capture process and produce U-236 and Pu-240.
      b. 24 of these neutrons induce fission.
        i. Assume the average value of ν is 2.5.
        ii. These 24 fissions produce $2.5(24) = 60$ neutrons (new fission neutrons).
    2. Assume 122 neutrons are absorbed by fertile material.
      a. 2 neutrons produce fast fission of fertile atoms.
        i. Assume the average value of ν of 2.5.
        ii. These 2 fissions produce $2.5(2) = 5$ neutrons (new fission neutrons).
      b. 120 neutrons are absorbed in the radiative-capture process and produce 120 Pu-239 atoms (new fuel atoms).
    3. Assume that 10 of the neutrons are absorbed by nonfuel and nonfertile materials in the core.
      a. 1 neutron is absorbed by cladding material.
      b. 2 neutrons are absorbed by the coolant.
      c. 3 neutrons are absorbed by fission products.
      d. 1 neutron is absorbed by structural material.
      e. 3 neutrons are absorbed by the control rods.

II. 710 of the 1000 original neutrons reach thermal energy.
  A. Assume that 27 of the thermal neutrons "leak" from the core.
  B. The balance of the thermal neutrons are absorbed by the in-core materials.
    1. Assume that 446 thermal neutrons are absorbed by the U-235 and Pu-239 atoms (burned fuel atoms).
      a. 72 of these neutrons induce the radiative-capture reaction, producing U-236 or Pu-240.
      b. 374 of the thermal neutrons cause fission.
        i. Assume the average value of ν is 2.5.
        ii. These reactions produce $2.5(374) = 935$ neutrons (new fission neutrons).
    2. Assume 196 of the thermal neutrons are absorbed by the fertile atoms (U-238 or Th-232).
      a. All of these reactions are radiative-capture reactions.
      b. These reactions will eventually produce 196 atoms of Pu-239 or U-233.
    3. Assume that 41 of the thermal neutrons are absorbed by the other materials in the reactor core.
      a. 6 neutrons are absorbed by the cladding material.
      b. 3 neutrons are absorbed by the coolant.
      c. 4 neutrons are absorbed by the moderator.
      d. 8 neutrons are absorbed by fission products.
      e. 2 neutrons are absorbed by structural material.
      f. 18 neutrons are absorbed by the control rods.

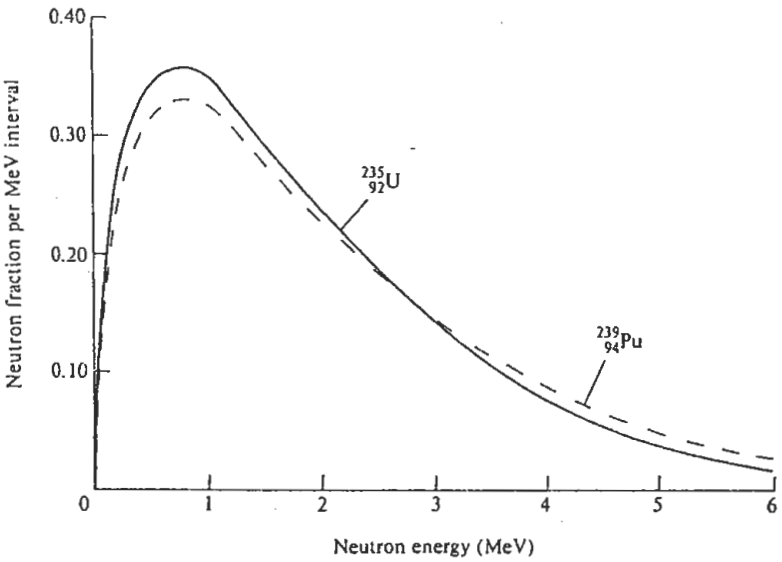


FIGURE 3.10
The energy spectrum of fission neutrons. (*From Steam: Its Generation and Use, 1972.*)

In order to estimate the multiplication factor k for a given reactor assembly, the modified one-group critical equation, obtained from reactor physics, may be used. This equation is

$$k = \frac{\eta f p \varepsilon \exp(-B^2\tau)}{1 + L^2B^2} \tag{3.26}$$

where η = number of neutrons produced per neutron absorbed by the fuel
f = thermal utilization factor = fraction of thermal neutrons absorbed by the fuel
p = resonance escape probability = probability that a fission neutron will reach thermal energy without being absorbed
ε = fast fission factor = ratio of total fissions to thermal fissions
B = reactor buckling, which is a function of the reactor size; increasing the reactor dimensions reduces the buckling; B has units of reciprocal meters
τ = Fermi age, which is a function of the moderating material, in meters squared
L = thermal diffusion length, which is a function of the diffusion coefficient and the thermal macroscopic absorption cross section of the core materials, in meters
$\exp(-B^2\tau)$ = fast nonleakage probability = probability that a fast neutron will not leak from the reactor core during the slowing-down process
$1/[1+L^2B^2]$ = thermal nonleakage probability = probability that a thermal neutron will not leak from the reactor core

Using the neutron balance presented in Table 3.3, the values for the parameters in the critical equation [Eq. (3.26)] become

ν = average number of neutrons produced from fission
$= 1000/(24+2+374) = 2.50$
η = (fission neutrons/fuel abs.) $= 2.50(374/446) = 2.0964$
f = (thermal fuel abs./total thermal abs.) $= 446/(710-27)$
$= 0.653$
p = fraction of fast neutrons not absorbed in the slowing-down process
$= (1000-130-160)/(1000-130) = 710/870 = 0.8161$
ε = total fissions/thermal fissions $= (374+2+24)/374$
$= 1.0695$
$\exp(-B^2\tau)$ = (total neutrons − fast leakage)/total neutrons
$= (1000-130)/1000 = 0.870$
$1/(1+L^2B^2)$ = (thermal neutrons − thermal leakage)/thermal neutrons
$= (710-27)/710 = 0.962$

$$\text{Multiplication factor} = k = [\eta f p \varepsilon \exp(-B^2\tau)]/(1+L^2B^2)$$
$$= (2.0964)(0.653)(0.8161)(1.0695)(0.870)(0.962)$$
$$= 1.000000$$

3.6.7 Composition of a Nuclear Power Reactor

REACTOR CORE. The reactor core is that part of the nuclear reactor which contains the fuel and fertile materials, and where almost all of the fission energy is released. The core volume includes not only the fuel and fertile materials but also the coolant, instrumentation, control elements, cladding, moderator (for thermal reactors), etc.

The core of homogeneous thermal reactors consists of fluid fuel and either a solid or liquid-solution moderator. The fuel of a homogeneous power reactor may be composed of molten plutonium, molten bismuth–uranium alloy, or a solution of molten fluoride salts. Aqueous solutions of uranyl nitrate or uranyl sulfate have been used in some experimental power and research reactors.

Heterogeneous power reactors have a core composed of solid fuel elements that are cooled by liquid or gas. The solid fissionable elements are metals at room temperature but are not stable during long periods of irradiation and thermal cycling. Only limited success has been achieved in the use of metallic fuel alloys as most of the alloys are also unstable.

Almost all of the present power reactors employ oxides of the fuel isotopes. The oxide compounds, uranium dioxide (UO_2) and plutonium dioxide (PuO_2), are compatible with the water coolant in LWRs. They are stable in the high radiation fields and they can undergo a high percentage of fuel burnup. About the only problem associated with these fuel compounds is that they have very low values of thermal conductivity which produce very high operating temperatures in the fuel. Fortunately, these materials have very high melting points

and can operate at these temperatures. Some research reactors use uranium dioxide particles dispersed in an aluminum matrix. Carbides of the fuel isotopes (plutonium carbide and uranium carbide) appear to be somewhat promising and a considerable amount of research has been done on these systems.

In any of the heterogeneous systems, the fuel is encapsulated in a structural material, called *cladding*. The purpose of the cladding material is to contain the fission products in the fuel element, thereby reducing the radioactive contamination of the coolant. Cladding materials should have good physical properties, including a high thermal conductivity, a high melting point, and good mechanical properties, and should be stable in a high neutron and gamma radiation environment. In addition, the cladding material should have a low macroscopic neutron absorption cross section so that the cladding does not compete with the fuel for the neutrons. The cladding material should be chemically stable so that it will experience little or no corrosion in the reactor, and it should be capable of being easily dissolved or stripped from the fuel during reprocessing of the fuel element.

A number of different structural materials have been employed as cladding materials. Aluminum has been used in a number of water-cooled, research reactors, but its relatively low melting point rules it out for application in power reactors. The British used a magnesium-based alloy in their Calder-Hall reactors, which were cooled with carbon dioxide. Stainless steels were used in some of the early water-cooled reactors, but these alloys have fairly high neutron absorption cross sections. The 300-series stainless steels are used as cladding and structural materials in sodium-cooled reactors because these alloys are compatible with alkali metals. Almost all of the water-cooled power reactors use a zirconium-based alloy as the cladding material. Most of the fuel elements are fabriacted from zirconium-alloy tubes filled with oxide fuel pellets and mounted in a square array. A typical LWR fuel element is shown in Fig. 3.11. Graphite is used as the cladding material in the HTGR fuel elements. While graphite has an excellent thermal conductivity and also has a very high melting point, it is fairly porous and fission products diffuse through it.

In a thermal-reactor system, some sort of moderating material is incorporated in the reactor core to slow down the fission neutrons. This material should have a high macroscopic neutron scattering cross section, a low macroscopic neutron absorption cross section, and a low atomic mass to get the maximum kinetic energy transfer from the neutrons to the moderator atoms. In addition, the moderator must be resistant to the high neutron and gamma radiation levels in the core, it should have good physical properties, and it should be compatible with the other materials in the core. Actually, only four isotopes or elements are used in materials to moderate neutrons. The moderator elements or isotopes are ordinary hydrogen (essentially H-1), heavy hydrogen or deuterium (H-2), beryllium, and carbon.

Ordinary hydrogen is often employed as the moderating material in the form of water, in solid and liquid organic compounds, and in the form of an intermetallic compound, zirconium hydride. While ordinary hydrogen is commonly used in thermal reactors, the light-hydrogen isotope has a sufficiently high

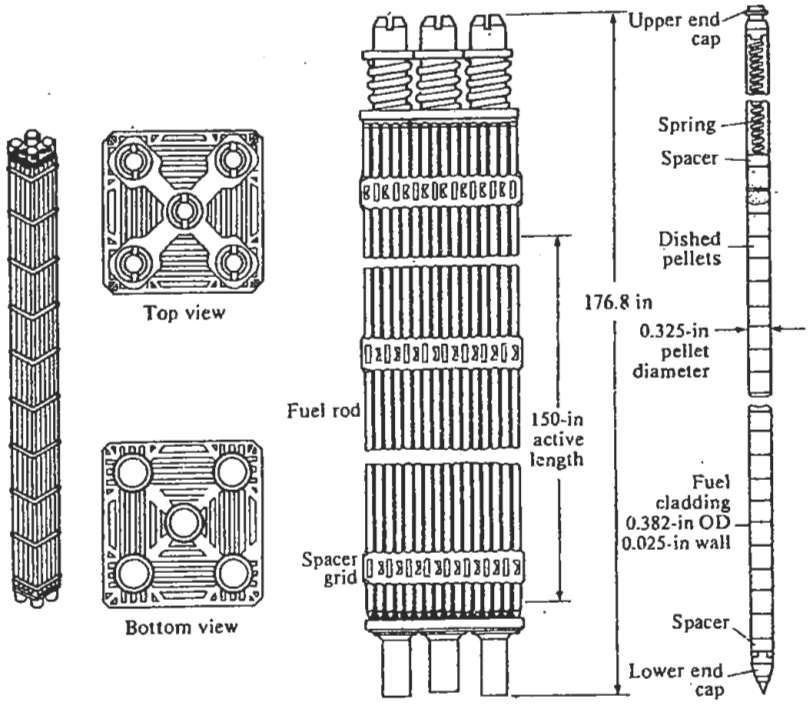


FIGURE 3.11
A typical fuel element for a light-water reactor (LWR). (*From Proceedings of the American Power Conference, 1974.*)

absorption cross section that reactors using it must employ enriched uranium. In many power and research reactors, light water is used as both the moderator and the coolant.

Heavy hydrogen is used as the moderating material in a number of thermal reactors in the form of heavy water or deuterium oxide, D_2O. The heavy hydrogen isotope has such a low absorption cross section that reactors moderated with it can employ natural-uranium fuel. Because of the high cost associated with the heavy water, most reactors use the heavy water only in the primary coolant system and employ ordinary water in the secondary cooling system. As discussed earlier, Canada is a major proponent of the heavy-water moderated and cooled reactor in their CANDU reactor system.

The other two moderators are solids at normal operating temperatures. Beryllium is the best metallic moderator and can be used in the form of either pure metal or as beryllium oxide, BeO. Beryllium is expensive and difficult to machine and consequently is not widely used in reactors. The other solid moderating material is carbon in the form of graphite. Although carbon has the highest atomic mass of any of the moderating materials, it is relatively inexpensive and

it has good high-temperature properties and excellent heat capacity. Carbon also has such a low neutron absorption cross section that it can be used to moderate thermal reactors fueled with natural uranium.

All heterogeneous reactors producing significant quantites of power employ coolants in the form of gases or liquids to transport thermal energy from the core. Coolants should have desirable physical properties, including a high thermal conductivity, a high specific heat, a high density, a low viscosity, and, if it is a liquid, a high boiling point, a low vapor pressure, and a low melting point. In addition, the coolant should be chemically compatible with the other in-core materials, it should not become highly radioactive, it should have a very low macroscopic neutron absorption cross section, and it should be stable when exposed to the intense in-core radiation field. Typical reactor coolants include light and heavy water, organic liquids, gases (helium), and liquid metals (sodium).

Another component found in any reactor core is the neutron source. The neutron source provides a supply of neutrons to bring the startup neutron level in the core to the point where it can be monitored by the in-core instrumentation. Thus, the reactor power and the rate of change of the neutron population can be checked at all times during the reactor startup period. Monitoring the neutron level during the startup period prevents any inadvertent power excursions during this interval.

There are two basic types of neutron sources. Both use beryllium as the basic material along with either an alpha-emitting radioisotope or a radioisotope that emits an energetic gamma ray. The (α, n) source is composed of a mixture of beryllium and an alpha emitting radioisotope, such as plutonium-238. The resulting alpha particles react with the beryllium nuclei to produce neutrons in the following reaction:

$$^{9}_{4}\mathrm{Be} + ^{4}_{2}\alpha \rightarrow {}^{13*}_{6}\mathrm{C} \rightarrow {}^{12}_{6}\mathrm{C} + {}^{1}_{0}n + \gamma_{\alpha}$$

The source is normally withdrawn from the core region into the low-flux region at low to moderate power levels to prevent "burnup" of the alpha source by the neutrons.

The other basic neutron source is the photoneutron or (γ, n) source. This is composed of a mixture of beryllium and a radioisotope that emits an energetic gamma ray. These gamma rays react with the beryllium nuclei in one of the following reactions:

$$\gamma + {}^{9}_{4}\mathrm{Be} \rightarrow {}^{9*}_{4}\mathrm{Be} \begin{cases} \rightarrow {}^{4}_{8}\mathrm{Be} + {}^{1}_{0}n + \gamma_{\gamma} \\ \rightarrow 2\,{}^{4}_{2}\alpha + {}^{1}_{0}n + \gamma_{\gamma} \end{cases}$$

In order for the photoneutron reaction to take place, the incident gamma-ray energy must exceed the threshold energy of 1.62 MeV. The isotope that is commonly used to produce such a high-energy gamma ray is antimony-124 (Sb-124). This radioisotope is produced by bombarding stable antimony (42.75% Sb-123) with neutrons to generate antimony-124 in the radiative-capture process. The antimony-124 radioisotope has a half-life of 60 days and emits an energetic gamma ray during the decay process. This source is normally left in the reactor

during operation in order to keep the neutron activation of the antimony at the "saturation" level.

All forms of instrumentation are employed in the core of a nuclear reactor, ranging from the usual flow nozzles or orifices and thermocouples to the more sophisticated neutron detectors and fission-product leak-detection systems. Of all this instrumentation, the neutron-detection systems are probably the most important for proper operation of the reactor. The detection of neutrons is difficult because they are not charged particles. In order to be detected, they must first react with some other nuclei in a reaction that produces a charged particle or particles. The resulting ionization by the charged particle is then detected.

Most nuclear reactors use gas-filled ionization chambers to detect the ionizing radiation. These chambers are similar to that shown schematically in Fig. 3.12. As ionizing radiation in the form of gamma rays or charged particles pass through the gas, they strip electrons from the gas molecules. This produces ion pairs along the path of the ionizing particle or radiation. If a voltage is applied across the center electrode and the casing, as indicated in Fig. 3.12, the resulting electric field can separate these ions before they have chance to recombine. When these ions reach the center electrode or case, they induce a voltage drop that is amplified and detected in the triode grid.

The response of a radiation-detection chamber to a fixed quantity of ionization as a function of the voltage difference across the electrodes is shown in Fig. 3.13. As the electrode voltage is increased to about 200 V, the signal or ionization collected in this region (region II in Fig. 3.13) levels off on a plateau called the *ionization-chamber region.* In this region, essentially all of the ion pairs along the path of the ionizing particle or radiation are separated by the electric field and are collected at the electrodes, producing a signal that is equal to the amount of ionization produced in the chamber.

As the electrode voltage is increased, the output signal also increases in the area of operation called the *proportional-chamber region* (region III in Fig. 3.13). The higher signal is generated because the separated primary ions, produced by the original radiation, are accelerated to the point where they produce secondary

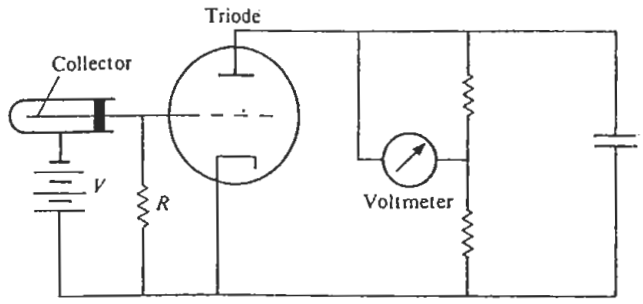


FIGURE 3.12
A typical radiation-detection chamber and electrical circuit. (*Glasstone and Sesonske, 1963.*)

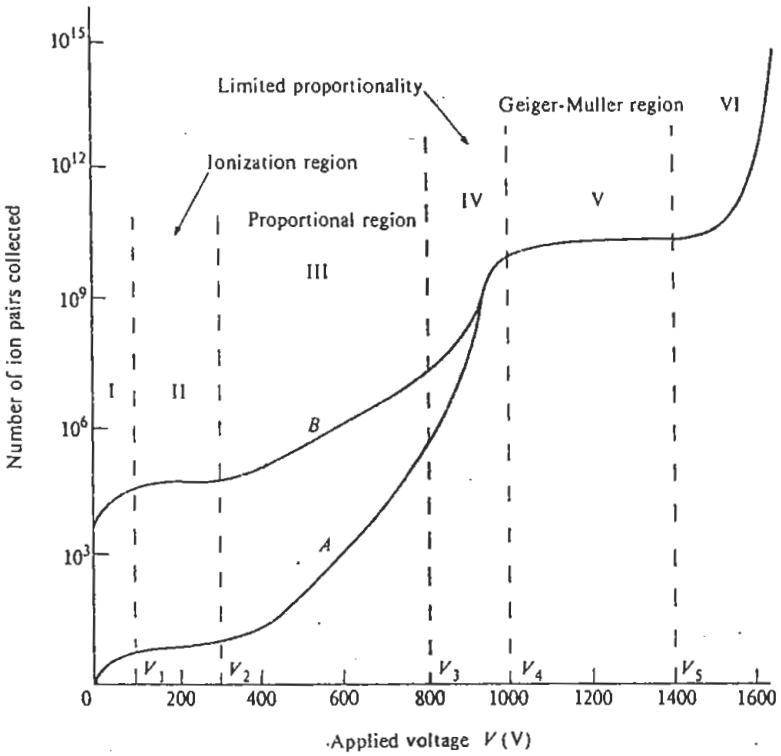


FIGURE 3.13
The response of a gas-filled radiation chamber to primary ionizations of 10 ion pairs (curve A) and 50,000 ion pairs (curve B). (*Foster and Wright, 1973.*)

ion pairs, thereby giving a higher signal. As the electrode voltage is increased further, another plateau, called the *Geiger–Muller* region (region V in Fig. 3.13), is attained. At this point, the gas in the tube is completely ionized and conducting due to the secondary ionization produced by the high voltage.

The Geiger–Muller region of operation is an excellent operational mode for the general detection of radiation because the production of one ion pair causes a complete discharge of the tube and generates a pulse. Consequently, geiger tubes are commonly employed for the general detection of the presence of radiation. However, since 1000 primary ions also generate one pulse, it is not possible to use these tubes to determine the amount of primary ionization produced by the ionizing particle or radiation.

In the reactor core, it is necessary to be able to discriminate between the heavy ionization caused by the charged particles generated by a neutron reaction and the ionization produced by the ever-present gamma radiation present in the reactor core. Consequently, almost all neutron detectors operate as ionization

chambers where the signal or pulse is directly proportional to the amount of primary ionization produced in the chamber.

There are three basic types of in-core neutron detectors. These include the fission chamber, the compensated-ion chamber, and the uncompensated-ion chamber. The fission chamber is a gas-filled ionization chamber that has the inside of the chamber casing plated with a thin layer of uranium-235. Some of the neutrons entering the chamber react with the U-235 atoms in the fission process. One of the resulting fission products, with an average kinetic energy of 80 MeV, enters the gas region where it produces very heavy ionization in the gas. It then becomes very easy to discriminate this single pulse from the ionization caused by the gamma radiation penetrating the chamber.

The fission chamber is used during the initial stages of reactor startup when there may be very few neutrons and a great deal of gamma radiation. This condition normally exists if the reactor has just been shut down. The fission chamber, like the (α, n) neutron source, is withdrawn into a shielded area as the reactor power is increased to prevent burnup of the fissile lining.

The compensated-ion chamber is actually a detector that is composed of two ion chambers. One chamber is filled with boron trifluoride (BF_3) gas. The neutrons entering the chamber react with the boron in an (n, α) reaction, and the resulting alpha particle causes considerable ionization in the chamber. The chamber with the BF_3 gas is sensitive to both neutrons and gamma radiation. The other chamber is filled with an inert gas with a low neutron absorption cross section so that it is sensitive to only gamma rays. The difference in the output of the two signals is proportional to the neutron level. The compensated-ion chamber is used from the intermediate power range to the full power range.

The uncompensated-ion chamber is a detector that is composed of a single BF_3 gas chamber. Since this chamber is sensitive to both neutrons and gamma radiation, it is used only during the high-power operation where the ionization caused by the high neutron flux in the (n, α) reaction overshadows that caused by the gamma radiation.

All reactors have some sort of in-core control system to regulate the fission rate and hence the reactor fission power level. There are two basic types of reactor control systems. One system employs the movement of fuel and/or moderating material, while the other uses the movement of neutron absorbers to control the system reactivity.

Insertion of fuel and/or moderator into the reactor core increases the reactivity of the reactor but these systems are difficult to design properly. Movement of the moderator alone does not usually have a great effect on the fission rate and, consequently, it is difficult to satisfy all the reactor control requirements with a system of this type. Movement of fuel into and out of the core does have a marked effect on the fission rate but a control system of this type is extremely difficult to design because of the problems associated heat generation and removal.

The control systems of most power reactors utilize some sort of absorber control. This system controls the fission rate by inserting or withdrawing a substance that has a high macroscopic neutron absorption cross section. This

respectively decreases or increases the system reactivity and the fission rate. While there is considerable heat generated in these rods, it is much smaller than that generated in a fuel element. A number of different absorber materials have been used in nuclear reactors, including hafnium, samarium, europium, gadolinium, cadmium, and indium, but the common absorber material is boron in the form of solid boron carbide (B_4C) pellets.

There are many kinds and shapes of absorber control rods employed in various reactors. The control rods commonly used in light-water power reactors are either *cruciform control rods* or the *finger control assemblies.* The cruciform rods are cross-shaped rods that slide between the fuel assumblies (see Fig. 5.9). The older PWR and all the BWR systems use this type of control rod. The newer PWR reactors use the finger control element assembly in which the control rods are inserted into guide tubes in several adjacent fuel elements. A typical control assembly of this type is shown in Fig. 3.14.

The control rods must be actuated from either the top or the bottom of the reactor core. Almost all of the PWRs use control-rod-drive systems that pull the control rods from the top of the reactor core with the use of electromagnets or magnetic jacks. In the event of an emergency, the magnet power is terminated and the rods fall into the core under the influence of gravity. This operation is called a *reactor SCRAM.* In a BWR, the top of the reactor is commonly filled with steam-drying equipment and consequently, the cruciform rods are driven from the bottom of the core. In the event of a reactor SCRAM, the rods are driven into the core by the potential energy stored in a hydraulic-accumulator-actuator.

The control rods essentially complete those components that are normally found in the reactor core except for structural material. In some power reactors, fertile material is loaded into certain regions of the core, and those regions are called *blankets.* This is done to improve the conversion ratio in the reactor.

COMPONENTS EXTERNAL TO THE REACTOR CORE. The core regions of almost all reactors are immediately surrounded by a neutron reflector. In thermal reactors, the reflector is composed of a moderating material while the reflector of a fast reactor is composed of heavy-mass material. The neutron reflector slows down and returns the leakage neutrons to the core of both of these systems, thereby reducing the critical mass and also reducing the maximum-to-average power ratio in the core. Reducing this ratio is desirable and improves the temperature or heat flux distribution in the reactor core.

Most power reactors employ a thermal shield or core barrel around the radial reflector. This shield attenuates the gamma and fast-neutron leakage fluxes so that they do not cause excessive heating and radiation damage in the containment vessel and the biological shield. Thermal shields are required in both fast and thermal power reactors. In a light-water reactor, the thermal shield is usually composed of alternate layers of water and steel.

The primary containment vessel is placed around the thermal shield and essentially contains the reactor coolant. This vessel, along with the rest of the

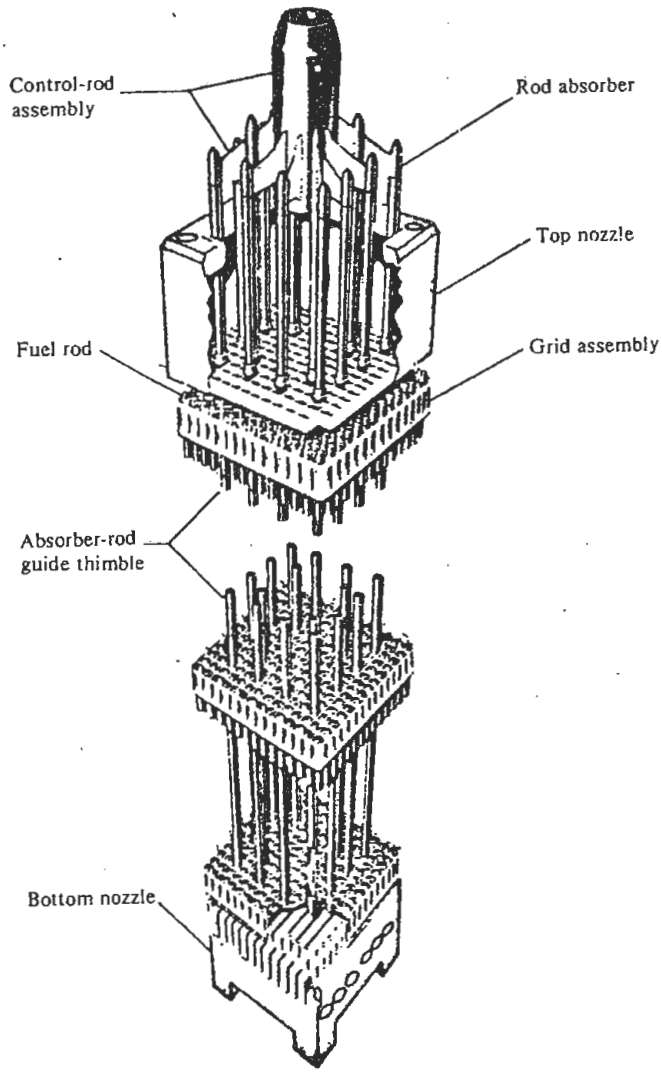


FIGURE 3.14
Cutaway of a typical pressurized-water, control-element assembly (CEA). (*Courtesy of Westinghouse Electric Corporation.*)

primary loop piping, provides the second barrier for the containment of fission products, with the fuel element cladding being the first barrier. In an LWR, the primary containment vessel is actually a large metallic pressure vessel. These vessels are usually fabricated from low-carbon steel, clad on the inside with stainless steel to minimize corrosion problems. The wall thickness of the pressure vessel normally runs from 8 to 10 in (20.3 to 25.4 cm) and the internal cladding

is nominally 0.5 in (1.27 cm) thick. These vessels range up to 21 ft in diameter and 40 to 60 ft (12 to 18 m) in length, with an overall weight of more than 700 tons (640 tonnes). They are so massive that they must normally be shipped by barge. A typical reactor pressure vessel and internals are shown in Fig. 3.15.

In the high-temperature, gas-cooled reactor, the containment vessel and biological shield are combined and constructed of prestressed concrete. This vessel is designed to contain the helium coolant, and all the heat-exchange equipment is located in the shield.

The biological shield is put around the reactor vessel to protect operating personnel from the radiation and neutrons emanating from the reactor core. This shield is normally constructed of concrete with a total thickness of 8 to 12 ft (2.4

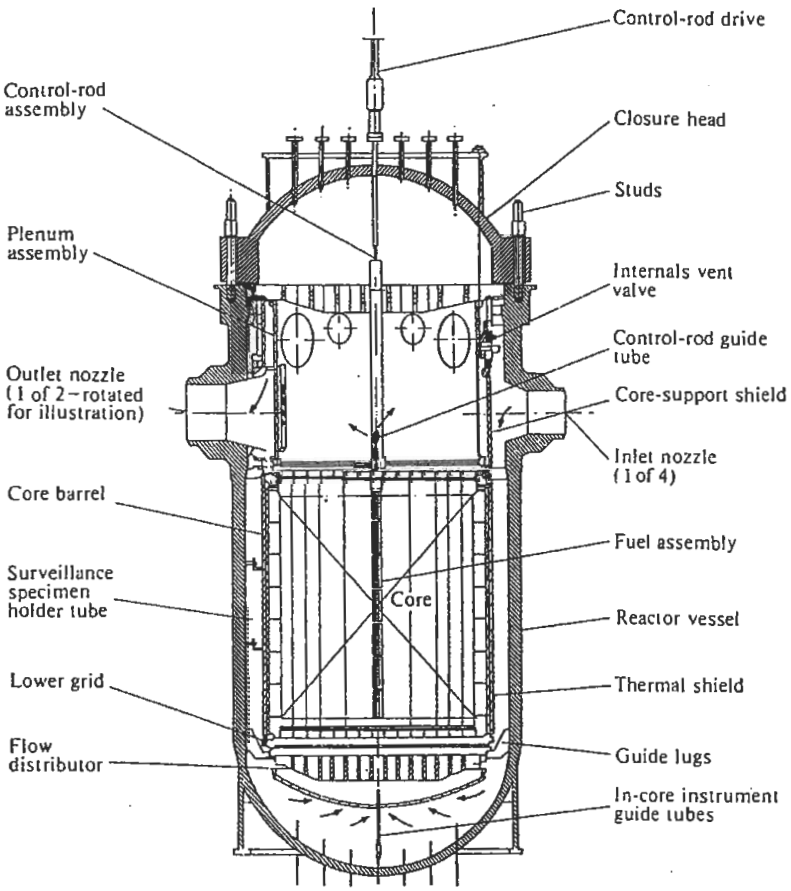


FIGURE 3.15
The primary pressure vessel of a pressurized-water reactor and its internals. (*From Steam: Its Generation and Use, 1972.*)

to 3.6 m). Heavy aggregate is sometimes used in the concrete to improve the gamma ray absorption and reduce the shield thickness. Heavy metals, such as lead or even depleted uranium, make excellent gamma shields, because of their high electron density, but they are not normally used in reactor shields because a light-mass material, such as the hydrated water in the concrete, is needed to attenuate the neutrons.

The final major system or component associated with a power reactor is the secondary containment system. This system is designed to contain all the coolant and fission products that might be released in the event of a sudden failure of the primary coolant system. In any LWR, this means that the secondary containment must hold all the steam generated from a sudden depressurization of the primary system plus that released from a simultaneous failure of the secondary cooling system of a PWR.

There are two basic types of secondary containment systems. One of these, like that shown in Fig. 3.16, uses a large volume to reduce the pressure to a value that can be tolerated by the secondary containment. These systems are the large spherical or cylindrical buildings (sometimes called *silos*) associated with many reactor installations. These structures are designed to be leaktight, and entry to and egress from the containment must take place through an air lock. This assures that the integrity of the secondary containment system is never violated. The

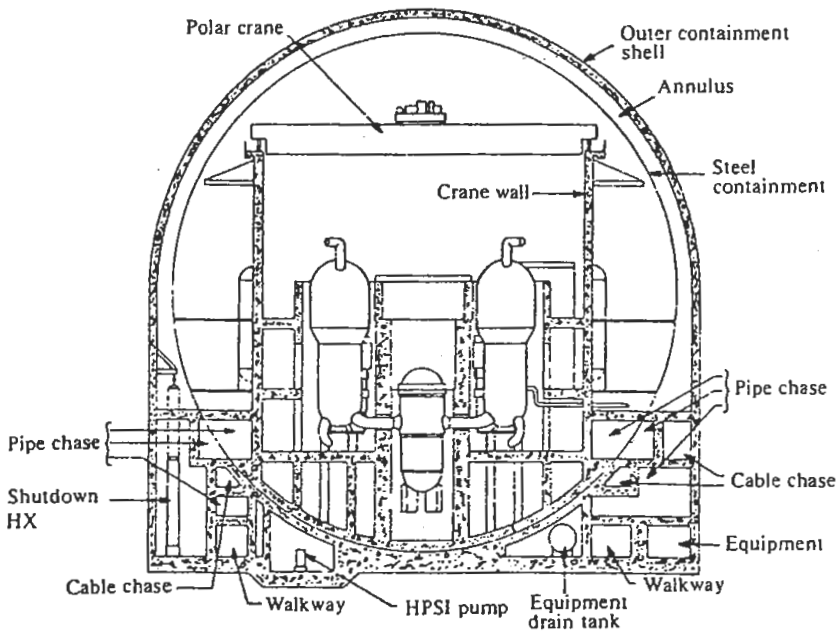


FIGURE 3.16
The spherical containment system for a pressurized-water reactor (PWR). (*From Proceedings of the American Power Conference, vol. 37, 1975.*)

LWR secondary containment vessels usually incorporate water sprays which are mounted high in the vessel to condense most of the steam generated in any accident and reduce the internal pressure as soon as possible.

The other type of secondary containment system is called the *vapor-suppression system.* In it, the primary pressure vessel and most of the piping are

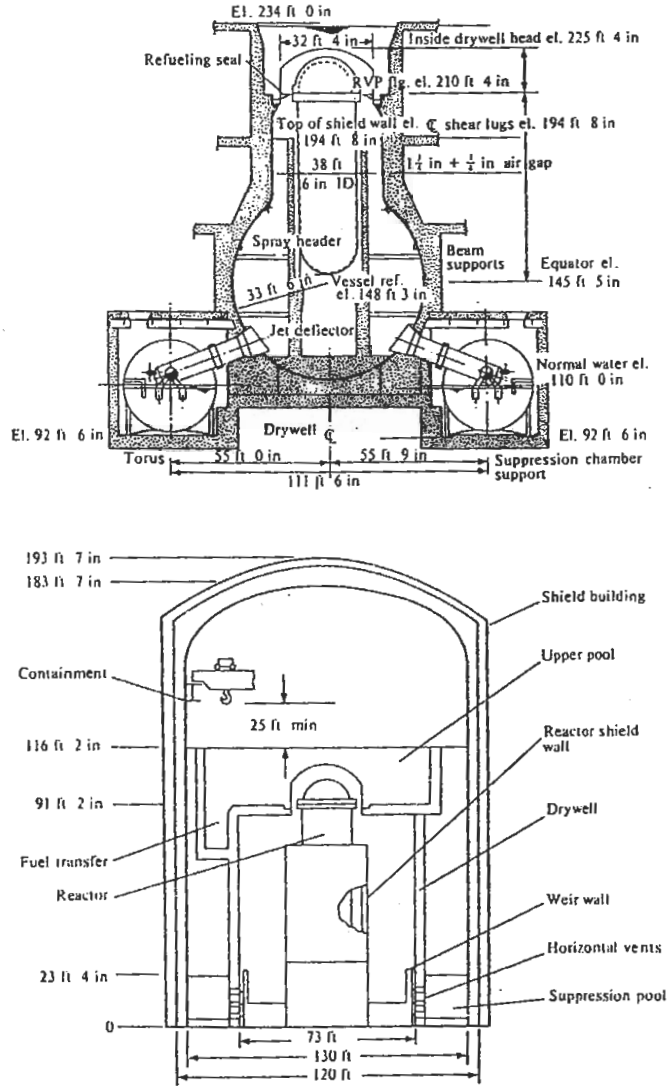


FIGURE 3.17
The water, vapor-suppression secondary containment system. (*From Proceedings of the American Power Conference, 1973.*)

contained in a "dry well" located within the biological shield. Any steam released from the primary system is forced to pass through a water moat (the General Electric system) or through a bed of ice (the Westinghouse system). These systems are designed to condense or "kill" most of the steam generated in a cooling-system failure and keep the maximum pressure in the external building to a minimum. Not only does the water and ice "kill" the steam, but it also removes a lot of the fission products that might be released with the steam from a failure of the cladding. Since the pressures generated outside the dry well are very low, the

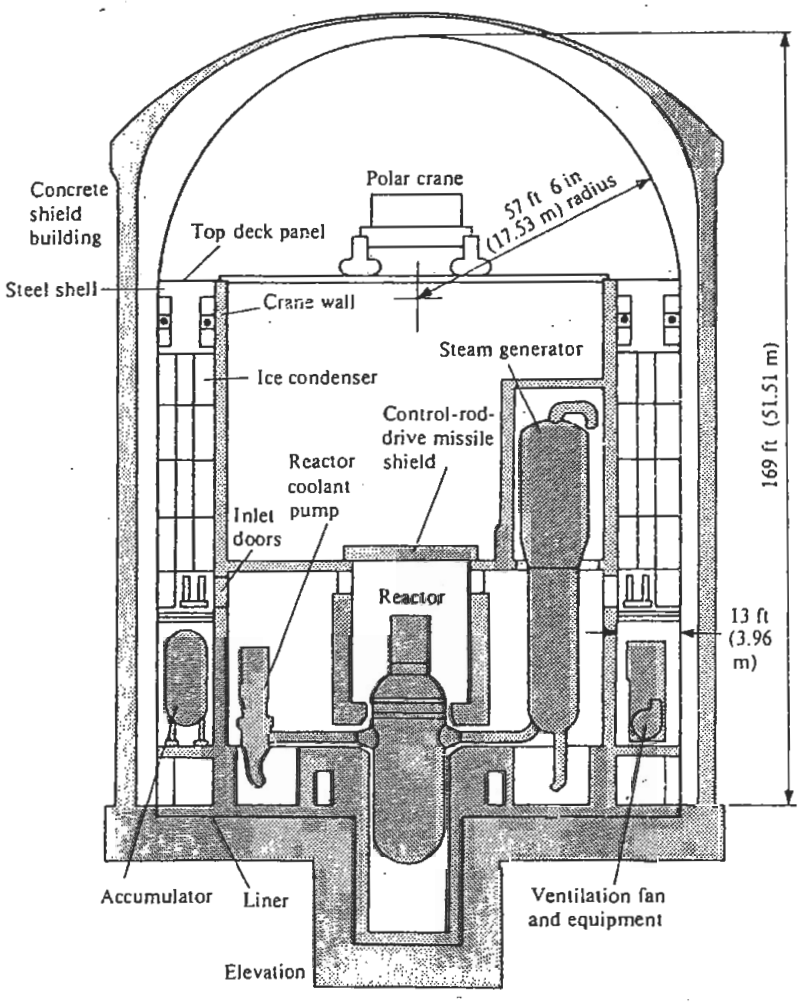


FIGURE 3.18
The ice, vapor-suppression secondary containment system. (*Courtesy of Westinghouse Electric Corporation.*)

balance of the secondary containment system is simply a leaktight building. Some of the vapor-suppression secondary containment systems are shown in Figs. 3.17 and 3.18.

LIST OF SYMBOLS

A	Ash fraction from the as-burned fuel analysis
$(A/F)_{A,G,D}$	Actual, gravimetric, dry, air–fuel ratio, kg air/kg fuel
$(A/F)_{A,G,W}$	Actual, gravimetric, wet, air–fuel ratio, kg air/kg fuel
$(A/F)_{A,M,D}$	Actual, molar, dry, air–fuel ratio, moles air/mole fuel
$(A/F)_{A,M,W}$	Actual, molar, wet, air–fuel ratio, moles air/mole fuel
$(A/F)_{T,G,D}$	Theoretical, gravimetric, dry, air–fuel ratio, kg air/kg fuel
$(A/F)_{T,G,W}$	Theoretical, gravimetric, wet, air–fuel ratio, kg air/kg fuel
$(A/F)_{T,M,D}$	Theoretical, molar, dry, air–fuel ratio, moles air/mole fuel
$(A/F)_{T,M,W}$	Theoretical, molar, wet, air–fuel ratio, moles air/mole fuel
B	Reactor buckling, 1/m
C	Carbon mass fraction, kg C/kg fuel
C_b	kg of carbon burned to CO and CO_2/kg of fuel burned
C_r	kg of unburned carbon in the refuse pit/kg of fuel burned
C_{ult}	Carbon mass fraction from the as-burned ultimate fuel analysis
e	Base of natural logarithms = 2.718
E	Energy, J
E_H	Upper energy limit for neutron energy group, MeV or eV
E_L	Lower energy limit for neutron energy group, MeV or eV
f	Isotopic abundance = atoms of isotope/atom of element
HHV	Higher heating value, kJ/kg fuel
HHV_m	Gravimetric higher heating value, kJ/kg fuel
H_2	Hydrogen mass fraction, kg H_2/kg fuel
i	Electric current, A
k	Reactor multiplication factor
l	Neutron lifetime, s
L	Diffusion length, m
M	Moisture mass fraction, kg H_2O/kg fuel
$\bar{n}$	Neutron density, neutrons/m^3
N	Number of atoms of a particular isotope
N_{fuel}	Number of fuel atoms
N_2	Nitrogen mass fraction, kg N_2/kg fuel
O_2	Oxygen mass fraction, kg O_2/kg fuel
P	Thermal power of the reactor, MW_{th}
Q	Energy release from a chemical reaction, kJ/kg · mol
R	Refuse mass fraction, kg R/kg fuel
R	Electrical resistance, ohms
S	Sulfur mass fraction in the fuel, kg S/kg fuel
t_r	Reactor period, s
T	Temperature, K

$T_{M,K}$	Moderator temperature, K
$T_{M,R}$	Moderator temperature, °R
v	Electrical potential, volts
V	Volume, m^3
$\bar{V}$	Neutron velocity, m/s
$\bar{V}_{ave}$	Average thermal neutron velocity, m/s
$\bar{V}_{mp}$	Most probable thermal neutron velocity, m/s
Z_C	Moles of carbon/mole of fuel
Z_H	Moles of elemental hydrogen/mole of fuel
Z_i	Moles of the ith element/mole of fuel
Z_N	Moles of elemental nitrogen/mole of fuel
Z_O	Moles of elemental oxygen/mole of fuel
Z_S	Moles of sulfur/mole of fuel
ε	Fast fission factor
η	Average number of neutrons/fuel absorption
ν	Average number of neutrons/fission
λ	Mean free path for the neutrons, neutron · m/reaction $\equiv 1/\Sigma$
ρ	Reactivity of the reactor core $\equiv (k-1)/k$
σ_i	Microscopic neutron cross section, ith reaction · barn/(atom)(neutron)
Σ_i	Macroscopic neutron cross section, ith reactions/neutron · m
τ	Fermi age, m^2
ϕ	Neutron flux, neutrons/m^2 · s
Φ	Average neutron flux, neutrons/m^2 · s
Φ_f	Average fast-neutron flux, neutrons/m^2 · s
Φ_{th}	Average thermal-neutron flux, neutrons/m^2 · s
ω	Humidity ratio of the atmospheric air, kg water vapor/kg dry air

PROBLEMS

3.1. Calculate the theoretical air-fuel ratios, in kg air/kg fuel, for the following fuels:
- (*a*) Bates County, Missouri, coal with $M = [7; 9.5; 12]$ percent and $A = [11; 13; 15]$ percent
- (*b*) Musselshell County, Montana, coal with $M = [2; 5; 8]$ percent and $A = [4; 7; 10]$ percent
- (*c*) Tulsa County, Oklahoma, coal with $M = [2; 5; 8]$ percent and $A = [4; 7; 10]$ percent
- (*d*) [Methyl; ethyl; propyl; butyl] alcohol
- (*e*) An LPG which is composed of [30; 40; 50; 60; 70] percent propane with the balance being butane
- (*f*) [Illinois; Indiana; Kansas; Kentucky; Missouri] natural gas
- (*g*) [Anthracite-producer; Blast-furnace; Coke-oven; Water; Illuminating; Carbureted-water] gas

3.2. In a pulverized-coal boiler, the amount of unburned carbon must be calculated separately from the refuse analysis of the ashpit and from the flyash carried up the exhaust duct in the flue gas and removed in the precipitator. Calculate the total

quantity of unburned carbon per kilogram of input coal (C_r) from the following data:

Ash content of the fuel (from the ultimate analysis) = 12.5 percent
Ashpit refuse fraction = 0.1 kg refuse/kg coal
HHV of ashpit refuse = [5000; 6000; 7000; 8000; 9000] kJ/kg
HHV of precipitator refuse = [8000; 9000; 10,000; 11,000; 12,000] kJ/kg

3.3. If Indiana County, Pennsylvania, coal with $M = 3$ percent and $A = 8.5$ percent is burned with [10; 12; 14; 16; 18] percent excess air, calculate the actual air fuel ratio and the ideal orsat analysis (no CO and no unburned carbon). Also, determine the theoretical orsat analysis if the HHV of the refuse is 5500 kJ/kg and the % CO in the dry flue gas is [0.2; 0.4; 0.6; 0.8; 1.0] percent of the dry flue gas.

3.4. For the system selected in Prob. 3.3, find the generation rate, in short tons per hour, of sulfur dioxide, carbon dioxide, and carbon monoxide if the coal is burned in a 1000-MW_e power plant with a heat rate of 8630 Btu/kWh.

3.5. Repeat Prob. 3.3 for a dilution coefficient of [1.15; 1.2; 1.25; 1.3; 1.35] if the % CO in the dry flue gas is 0.86 and the HHV of the refuse is [2500; 3000; 3500; 4000; 4500] kJ/kg.

3.6. For the condition in Prob. 3.5, find the generation rate, in short tons per hour, of sulfur dioxide, carbon dioxide, and carbon monoxide if the coal is burned in a 1000-MW_e power plant with a thermal efficiency of 38.2 percent.

3.7. The Bruce Mansfield plant of the Pennsylvania Power Company is a three-unit, coal-fired system with a total output of 2757 MW_e (three 919-MW_e units). Assume that the system burns Elk County, Pennsylvania, coal with moisture and ash fractions of 0.03 and 0.09, respectively. The heat rate of the plant is [8800; 8900; 9000; 9100; 9200] Btu/kWh and the higher heating value of the refuse, in kJ/kg, and the percent CO_2, O_2, and CO in the orsat analysis are respectively given as follows: [(1058 kJ/kg, 13.77%, 4.4%, 1.24%); (2485 kJ/kg, 12.78%, 5.73%, 0.86%); (3068 kJ/kg, 13.53%, 4.80%, 0.98%); (2838 kJ/kg, 12.97%, 5.36%, 1.08%)]. Find:

(*a*) The percent excess air
(*b*) The maximum combustion-air rate through the plant, in ton/min of full-power operation
(*c*) The amount of SO_2 generated, in ton/h of full-power operation

3.8. A coke-oven gas has the following molar composition: $CO_2 = 1$ percent, CO = 8 percent, $CH_4 = 25$ percent, $H_2 = [44; 46; 48; 50; 52]$ percent, with the balance being nitrogen. Calculate the actual air-fuel ratio in lbm air/lbm gas and determine the ideal orsat analysis (no CO) when the gas is burned with [12; 15; 18; 21; 24] percent excess air.

3.9. Illinois natural gas is burned in a 2000-MW_{th} power plant with a dilution coefficient of [1.1; 1.15; 1.2; 1.25; 1.3] and a CO mole percentage in the dry flue gas of [0.3; 0.4; 0.5; 0.6; 0.7] percent. Determine the theoretical orsat analysis, the combustion-air rate through the furnace, in ton/min, and the tons of CO generated during each hour of full-power operation.

3.10. A producer gas with the following molar composition is burned in a furnace: 21% CO, 31% H_2, and 48% N_2. The orsat analysis of the flue gas gives [(8.6% CO_2, 6.4% O_2, 0.2% CO); (8.89% CO_2, 4.32% O_2, 1.46% CO); (8.59% CO_2, 5.71% O_2, 0.76% CO); (8.80% CO_2, 4.88% O_2, 1.14% CO); (7.26% CO_2, 8.33% O_2, 0.44% CO)]. If this furnace supplies heat to a 50-MW_e power system with a thermal efficiency of [32; 34; 36; 38; 40] percent, find the dry air rate, in ton/day of full-power operation.

3.11. A natural gas with following composition is burned in a furnace: $CO_2 = 2.3$ percent, $N_2 = 0.4$ percent, with the balance methane. The orsat analysis of the flue gas reads: [(8.5% CO_2, 5.6% O_2, 0.1% CO); (9.12% CO_2, 4.16% O_2, 0.38% CO); (9.46% CO_2, 2.19% O_2, 1.36% CO); (9.33% CO_2, 3.08% O_2, 0.88% CO); (9.20% CO_2, 3.84% O_2, 0.64% CO)]. Find the actual dry-air rate, in tons of air per day of full-power operation, if this gas is burned in a 100-MW_e power plant with a heat rate of [8500; 8650; 8800; 8950; 9100] Btu/kWh.

3.12. If 1 kg of propanol (propyl alcohol, C_3H_7OH) with a HHV of 33,492 kJ/kg is used as a fuel, find the ideal orsat analysis and the energy released in an ideal (no oxygen) combustion process if it is burned with:
(*a*) A dilution coefficient of [0.95; 0.9; 0.85; 0.8; 0.75; 0.7; 2/3].
(*b*) A dilution coefficient of [0.65; 0.6; 0.55; 0.5; 0.45; 0.4; 1/3].

3.13. For the conditions of Prob. 3.12, find the energy release in Btu/gal of propanol if the specific gravity of the liquid is 47°Bé.

3.14. Determine the temperature, in °C, of a block of graphite containing thermal neutrons with a/an ["most probable"; "average"] velocity of [2400; 2600; 2800; 3000; 3200; 3400; 3600; 3800; 4000] m/s. Also, evaluate the other velocity (either the "average" or "most probable") if the energy distribution of the neutrons is a Maxwell-Boltzmann distribution.

3.15. Calculate the average thermal absorption, fission, and scattering neutron cross sections for [Th-232; U-233; U-234; U-235; U-238; Pu-239] for a moderator temperature of [300; 400; 500; 600; 700; 800; 900; 1000] °F. Use the cross-section data from Table 3.1 and assume that σ_S for U-233 is 10 barns.

3.16. Assuming that the materials in Prob. 3.15 are in the form of ThO_2, UO_2, or PuO_2, and are composed of 100 percent of the isotope of interest, calculate the average thermal macroscopic fission, radiative-capture, absorption, scattering, and total neutron cross sections. Assume the density of each oxide is 10,000 kg/m^3. Do this only for the isotopes assigned in Prob. 3.15.

3.17. The University of Missouri-Columbia has one of the highest-powered research reactors in the country and operates at a power of 10 MW_{th}. If the average water and beryllium-island temperature is [40; 45; 50; 55; 60] °C and the fuel loading is 6 kg of uranium-235, find the average thermal-neutron flux in the reactor fuel at a thermal power of [2; 4; 6; 8; 10] MW.

3.18. A 3800-MW_{th} pressurized-water power reactor operates at an average thermal flux of [5; 7; 9; 11; 13] $\times 10^{17}$ neutrons/$m^2 \cdot s$ and the average water temperature is 343°C (650°F). The reactor is fueled with uranium dioxide (UO_2) that is enriched to [2.1; 2.3; 2.5; 2.7; 2.9] percent. Find the mass of uranium dioxide in the reactor

3.19. A boiling-water reactor power plant produces 1200 MW_e with a heat rate of 10,200 Btu/kWh. If the system is fueled with [2.0; 2.2; 2.4; 2.6; 2.8] percent enriched uranium in the form of uranium dioxide (UO_2) and operates at a saturation pressure of 8.5 MPa with an average thermal-neutron flux of [2; 4; 6; 8; 10] $\times 10^{1}$ neutrons/$m^2 \cdot s$, find the total loading of U-235 and UO_2, in tons. If the UO_2 has a density of 9600 kg/m^3, find the total volume of fuel in the reactor core, in ft^3, and determine the volume fraction of the fuel in the core if the core is a cylinder 4 m long and 4 m in diameter.

3.20. If boiling light water has a mean density of [700; 750; 800; 850; 900] kg/m^3 calculate the total average distance traveled by a thermal neutron in an infinit

medium (no leakage) and the average distance that a thermal neutron travels before some event (absorption or scattering) occurs, and determine the average thermal-neutron lifetime if the water is at [250; 275; 300; 325; 350]°C.

3.21. Repeat Prob. 3.20 for graphite with a density of [1200; 1300; 1400; 1500; 1600] kg/m^3 and an operating temperature of [1250; 1300; 1350; 1400; 1450]°F.

3.22. Repeat Prob. 3.20 for beryllium oxide (BeO) with a density of [2600; 2700; 2800; 2900; 3000] kg/m^3 and an operating temperature of [1040; 1140; 1240; 1340; 1440]°F.

3.23. Calculate the total neutron reaction rate, the absorption rate, the capture rate, the scattering rate, and the thermal power in W/cm^3 of uranium dioxide (UO_2). The density of uranium dioxide is 10,300 kg/m^3, the moderator temperature is [600; 650; 700; 750; 800]°F, and the average thermal-neutron flux is [4; 5; 6; 7; 8] $\times 10^{17}$ neutrons/m$^2 \cdot$ s. Assume that the uranium is natural uranium and the total fuel volume is 10 m^3. In addition to the quantities asked for earlier, determine the average neutron lifetime ($1/\Sigma_a V_{ave}$) and the breeding ratio [(U-238 abs.+ U-234 abs.)/(U-235 abs.)].

3.24. 100,000 thermal neutrons are inserted into an infinite lattice of uranium nitride (U_3N_4) at a temperature of [250; 300; 350; 400; 450]°C using uranium with an enrichment (e) of [0.71; 1.0; 1.5; 2.0; 2.5] percent. Assume that the ratio of U-234 to U-235 atoms remains constant in the enrichment process and that the density of U_3N_4 is 9,500 kg/m^3. Find:

(a) The average macroscopic scattering, absorption, fission, and total neutron cross sections

(b) The average neutron lifetime, $1/\Sigma_a \bar{V}_{ave}$

(c) The number of original neutrons absorbed by each of the three uranium isotopes and by the nitrogen atoms

(d) The multiplication factor for the lattice, assuming the fission neutrons are produced at thermal energy

(e) The breeding/conversion ratio for this lattice

Assume that the uranium isotopic abundance values (f) may be calculated as follows:

$$f_{235} = \frac{238e}{235}$$

$$f_{234} = \frac{0.00006 f_{235}}{0.0072}$$

$$f_{238} = 1 - f_{234} - f_{235}$$

3.25. A 0.325-in-outside-diameter by 0.500-in-long reactor fuel pellet is composed of uranium dioxide with an average density of 10,300 kg/m^3. The uranium is enriched to an enrichment of [2.0; 2.2; 2.4; 2.6; 2.8] percent and the pellet is exposed to an average thermal-neutron flux of [5; 6; 7; 8; 9] $\times 10^{17}$ neutrons/m$^2 \cdot$ s. If the average moderator temperature is 650°F, find the thermal power in the fuel pellet, in kW_{th}.

REFERENCES

Bonilla, C. F. (ed.): *Nuclear Engineering*, McGraw-Hill, New York, 1957.

De Lorenzi, Otto (ed.): *Combustion Engineering*, Combustion Engineering Superheater, New York, 1952.

Dillo, C. C., and E. P. Nye: *Thermal Engineering*, International Textbook Company, Scranton, Pa., 1963.

Foster, A. R., and R. L. Wright, Jr: *Basic Nuclear Engineering*, Allyn and Bacon, Boston, 1973.

Glasstone, S., and A. Sesonske: *Nuclear Reactor Engineering*, D. Van Nostrand Company, New York, 1963.

Lish, K. C.: *Nuclear Power Plant Systems*, Industrial Press, New York, 1972.

Nuclear News, a publication of the American Nuclear Society, November 1988.

Potter, P. J.: *Steam Power Plants*, The Ronald Press, New York, 1972.

Proceedings of the American Power Conference, vol. 35, pp. 110–124, Illinois Institute of Technology, Chicago, 1973.

Proceedings of the American Power Conference, vol. 36, pp. 70–134, Illinois Institute of Technology, Chicago, 1974.

Proceedings of the American Power Conference, vol. 37, pp. 113–121, Illinois Institute of Technology, Chicago, 1975.

Skrotski, B. G. A., and W. A. Vopat: *Power Station Engineering and Economy*, McGraw-Hill, New York, 1960.

Steam: Its Generation and Use, 38th ed., Babcock and Wilcox Company, New York, 1972.

CHAPTER 4

FOSSIL-FUEL SYSTEMS

4.1 INTRODUCTION

This chapter presents a more detailed description and the principles of operation of fossil-fuel, steam-generating systems and their associated auxiliary equipment. Specifically, this material covers the fluid machinery needed in the operation of the steam generator, including pumps and fans, the different types of combustion systems, and, finally, the types of boilers and the operational problems associated with them.

4.2 FLUID-MOVING SYSTEMS

4.2.1 Introduction

Two basic fluid moving systems are employed in almost all steam-generator systems. These are the pumps needed to supply the working fluid to the steam generator and the air compressors or fans needed to supply combustion air to the furnace. An important parameter for these systems is the mechanical efficiency η_{mech}, which is a measure of the machine's ability to transmit mechanical work to the fluid flowing through the device. The relationship for the mechanical efficiency for fluid-moving systems is given by:

$$\eta_{mech} = \frac{\text{ideal work input}}{\text{actual work input}} \qquad (4.1a)$$

The relationship for a driven machine is the reciprocal of the equation for the mechanical efficiency of a prime mover where the fluid is driving the machine.

For a prime mover, such as a turbine, the mechanical efficiency is:

$$\eta_{mech} = \frac{\text{actual work output}}{\text{ideal work output}} \tag{4.1b}$$

Since the boiler feed pumps handle relatively incompressible liquids and the fans operate over a very narrow pressure range, both of these systems can be assumed to pump an incompressible fluid. For geometrically similar centrifugal machines, operating at the same efficiencies, the pressure rise Δp across the device, the volumetric flow rate Q through the device, and the input power requirements P are related by the following equations:

$$Q = K_1 N D^3 \tag{4.2}$$

$$\Delta p = K_2 \rho N^2 D^2 \tag{4.3}$$

$$P = K_3 Q \Delta P = K_4 \rho N^3 D^5 \tag{4.4}$$

where ρ is the fluid density, N is the angular velocity, and D is the diameter of the impeller. These relationships are used to develop the so-called fan or pump laws.

4.2.2 Boiler Feed Pumps

The boiler feed pump supplies high-pressure liquid water to the boiler and commonly operates over a wide range of pressures. The centrifugal pump is commonly used for this purpose and the performance of these systems is usually expressed in terms of the *specific speed* N_S of the pump. The specific speed of a given pump is defined as the angular velocity, in r/min, of a geometrically similar pump, reduced in size, which will produce a volumetric flow rate of 1 gal/min against a total pressure rise of 1 lb/in^2. The specific speed of a given pump can be determined from a known volumetric flow rate of Q gal/min over a pressure rise of Δp lb/in^2 at an angular velocity of N r/min:

$$N_S = \frac{NQ^{1/2}}{(\Delta p^3)^{1/4}} \tag{4.5}$$

The general relationship between the shape of an impeller and the specific speed of the pump is shown in Fig. 4.1.

There is a certain condition that should be avoided during the operation of any liquid pump. This condition is called *cavitation.* Cavitation occurs when the liquid pressure on the surface of the impeller falls below the vapor pressure of the fluid. This causes vapor bubbles to form on the surface of the impeller and these bubbles collapse as they move into a region of higher pressure. The sudden collapse of these bubbles causes severe impact loads on the impeller and this action can cause severe erosion of the impeller surface. Not only can cavitation

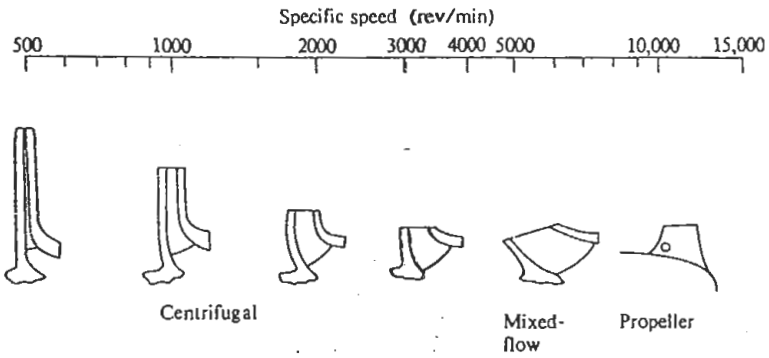


FIGURE 4.1
The variation of the specific speed of a pump with impeller shape. (*From Skrotzki and Vopat, 1960.*)

physically damage the pump but it also drastically lowers the mechanical efficiency of the pump and makes it noisy.

Cavitation can be alleviated by increasing the fluid-pressure at the pump inlet. This pressure, minus the vapor pressure of the liquid, is called the *net positive suction head* or *NPSH*. The minimum value of the NPSH to assure cavitation-free operation is commonly specified by the pump manufacturer.

Some of the boiler feed pumps are very large components, with input power requirements of more than 60,000 hp. A list of some high-pressure, high-power pumps is given in Table 4.1. A cross-sectional view of a typical, multistage feed pump is shown in Fig. 4.2. These large boiler feed pumps are usually driven by steam turbines.

TABLE 4.1
Large boiler feed pumps

Power Station	Pump speed, r/min	Flow rate, gal/min	Discharge pressure, lb/in^2	Pump power, hp
Glen Lyn 6	5500	3,200	2452	5,650
Muskingham River 4	5500	3,200	2503	5,650
Clinch River 3	5500	3,200	2490	6,300
Breed 1	3600	7,200	4500	21,600
Philip Sporn 5	3500	3,600	4500	10,800
Big Sandy 1	5500	4,400	2868	8,500
Tanners Creek 4	4500	8,900	4575	26,800
Cardinal 1 and 2	4560	9,500	4695	29,100
John E. Amos 1 and 2	4840	12,550	4570	37,500
Gen. James M. Gavin 1 and 2	4160	21,600	4625	63,000

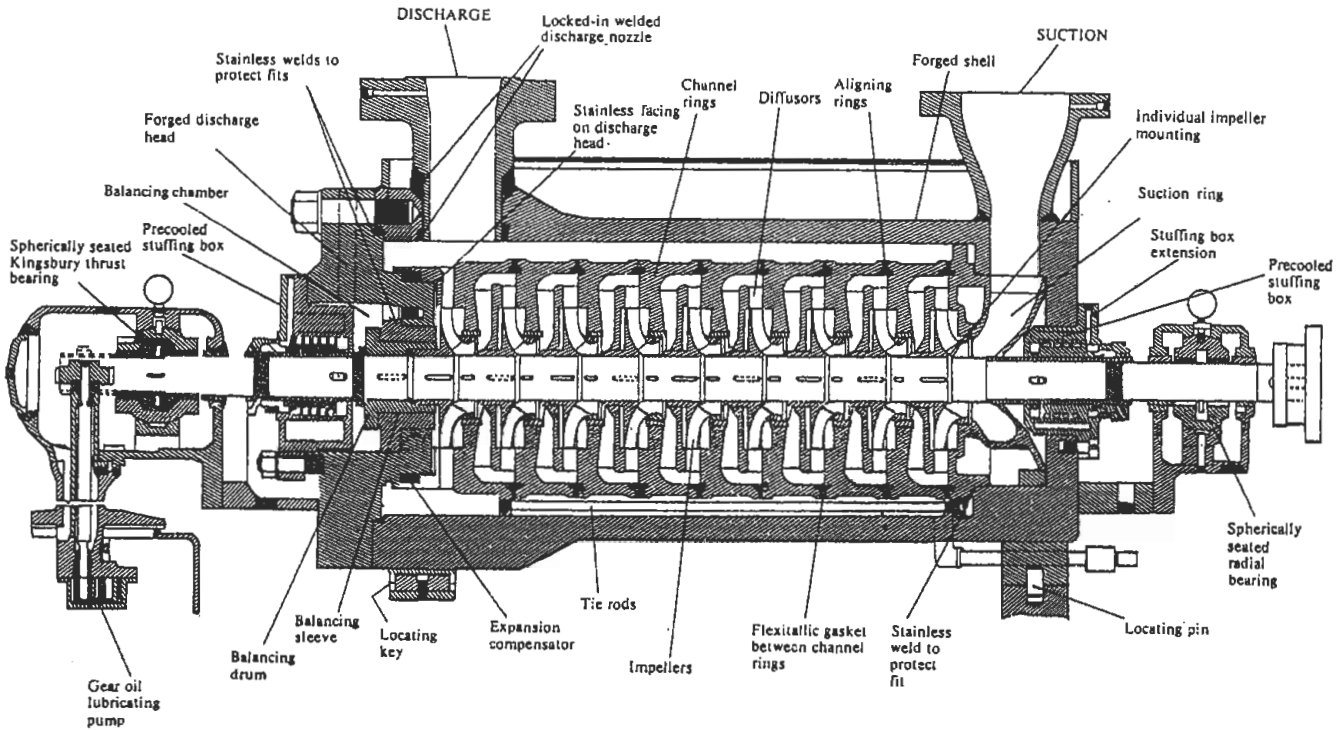


FIGURE 4.2
Cross section of a large boiler feed pump. (*Courtesy of Ingersoll-Rand Company.*)

4.2.3 Combustion Air Systems

There are two general types of air compressors—positive-displacement air compressors and dynamic air compressors. In the positive-displacement compressor, the impeller or piston forcibly displaces the air volume to compress it. A common positive-displacement air compressor is the reciprocating compressor, which is characterized by relatively low capacity, high head, and pulsating flow. These machines are commonly used to supply high-pressure station air for control and other purposes but they are not normally used to supply combustion air.

The rotary air compressors are also positive-displacement machines and include the sliding-vane air compressor, the Roots blower, the screw compressor, etc. These machines are characterized by moderate pressure rises, medium capacity, and continuous flow. Rotary compressors are used to supply air to supercharge engines but they are not widely used to supply combustion air to large combustion systems.

In the dynamic air compressor, the high-velocity impeller transfers momentum from the impeller to the air. The two categories of dynamic air compressors are the axial-flow and centrifugal compressors. These machines are characterized by relatively high capacity, low head, and steady flow. The axial-flow compressors are commonly used in the gas turbine and turbojet engines and they are becoming increasingly popular for large combustion systems. Centrifugal compressors, commonly called *fans*, are widely used to supply the large volumes of combustion air for fossil-fuel combustion in power plants.

Combustion-air fans usually have very high flow rates but total pressure rises of less than 15 to 20 kPa (2 to 3 psia). The three types of centrifugal fans include those with backward-inclined blades, those with radial blades, and those with forward-inclined blades. The different blade orientations give the fans different operating characteristics. A comparison of the operating characteristics of the fans is given in Table 4.2.

Since the pressure rise across any fan is relatively small, the air flow through the fan can be assumed to be incompressible. In this case, the volumetric flow rate Q, the pressure rise across the fan Δp, and the power requirement of the fan,

TABLE 4.2
Operating characteristics of centrifugal fans

Quantity	Backward-inclined blades	Radial blades	Forward-inclined blades
Size of impeller	Medium	Medium	Medium
Mechanical efficiency	High	Average	Average
Stability	Good	Good	Poor
Fan speed, r/min	High	Average	Low
Impeller—tip speed	High	Medium	Low
Resistance to erosion	Medium	Good	Poor

P, vary according to the so-called fan laws. These laws are essentially the same as Eqs. (4.2), (4.3), and (4.4) except that the impeller diameter is constant.

Some of the newer fossil-fuel combustion systems are using very large axial-flow fans to supply combustion air to the furnace. The Martins Creek Power Station of the Pennsylvania Power and Light Company has two 820-MW_e coal-fired units that employ axial-flow fans for both the forced-draft and the induced-draft fans. Axial-flow fans are used instead of centrifugal fans because the gas flow rate can be regulated by varying the pitch of the fan blades. This permits these units to operate at much higher efficiencies than comparable centrifugal units operating at off-load conditions. Figure 4.3 shows the single-stage, forced-

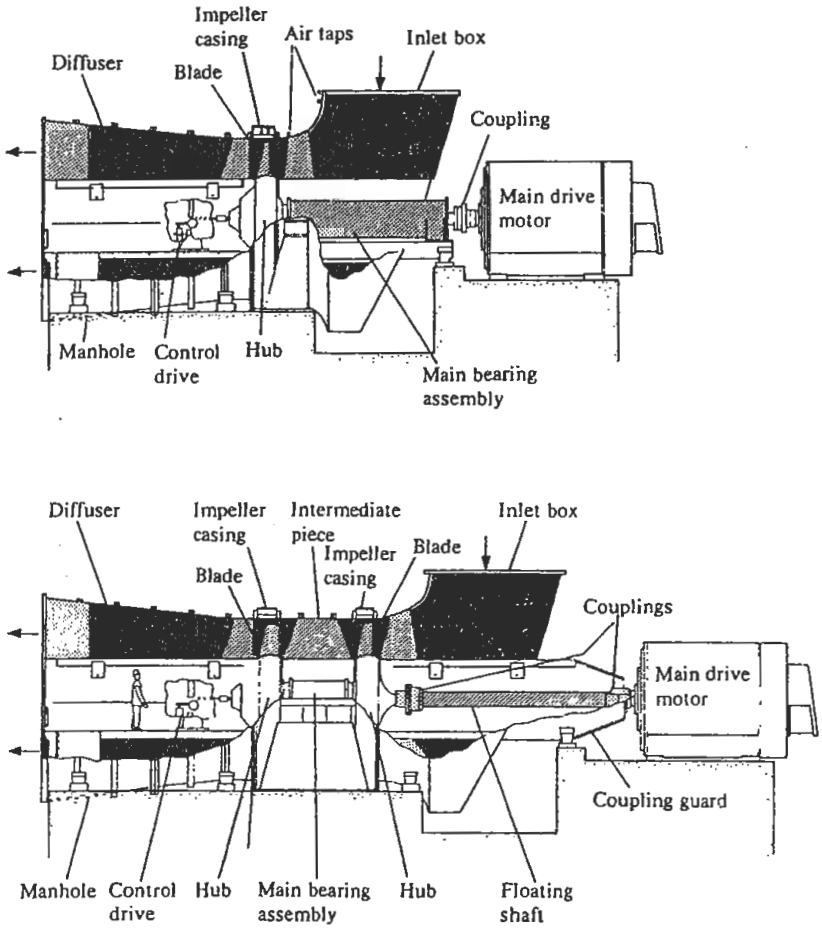


FIGURE 4.3
A single-stage, 5000 hp, forced-draft fan and a two-stage, 12,000-hp, induced-draft fan. (*From Editors of Power Magazine, 1976.*)

draft fan and the two-stage, induced-draft fan used in the Martins Creek station. This station has two forced-draft and two induced-draft fans.

4.2.4 Draft Systems

The air required for combustion can be supplied by a natural-draft system, by a mechanical-draft system, or, as is usually the case, by a combination of these two systems. In the natural-draft system, the air flow is produced by a driving force which is established by the difference in the specific weights of the stack exhaust gas and the atmospheric air. The driving force is equal to the product of the specific-weight difference and the effective height of the stack or chimney. The driving force is balanced by the pressure drop in the draft system, the furnace, and the exhaust system.

The air-flow rate in a natural-convection system can be increased by raising the exhaust-gas temperature and/or by increasing the stack height. An increase in exhaust-gas temperature decreases the gas density (specific weight), thereby increasing the driving heat, but it also increases the system heat losses, which is undesirable. Increasing the stack height not only increases the gas-flow rate but it improves the dispersion of exhaust products. Stack heights from 700 to 1200 ft (210 to 365 m) are fairly common. Despite the use of very tall stacks or chimneys, the natural-draft systems cannot normally supply sufficient air flow for good combustion. Consequently, some sort of mechanical-draft system is normally required.

There are two basic types of mechanical-draft systems—the forced-draft (f-d) system and the induced-draft (i-d) system. In the forced-draft system, the fan pumps only combustion air into the furnace. The forced-draft fan pumps only cold, clean combustion air, and the resulting positive pressure in the combustion chamber improves the gas-side convection coefficient. Unfortunately, the positive pressure in the furnace produces a major problem because any leakage from the furnace is likely to cause the combustion products to be released in areas where personnel may be working. This is a major drawback of the forced-draft system when it is used alone.

The minimum ideal mass flow rate of the forced-draft fan is equal to the product of the actual mass air-fuel ratio and the fuel rate:

$$\text{Minimum mass rate for f-d fan} = (\text{fuel rate})\left(\frac{A}{F}\right)_{A,G,W} \tag{4.6}$$

The gravimetric air–fuel ratio used in Eq. (4.6) includes the moisture in the air and it is normal practice to increase this rate by 20 to 40 percent to account for leakage from the supply ducts. If centrifugal fans are used in the forced draft system, they are usually high-speed fans with backward-curved blades.

Many large positive-pressure or "pressurized" furnaces use another large fan along with the force-draft fan. This fan, called a *gas recirculation fan*, draws combustion gas from the exhaust ductwork and pumps it back into the combustion chamber. This is done to cool the chamber and control the rate of energy

deposition on the heat-transfer surfaces in the boiler. This procedure also provides some control of the nitrogen oxide (NO_x) emissions. This fan pumps relatively hot exhaust gas which may contain a lot of flyash but it handles only a small portion of the total exhaust gas flow.

In the induced-draft system, the fan draws combustion products from the combustion chamber and discharges them into the stack. This produces a negative pressure in the combustion chamber, eliminating the leakage problem. This fan, like the exhaust gas recirculation fan, handles hot, ash-loaded combustion products. The high gas temperature drastically increases the volumetric flow rate through the i-d fan and the ash can cause a severe erosion problem and/or a vibration problem due to the deposition of ash on the fan blades. For a given combustion rate in the furnance, the mass flow rate through the induced-draft fan is around 10 percent higher than the mass flow rate through the forced-draft fan. Theoretically, for each kilogram of fuel burned the forced-draft pumps on the actual air-fuel ratio, but the induced-draft fan pumps the actual air-fuel ratio plus all of the 1 kg of fuel except for the refuse fraction, R:

$$\text{Minimum mass rate for i-d fan} = (\text{fuel rate})\left[\left(\frac{A}{F}\right)_{A,G,W} + 1.0 - R\right] \tag{4.7}$$

As in the case for the forced-draft fan, the flow rate given by Eq. (4.7) is a minimum and should be increased by 20 percent or so to account for infiltration due to leakage into the furnace and ductwork.

The volumetric flow rates for the forced-draft and induced-draft fans can be obtained by dividing the mass flow rates from Eqs. (4.6) and (4.7) by the inlet gas density for each fan:

$$\text{Volumetric flow rate} = \frac{\text{mass flow rate}}{\text{inlet gas density}}$$

$$= (\text{mass flow rate})\left(\frac{R_u T}{p(\text{MW of gas})}\right) \tag{4.8}$$

For the f-d fan, Eq. (4.8) should be modified to consider both the air and the water vapor separately because they have such different molecular weights (MW) (18 to 29). If ω is the humidity ratio of the atmospheric air, Eq. (4.8) becomes:

$$\text{Volumetric flow rate for f-d fan} = Q_{FD}$$

$$Q_{FD} = (\text{fuel rate})\left(\frac{A}{F}\right)_{A,G,D}\left(\frac{R_u T}{p}\right)\left(\frac{1}{28.97} + \frac{\omega}{18.016}\right) \tag{4.9}$$

The volumetric flow rate through the i-d fan is calculated from Eq. (4.8) but a difficult problem encountered is to determine the molecular weight of the flue gas. Sometimes, it is assumed that the molecular weight of the flue gas is 28.97 or the same as that of air. This is usually a pretty good approximation, but it can also be determined directly, as is done in Example 4.1.

Many combustion systems employ both forced-draft and induced-draft fans to produce a "balanced-draft" system. In this system, the combustion chamber operates at or slightly below atmospheric pressure. The forced-draft fan overcomes the pressure drops in the fuel-handling equipment and the air-supply ductwork while the induced-draft fan and the stack overcome the pressure drops in the exhaust gas system, including the precipitator or baghouse and the scrubber, if they are used. With the balanced-draft system, it is possible to do firebox inspections and minor maintenance on the furnace while the unit is in operation. This is almost impossible to do in a positive-pressure furnace.

As was mentioned earlier, most forced-draft fans are high-speed, centrifugal fans with backward-inclined blades or they are axial-flow fans. Induced-draft fans, on the other hand, are either axial-flow fans or low-speed, centrifugal fans with forward-curved blades. The low-speed fans reduce the erosion problem in the induced-draft fans.

The fans used to supply air and pump exhaust gas for a typical fossil-fueled power plant are large, expensive machines. The Labadie Power Station of the Union Electric Company (St. Louis) has four 600-MW_e units and each unit has two 1750-hp forced-draft fans and two 4000-hp induced-draft fans. These fans are driven by large alternating current induction motors. A typical combustion air fan is shown in Fig. 4.4 along with a diagram showing the air and flue-gas distribution in a large coal-fired generator.

Example 4.1. A 600-MW_e power plant burns Lafayette County, Missouri, coal with average moisture and ash fractions of 14 and 11 percent, respectively. This plant operates with a heat rate of 8863 Btu/kWh. An analysis of the refuse pit gives a higher heating value of 2605 kJ/kg. An orsat analysis of the flue gas gives 13.78% CO_2, 4.49% O_2, and 0.75% CO. Find:

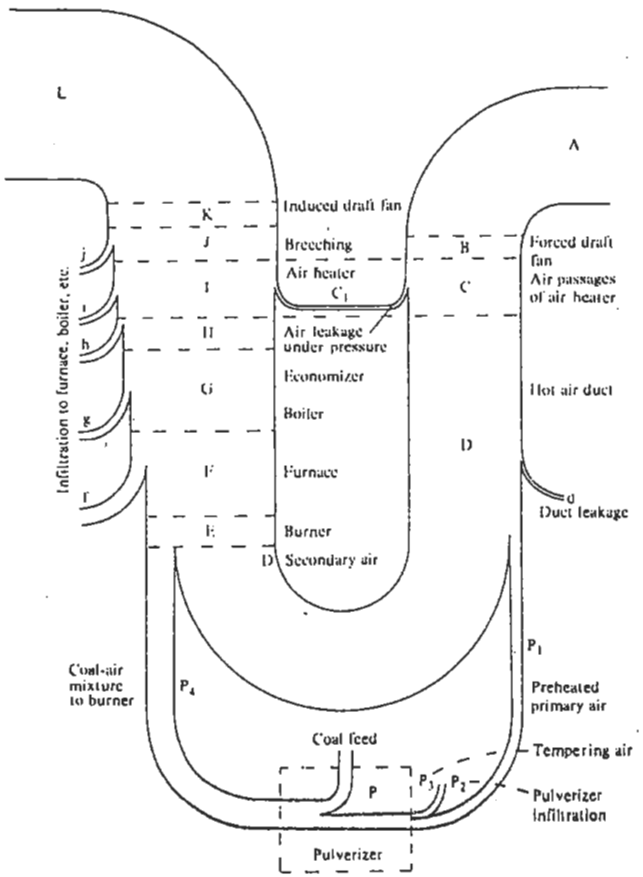
(*a*) The thermal efficiency of the power plant
(*b*) The coal rate
(*c*) The dilution coefficient and the percent excess air
(*d*) The capacity of the f-d fan, in kg/min and ft^3/min, if atmospheric conditions are 50°C, 0.93 atm, and a relative humidity of 50 percent
(*e*) The capacity of the i-d fan, in kg/min and ft^3/min, if the exhaust gas is at 288°C and 0.88 atm
(*f*) The size of the motors required to drive the i-d and the f-d fans, in hp, if there is a 25-in water differential across each unit and the mechanical efficiency of each fan is 86 percent
(*g*) The dew-point temperature of the exhaust gas leaving the i-d fan

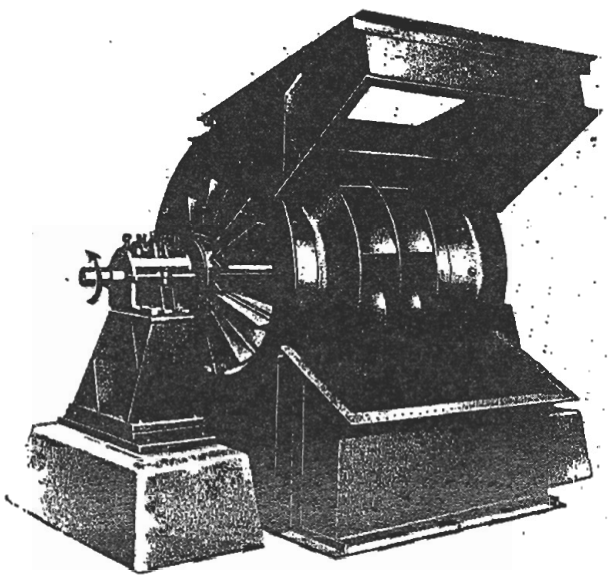
Solution. Given: $T_{in} = 50°C = 122°F$, $T_{out} = 288°C = 550.4°F$, HR = heat rate = 8863 Btu/kW · h.

(*a*)

$$\text{Thermal efficiency of plant} = \eta_{th} = \frac{3412}{\text{HR}} = \frac{3412}{8863}$$

$$= 0.3850 = 38.50\%$$


L
A
K
J
I
H
G
F
E
D
Induced draft fan
Breeching
Air heater
C_1
Air leakage under pressure
Economizer
Boiler
Furnace
Burner
Secondary air
B
C
D
Forced draft fan
Air passages of air heater
Hot air duct
Duct leakage
Infiltration to furnace, boiler, etc.
Coal-air mixture to burner
P_4
P_1
Preheated primary air
Coal feed
Tempering air
P
P_3
P_2
Pulverizer infiltration
Pulverizer



(*b*) Coal analysis (from App. E): 78.6% C, 5.6% H_2, 9.3% O_2, 1.3% N_2, 5.2% S, HHV = 33,160 kJ/kg. Refuse analysis: (HHV of refuse) = 2605 kJ/kg.

$$\frac{C_r}{R} = \frac{HHV_R}{HHV_C} = \frac{2605}{32{,}778} = 0.0795 \text{ kg } C_r/\text{kg } R$$

$$\frac{A}{R} = 1.0 - \frac{C_r}{R} = 1.0 - 0.0795 = 0.9205 \text{ kg } A/\text{kg } R$$

$$R = \frac{A_{ult}}{A/R} = \frac{0.11}{0.9205} = 0.1195 \text{ kg refuse/kg coal}$$

$$C_r = R - A = 0.1195 - 0.11 = 0.0095 \text{ kg } C_r/\text{kg coal}$$

$$C_b = C_{ult} - C_r = 0.786\,(1 - 0.14 - 0.11) - 0.0095$$

$$= 0.5895 - 0.0095 = 0.58 \text{ kg C burned/kg coal}$$

$$\text{Coal rate} = \frac{\text{thermal power}}{\text{as-burned HHV of fuel}}$$

$$\text{Coal rate} = \frac{(600{,}000 \text{ kW}_e)(1 \text{ kJ}_e/\text{kW}_e \cdot \text{s})(3600 \text{ s/h})}{(0.3851 \text{ kJ}_e/\text{kJ}_{th})(33{,}160 \text{ kJ}_{th}/\text{kg})(1 - 0.14 - 0.11)}$$

$$= 225{,}600 \text{ kg/h} = 225.6 \text{ tonne/h} = 248.7 \text{ ton/h}$$

(*c*) Theoretical, gravimetric, dry air-fuel ratio $= \left(\frac{A}{F}\right)_{T,G,D}$:

$$\left(\frac{A}{F}\right)_{T,G,D} = \frac{(2.66\,C + 7.94\,H_2 + 0.998\,S - O_2)(1 - M - A)}{0.232}$$

$$= [2.66(0.786) + 7.94(0.056) + 0.998(0.052) - 0.093]$$

$$\times \frac{(1 - 0.11 - 0.14)}{0.232} = 8.063 \text{ kg air/kg coal}$$

Actual, gravimetric, dry air-fuel ratio $= \left(\frac{A}{F}\right)_{A,G,D}$:

$$\left(\frac{A}{F}\right)_{A,G,D} = \frac{2.332(\%N_2)(C_b)/(\%CO + \%CO_2) - N_{2,ult}}{0.768}$$

$$\%N_2 \text{ (from orsat)} = 100 - 13.78 - 4.49 - 0.75 = 80.98\%$$

$$(1 - M - A) = 1.0 - 0.11 - 0.14 = 0.75$$

$$\left(\frac{A}{F}\right)_{A,G,D} = \frac{2.332(80.98)(0.58)/(0.75 + 13.78) - 0.013(0.75)}{0.768}$$

$$= 9.803 \text{ kg air/kg coal}$$

FIGURE 4.4
The air and flue-gas distribution in a large boiler and a typical large centrifugal fan with backward-curved blades. (*From Editors of Power Magazine, 1969.*)

$$\text{Dilution coefficient} = \frac{(A/F)_{A,G,D}}{(A/F)_{T,G,D}} = \frac{9.80}{8.06}$$

$$= 1.216$$

$$\text{Percent excess air} = (\text{dilution coefficient} - 1.0)(100)$$

$$= (1.216 - 1.0)(100) = 21.6\%$$

(*d*) Moisture in the combustion air: relative humidity = $\phi = 0.5$; saturation pressure at DBT from steam tables = 1.7891 lb/in^2; partial pressure of H_2O in air = $p_w = \phi p_{sat} = 0.5(1.7891) = 0.8946$ lb/in^2.

$$\text{Humidity ratio} = \omega = \frac{0.622\, p_w}{p_{air}}$$

$$= \frac{0.622(0.8944)}{14.7(0.93) - 0.8946}$$

$$= 0.04355 \text{ kg } H_2O/\text{kg dry air}$$

Mass gas rate for f-d fan = (coal rate)$(1+\omega)(A/F)_{A,G,D} = \dot{m}_{f\text{-}d}$:

$$\dot{m}_{f\text{-}d} = \left(\frac{225{,}600}{60}\right)(1 + 0.04355)(9.803) = 38{,}460 \text{ kg/min}$$

Volumetric gas rate for f-d fan = $Q_{f\text{-}d}$:

$$Q_{f\text{-}d} = (\text{coal rate})\left(\frac{A}{F}\right)_{A,G,D}\left(\frac{1}{28.97} + \frac{\omega}{18.02}\right)\left(\frac{R_u T}{p_{in}}\right)$$

$$= \frac{(248.7)(2000)}{60}(9.803)\left(\frac{1}{28.97} + \frac{0.04355}{18.02}\right)$$

$$\times \frac{(1545)(122 + 460)}{(144)(0.93)(14.7)}$$

$$= 1{,}371{,}000 \text{ ft}^3/\text{min}$$

(*e*) Mass rate through i-d fan = $\dot{m}_{i\text{-}d}$:

$$\dot{m}_{i\text{-}d} = (\text{coal rate})\left[\left(\frac{A}{F}\right)_{A,G,D}(1+\omega) + 1 - R\right]$$

$$= \frac{225{,}600}{60}[9.803(1 + 0.04355) + 1.0 - 0.1195]$$

$$= 41{,}780 \text{ kg exhaust/min}$$

$$\text{Moles of dry exhaust/kg coal} = \frac{100(C_b/12.01)}{\%CO + \%CO_2}$$

$$= \frac{(100)(0.58/12.01)}{0.75 + 13.68}$$

$$= 0.33467 \text{ moles dry exhaust/kg coal}$$

$$\text{Moles } H_2O/\text{kg coal} = \frac{M + \omega(A/F)_{A,G,D} + 9\ H_2}{(18.02)}$$

$$= \frac{0.14 + 0.04355(9.8) + 9(0.75)(0.056)}{18.02}$$

$$= 0.05244 \text{ moles } H_2O/\text{kg coal}$$

$$\text{Moles } SO_2/\text{kg coal} = \frac{S}{32.06} = \frac{0.75(0.052)}{32.06}$$

$$= 0.00122 \text{ moles } SO_2/\text{kg coal}$$

$$\text{Moles wet exhaust/kg coal} = 0.33467 + 0.05244 + 0.00122$$

$$= 0.38833 \text{ moles wet exhaust/kg coal}$$

$$\text{Total mass exhaust/kg coal} = \left(\frac{A}{F}\right)_{A,G,D}(1+\omega) + 1.0 - R$$

$$= 9.80(1 + 0.04355) + 1.0 - 0.1195$$

$$= 11.11 \text{ kg exhaust/kg coal}$$

$$\text{Molecular weight of exhaust} = \frac{11.11}{0.3883}$$

$$= 28.61 \text{ kg exhaust/kg} \cdot \text{mol of exhaust}$$

$$\text{Density of exhaust gas} = \frac{p_{out}}{RT_{out}} = \frac{(p_{out})(MW)}{R_u T_{out}}$$

$$= \frac{(0.88)(14.7)(144)(28.61)}{(1545)(1010)}$$

$$= 0.03414 \text{ lbm/ft}^3$$

Volumetric flow rate through i-d fan = $Q_{i\text{-}d}$:

$$Q_{i\text{-}d} = \frac{\text{mass flow rate of gas}}{\text{gas density}}$$

$$= \frac{41{,}780 \text{ kg/min}}{(0.03414 \text{ lbm/ft}^3)(0.4536 \text{ kg/lbm})}$$

$$= 2{,}697{,}000 \text{ ft}^3/\text{min}$$

(f) Pressure rise across fans = $\Delta p_{fan} = 25$ in H_2O; $\Delta p_{fan} = (25/12)(62.4) = 130$ lb/ft^2.

$$\text{Power of f-d fan} = \frac{Q_{f\text{-}d}\Delta p_{fan}}{33{,}000\ \eta_{mech}} = \frac{(1{,}371{,}000)(130)}{(33{,}000)(0.86)} = 6280 \text{ hp}$$

$$\text{Power of i-d fan} = \frac{Q_{i\text{-}d}\Delta p_{fan}}{33{,}000\ \eta_{mech}} = \frac{(2{,}697{,}000)(130)}{(33{,}000)(0.86)} = 12{,}350 \text{ hp}$$

(g) Mole fraction of H_2O in exhaust gas = $(MF)_w$:

$$(MF)_w = \frac{\text{moles } H_2O/\text{kg coal}}{\text{moles wet exhaust/kg coal}}$$

$$= \frac{(0.05244)}{0.3883} = 0.1350 \text{ moles } H_2O/\text{mole exhaust}$$

$$\text{Exhaust gas pressure leaving i-d fan} = 0.88(14.7) + \frac{130}{144}$$

$$= 13.84 \text{ psia}$$

Partial pressure of H_2O in exhaust gas = p_w:

$$p_w = (\text{exhaust gas pressure})(MF)_w = (13.84)(0.1350)$$

$$= 1.868 \text{ psia}$$

Dew-point temperature of exhaust gas = DPT:

$$\text{DPT} = \text{saturation temperature for } p_w = 1.868 \text{ psia}$$

$$= 124°\text{F} = 51°\text{C (from steam tables)}$$

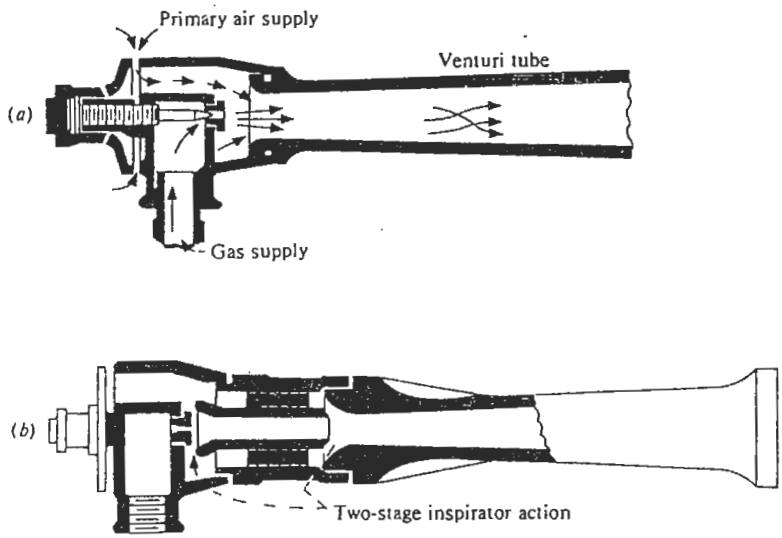


FIGURE 4.5
Atmospheric gas burners. (a) Atmospheric gas burners pull in their primary air for combustion by the action of a stream of low-pressure gas expanding through an orifice. (b) Two-stage burner operates on high-pressure gas; passes it through two venturi sections in series. Primary air enters shutter, at left under induction. (*From Bender, 1964.*)

4.3 COMBUSTION METHODS AND SYSTEMS

4.3.1 Gas-Fired Systems

Gaseous fuels, including natural gas, are the easiest fossil fuels to burn. The fuel gas needs little or no preparation before combustion. It must be simply proportioned, mixed with air, and ignited. This can be accomplished in several ways.

The atmospheric gas burner is one of the more common gas burners. In these systems, the momentum of the incoming gas is used to draw the primary air into the burner in a process called *aspiration*. The operation of these systems is normally satisfactory, with a primary air-fuel gas premix from 30 to 70 percent. Secondary air is drawn in around the burner to complete the combustion process. Two typical atmospheric gas burners are shown in Fig. 4.5.

Refractory gas burners are commonly used in steam generators. The combustion air is drawn in around the burner, which has multiple gas jets that produce

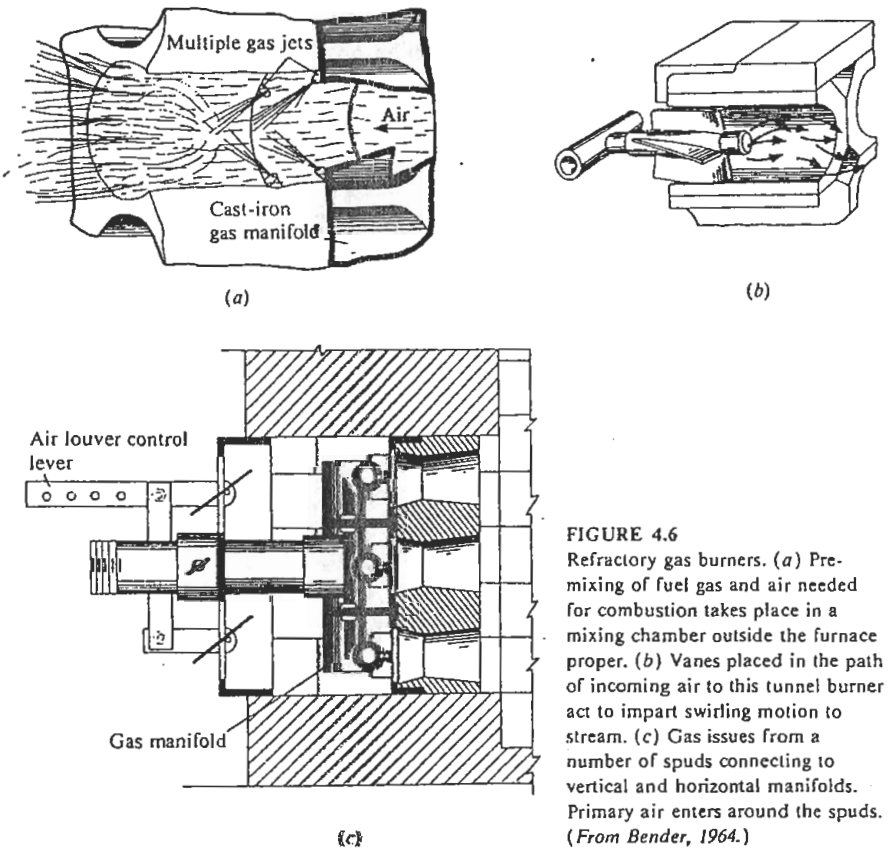


FIGURE 4.6
Refractory gas burners. (*a*) Premixing of fuel gas and air needed for combustion takes place in a mixing chamber outside the furnace proper. (*b*) Vanes placed in the path of incoming air to this tunnel burner act to impart swirling motion to stream. (*c*) Gas issues from a number of spuds connecting to vertical and horizontal manifolds. Primary air enters around the spuds. (*From Bender, 1964.*)

good mixing. The gas–air mixture is then discharged into a short mixing tube or tunnel of refractory material. The refractory tube protects the metal burner from the high temperature. Three refractory gas burners are shown in Fig. 4.6.

Another common gas burner is the fan-mix burner. In this system, the fuel gas is introduced from nozzles mounted at an angle in a rotating "spider" burner and the resulting reaction force turns the spider plus an attached fan. This fan produces thorough mixing and the combustion occurs very close to the burner. A typical fan-mix burner is shown in Fig. 4.7.

4.3.2 Oil-Fired Systems

Oil is somewhat more difficult to burn than natural gas because the burner must prepare the fuel for combustion as well as proportion it, mix it with air, and burn it. This is particularly true when the unit is fired with a residual fuel oil. There are several ways to prepare the fuel oil for combustion, including vaporization or gasification by heating it within the burner or by atomization in the combustion-air stream. The vaporization technique is particularly well suited for the light fuel oils.

Atomization of the oil droplets can be accomplished with the use of high-pressure air or steam, or the liquid oil film can be torn apart by centrifugal force. Examples of two atomizing burners using high-pressure air and steam are shown

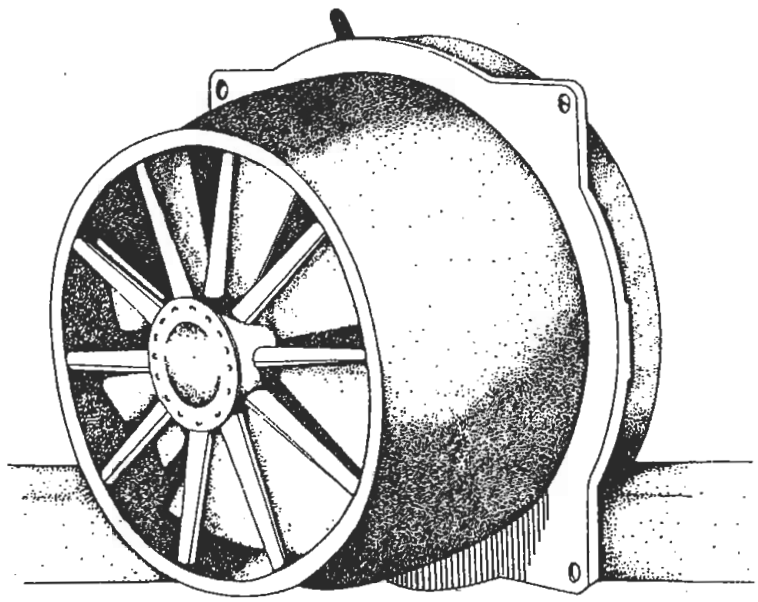


FIGURE 4.7
The fan-mix burner. (*From Bender, 1964.*)

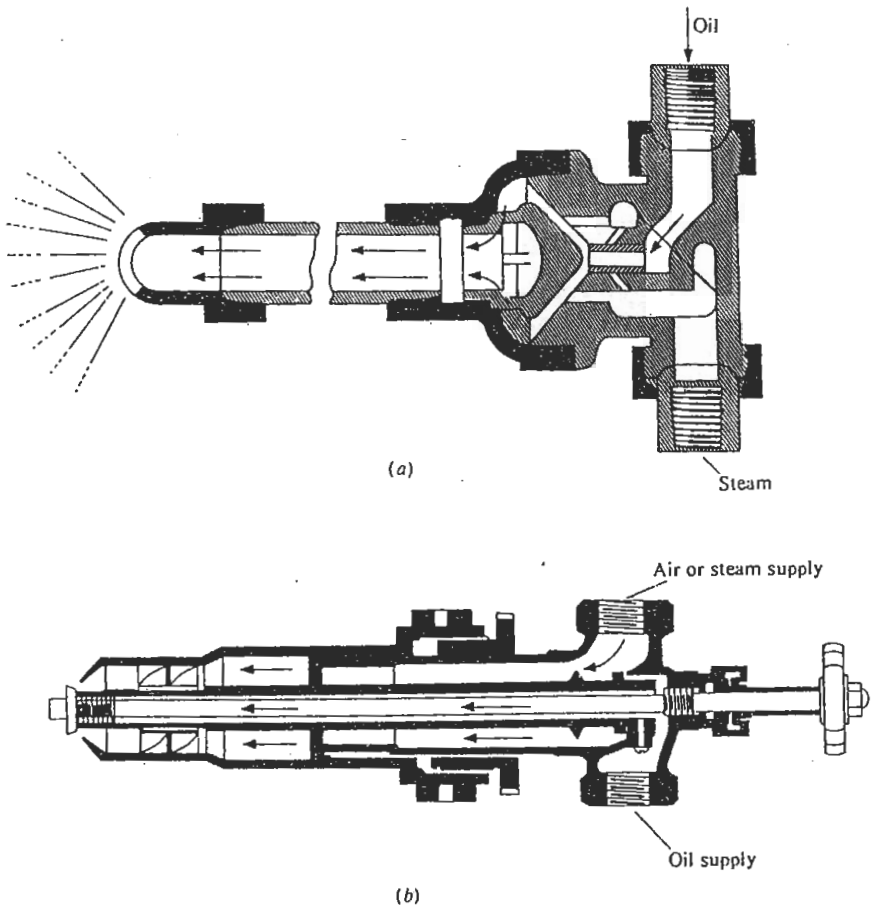


FIGURE 4.8
Atomizing oil burners. (*a*) In typical design of internal-mixing, steam-atomizing burner, changing tip alters the range of capacities handled. (*b*) Steam-atomizing burner of external-mixing type brings oil and atomizing medium steam together at the burner tip. (*From Skrotzki and Vopat, 1960.*)

in Fig. 4.8. Steam or air atomization is best suited for variable loads and can cover a wide range of capacity without changing the tip or gun assembly. Mechanical atomization is best suited for steady loads and high capacities but has a fairly limited capacity range. A common rotary-cup burner is shown in Fig. 4.9. This burner employs a high-speed (3500-r/min) horizontal rotary cup to spin oil off the rim and into the air stream by centrifugal force. This particular mechanical burner has a very wide capacity range (16 to 1).

Any fuel-oil combustion system is commonly composed of an oil-storage tank, pumping and heating equipment, an oil-supply header, the burners, and

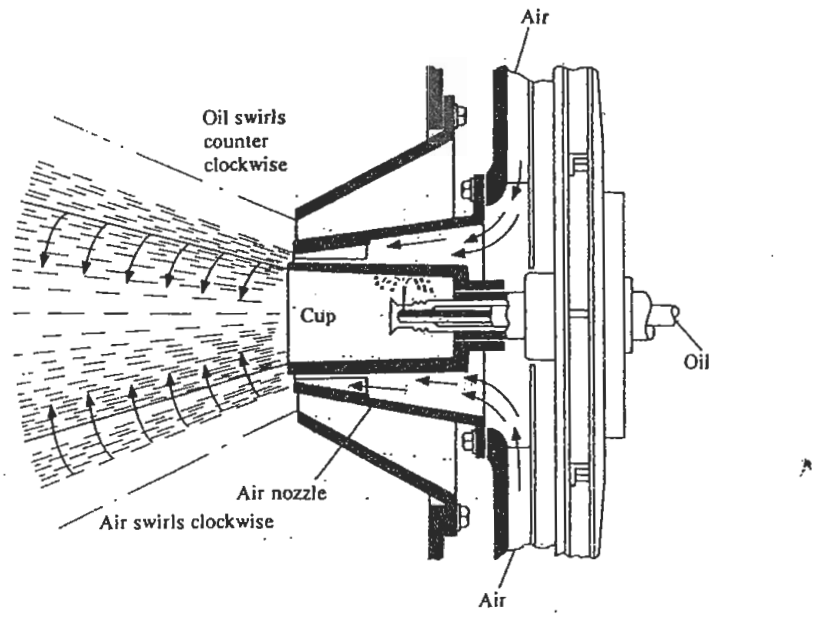


FIGURE 4.9
Rotary-cup oil burner. Cup revolving counterclockwise breaks up oil film at rim by centrifugal force and discharges it into a clockwise airstream. (*From Bender, 1964.*)

an oil-return line. The schematic diagrams of two fuel oil supply systems are shown in Fig. 4.10.

4.3.3 Coal-Combustion Systems

STOKER FURNACES. The stoker furnace is one of the oldest type of coal furnaces and is still in use, today. Its somewhat limited capacity does not lend this type of furnace to large power applications but it is widely used in industrial plants where relatively limited amounts of process steam are desired. In this unit, the coal is introduced on a grate and it is finally burned in a stationary bed. The stoker furnace burns coarsely crushed coal. Part of the combustion air, called *primary air*, is introduced below the burning bed. The primary air initiates the combustion process and also cools the grate. The balance of the combustion air, called *secondary air* or *overfire air*, is introduced above the burning bed to complete the combustion process.

There are several different types of stoker furnaces. The more common include the chain-grate and traveling-grate stokers, the vibrating-grate stoker, the underfeed stoker, and the spreader stoker. The chain-grate or traveling-grate stoker is the simplest and least expensive of the stoker furnaces and a typical unit is shown in Fig. 4.11. In this system, crushed coal is fed into a coal hopper

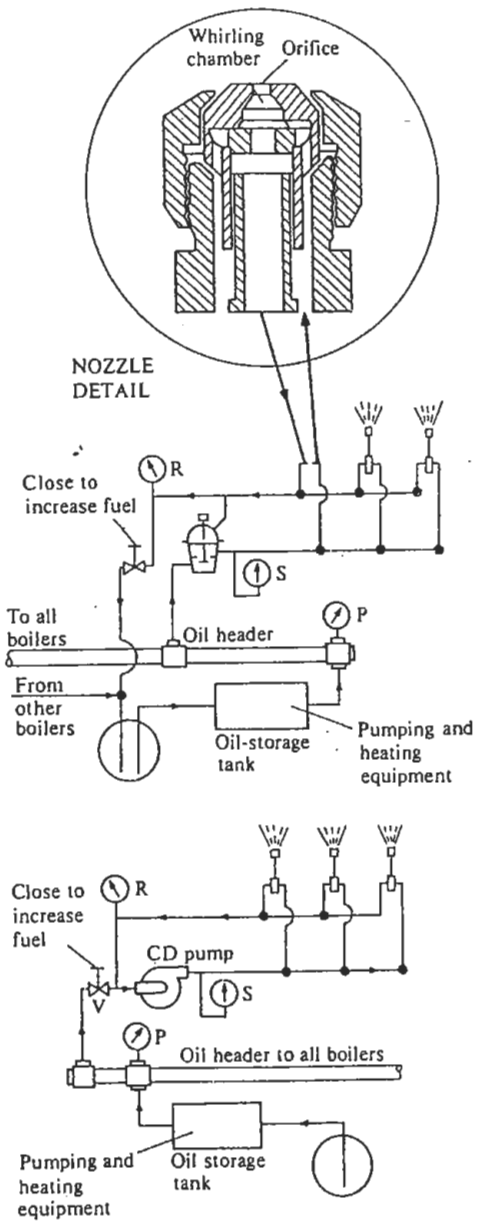


FIGURE 4.10
Fuel-oil supply and distribution systems. (*From Skrotzki and Vopat, 1960.*)

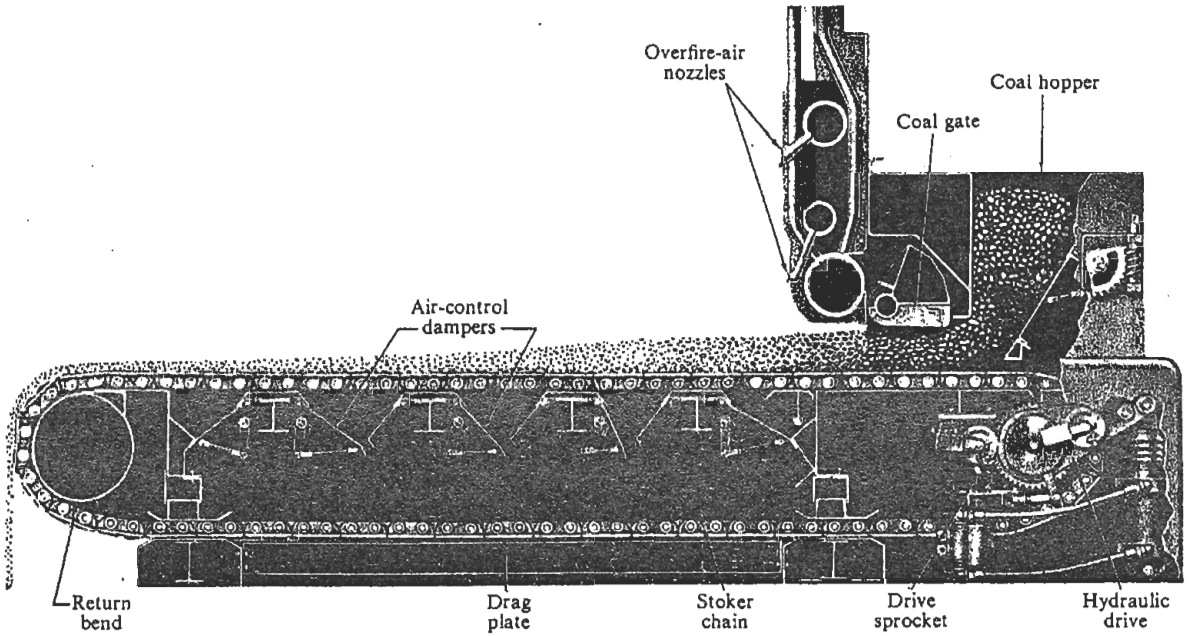


FIGURE 4.11
The Babcock and Wilcox jet-ignition, chain-grate stoker. (*From Steam: Its Generation and Use, 1972.*)

by means of conveyor belts. The coal flows by gravity from the hopper onto the grate. The coal depth is fixed by a "gate" and the combustion rate is fixed by varying the coal depth with the gate and/or by varying the grate speed. The grate is composed of a continuous traveling link chain composed of pinned cast-iron bars with narrow gaps between the links to allow the flow of primary air into the furnace. This particular unit is not well suited to the combustion of caking coals because there is insufficient agitation of the burning bed to break up the fused burning coal lumps.

The vibrating-grate stoker is very similar to the chain-grate stoker, except in the operation and the orientation of the grate. In this unit, the coal grate does not move continuously in one direction. Instead, the grate is inclined toward the ashpit and the grate is vibrated. The raw coal flows from the storage-inlet hopper to the grate and then the particles move down the grate under the influence of the vibration and gravity. The coal particles burn as they move down the grate and hopefully nothing but ash falls off the back of the grate into the ashpit. Since there is considerable agitation of the fuel bed, this unit can burn most caking coals.

The underfeed stoker furnace is one of the more common types of high-capacity stoker furnaces. In it, the coal is pushed into the bottom of the fuel bed in one or more feed troughs, called *retort trenches.* The coal is advanced in the retort trench by rams, pusher rods, or Archimedes' screws. A single retort trench stoker furnace is shown in Fig. 4.12. In the horizontal-feed, underfeed unit in Fig. 4.12, the ash flows off the sides of the grate. In the gravity-feed, underfeed stoker furnace, the grate is inclined at an angle of 20° to 25° and the ash falls off the back of the grate. Multiple-retort furnaces have grate release rates as high as 720,000 Btu/hft^2. Because of the ramming action in the bottom of the coal bed, the agitation probably makes this particular unit the best system for burning caking coals.

The newest type of stoker furnace is the spreader stoker and this unit has found widespread application because of its relative simplicity. This system has high capacity, it is low in initial cost, and it is relatively insensitive to the coal characteristics. In this stoker furnace, the raw coal is literally thrown over the bed by rotating paddles or vanes, or it is blown over the bed by a pneumatic spreader system powered by high-pressure air or steam. The coal then falls on a moving or traveling grate, similar to that of a chain-grate stoker, except that the grate moves back toward the coal injector and the ashpit lies directly below the coal hopper, as shown in Fig. 4.13. A typical injection system for the spreader stoker is also shown in Fig. 4.13. This furnace has a faster response than the other stoker furnaces but it also requires more combustion air and it has greater problems with flyash emissions than the other stoker units.

CYCLONE FURNACES. The cyclone furnace is a combustion system that employs a number of independent combustion chambers (as many as 16 in a large power boiler) all of which feed hot exhaust gas into a large, water-cooled boiler. A typical cyclone, like that shown in Fig. 4.14, consists of a small cylindrical chamber (about 4 ft in diameter) that feeds a large (15 to 18 ft in diameter) insulated

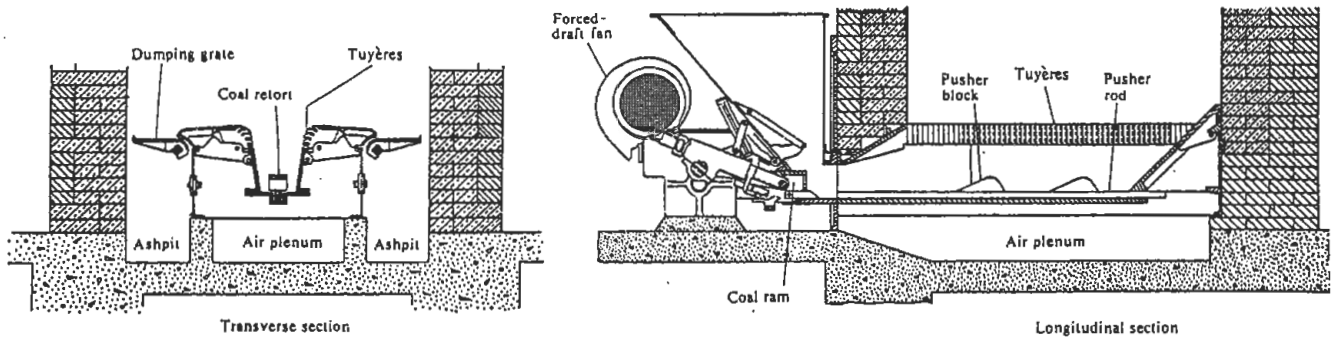


FIGURE 4.12
A single-retort horizontal-feed, underfeed stoker furnace. (*From Steam: Its Generation and Use, 1972.*)

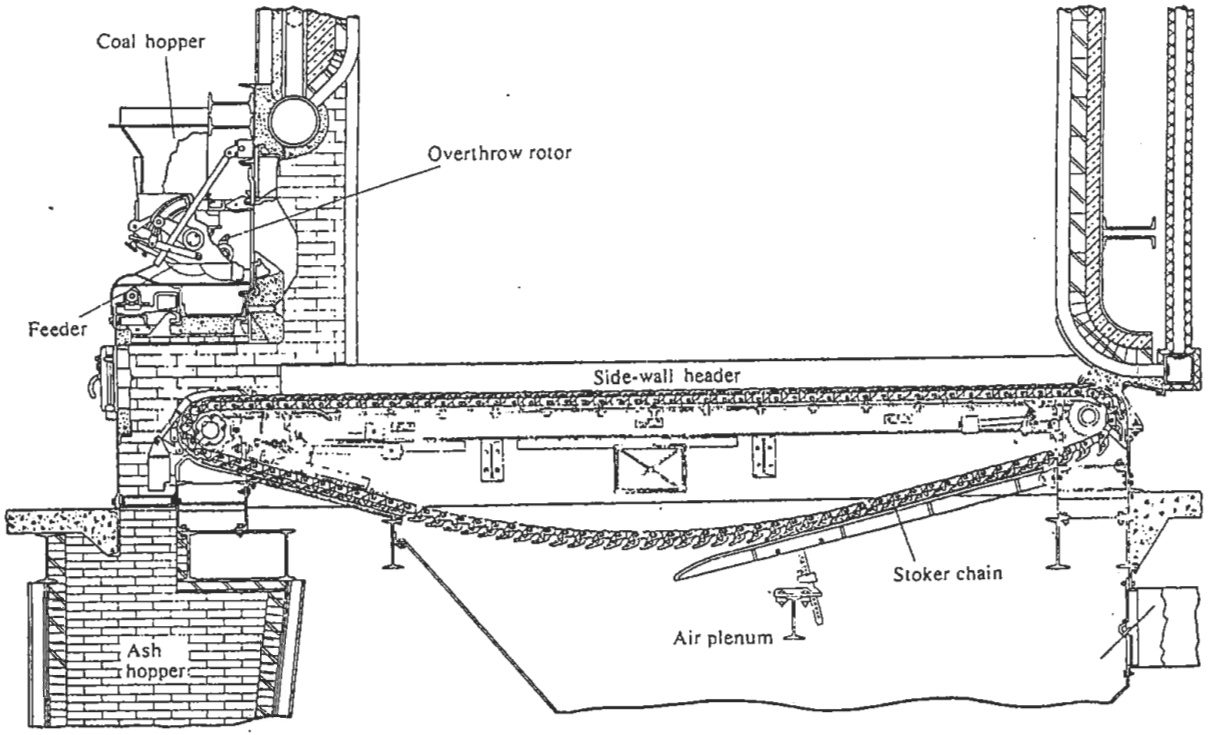


FIGURE 4.13
The spreader stoker furnace and the coal-injection system. (*From Steam: Its Generation and Use, 1972.*)

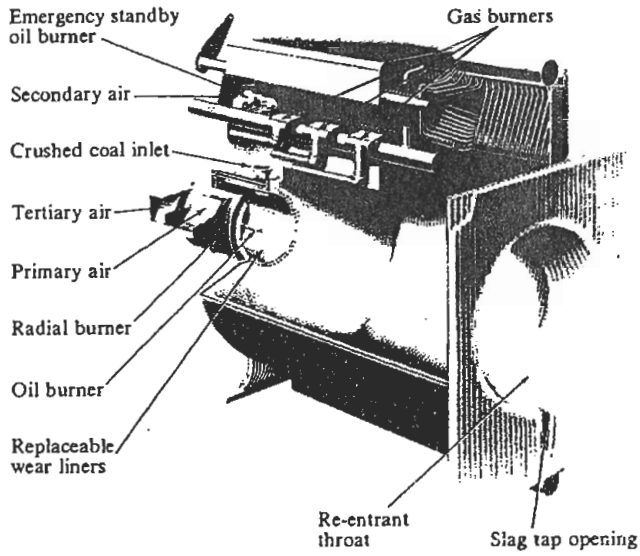


FIGURE 4.14
The cyclone coal combustion system. (*From Steam: Its Generation and Use, 1972.*)

chamber from which the hot gases are discharged into the heat-transfer section of the boiler.

The cyclone furnace burns coarsely crushed coal (1-in diameter or less). The coal and the primary air are fed tangentially into the small combustion chamber, which is lined with cast-iron "wear" blocks, and the secondary air is introduced tangentially into the large insulated cylindrical chamber. Molten ash collects on the walls of the large chamber. A small quantity of air, called *tertiary air*, is introduced into the vortex of the cyclone to break up the vacuum.

The strong vortex flow throws any large unburned chunks of coal into the molten ash collecting on the side of the cylindrical wall where the secondary air completes the combustion process. The main combustion chamber of a cyclone unit operates at a temperature of 1750°C (3200°F) and the molten ash runs out of the cyclone burner through a slag-tap opening onto the furnace floor. Once on the furnace floor, the molten ash falls through an opening, called the *monkey*, into a water-filled slag tank. This furnace traps approximately 75 percent of the total ash in the molten slag, reducing the particulate-emission problems.

The cyclone furnace commonly operates as a positive-pressure furnace. The draft system for these units is composed of one or two large forced-draft fans plus several intermediate-sized, gas-recirculation fans. The positive-pressure firebox does present some problems with respect to leakage and maintenance. Consequently, some of these units have been retrofitted with induced-draft fans so that the furnace can operate as a balanced-draft system.

Cyclone furnaces became very popular in the 1950s and 1960s but they are no longer being built because of two major problems associated with the environment. First, they have difficulty burning low-sulfur coals because of ash-slagging problems. Second, because of the high combustion temperature required in each combustion chamber, a significant amount of NO_x is formed, and these nitrogen oxides are important atmospheric pollutants.

PULVERIZED-COAL FURNACES. The pulverized-coal furnace burns finely powdered coal and air in a gaseous torch. This combustion system can produce much higher capacities than the stoker furnaces, it gives fast response since there is little unburned fuel in the combustion chamber, it reduces the amount of excess air required for combustion and this reduces the NO_x emissions, it can burn all ranks of coal from anthracitic to lignitic, and it permits combination firing. The term "combination firing" refers to the capability of burning coal, oil, or natural gas in the same burner. Normally, only one type of fuel is burned at a time although two different fuels can be simultaneously burned for short periods of time. The pulverized-coal furnace finds widespread application in coal-fired power plants.

Despite the numerous advantages listed above, the pulverized-coal system has a number of problems associated with it. It requires a complicated coal pulverizer with its accompanying power demand and associated higher maintenance costs. Flyash erosion and pollution also complicate the operation of the unit and increase the required maintenance of the exhaust system. The pulverized-coal systems have higher initial cost and require larger furnace volumes for the combustion process.

There are many different kinds of coal pulverizers but they all employ one or a combination of three basic pulverizing actions—crushing, impact, and attrition. Crushing and impact are self-explanatory while attrition is the pulverizing action produced by rubbing two coal particles together or by rubbing a coal particle against a solid surface, such as a wall. The common coal pulverizer grinds the coal to a consistency finer than most face powders. The standard pulverizer specifications require that at least 98 percent of the output particles pass through a 50-mesh screen (50 wires/in), yielding a maximum particle diameter of less than 0.3 mm. Not only does the pulverizer grind the coal to a fine powder, but it also dries it. The primary air is usually heated to 260 to 315°C (500 to 600°F) and is pumped by a separate fan through the pulverizer, where it dries the coal and transports it to the burner.

The simplest type of coal pulverizer is the ball mill or the ball-and-tube mill. This system is composed of a large drum rotating on its horizontal axis partially filled with steel balls and/or tubes. The most widely used coal pulverizers are probably the ball-race mills, the roll-and-race mills, and the bowl mills. These mills have a series of large steel balls or rollers running against a rotating race or drum. There are a number of other kinds of pulverized-coal mills, including hammer-mill pulverizers and the steam-jet pulverizers, among others. Some of the common coal pulverizers are shown in Fig. 4.15.

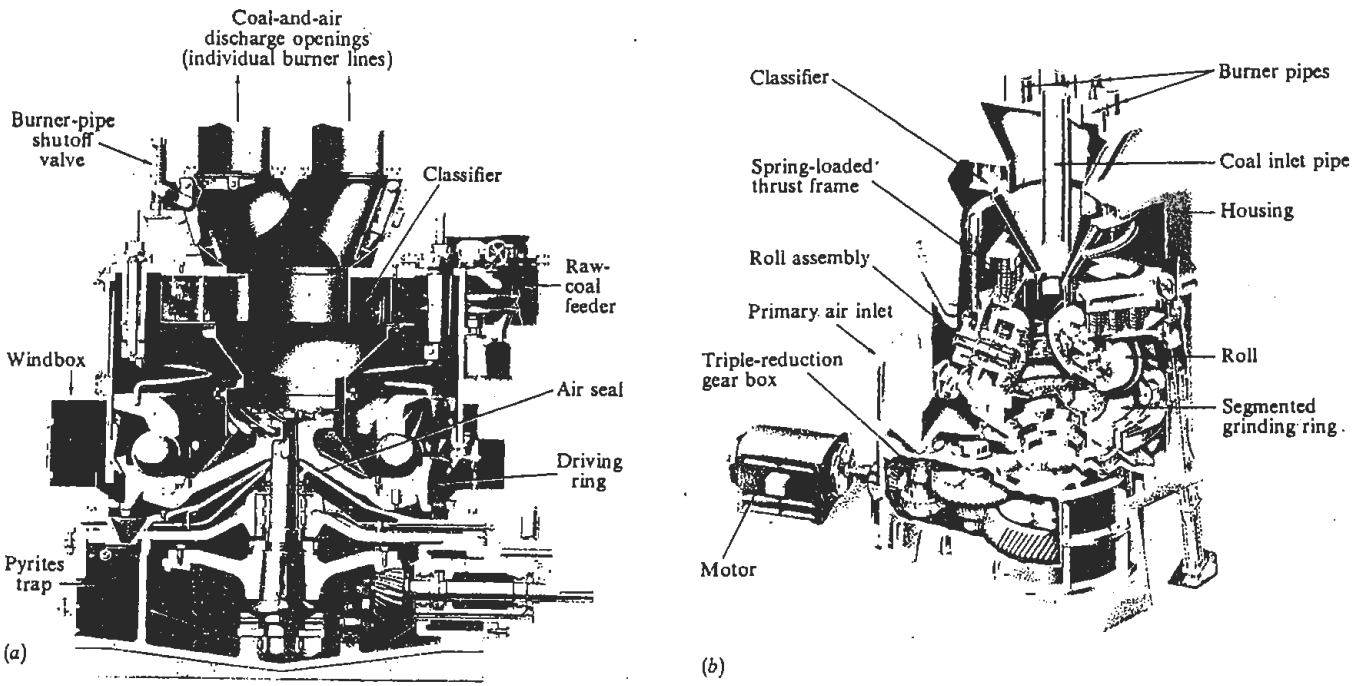


FIGURE 4.15
Some common coal pulverizers. (*a*) the Babcock and Wilcox type EL, single-row, ball-and-race pulverizer. (*b*) The Babcock and Wilcox type MPS mill. (*From Steam: Its Generation and Use, 1972.*)

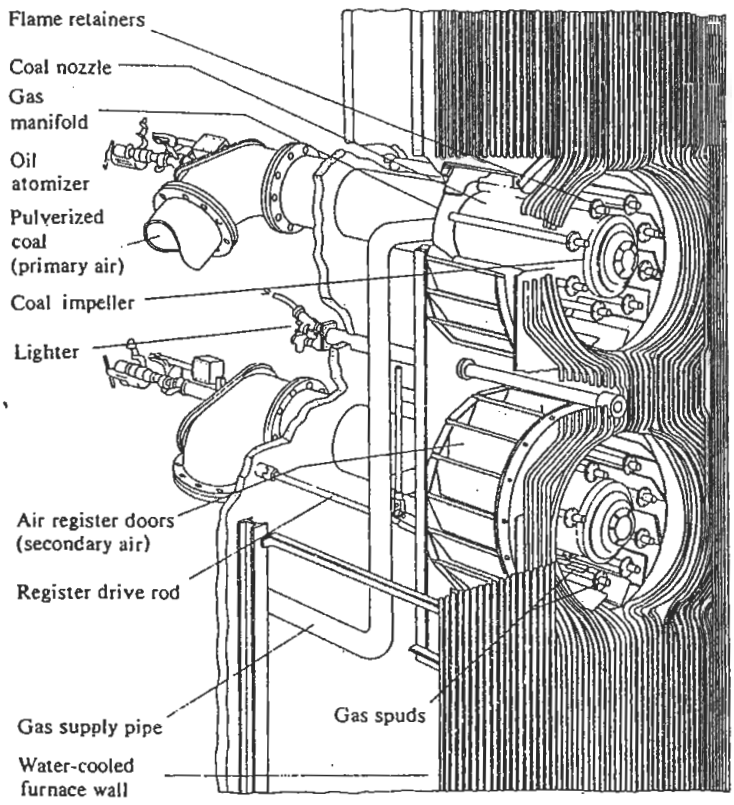


FIGURE 4.16
Pulverized-coal burners. (*From Bender, 1964.*)

There are many types of pulverized-coal burners, but the circular and cell types are commonly employed because they are capable of combination firing. A typical burner of this type is shown in Fig. 4.16. These burners usually fire horizontally and are commonly either fired from the corners of a square combustion chamber so that the flames are directed toward an imaginary circle (tangential firing), or they are mounted in the long walls of a rectangular combustion chamber, opposite each other, and these pairs of burners are fired in tandem (opposed firing) so that a sheet of flame is produced in the center of the furnace. This keeps the flyash particles from eroding the boiler tubes.

In many pulverized-coal furnaces, the burners can be tilted up or down to permit some control of the energy deposition in the boiler. If the burners are tilted down, more heat is transferred to the evaporator section in the lower part of the boiler adjacent to the burners and less heat is transferred to the pendant superheaters and reheaters in the top of the boiler. If the burners are tilted up, less heat is transferred to the evaporator section and more heat is transferred to

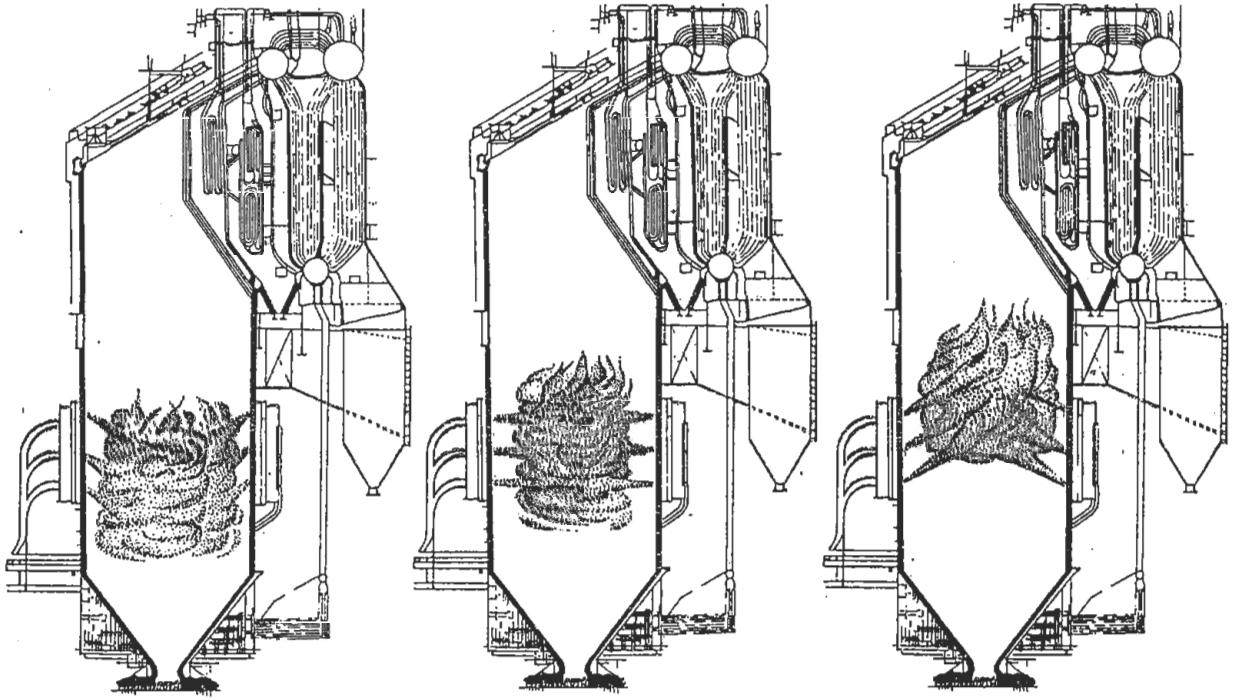


FIGURE 4.17
Operation of a tangentially fired, pulverized-coal furnace with tiltable burners. (*From Skrotzki and Vopat, 1960.*)

the superheat and reheat sections. See the tangentially fired pulverized-coal furnace in Fig. 4.17.

The ash from a pulverized-coal furnace can be handled in one of two ways. In the *wet-bottom* or *slag-tap furnace*, the ash is handled in molten or liquid form. The combustion chamber of this unit is normally insulated and the burners might be directed toward the molten ash on the furnace floor to facilitate ash collection. A coal with a low-ash-softening temperature is desired for this system and the slag pool must be maintained at a high enough temperature to assure that the hot slag flows continuously over a water-cooled weir or ring into a quenching tank filled with water. Approximately 50 percent of the flyash is usually trapped in the pool of molten slag.

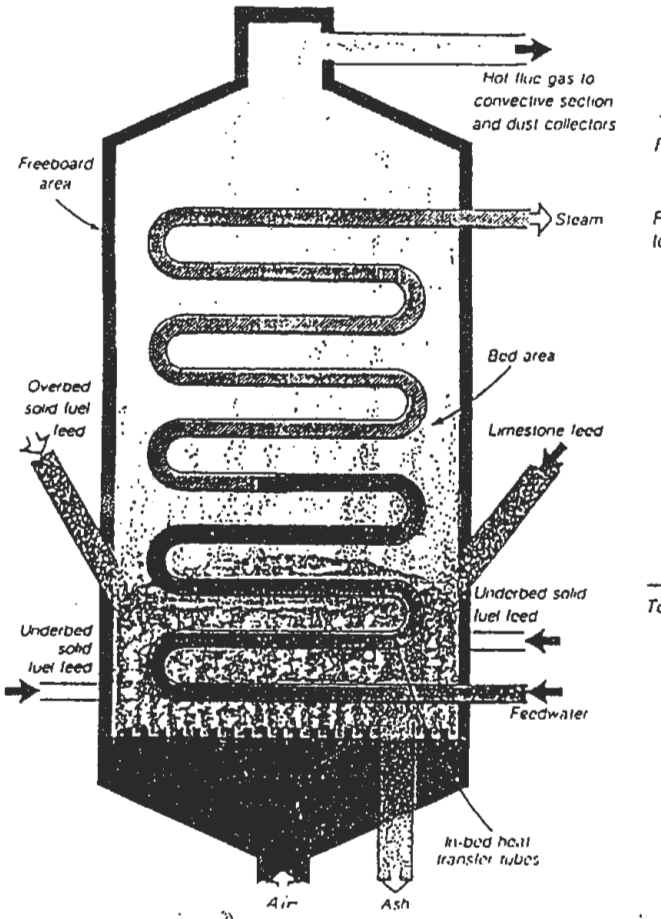
The other general ash system handles the ash in solid form and is called the *dry bottom furnace*. The coal used in this furnace should have a high ash-softening temperature (at least 1300°C or 2400°F). The walls of the combustion chamber are water-cooled and the ash particles are cooled in suspension. Some of the ash settles to the furnace floor but about 80 percent of it leaves with the exhaust gas, entrained as flyash. Because of the high flyash concentration in the flue gas, this system will probably require one or more mechanical dust collectors (see Chap. 6) plus an electrostatic precipitator, baghouse filter, or their equivalent.

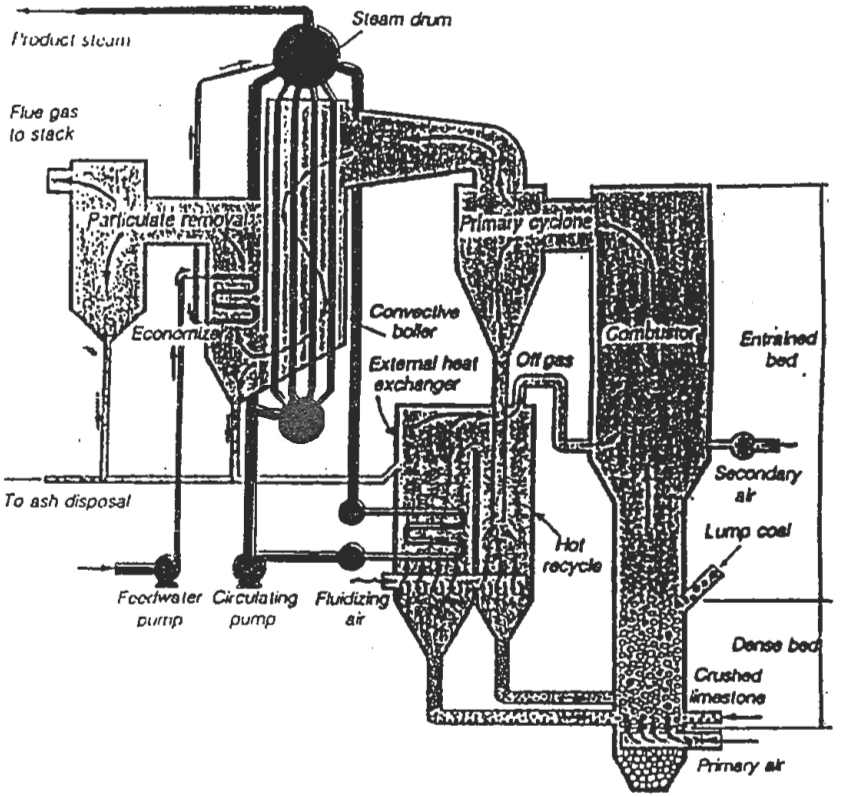
At the present time, the dry-bottom, pulverized-coal furnace is the most popular furnace used in large coal-fired power plants. The low-temperature combustion process combined with the low air-fuel ratios used in this system reduces the formation of NO_x.

FLUIDIZED-BED COMBUSTION SYSTEM. The fluidized-bed furnace is a radically new type of combustion system that has been under development and testing during the last 20 years. In this unit, crushed coal and either crushed dolomite or limestone are mixed in a bed that is then levitated by the combustion air entering the bottom of the furnace. The boiler evaporator tubes are immersed directly in the fluidized bed and the direct contact between the burning coal particles and the water tubes produces very high heat-transfer rates, reducing the size of the unit. This arrangement also produces very low combustion temperatures.

There are several different types of fluidized-bed combustion systems. These include pressurized versus atmospheric bed systems and circulating versus stationary bed systems. Pressurized bed systems have a number of advantages but they are especially suited to serve as heat sources for combustion turbines. In stationary bed systems, almost all the coal particles stay in the furnace, while in the circulating bed systems, a good portion of the particles exit the furnace with the flue gas. These particles are then separated from the exhaust and reinjected into the fluidized-bed system.

The major advantage of the fluidized-bed system lies in the area of pollution control and abatement. The relatively low combustion temperatures of 820 to 950°C (1500 to 1600°F) produced by the placement of the evaporator tubes directly in the burning bed greatly inhibits the formation of nitrogen oxides. The addition


Hot flue gas to convective section and dust collectors
Freeboard area
Steam
Bed area
Overbed solid fuel feed
Limestone feed
Underbed solid fuel feed
Underbed solid fuel feed
Feedwater
In-bed heat transfer tubes
Air
Ash


Steam drum
Product steam
Flue gas to stack
Particulate removal
Primary cyclone
Economizer
Convective boiler
External heat exchanger
Off gas
Combustor
Entrained bed
Secondary air
To ash disposal
Hot recycle
Lump coal
Feedwater pump
Circulating pump
Fluidizing air
Dense bed
Crushed limestone
Primary air

of either dolomite (a calcium-magnesium carbonate, $MgCO_3$) or limestone (a calcium carbonate, $CaCO_3$) produces a chemical reaction between the calcium and/or magnesium and the sulfur from the coal-producing sulfites and sulfates. These calcium and/or magnesium sulfur salts are solids and remain in the combustion chamber. Thus, the fluidized-bed combustion system, similar to that shown in Fig. 4.18, traps the sulfur in the furnace, thereby permitting the utilization of high-sulfur coal.

There are several disadvantages associated with the use of fluidized-bed combustion systems. There are problems associated with the distribution of the coal and dolomite or limestone, there are erosion problems caused by the particles in the furnace rubbing the evaporator tubes, and the system requires about 50 percent more dolomite or limestone than a flue-gas scrubber system for the same sulfur removal. Also, the system appears to be best suited for relatively low-power applications and would require many units in parallel to produce the power needed for a large power plant.

Another disadvantage of this particular system is due to the fact that the combustion air must be supplied at a high enough pressure that it can support the fluidized bed. This means that the pressure rise across the fan or compressor must be higher than that for a conventional coal-fired furnace with an accompanying increase in the required fan power. Another disadvantage (or maybe advantage?) associated with the fluidized-bed system is the fact that it is a relatively new concept and, as such, has not been as fully developed as the other types of combustion systems.

Despite some problems associated with the use of fluidized-bed combustion systems, they still appear to be one of the more promising combustion systems of the future. The advantages associated with reduced emission of pollutants and the utilization of high-sulfur coal make this system very attractive.

4.4 STEAM GENERATORS

4.4.1 General

The steam generator or boiler is a combination of systems and equipment for the purpose of converting chemical energy from fossil fuels into thermal energy and transferring the resulting thermal energy to a working fluid, usually water, for use in high-temperature processes or for partial conversion to mechanical energy in a turbine. In most modern large power plants, one boiler is used to supply steam to one steam-turbine generator unit. The boiler complex includes the ductwork and air-handling equipment, the fuel-handling and processing equipment, the furnace, the water supply and treatment system, the steam drums and piping, the exhaust gas system, and the pollution control systems including scrubber and electrostatic precipitator or baghouse filter.

FIGURE 4.18
The fluidized-bed combustion system and schematic diagram of a circulating-bed system.

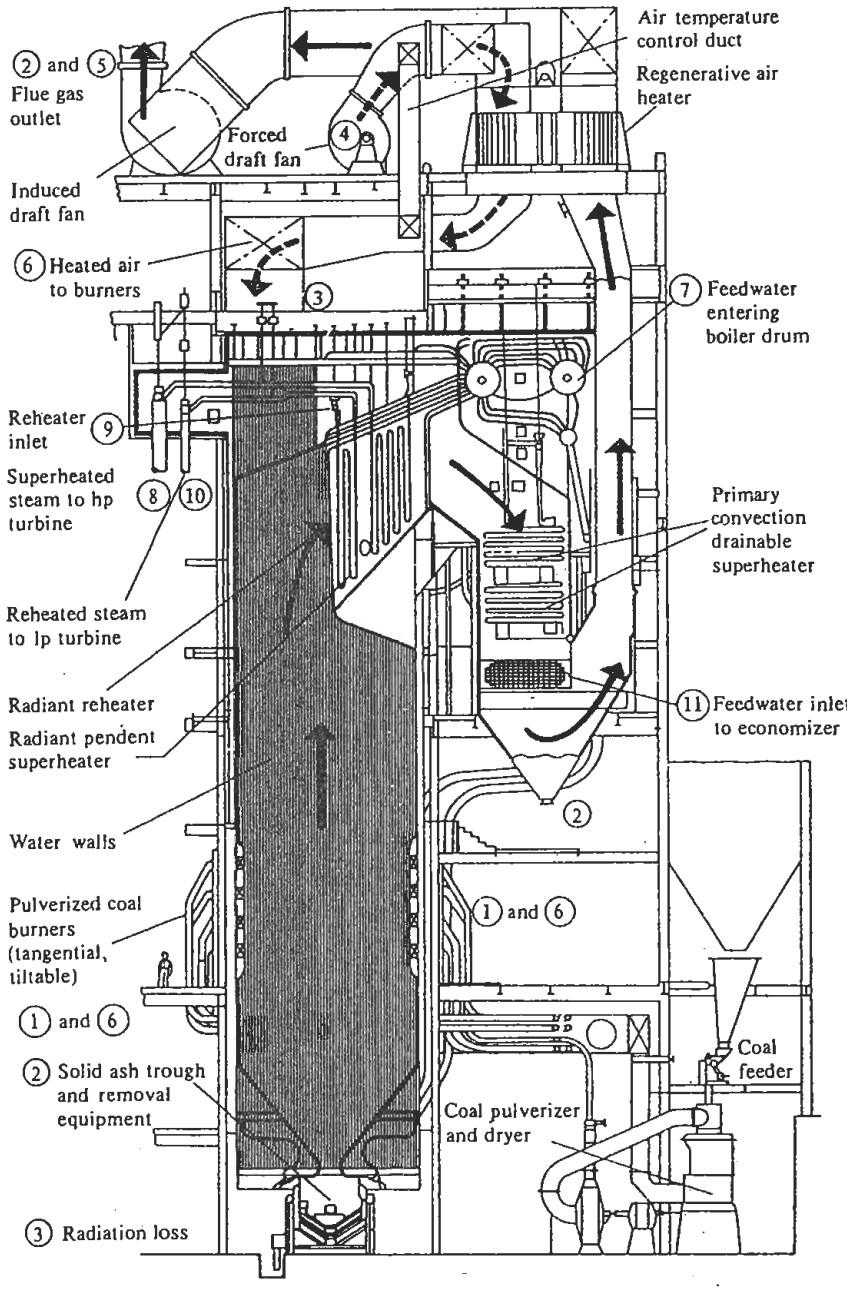


FIGURE 4.19
Schematic diagram of a large pulverized-coal steam generator.

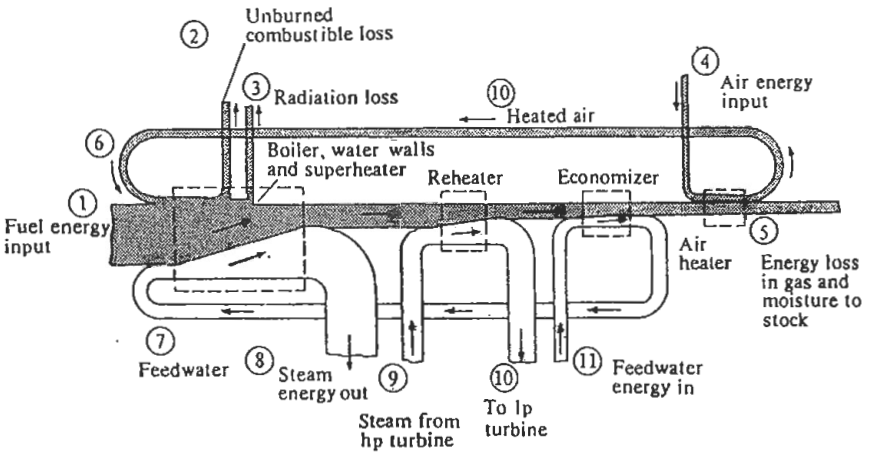


FIGURE 4.20
The energy flow diagram for a typical pulverized-coal steam generator. (*From Bender, 1964.*)

The heat-transfer sections of a large boiler include the evaporator, the superheater, the reheater, the air preheater, and the economizer sections. The evaporator, superheater, and reheater surfaces are called *primary heat-transfer surfaces*, while the air preheater and economizer are called *secondary heat-transfer surfaces*. A schematic of a typical, large, pulverized-coal steam generator is depicted in Fig. 4.19. An energy flow diagram for a typical large steam generator is shown in Fig. 4.20.

4.4.2 Boiler Types and Classifications

Steam boilers can be classified many ways but there are actually two basic types of steam generators, depending on the orientation of the water-steam and hot-gas flow paths. These two general classifications are the *fire-tube boilers* and the *water-tube boilers*. The common fire-tube boiler is essentially composed of a water-filled pressure vessel containing a number of tubes which are the passageways for the hot exhaust gas and through which heat is transferred from the hot gas to the water in the vessel. This system is the simplest and probably the least expensive of all the steam generators.

In the fire-tube system, the high-pressure water is placed on the external surface of the tubes. Since most pressure-vessel codes will limit the external pressure on a tube to half that for internal pressure, the fire-tube systems are limited to relatively low steam pressures. The maximum drum diameter is around 2.5 m (8 ft) and the maximum steam pressure is limited to about 1.7 MPa (250 psia), although most of the systems normally operate at a pressure of about 1 MPa (150 psia).

Another problem associated with the fire-tube boiler is the consequence of a major tube failure. In the event of a sudden tube failure, the high-pressure

water flows into the hot combustion chamber, generating large quantities of steam in the furnace. This is likely to produce a steam explosion in the furnace.

The entire heating surface in the drum of a fire-tube boiler is devoted to the production of saturated steam, although a separate superheater section can be added. There are several different kinds of fire-tube boilers but the horizontal-return-tubular (hrt) boiler is one of the more popular types. The fire-tube steam generator is commonly employed in small industrial plants, and these systems can be purchased in the form of complete operational packages. A typical two-pass, packaged, fire-tube steam generator is shown in Fig. 4.21.

The water-tube boilers are best suited for high-pressure, high-capacity steam generators. The high-pressure water and the steam flows from tube headers or drums through tubes in the furnace walls or in tube bundles mounted in the exhaust gas duct. These tubes range from 0.05 to 0.1 m (2 to 4 in) in diameter and can withstand boiler pressures up to 35 MPa (5000 psia). The water-tube steam generators can be classified according to the shape of the tubes, the position of the drums, the number of drums, the method of circulation, the type of service (stationary or marine), or the capacity and thermal conditions of the outlet steam. Because of the large exhaust gas ductwork in a water-tube steam generator, danger of a steam explosion in the event of a catastrophic tube failure is lessened.

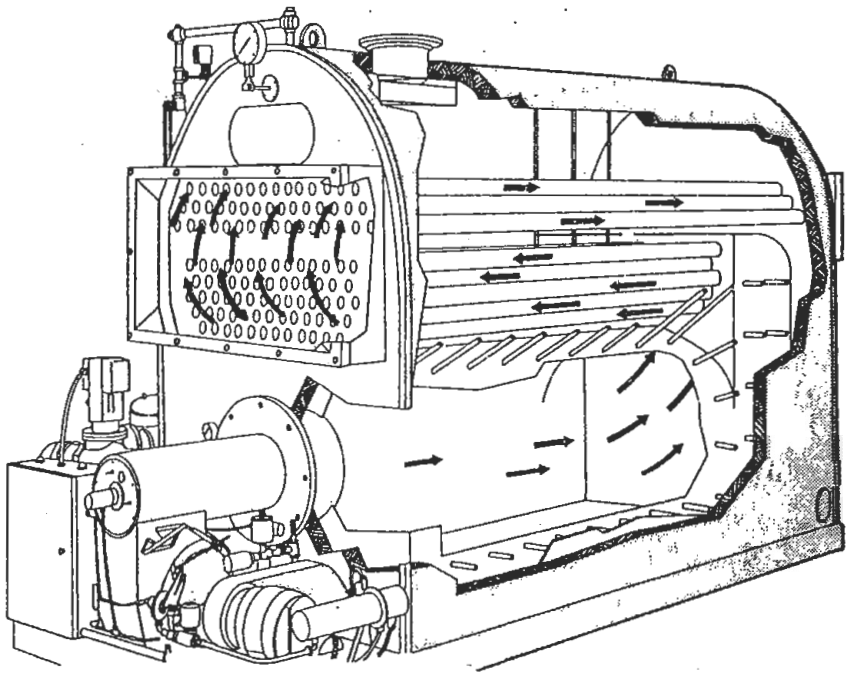


FIGURE 4.21
A typical two-pass, packaged, fire-tube, steam generator. (*From Bender, 1964.*)

Normally, a tube failure necessitates a boiler shutdown only because of excessive water loss.

The water-tube steam generators may be classified as either natural-circulation systems or forced-circulation boilers. Most of the older steam generators are natural-circulation systems. In these units, the fluid flow is induced by the difference in the specific weight of the water in the vertical supply tubes and the average specific weight of the water-steam mixture in the evaporator tubes where the water is boiled. The driving force for fluid flow through the evaporator section is equal to the product the difference in the average specific weights and the height of the evaporator tubes. This driving force is balanced by the frictional pressure drop in the supply and evaporator tubes. Most of the pressure drop occurs in the evaporator tubes as the result of the two-phase flow of water and steam.

The principle of circulation in any natural-circulation boiler is shown in Fig. 4.22. The saturated water flows from the steam drum high in the boiler, through the supply or "downcomer" tubes located in the cooler part of the boiler, to the bottom or "mud" drum. From the mud drum, the water flows back to the steam drum through the evaporator or "riser" tubes. In the steam drum, the steam and water are separated and the steam is washed and dried before it is sent to the superheater. The internals of a typical steam drum are also presented in Fig. 4.22. The lower drum is commonly called the *mud drum* because any water impurities naturally gravitate to this drum. Periodically, some of the water in the mud drum is vented ("blown down") to the atmosphere and fresh boiler feed ("makeup") is added to lower the overall concentration of impurities in the water system.

As the steam pressure is increased, the density and specific weight difference between the saturated water and steam decreases, requiring a greater height (up to 15 stories high) for adequate flow. At the critical point of water, 374.1°C and 22.09 MPa (705.4°F and 3206.2 psia), the difference is zero and there is no natural-circulation driving force. Actually, at pressures greater than 16.5 MPa (2400 psia), the density difference is effectively too small for natural-circulation units and these systems must employ forced circulation.

In a forced-circulation boiler, the fluid is pumped through the evaporator section of the boiler. This permits operation of the power cycle at very high pressures, even above the critical pressure. High-pressure operation theoretically improves the efficiency of the basic steam cycle. The forced-circulation system eliminates the need for boiler height, it is lighter in weight, it uses smaller tubes and drums or no drums at all, and the lower total water content in the boiler reduces the danger of a steam explosion. In addition to the problems associated with the main circulation pump and potentially higher operating pressures, some of these systems also require extremely pure water—orders of magnitude purer than that required for natural-circulation systems.

There are many different kinds of forced-circulation boilers, depending upon the circulation paths in the evaporator. The most widely used forced-circulation boiler system in the United States is the *universal-pressure* (*UP*) or

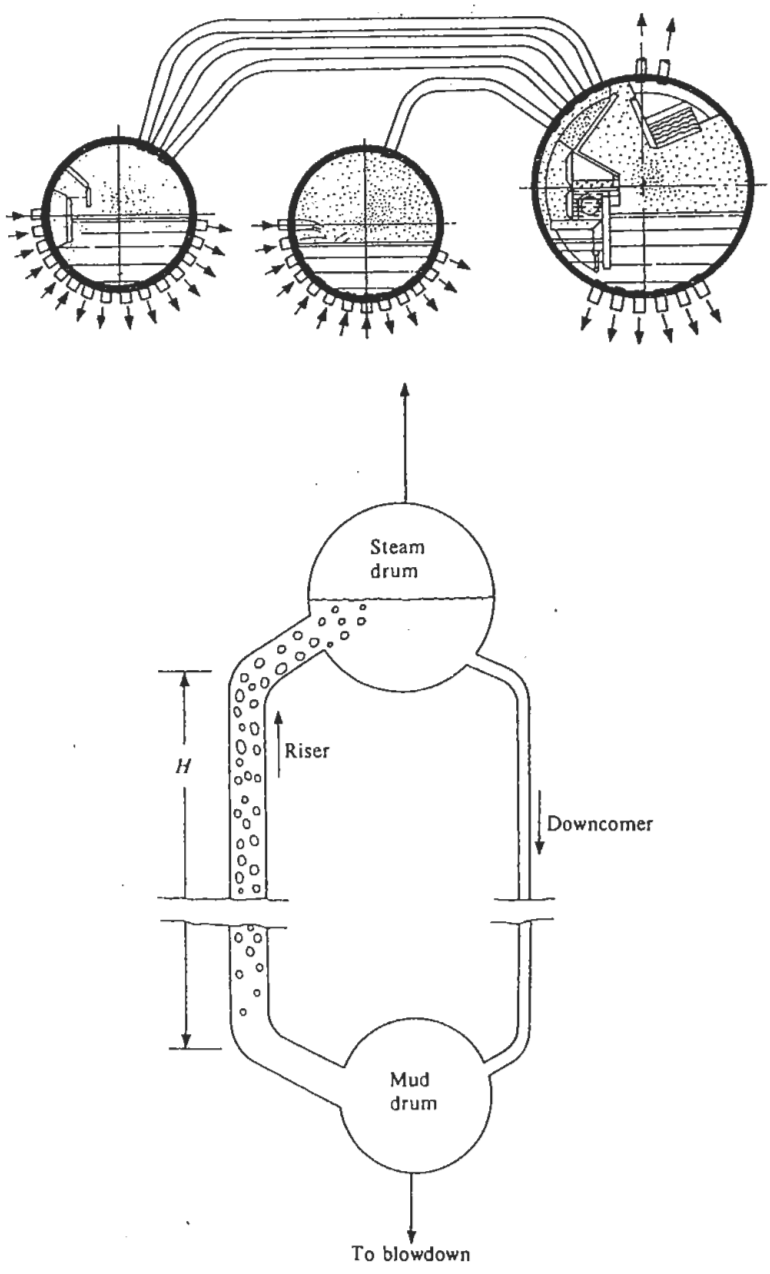


FIGURE 4.22
A typical steam drum and schematic diagram for a natural-circulation boiler. (*From Bender, 1964.*)

Benson boiler. A schematic diagram of the Benson boiler is shown in Fig. 4.23, along with schematics of a number of other forced-circulation units.

In the Benson boiler, the water is pumped to about 35 MPa (5000 psia) in the main feed pump. This compressed water is then piped to the economizer section, through the evaporator tubes, through a transition section, and finally

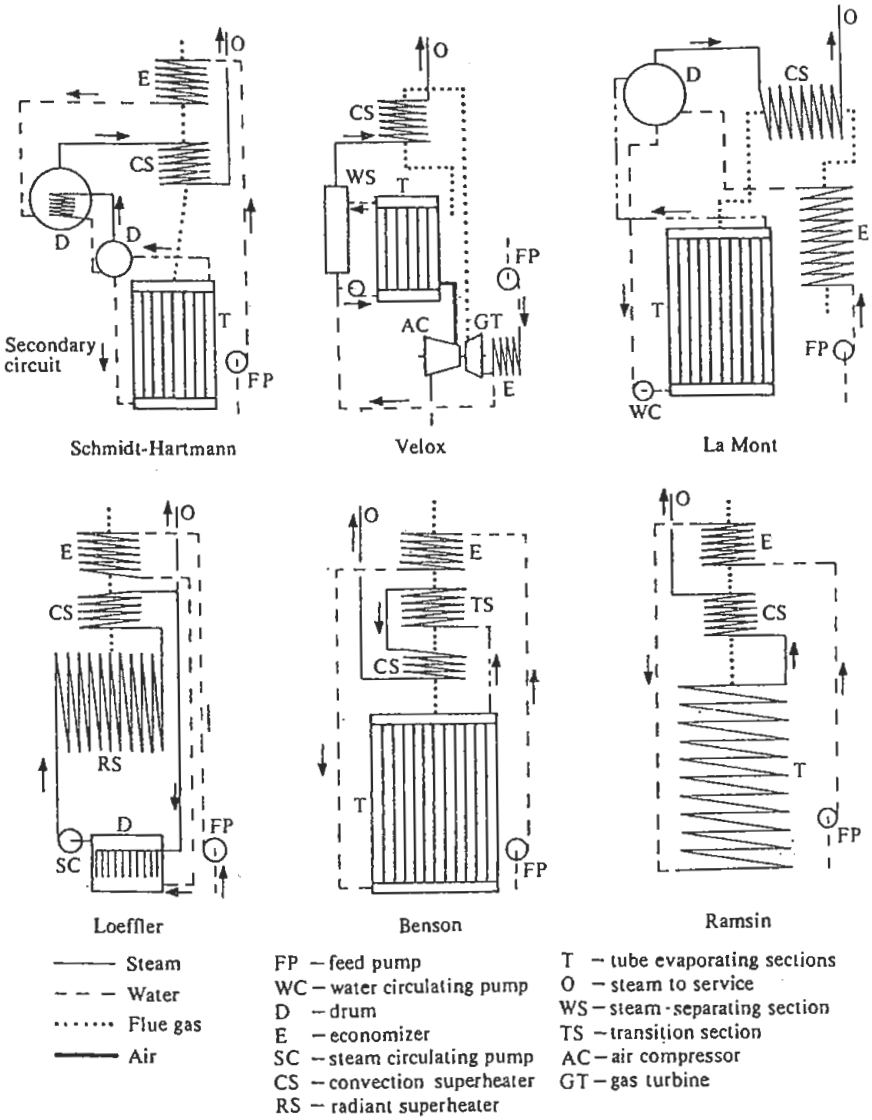


FIGURE 4.23
Schematic diagrams of forced-circulation boilers. (*From Skrotzki and Vopat, 1960.*)

through a convection superheater, where it is exhausted to the turbine at a pressure of around 24 MPa (3500 psia). This supercritical boiler system requires extremely pure water. The impurity concentration must be no higher than a few parts per billion because any impurity in the water will normally be deposited in the boiler tubing. The Ramsin boiler is essentially identical to the Benson boiler except that the evaporating section is composed of inclined T-bundle coils arranged in a spiral array.

The LaMont boiler, shown schematically in Fig. 4.23, closely resembles the natural-circulation boilers because it has a steam drum. Since the water-steam mixture is separated in this drum, the system must operate at a pressure below the critical pressure. The Velox boiler is an interesting unit because it combines the steam or Rankine power cycle with the gas-turbine or Brayton power cycle. This system is very different from the so-called combined-cycle systems that are becoming increasingly popular. In these latter systems, the gas turbine discharge is used as the source of hot combustion air in the steam generator. In the Velox system, the combustion air is compressed to 200 to 300 kPa (29 to 44 psia) in an air compressor that is driven by the gas turbine. The air is then heated and passed through the steam generator before it is discharged to the gas turbine. This unit produces steam at 1.4 to 8 MPa (200 to 1200 psia). It has a relatively high overall thermal efficiency but the steam-generator casing is essentially a pressure vessel which significantly increases the capital cost of the system.

As mentioned earlier, some of the forced-circulation systems require ultra-pure water but the Loeffler and the Schmidt-Hartmann boilers can operate while using feedwater with relatively high impurity levels. Both of these units must operate at pressures below the critical pressure. In the Loeffler boiler, the water is evaporated by part of the superheated steam and the resulting saturated steam is pumped through the superheater section. In the Schmidt-Hartmann boiler, the water is boiled by condensing steam in a higher-pressure, closed, natural-circulation, secondary system.

Despite some of the advantages realized by the forced-circulation boiler systems, the only unit that has seen widespread application in the United States is the universal-pressure or Benson boiler. Forced-circulation systems are fairly common in Europe where land is at a premium. Recently, difficulties encountered in the operation of universal-pressure boilers in the United States have reversed the trend of employing these systems. Many utilities are presently returning to the use of 16.5-MPa (2400-psia) natural-circulation boilers.

4.4.3 Primary Boiler Heat-Transfer Surfaces

The primary heat-transfer surfaces in the boiler include the evaporator section, the superheater section, and the reheat section if the power cycle employs reheat. The evaporative surface is usually located in the hottest part of the boiler near the combustion zone because the boiling water in the tubes protects the tube material from the excessive temperatures. The evaporator sections include the water walls, the water floor, and the water screens which are used to direct the

flow of the hot exhaust gases in the boiler. Three general types of water-wall surfaces are shown in Fig. 4.24. These include bare tubes, tubes with extended surfaces or metal-block facing, and studded tubes packed with refractory insulation or tile facing. The studded tubes with insulation are used where little heat transfer is desired such as in the large cylinder of a cyclone burner.

Superheater sections are the heat-transfer surfaces in which heat is transferred to the saturated steam to increase its temperature and available energy. Superheaters are particularly important in the production of turbine steam to reduce the moisture content of the steam as it passes through the turbine. Superheaters are commonly classified as either radiant, convection, or combined, depending on how they absorb thermal energy from the combustion products. It is usually desirable that the final steam temperature stay essentially constant over a wide range of boiler loads. When the exit steam temperature becomes

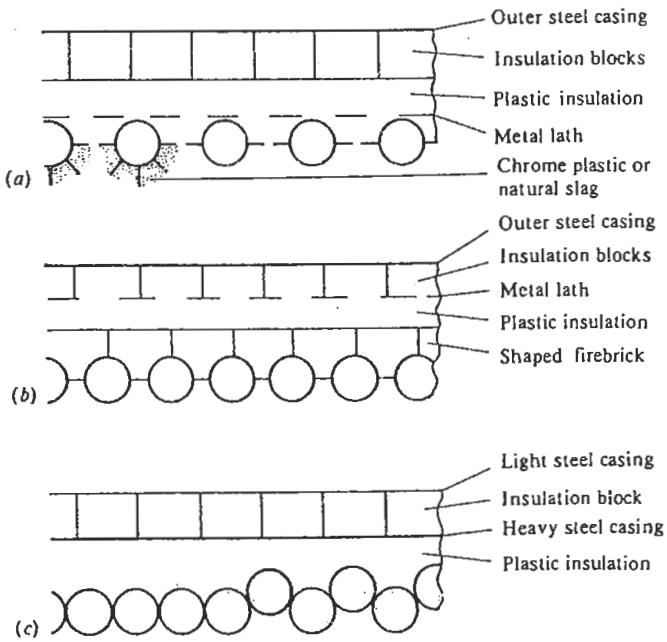


FIGURE 4.24
Evaporation water-wall surfaces used in steam boilers. (*a*) Steel lugs or longitudinal fins are often welded to nontangent wall tubes. In some designs, the lugs protrude from the tube into the furnace and are covered with a chrome-based refractory or slag. To assure furnace tightness, adjacent fins are often welded. (*b*) With moderate cooling a key requirement, this design has tubes spaced apart and wall surface composed of part firebrick. Brick is backed with several layers of insulation and a strong steel casing. Reinforcing metal lath is often used in wall construction. (*c*) Tangent tubes are favored in furnaces of many small and large boilers. In some designs, tubes are staggered. This arrangement offers high-heat-absorbing surface that is backed by solid block or plastic insulation and a strong steel external casing. (*From Bender, 1964.*)

excessive, some units employ an attemporator or desuperheater, in which compressed feedwater is sprayed into the superheated steam to lower its temperature. Many superheater sections are pendant-type units in which bundles of tubes are suspended in the exhaust gas ductwork.

The reheat section of a large boiler is that portion of the boiler in which all of the steam exhausting from the high-pressure turbine is returned for additional superheat before it is sent to the intermediate-pressure turbine or turbine section. The optimum reheat pressure is established by the maximum reheat temperature and the turbine exhaust conditions. It is normally around one-fourth the maximum superheater pressure. The reheat section is very similar to the superheater in appearance and location in the boiler.

4.4.4 Secondary Boiler Heat-Transfer Surfaces

The secondary heating surfaces recover heat from the flue gas after it has passed over the primary heat-transfer surfaces. In order to achieve a high boiler efficiency, it is desirable to lower the temperature of the exhaust gas as much as possible. There are two kinds of secondary heat-transfer surfaces—the economizer and the air preheater. The economizer transfers heat from the flue gas to the incoming boiler feedwater while the air preheater (sometimes simply called the *air heater*) transfers the flue-gas energy to the incoming combustion air.

While a low exhaust gas outlet temperature improves the boiler efficiency, the temperature should not be lowered much more than 85C° (≈150F°) above the dew-point temperature of the exhaust gas. If the temperature is lowered below this point, condensation will probably occur on the cold surfaces of the exhaust gas system. Any condensation in the flue-gas system is extremely undesirable since the liquid will be strongly acidic and corrosive because of the sulfur dioxide and sulfur trioxide in the exhaust. Unfortunately, the presence of small quantities of sulfur dioxide and particularly sulfur trioxide in the flue gas drastically raises the dew-point temperature of the gas over that of pure water vapor. The dew-point temperature can be increased from 40 to 50°C (104 to 122°F) to as high as 120 to 180°C (250 to 360°F) by the presence of SO_2 and SO_3.

The economizer is normally a cross-flow heat exchanger in which the heat is transferred from the flue gas to the incoming feedwater. It has been estimated that an increase of 6 to 7C° (10 to 12F°) in the temperature of the feedwater produced from the heat recovery in the economizer will increase the boiler efficiency about 1 percent. The flue gas leaving the economizer should be at least 80C° (≈150F°) above the dew-point temperature of the flue gas to prevent condensation and the boiler feed should be at least 30C° (≈50F°) below the saturation temperature of the boiler feed. This prevents any boiling and resulting two-phase flow with the accompanying high pressure drop in the economizer as the result of minor pressure fluctuations in the boiler.

In the design of economizer systems, the high-pressure water is put inside the economizer tubes. Since the gas-side, heat-transfer convection coefficient is low and is the controlling heat-transfer coefficient in the system, it is common

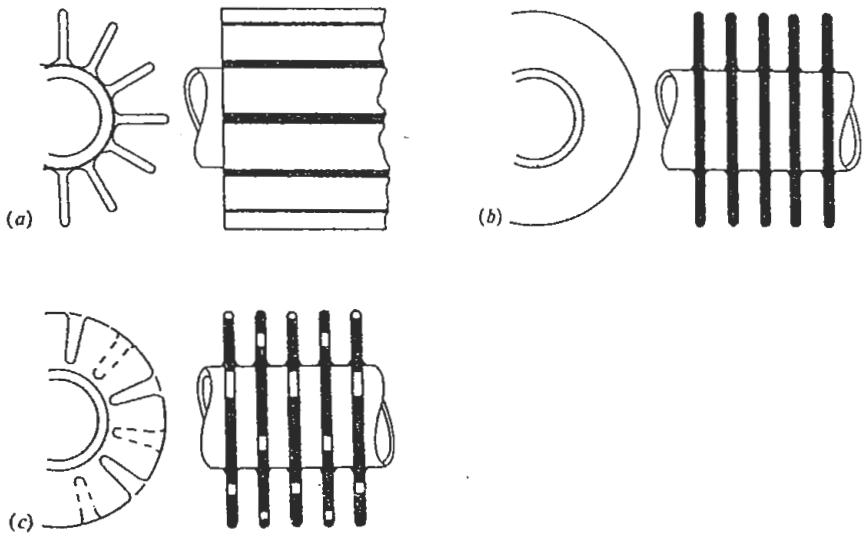


FIGURE 4.25
Economizer heat-transfer sections. (*a*) Welding continuous fins onto tubes lengthwise increases heat transfer. This design also improves antisag feature. Typical fins used today may be 0.25 in thick, 2 in high. (*b*) Another extended heating surface consists of gilled ring tubing made of cast iron or steel. Fins may be square-shaped, totally independent, or a continuous spiral. (*c*) One design favors separate lentil-shaped steel lugs that are welded around the tube. They keep soot from accumulating and are easy to keep clean. (*From Bender, 1964.*)

practice to use fins or extended surfaces in the economizer tubes. Some typical economizer sections are shown in Fig. 4.25.

One problem associated with any coal-fired boiler system, particularly a pulverized-coal system, is the ash content of the flue gas and the resulting buildup of ash or slag deposits on the heat-transfer surfaces of the boiler, both the primary and the secondary surfaces. The buildup of these deposits is particularly severe for those heating surfaces employing extended surfaces. It is common practice in coal-fired boilers to incorporate devices, called *soot blowers*, to remove the ash deposits from the tubes. These systems can be composed of stationary nozzles or retractable lances with rotating nozzles. Most of the soot blowers are powered with high-pressure air or steam. Some of these soot-blower systems are shown in Fig. 4.26.

In recent years, ash deposits also have been removed from the tube surfaces with the use of large acoustic horns. These stainless steel horns operate at a relatively low frequency of 250 Hz at a level of 145 dB. They are powered with 80-psia air and appear to be quite effective in removing the ash deposits.

The air preheater transfers thermal energy from the exhaust gas to the cold combustion air. There are two broad classes of air preheaters—the regenerative heaters and the recuperative heaters. The recuperative heater is a plate-type or

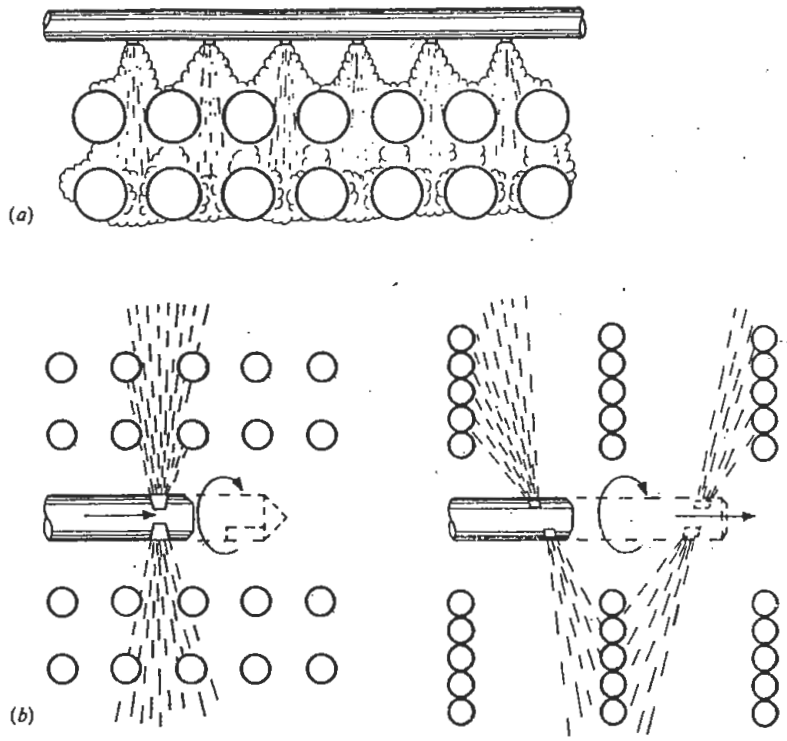


FIGURE 4.26
Soot-blower systems. (*a*) Stationary soot blowers employing straight nozzles clean banks of in-line tubes. With staggered tubes, the nozzles are offset for improved penetration. (*b*) Retractable blower lance, driven by two motors, traverses boiler at one speed, retracts at twice that speed. Result: about a 26 percent saving in cleaning time and in blowing medium. Speed of lance rotation is held throughout the cycle. (*From Bender, 1964.*)

tubular heat exchanger operating as either a counterflow or crossflow unit. A typical recuperative air preheater is shown in Fig. 4.27. A shot-cleaning system, rather than a soot-blower system, is commonly used to clean the flue-gas side of these heat exchangers. The shot-cleaning system operates by dropping 0.5-in, porous steel shot from the top of the exchanger. The shot knocks off the ash deposits as it trickles through the tubing. The shot is then separated from the flyash and returned to the top of the exchanger by a pneumatic transfer system. A typical shot-cleaning system is shown in Fig. 4.28.

The regenerative air preheater, or Ljungstrum heater, employs a large rotor assembly with approximately half of the element mounted in the exhaust gas duct and the other half in the supply air duct. The rotating element, which usually turns 2 to 4 r/min, contains many corrugated lamina that are alternately heated by the flue gas and cooled by the combustion air. The corrugated elements are

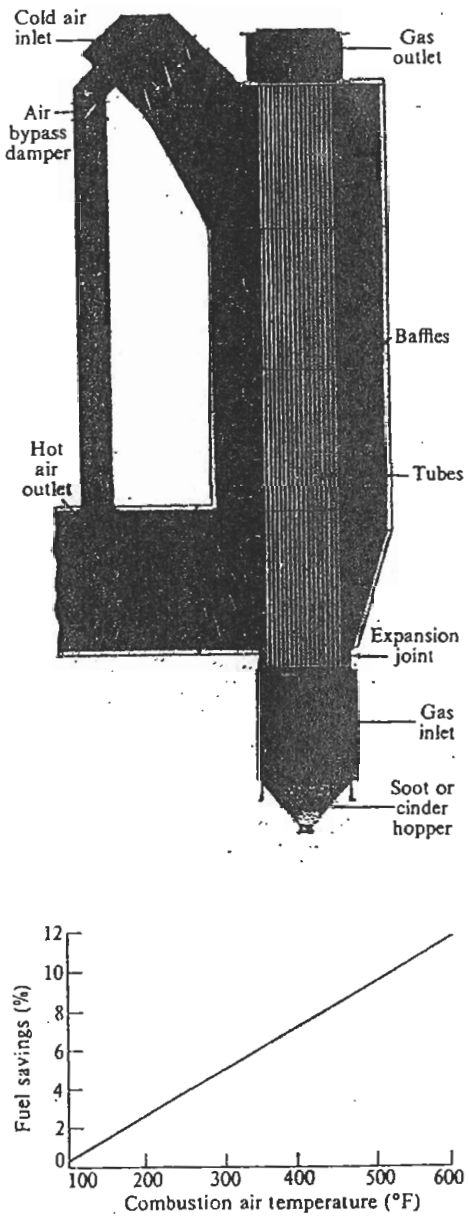


FIGURE 4.27
A cross-flow, recuperative air heater. (*From Bender, 1964.*)

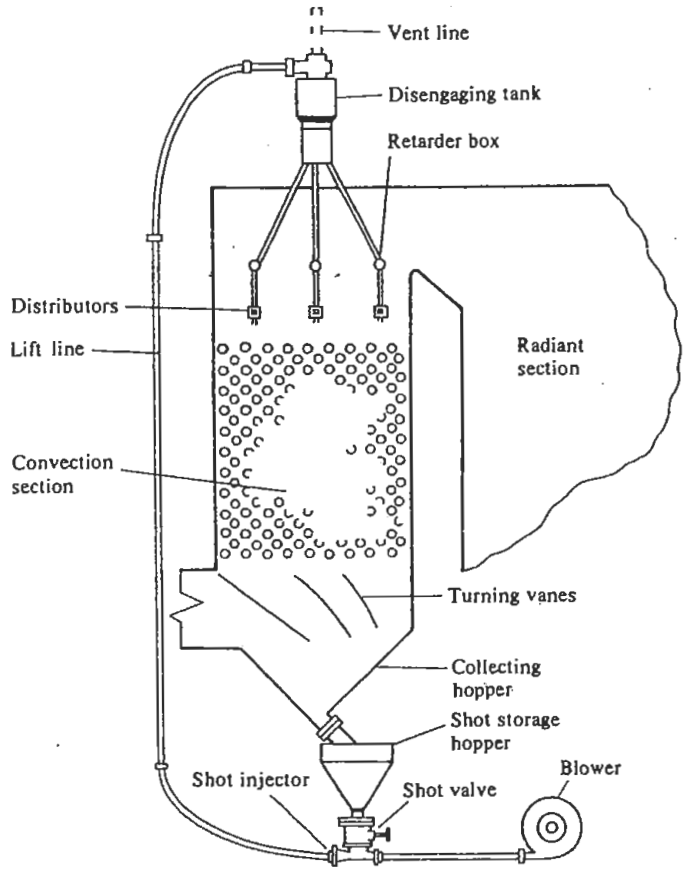


FIGURE 4.28
A shot-cleaning system. This technique calls for cascading metal balls onto heating surfaces. The cycle is automatic, utilizing pneumatic lift. (*From Bender, 1964.*)

commonly divided into upper and lower segments so that the coldest portion can be replaced periodically. The coldest part of the air preheater is a likely place where condensation occurs, with its corresponding increased corrosion. Radial seals and diaphragms keep leakage to a minimum but some leakage still occurs (in both directions) because of gas entrainment in the rotating lamina. A typical regenerative air preheater is shown in Fig. 4.29.

The air preheaters are useful in other ways than just improving the overall efficiency of the unit. They reduce the time required for fuel ignition, thereby improving fuel combustion. The maximum combustion-air temperature depends upon the type of furnace used. The inlet air for stoker furnaces is normally limited to a maximum temperature of 120 to 175°C (250 to 350°F) because this air is

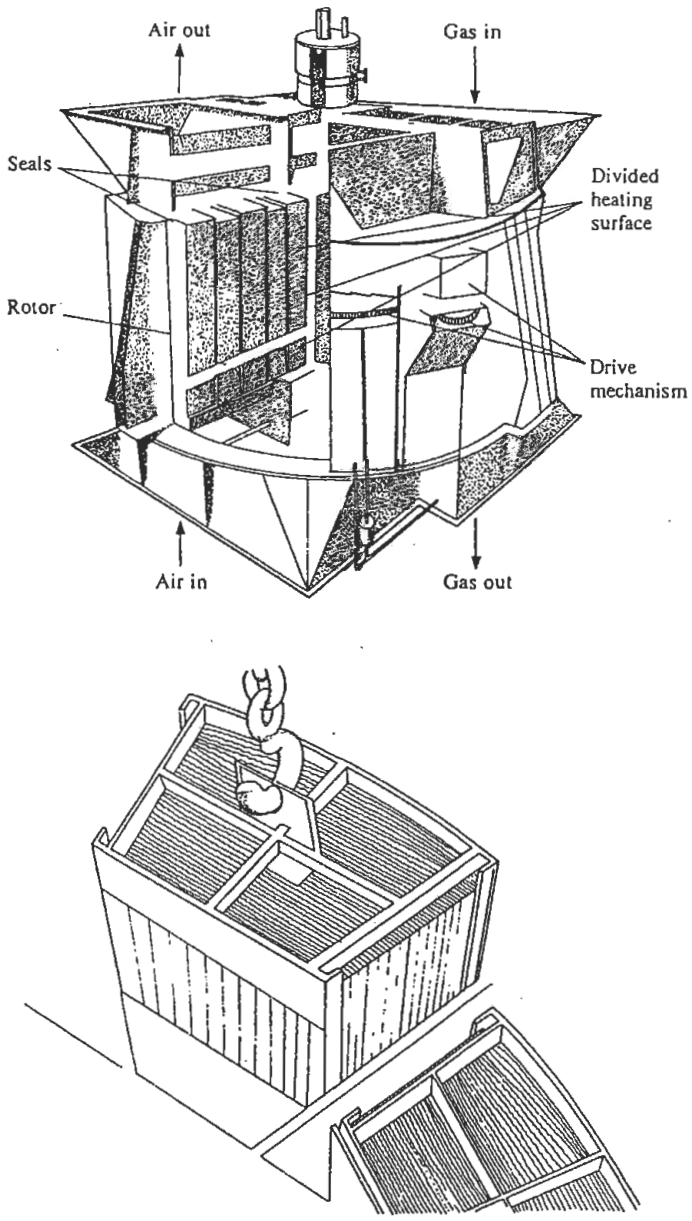


FIGURE 4.29
The regenerative air preheater. (*From Bender, 1964.*)

used to cool the stoker grates. The inlet air for a pulverized-coal furnace is limited to 290 to 315°C (550 to 600°F).

If one must choose only one of the two types of secondary heat-transfer surfaces, either the economizer or air preheater, the optimum choice is dictated by the type of system used. For large pulverized-coal or cyclone systems, the preheater surface is usually cheaper than the economizer surface for a given heat recovery. The effectiveness of an economizer may also be limited by the use of many feedwater heaters. For small stoker units where air heating is limited and only one deaerating feedwater heater is used, the economizer surface is normally less expensive for a given heat recovery than the preheater surface.

4.4.5 Boiler Ratings and Performance

In the early part of the twentieth century, an attempt was made to relate the output of the boiler to the output of the steam prime mover, which at that time was the reciprocating steam engine. This produced a unit of boiler output called a *boiler horsepower*, often abbreviated bhp. One bhp was supposed to produce 1 hp of mechanical energy. At that time, 1 bhp was defined as the generation of 34.5 lbm of steam per hour from water at 100°C (212°F). This resulted in a value of 33,500 Btu/h · bhp. At the same time that the boiler horsepower was developed, another term, called the *boiler rating*, was defined. A boiler with a rating of 100 percent was supposed to develop 1 bhp for each 10 ft^2 of evaporative heating surface, excluding the superheating and economizer surfaces.

Both the boiler horsepower and the boiler rating terms are antiquated quantities, as most modern steam generators have ratings in excess of 400 percent. If 1 bhp produces only 1 hp of mechanical energy, the thermal efficiency of the power system is only 7.6 percent. However, one still finds some small units, particularly small packaged boilers, that are rated in units of boiler horsepower. Most of the modern steam generators are rated in terms of steam capacity (usually lbm/h) along with the steam outlet pressure and temperature. There is no attempt, at present, to relate the turbine or generator output to the output of the boiler.

The figure of merit for operation of a boiler is the boiler or steam-generator efficiency η_{sg}. This quantity is defined as the fraction the input chemical energy that is transferred to the working fluid. The boiler efficiency commonly ranges from 70 to 90 percent and usually is highest at low boiler loads. There are two ways to calculate the boiler efficiency—the direct method and the indirect method.

In the direct method, the total heat added to the working fluid in the economizer, evaporator, superheater, and reheat sections of the boiler is evaluated and this quantity is divided by the total fuel-input energy:

$$\text{Boiler efficiency} = \eta_{sg} = 100\left(\frac{\text{total energy added to the working fluid}}{\text{total fuel input energy}}\right)$$

$$= 100\,\frac{\dot{m}_s(h_2 - h_1) + \dot{m}_r(h_4 - h_3)}{\dot{m}_f(\text{HHV})_{\text{fuel}}} \quad \text{percent} \qquad (4.10)$$

where $\dot{m}_f$ is the mass flow rate of the fuel, $\dot{m}_r$ is the mass flow rate of the steam

to the reheater, $\dot{m}_s$ is the mass flow rate of boiler feed to the steam generator, h_1 is the specific enthalpy of the boiler feedwater, h_2 is the specific enthalpy of the steam leaving the superheater, h_3 is the specific enthalpy of the steam entering the reheater, and h_4 is the specific enthalpy of the steam leaving the reheater. Since it is very difficult to measure the fuel and fluid flow rates much more accurately than ±5 percent, the direct method of evaluating the steam-generator efficiency is not too accurate and is not used in common practice.

Most boiler efficiency calculations are made using the indirect method of calculation. In this system, it is assumed that the total fuel-input energy is either transferred to the working fluid or is lost in a number of ways. These losses can be readily determined. There are a total of six boiler heat losses and all of them are calculated in terms of energy lost per unit mass of fuel (kJ/kg or Btu/lbm). Using this system, the steam-generator efficiency becomes:

$$\eta_{sg} = 100\left(\frac{\text{higher heating value of fuel} - \text{total losses}}{\text{higher heating value of fuel}}\right)$$

$$= 100\,\frac{\text{HHV}_{\text{fuel}} - \text{total losses}}{\text{HHV}_{\text{fuel}}} \tag{4.11}$$

The six major boiler losses are the dry-gas loss (DGL), the moisture loss (ML), the moisture-in-combustion-air loss (MCAL), the unburned-carbon loss (UCL), the incomplete-combustion loss (ICL), and the radiation and unaccounted loss (RL). These losses are determined by using the ultimate analysis of the fuel, the orsat analysis of the flue gas, and the refuse analysis when the system is coal-fired, along with the pressures and temperatures of the fluids in the steam generator. Since these measurements can be made much more accurately than the steam flow rates, the indirect calculational method normally gives a more reliable estimate of the boiler efficiency than the direct method. Moreover, a relatively large error in one of these losses has a small effect on the calculation of the boiler efficiency.

The dry-gas loss (DGL) is that portion of the boiler losses that can be attributed to the combustion air supplied to the steam generator. Since this energy is all sensible heat, it can be estimated by using the actual, dry, gravimetric air-fuel ratio and the gas temperatures. The mass of dry flue gas generated per unit fuel mass is equal to the actual, dry, gravimetric air-fuel ratio plus the unit fuel mass less the refuse mass fraction and the mass of water present (M) and formed ($9H_2$) during the combustion process:

$$\text{DGL} = w_g c_p (T_{g,\text{out}} - T_{g,\text{in}})$$

$$= \left[\left(\frac{A}{F}\right)_{\text{A,G,D}} + 1.0 - R - M - 9\text{H}_2\right] c_p (T_{g,\text{out}} - T_{g,\text{in}}) \tag{4.12}$$

where $w_g = (A/F)_{\text{A,G,D}} + 1.0 - R - M - 9\text{H}_2$, kg of dry flue gas/kg fuel

c_p = specific heat of the flue gas (assumed to be the same as that of air) = 1.0035 kJ/kg · C°

$T_{g,\text{in}}$ = inlet air temperature, °C

$T_{g,\text{out}}$ = outlet flue-gas temperature, °C

and R, M, and H_2 are the refuse, moisture, and hydrogen mass fractions as determined from the refuse and as-burned ultimate analyses. The dry-gas loss is almost always one of the major boiler lossess in any combustion system.

The moisture loss (ML) includes the loss due to vaporizing the moisture in the fuel and the loss due to the latent heat of the moisture produced from the combustion of the hydrogen in the fuel:

$$\mathrm{ML} = (M + 9\mathrm{H}_2)(h_s - h_w) \tag{4.13}$$

where h_s = specific enthalpy of superheated steam at $T_{g,out}$ and a pressure of 7 kPa (the approximate partial pressure of the water vapor in the flue gas), kJ/kg

h_w = specific enthalpy of water at the inlet gas temperature, $T_{g,in}$, kJ/kg

If $T_{g,out}$ exceeds 300°C,

$$h_s - h_w \approx 2442 + 2.093\,T_{g,out} - 4.187\,T_{g,in} \tag{4.14}$$

If $T_{g,out}$ is less than or equal to 300°C,

$$h_s - h_w \approx 2492.6 + 1.926\,T_{g,out} - 4.187\,T_{g,in} \tag{4.15}$$

The values of M and H_2 are the fuel mass fractions of moisture and hydrogen, respectively, from the as-burned ultimate fuel analysis, $h_s - h_w$ is the enthalpy difference, in kJ per kg, and the temperatures are in °C. The moisture loss is a major loss in most boilers and is higher for natural-gas fired units because of the higher hydrogen content.

Another but much smaller moisture loss is the moisture-in-combustion-air loss (MCAL) (the latent heat is not involved in this calculation as this moisture enters and leaves the combustion process as a superheated vapor):

$$\mathrm{MCAL} = \left(\frac{A}{F}\right)_{A,G,D} \omega c_{p,w}(T_{g,out} - T_{g,in}) \tag{4.16}$$

In Eq. (4.16), ω is the humidity ratio of the entering air, in kg of moisture/kg of dry air, and $c_{p,w}$ is the specific heat of water vapor, or 1.926 kJ/kg · °C.

The specific humidity can be evaluated from Fig. 4.30 as a function of the dry-bulb and the wet-bulb temperatures, in °F. It can also be calculated from Eq. (4.17) if the relative humidity ϕ and the total atmospheric pressure p_{atm}, are known:

$$\omega = \frac{0.622\phi p_{sat}}{p_{atm} - \phi p_{sat}} \tag{4.17}$$

In this equation, p_{sat} is the saturation pressure of the water vapor at $T_{g,in}$ and ϕp_{sat} is the partial pressure of the water vapor in the air. The moisture-in-combustion-air loss is normally one of the smaller boiler losses—at least an order of magnitude lower than the moisture and dry-gas losses for most fuels.

The unburned-carbon loss (UCL) is the boiler loss associated with the appearance of carbon in the refuse. This loss is equal to the product of the mass of unburned carbon per unit mass of fuel in the refuse (C_r) and the higher heating

4.4. During the test of a [460; 480; 500; 520; 540]-hp Babcock and Wilcox boiler, the following data were obtained:

Coal rate = [975; 1000; 1025; 1050; 1075] kg/h
Coal to refuse ratio = 5.37
Percentage of combustible in the refuse = 22.84%
Ultimate coal analysis: C = 60.31%, H_2 = 4.06%, O_2 = 6.71%, N_2 = 1.13%, S = 5.23%, A = 22.56%
Orsat analysis of flue gas: 10.58% CO_2, 8.41% O_2, and 0.23% CO

Find: (*a*) the boiler efficiency if 1 bhp = 33,500 Btu/h; (*b*) the percentage of excess air; (*c*) the mass of flyash going up the stack, in kg/h.

4.5. A 2284-MW_e power plant burns Linn County, Missouri, coal with *M* and *A* of 12 percent and 8 percent, respectively, and the heat rate is [8800; 9000; 9200; 9400; 9600] Btu/kWh. This plant has eight f-d fans and eight i-d fans. The f-d fans are designed to pump air at [32; 36; 40; 44; 48]°C and 93 kPa across a pressure rise of 3.5 kPa, and the i-d fans are designed to pump exhaust gas at 150°C and 88 kPa across a pressure rise of [3.5; 4.0; 4.5; 5.0; 5.5] kPa. Assume that the mechanical efficiency of each fan is 80 percent. An analysis of the refuse pit shows that the higher heating value of the refuse is 3280 kJ/kg. An orsat analysis of the flue gas yields: 14.36% CO_2, 4.01% O_2, and 0.78% CO.

Find: the percentage of excess air for this system as well as the fan capacities in ft^3/min and the horsepower requirements for the fans.

4.6. When St. Clair County, Illinois, coal (*M* = 10 percent and *A* = 12 percent) is burned in a [200; 400; 600; 800; 1000]-MW_e power plant with a heat rate of [8800; 9000; 9200; 9400; 9600] Btu/kWh, the heating value of the refuse is 4685 kJ/kg and the orsat analysis gives: 12.45% CO_2, 5.45% O_2, and 1.43% CO.

(*a*) Find the coal rate for the unit in tonne/h and in ton/h.
(*b*) Find the mass (kg/h) and volumetric (ft^3/h) flow rates of combustion air required to burn the fuel if atmospheric air is at 95 kPa and 40°C.
(*c*) Repeat part (*b*) for the exhaust gas if it leaves at 88 kPa and 240°C.
(*d*) Find the horsepower requirements of the i-d and f-d fans if the pressure rise across each fan is 6 kPa and the fan efficiencies are 80 percent.
(*e*) Find the dew-point temperature of the exhaust gas.

4.7. A boiler consumes [100; 150; 200; 250; 300] tons of coal per hour. The coal has the following ultimate analysis: C = 71.89 percent, H_2 = 6.69 percent, S = 1.91 percent, O_2 = 1.17 percent, N_2 = 2.68 percent, *M* = 8.82 percent, and *A* = 6.84 percent. The higher heating value of the refuse is 4333 kJ/kg and the orsat analysis is: 11.27% CO_2, 6.62% O_2, and 1.32% CO. Assume the air enters the f-d fan at 94 kPa and 45°C and the flue gas enters the i-d fan at 87 kPa and 310°C. If the mechanical efficiency of each fan is 80 percent, find the required power of each fan, in kW and in hp, and the capacity of each fan, in ft^3/min. Assume the pressure rise across each fan is [3.5; 4.0; 4.5; 5.0; 5.5] kPa. Also, determine the percentage of excess air and the dew-point temperature of the exhaust gas and estimate the electrical power output of the plant if the overall heat rate is 9750 Btu/kWh.

4.8 If the relative humidity of the incoming air is [30; 35; 40; 45; 50] percent and all four walls of the furnace are water-cooled, determine the boiler heat balance and the boiler efficiency for the system in Prob. 4.7.

4.9. The following data were taken during a boiler test:

Ultimate analysis of dry coal: 75.97% C, 4.83% H_2, 1.39% N_2, 5.70% O_2, 2.48% S, 12.63% *A*, and HHV = 30,724 kJ/kg
Moisture content, as fired = 4.6 percent
Orsat analysis: 12.93% CO_2, 6.03% O_2, and 0.08% CO
Temperature of the flue gas = [180; 190; 200; 210; 220]°C
HHV of refuse = 2472 kJ/kg
Atmospheric conditions: 21°C, 92 kPa, and a relative humidity of [70; 75; 80; 85; 90] percent

The boiler is a 40-MBtu/h unit with water tubes on three sides of the unit which is operated at 10 MBtu/h during the test. Estimate the boiler efficiency.

4.10. The following data were collected during operation of a [400; 500; 600; 700; 800] MW_e power plant operating at a heat rate of [9000; 9200; 9400; 9600; 9800] Btu/kWh:

Coal (as fired): Williamson County, Illinois, coal with $M = 8$ percent and $A = 12$ percent
Orsat analysis: 13.8% CO_2, 4.8% O_2, and 0.7% CO
Combustion-air conditions: 90°F DBT and 81°F WBT
Outlet flue-gas temperature: 260°C
Percentage of combustible in the refuse = 17.8 percent
System power during the test = 400 MW_e

Determine:

(*a*) The coal rate in tonne/h and ton/h
(*b*) The percent excess air
(*c*) The energy losses for the boiler, including the radiation loss, if only two of the furnace walls are cooled
(*d*) The boiler efficiency (using the indirect method)
(*e*) The dew-point temperature of the exhaust gas (assuming a maximum flue-gas pressure of 92 kPa)

4.11. Calculate the boiler heat balance and the boiler efficiency from the following data:

Ultimate as-burned coal analysis: 10.48% *A*, 1.1% S, 4.1% H_2, 77.39% C, 1.62% N_2, 5.31% O_2, and HHV = 30,866 kJ/kg
Duration of test: 24 h
Fuel fired during the test = 382.18 tonne
Heating value of the refuse = 1872 kJ/kg
Water supplied to boiler during the test = 4075,732 kg
Outlet steam conditions: 400°C and 5.8 mPa
Inlet water temperature = 190°C
Fuel and air temperature = [25; 29; 33; 37; 41]°C
Relative humidity of the inlet air = 50%
Outlet gas temperature = [225; 250; 275; 300; 325]°C
Orsat analysis: 14.7% CO_2, 3.7% O_2, and 0.2% CO

4.12. The following data were obtained from a boiler evaporation test:

Boiler efficiency = 77 percent
Ultimate as-burned coal analysis: 65% C, 4% H_2, 8% O_2, 2% S, 10% *A*, 1% N_2, 10% *M*, and HHV = 26,352 kJ/kg

Refuse analysis: 20% combustible
Orsat analysis: 14.18% CO_2, 3.55% O_2, and 1.42% CO
Combustion-air conditions: [25; 27; 29; 31; 33]°C DBT and 22°C WBT
Flue-gas temperature = [220; 230; 240; 250; 260]°C
Boiler steam temperature = 180°C

Find the individual boiler losses and the dilution coefficient, and estimate the dew-point temperature of the flue gas leaving the boiler if the flue gas has a maximum pressure of 14.8 psia.

4.13. An 80-MW_e power plant operates at an average heat rate of [8700; 8900; 9100; 9300; 9500] Btu/kWh. Two sides of the firebox are cooled and the system is fired with Coal County, Oklahoma, coal with M and A of 6 percent and 10 percent, respectively. During a test with the boiler operating at 30 percent capacity, the following data were taken:

Refuse analysis: HHV = 7188 kJ/kg
Orsat analysis: 13.83% CO_2, 4.21% O_2, and 1.15% CO
Exhaust gas temperature: [260; 280; 300; 320; 340]°C
Air conditions: 32°C, 98 kPa, and 50 percent relative humidity

Estimate the boiler efficiency and the percentage of excess air.

4.14. Data from a boiler test are as follows:

Ultimate analysis of coal: 60% C, 4% H_2, 6% O_2, 1% N_2, 3% S, 12% M, and 14% A
Refuse analysis: HHV = 6770 kJ/kg
Orsat analysis: 13.57% CO_2, 4.37% O_2, and 1.18% CO
Air conditions: [21; 24; 27; 30; 33]°C DBT and 16°C WBT
Flue-gas temperature: [180; 210; 240; 270; 300]°C

Calculate the percent excess air and the boiler efficiency if the radiation loss is 3 percent of the input energy. Use Dulong's formula to determine the HHV of the fuel.

4.15. The Bruce Mansfield power plant of the Pennsylvania Power Company is a three-unit, pulverized-coal system with a total output of 2751 MW_e. Each unit has two f-d fans and eight i-d fans. The f-d fans have a pressure rise of 8 kPa with dry inlet air at 1 atm and 27°C. The i-d fans have a pressure rise of 8.5 kPa with 48°C and 0.9135-kg/m^3 flue gas. Assume that the system burns Elk County, Pennsylvania, coal with moisture and ash fractions of 0.03 and 0.09, respectively. The plant heat rate is [8500; 8800; 9100; 9400; 9700] Btu/kWh and the HHV of the refuse is 1058 kJ/kg. The orsat analysis gives: 13.77% CO_2, 4.40% O_2, and 0.99% CO.

Find:

(*a*) The maximum coal rate for the plant at full power, in ton/h
(*b*) The percent excess air
(*c*) The horsepower requirement for each of the six f-d fans
(*d*) The horsepower requirement for each of the 18 i-d fans
(*e*) The energy losses for the boiler when the three of the furnace walls are cooled and the test data are:
  Power during boiler test = rated power of one unit/3
  Air conditions: 32°C and 80 percent relative humidity
  Exit flue gas temperature = [240; 260; 300; 340; 380]°C
(*f*) The boiler efficiency (using the indirect method)
(*g*) The dew-point temperature of the flue gas

REFERENCES

Bender, R. J.: "Steam Generation," a *Power Magazine* special report, McGraw-Hill, New York, June 1964.

Dillio, C. C., and E. P. Nye: *Thermal Engineering*, International Textbook Company, Scranton, Pa., 1963.

Editors of *Power Magazine*: "Axial Fans Reduce Operating Costs," in *Generation Planbook*, McGraw-Hill, New York, 1976.

Engineers Reference Library: "Fans," by the Editors of *Power Magazine*, the magazine of generation and plant utilities engineering, McGraw-Hill, 1969.

Fritsch, T. J.: "World's Largest Boiler Feed Pump," *Proceedings of the American Power Conference*, vol. 36, pp. 539–546, Illinois Institute of Technology, Chicago, 1974.

Hays, T. C., B. C. Krippene, G. J. Clessuras, and G. E. McMackin: "Development of Large Components for Large Steam Generators," *Proceedings of the American Power Conference, 1973*, vol. 35, pp. 616–625, Illinois Institute of Technology, Chicago, 1973.

Lorenzi, Otto de (ed.): *Combustion Engineering*, Combustion Engineering-Superheater, New York, 1952.

Mesko, J. E., and R. L. Gamble: "Atmospheric Fluidized-Bed Steam Generators for Electric Power Generation," *Proceedings of the American Power Conference*, vol. 36, pp. 491–499, Illinois Institute of Technology, Chicago, 1974.

Skrotski, B. G. A., and W. A. Vopat: *Power Station Engineering and Economy*, McGraw-Hill, New York, 1960.

Steam: Its Generation and Use, 38th ed., Babcock and Wilcox Company, New York, 1972.

Wilhem, B. W., et al.: "The Effect of Water Jet Lancing on Furnace Walls," *Proceedings of the American Power Conference*, vol. 37, pp. 410–420, Illinois Institute of Technology, Chicago, 1975.

CHAPTER 5

NUCLEAR REACTOR DESIGN AND OPERATION

5.1 INTRODUCTION

Of all the fuel sources, nuclear fission probably has the poorest public relations and, as a result, the lowest public acceptance. In fact, in a 1986 public-opinion poll, the general public rated nuclear power as the No. 1 technological hazard to health—ranking it above smoking and motor-vehicle accidents. Energy experts, in the same poll, ranked smoking No. 1 followed by motor vehicles. These same experts ranked conventional combustion power systems ninth and they ranked nuclear units No. 20 among the 30 listed life-threatening technologies.

Despite an excellent safety record in the United States, in which there are no known deaths among the general public from the operation of the more than 100 commerical nuclear power plants currently in operation, there have been no new nuclear power plants ordered since the Three Mile Island (TMI) accident in 1978. There were a number of plant workers and firemen killed and injured in the U.S.S.R. as the result of the Chernobyl disaster of 1986. However, the 20,000 lives originally reported as lost because of Chernobyl by some of the media in this country appear to have been grossly exaggerated by several orders of magnitude. During the first 12 months after the accident, the Soviets reported a total of 31 deaths, but undoubtedly more will occur in the future.

The TMI incident, in 1978, was a major reactor accident and a financial disaster to the utility. Even though it was the worst reactor accident in the United States to date, and received prime-time coverage by the air and print media for

many months, it ranks as one of the few major disasters in which there is no known loss of life—plant workers or civilians. With the exception of a few minor controlled releases of radioactive gases, the built-in safety systems contained all of the radioactivity within the reactor complex. If the plant operating personnel had not mistakenly shut down the emergency core cooling system (one of the automatic safety systems), there would have been little or no damage to the plant.

The principal "fallout" from the TMI accident was not the radioactive material released but instead the myriad of new safety requirements and regulations imposed by the Nuclear Regulatory Commission (NRC). Some of these new rules were probably warranted, but many others were of questionable value. The new regulations increased the time to build a nuclear power system from 7 or 8 years to 12 to 15 years. The resulting delays have drastically increased the cost of nuclear power (see the example in Prob. 1.4), and unless the construction time can be drastically reduced, it will be some time before a utility is likely to build a new nuclear power plant in the United States. In 1988, the antinuclear hysteria led to the purchasing of the completed Shoreham Nuclear Station by the state of New York to prevent its operation. The cost of this acquisition was then passed on to the customers of the utility.

An electrical utility in France can put a new nuclear plant "on line" in 5 years, and consequently nuclear power costs there are considerably less than the

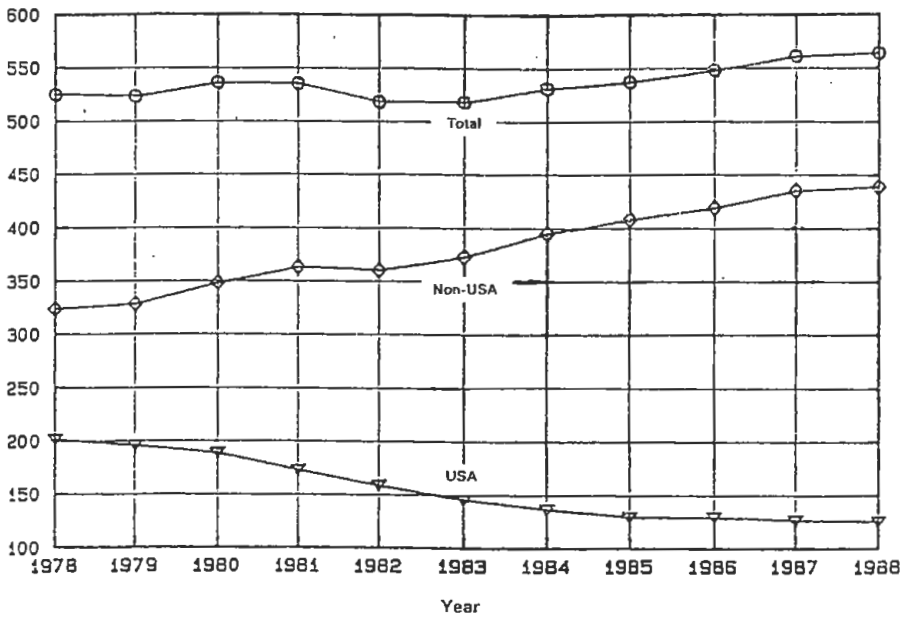


FIGURE 5.1
The total number of nuclear reactors planned, under construction, and in operation in the United States and the rest of the world since the Three Mile Island accident.

cost of power from fossil fuel. By 1986, nuclear power accounted for more than 60 percent of the electrical capacity of France, which is the world's leader in liquid-metal fast-breeder reactor (LMFBR) technology. Meanwhile, the United States (once the world's leader) had terminated the breeder reactor development. It should be noted, however, that concern about the "greenhouse effect" caused by the atmospheric release of CO_2 may accelerate interest in nuclear power in the United States.

This chapter covers the various power reactor systems currently in use in the United States and France as well as some of the problems associated with the thermal design and operation of these systems. It is assumed that the student is familiar with the general reactor terminology and the operational principles presented in Chap. 3. The growth and decline of the number of nuclear reactors under construction or in operation in the world and the United States, since the TMI accident (1979) is depicted in Fig. 5.1.

5.2 POWER REACTOR SYSTEMS

5.2.1 Light-Water Reactors

INTRODUCTION. All but one of the more than 100 nuclear power reactors currently operating in the United States are light-water reactors (LWRs). These are thermal reactor systems in which the water serves as both the coolant and the moderator. The use of ordinary water in these systems means that they must employ uranium fuel which is enriched to 2 to 3 percent. All LWR power systems employ cylindrical fuel rods mounted in a square fuel array, similar to that shown in Fig. 3.10. There are two basic types of light-water reactors, including the pressurized-water reactor (PWR) and the boiling-water reactor (BWR). In 1973, the Atomic Energy Commission (forerunner of the Nuclear Regulatory Commission) issued its Standardization Policy which set the maximum power of any power reactor system at 3800 MW_{th} plus the core power needed to drive the reactor's auxiliary equipment.

PRESSURIZED-WATER REACTORS. The pressurized-water reactor (PWR) is most prevalent of all the reactor systems currently being built in this country. It is also the basic power system employed in the Naval Reactor Program. The PWR is offered commercially by Westinghouse, Babcock and Wilcox, and Combustion Engineering.

There is no bulk boiling permitted in the reactor core of the PWR as the water is pressurized to about 15.5 MPa (2250 psia). The hot water from the reactor flows to a steam generator, where the heat is transferred to water and steam in a secondary cooling system that operates at lower pressure. The primary coolant then flows from the steam generator to the primary cooling pump, where it is pumped back to the reactor. A typical PWR primary cooling system is shown in Fig. 5.2, along with the secondary steam system. The operational parameters for the 800-MW_{th} PWR systems are given in Table 5.1.

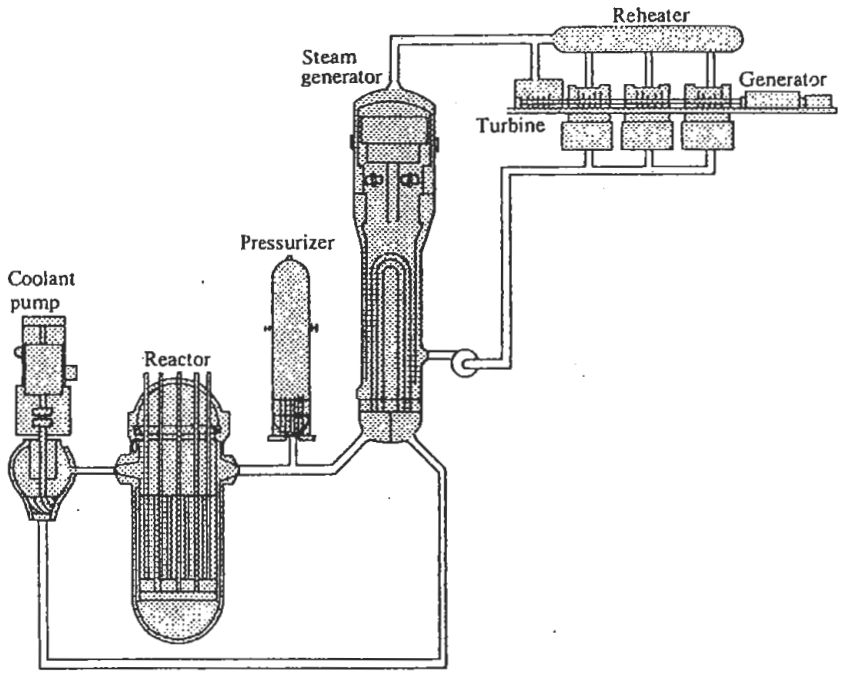


FIGURE 5.2
The primary and secondary cooling systems for a typical PWR. (*Courtesy of Westinghouse Electric Corporation.*)

The PWR primary system shown in Fig. 5.2 contains one component not discussed previously—the pressurizer. This system is simply a pressure vessel with a heater at the bottom and a water spray at the top. The top of the pressurizer is filled with steam at the primary-system pressure. If the primary-system pressure drops, the heater is energized to increase the steam content in the pressurizer thereby increasing the pressure of the primary cooling system. If the primary-system pressure is too high, cold pressurized water is sprayed into the steam volume to condense the steam and reduce the primary-system pressure.

Each PWR normally has two to four primary cooling loops but only one pressurizer. Each cooling loop contains a large steam generator and one or two primary pumps. The pressurizer for the Babcock and Wilcox PWR, which is typical for most PWRs, is shown in Fig. 5.3.

Two different kinds of steam generators are employed in PWR systems. The Westinghouse and Combustion Engineering system use a "U-tube" steam generator design which produces saturated secondary steam for the turbine. Babcock and Wilcox employs a once-through counterflow steam generator in which the hot primary water from the reactor actually produces superheated steam in the

TABLE 5.1
Operational and design parameters for 3800-MW_{th} pressurized-water reactor (PWR) systems

Nuclear Steam Supply System vendor	Westinghouse	Combustion Engineering	Babcock and Wilcox
System designation	Westinghouse 3817	System 80	Babcock 241
Core power, MW_{th}	3817	3817	3815
Number of primary coolant pumps	4	4	4
Pump power, hp	8000 (5970 kW)	8991 (6700 kW)	6870 (5125 kW)
Primary system pressure, lb/in^2 abs	2250 (15.5 MPa)	2250 (15.5 MPa)	2250 (15.5 MPa)
Number of fuel-element assemblies	193	241	241
Active core length, in	164 (4.165 m)	150 (3.81 m)	143 (3.632 m)
Number of control rod assemblies	61	89	84
Reactor-inlet temperature, °F	559 (293°C)	564.5 (295.8°C)	573.5 (300.8°C)
Reactor-outlet temperature, °F	623 (328.3°C)	621.5 (327.5°C)	629.4 (331.9°C)
Coolant flow rate, 10^6 lbm/h	147 (667 Gg/h)	164 (744 Gg/h)	159 (721 Gg/h)
Number of primary loops	4	2	2
Secondary steam pressure, lb/in^2 abs	1100 (7.58 MPa)	1070 (7.38 MPa)	1135 (7.82 MPa)
Turbine steam temperature, °F	556 (291.1°C) (sat)	553 (289.4°C) (sat)	603 (317.2°C) (sup)
Nominal electrical rating, MW_e	1300	1300	1322

secondary loop. This improves the turbine performance and the overall performance of the system. The two kinds of steam generators are shown in Fig. 5.4.

The reactor core of a PWR system is enclosed in a large pressure vessel. These vessels are up to 21 ft in diameter and more than 40 ft in length. The walls are constructed of 8 to 10 in (0.203 to 0.254 m) of carbon steel with approximately $\frac{5}{16}$ in of stainless steel welded to the inside surface to provide corrosion protection from the hot water. All nozzles and major penetrations to the reactor pressure vessel are made above the reactor core to prevent the complete loss of coolant in the event of a failure of the primary-system piping. The cold water enters the reactor vessel above the fuel region, flows down the annular region between the core and the pressure vessel, and then flows up through the fuel elements where the fission energy is transferred to the water. The hot water is then piped to the steam generator.

The control rods in a PWR enter from the top of the reactor core and are actuated by a magnetic drive system. The absorber rods are pulled from the core by a magnetic "jack" or by a system containing an electromagnet. The reactor is "scrammed" by simply terminating the power to the magnets, letting the rods drop into the core under the influence of gravity. The older PWR systems employed "cruciform rods," similar to that shown in Fig. 5.10, while the newer systems use a control-element assembly similar to that shown in Fig. 3.14. The newer system puts cylindrical control rods into a number of different fuel assemblies. The basic PWR pressuure vessel and internal equipment are shown in Fig. 5.5.

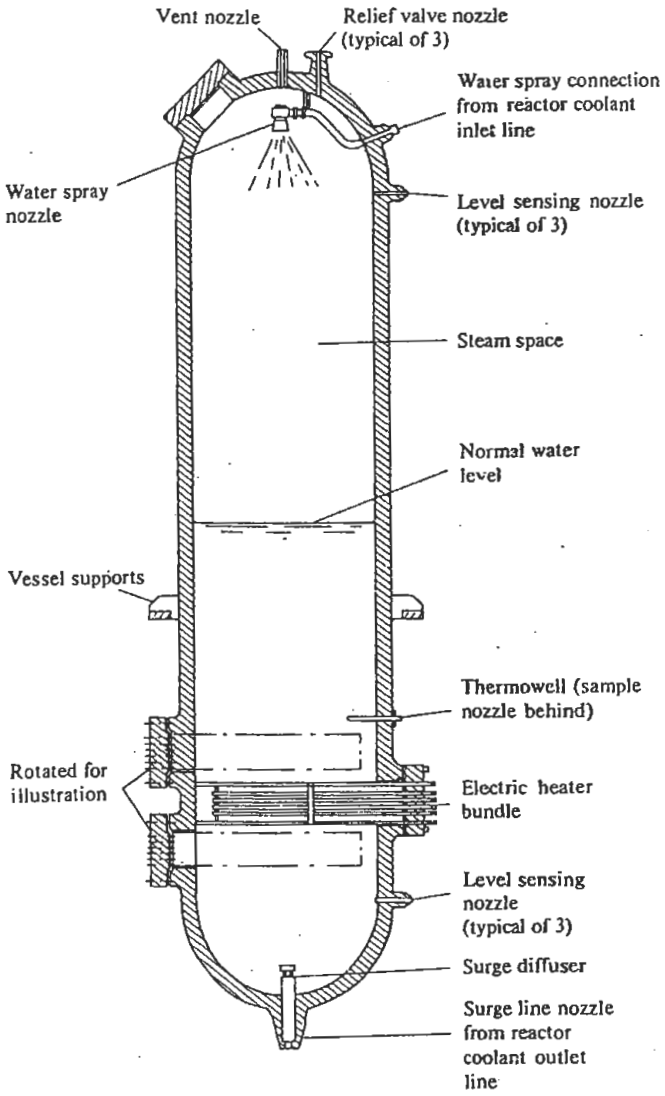
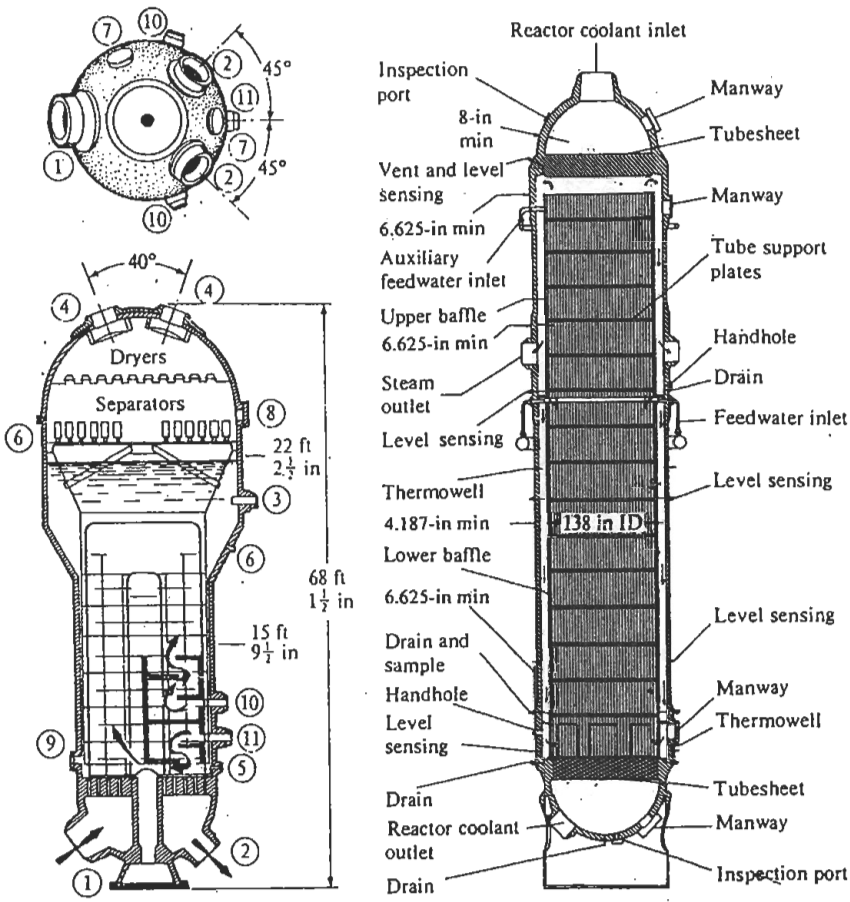


FIGURE 5.3
A typical pressurizer for the primary cooling loop of a PWR. (*From Steam: Its Generation and Use, 1972.*)

No.	Service
1	Primary inlet
2	Primary outlet
3	Auxiliary feedwater
4	Steam outlet
5	Blowdown
6	Liquid level
7	Primary manway
8	Secondary manway
9	Handhole
10	Upper feedwater
11	Lower feedwater



"U-tube" steam generator

"Once-through" steam generator

FIGURE 5.4
The large PWR steam generators. (*From Bevilacqua and Gibbons, 1974; and from Steam: Its Generation and Use, 1972.*)

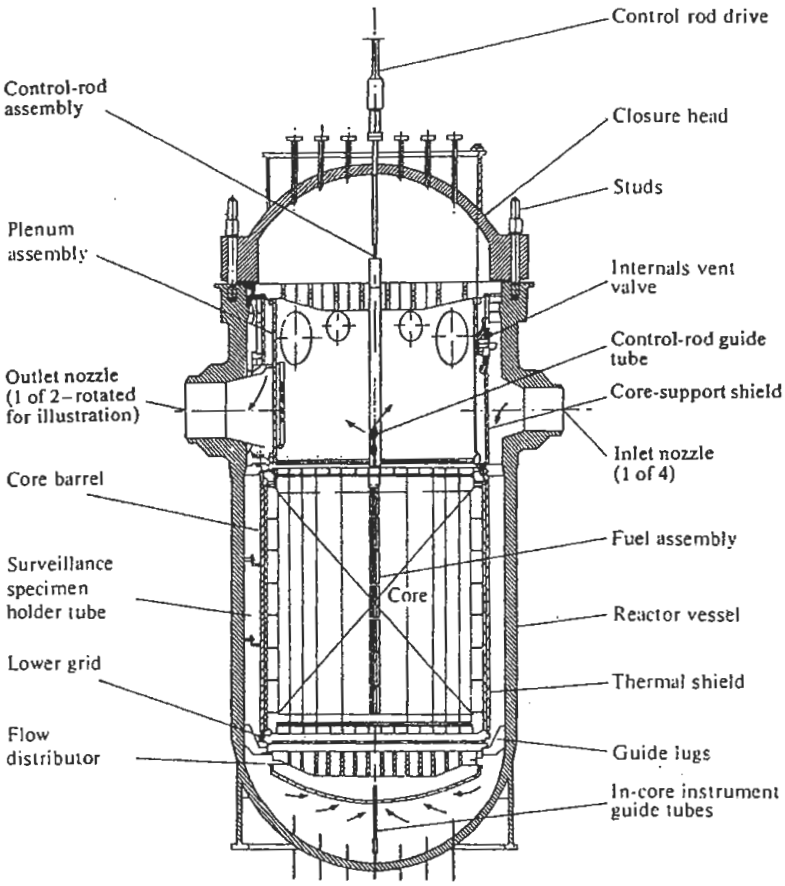


FIGURE 5.5
The PWR pressure vessel and internals. (*From Steam: Its Generation and Use, 1972.*)

BOILING-WATER REACTORS. In the boiling-water reactor (BWR), saturated steam is generated in the reactor core and this steam is dried and sent directly to the steam turbine. This system eliminates the large, expensive, high-maintenance steam generators of the PWR systems although some of the early BWR units used small steam generators for control purposes. These reactor systems have had some problems with the carryover of radioactive material into the turbine and also with in-core vibration. The boiling-water reactor is promoted by the General Electric Company.

The early BWRs were called *dual-cycle flow systems* because they generated most of the turbine steam directly in the reactor core, but they also generated a portion of the turbine steam in a secondary steam generator at lower pressure

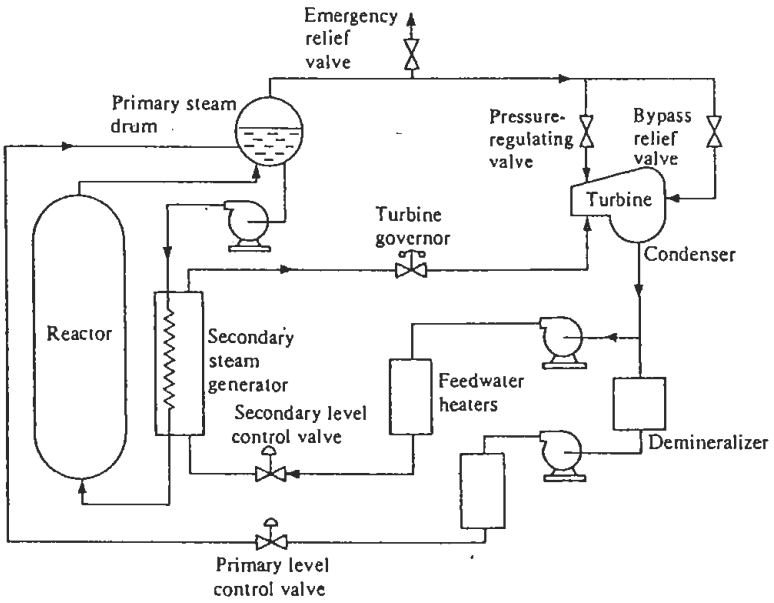


FIGURE 5.6
Schematic diagram of the dual-cycle BWR system. (*Courtesy of the General Electric Company.*)

for control purposes. A schematic diagram of the dual-cycle BWR system is shown in Fig. 5.6.

In a BWR, the amount of steam bubbles in the reactor core essentially controls the reactor power. Since the water coolant also moderates (slows down) the fast neutrons, an increase in the steam ("void") fraction in the core displaces water in the core, increasing the fast-neutron leakage, which reduces the reactor power unless the control rods are withdrawn. If the reactor steam is supplied to the turbine through a throttling valve and the valve is opened to increase the turbine power, the immediate effect is to lower the steam pressure in the reactor. The decrease in steam pressure increases the steam volume in the core and this results in a lower reactor power—just the opposite of the desired effect. This condition can be remedied by using a small secondary steam generator and placing the turbine throttle valve on the secondary steam supply line. In this case, opening the throttle valve reduces the secondary steam pressure and temperature, increasing the heat transfer from the primary water. The increased heat transfer lowers the coolant temperature entering the reactor and this condenses some of the in-core steam, thereby increasing the reactor power. This arrangement essentially gives the reactor an inherent load-following capability.

The latest BWR systems are single-cycle power reactors and require no secondary steam generators. The reactor power is controlled by varying the recirculation rate through the reactor core with a series of jet pumps that surround

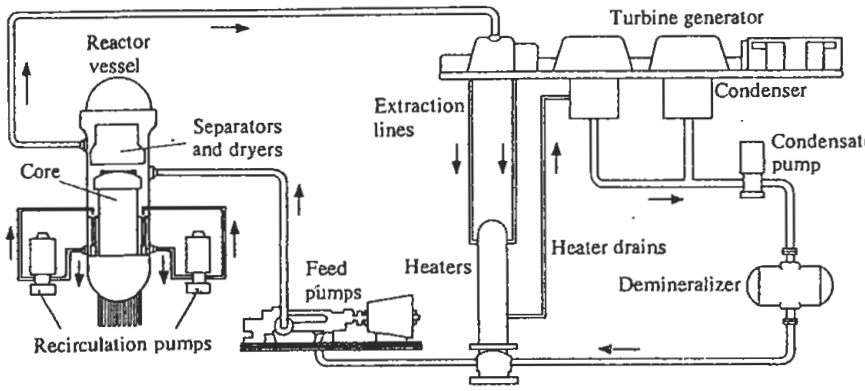


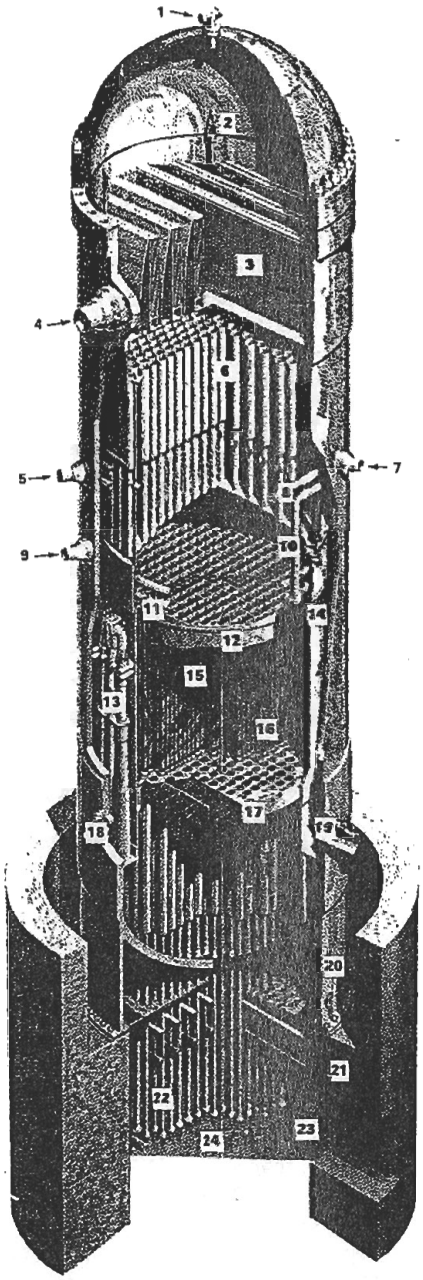
FIGURE 5.7
Schematic diagram of the single-cycle BWR system. (*Courtesy of the General Electric Company.*)

the core. When the power demand increases, the water recirculation rate through the core is increased and this sweeps the steam bubbles from the core, increasing the reactor power. The use of jet pumps around the periphery of the reactor core eliminates any moving parts inside the primary pressure vessel. A detailed illustration of the reactor system is shown in Fig. 5.7. Some of the design parameters for the latest 3800-MW_{th}, single-cycle BWR system, as offered by the General Electric Company, are listed in Table 5.2.

The pressure vessel for the BWR system is considerably larger than the PWR vessel although it operates at a pressure of only 6.9 MPa (1000 psia), which is less than half the operating pressure in the PWR. The top of the BWR vessel is filled with steam-drying equipment (see Fig. 5.8) and the control rods enter from the bottom of the core because the top is filled with steam equipment. Since the control rods cannot rely on gravity for emergency insertion ("SCRAM") as do the PWR systems, a hydraulic accumulator system is employed for each rod.

TABLE 5.2
Operational and design parameters for the 3800-MW_{th} boiling water reactor (BWR) system

Reactor designation	GE/BWR/6
Core power, MW_{th}	3,833
Number of fuel elements	784
Number of control rods	193
Pressure vessel ID, in	251 (6.375 m)
Recirculation pipe size, in	24 (0.61 m)
Core flow rate, 10^6 lbm/h	113.5 (250.2 Mg/h)
Recirculation-pump flow, gal/min	44,900 (10.2 Ml/h)
Pump power, hp	7,290 (5,440 MW)
Motor rating, hp	7,700 (5,740 MW)



BWR/6
REACTOR ASSEMBLY

1. Vent and head spray
2. Steam dryer lifting lug
3. Steam dryer assembly
4. Steam outlet
5. Core spray inlet
6. Steam separator assembly
7. Feedwater inlet
8. Feedwater sparger
9. Low-pressure-coolant injection inlet
10. Core spray line
11. Core spray sparger
12. Top guide
13. Jet pump assembly
14. Core shroud
15. Fuel assemblies
16. Control blade
17. Core plate
18. Jet pump/recirculation water inlet
19. Recirculation water outlet
20. Vessel support skirt
21. Shield wall
22. Control-rod drives
23. Control-rod drive hydraulic lines
24. In-core flux monitor

FIGURE 5.8
The BWR pressure vessel and internals. (*Courtesy of the General Electric Company.*)

Each of the "accumulators" has enough stored compressed fluid energy to drive the rod into the core in the event of a SCRAM condition.

Care must be taken in the operation of any liquid-cooled reactor, but particularly in the design of a BWR system, to assure that the maximum heat flux (W/m^2) from the surface of the reactor fuel does not exceed the value of the *departure from nucleate boiling* or *DNB*. A typical boiling heat-transfer curve is shown in Fig. 5.9. At relatively low heat fluxes, the heat-transfer process is called *nucleate boiling*. In this region, vapor bubbles are produced at the surface of the fuel element and break away, producing a lot of agitation in the boundary layer. This produces very high heat-transfer rates (very high convective heat-transfer coefficients) and small temperature differences between the surface and the saturation temperature of the coolant.

As the heat flux is increased, however, the vapor-bubble formation rate increases until the entire surface of the fuel element surface is eventually covered with vapor. When the surface is completely covered with vapor, the vapor acts as an insulating layer and the surface temperature increases dramatically. This heat-transfer mode is called *film boiling* and, unless the heat flux at the surface is reduced, the surface will actually melt. The transition from nucleate to film boiling essentially takes place at the departure from nucleate boiling (DNB).

Since a nuclear reactor has no theoretical maximum temperature, power, or heat-flux limit as long as a supercritical assembly can be maintained, care must be taken in the design and operation of any reactor to assure that the maximum heat flux is below the DNB value. This consideration is important in

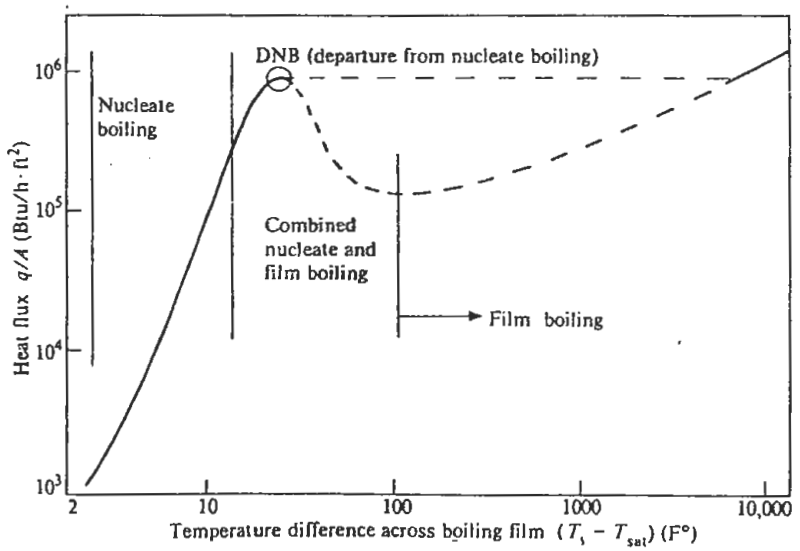


FIGURE 5.9
Typical boiling heat-transfer relationships.

all liquid-cooled systems but it is particularly important for the boiling-water reactor since the phase change is already taking place in the reactor core.

Most of the boiling-water reactors are designed to operate well below the value of the DNB. To accomplish this, it may be necessary to limit the power generation in those fuel element tubes adjacent to the water gap created when the control rod is withdrawn. A typical cross section of the core of an early BWR, including the fuel elements and control rods, is presented in Fig. 5.10. When the

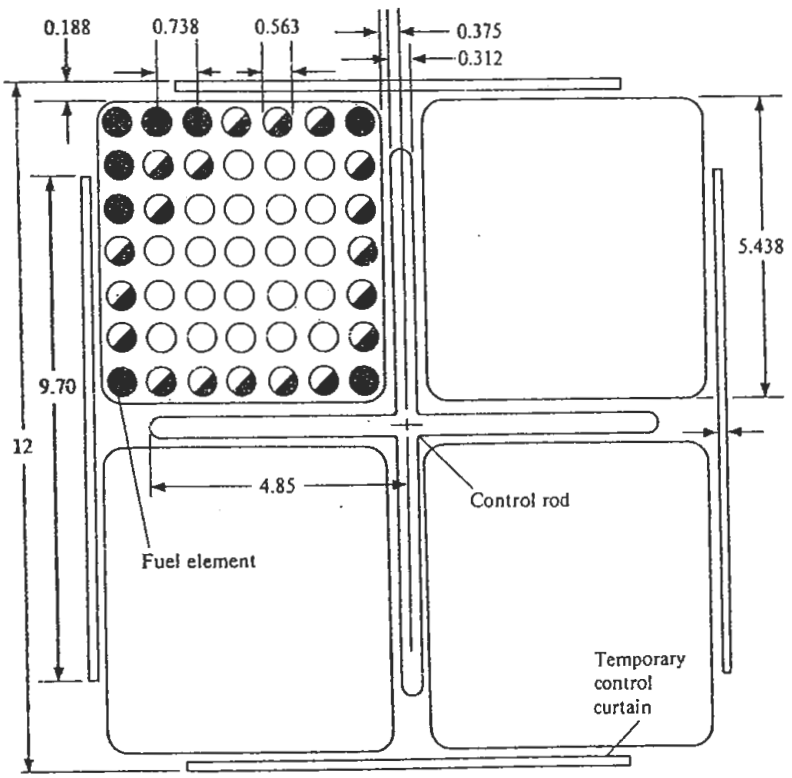


FIGURE 5.10
A typical in-core section of an older BWR fuel module consisting of four fuel elements surrounding a cruciform control rod. Newer fuel modules have an 8×8 array of fuel rods. (*Courtesy of the General Electric Company.*)

cruciform control rods are withdrawn from the reactor core, the thermal neutrons tend to pile up or "peak" in the gap. The high thermal-neutron flux can cause excessive fission heating in those fuel rods at the edge of the fuel element. To limit the power generation in these rods, lower fuel enrichments are employed in these rods than are used in the center of the fuel element. The different "cross hatching" in the rods of the upper-right element, in Fig. 5.10, represent different fuel enrichments.

The operating boiling-water reactor systems have developed some minor generic problems. In-core vibration brought about by the boiling process has caused failure of some of the lines to the in-core instrumentation. Several of the operating BWRs have also developed cracks in the 2-ft recirculation water lines that transfer water to the jet pumps surrounding the core. Repair of these lines have been made and the reactor put into operation with little difficulty.

5.2.2 Gas-Cooled Reactors

The earliest commercial gas-cooled reactors were the *Calder-Hall* systems developed in the early 1950s by the United Kingdom. These units were moderated with graphite and cooled with carbon dioxide since helium was unavailable to the British at that time. A total of 33 of these units were still in operation during 1987. The British have also developed a number of helium-cooled, graphite-moderated reactors (advanced gas-cooled reactors or AGRs) following the discovery of helium in the North Sea gas fields.

Two gas-cooled, commercial power reactors have been built in the United States. One of these systems was a small 40-MW_e prototype reactor (Peach Bottom I) built for the Philadelphia Electric Company. The other was a 330-MW_e power reactor (Ft. St. Vrain Reactor) built by the Public Service Company of Colorado. These systems are cooled with helium and moderated with graphite and are called *high-temperature, gas-cooled reactors* or simply *HTGRs*. The entire core is constructed of nonmetallic materials (primarily graphite) so that very high temperatures can be tolerated in this system. In addition, the large amount of graphite in the core has such a high heat capacity that it can absorb the fission-product decay heat without the problem of a core meltdown. This reactor type has been developed and is being promoted by Gulf General Atomics, a division of the Gulf Oil Corporation.

The HTGR is completely contained within a prestressed-concrete pressure vessel (PCPV) along with the helium coolant and the steam-generating and superheating equipment. A schematic diagram of the HTGR power system is shown in Fig. 5.11 and the pertinent operational parameters are presented in Table 5.3. The proposed reactor for a 3800-MW_e HTGR is shown in Fig. 5.12.

It will be noted that this system produces high-temperature (955°F), high-pressure (2400-psig) steam at the turbine inlet. These steam conditions are comparable to those from a high-performance, fossil-fueled system. The resulting thermal efficiency of the HTGR plant is around 38 percent, which compares favorably with the thermal efficiency of the best fossil units. This efficiency is

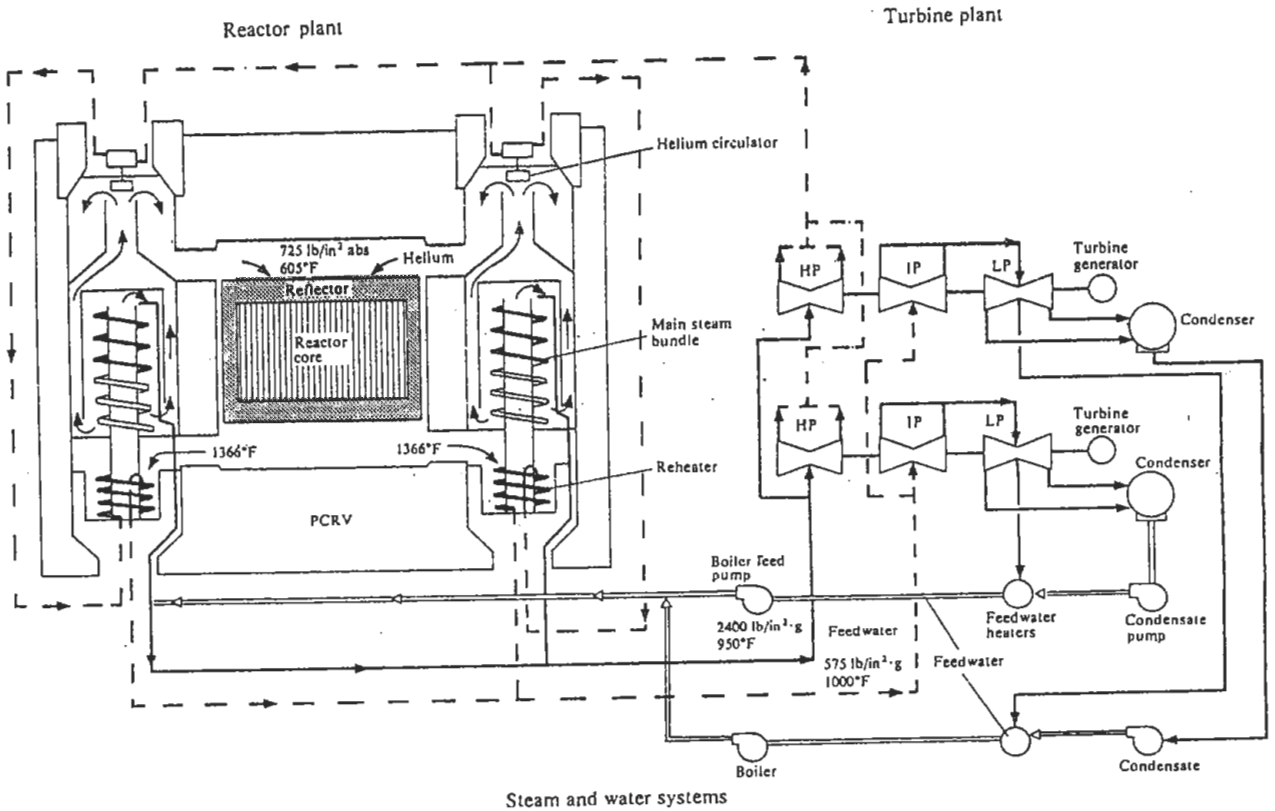


FIGURE 5.11
Schematic diagram for the HTGR power system. (*From Waage et al. 1974.*)

TABLE 5.3
Operational parameters for the 3800-MW_{th} high-temperature, gas-cooled (HTGR) reactor

Core power, MW_{th}	3800
Net thermal output, MW_{th}	3764
Primary coolant helium) pressure, lb/in^2 abs	725 (5 MPa)
Helium-inlet temperature, °F	605 (318.3°C)
Helium-outlet temperature, °F	1366 (741.1°C)
Throttle-steam conditions, lb/in^2 gage/°F	2400/950 (16.54 MPa/510°C)
Reheat-steam conditions, lb/in^2 gage/°F	575/1000 (4 MPa/538°C)
Net electrical output, MW_e	1450
Net thermal efficiency, %	38.2

much higher than the typical thermal efficiency values of 32 to 33 percent for the LWR plants.

The HTGR has many attractive features and, by 1974, six 1100-MW_e systems had been ordered by various electrical utilities. However, in-core vibration problems that were present in the Ft. St. Vrain reactor led to major revisions with a corresponding escalation of the cost so that all six of the HTGRs on order were canceled by early 1976. The initial operating problems present in the Ft. St. Vrain reactor prevented the system from reaching the design power of 330-MW_e until late 1981 although it first went into operation in spring of 1979. Considerable research and design have been directed toward the possibility of adapting the HTGR to a Brayton-cycle (gas-turbine) system in order to achieve higher thermal efficiencies.

5.2.3 Liquid-Metal, Fast-Breeder Reactors

One of the major casualities of the Three Mile Island fiasco was the liquid-metal, fast-breeder reactor (LMFBR) program in the United States. The United States was the world leader in this technology until the mid 1970s, when President Carter and congress decided that this reactor type was not needed. The first LMFBR (Experimental Breeder Reactor I) was built in the United States in 1954. The LMFBR commercial power program lost all governmental support in the mid 1980s, and this terminated the Clinch River Breeder Reactor (CRBR) which was a 975-MW_{th} demonstration LMFBR plant that was to be operated by the Tennessee Valley Authority (TVA). Despite the demise of the LMFBR power program in the United States, a considerable amount of LMFBR research continues at various national laboratories, along with continued operation of the Experimental Breeder Reactor II in Idaho and the Fast Flux Test Facility in Washington State.

Although the LMFBR program was terminated in the United States, in the mid-1980s, the U.S. Department of Energy authorized two groups of reactor suppliers to design the power reactor of the future. Both of these developed relatively low-powered (200- to 400-MW_e) reactor modules that were essentially

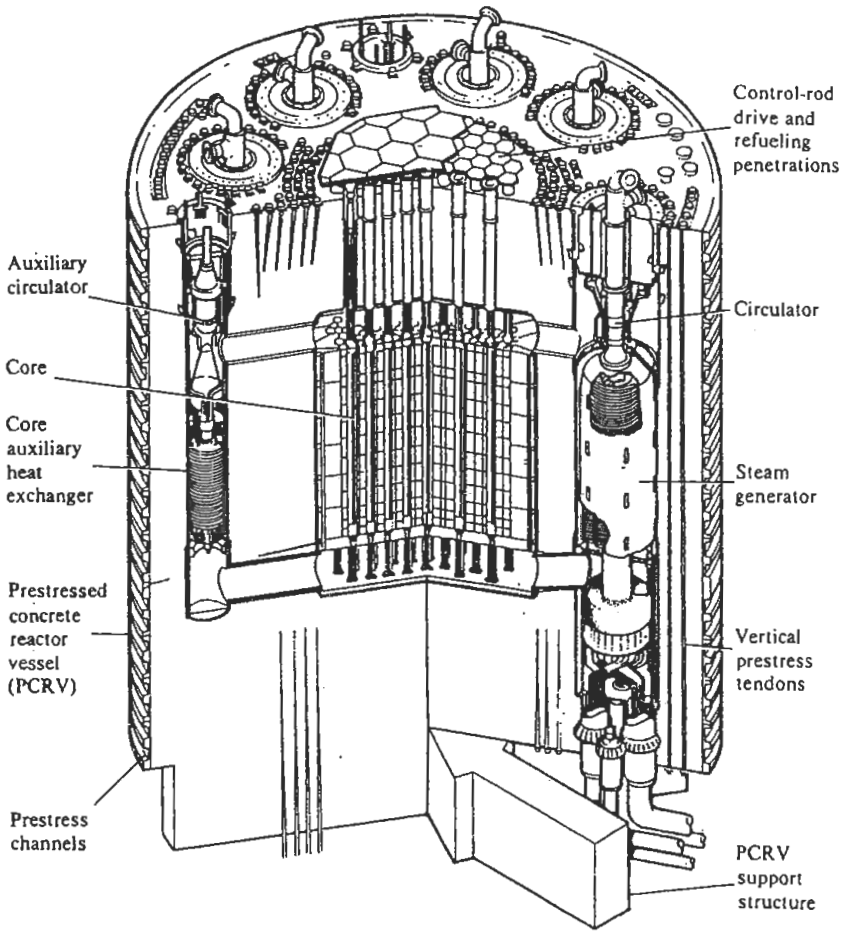


FIGURE 5.12
The arrangement of the reactor core and heat-exchange equipment in the prestressed concrete pressure vessel of the HTGR. (*From Waage et al. 1974.*)

pool-type LMFBRs. While the LMFBR program in the United States is currently at a standstill, liquid-metal, fast-breeder reactor technology is nevertheless likely to provide the next generation of new power reactors barring a technical breakthrough by another reactor type.

The other major industrial countries of the world are continuing development of the LMFBR. Great Britain, Russia, and France have LMFBR prototypes in operation while West Germany and Japan have prototype LMFBR units under construction. At this time, France is probably the world's leader in LMFBR technology, and it is in the process of starting up the Creys Malville LMFBR,

called *Superphoenix*. Superphoenix is a full-sized (1200-ME_e) LMFBR power system.

There are two major types of LMFBR systems—the *loop* reactors and the *pool* reactors. In the loop reactors, the liquid sodium is pumped directly through the reactor core to the intermediate sodium heat exchanger and then back to the pump in one of several primary cooling loops. In the pool reactors, the reactor core and intermediate sodium heat exchangers are submerged in a large sodium pool. The cold primary sodium coolant from the pool is pumped through the core and the hot sodium goes through the intermediate sodium heat exchangers and then back into the large pool.

The advantage of the loop reactor system is that the reactor vessel is much smaller, which simplifies shielding, etc. The main advantage of the pool reactor

TABLE 5.4
Operating characteristics of the Crey's-Malville fast-breeder reactor (Superphoenix)

General:
- Rated electrical output = 1240 MW_e
- Rated thermal power = 3000 MW_e
- Thermal efficiency = 41.3%
- Construction time = 68 months

Core parameters:
- Average fast flux = 6.2×10^{19} $n/m^2 \cdot s$
- Core volume = 10,820 L = 382.2 ft^3
- Fuel element length = 5.5 m = 18.05 ft
- Number of fuel pins per element = 271
- Outside diameter of fuel pins = 8.65 mm = 0.341 in
- Active fuel length = 1 m = 3.28 ft

Primary containment vessel:
- Material: Austenitic stainless steel
- Diameter = 21 m = 68.9 ft
- Primary sodium inventory = 3300 tonne

Primary cooling system:
- Number of pumps (mounted in the primary vessel) = 4
- Reactor sodium inlet temperature = 395°C = 743°F
- Reactor sodium outlet temperature = 545°C = 1031°F
- Total sodium flow rate in core = 16,400 kg/s = 1.3×10^8 lbm/h
- Number of sodium-to-sodium heat exchangers (IHXs), mounted in primary containment vessel = 8

Secondary cooling system:
- Number of pumps = 4
- Secondary sodium outlet temperature = 525°C = 977°F
- Secondary sodium flow rate = 13,200 kg/s = 1.05×10^8 lbm/h
- Total secondary sodium inventory = 1700 tonne

Turbine steam system:
- Number of sodium-to-water steam generators = 4
- Outlet steam temperature = 490°C = 914°F
- Outlet steam pressure = 18 MPa = 2611 psia
- Steam rate = 1360 kg/s = 1.08×10^8 lbm/h

system is that the large sodium inventory in the pool provides a large heat sink for absorption of fission-product decay heat in case of a loss of coolant accident. Another advantage of the pool reactor system is that the radioactive primary sodium does not leave the pool.

The operational characteristics of the Superphoenix reactor are given in Table 5.4. A layout of the Superphoenix fast-reactor system is shown in Fig. 5.13.

5.3 REACTOR THERMAL DESIGN

5.3.1 Reactor In-Core Power Distribution

In the design or operation of any nuclear reactor, there is normally some maximum operating temperature (e.g., the melting point of the fuel) or heat flux (e.g., the value of DNB) that limits the reactor power. The maximum heat flux is a function of the fission rate per unit volume or the power density in the fuel material. The maximum possible safe reactor power that can be attained is realized when the entire reactor core is operating at the limiting temperature or heat flux. Likewise, the safest operating condition occurs at lower powers when the entire core is operating at the same temperature or the same heat flux in order to achieve as large a margin of safety as possible.

The local fission rate per unit volume or power density is equal to the product of the local atomic density of the fuel N_{fuel}/V, the average microscopic fission cross section σ_f, and the local value of the neutron flux causing fission, ϕ. Since the fission cross section is essentially constant, the local power density varies as the product of the local neutron flux and the atomic concentration of the fuel if the reactor has a variable fuel loading. If the reactor is uniformly loaded, the local power density is the same as the distribution of the neutrons causing fission, i.e., the fast flux in a fast reactor and the thermal flux in a thermal reactor.

A uniform temperature or heat flux can be achieved in a reactor core either by employing a nonuniform fuel distribution or by using absorber rods to shape the power. Most LWR systems move the partially burned fuel from the outer edge of the reactor to the center of the core and insert the new fuel at the edge of the core in order to level-out and improve the radial power distribution. The use of absorber rods to shape the reactor power is not as efficient as varying the reactor fuel loading.

The use of a variable fuel loading is very difficult to analyze because the local neutron flux and local fuel loading are not independent variables. As the fuel concentration is increased in a given region, the power increases but not proportionally to the fuel loading. This is because the addition of more fuel into a given region of the core increases the absorption cross section which, in turn, decreases the neutron flux in that region. The local fuel concentration at a given point can be increased by putting more fuel material in that volume and/or by varying the enrichment of the fuel. An analysis of the nonuniform fuel loading condition is beyond the scope of this text and is even beyond the scope of most

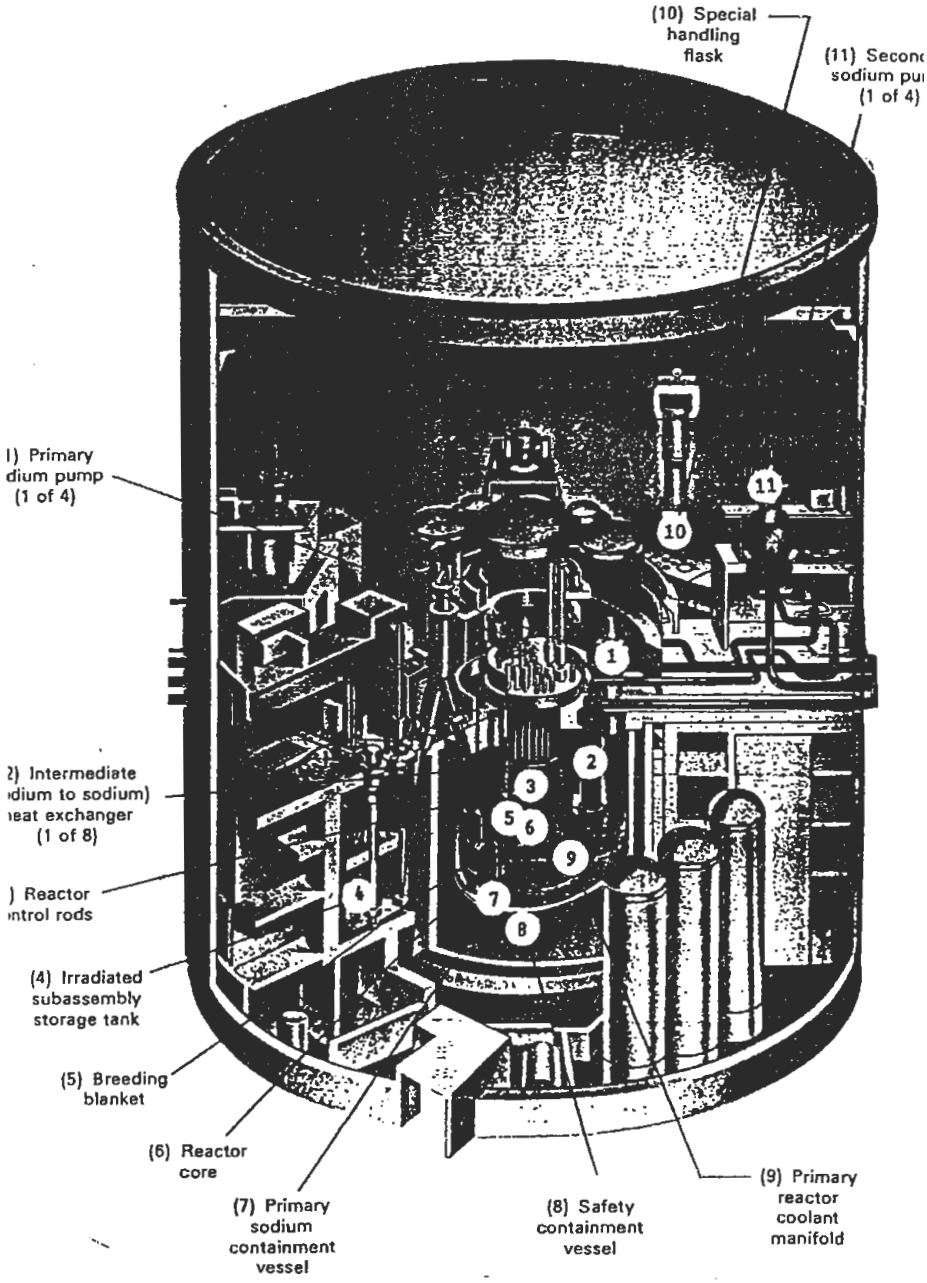


FIGURE 5.13
The Superphoenix, liquid-metal, fast-breeder reactor (LMFBR).

textbooks on reactor physics. It is usually accomplished with the use of a high-speed digital computer.

While uniformly loaded reactor systems are not common in power reactors, they are common in low-powered research reactors. These systems can be studied analytically and they allow the student to obtain some idea of the analytical approach to the actual system analysis. In fact, this text treats the simplest type of reactor, which is the uniformly loaded, bare reactor system, and starts with the neutron-flux distributions as developed from reactor physics.

In a bare, uniformly loaded reactor, the neutron flux is a maximum at the center of the assembly and drops off at the boundaries because of neutron leakage. It is common practice to extrapolate the flux distribution to zero at some point outside the core, called the *extrapolated core boundary.* Using the simple approximation of diffusion theory from reactor physics, in which the neutrons are treated as gas atoms, the neutron-flux distributions can be obtained from some simple "bare" reactor geometries.

For an infinite slab reactor, as shown in Fig. 5.14, the neutron flux is given by the following equation, where x is the distance from the center of the reactor:

$$\phi(x) = \phi_{max} \cos \frac{\pi x}{a_0} \tag{5.1}$$

where a_0 is the total extrapolated core boundary, as shown in Fig. 5.14. a_0 is equal to the actual core thickness a_b, plus twice the extrapolation distance, $2d$. Since the power and the neutron-flux distributions for a uniformly loaded reactor

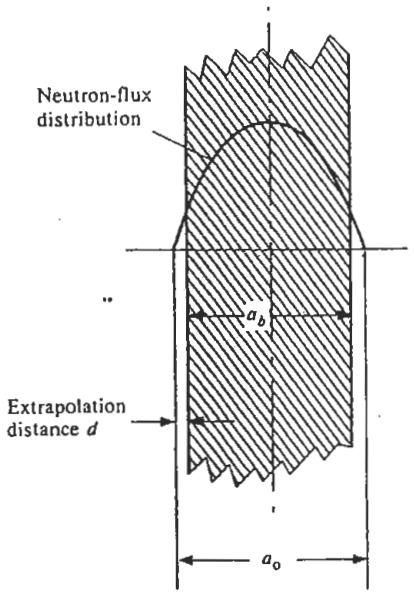


FIGURE 5.14
The neutron flux distribution in an infinite, bare, uniformly-loaded slab reactor.

are the same, the power distribution for an infinite bare slab reactor is

$$P(x) = P_{max} \cos \frac{\pi x}{a_0} \tag{5.2}$$

For a bare, infinitely long (infinite), uniformly loaded cylindrical reactor, whose cross section is shown in Fig. 5.15, the neutron flux, as a function of r, is given by the following equation:

$$\phi(r) = \phi_{max} J_0 \frac{2.405r}{r_0} \tag{5.3}$$

where J_0 is the zeroth-order Bessel function of the first kind and r_0 is the extrapolated core radius. In this case, the extrapolated core radius r_0 is equal to the sum of the reactor core radius r_b and the extrapolation distance d. The properties of the zeroth-order Bessel function of the first kind are such that $J_0(0) = 1.0$ and $J_0(2.405) = 0$. The power distribution has the same general equation and is equal to

$$P(r) = P_{max} J_0 \frac{2.405r}{r_0} \tag{5.4}$$

For a uniformly loaded, bare spherical reactor, the distribution is similar to that shown in Fig. 5.15 and is given by the following equation:

$$\phi = \frac{A_0}{r} \sin \frac{\pi r}{r_0} \tag{5.5}$$

where A_0 is a constant but it is not the maximum flux, and r_0 is the extrapolated core radius which is equal to the sum of the actual radius r_b, and the extrapolation distance d. The value of A_0 is obtained by setting the value of the neutron flux

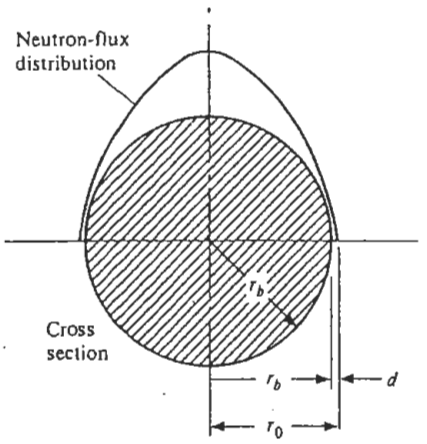


FIGURE 5.15
The neutron-flux distribution in an infinite, bare, uniformly-loaded, cylindrical reactor.

at the center of the reactor ($r = 0$) to the maximum neturon flux in the core, ϕ_{max};

$$\phi(\text{at } r = 0) = \phi_{max} = \lim_{r \to 0} \left(\frac{A_0}{r} \sin \frac{\pi r}{r_0} \right) = \frac{0}{0} \text{ (indeterminate)}$$

Applying L'Hospital's rule,

$$\phi(\text{at } r = 0) = \phi_{max} = \lim_{r \to 0} \left(\frac{A_0 \pi}{r_0} \cos \frac{\pi r}{r_0} \right) = \frac{A_0 \pi}{r_0} \tag{5.6}$$

or

$$\phi_{max} = \frac{A_0 \pi}{r_0} \qquad \text{and} \qquad A_0 = \frac{\phi_{max} r_0}{\pi} \tag{5.7}$$

Substituting Eq. (5.7) into Eq. (5.5) gives

$$\phi(r) = \frac{\phi_{max} r_0}{\pi r} \sin \frac{\pi r}{r_0} \tag{5.8}$$

Since the power and neutron-flux distributions are the same in a uniformly loaded reactor,

$$P(r) = \frac{P_{max} r_0}{\pi r} \sin \frac{\pi r}{r_0} \tag{5.9}$$

The reactor design engineer needs the ratio of P_{max} to P_{ave} in order to evaluate the maximum temperature and/or heat flux in the reactor core. In order to determine this power ratio, the average power P_{ave} must be obtained by integrating over the volume of the reactor core. The average power in the core can be found from the following equation:

$$P_{ave} = \frac{\int_{vol} P(V)\, dV}{\int_{vol} dV} \tag{5.10}$$

For the infinite-slab reactor, $V = Ax$ and $dV = A\, dx$, where A is the cross-sectional area of the slab (in this case infinity). Substituting the expressions for dV and $P(V)$ into Eq. (5.10), the area cancels and Eq. (5.10) reduces to

$$P_{ave} = \frac{\int_{-a_b/2}^{a_b/2} P_{max} \cos(\pi x / a_0)\, dx}{\int_{-a_b/2}^{a_b/2} dx} \tag{5.11}$$

Integrating this equation and substituting the limits gives

$$\frac{P_{max}}{P_{ave}} = \frac{\pi a_b / 2a_0}{\sin(\pi a_b / 2a_0)} \tag{5.12}$$

The maximum possible value (the upper limit) of the power ratio, $(P_{max}/P_{ave})_{max}$, occurs when the extrapolation distance d is small compared to the core dimension a_b. When $a_b \to a_0$, Eq. (5.12) reduces to

$$\left(\frac{P_{max}}{P_{ave}} \right)_{\text{max (infinite bare slab)}} = \frac{\pi}{2} = 1.57 \tag{5.13}$$

While the power engineer will never encounter an infinite-slab reactor, the same results can be used to estimate the maximum-to-average power ratio for a bare, rectangular parallelepiped reactor. In this system, it is common practice to assume that the neutron flux and the power distributions are variable separable, or

$$\phi(x, y, z) = \phi_{max} \cos \frac{\pi x}{a_0} \cos \frac{\pi y}{b_0} \cos \frac{\pi z}{c_0} \tag{5.14}$$

and

$$P(x, y, z) = P_{max} \cos \frac{\pi x}{a_0} \cos \frac{\pi y}{b_0} \cos \frac{\pi z}{c_0} \tag{5.15}$$

where a_0, b_0, and c_0 are the respective extrapolated core dimensions in the x, y, and z directions. Integrating either of these last two expressions over the extrapolated core boundaries in each direction gives a power ratio of 1.57 in each direction, or

$$\left(\frac{\phi_{max}}{\phi_{ave}}\right)_{max\ (parallelepiped)} = \left(\frac{P_{max}}{P_{ave}}\right)_{max} = (1.57)^3 = 3.87 \tag{5.16}$$

For an infinite bare cylindrical reactor, $V = \pi r^2 L$ or $dV = 2\pi r L\, dr$. Substituting this expression into Eq. (5.10), along with the power distribution given by (5.4), gives

$$P_{ave} = \frac{\int_0^{r_b} P_{max} J_0(2.405 r/r_0) 2\pi r L\, dr}{\int_0^{r_b} 2\pi r L\, dr} \tag{5.17}$$

Integrating this equation and substituting the limits yields

$$\frac{P_{max}}{P_{ave}} = \frac{2.405 r_b / 2 r_0}{J_1(2.405 r_b / r_0)} \tag{5.18}$$

The maximum-to-average power ratio occurs when the extrapolation distance is negligible and $r_b \to r_0$. In this case, Eq. (5.18) reduces to

$$\left(\frac{P_{max}}{P_{ave}}\right)_{max\ (cylinder)} = \frac{2.405/2}{J_1(2.405)} = \frac{1.2025}{0.5191} = 2.32 \tag{5.19}$$

For a bare, uniformly loaded right circular cylinder, the neutron flux and power are assumed to be variable separable, so that

$$\phi(r, z) = \phi_{max} J_0 \frac{2.405 r}{r_0} \cos \frac{\pi z}{c_0} \tag{5.20}$$

and

$$P(r, z) = P_{max} J_0 \frac{2.405 r}{r_0} \cos \frac{\pi z}{c_0} \tag{5.21}$$

Integrating either of these two expressions over all the extrapolated core boun-

daries ($r_b \to r_0$ and $c_b \to c_0$), gives

$$\left(\frac{\phi_{max}}{\phi_{ave}}\right)_{max} = \left(\frac{P_{max}}{P_{ave}}\right)_{max} = \left(\frac{P_{max}}{P_{ave}}\right)_{max,cyl}\left(\frac{P_{max}}{P_{ave}}\right)_{max,slab}$$

$$= (2.32)(1.57) = 3.64 \tag{5.22}$$

This value is lower (and better) than the value of 3.87 obtained for the rectangular parallelepiped reactor.

For a bare, uniformly loaded spherical reactor, $V = 4\pi r^3/3$ and $dV = 4\pi r^2\, dr$. Substituting this expression for dV into Eq. (5.10) along with Eq. (5.9) for the power distribution of a sphere as a function of r, gives

$$P_{ave} = \frac{\int_0^{r_b} (P_{max} r_0/\pi r)[\sin(\pi r/r_0)(4\pi r^2)\, dr}{\int_0^{r_b} 4\pi r^2\, dr} \tag{5.23}$$

Integrating this equation by parts and substituting the limits yields

$$\frac{P_{max}}{P_{ave}} = \frac{(\pi r_b/r_0)^2}{3[-\cos(\pi r_b/r_0) + (r_0/\pi r_b)\sin(\pi r_b/r_0)]} \tag{5.24}$$

The maximum possible power ratio occurs when the extrapolation distance is negligible and $r_b \to r_0$:

$$\left(\frac{P_{max}}{P_{ave}}\right)_{max\ (sphere)} = \frac{\pi^2}{3} = 3.29 \tag{5.25}$$

For a bare, uniformly loaded sphere, the value of 3.29, given by Eq. (5.25) is considerably lower and better than the values for either the right circular cylinder or the rectangular parallelepiped.

Again, it should be emphasized that the maximum power ratios, as given by Eqs. (5.16), (5.22), and (5.25), are indeed maximum values and the actual ratio of maximum-to-average power will be significantly less. For instance, if $r_b = 0.9r_0$ for the bare spherical system, the value of P_{max}/P_{ave} becomes 2.513, instead of 3.29.

Example 5.1. If the maximum thermal-neutron flux in a 4-m-diameter bare, uniformly loaded sphere is 10^{17} n/m$^2 \cdot$ s and the flux at the core boundary is 2×10^{16} n/m$^2 \cdot$ s, find the average thermal-neutron flux and the extrapolation distance d.

Solution. Given:

$$\phi_{max} = 10^{17}\ \text{n/m}^2 \cdot \text{s} \qquad \phi(\text{at } r = r_b) = 2 \times 10^{16}\ \text{n/m}^2 \cdot \text{s} \qquad r_b = 2\ \text{m}$$

$$\phi(\text{at } r = r_b) = 0.2 \times 10^{17} = \phi_{max}\left(\frac{r_0}{\pi r_b}\right)\sin\left(\frac{\phi r_b}{r_0}\right)$$

$$= 10^{17}\left(\frac{r_0}{\pi r_b}\right)\sin\left(\frac{\pi r_b}{r_0}\right)$$

$$\frac{\sin(\pi r_b/r_0)}{(\pi r_b/r_0)} = 0.2 \Rightarrow \text{(a transcendental equation)}$$

Since $r_0 > r_b$, $\pi r_b/r_0 < \pi$ rad.

By trial and error, $(\pi r_b/r_0) = 2.595$ rad. Thus

$$r_0 = \frac{r_b \pi}{2.595} = \frac{2\pi}{2.595} = 2.421 \text{ m}$$

Extrapolation distance $= d = r_0 - r_b = 2.421 - 2 = 0.421$ m. Thus

$$\frac{P_{max}}{P_{ave}} = \frac{\phi_{max}}{\phi_{ave}}$$

$$= \frac{(\pi r_b/r_0)^2}{3[-\cos(\pi r_b/r_0) + (r_0/\pi r_b)\sin(\pi r_b/r_0)]}$$

$$= \frac{(2.595)^2}{3[-\cos(2.595) + (1/2.595)\sin(2.595)]} = 2.128$$

$$\text{Average thermal-neutron flux} = \phi_{ave} = \Phi_{th} = \frac{\phi_{max}}{2.128} = \frac{10^{17}}{2.128}$$

$$= 4.699 \times 10^{16} \text{ n/m}^2 \cdot \text{s}$$

Neglecting coolant temperature changes, the design engineer desires a maximum-to-average power ratio of unity in the reactor core to achieve a uniform maximum temperature or heat flux. If the coolant temperature increases significantly as it passes through the core, it is desirable to increase the power density in the cold part of the reactor, if possible. If the radial power distribution cannot be shaped to achieve a uniform maximum temperature, it may be desirable to orifice the coolant flow so that those elements operating at higher than average power receive a higher coolant flow than those operating at lower power densities.

The maximum-to-average power ratio in a nuclear reactor can be improved (decreased) by putting a reflector around a bare core. The reflector essentially reduces the neutron leakage by returning neutrons to the reactor core as the result of neutron scattering. Not only does the reflector return leakage neutrons to the core but it also reduces the kinetic energy of the fast and intermediate neutrons. This makes these neutrons more effective in inducing fission and producing fission energy at the outer regions of the core.

The effect of adding a reflector to a bare thermal reactor is shown in Fig. 5.16. It will be noted that the reflector is very effective in raising the neutron flux and hence the power density at the edges of the core. In some systems, the addition of a reflector may actually cause the peak power to occur at the edge of the reactor core rather than at the center of the reactor.

The addition of a reflector to a bare reactor core accomplishes two things. It reduces the critical mass of the reactor by decreasing the neutron leakage rate. If the same fuel concentration is used, the reactor can be made smaller, or if the same dimensions are maintained, the fuel concentration or enrichment can be lowered. The addition of a reflector also causes a marked improvement in the ratio of maximum-to-average power in the core by raising the neutron flux and hence the power generation at the core boundary. A typical value of P_{max}/P_{ave} for a reflected assembly is about 2.4.

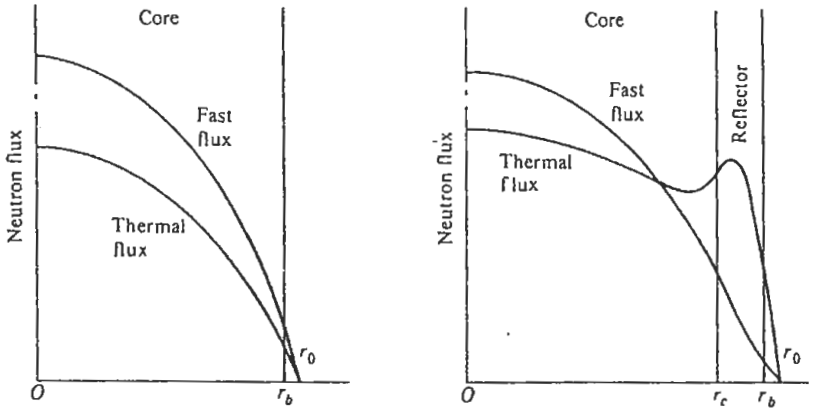


FIGURE 5.16
The thermal neutron-flux distribution in a bare and a reflected reactor core.

5.3.2 Fuel Element Temperatures and Heat Fluxes

GENERAL. Once the power distribution in the reactor core has been determined, it is a relatively simple matter to estimate the maximum temperatures and heat flux in the core. Two basic types of fuel elements are commonly employed in nuclear reactors. The flat-plate element is used in many research reactors and the pellet-in-tube element is used in most power reactors. Both elements are analyzed in this section.

In the design of any fuel element, it is normally assumed that all of the fission energy is generated in the fuel material and that it is distributed uniformly throughout the volume of the fuel material in a given plate or pellet. This is actually a conservative assumption as the heat generation rate in the fuel is highest at the outer edges of the fuel plate or pellet because of the neutron-flux depression in the fuel material due to its high neutron-absorption cross section. Assuming that the volumetric heat-generation rate q' is uniform produces results that predict higher temperatures than actually occur.

Normally, the maximum temperature and maximum heat flux are found at the location of the maximum heat-generation rate or power density. The maximum temperatures may occur downstream of the location of the maximum power density if the coolant undergoes a significant temperature rise as it passes through the core. The maximum volumetric heat-generation rate in the core, q', is given by the following equations:

$$q' = \left(\frac{P_{th}}{V_{fuel,m^3}}\right)\left(\frac{P_{max}}{P_{ave}}\right) \qquad \text{kW/m}^3 \tag{5.26}$$

or

$$q' = \left(\frac{3412 P_{th}}{V_{fuel,ft^3}}\right)\left(\frac{P_{max}}{P_{ave}}\right) \qquad \text{Btu/h} \cdot \text{ft}^3 \tag{5.27}$$

where P_{th} is the thermal power of the reactor in kilowatts, $V_{fuel,cm}$ is the volume of the fuel material in cubic meters, and V_{fuel,ft^3} is the fuel volume in cubic feet.

Once the internal heat-generation rate has been determined, the temperature distribution in the fuel element can be determined with the use of the heat conduction equation and the convection heat-transfer relationship. For constant thermal conductivity k, the heat conduction equation is

$$\nabla^2 T + \frac{q'}{k} = \frac{1}{\alpha}\frac{\partial T}{\partial t} \tag{5.28}$$

where T is the temperature, α is the thermal diffusivity of the material, t is the time, and ∇^2 is the Laplacian operator. Since the design engineer is normally concerned with steady-state conditions, $\partial T/\partial t = 0$, and Eq. (5.28) reduces to

$$\nabla^2 T + \frac{q'}{k} = 0 \tag{5.29}$$

For cartesian coordinates,

$$\nabla^2 T = \frac{\partial^2 T}{\partial x^2} + \frac{\partial^2 T}{\partial y^2} + \frac{\partial^2 T}{\partial z^2} \tag{5.30}$$

For cylindrical coordinates,

$$\nabla^2 T = \frac{\partial^2 T}{\partial r^2} + \frac{1}{r}\frac{\partial T}{\partial r} + \frac{1}{r^2}\frac{\partial^2 T}{\partial \theta^2} + \frac{\partial^2 T}{\partial z^2} \tag{5.31}$$

For spherical coordinates,

$$\nabla^2 T = \frac{\partial^2 T}{\partial r^2} + \frac{2}{r}\frac{\partial T}{\partial r} + \frac{1}{r^2}\frac{\partial^2 T}{\partial \theta^2} + \frac{\cos\theta}{r^2 \sin\theta}\frac{\partial T}{\partial \theta} + \frac{1}{r^2 \sin^2\theta}\frac{\partial^2 T}{\partial \psi^2} \tag{5.32}$$

PLATE-TYPE FUEL ELEMENTS. The plate-type or slab fuel element is composed of a thin slab of fuel material clad on each side with structural material, called *cladding.* The structural material is metallurgically bonded to the fuel material so that there is a very small temperature drop across the fuel-clad interface. The fuel plates are thin enough so that a single plate can be approximated by a one-dimensional infinite slab as pictured in Fig. 5.17. The origin of the axis is established at the centerline of the fuel, the values of $x = \pm a$ mark the fuel-clad boundaries, and the values of $x = \pm b$ mark the outer boundaries of the cladding material.

In the fuel material of the infinite slab, Eq. (5.29) reduces to

$$\frac{d^2 T}{dx^2} + \frac{q'}{k_f} = 0 \tag{5.33}$$

Assuming a symmetrical temperature distribution in the fuel material (maximum temperature at the center of the fuel) gives the following relationship in the fuel:

$$T_x - T_a = \frac{q'(a^2 - x^2)}{2k_f} \qquad \text{for } 0 \le x \le a \tag{5.34}$$

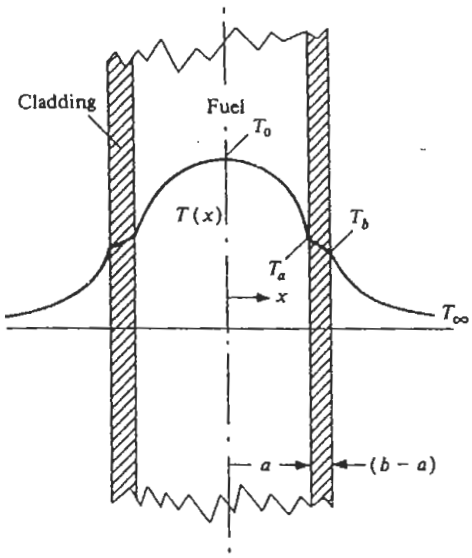


FIGURE 5.17
Temperature distribution in a plate-type fuel element.

where T_a is the temperature of the fuel at the fuel-clad interface and k_f is the thermal conductivity of the fuel material. Thus, the temperature at the center of the fuel ($x=0$), T_0, is the maximum temperature and is equal to

$$T_0 = T_a + \frac{q'a^2}{2k_f} \tag{5.35}$$

The steady-state heat-transfer rate q through the fuel-clad interface, the layer of cladding, and the coolant film is a constant and is equal to

$$q = -k_f A\left(\frac{dT}{dx}\right)_{\text{at } x=a} = aAq' \qquad W \text{ or Btu/h} \tag{5.36}$$

where A is the surface area normal to the flow of heat. Using this equation, along with the assumption that there is no heat generation in the cladding, gives

$$T_a - T_b = \frac{q(b-a)}{Ak_c} = \frac{q'a(b-a)}{k_c} \tag{5.37}$$

where T_b is the surface temperature of the element and k_c is the thermal conductivity of the cladding material. Again, employing Eq. (5.36), along with the Newton equation for convective heat transfer, gives the following temperature drop across the fluid film:

$$T_b - T_\infty = \frac{q}{hA} = \frac{q'a}{h} \tag{5.38}$$

where T_∞ is the bulk temperature of the coolant and h is the surface conductance of the coolant.

The total temperature drop from the center of the fuel to the coolant is obtained by adding Eqs. (5.35), (5.37), and (5.38). This gives

$$T_0 - T_\infty = q'a\left(\frac{a}{2k_f} + \frac{b-a}{k_c} + \frac{1}{h}\right) \tag{5.39}$$

CYLINDRICAL FUEL ELEMENTS. The cylindrical fuel element shown in Fig. 5.18 is commonly employed in most of the current power reactors. The fuel rods are less than 0.5 in in diameter and over 12 ft long. Consequently, the heat flow from the fuel rods can be approximated by a one-dimensional, infinite cylinder. For a one-dimensional cylinder, the steady-state heat conduction equation (5.29) reduces to:

$$\frac{d^2T}{dr^2} + \frac{1}{r}\frac{dT}{dr} = -\frac{q'}{k_f} \tag{5.40}$$

The heat flow through the cylindrical fuel element is complicated by an additional thermal resistance term that is not encountered in the slab fuel element. In the slab element, the fuel and cladding are metallurgically bonded to each other in a hot rolling process that produces a very low thermal resistance. In the fabrication of the cylindrical elements, on the other hand, the ceramic fuel pellets are placed inside the cladding tube. This means that there is a small gap between the pellet and the wall of the cladding. This gap produces a significant thermal resistance because of the poor contact between the pellet and the inside wall of the cladding. For the purpose of this study, it will be assumed that the heat flow

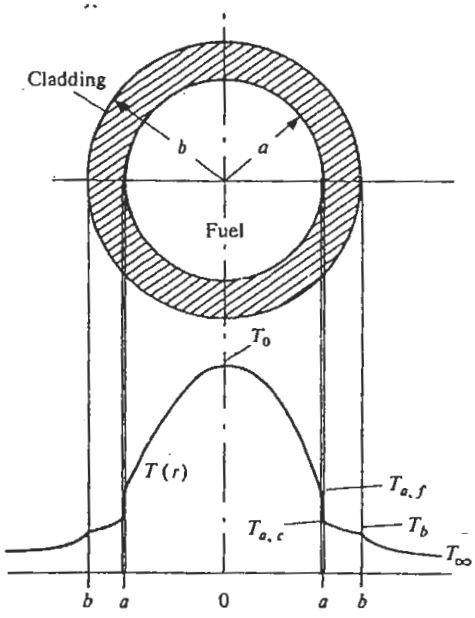


FIGURE 5.18
Temperature distribution in a cylindrical fuel element.

through this contact resistance can be found by using the Newton heat-flow equation and employing an effective surface conductance h for the flow of heat. Despite the gap that exists between the pellet and the tube, and the actual gap changes as the reactor operates over a long period of time, it will be assumed that the outer radius of the fuel pellet and the inner radius of the tube are both equal to a.

Equation (5.40) can be integrated twice to determine the temperature drop in the fuel pellet. For the condition of symmetrical cooling, this equation gives

$$T_r - T_{a,f} = \frac{q'(a^2 - r^2)}{4k_f} \qquad 0 \le r \le a \tag{5.41}$$

where T_r is the temperature at any fuel radius and $T_{a,f}$ is the temperature at the surface of the fuel pellet. The maximum temperature drop in the fuel pellet is then obtained by setting $r = 0$. This gives

$$T_0 - T_{a,f} = \frac{q'a^2}{4k_f} \tag{5.42}$$

At steady state, all of the heat that is generated in the fuel pellets must be transferred through the contact resistance, through the cladding, and then to the coolant. Since it is assumed that all of the fission energy is generated in the fuel, the standard heat-transfer equations are applicable outside the fuel material. The steady-state heat transfer is equal to the product of the fuel volume and the volumetric heat generation rate q':

$$q = q'\pi a^2 L \tag{5.43}$$

Applying Eq. (5.43) to the Newton convection equation gives the temperature drop between the outer surface of the fuel pellet, $T_{a,f}$, and the inside surface of the cladding, $T_{a,c}$:

$$T_{a,f} - T_{a,c} = \frac{q}{2\pi a L h_a} = \frac{q'a}{2h_a} \tag{5.44}$$

Substituting Eq. (5.43) into the equation for conduction heat flow through a cylindrical wall gives the following equation for the temperature drop across a tube wall with an inner radius of a and an outer radius of b:

$$T_{a,c} - T_b = \frac{q}{2\pi k_c L} \ln \frac{b}{a} = \frac{q'a^2}{2k_c} \ln \frac{b}{a} \tag{5.45}$$

The temperature drop across the coolant film can be obtained in the same manner as Eq. (5.34):

$$T_b - T_\infty = \frac{q}{2\pi b L h_b} = \frac{q'a^2}{2bh_b} \tag{5.46}$$

The maximum temperature drop across the cylindrical fuel rod is obtained by

adding Eqs. (5.42), (5.44), (5.45), and (5.46). This gives

$$T_0 - T_\infty = \frac{q'a^2}{2}\left(\frac{1}{2k_f} + \frac{1}{ah_a} + \frac{1}{k_c}\ln\frac{b}{a} + \frac{1}{bh_b}\right) \tag{5.47}$$

If the maximum fuel temperature $T_{0,\max}$ is desired, it can be estimated from either (5.39) or (5.47) along with the exit coolant temperature $T_{\infty,\max}$. In some systems, particularly the boiling-water reactors, the maximum heat flux at the surface of the cylindrical fuel element is the condition that limits the reactor power. This quantity can be obtained by dividing the maximum heat-transfer rate in the core by the surface area of the cladding. This gives

$$\left(\frac{q}{A}\right)_{\max} = \frac{q'\pi a^2 L}{2\pi bL} = \frac{q'a^2}{2b} \tag{5.48}$$

Example 5.2. A cylindrical fuel element in a BWR is composed of zircoloy-2 tubes filled with UO_2 pellets. The tubes have an outside diameter (OD) of 12.5 mm and an inside diameter (ID) of 10.8 mm. If the thermal conductivity of the fuel and cladding are 1.8 and 14.0 W/m · °C, respectively, the thermal conductance of the pellet-clad interface is 5500 W/m² · °C, the surface temperature is 520°C, and the heat flux at the cladding surface is 950,000 W/m², find the maximum temperature in the fuel pellet and average thermal-neutron flux in the fuel. Assume the UO_2 has a density of 10 g/cm³ and a U-235 enrichment of 2.2 percent, and assume the average coolant temperature is 305°C.

Solution. Given:

$$a = \frac{10.8}{2} = 5.4 \text{ mm} = 0.0054 \text{ m} \qquad b = \frac{0.0125}{2} = 0.00625 \text{ m}$$

Heat-transfer rate through the clad is

$$q = \frac{q}{A}A = \left(\frac{q}{A}\right)_b (2\pi bL)$$

$$\frac{q}{L} = 950{,}000(2\pi)(0.00625) = 37{,}306 \text{ W/m}$$

Volume of the fuel is

$$\pi a^2 L = (0.0054)^2 \pi L = 0.0000916L \text{ m}^3 = V_{\text{fuel}}$$

$$q' = \frac{q/L}{V_{\text{fuel}}/L} = \frac{37{,}306}{0.0000916} = 4.072 \times 10^8 \text{ W/m}^3$$

$$k_f = 1.8 \text{ W/m} \cdot °\text{C} \qquad h_a = 5500 \text{ W/m}^2 \cdot °\text{C} \qquad k_c = 14.0 \text{ W/m} \cdot °\text{C}$$

$$T_0 - T_b = (4.072 \times 10^8)\frac{0.0054}{2}\left[\frac{0.0054}{2(1.8)} + \frac{1}{5500} + \left(\frac{0.0054}{14}\right)\ln\left(\frac{0.00625}{0.0054}\right)\right]$$

$$= (1.099 \times 10^6)(0.0015 + 0.0001818 + 0.0000564)$$

$$= (1.099 \times 10^6)(0.0017382) = 1910°\text{C}$$

$$T_0 = T_b + 1910 = 520 + 1910 = 2430°\text{C}$$

For a unit meter of tubing:

$$\text{Fission rate} = \bar{\sigma}_f N_{\text{fuel}} \Phi_{\text{th}} = (3.1 \times 10^{10} \text{ fission/W} \cdot \text{s})(37{,}306 \text{ W})$$

$$= 1.1565 \times 10^{15} \text{ fissions/s}$$

$$\text{Average U-235 fission cross section} = \bar{\sigma}_f = \frac{582[293/(305+273)]^{1/2}}{1.128}$$

$$= 367.4 \text{ barns} = 3.674 \times 10^{-26} \text{ m}^2$$

$$N_{\text{fuel}} = \frac{V_{\text{fuel}} \rho_{\text{fuel}}[238/(238+32)](\text{Avogadro's number})(\text{enrichment})}{235}$$

$$= \frac{(91.6 \text{ cm}^3)(10 \text{ g/cm}^3)(238/270)(0.6022 \times 10^{24})(0.022)}{235}$$

$$= 4.533 \times 10^{22} \text{ atoms of U-235}$$

$$\Phi_{\text{th}} = \frac{1.1565 \times 10^{15}}{(4.553 \times 10^{22})(367.4 \times 10^{-28})} = 6.914 \times 10^{17} \text{ n/m}^2 \cdot \text{s}$$

AXIAL TEMPERATURE DISTRIBUTIONS. The maximum heat flux in a reactor fuel element occurs at the location of the maximum heat-generation rate which is at the center of a uniformly loaded reactor. The maximum fuel element temperature, however, does not necessarily occur at the center of the reactor because of the heating of the reactor coolant as it passes through the reactor core. It is commonly assumed that the axial power distribution (in the direction of coolant flow) is a "chopped-sine distribution," as is shown in Fig. 5.20. The power and heat-generation rate, as a function of axial position, is given as follows:

$$P(x) = P_{\max} \sin \frac{\pi(x+d)}{L+2d} = P_{\max} \sin \frac{\pi(x+d)}{\chi} \tag{5.49}$$

and

$$q'(x) = q'_{\max} \sin \frac{\pi(x+d)}{L+2d} = q'_{\max} \sin \frac{\pi(x+d)}{\chi} \tag{5.50}$$

where L is the core length, d is the extrapolation distance, and χ is defined as $L+2d$.

The axial distribution of the coolant temperature can be obtained by integrating the axial power distribution and setting it equal to $mc_p(T_{\infty,x} - T_{\infty,0})$, which is the thermal energy transferred to the coolant. Solving for the temperature rise of the coolant gives

$$T_{\infty,x} - T_{\infty,0} = \frac{1}{mc_p} \int_0^V q'(V)\, dV = \frac{\pi a^2 q'_{\max}}{mc_p} \int_0^x \sin \frac{\pi(x'+d)}{\chi}\, dx'$$

$$= \frac{q'_{\max} a^2 \chi}{mc_p} \left[\cos \frac{\pi d}{\chi} - \cos \frac{\pi(x+d)}{\chi} \right] \tag{5.51}$$

At a given axial position along a fuel rod, the temperature increases from the coolant temperature to the various radial positions in the element are given by the following equations:

$$T_{b,x} - T_{\infty,x} = T_{3,x} - T_{\infty,x} = \frac{q'_{max} a^2}{2} C_3 \sin \frac{\pi(x+d)}{\chi} \tag{5.52a}$$

$$T_{ac,x} - T_{\infty,x} = T_{2,x} - T_{\infty,x} = \frac{q'_{max} a^2}{2} C_2 \sin \frac{\pi(x+d)}{\chi} \tag{5.52b}$$

$$T_{af,x} - T_{\infty,x} = T_{1,x} - T_{\infty,x} = \frac{q'_{max} a^2}{2} C_1 \sin \frac{\pi(x+d)}{\chi} \tag{5.52c}$$

$$T_{0,x} - T_{\infty,x} = T_{0,x} - T_{\infty,x} = \frac{q'_{max} a^2}{2} C_0 \sin \frac{\pi(x+d)}{\chi} \tag{5.52d}$$

where

$$C_0 = C_1 + \frac{1}{2k_f} = \frac{1}{bh_b} + \frac{\ln(b/a)}{k_c} + \frac{1}{ah_a} + \frac{1}{2k_f} \tag{5.53a}$$

$$C_1 = C_2 + \frac{1}{ah_a} = \frac{1}{bh_b} + \frac{\ln(b/a)}{k_c} + \frac{1}{ah_a} \tag{5.53b}$$

$$C_2 = C_3 + \frac{\ln(b/a)}{k_c} = \frac{1}{bh_b} + \frac{\ln(b/a)}{k_c} \tag{5.53c}$$

$$C_3 = \frac{1}{bh_b} \tag{5.53d}$$

Adding Eq. (5.51) to Eqs. (5.52) gives the element temperatures in terms of the inlet coolant temperature $T_{\infty,0}$, or

$$T_{i,x} - T_{\infty,0} = \frac{q'_{max} a^2 \chi}{\dot{m} c_p} \left(\cos \frac{\pi d}{\chi} - \cos \frac{\pi(x+d)}{\chi} \right) + \frac{q'_{max} a^2}{2} C_i \sin \frac{\pi(x+d)}{\chi} \tag{5.54}$$

The location (value of x) of the maximum value of T_i can be determined by differentiating Eq. (5.54) with respect to x, setting the derivative to zero, and solving for the position of the maximum temperature $T_{i,max}$. This gives

$$x_{\max T_i} = \frac{\chi}{\pi} \tan^{-1} \left[-\frac{\dot{m} c_p C_i}{2\chi} \right] - d \tag{5.55}$$

Once the location of the maximum temperature is known, the actual maximum temperatures can be determined from Eqs. (5.52).

Example 5.3. Use the values in Example 5.2, except assume that the system is a PWR with inlet and exit water temperatures of 290°C and 340°C, the surface conductance of the water coolant is 6000 W/m^2 · °C, the maximum-to-average axial power ratio is 1.4, and the core length is 3.66 m. Calculate the maximum surface temperature T_b, the maximum cladding temperature T_{ac}, the maximum surface temperature of the fuel pellet T_{af}, and the maximum pellet temperature T_0.

Solution. From Example 5.2: $a = 0.0054$ m; $b = 0.00625$ m; $k_f = 1.8$ W/m^2 · °C; $k_c = 14$ W/m^2 · °C; $q'_{ave} = 4.072 \times 10^8$ W/m^3; $h_a = 5500$ W/m^2 · °C. Also, $h_b = 6000$ W/m^2 · °C and $L = 3.66$ m. Thus

$$\dot{m}c_p = \frac{q'_{ave}a^2\pi L}{\Delta T} = \frac{(4.072 \times 10^8 \text{ W/m}^3)(0.0054 \text{ m})^2\pi(3.66 \text{ m})}{50°\text{C}}$$

$$= 2730 \text{ W/°C}$$

$$q'_{max} = 1.4q'_{ave} = 1.4(4.072 \times 10^8) = 5.7 \times 10^8 \text{ W/m}^3$$

$$P_{ave} = \frac{P_{max}}{1.4} = \int_0^L P_{max} \frac{\sin[\pi(x+d)/(L+2d)]}{L}\,dx$$

$$= P_{max}\left[\frac{(L+2d)}{\pi L}\right]\left(\cos\frac{\pi d}{L+2d} - \cos\frac{\pi(L+d)}{L+2d}\right)$$

$$d = \frac{\pi L}{2.8}\left(\cos\frac{\pi d}{L+2d} - \cos\frac{\pi(L+d)}{L+2d}\right)^{-1} - \frac{L}{2}$$

By trial and error, $d = 0.2643$ m.

$$\chi = L + 2d = 4.1885 \text{ m}$$

Location of maximum temperatures:

Thermal constants:

$$C_3 = \frac{1}{bh_b} = \frac{1}{(0.00625)(6000)} = 0.026667 \text{ m} \cdot °\text{C/W}$$

$$C_2 = C_3 + \frac{\ln(b/a)}{k_c} = 0.026667 + \frac{\ln(0.00625/0.0054)}{14}$$

$$= 0.026667 + 0.010442 = 0.037109 \text{ m} \cdot °\text{C/W}$$

$$C_1 = C_2 + \frac{1}{ah_a} = 0.037109 + \frac{1}{(0.0054)(5500)}$$

$$= 0.037109 + 0.03367 = 0.070779 \text{ m} \cdot °\text{C/W}$$

$$C_0 = C_1 + \frac{1}{2k_f} = 0.070779 + \frac{1}{3.6} = 0.348556 \text{ m} \cdot °\text{C/W}$$

$$x_{max,T_i} = \frac{\chi}{\pi}\tan^{-1}\left[\frac{-C_i\dot{m}c_p}{2\chi}\right] - d$$

$$= \frac{4.1885}{\pi}\tan^{-1}\left[\frac{-C_i(2730)}{2(4.1885)}\right] - 0.2643$$

$$= (1.3332)\tan^{-1}(-325.89C_i) - 0.2643$$

$$x_{max,T_b} = 1.3332\tan^{-1}[-325.89(0.026667)] - 0.2643 = 1.983 \text{ m}$$

$$x_{max,T_{a_1}} = 1.3332\tan^{-1}[-325.89(0.037109)] - 0.2643 = 1.940 \text{ m}$$

$$x_{max,T_{a_f}} = 1.3332\tan^{-1}[-325.89(0.070779)] - 0.2643 = 1.888 \text{ m}$$

$$x_{max,T_0} = 1.3332\tan^{-1}[-325.89(0.348556)] - 0.2643 = 1.842 \text{ m}$$

Maximum temperatures:

$$T_{i,x} - T_{\infty,0} = q'_{\max} a^2 \left(\frac{\chi}{\dot{m} c_p} \cos \frac{\pi d}{\chi} - \frac{\chi}{\dot{m} c_p} \cos \frac{\pi(x+d)}{\chi} + \frac{C_i}{2} \sin \frac{\pi(x+d)}{\chi} \right)$$

$$T_{i,x} = 290 + (5.7 \times 10^8)(0.0054^2) \left(\frac{4.1885}{2730} \cos \frac{0.2643\pi}{4.1885} + \frac{4.1885}{2730} \cos \frac{\pi(x+0.2643)}{4.1885} + \frac{C_i}{2} \sin \frac{\pi(x+0.2643)}{4.1885} \right)$$

$$T_{i,x} \simeq 290 + 25.0 - 25.5 \cos \frac{(x+0.2643)}{1.3332} + (8310.6 C_i) \sin \frac{(x+0.2643)}{1.3332}$$

$$T_{b,\max} = 315 - 25.5 \cos \frac{1.983 + 0.2643}{1.3332} + 8310.6(0.026667) \sin \frac{1.983 + 0.2643}{1.3332}$$

$$= 315 + 2.9 + 220.2 = 538.1°C$$

$$T_{ac,\max} = 315 - 25.5 \cos \frac{1.940 + 0.2643}{1.3332} + 8310.6(0.03711) \sin \frac{1.940 + 0.2643}{1.3332}$$

$$= 315 + 2.1 + 307.4 = 624.5°C$$

$$T_{af,\max} = 315 - 25.5 \cos \frac{1.888 + 0.2643}{1.3332} + 8310.6(0.070779) \sin \frac{1.888 + 0.2643}{1.3332}$$

$$= 315 + 1.1 + 587.7 = 903.8°C$$

$$T_{0,\max} = 315 - 25.5 \cos \frac{1.842 + 0.2643}{1.3332} + 8310.6(0.34856) \sin \frac{1.842 + 0.2643}{1.3332}$$

$$= 315 + 0.2 + 2896.6 = 3211.8°C$$

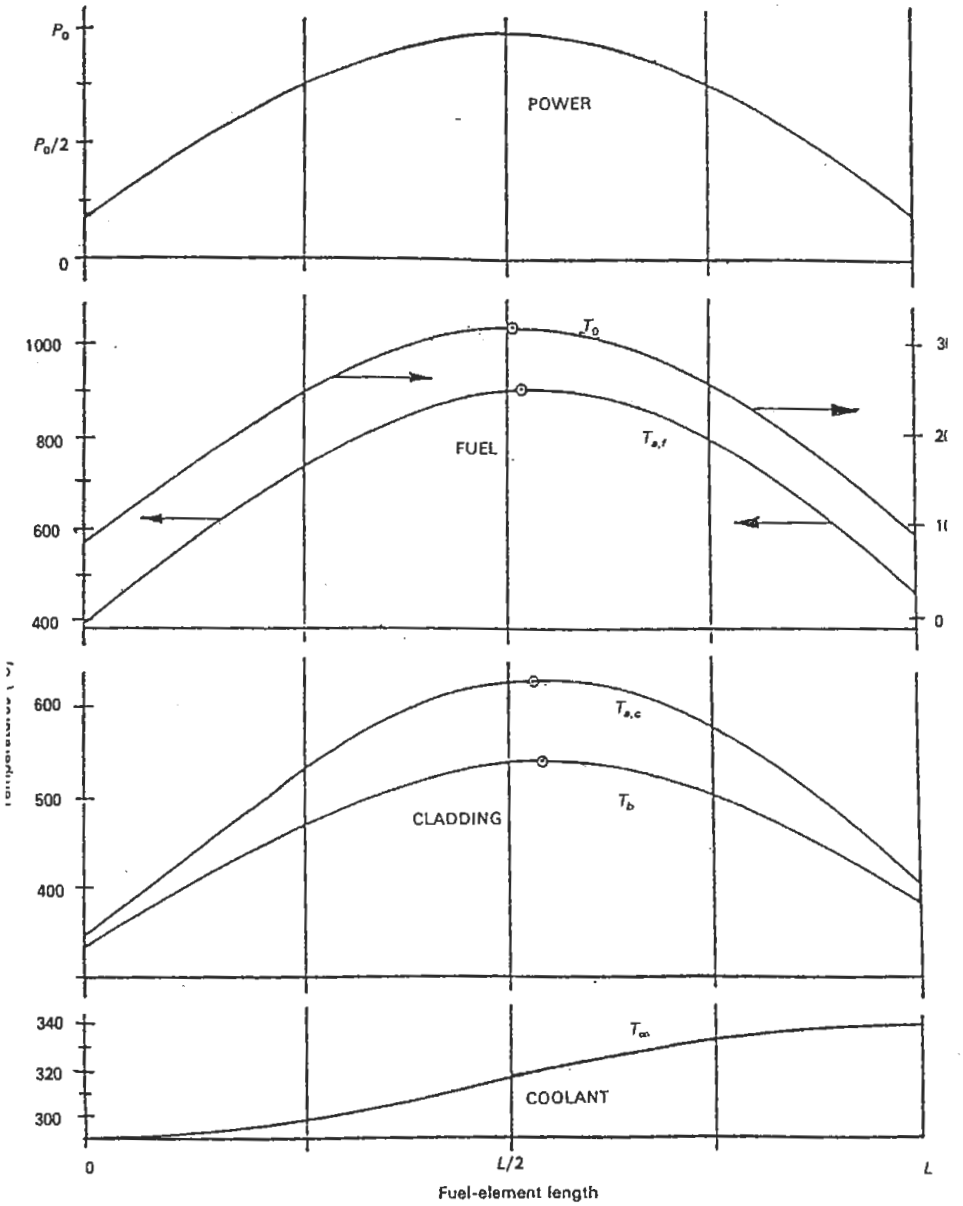
The axial temperature distributions for each of these locations are shown in Fig. 5.19.

5.4 REACTOR OPERATIONS

5.4.1 Reactor Kinetics

A term commonly encountered in the operation of any nuclear reactor is the *reactor period* t_r. The reactor period is defined as the time required for the reactor power or the neutron flux to *increase* by a factor e, the base of natural logarithms. In a supercritical reactor, the multiplication factor is greater than unity, the reactivity ρ is positive, and the reactor period t_r is positive. In a critical reactor, the multiplication factor is exactly unity, the reactivity is zero, and the reactor period is equal to infinity. In a subcritical reactor, the multiplication factor is less than unity, the reactivity is negative, and the reactor period is negative.

An important parameter in the determination of the reactor period is the lifetime of the average neutron in the reactor because this is also equal to the average generation time for the neutrons in the chain reaction. The average neutron lifetime is defined as the time between the instant that the fission occurs



⊙—Location of maximum temperature.

FIGURE 5.19
The axial temperature and power distributions in a reactor fuel element.

that produces the neutron until this average neutron is lost from the reactor core as the result of absorption or leakage. In a thermal reactor system, the lifetime of the thermal neutrons is equal to the sum of the production time l_{pr}, the slowing-down time l_s, and the thermal diffusion time l_{th}, or

$$\text{Average neutron lifetime} = l_{pr} + l_s + l_{th} \tag{5.56}$$

The production time l_{pr} is the time from the instant that the fission occurs until the fission neutron appears. For most of the reactor neutrons, the production time is very short, within 10^{-14} s. These neutrons are called *prompt neutrons* and, because of the extremely short production time, this time is normally neglected when calculating the average lifetime. A small number of fission neutrons, called *delayed neutrons*, have a long production time because they are produced as the result of radioactive decay of certain fission products. These fission products are halogen atoms (isotopes of iodine and bromine) and are called *delayed-neutron precursors*. Although these neutrons make up less than 1 percent of all the fission neutrons, the production time of them is so long that they are very important in evaluating the average neutron lifetime in the reactor.

The slow-down time l_s is relatively short, ranging from around 10^{-5} s in a large graphite or heavy-water moderated reactor to less than 10^{-8} s in a small fast reactor. This time is normally neglected in most thermal-reactor systems because it is several orders of magnitude lower than the thermal-diffusion time. In a fast reactor, however, the average lifetime of prompt neutrons is essentially the same as the slowing-down time since the production time is very short and the thermal-diffusion time is zero.

The thermal-diffusion time l_{th} is the average time that the thermal neutrons spend in a thermal reactor until they are either absorbed or they leak from the core. This time ranges from about 10^{-4} s for LWR systems to around 10^{-3} s for the large graphite- or heavy-water-moderated systems. If the thermal-neutron leakage is small, the thermal-diffusion time in a homogeneous assembly is equal to

$$l_{th} = \frac{\lambda_a}{\bar{V}_{th}} = \frac{1}{\bar{\Sigma}_a \bar{V}_{th}} \tag{5.57}$$

where $\bar{\Sigma}_a$ is the total macroscopic neutron-absorption cross section and $\bar{V}_{th}$ is the average velocity of thermal neutrons.

For prompt neutrons, the average lifetime is called the *prompt-neutron lifetime* l_p. Since l_{pr} is very small, the prompt-neutron lifetime for fast reactors is equal to l_s, while that for thermal neutrons is approximately equal to l_{th}. For fast-reactor systems,

$$10^{-8} < l_p < 10^{-7} \text{ s}$$

For thermal-reactor systems,

$$10^{-4} < l_p < 10^{-3} \text{ s}$$

The lower values in each case represent values for small, highly loaded reactors where the leakage and/or the absorption cross section is high.

For the delayed neutrons, the delayed-neutron lifetime l_d is approximately equal to the production time because it is much longer than either the slowing-down time or the thermal-diffusion time. The production time of these neutrons is equal to the average lifetime of the precursor isotopes. There are six groups of delayed-neutron precursors with half-lives ranging from a minimum of 0.23 s to a maximum of 55.72 s. According to Eq. (2.23), the average lifetime of any radioisotope is equal to the reciprocal of the decay constant of the radioisotope. Thus, the production time for the ith group of delayed neutrons is

$$l_{d,i} = l_{pr,i} = \frac{1}{\lambda_i} = \frac{t_{1/2,i}}{\ln 2} \tag{5.58}$$

where $t_{\frac{1}{2},i}$ is the half-life of the ith group of delayed-neutron precursors. The production times and hence the delayed-neutron lifetimes range from 0.332 s for the first or shortest-lived group to 80.4 s for the sixth or longest-lived group.

Table 5.5 lists the average kinetic energy, the half-lives of the delayed-neutron precursors, and the fraction β_i of the total fission neutrons produced by each of the delayed-neutron precursors. These values are tabulated for each of the common fuel isotopes. It will be noted that uranium-235 has the largest delayed-neutron fraction while plutonium-239 has the smallest fraction.

The average lifetime of all the fission neutrons can be estimated by summing the products of the fraction of each group of neutrons and their respective average lifetimes. Since the total fraction of delayed neutrons is equal to β, where β is the summation of β_i over all six delayed-neutron groups, the fraction of fission neutrons that are prompt neutrons is $1-\beta$. The average lifetime of all the fission neutrons, $\bar{l}$, is given by the following equation:

$$\bar{l} = (1-\beta)l_p + \sum_{i=1}^{6} \beta_i l_{d,i} = (1-\beta)l_p + \frac{\sum_{i=1}^{6} \beta_i t_{1/2,i}}{\ln 2} \tag{5.59}$$

TABLE 5.5
Delayed-neutron parameters for the common fuel isotopes

Group, i	Energy for uranium-235 fission, MeV	Half-life, s	Total neutrons from fission, %		
			Uranium-235	Uranium-233	Plutonium-239
Prompt	≈2.00	<0.001	99.359	99.736	99.790
1	0.25	55.72	0.021	0.023	0.007
2	0.56	22.72	0.140	0.079	0.063
3	0.43	6.22	0.126	0.066	0.044
4	0.62	2.30	0.253	0.073	0.069
5	0.42	0.61	0.074	0.014	0.018
6		0.23	0.027	0.009	0.009
	Total delayed-neutron fraction =		0.641	0.264	0.210

The maximum value of $(1-\beta)l_p$ is less than 0.001 s while the value of the second term or the summation of $\beta_i(t_{1/2,i})/(\ln 2)$ ranges from 0.0832 s for uranium-235 to 0.0327 s for plutonium-239. Thus, the delayed neutrons are very effective in increasing the average-neutron lifetimes. The average-neutron lifetimes are essentially independent of the prompt-neutron lifetimes and depend only on the type of fuel used in the reactor. As will be discussed later, however, there are some modes of operation where the prompt-neutron lifetime is very important.

If it is assumed that all the neutrons have one lifetime, it is relatively simple to develop an equation relating the transient response of the reactor to the reactor multiplication factor k or the system reactivity ρ. The average-neutron lifetime is also the average-neutron generation time since a fission cannot occur until the neutron is absorbed in the fission process.

The rate of change of neutrons with time, dn/dt, is

$$\frac{dn}{dt}=\frac{n_1-n}{\bar{l}}=\frac{n[(n_1/n)-1]}{\bar{l}} \tag{5.60}$$

where n_1 is the number of neutrons produced in one generation and n is the number produced in the preceding generation. The ratio of n_1/n is the definition of the multiplication factor k. Since $k-1$ is approximately equal to the reactivity ρ for values of k close to unity, eq. (5.60) reduces to

$$\frac{dn}{dt}=\frac{n(k-1)}{\bar{l}}\approx\frac{n\rho}{\bar{l}} \tag{5.61}$$

For small step changes in k or ρ, this equation can be integrated to yield

$$n=n_0\exp\left(\frac{\rho t}{\bar{l}}\right) \tag{5.62}$$

where n is the number of neutrons at some arbitrary time t and n_0 is the number that was present at some arbitrary time $t=0$. The population n in the reactor core is directly proportional to the neutron flux and also to the reactor power. Consequently, Eq. (5.62) may also be written as either

$$\phi=\phi_0\exp\left[\frac{(k-1)t}{\bar{l}}\right]=\phi_0\exp\left(\frac{\rho t}{\bar{l}}\right) \tag{5.63}$$

or

$$P=P_0\exp\left[\frac{(k-1)t}{\bar{l}}\right]=P_0\exp\left(\frac{\rho t}{\bar{l}}\right) \tag{5.64}$$

In practice, Eqs. (5.63) and (5.64) have a fairly limited range of application because all the fission neutrons do not have the same lifetime. In a uranium-235-fueled reactor, these equations are applicable for reactivity values in the range of ± 0.001. The reactor period t_r is defined as the time required for the power to increase by a factor e. Substituting this definition into the previous equation yields

$$n=n_0\exp\frac{t}{t_r}\qquad\text{or}\qquad\phi=\phi_0\exp\frac{t}{t_r}\qquad\text{or}\qquad P=P_0\exp\frac{t}{t_r} \tag{5.65}$$

where

$$t_r = \frac{\bar{l}}{\rho} \tag{5.66}$$

As mentioned above, these equations are applicable for uranium-235-fueled reactors ($\bar{l} = 0.0832$ s) for step changes in reactivity ranging from -0.001 to $+0.001$. Using the upper limit of $\rho = +0.001$, the simple equation gives a stable reactor period of 83.2 s. A rigorous calculation of the stable period for the same reactivity insertion gives a value of about 60 s.

Figure 5.20 gives a plot of the stable reactor period for uranium-235-fueled reactors as a function of a step change of reactivity and also as a function of the prompt-neutron lifetime. A rigorous solution of the reactor transient equations for a step change in reactivity involves the solution of a seventh-order equation to find the seven roots. There is one root for each of the six groups of delayed neutrons plus the prompt-neutron group. These roots, a_i, yield a general flux equation of the following form:

$$\phi(t) = A_0 \exp(a_0 t) + A_1 \exp(a_1 t) + A_2 \exp(a_2 t) + A_3 \exp(a_3 t) + A_4 \exp(a_4 t) + A_5 \exp(a_5 t) + A_6 \exp(a_6 t) \tag{5.67}$$

For positive insertions of reactivity, one root, a_0, and one coefficient, A_0, are positive while all the other roots and coefficients are negative. All the terms involving the negative roots decay exponentially with time and the stable reactor period is $1/a_0$. For small negative changes, the stable period is $1/a_0$, while for

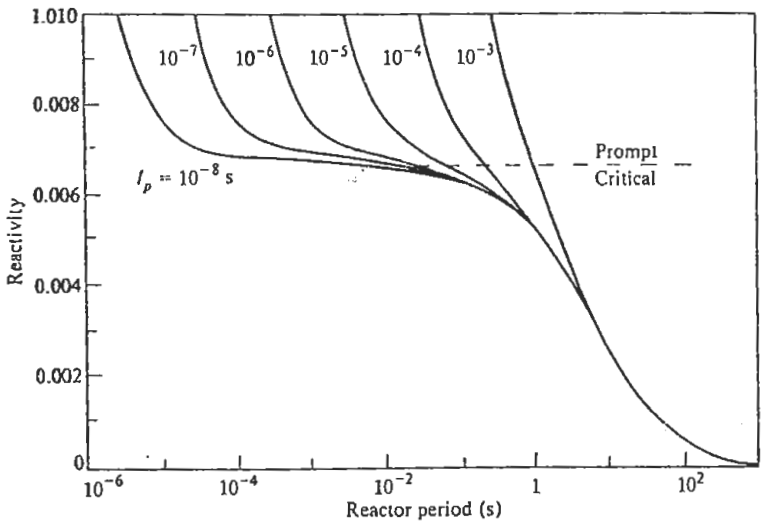


FIGURE 5.20
The stable reactor period for a step increase in reactivity in a U-235-fueled reactor.

large negative reactivity changes, such as that which occurs in a reactor scram, it is −80.4 s. This period corresponds to the lifetime of the longest-lived group of delayed-neutrons precursors.

Before considering the response of the actual reactor to step changes in reactivity, consider the importance of the delayed neutrons to reactor control. As was discussed earlier, for a uranium-235-fueled reactor and reactivity values ranging between ±0.001, the stable reactor period is $t_r = \bar{l}/\rho$. If there were no delayed neutrons, the average-neutron lifetime would be equal to the prompt-neutron lifetime l_p, and the stable and only period would become $t_r = l_p/\rho$. A small fast reactor with a prompt-neutron lifetime of 10^{-8} s would achieve a reactor period of 10^{-5} s for a step decrease in reactivity of +0.001. This means that the reactor would go from a thermal power of 1 W to a power of more than 5×10^{15} MW in a 1-s time interval. This response approaches or exceeds that of an atomic bomb. The presence of delayed neutrons increases the actual period to about 60 s, which means that the power actually increases from 1 to 2.718 W in a 1-min interval. If it were not for the presence of delayed neutrons, reactor control would be essentially impossible.

As discussed above, the actual response to a step change in reactivity is difficult to calculate explicitly. However, some general trends can be examined. For a step insertion of positive reactivity into a critical reactor at some arbitrary time $t = 0$, the power will start to increase with an initial period of $t_r = l_p/\rho$, but then the rate of increase will slow until the stable period is attained. This response is shown in the semilog plot of power versus time in Fig. 5.21. The exponential relationship such as that given by Eq. (5.65) plots as a straight line on semilog graph paper.

For large negative step changes, such as occur during a reactor scram when the control rods are dropped into the core, there is an initial rapid transient drop

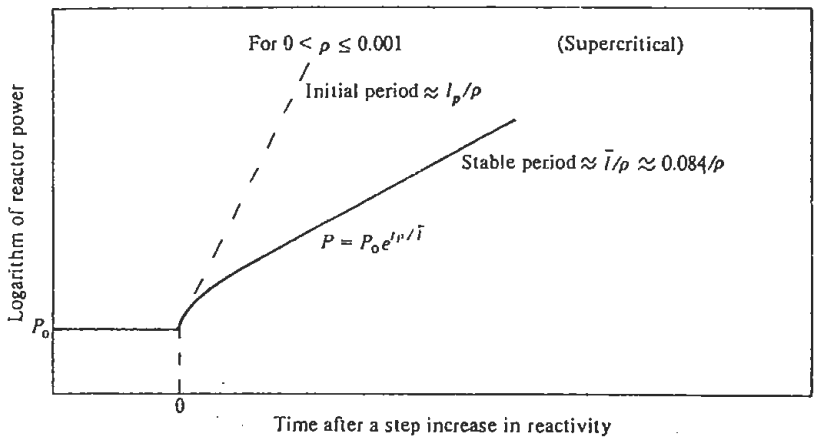


FIGURE 5.21
Reactor power following a step increase of reactivity in a critical reactor fueled with U-235.

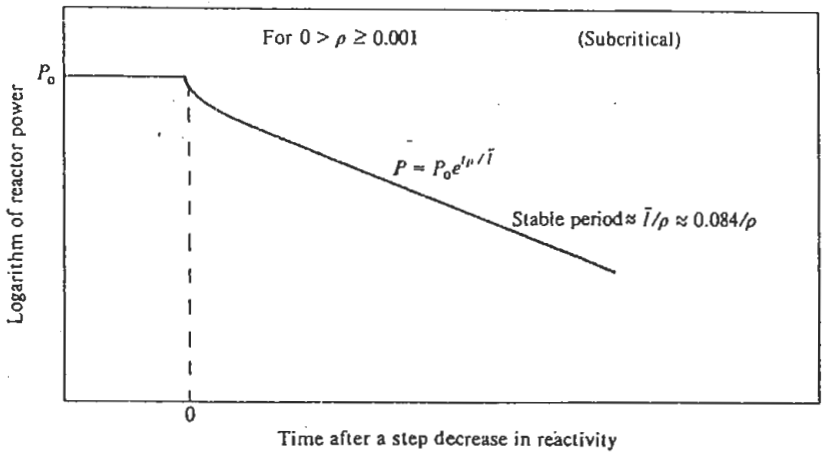


FIGURE 5.22
Reactor power following a step decrease of reactivity in a critical reactor fueled with U-235.

in power and then the power eventually decays with a stable period of −80 s. The reactor response to a small step decrease in reactivity of a critical reactor is shown in Fig. 5.22.

For large positive values of reactivity insertions, the prompt-neutron lifetime l_p becomes very important. If the amount of positive reactivity is equal to the delayed-neutron fraction, or $\rho = \beta$, the multiplication factor k is approximately $1+\beta$. This means that the delayed neutrons could be discarded and the reactor would still be critical. When this happens, the reactor is said to be *prompt critical* because the reactor could be critical on prompt neutrons alone. If the system reactivity exceeds β, the stable reactor period approaches

$$t_r < \frac{l_p}{\rho - \beta} \tag{5.68}$$

The prompt-critical condition is normally avoided in all power reactors but it is especially severe in small fast reactors because of the very short prompt-neutron lifetimes. The super-prompt-critical condition is normally attained in the detonation of atomic bombs to achieve a high energy release or "yield" before the assembly is blown apart. There are a few pulsed research reactors that operate above the prompt-critical condition in order to achieve very high power pulses. These systems depend on the temperature increase to limit the total energy release to tolerable levels before meltdown.

Some opponents of fast reactors point to the response of fast reactor systems to the prompt-critical condition as a major disadvantage. However, it should be pointed out that for small changes in reactivity, the response of fast and thermal reactors is about the same because the delayed neutrons produce about the same value of stable reactor period. Moreover, it is much more difficult to achieve the

prompt-critical condition in a fast reactor system as compared to thermal reactors. Actually, the possibility that any reactor system might detonate like an atomic bomb is zero. However, there is a possibility that a fast transient could cause a reactor meltdown or the sudden vaporization of the reactor coolant which could result in considerable damage to the reactor complex.

Throughout this discussion, the delayed-neutron fractions were assumed to be constant for a given fuel, as listed in Table 5.5. Actually, this is true for only heterogeneous reactor systems. In homogeneous reactors, where the fuel solution is circulated outside the core, some of the delayed neutrons will be produced in the external piping where they have no effect on the system reactivity. Thus, the effective delayed-neutron fractions and the prompt-critical value of reactivity are somewhat less than the actual delayed-neutron fraction β.

There are several units of reactivity in common use today. The *in-hour* of reactivity, Ih, is a small unit of reactivity and is equal to the amount of reactivity that will put a critical reactor on a stable period of 1 h or 3600 s. The term *in-hours* is a contraction of "inverse hours," and for small changes in reactivity, the stable period is

$$t_r = \frac{3600}{\text{Ih}} \qquad \text{for Ih} \leq 50 \tag{5.69}$$

The other common unit of reactivity is the *dollar of reactivity*. One dollar of reactivity inserted into a critical reactor will make the reactor just prompt critical. For heterogeneous reactors, a dollar's worth of reactivity is equal to the delayed-neutron fraction, but it is less than this quantity for a homogeneous reactor. One *cent of reactivity* is equal to one-hundredth of a dollar.

Example 5.4. Find the stable reactor period and the excess reactivity, in percent, and in in-hours of reactivity, if 5 cents of reactivity are inserted into a critical thermal reactor fueled with Pu-239. How long will it take the critical reactor to go from a power of 100 W to 3800 MW after the reactivity insertion? Also, evaluate the time required to go from 3800 to 500 MW if the reactor is scrammed and the initial transient is neglected.

Solution. Use the values from Table 5.5. Thus the delayed neutron fraction for Pu-239 = $\beta = 0.210$ percent = 0.0021.

$$5 \text{ cents of reactivity} = 0.05\beta = 0.05(0.0021) = 0.000105$$

$$\text{Excess reactivity} = \rho = 0.000105 = 0.0105\%$$

Average-neutron lifetime for Pu-239 is

$$\bar{l} \approx \frac{\sum_{i=1}^{6} \beta_i (t_{1/2})_i}{\ln 2}$$

$$= [55.72(0.00007) + 22.72(0.00063) + 6.22(0.00044) + 2.3(0.00069) + 0.61(0.00018) + 0.23(0.00009)]/\ln 2$$

$$= 0.0327 \text{ s}$$

$$\text{Stable reactor period} = t_r = \frac{\bar{l}}{\rho} = \frac{0.0327}{0.000105} = 311.4 \text{ s}$$

$$\text{In-hours of reactivity} = \frac{3600}{t_r} = \frac{3600}{311.4} = 11.56 \text{ lh}$$

Time required to go from 100 W to 3800 MW:

$$P = P_0 \exp \frac{t}{t_r} \quad \text{or} \quad t = t_r \ln \frac{P}{P_0}$$

$$t = 311.4 \ln \frac{3800 \times 10^6}{100} = 311.4(\ln 38{,}000{,}000) = 5435 \text{ s}$$

$$= 90.58 \text{ min} = 1.51 \text{ h}$$

The time required to go from 3800 to 500 MW when the reactor is scrammed and the initial transient is neglected can be determined as follows. The stable reactor period is equal to the lifetime of the longest-lived group of delayed neutrons:

$$t_r = \frac{-(t_{1/2})_{\text{long-lived}}}{\ln 2} = \frac{-55.72}{\ln 2} = -80.38 \text{ s}$$

$$t = t_r \ln \frac{P}{P_0} = -80.38 \ln \frac{500}{3800} = -80.38 \ln 0.2669$$

$$= 163 \text{ s} = 2.72 \text{ min}$$

It should be stressed here that this is not a realistic value because the initial transients will significantly reduce the calculated value.

5.4.2 Reactivity Coefficients

Reactivity coefficients are very important in the operation of reactors because they indicate how the system reactivity ρ changes with respect to a change in certain operating parameters such as power, temperature, pressure, etc. Actually, the reactivity coefficient of greatest interest is the power coefficient of reactivity α_P, which gives the rate of change of reactivity with power:

$$\alpha_P = \frac{\partial \rho}{\partial(\text{power})} \tag{5.70}$$

For ease of control, the power coefficient of reactivity should be large in absolute magnitude and negative in arithmetic sign at the operating point. With this condition, the reactor will be very stable because an increase in power causes a decrease in reactivity which, in turn, limits the reactor power. A positive power coefficient, on the other hand, gives positive feedback and a diverging power condition. It is usually difficult to predict the value of the power coefficient directly because it is a function of many variables. Instead, some of the other reactivity coefficients are evaluated because they are closely related to the power coefficient.

One of the more important reactivity coefficients for ease of reactor control is the temperature coefficient of reactivity, α_T. This coefficient gives the rate of change of reactivity with the reactor temperature:

$$\alpha_T = \frac{\partial \rho}{\partial T} \tag{5.71}$$

As is the case for all reactivity coefficients, for ease of control, α_T should be large in magnitude and negative in sign at the operating point. If α_T is positive, an unstable condition exists because an increase in temperature would cause an increase in reactivity which would, in turn, cause an increase in power and temperature, producing an additional increase in reactivity, etc.

An important temperature phenomenon encountered in the operation of some reactors is *doppler broadening*. Doppler broadening effectively causes a neutron cross-section peak or resonance, commonly found in the intermediate-energy range, to decrease in magnitude but increase in energy width. The effect is caused by the relative motion between the incident neutrons and the target nuclei. Above absolute zero, all nuclei in a solid are vibrating about a fixed lattice position, and, as the temperature increases, the molecular (nuclear) kinetic energy increases directly with the absolute temperature. If the incident neutron reacts with the target nucleus while they are moving in the same direction, the apparent kinetic energy of the incident neutron with respect to the target nucleus is less than its absolute kinetic energy. If the neutron and the target nucleus collide while they are going in opposite directions, the apparent kinetic energy of the reacting neutron with respect to the target nucleus is greater than its absolute kinetic energy. Thus, some of the neutrons having energies slightly above or below the resonance energy band will appear to fall within the resonance energy due to the motion of the target nucleus. The doppler broadening effectively increases the neutron reaction rate with a given nucleus because of an increase in temperature.

The doppler broadening effect can be very important in the control of some reactors, particularly fast reactors. If most of the cross-section resonances are fission resonances, an increase in temperature increases the fission rate because of the doppler broadening of those resonances. The increased fission rate produces a positive temperature coefficient of reactivity and this makes the reactor very difficult to control unless there are other effects, such a fuel expansion, etc., that make the overall temperature coefficient negative.

Typical values of the temperature coefficient of reactivity range from -10^{-4} to $-10^{-8}\ \Delta\rho/\mathrm{C}^\circ$. Homogeneous reactors normally have values of α_T approaching $-10^{-4}\ \Delta\rho/\mathrm{C}^\circ$ because any increase in reactor temperature causes the fuel solution to expand, and this removes fuel from the reactor core. Fast heterogeneous reactors, on the other hand, commonly have an α_T of about $-10^{-8}\ \Delta\rho/\mathrm{C}^\circ$ and the doppler coefficient may be a prime component of the overall temperature coefficient of reactivity in these systems.

For operational purposes, the overall temperature coefficient of reactivity is further divided into a prompt component of the temperature coefficient and a

delayed component. The prompt temperature coefficient is that portion of the overall temperature coefficient which is associated with fuel effects, such as fuel expansion, doppler broadening, etc. The delayed temperature coefficient is that part of the overall coefficient that is associated with the temperature effects on the coolant, moderator, and other nonfuel materials in the core.

If the prompt temperature coefficient of reactivity is positive, it can cause operational problems during fast positive transients when the reactor period is very short. In fact, the experimental breeder reactor I (EBR-I), which had a negative overall temperature coefficient, actually had an unknown positive prompt coefficient due to bowing of the fuel rods as the result of fuel expansion. During some fast transient tests that were carried out just before the reactor was to be shut down for dismantling, the positive prompt temperature coefficient produced an unexpectedly high power excursion that resulted in a core meltdown.

Another important reactivity coefficient in the operation of liquid-cooled reactors is the void coefficient of reactivity α_V. The void coefficient gives the rate of change of reactivity with the percentage of voids in the core:

$$\alpha_V = \frac{\partial \rho}{\partial(\%\ \text{voids})} \tag{5.72}$$

Vaporization of the coolant in any liquid-cooled reactor essentially introduces voids into the reactor core. Thus, the void coefficient of reactivity is particularly important in the normal operation of BWR systems. For stable operation, the void coefficient should be large in absolute magnitude and negative in sign at the desired operating point. While this coefficient is particularly important in boiling-water systems, it is also important in the operation of any liquid-cooled reactor. A power excursion in any of these systems can produce localized or general boiling of the coolant. This sudden vaporization of the coolant can aggravate or reduce the power excursion, depending on whether the void coefficient is positive or negative.

5.4.3 Fission-Product Poisoning

GENERAL POISONING EFFECTS. During the operation of any nuclear fission reactor, the system reactivity decreases as the system is operated. This is due to the fact that the fuel is being consumed and also because fission products are accumulating in the reactor core and they absorb some neutrons. While all fission products absorb some neutrons and consequently "poison" the reactor, some of them have extremely high microscopic absorption cross sections and present some interesting operating problems. This section investigates the effect of the buildup of fission products on the reactivity and the operation of the reactor. The effect of fuel burnup will be studied in Sec. 5.4.4.

An examination of the modified, one-group, critical equation (3.26) shows that the only terms strongly influenced by the buildup of fission-product poisons are the thermal diffusion length L and the thermal utilization factor f. The thermal diffusion length appears in the thermal nonleakage probability function. This

term, $1/(1+L^2B^2)$, is approximately unity for most thermal reactors and the product L^2B^2 is much smaller than unity. For most systems, therefore, this means that the variation of the multiplication factor with respect to the buildup of fission products essentially occurs only in the thermal utilization factor f.

The thermal utilization factor is the fraction of thermal neutrons that are absorbed by the fuel. As fission products accumulate in the core, they absorb some of the thermal neutrons, reducing f and therefore k. The multiplication factor equation can be written as follows:

$$k = K_1 f \tag{5.73}$$

where $K_1 = \eta p \varepsilon [\exp(-B^2\tau)]/(1+L^2B^2)$.

For a "clean" reactor, one in which there are no fission products in the core, the total thermal-neutron absorption rate in the reactor core is equal to

$$\begin{aligned}(\bar{\Sigma}_a \Phi_{th} V)_{total} = {} & (\bar{\Sigma}_a \Phi_{th} V)_{fuel} (\bar{\Sigma}_a \Phi_{th} V)_{clad} + (\bar{\Sigma}_a \Phi_{th} V)_{mod} \\ & + (\bar{\Sigma}_a \Phi_{th} V)_{cool} + (\bar{\Sigma}_a \Phi_{th} V)_{rods} + (\bar{\Sigma}_a \Phi_{th} V)_{struct} \\ & + \cdots \end{aligned} \tag{5.74}$$

Lumping the absorptions by the nonfuel material (moderator, coolant, etc.) into one term and assuming that the average-neutron flux in all the materials is about the same (not a very good assumption in some heterogeneous reactors), the absorption rate equation (5.67) reduces to

$$\bar{\Sigma}_{a,total} = \bar{\Sigma}_{a,fuel} + \bar{\Sigma}_{a,other} \tag{5.75}$$

The thermal utilization factor for the clean reactor, f_c, becomes

$$f_c = \frac{\bar{\Sigma}_{a,fuel}}{\bar{\Sigma}_{a,total}} = \frac{\bar{\Sigma}_{a,fuel}}{\bar{\Sigma}_{a,fuel} + \bar{\Sigma}_{a,other}} = \frac{1}{1+\delta} \tag{5.76}$$

where $\delta \equiv \bar{\Sigma}_{a,other}/\bar{\Sigma}_{a,fuel}$.

Substituting Eq. (5.76) into Eq. (5.73) gives

$$k_c = K_1 f_c = \frac{K_1}{1+\delta} \tag{5.77}$$

and the resulting reactivity for the clean reactor, ρ_c, becomes

$$\rho_c = \frac{k_c - 1}{k_c} = 1 - \frac{1}{k_c} = 1 - \frac{1+\delta}{K_1} = \frac{K_1 - 1 - \delta}{K_1} \tag{5.78}$$

In a "dirty" reactor, which is one containing fission products, the thermal utilization factor is reduced because of the absorption by the fission products. In this case, Eq. (5.75) becomes

$$\bar{\Sigma}_{a,total} = \bar{\Sigma}_{a,fuel} + \bar{\Sigma}_{a,other} + \bar{\Sigma}_{a,fission\ products} \tag{5.79}$$

The thermal utilization factor for the dirty reactor, f_d, is

$$f_d = \frac{1}{1+\delta+\theta} \tag{5.80}$$

where θ is called the *fission-product poisoning* and is given by

$$\theta = \frac{\bar{\Sigma}_{a,\text{fission products}}}{\bar{\Sigma}_{a,\text{fuel}}} \tag{5.81}$$

The multiplication factor for the dirty reactor, k_d, becomes

$$k_d = K_1 f_d = \frac{K_1}{1+\delta+\theta} \tag{5.82}$$

and the reactivity for the dirty reactor, ρ_d, is

$$\rho_d = \frac{k_d - 1}{K_d} = 1 - \frac{1}{k_d} = \frac{K_1 - 1 - \delta - \theta}{K_1} \tag{5.83}$$

The change in reactivity that occurs in going from the "clean" to the "dirty" condition, $\Delta\rho_{fp}$, is equal to

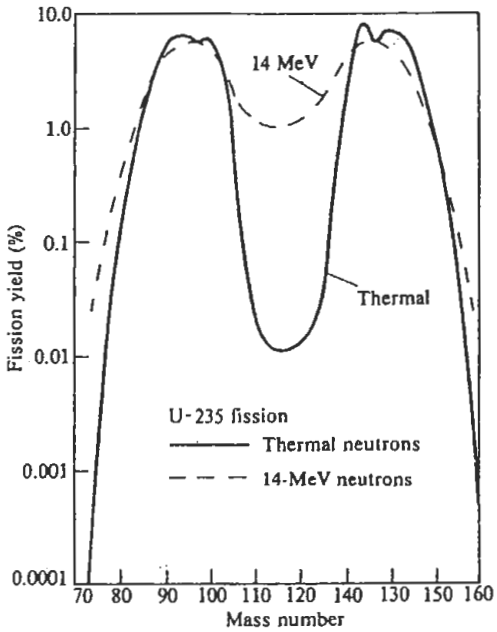
$$\Delta\rho_{fp} = \rho_d - \rho_c = \frac{K_1 - 1 - \delta - \theta}{K_1} - \frac{K_1 - 1 - \delta}{K_1} = \frac{-\theta}{K_1} \tag{5.84}$$

If the fuel is the principal absorber in the core, $\delta \ll 1.0$, and K_1 approaches unity, the change in reactivity due to the buildup of fission products in the core approaches $-\theta$, the fission-product poisoning term. While this derivation is carried out for thermal reactors, the result is also applicable to fast reactor systems.

THERMAL-REACTOR POISONS. There are two fission products that are important in the operation of thermal reactors because of their high microscopic neutron-absorption cross sections. These two thermal-reactor poisons are xenon-135 and samarium-149. To determine the atomic density and the fission-product poisoning due to these two isotopes, the production and depletion rates of the various isotopes appearing in the fission-product decay chains must be examined. On the average, the first or primary fission products produced from fission undergo three stages of beta decay before they reach a stable configuration. The first isotope appearing in the fission-product chain is called the *primary fission product* for that particular chain. All the other products appearing in the radioactive-decay chain are called *secondary fission products.*

The production rate of a primary fission product is directly proportional to the fission rate. The constant of proportionality is called the *fission yield constant*, γ_i, and is experimentally determined. Since there are two fission products produced in the fission process, the summation of all values of γ_i total 2. The typical double-humped yield curve for uranium-235 fission is shown in Fig. 5.23. The production rate of a primary fission product is equal to the yield constant times the fission rate, or $\gamma_i N_{\text{fuel}} \bar{\sigma}_f \Phi_{\text{th}}$.

The primary fission product is lost as the result of radioactive decay and as the result of neutron burnup. The radioactive-decay rate of any radioisotope is equal to the product of the number of atoms N_i and the decay constant λ_i, or $\lambda_i N_i$. The neutron burnup rate of a secondary fission product is equal to the



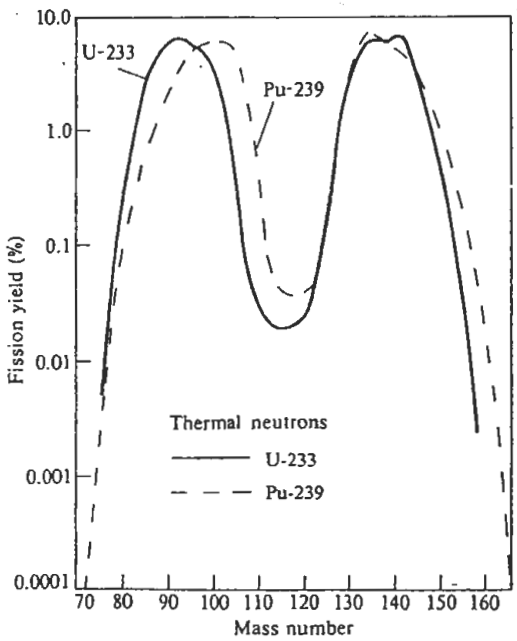


FIGURE 5.23
The mass distribution of fission products from the fission of U-235, U-233, and Pu-239. (*From Steam: Its Generation and Use, 1972.*)

product $N_i\bar{\sigma}_{a,i}\Phi_{th}$. The production rate of any secondary fission product is equal to the decay rate of the precursor product in the decay chain.

The xenon-135 fission product isotope has the highest microscopic neutron absorption cross section of any known material, with $\sigma_{a,th}$ equal to 3.2×10^6 barns. This isotope is both a primary and a secondary fission product and is also radioactive, with a half-life of 9.2 h. The fission-product decay chain containing xenon-135 is shown below:

Fission ↓ Fission ↓

$$_{52}\text{Te}^{135} \xrightarrow[2\text{ min}]{\beta^-} {}_{53}\text{I}^{135} \xrightarrow[6.7\text{ h}]{\beta^-} {}_{54}\text{Xe}^{135} \xrightarrow[9.2\text{ h}]{\beta^-} {}_{55}\text{Cs}^{135} \xrightarrow[2000\text{ years}]{\beta^-} {}_{56}\text{Ba}^{135} \quad \text{(Stable)}$$

The design or operating engineer is normally interested in the maximum values of fission-product poisoning. During reactor operation, this occurs when equilibrium conditions are attained. To find the equilbirium xenon-135 concentration, the equilibrium concentrations of the preceding products in the chain must be determined first. The rate of change of the number of telurium-135 atoms with time is:

$$\frac{d(\text{Te})}{dt} = \gamma_{\text{Te}} N_{\text{fuel}} \bar{\sigma}_f \Phi_{th} - \lambda_{\text{Te}}(\text{Te}) - (\text{Te})\bar{\sigma}_{a,\text{Te}}\Phi_{th} \tag{5.85}$$

At equilibrium, $d(\text{Te})/dt$ is zero and the burnup term in the above equation happens to be negligible when compared to the radioactive-decay term. Substituting these relationships into (5.85) gives the equilibrium number of tellurium atoms, $(\text{Te})_\infty$:

$$(\text{Te})_\infty = \frac{\gamma_{\text{Te}} N_{\text{fuel}} \bar{\sigma}_f \Phi_{th}}{\lambda_{\text{Te}}} \tag{5.86}$$

A similar approach can be used to develop an equation for the secondary fission product, iodine-135. The rate of change of iodine-135 is given by the following equation:

$$\frac{d(I)}{dt} = \lambda_{\text{Te}}(\text{Te}) - \bar{\sigma}_{a,I}(I)\Phi_{th} - \lambda_I(I) \tag{5.87}$$

At equilibrium in the reactor,

$$\frac{d(I)}{dt} = 0 \qquad \text{and} \qquad (\text{Te}) = (\text{Te})_\infty \tag{5.88}$$

As in the case for tellurium, $\sigma_{a,I}$ is so small (about 7 barns) that the neutron-burnup term is several orders of magnitude smaller than the radioactive-decay rate. The equilibrium number of iodine atoms, $(I)_\infty$, in the reactor becomes

$$(I)_\infty = \frac{(\text{Te})_\infty \lambda_{\text{Te}}}{\lambda_I} = \frac{\gamma_{\text{Te}} N_{\text{fuel}} \bar{\sigma}_f \Phi_{th}}{\lambda_I} \tag{5.89}$$

The differential equation for the variation of xenon-135 atoms with time is somewhat more complicated than those for tellurium and iodine because xenon-135 is both a primary and a secondary fission product:

$$\frac{d(\mathrm{Xe})}{dt} = \lambda_I(\mathrm{I}) + \gamma_{\mathrm{Xe}} N_{\mathrm{fuel}} \bar{\sigma}_f \Phi_{\mathrm{th}} - \lambda_{\mathrm{Xe}}(\mathrm{Xe}) - (\mathrm{Xe})\bar{\sigma}_{a,\mathrm{Xe}}\Phi_{\mathrm{th}} \tag{5.90}$$

The neutron-burnup term in this equation cannot be neglected, because of the extremely large value of the microscopic neutron-absorption cross section of xenon-135, unless the neutron flux is very low (less than 10^{15} n/m$^2 \cdot$ s). In fact, if the average-neutron flux exceeds 10^{19} n/m$^2 \cdot$ s, the neutron-burnup term in Eq. (5.90) overshadows the xenon decay-rate term. At equilibrium, $d(\mathrm{Xe})/dt$ is zero and the iodine will have already attained equilibrium concentration, $(\mathrm{I})_\infty$, because of its shorter half-life. Thus, the equilibrium number of xenon-135 atoms, $(\mathrm{Xe})_\infty$, in the core is

$$(\mathrm{Xe})_\infty = \frac{(\gamma_{\mathrm{Te}} + \gamma_{\mathrm{Xe}}) N_{\mathrm{fuel}} \bar{\sigma}_f \Phi_{\mathrm{th}}}{\bar{\sigma}_{a,\mathrm{Xe}}\Phi_{\mathrm{th}} + \lambda_{\mathrm{Xe}}} \tag{5.91}$$

The equilibrium poisoning value of xenon-135, $\theta_{\mathrm{Xe},\infty}$, is obtained from the following equation:

$$\theta_{\mathrm{Xe},\infty} = \frac{\Sigma_{a,\mathrm{Xe},\infty}}{\Sigma_{a,\mathrm{fuel}}} = \frac{(\mathrm{Xe})_\infty \bar{\sigma}_{a,\mathrm{Xe}} / V}{N_{\mathrm{fuel}} \bar{\sigma}_{a,\mathrm{fuel}} / V} \tag{5.92}$$

Substituting Eq. (5.91) into Eq. (5.92) gives

$$\theta_{\mathrm{Xe},\infty} = \frac{\bar{\sigma}_{a,\mathrm{Xe}} (\sigma_f / \sigma_a)_{\mathrm{fuel}} \Phi_{\mathrm{th}} (\gamma_{\mathrm{Te}} + \gamma_{\mathrm{Xe}})}{\bar{\sigma}_{a,\mathrm{Xe}}\Phi_{\mathrm{th}} + \lambda_{\mathrm{Xe}}} \tag{5.93}$$

For a uranium-235-fueled thermal reactor, $\gamma_{\mathrm{Te}} = 0.056$, $\gamma_{\mathrm{Xe}} = 0.003$, $\sigma_f = 582$ barns, and $\sigma_a = 683$ barns, so that Eq. (5.93) reduces to

$$\theta_{\mathrm{Xe},\infty,\mathrm{U\text{-}235}} = \frac{1.7 \times 10^{-23}\Phi_{\mathrm{th}}}{3.2 \times 10^{-22}\Phi_{\mathrm{th}} + 2.1 \times 10^{-5}} \tag{5.94}$$

Again, it will be noted in Eq. (5.94) that if the average thermal-neutron flux in the core is 10^{15} n/m$^2 \cdot$ s, or less, the first term in the denominator is negligible when compared to the second term and consequently the equilibrium xenon poisoning is directly proportional to the average thermal-neutron flux. However, when the thermal flux exceeds 10^{19} n/m$^2 \cdot$ s, the first term in the denominator of (5.94) becomes the dominate term and the poisoning value is then independent of the neutron flux and is constant at 0.053 or 5.3 percent or more than 8 dollars worth of reactivity. The equilibrium xenon-poisoning values in a uranium-235-fueled reactor and shown as a function of the average thermal-neutron flux in the core in Table 5.6. Most power reactors operate with average thermal-neutron fluxes ranging between 10^{17} and 5×10^{18} n/m$^2 \cdot$ s.

It is interesting to examine the variation of xenon poisoning during the normal operation of the reactor. If the reactor is a high-flux (high-powered) system, the xenon-poisoning value may be similar to the plot shown in Fig. 5.24.

TABLE 5.6
Equilibrium xenon-poisoning values

Average operating thermal flux, Φ_{th}, $n/m^2 \cdot s$	10^{15}	10^{16}	10^{17}	10^{18}	10^{19}
Equilibrium xenon poisoning, $\theta_{Xe,\infty,U\text{-}235}$	0.0008	0.007	0.032	0.050	0.053

Because the yield of tellurium is larger than the yield of xenon, most of the xenon comes from the decay of iodine. An increase in reactor power causes an immediate increase in the thermal flux which, in turn, causes an immediate increase in the neutron burnup term. There is a lag, however, in the increased production rate of xenon from iodine decay and consequently the xenon production rate increases rather slowly. This means that there will be an immediate but temporary decrease in the reactor xenon poisoning. If the thermal power is reduced, on the other hand, the Xe-burnup term goes down immediately but the production rate from iodine decay decreases later. This produces an immediate but temporary increase in reactor xenon poisoning, as indicated in Fig. 5.24.

It will be noted in Fig. 5.24 that the xenon poisoning in a high-flux reactor goes through a maximum following reactor shutdown. A maximum in xenon poisoning occurs only if the average thermal flux exceeds 3.2×10^{15} $n/m^2 \cdot s$. This maximum poisoning value occurs because the iodine decays at a faster rate than the xenon, following reactor shuntdown. When the two decay rates are the same, the poisoning is a maximum. The maximum shutdown xenon-135-poisoning values, $\theta_{Xe,S,max}$, in a high-flux thermal reactor is normally reached 10 to 12 h

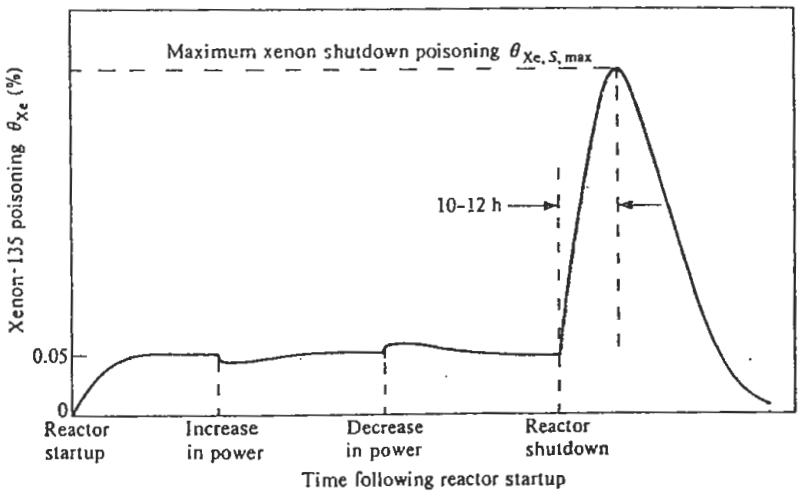


FIGURE 5.24
The operating xenon-135 poisoning in a high-flux reactor fueled with U-235.

TABLE 5.7
Maximum xenon-poisoning values in a uranium-235-fueled thermal reactor following shutdown

Average thermal-neutron flux Φ_{th}	Time following shutdown for maximum xenon poisoning, h	Maximum shutdown xenon poisoning, $\theta_{Xe,S,max}$
5×10^{15}	0.30	0.00378
10^{16}	0.98	0.00751
5×10^{16}	4.39	0.0255
10^{17}	6.40	0.0420
5×10^{17}	9.82	0.1512
10^{18}	10.88	0.2830
5×10^{18}	11.11	1.334
10^{19}	11.20	2.884
∞	11.28	∞

following reactor shutdown. The maximum xenon-135 shutdown poisoning values are tabulated in Table 5.7 as a function of the thermal-neutron flux.

The maximum xenon shutdown poisoning can sometimes be a major problem in the operation of a high-flux reactor. Consider the xenon poisoning shown in Fig. 5.25, for a reactor with an average thermal-neutron flux of 10^{18} n/m$^2 \cdot$ s. If the reactor control system has a maximum reactivity worth of 15 percent, the reactor may be started until the maximum xenon poisoning reaches 15 percent. After this time, the xenon poisoning prevents startup of the reactor even though all the control rods are withdrawn from the core. This condition continues until

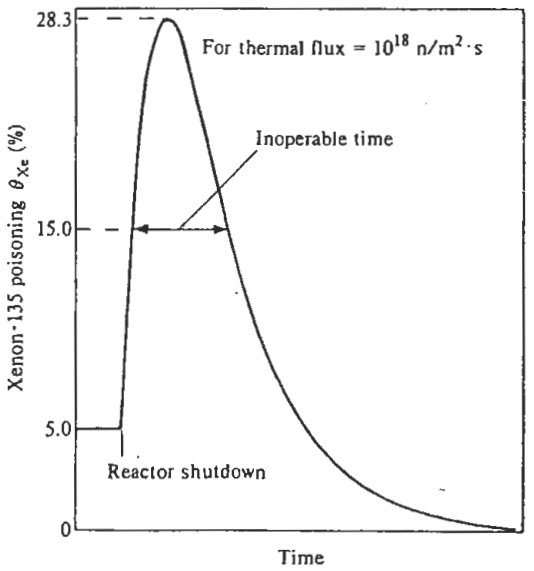


FIGURE 5.25
The shutdown xenon-135 poisoning in a high-flux, thermal reactor fueled with U-235.

the xenon poisoning has decayed to 15 percent, at which time the reactor can be restarted. This means there is some time interval during which the zero-power reactor cannot be operated. While this condition may not be too bad for many systems, it may be intolerable for a nuclear-powered submarine sitting on the ocean floor.

Another xenon operational problem encountered in some large, high-powered reactors is called the *xenon instability*. This problem is caused by the increased production of xenon in the region of the reactor core where the power density is the highest. As the xenon builds up in that region, it poisons that part of the core, reducing the thermal-neutron flux and the power generation in that volume. As a result, the location of the maximum power in the core of these systems tends to move around because of the xenon instability.

The other fission product that is important in the operation of thermal reactors is samarium-149. This isotope is a secondary fission product that appears at the end of the fission-product decay chain because it is stable. Samarium-149 has a microscopic neutron-absorption cross section of 66,000 barns for 0.0253-eV neutrons. The fission-product chain that produces this isotope is

$$\text{Fission} \downarrow \quad {}_{60}\text{Nd}^{149} \xrightarrow[1.7\text{ h}]{\beta^-} {}_{61}\text{Pm}^{149} \xrightarrow[47\text{ h}]{\beta^-} {}_{62}\text{Sm}^{149} \qquad \text{(Stable)}$$

As in the case of xenon-135, only the equilibrium operating values will be developed here. The rate equation for the primary fission-product isotope, neodynium-149, is

$$\frac{d(\text{Nd})}{dt} = \gamma_{\text{Nd}} N_{\text{fuel}} \bar{\sigma}_f \Phi_{\text{th}} - \lambda_{\text{Nd}}(\text{Nd}) - (\text{Nd})\bar{\sigma}_{a,\text{Nd}} \Phi_{\text{th}} \tag{5.95}$$

As was the case for the precursors in the xenon chain, the neutron burnup term in this equation is negligible compared to the radioactive decay-rate term and, at equilibrium, the fission production rate is equal to the decay rate. Thus, the equilibrium concentration of neodymium-149, is

$$(\text{Nd})_\infty = \frac{\gamma_{\text{Nd}} N_{\text{fuel}} \bar{\sigma}_f \Phi_{\text{th}}}{\lambda_{\text{Nd}}} \tag{5.96}$$

The rate equation for promethium-149, the first secondary product in the decay chain, is

$$\frac{d(\text{Pm})}{dt} = \lambda_{\text{Nd}}(\text{Nd}) - \lambda_{\text{Pm}}(\text{Pm}) - (\text{Pm})\bar{\sigma}_{a,\text{Pm}} \Phi_{\text{th}} \tag{5.97}$$

Again, neglecting the neutron-burnup term, the above equation gives the equilibrium concentration of promethium-149, as follows:

$$(\text{Pm})_\infty = \frac{(\text{Nd})_\infty \lambda_{\text{Nd}}}{\lambda_{\text{Pm}}} = \frac{\gamma_{\text{Nd}} N_{\text{fuel}} \bar{\sigma}_f \Phi_{\text{th}}}{\lambda_{\text{Pm}}} \tag{5.98}$$

The rate equation for samarium-149 is

$$\frac{d(\mathrm{Sm})}{dt} = \gamma_{\mathrm{Pm}}(\mathrm{Pm}) - (\mathrm{Sm})\bar{\sigma}_{a,\mathrm{Sm}}\Phi_{\mathrm{th}} \tag{5.99}$$

In this equation, the burnup term cannot be neglected because it is the only way that samarium is lost. The equilibrium samarium-149 concentration, $d(\mathrm{Sm})/dt = 0$, in the reactor core is

$$(\mathrm{Sm})_{\infty} = \frac{\gamma_{\mathrm{Nd}} N_{\mathrm{fuel}} \sigma_f}{\sigma_{a,\mathrm{Sm}}} \tag{5.100}$$

It will be noted in Eq. (5.100) that the number of samarium atoms in the core is independent of the thermal-neutron flux. The equilibrium samarium-poisoning value is found to be equal to

$$\theta_{\mathrm{Sm},\infty} = \frac{\bar{\Sigma}_{a,\mathrm{Sm}}}{\bar{\Sigma}_{a,\mathrm{fuel}}} = \gamma_{\mathrm{Nd}}\left(\frac{\sigma_f}{\sigma_a}\right)_{\mathrm{fuel}} \tag{5.101}$$

For uranium-235, γ_{Nd} is 0.014, $\sigma_a = 683$ barns, and $\sigma_f = 582$ barns, which gives an equilibrium poisoning of 0.012 or about 2 dollars of reactivity. While the equilibrium samarium poisoning is independent of the neutron flux and hence is the same in all reactors, it takes a long time to reach the equilibrium poisoning value in a low-powered reactor.

The poisoning due to samarium-149 actually becomes more important following shutdown of the reactor because it is stable. Following shutdown, all the neodymium-149 and the promethium-149 atoms in the reactor core decay to samarium-149. Consequently, the samarium poisoning does not go through a maximum and then to zero like the xenon poisoning but, instead, it builds up to some asymptotic value. The maximum samarium poisoning is a function of the neutron flux because the equilibrium concentrations of neodymium-149 and promethium-149 are directly proportional to the average thermal flux in the core. For a uranium-235-fueled reactor, the maximum shutdown value of samarium poisoning is

$$\theta_{\mathrm{Sm},S,\mathrm{U}\text{-}235} = 0.012 + 2 \times 10^{-20}\Phi_{\mathrm{th}} \tag{5.102}$$

One high-flux research or production reactor (the high-intensity flux reactor, HIFR, at Oak Ridge) normally operated for a 2-week period before refueling. If this system experienced an unscheduled shutdown partway through the run, it had to be restarted within 20 min or the xenon poisoning prevented startup. By the time the xenon had decayed to tolerable levels, the samarium poisoning had increased to the point where it prevented startup of the reactor. In order to restart this system, a portion of the core had to be refueled.

5.4.4 Fuel Requirements for a Nuclear Reactor

Almost all nuclear reactors must be initially loaded with more fuel than the actual critical mass to compensate for fuel burnup, for the effect of reactivity coefficients,

and for fission-product poisoning. In the case of fuel burnup, the mass of fuel needed to compensate for neutron burnup can usually be estimated from the reactor power and the operating time. In the case of the reactivity coefficients and the fission-product poisoning, the change in reactivity can normally be estimated from the various relationships developed earlier.

The amount of fuel that must be added to a reactor to compensate for neutron burnup depends on the kinetic energy of the neutrons causing fission, the type of fuel used, the operating period of the reactor, the average power of the reactor, and the conversion or breeding ratio of the reactor. Approximately 1 g of any of the three fissionable isotopes, completely fissioned, produces 1 MW · day of thermal energy. Actually it takes more than 1 g to produce this much energy because some of the fuel is destroyed in the radiative-capture and other nonfission neutron absorption reactions.

The mass of fuel, in grams, consumed during the operation of a reactor depends on the average thermal power of the reactor, P_{ave}, in megawatts, over the operating period of t_{op} days. The burnup mass, m_{bu}, in grams, is

$$m_{bu} = K_2 P_{ave} t_{op} \tag{5.103}$$

The constant, K_2, is a function of the type of fuel used and the average kinetic energy of the neutrons causing fission. The values of K_2 are listed in Table 5.8.

In a reactor loaded with fully enriched fuel, Eq. (5.103) can be used to evaluate the fuel-burnup requirements for the reactor. However, if the core contains any fertile material at all, some new fuel atoms will be generated and burned as the reactor operates and this reduces the required burnup mass. It is possible to use a simplified approach to estimate the fuel requirements for a uranium-235-fueled reactor. This method assumes that the average reactor power P_{ave}, the average thermal-neutron flux Φ_{th}, and the conversion ratio of the reactor, r, are all constant during reactor operation. Solving the fuel-burnup differential equation yields the data presented in Fig. 5.26. Using this method for a uranium-235-fueled reactor operating for a total of t_{op} days, the amount of uranium-235 that must be added to the core to compensate for neutron burnup m_{bu} can be obtained from the following equation:

$$m_{bu} = P_{ave}(1.23 t_{op} - rS) \tag{5.104}$$

where S is the value obtained from the graph in Fig. 5.26.

TABLE 5.8
Values of K_2

Fissionable isotope	Thermal reactors	Fast reactors
U-233	1.14	1.05
U-235	1.23	1.11
Pu-239	1.49	1.10

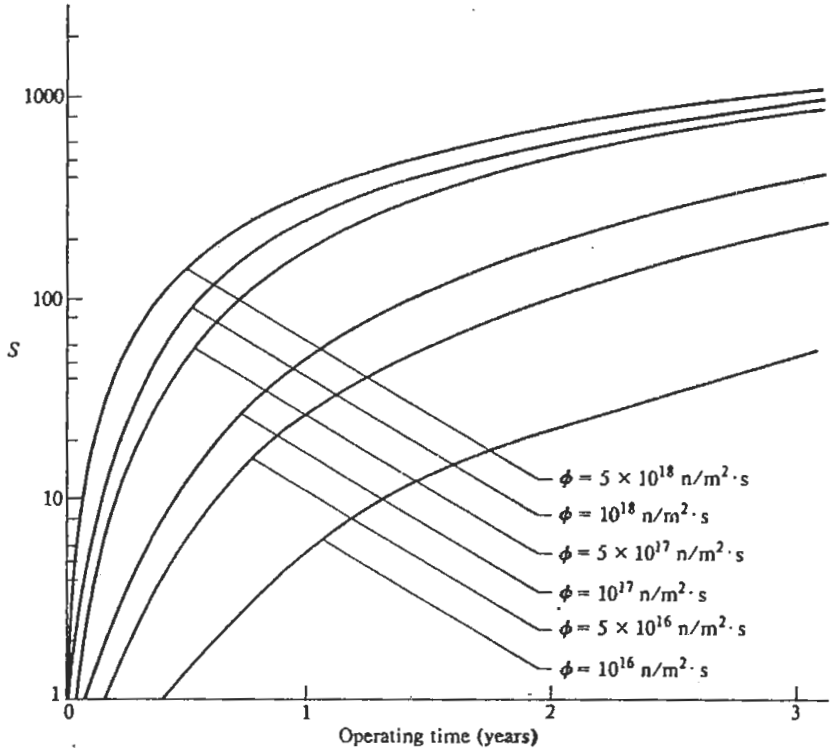


FIGURE 5.26
Fuel-burnup parameters for a thermal converter reactor fueled with U-235.

The increase in the reactivity of a reactor caused by the addition of the fuel needed for burnup is evaluated by adding this burnup mass to the critical mass of the reactor and then calculating the value of the multiplication factor k from the critical equation. For the same burnup mass, the increase in reactivity caused by the addition of the extra burnup mass is larger for reactors with small critical masses than for those that have high critical masses (like fast reactors).

Additional fuel must be initially loaded into the reactor to overcome the effect of the reactivity coefficients in going from the ambient condition to the operating condition. If all the reactivity coefficients are negative, the system reactivity decreases as the reactor is brought to power. This means that the cold reactor will have a higher reactivity than the hot reactor.

Unlike the burnup mass calculations, the amount of extra fuel that must be added to a cold reactor to compensate for the reactivity coefficients cannot be explicitly evaluated. Instead, the decrease in system reactivity can be evaluated and the mass of fuel needed to compensate for these coefficients must be determined from the criticality equation.

If the average power coefficient of reactivity, $\bar{\alpha}_P$, is known for a particular reactor, the excess reactivity $\Delta\rho_{pc}$ needed to overcome the power coefficient of reactivity is

$$\Delta\rho_{pc} = \bar{\alpha}_P P_{op} \tag{5.105}$$

where P_{op} is the operating power of the reactor. In a fluid-cooled reactor in which there is no phase change, the power coefficient of reactivity is closely related to the temperature coefficient of reactivity. Thus, the change in reactivity, $\Delta\rho_{tc}$, caused by the temperature increase is equal to the product of the average temperature coefficient $\bar{\alpha}_T$ and the temperature rise (usually the rise in coolant temperature), or

$$\Delta\rho_{tc} = \rho_{hot} - \rho_{cold} = \bar{\alpha}_T(T_{op} - T_{amb}) \tag{5.106}$$

where T_{op} is the operating temperature of the coolant and T_{amb} is the ambient temperature.

If there is any boiling in the reactor core, there will be an additional decrease in system reactivity if the void coefficient of reactivity, α_V, is negative. The change in reactivity due to the vapor bubbles is equal to the product of the average void coefficient α_V and the percentage of "voids" in the core:

$$\Delta\rho_{vc} = \bar{\alpha}_V(\text{percent voids}) \tag{5.107}$$

The total change in reactivity of a BWR system due to the reactivity coefficients is

$$\Delta\rho_{rc} = \rho_{op} - \rho_{amb} = \bar{\alpha}_T(T_{sat} - T_{amb}) + \bar{\alpha}_V(\text{percent voids}) \tag{5.108}$$

If the operating value of reactivity, ρ_{op}, is zero, the cold or ambient reactivity ρ_{amb} must be

$$\rho_{amb} = -\bar{\alpha}_T(T_{sat} - T_{amb}) - \bar{\alpha}_V(\text{percent voids}) \tag{5.109}$$

In addition to fuel-burnup and reactivity coefficients, extra fuel must be added to a critical reactor to compensate for the decrease in reactivity caused by the buildup of fission products. Fission products "poison" all reactors but they are particularly important in the operation of high-flux thermal systems because of the xenon-135 and samarium-149 fission products. As discussed earlier, the decrease in reactivity in going from the "clean" reactor with no fission products to the "dirty" system is approximately equal to the value of the fission-product poisoning. In high-powered thermal reactors in which the flux exceeds 10^{19} n/m$^2 \cdot$ s, the decrease in reactivity is approximately equal to

$$\Delta\rho_{fp} = (\rho_{dirty} - \rho_{clean})_{max} = -\theta_{Xe,\infty} - \theta_{Sm,\infty} = -0.053 - 0.012 = -0.065 \tag{5.110}$$

This means that the clean multiplication factor must be greater than 1.069 to compensate for the buildup of these products. If the average thermal flux in the core is less than 10^{19} n/m$^2 \cdot$ s, the xenon-135 poisoning will be less than 5.3 percent and should be calculated from Eq. (5.93). Again, it should be stressed that the numerical values in the previous equations are applicable only for uranium-235-fueled thermal reactors.

Some nuclear reactors, particularly military systems and other systems where continuity of operation is important, must have the capability of being started at any time. This means that the reactor must have enough excess reactivity that it can override the buildup of fission-product poisoning following reactor shutdown. If the reactor is a high-flux system, this means that the reactor must have a lot of excess reactivity to override the buildup of xenon and samarium.

The maximum excess reactivity for most reactor systems occurs for the cold, clean reactor if all the reactivity coefficients are negative. At the end of the reactor operating period, the system reactivity should be equal to zero or equal to the reactivity for fission-product override if this quantity is included in the design of the reactor system. This means that the reactivity of the cold, clean reactor, is

$$\rho_{\text{cold,clean}} = \Delta\rho_{\text{burnup}} + \Delta\rho_{\text{void}} + \Delta\rho_{\text{steady-state fp}} + \Delta\rho_{\text{fp override}} + \Delta\rho_{\text{temp}} \quad (5.111)$$

For a high-flux thermal reactor, Eq. (5.111) becomes

$$\rho_{\text{cold,clean}} = \Delta\rho_{\text{burnup}} - \bar{\alpha}_T \Delta T - \bar{\alpha}_V(\text{percent voids}) + 0.65 + \Delta\rho_{\text{fp override}} \quad (5.112)$$

Since $k = 1/(1-\rho)$, the cold, clean value of reactivity can be used to evaluate the cold, clean multiplication factor. Once this value is known, the criticality relationships can be used to estimate the required fuel loading for the reactor.

The reactor control system must be able to handle all the excess reactivity with a significant margin of safety. Some reactors control the excess reactivity with a large number of control rods. At the beginning of reactor operation, almost all of the rods are partially inserted into the core and then withdrawn as the reactor is operated and the reactivity decreases. These rods can be programmed to shape the power distribution in the reactor core to improve the maximum-to-average power ratio. When all the rods have been withdrawn and the reactor power starts to drop, it is time to refuel the core.

Some reactors, particularly PWRs, employ a "burnable poison" to reduce the reactivity requirement of the control system. In a high-powered reactor system, most of the excess fuel is used to overcome the problem of fuel burnup. Theoretically, the burnable poison is supposed to compensate for the decrease in reactivity caused by the depletion of the fuel. Boron is commonly used as the burnable poison and may be incorporated in either the fuel element or in the reactor coolant. Some PWR systems employ a boric-acid solution in the water coolant.

Unfortunately, boron has a slightly higher absorption cross section than the uranium-235 fuel so that it burns at a faster rate than the fuel. This means that the overall reactivity of the system initially rises until the two burnout rates are the same and then the reactivity drops. The maximum system reactivity that must be handled by the control system with a solid burnable poison commonly occurs near the midlife of the reactor system.

Example 5.5. A 3800-MW_{th} BWR operates with a critical mass of 3 tons of U-235 and a conversion ratio of 0.8. The average core temperature of the coolant (the saturation temperature of the water) is 340°C and the average in-core steam fraction

is 20 percent. This system is designed to be completely refueled at 18-month intervals while operating at an average capacity factor of 80 percent. The system has an average temperature coefficient of $+3\times10^{-6}\,\Delta\rho/°\text{Celsius}$ and an average void coefficient of $-3\times10^{-4}\,\Delta\rho/\text{void percent}$. Assuming that the multiplication factor of the reactor is equal to the cube root of the ratio of the actual fuel mass to the critical fuel mass, find the initial U-235 loading, the value of the cold-clean and maximum reactivities, and the multiplication factors. Also, find the maximum reactivity worth of the control system if it must have the capability of reducing the system multiplication factor to 0.95 at any point during operation of the reactor. Assume that no provision is made for overriding the fission-product poisons.

Solution. Average fission cross section is

$$\bar{\sigma}_f = \frac{584[293/(273+340)]^{1/2}}{1.128}$$
$$= 357.9 \text{ barns}$$

Number of fuel atoms in the critical mass is

$$N_{\text{fuel,c}} = \frac{3(2000)(0.4536)(0.6022\times10^{27})}{235} = 6.974\times10^{27} \text{ atoms}$$

Maximum neutron flux (based on the critical mass) is

$$\Phi_{\text{th,max}} = \frac{3.1\times10^{16}\,P_{\text{th,max}}}{\bar{\sigma}_f N_{\text{fuel,c}}}$$
$$= \frac{3.1\times10^{16}(3800)}{(357.9\times10^{-28})(6.974\times10^{27})}$$
$$= 4.719\times10^{17}\ \text{n/m}^2\cdot\text{s}$$

Average neutron flux over the operating period is

$$\Phi_{\text{th,ave}} = 0.8(4.719\times10^{17}) = 3.776\times10^{17}\ \text{n/m}^2\cdot\text{s}$$

(Use this value for the burnup calculations, but use the maximum value for the xenon poisoning.)

Fuel burnup calculations:

$$P_{\text{ave}} = 0.8\,P_{\text{max}} = 0.8(3800) = 3040\ \text{MW}_{\text{th}}$$
$$t_{\text{op}} = 365.25(1.5) = 547.9 \text{ days}$$
$$r = 0.8$$

S (from Fig. 5.25) = 290. Thus

$$m_{\text{bu}} = P_{\text{ave}}(1.23t_{\text{op}} - rS) = 3040[1.23(547.9) - 0.8(290)]$$
$$= 1.343\times10^{6}\ \text{g} = 1.481 \text{ tons U-235}$$
$$k_{\text{bu}} = \left(\frac{m_{\text{hu}}+m_c}{m_c}\right)^{1/3} = \left(\frac{1.481+3}{3}\right)^{1/3} = 1.1431$$
$$\rho_{\text{burnup}} = \frac{k_{\text{bu}}-1}{k_{\text{bu}}} = \frac{1.143-1}{1.143} = 0.1252$$

Reactivity compensation for the temperature coefficient is

$$\Delta\rho_{tc} = \rho_{hot} - \rho_{cold} = \bar{\alpha}_T(T_{op} - T_{amb}) = 3\times10^{-6}(340-20) = 0.00096$$

This is positive because the reactor is "overmoderated" and the water acts as a poison. Water expansion removes some of the water (poison) and improves the system reactivity.

Reactivity compensation for fission-product poisoning is

$$\Delta\rho_{fp} = \rho_{clean} - \rho_{dirty} = \theta_{Sm,\infty} + \theta_{Xe,\infty}$$

$$= 0.012 + \frac{1.7\times10^{-23}\Phi_{max}}{3.2\times10^{-22}\Phi + 2.1\times10^{-5}}$$

$$= 0.012 + \frac{(1.7)(4.719\times10^{17})}{32(4.719\times10^{17}) + 2.1\times10^{18}}$$

$$= 0.012 + 0.04666 = 0.05866$$

Reactivity compensation for the void coefficient is

$$\Delta\rho_{vc} = \bar{\alpha}_V(\text{percent voids}) = -3\times10^{-4}(20) = -0.006$$

Reactivity for the cold, clean reactor is

$$\rho_{c,c} = \rho_{burnup} + \Delta\rho_{fp} - \bar{\alpha}_T\Delta T - \alpha_V(\text{percent voids})$$

$$= 0.1252 + 0.05866 - 0.00096 + 0.006$$

$$= 0.18890$$

Reactivity for the hot, clean reactor is

$$\rho_{h,c} = \rho_{c,c} + \Delta\rho_{tc}$$

$$= 0.18890 + 0.00096 = 0.18986$$

$$\text{Reactivity of the hot, clean reactor with voids} = 0.18986 - 0.006$$

$$= 0.18386$$

The maximum reactivity and multiplication factors are the values for the hot, clean reactor with no voids is

$$\rho_{max} = \rho_{hot,clean} = 0.18986$$

$$k_{max} = \frac{1}{1-\rho_{h,c}} = 1.23435$$

$$\text{Total fuel loading} = (\text{critical mass})(k_{max})^3 = 3(1.23435)^3$$

$$= 5.642 \text{ tons U-235}$$

$$\text{Shutdown reactivity margin} = \frac{k-1}{k} = \frac{(0.95-1)}{0.95} = -0.0526$$

$$\text{Required worth of control system} = \rho_{max} + 0.0526$$

$$\text{Required worth of control system} = 0.18986 + 0.0526 = 0.24246$$

LIST OF SYMBOLS

a	Slab reactor thickness or half-thickness of fuel in plate-type fuel element, m
a	Outer fuel pellet radius and inner cladding radius, m
a_h	Thickness of slab-reactor core, m
a_0	Extrapolated core thickness for slab reactor, m
A	Surface area, m^2
A_0	Spherical reactor flux constant, m
b	Outer radius of cladding tube or half-thickness of flat-plate fuel element, m
B	Reactor buckling, m^{-2}
c_p	Specific heat at constant pressure, $J/kg \cdot C°$
C_i	Geometrical heat transfer constants, $m \cdot C°/W$
d	Extrapolation distance, m
f	Thermal utilization factor
h	Heat-transfer coefficient or surface conductance, $W/m^2 \cdot C°$
h_a	Thermal conductance across the fuel-clad interface, $W/m^2 \cdot C°$
h_b	Thermal conductance across coolant film, $W/m^2 \cdot C°$
Ih	Unit of reactivity, in in-hours
J_0	Zeroth-order Bessel function of the first kind
k	Multiplication factor
k	Thermal conductivity, $W/m \cdot C°$
k_c	Thermal conductivity of cladding material, $W/m \cdot C°$
k_f	Thermal conductivity of fuel material, $W/m \cdot C°$
K_1	Constant for critical equation
K_2	Constant for burnup calclations
l	Neutron lifetime, s
l_p	Prompt neutron lifetime, s
l_{pr}	Neutron production time, s
l_s	Neutron slowing-down time, s
l_{th}	Thermal-neutron diffusion time, s
L	Core length, m
L	Thermal diffusion length, m
$\dot{m}$	Mass flow rate, kg/h
n	Neutron density, n/m^3
N	Total number of atoms
N_{fuel}	Total number of fuel atoms
p	Resonance escape probability
P	Power, W or MW
P_{ave}	Average thermal power, W or MW
P_0	Initial power (@ $t=0$), W or MW
P_{max}	Maximum thermal power, W or MW
q	Heat-transfer rate, W
q'	Volumetric heat generation rate, W/m^3

q'_{max}	Maximum volumetric heat generation rate, W/m^3
r	Conversion ratio
r	Radius, m
r_0	Extrapolated core radius, m
S	Burnup factor (from Fig. 5.27)
t	Time, s
t_r	Reactor period, s
$t_{1/2}$	Half-life of a radioisotope, s
T	Temperature, K or °C
T_a	Minimum fuel temperature at a given axial position, K or °C
T_b	Maximum fuel temperature at a given axial position, K or °C
T_0	Maximum fuel temperature at a given axial position, K or °C
T_∞	Bulk coolant temperature, K or °C
V	Volume, m^3
x	Variable in slab-reactor geometry or axial position in cylindrical reactor, m
$x_{max,TI}$	Axial position of maximum temperature in a cylindrical reactor, m
α	Thermal diffusivity, s/m^2
α_P	Power coefficient of reactivity, 1/W
α_T	Temperature coefficient of reactivity, $1/C^\circ$
α_V	Void coefficient of reactivity, 1/(percent voids)
β	Total delayed-neutron fraction
β_i	Delayed-neutron fraction of the ith group of delayed neutrons
γ	Fission yield constant
∂	Partial derivative
δ	Poisoning, $\Sigma_{a,other}/\Sigma_{a,fuel}$
ε	Fast fission factor
η	Average number of neutrons produced per neutron absorbed by the fuel
θ	Angle used in cylindrical and spherical geometry
θ	Fission-product poisoning
λ	Radioactive-decay constant, 1/s
ρ	Density, kg/m^3
ρ	System reactivity
$\Delta\rho_{fp}$	Change in reactivity due to fission-product poisoning
$\Delta\rho_{pc}$	Change in reactivity due to power coefficient, 1/W
$\Delta\rho_{tc}$	Change in reactivity due to temperature coefficient, $1/C^\circ$
$\Delta\rho_{vc}$	Change in reactivity due to void coefficient, 1/(percent voids)
σ_a	Microscopic absorption neutron cross section, m^2 or barns
σ_F	Microscopic fission cross section, m^2 or barns
Σ_a	Macroscopic absorption neutron cross section, 1/m
τ	Fermi age, m^2
ϕ	Local neutron flux, $n/m^2 \cdot s$
ϕ_{max}	Maximum neutron flux, $n/m^2 \cdot s$
Φ	Average neutron flux, $n/m^2 \cdot s$
χ	Extrapolated core length $= L+2d$

ψ Angle used in spherical geometry
∇^2 Lapacian operator

PROBLEMS

5.1. A bare, cubical reactor [1.0; 1.2; 1.4; 1.6; 1.8] m on a side, has neutron flux at the center of any outside face which is [0.15; 0.20; 0.25; 0.30; 0.35] times the flux at the center of the core. Find the maximum-to-average power ratio in the reactor core and determine the extrapolation distance for the reactor.

5.2. A bare, spherical homogeneous reactor has a core with a diameter of [50; 100; 150; 200; 250] cm and operates at a thermal power of 2 MW. If the power at the edge of the sphere is [12; 14; 16; 18; 20] percent of the maximum power, find the maximum power density, in W/cm^3, in the reactor.

5.3. A bare, spherical reactor has a core diameter of [2.0; 3.0; 4.0; 5.0; 6.0] m and operates at a thermal power of 1000 MW. If the power density at the edge of the core is [8; 12; 16; 20; 24] percent of the value of the maximum power density, determine the value of the maximum power density, in W/cm^3, and the extrapolation distance for the system.

5.4. A bare, spherical, homogeneous thermal reactor has a core with a diameter of 2 m. The reactor operates at a thermal power of 300 MW with an average moderator temperature of [240; 260; 300; 340; 380]°C. If the maximum thermal-neutron flux is $[5; 6; 7; 8; 9] \times 10^{18}$ $n/m^2 \cdot s$ and the flux at the core boundary is 1.8×10^{18} $n/m^2 \cdot s$, find the mass of U-233 needed to fuel the reactor, the maximum and average power densities, in W/cm^3, and the average specific power, in kW/kg of fuel.

5.5. Repeat Prob. 5.4. except assume that the reactor is fueled with [Pu-239; U-235] fuel.

5.6. A reactor fuel plate is fabricated with 1.5 mm of (8; 10; 12; 14; 16] percent UO_2 by weight, and the balance an aluminum alloy as fuel with 0.4 mm of aluminum cladding on each side. Assume that the conductivity of the fuel and the aluminum are 173 and 208 $W/m \cdot C°$, respectively, and the densities are 3.3 and 2.7 g/cm^3. The uranium is 20 percent enriched and the peak thermal-neutron flux is $[1.0; 2.0; 3.0; 4.0; 5.0] \times 10^{18}$ $n/m^2 \cdot s$. The surface conductance at the outer surface of the plate is 4300 $W/m^2 \cdot C°$ and the coolant temperature is 180°C. Determine the peak heat flux at the surface of the element and also find the temperature at the center of the fuel plate, plus the temperature at the plate surface for the same location.

5.7. A BWR fuel rod is filled with UO_2 ($k = 1.8$ $W/m \cdot C°$) pellets that have a diameter of [8.5; 9.0; 9.5; 10.0; 10.5] mm and a cladding thickness of 0.5 mm of zirconium alloy ($k = 24.2$ $W/m \cdot C°$). The surface conductance between the surface of the fuel pellet and the internal surface of the cladding tube is $[5.3; 5.5; 5.7; 5.9; 6.1] \times 10^3$ $W/m^2 \cdot C°$. The outside film conductance is 12,000 $W/m^2 \cdot C°$ and the boiling water has a temperature of 340°C. If the maximum allowable fuel temperature is 2500°C, find the maximum power output of the rod, in kilowatts per foot, and the maximum heat flux at the surface of the rod, in W/m^2.

5.8. A plate-type fuel element is composed of a 1-mm layer of a UO_2 dispersion in an aluminum matrix, which is clad on each side with a 0.5-mm layer of aluminum. The fuel dispersion contains [21; 23; 25; 27; 29] percent UO_2, by weight, and the uranium is enriched to a level of 98 percent. The thermal conductivities of both the fuel and cladding may be assumed to be 204 $W/m \cdot C°$. The density of pure UO_2 is

about 10 g/cm^3 while that of the aluminum is 2.7 g/cm^3. The thermal-neutron flux in the fuel region is [0.8; 1.0; 1.2; 1.4; 1.6] $\times 10^{18}$ n/m$^2 \cdot$ s. The plate is cooled on both sides with water at 38°C and the convective film coefficient is 40,000 W/m$^2 \cdot$ C°. Calculate the maximum fuel and cladding temperatures and determine the surface temperature of the cladding.

5.9. A BWR core contains 560 fuel elements and operates at a thermal power of [2000; 2400; 2800; 3200; 3600] MW_{th}. Each element consists of an 8×8 array of fuel rods and the maximum-to-average power ratio in the core is [2.2; 2.3; 2.4; 2.5; 2.6]. The UO_2 fuel pellets ($k = 2$ W/m $\cdot$ C°) have an OD of 10.8 mm and an active length of 3.66 m. The cladding is 1 mm of zircaloy-2 ($k = 14.7$ W/m $\cdot$ C°). The surface-conductance between the fuel pellet and cladding is 4000 W/m$^2 \cdot$ C°, the boiling heat transfer coefficient is 80,000 W/m$^2 \cdot$ C°, and the saturation temperature of the water is 360°C. Estimate the maximum heat flux at the cladding surface and the maximum temperature in the core.

5.10. A [2.0; 2.5; 3.0; 3.5; 4.0] percent enriched uranium fuel rod is 19.1 mm in diameter and is clad with 0.76 mm of aluminum. Assume that the thermal conductivities of the fuel and cladding materials are 29.4 and 200 W/m $\cdot$ C°, respectively. If the fuel element is cooled with air at 90°C and the average convective heat-transfer coefficient is 115 W/m$^2 \cdot$ C°, find the maximum neutron flux that can be tolerated when the maximum fuel temperature is limited to [375; 400; 425; 450; 475]°C. Assume that the density of the uranium is 18.7 g/cm^3, that the temperature of the graphite moderator is 200°C, and that the neutron flux is constant throughout the fuel material.

5.11. If the axial maximum-to-average power distribution for the system of problem 5.10 is 1.35 and the coolant air enters the reactor at 0°C and leaves at 180°C, determine the maximum cladding and surface temperatures. Use q' from Prob. 5.10, and take the length of the fuel channel to be 8 m.

5.12. A fuel rod of UO_2 ($k = 2$ W/m $\cdot$ C°) has a diameter of 9.5 mm and is clad with 0.4 mm of 304 stainless steel ($k = 15.6$ W/m $\cdot$ C°). The surface conductance between the surface of the fuel pellet and the internal surface of the cladding is [2000; 3000; 4000; 5000; 6000] W/m$^2 \cdot$ C°. The rod is to develop 20 kW_{th}/m at the point under consideration. The outside film coefficient is [7000; 9000; 11,000; 13,000; 15,000] W/m$^2 \cdot$ C° and the boiling water has a temperature of 340°C. Calculate the temperature at the center of the rod and determine the heat flux at the surface of the cladding.

5.13. Determine the relative energy of a [0.5; 0.7; 0.9; 1.1; 1.2]-eV neutron if it collides with a Pu-239 nucleus which is moving toward the neutron at the most probable velocity corresponding to a temperature of [1500; 2000; 2500; 3000; 3500]°C at the instant of collision.

5.14. Repeat Prob. 5.13 except assume that the nucleus is moving away from the Pu nucleus at the instant of collision.

5.15. Estimate the percentage increase in reactivity, in cents, and reactivity, in Ih, that will result in a stable reactor period of [2.5; 5.0; 7.5; 10.0; 12.5; 15] min in reactors fueled by the [U-233; U-235; Pu-239] fuel isotope.

5.16. Considering only the stable reactor period due to the longest delayed-neutron group, estimate the minimum time required to reduce the reactor power so that the average-neutron flux drops from [8; 7; 6; 5; 4] $\times 10^{18}$ to [9; 7; 5; 3; 1] $\times 10^6$ n/m$^2 \cdot$ s.

5.17. Using the data in Table 5.5, find the stable reactor period and the percent increase in reactivity and cents of reactivity that result from an insertion of [15; 20; 25; 30; 35; 40] Ih of reactivity into a critical reactor fueled with [U-233; U-235; Pu-239].

5.18. What is the reactivity, in cents and Ih, of a carbon-moderated [U-233; U-235; Pu-239]-fueled reactor that will produce a stable reactor period of [2; 4; 6; 8; 10; 12] min.

5.19. If [5; 10; 15; 20; 25; 30] cents of reactivity are inserted into a critical reactor which is fueled with [U-233; U-235; Pu-239], find the stable reactor period and the reactivity insertion in percentages and in Ih.

5.20. Due to meteorite damage, it is found that the automatic control system of a nuclear reactor on board a spacecraft is inoperable and during a time of 15 min a constant value of reactivity of $-[1; 3; 5; 7; 9] \times 10^{-5}$ has existed. The astronauts are instructed to manually restore the power level to that prior to the malfunction. If the power is to be restored within [5; 7; 9; 11; 13] min, find the amount of excess reactivity required. Assume that the reactor is fueled with U-235, and find the percentage drop in power while the malfunction was in effect.

5.21. A high-flux research reactor is fueled with fully enriched U-235 and has an operational cycle such that it operates at a power of [160; 170; 180; 190; 200] MW_{th} for a 1-week period before refueling. At the time of shutdown, the reactor has an average thermal neutron flux of 10^{19} n/m$^2 \cdot$ s and the average temperature coefficient of reactivity is $-[2.0; 2.5; 3.0; 3.5; 4.0] \times 10^{-5}\ \Delta\rho/C°$. If the reactor operates at a maximum temperature of 190°C, estimate the mass of fuel left in the reactor when it is shut down for refueling. Find the cold, clean value of multiplication factor, the total excess reactivity that must be contained by the control system, and the initial fuel loading in the reactor if the multiplication factor is approximately equal to the cube root of the ratio of the actual fuel mass divided by the critical mass.

5.22. A 1000-MW_e BWR has an overall thermal efficiency of [30; 31; 32; 33; 35] percent and a critical mass of 100 ton of 2.2 percent-enriched UO_2. The system has an average temperature coefficient of reactivity of $-10^{-6}\ \Delta\rho/C°$ and an average void coefficient of reactivity of $-[5; 7; 9; 11; 13] \times 10^{-5}\ \Delta\rho$/percent voids. The plant is designed to operate at a pressure of 10 MPa with a nominal steam fraction in the core of 15 percent. The average conversion ratio is 0.8, and the system is designed to operate for a period of 18 months with a capacity factor of 70 percent before refueling. If the multiplication factor k is approximately equal to the cube root of the ratio of the actual fuel loading to the critical mass, find: (a) the maximum system reactivity that must be controlled, (b) the total UO_2 loading for the system, (c) the initial average thermal-neutron flux in the reactor core, and (d) the average thermal-neutron flux at the end of 18 months. Base the fission-product poisoning on the flux obtained by using the critical mass.

5.23. An 800-MW_e boiling-water reactor has a thermal efficiency of 32 percent and a critical mass of 90 tons of 2.4 percent-enriched UO_2, and is designed to operate at a capacity factor of [60; 65; 70; 75; 80] percent for 450 days before refueling. The system has an average temperature coefficient or reactivity of $-5.4 \times 10^{-6}\ \Delta\rho/C°$ and a void coefficient of reactivity of $-5 \times 10^{-4}\ \Delta\rho$/percent voids. The plant is designed to operate at a pressure of 6.8 MPa with a nominal steam fraction in the core of [15; 16; 17; 18; 19] percent and a conversion ratio of 0.75. Assuming that the multiplication factor is approximately equal to the cube root of the ratio of the

actual fuel loading to the critical mass, find: (*a*) the total loading of UO_2 required for this system, (*b*) the maximum system reactivity that must be controlled during startup, (*c*) the initial average thermal-neutron flux in the reactor, and, (*d*) the average thermal-neutron flux at the end of 450 days.

REFERENCES

Bevilacqua, F., and J. F. Gibbons: "System 80; Combustion Engineering's Standard 3800 MWT PWR," *Proceedings of the American Power Conference*, vol. 36, pp. 70–97, Illinois Institute of Technology, Chicago, 1974.

El-Wakil, M. M.: *Nuclear Heat Transport*, International Textbook Company, Scranton, Pa., 1971.

Foster, A. R., and R. L. Wright, Jr.: *Basic Nuclear Engineering*, 3d ed., Allyn and Bacon, Boston, 1977.

Geurts, J. R., D. R. Patterson, and E. P. Schlinger: "BWR Plant Standardization Utilizing GESSAR and STRIDE," *Proceedings of the American Power Conference*, vol. 36, pp. 107–116, Illinois Institute of Technology, Chicago, 1974.

Glasstone, S., and A. Sesonske: *Nuclear Reactor Engineering*, D. Van Nostrand Company, New York, 1963.

MacMillan, J. H., and T. O. Johnson: "Once Through Performance at 3800 MWT—The Babcock 241 Standardized Nuclear Steam System," *Proceedings of the American Power Conference*, vol. 36, pp. 98–106, Illinois Institute of Technology, Chicago, 1974.

Nuclear News, a publication of the American Nuclear Society, vol. 31, no. 10, August 1988.

Steam: Its Generation and Use, 38th ed., Babcock and Wilcox Company, New York, 1972.

"Superphoenix: A Full-scale Breeder Reactor," *Scientific American*, vol. 236, no. 3, pp. 26–35, March 1977.

Toth, G. P., and R. J. Nath: "Westinghouse 3817-MW NSSS," *Proceedings of the American Power Conference*, vol. 36, pp. 98–106, Illinois Institute of Technology, Chicago, 1974.

U.S. Atomic Energy Commission: *Reactor Physics Constants*, ANL publication 5800, 2d ed., Argonne National Laboratory, Chicago, July 1963.

Waage, J. M., et al.: "General Atomics 1500 MWe High Temperature Gas-Cooled Reactor," *Proceedings of the American Power Conference*, vol. 36, pp. 125–134, Illinois Institute of Technology, Chicago, 1974.

CHAPTER 6

ENVIRONMENTAL IMPACT OF POWER PLANT OPERATION

6.1 INTRODUCTION

The design, location, construction, and operation of electrical power generation facilities have been markedly affected by the concern for the environment. As was discussed earlier, the power engineer of today must have a sincere concern for the environment but must also be concerned with producing enough power to meet the public demand with as low a cost as possible. The power engineer must also be knowledgeable about the rules and laws governing power plant operation and keep in mind what the public will or will not accept. Meeting all five of these considerations, i.e., the "five P's" of energy conversion (power, pennies, pollution, politics, and prejudice), is one of the major problems facing modern society.

While ecology is very important, many of the self-proclaimed "environmentalists" are not true environmentalists but are simply antinuclear or even antipower advocates. These people fight the siting and construction of new power plants with long and costly litigation, producing serious delays and even cancellations of some plants. These same people are the first to complain about the brownouts, blackouts, and rate increases brought about by the delays.

During the late 1980s, concern arose about the "greenhouse effect." This effect is due primarily to the combustion of carbon in fossil fuels. The resulting carbon dioxide, when discharged to the atmosphere, lets the short-wavelength,

solar radiation through the atmosphere to be absorbed by the earth's surface. However, when the earth's surface reradiates long-wavelength radiation, the CO_2 absorbs this reradiated energy. This results in heating of the atmosphere with resulting climatic changes. In addition, it is estimated that an increase of 2 to 3F° (1 to 1.5C°) of the earth's atmospheric temperature will melt the south polar icecap. This will raise the average sea level about 9 m (30 ft), flooding most coastal cities. A large, coal-fired power plant will discharge approximately 6 to 8 million tons of CO_2 to the atmosphere each year. It is estimated that a worldwide total of about 18 billion tons of CO_2 are released to the atmosphere each year. At the present time, there are no legal limits on the amount of CO_2 that can be discharged to the atmosphere. Any legal limitations will probably preclude the use of fossil and biomass fuels as sources of fuel energy. If this happens, the human race will have to depend upon nuclear power, solar power (direct and indirect), geothermal energy, and possibly the combustion of hydrogen as energy sources. When one looks objectively at these alternatives, nuclear power would appear to be the best solution from the standpoint of safety, reliability, and cost. The approximate amounts of various pollutants generated by the common power sources are presented in Table 6.1.

Federal and state governments have passed environmental legislation that limits the amount of certain solid and gaseous pollutants that can be discharged to the atmosphere along with the amount of thermal energy that can be discharged to natural waters. Because of public pressure, some state governments have passed laws which make it unlawful to build a nuclear power plant—probably the safest and most environmentally acceptable method of producing large quantities of electrical energy.

TABLE 6.1
Typical generation of pollutants in a 1000-MW_e power system

	Coal	Oil	Nuclear
CO_2 generation rate, ton/year	7,800,000 (7,076,000 tonnes/y)	4,700,000 (4,264,000 tonnes/y)	0
SO_2 generation rate, ton/year	40,000 (36,000 tonnes/y)	91,000 (82,600 tonnes/y)	0
NO_x generation rate, ton/year	9,500 (8,620 tonnes/y)	6,500 (5,900 tonnes/y)	0
Radiation dose to population living in vicinity, mrem/h†	1	0	20
Solid-waste generation rate, ton/year	330,000 (ash) (299,400 tonnes/y) 6,000 (dust) (5,440 tonnes/y)	6,500 (dust) (5,900 tonnes/y)	0.9 (FP)‡ 30.0 (SF)‡ 9.1 (LLW)‡

† The average "background" radiation dose rate to the general public from the environment is 300 millirems/hour (mrem/h).

‡ Legend for nuclear solid wastes: FP = fission products, SF = spent fuel, and LWW = low-level waste (similar to that produced by hospitals and currently buried).

The federal government passed the Clean-Air Act of 1970, which set a number of standards limiting the amount of certain gaseous and particulate emissions that can be legally discharged from any new steam-generating units or any plant construction or modification started after August 17, 1971, that has a thermal input of more than 250 million Btu/h. The original standards were:

I. Particulate matter
   A. The maximum 2-h average permitted is 0.1 lbm of particulate matter per million Btu of input energy.
   B. The visible emissions from the stack shall not exceed 20 percent opacity, except for 2 min in any one hour, when emission may be as great as 40 percent opacity, as determined by the standard Ringlemann charts. These charts are simply lined plastic cards that the inspector holds up to the sky and compares to the effluent. Examples of these charts are given in Fig. 6.1.

II. Sulfur oxides (primarily sulfur dioxide)
   A. The maximum 2-h average for an oil-fired system is 0.8 lbm of SO_2 per million Btu of input thermal energy.
   B. The maximum 2-h average for a coal-fired system is 1.2 lbm of SO_2 per million Btu of input thermal energy.

III. Nitrogen oxides (nitric oxide and nitrogen dioxide)
   A. The maximum 2-h average for a gas-fired system is 0.20 lbm per million Btu of input thermal energy.
   B. The maximum 2-h average for an oil-fired system is 0.30 lbm per million Btu of input thermal energy.
   C. The maximum 2-h average for a coal-fired system is 0.70 lbm per million Btu of input thermal energy.

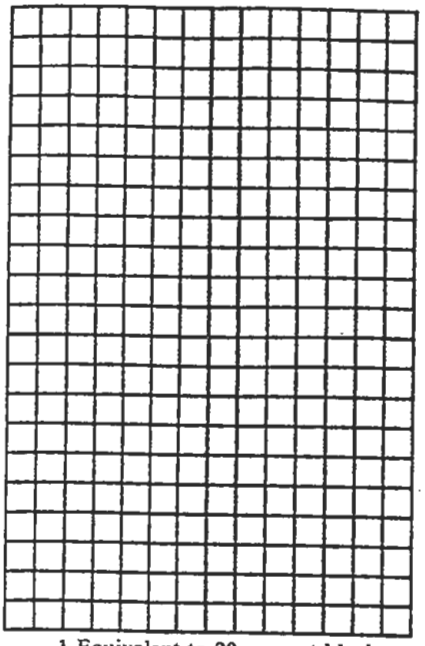
These rules are enforced by the Environmental Protection Agency (EPA). In the generation of electricity, these rules are applicable to any system producing more than around 25 MW_e of electrical energy.

Some utilities used to be able to meet these requirements without using some kind of sulfur removal system by burning coal with a sulfur content of 1 percent or less. As a consequence, the demand for low-sulfur coal skyrocketed while the demand for high-sulfur coal plummeted.

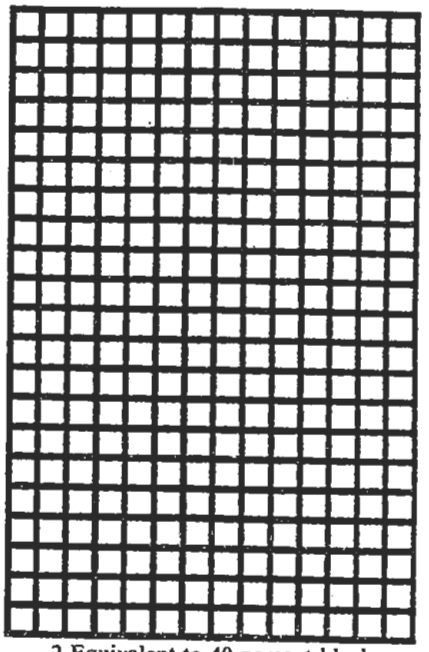
In 1983, the EPA tightened the SO_x and particulate emission requirements to increase the demand for high-sulfur coal. According to the new regulations, the allowable release of particulate matter: The maximum 2-h average permitted is 0.03 lbm of particulate matter per million Btu of input thermal energy (30 percent of the original value).

The new allowable SO_x emission rate is a function of the theoretical SO_2 production rate, $\mathscr{P}_x$, in units of lbm/MBtu input. The value of $\mathscr{P}_x$ can be determined from the following equation:

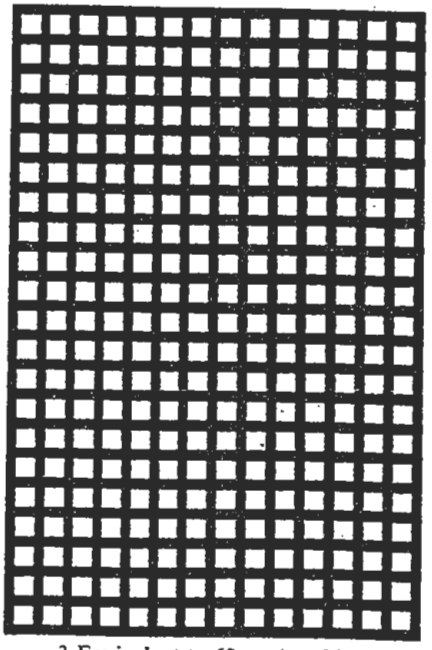
$$\mathscr{P}_x = (2 \times 10^6)S/HHV_{Btu} = (4.65 \times 10^6)S/HHV_{kJ} \qquad (6.1)$$



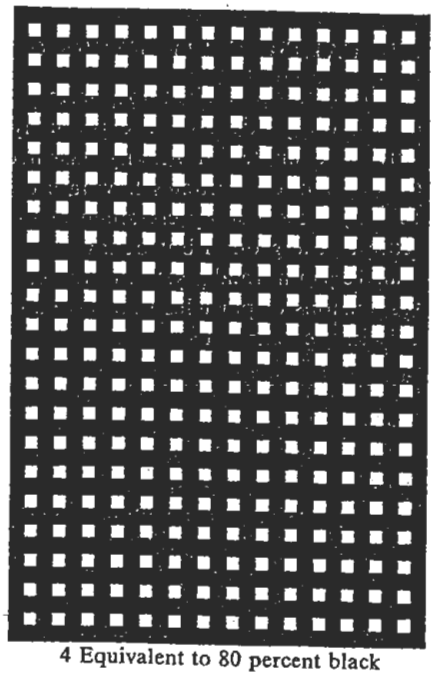
1 Equivalent to 20 percent black



2 Equivalent to 40 percent black



3 Equivalent to 60 percent black



4 Equivalent to 80 percent black

where S is the sulfur mass fraction of the coal, $(HHV)_{Btu}$ is the higher heating value in Btu/lbm, and $(HHV)_{kJ}$ is the higher heating value in kJ/kg of the coal. Values of S and HHV can be used on any basis, as long as they are consistent. Thus, dry, ash-free values from App. E can be used directly in Eq. (6.1).

Once the SO_2 production rate $\mathscr{P}_s$ has been evaluated, the allowable SO_2 release rate R_s, in lbm/MBtu, can be determined from one of the following equations.

For $\mathscr{P}_s < 2.0$ lbm SO_2/MBtu,

$$R_s = 0.3\mathscr{P}_s \quad \text{lbm/MBtu} \tag{6.2a}$$

For $2.0 < \mathscr{P}_s < 6.0$ lbm SO_2/MBtu,

$$R_s = 0.6 \quad \text{lbm/MBtu} \tag{6.2b}$$

For $6.0 < \mathscr{P}_s < 12.0$ lbm/MBtu,

$$R_s = 0.1\mathscr{P}_s \quad \text{lbm/MBtu} \tag{6.2c}$$

For $\mathscr{P}_s > 12.0$ lbm/MBtu,

$$R_s = 1.2 \quad \text{lbm/MBtu} \tag{6.2d}$$

Thus, the EPA requires that all new combustion systems remove a minimum of 70 percent of the sulfur in the fuel.

6.2 PARTICULATE EMISSIONS

Of the three general atmospheric pollutants emitted from fossil-fueled power plants, the particulates are probably the easiest of the pollutants to control. Particulate matter is normally classified either according to the size of the particles or their source. Particles having a diameter of less than 1 micrometer (1 μm = 10^{-6} m) are generally classified as dust and are small enough that they do not settle to the ground but behave as aerosols. Particles with a diameter of more than 10 μm normally settle to the ground. Smoke is usually composed of stable suspensions of particles that have a diameter of less than 10 μm and are visible only in the aggregate.

FIGURE 6.1
Standard Ringelmann charts.

Note:

1. Light shining on chart should be the same light that is shining on smoke being examined: for best results, sun should be behind observer.
2. Match smoke as closely as possible with corresponding grid on chart.
3. To compute smoke density, use the following formula:

$$\frac{\text{Equivalent units of No. 1 smoke} \times 0.20}{\text{Number of observations}} = \text{percentage smoke density}$$

(*Source: U.S. Bureau of Mines Information Circular 8333, 1967.*)

Fumes are very small particles resulting from chemical reactions and are normally composed of metals or metallic oxides. The ash particles that are found in the flue gas of a fossil-fueled boiler with diameters of 100 μm, or less, are called *flyash* while larger particles are called *cinders.* The size ranges of various particles, fumes, aerosols, etc., are shown in Fig. 6.2.

There are many ways of removing particulates from the flue gas. The performance parameter of a particular removal system is called the *collection efficiency* of the system and is defined by the following equation:

$$\text{Collection efficiency} = \frac{(100)(\text{mass of dust removed})}{\text{mass of dust present}} \tag{6.3}$$

The collection efficiency varies considerably from system to system but normally ranges from 50 percent for some of the simpler mechanical systems to as high as 99 percent or more for the electrostatic precipitator or baghouse filter.

Some typical mechanical systems for the removal of particles are shown in Fig. 6.3. These include (1) a sudden decrease in gas velocity, (2) an abrupt change in the direction of gas flow, (3) the impingement of the gas stream on a series of baffles, and (4) the use of centrifugal force, as in the "cinder-vane" fan. The

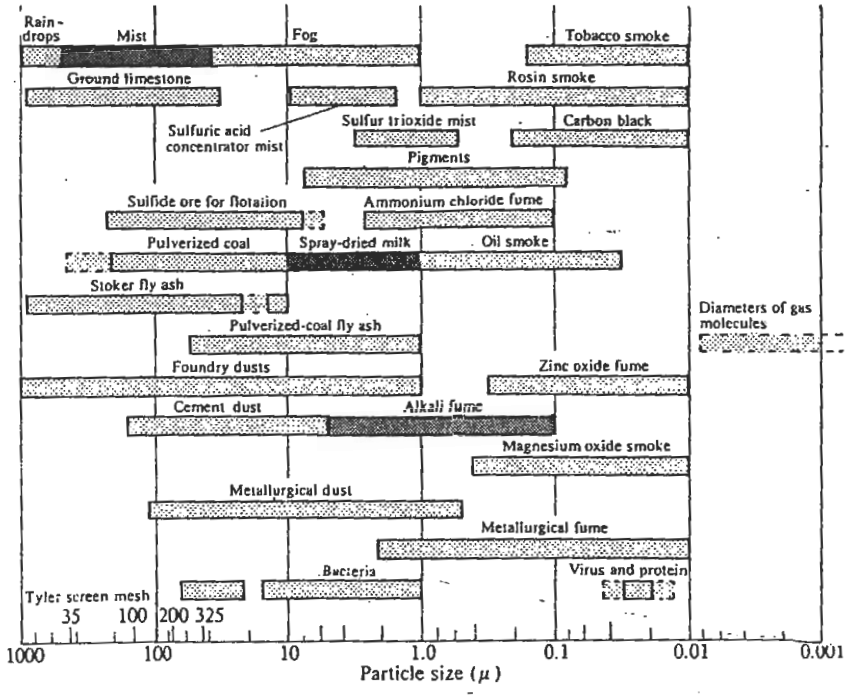


FIGURE 6.2
Size of particulate pollutants.

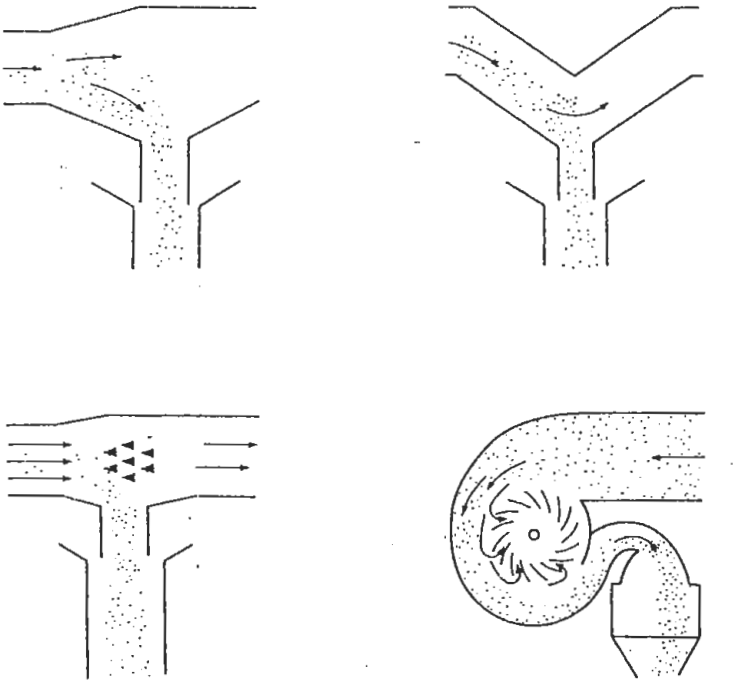


FIGURE 6.3
Mechanical dust collection systems. (*From Skrotski and Vopat, 1960.*)

first three systems in Fig. 6.3 are called *cinder catchers* and are commonly used on stoker and small cyclone furnaces, where crushed coal is burned rather than the very fine pulverized coal. Cyclone and mechanical separators, similar to that shown in Fig. 6.4, are also employed when the greater collection efficiencies are desired. The collection efficiency of the cinder catchers and the cinder-vane fan (of Fig. 6.3) range from 50 to 75 percent. The cyclone separators give collection efficiencies as high as 85 percent.

Wet scrubbers, similar to that shown in Fig. 6.5, are commonly used to remove particulates from process gases in the chemical and the grain-milling industry. Some of the problems associated with the use of wet scrubbers in the flue gas system are that the gas is cooled so much that it must be reheated before it is put up the stack; the resulting pressure drop across the scrubber is quite high; the water, which is used as the scrubber fluid, becomes contaminated with sulfurous and sulfuric acid if the exhaust contains any sulfur oxides, and this can cause corrosion problems. The collection efficiency of wet scrubbers is around 90 percent.

While wet scrubbers are not commonly used to remove particulate matter from the flue gas, more and more power plants are employing them in the flue

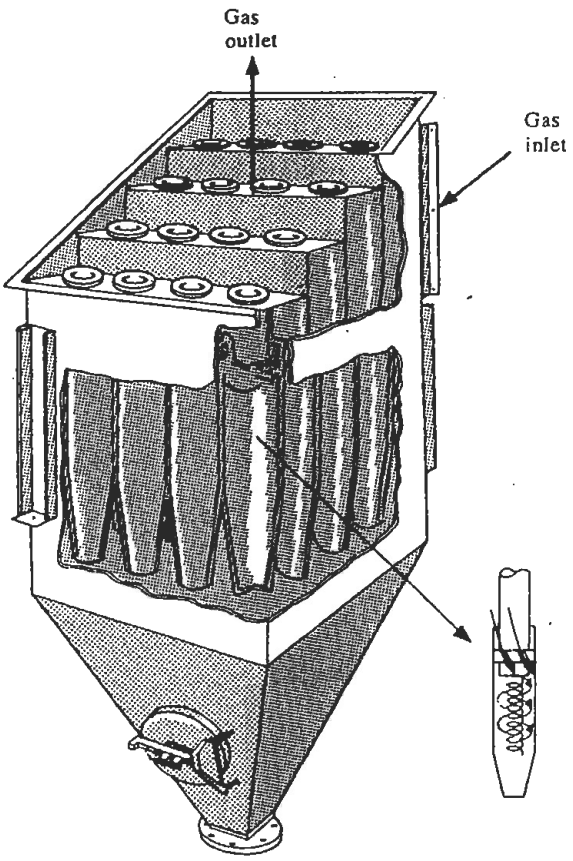


FIGURE 6.4
A cyclone particulate-removal system. (*Courtesy of Western Precipitation Company.*)

gas system to remove sulfur oxides from the gas. The use of lime or limestone solutions in these scrubbers neutralizes the sulfur acids. While it might be expected that sulfur dioxide and the particulates could be removed in the same wet-scrubber system, a separate particulate-removal system is commonly employed ahead of the SO_2 scrubber because the simultaneous removal of both pollutants adversely affects the performance of the SO_2 removal system.

In the past, most large, pulverized-coal and large cyclone furnaces used a large electrostatic precipitator for final cleanup of particulate matter from the flue gas. A cutaway diagram of one of these systems is shown in Fig. 6.6. In the electrostatic precipitator, highly charged (30,000 to 60,000 V) wires are suspended in a gas-flow passage between two grounded plates. The particles in the gas stream acquire a charge from the negatively charged wires and are then attracted to the grounded plates. The grounded plates are periodically rapped by a steel

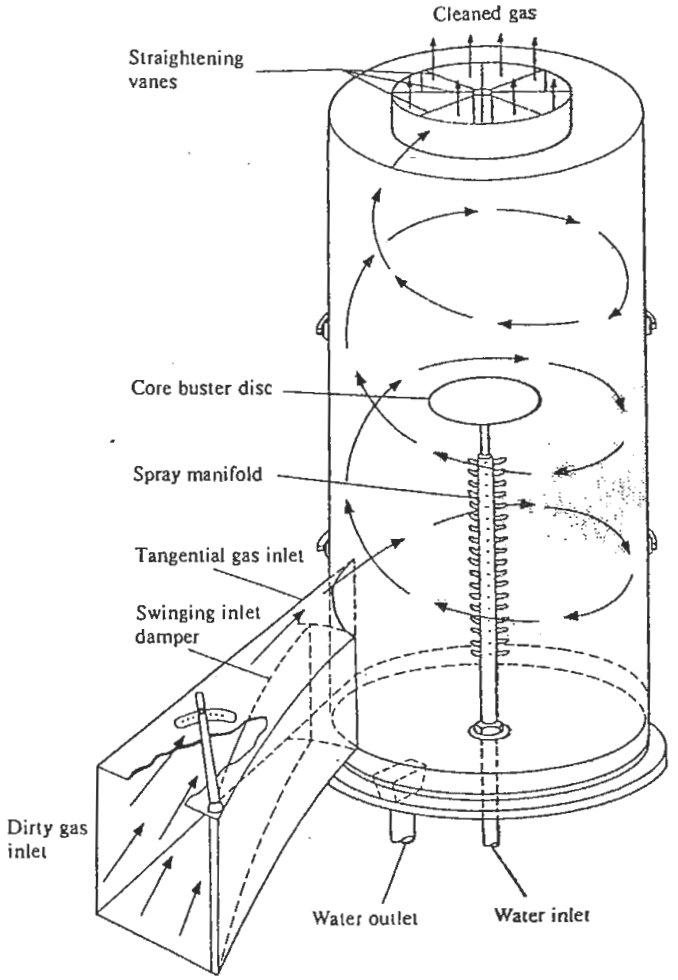


FIGURE 6.5
A cyclonic wet-scrubber system. (*From Faith, 1959.*)

plug which is raised and dropped by an electromagnet and the collected dust particles fall into hoppers below the plate.

Care must be taken in the operation of any electrostatic precipitator to assure that there is no possibility that a large charge of unburned gas enters the precipitator. If such a charge does enter, power to the unit should be terminated immediately because there is constant arcing between the wires and plates which will trigger an explosion of the unburned gas.

While electrostatic precipitators have been commonly accepted throughout the power industry and have collection efficiencies in excess of 99 percent, they

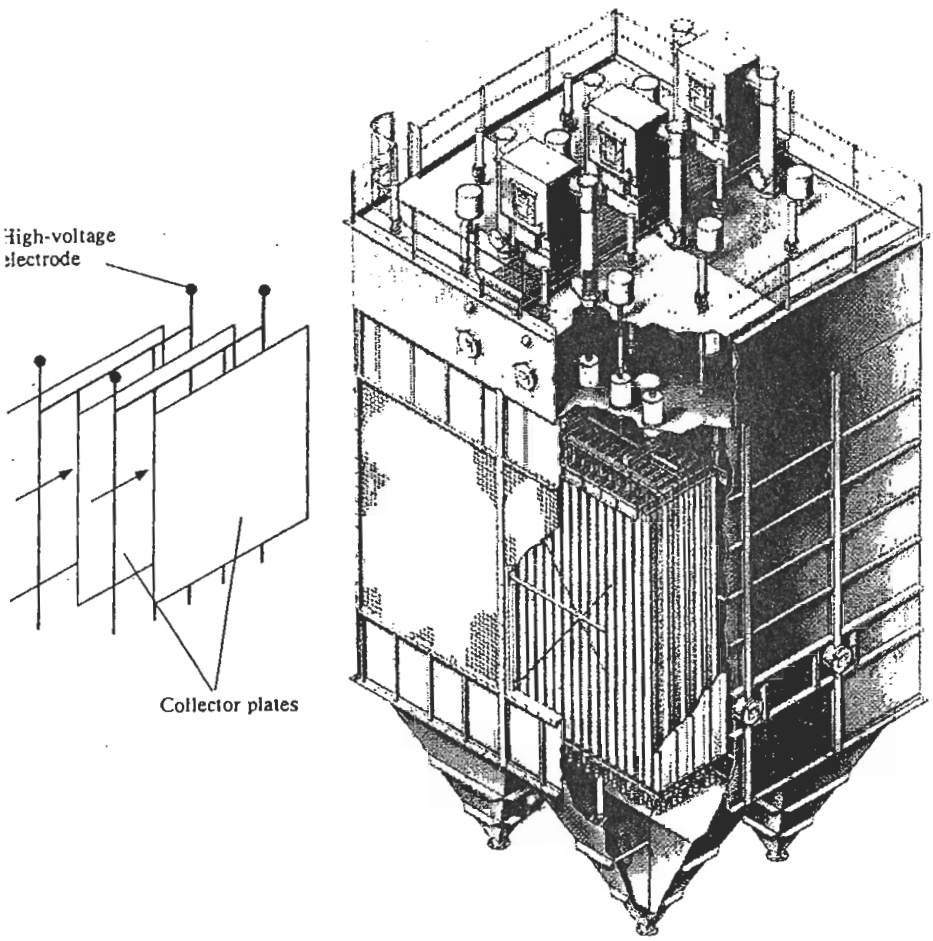


FIGURE 6.6
The electrostatic precipitator. (*Courtesy of Babcock and Wilcox and Research Cottrell, Inc.*)

do not work well when the flyash has a high electrical resistivity. High-resistivity flyash commonly results from the combustion of low-sulfur coal. One solution to this problem that has actually been used is to inject sulfur trioxide (SO_3) gas into the exhaust gas to improve the conductivity of the flyash. This solution is hardly an environmentally acceptable solution because of the increased emission of sulfur oxides.

Because of the problem encountered with electrostatic precipitators and systems burning low-sulfur coal and because of the increased consumption of low-sulfur coal, more and more utilities have resorted to the use of large baghouse

filters for the final cleanup of particulates from the flue gas. Schematic diagrams of this system are shown in Fig. 6.7 and a photograph is shown in Fig. 6.8.

A major problem associated with the use of baghouse filters is the high maintenance cost associated with the cloth bags. The bags, which represent up

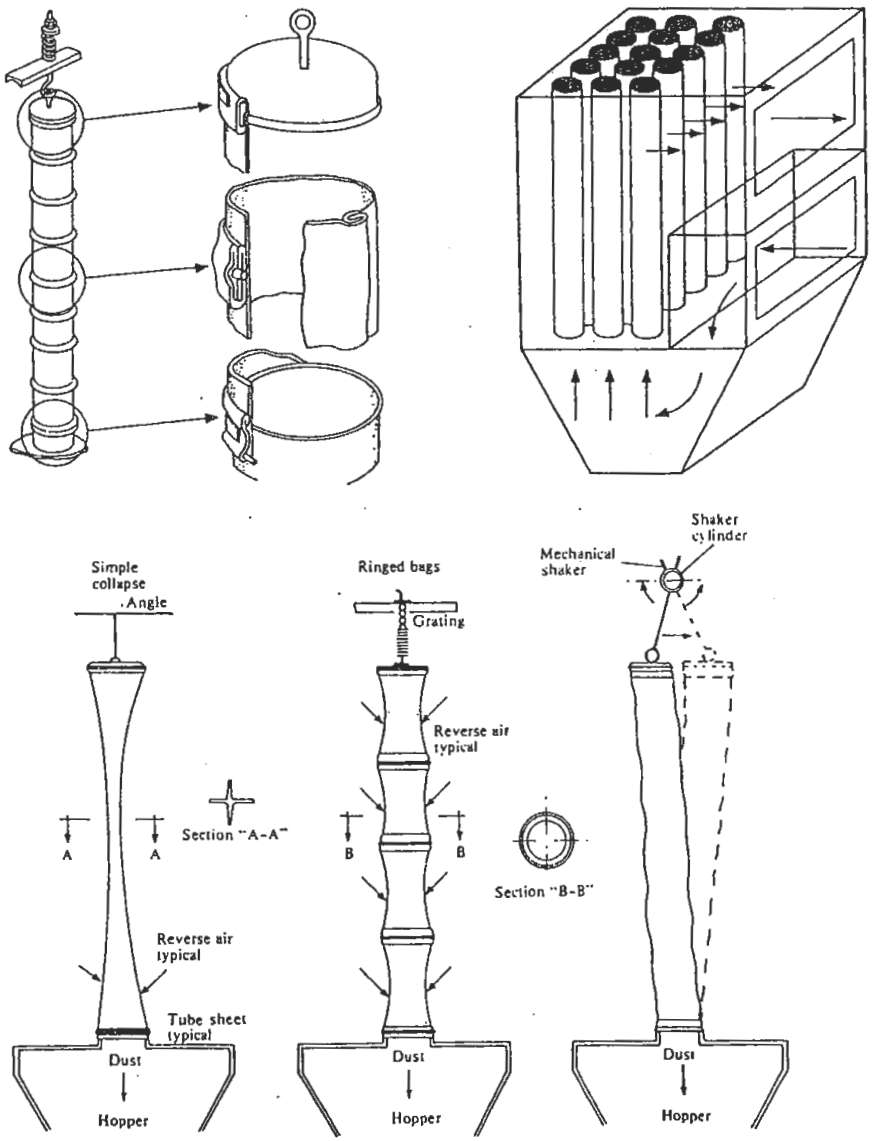


FIGURE 6.7
Schematic diagrams of the baghouse filter system.

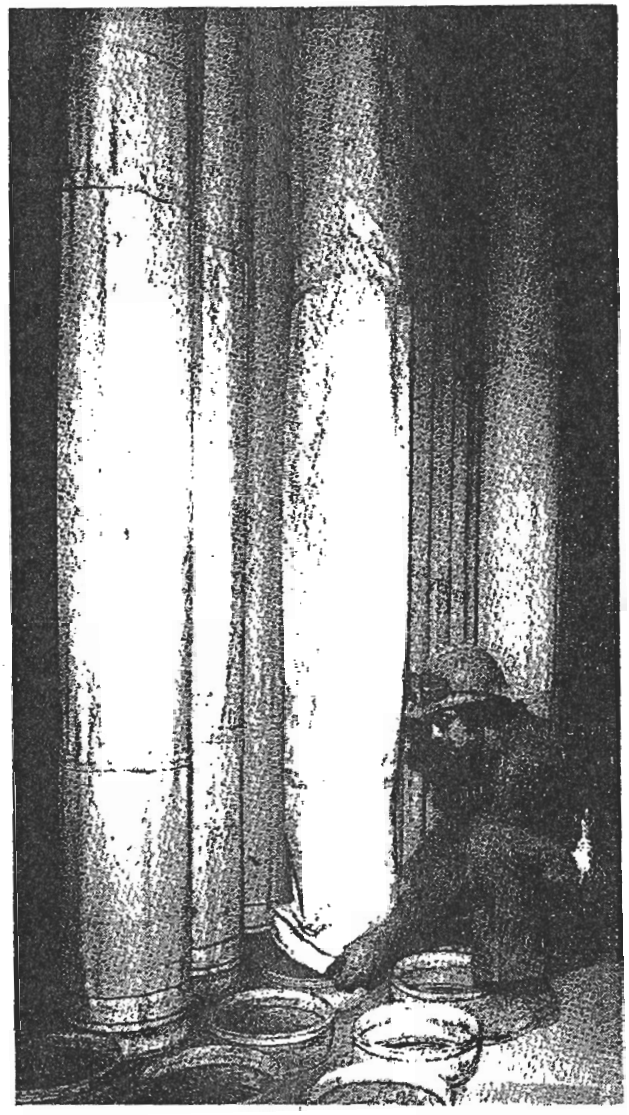


FIGURE 6.8
A baghouse filter system. (*From Helfritch and Beach, 1976.*)

to 20 percent of the erected cost of the baghouse, have an average life of 18 to 36 months. There are two basic types of bag materials in common use. Both are well suited for use in high-temperature, dust-laden environments. The two types are the felted bags like those fabricated from Teflon® and the woven bags

fabricated from glass fibers with various coatings. The baghouse unit is normally cleaned by shaking the bags or by flushing the system with a reversed flow of atomospheric air. The felted bag is difficult to clean and creates a large pressure drop, while the woven bag loses its dust precoating when cleaned. This produces a temporary drop in the collection efficiency. In fact, the collection efficiency of a baghouse filter normally increases as the system operates but the pressure drop also increases.

Baghouse filters are inherently large structures and require a minimum of $70\ ft^2/MW_e$. Despite the maintenance problems and the large collection volumes required for these units, baghouse filters are finding wider and wider acceptance in coal-fired power systems.

6.3 GASEOUS POLLUTANTS

SULFUR OXIDES (SO_x). The emission of sulfur oxides, primarily sulfur dioxide (SO_2) with some sulfur trioxide (SO_3), is a primary source of atmospheric pollution from fossil-fired electrical generation plants. It is estimated that more than 90 million tons of sulfur dioxide are discharged to the atmosphere each year. The EPA now regulates how much sulfur oxide that a new power plant can legally discharge to the environment. As was discussed earlier, the original limit was 1.2 lbm SO_2 per million Btu of input energy. Many utilities met this requirement by simply burning coal with low-sulfur content (>1% sulfur). Most of this coal is found in Montana and Wyoming, so its use normally entails a significant transportation charge.

In an effort to reduce the demand for low-sulfur coal the EPA revised the original standards such that regardless of the sulfur content of the coal, any new installation must remove a minimum of 70 percent of the sulfur. The allowable release of sulfur oxides depends on the amount of sulfur in the fuel as defined by Eqs. (6.2). The sulfur can be removed before or at any time during the combustion process as far as the EPA is concerned.

The sulfur found in coal is either in the form of inorganic sulfur, commonly iron pyrite (FeS_2), or in the form of organic sulfur. The inorganic sulfur has a much higher density than the rest of the coal and much of it can be removed as the result of some sort of flotation process. Unfortunately, a maximum of only 50 percent of the sulfur can be removed in this process, which is still below the minimum removal required by the EPA. It is also possible to remove sulfur from crude oil but it adds significantly to the cost of the crude.

As discussed in Chap. 4, the sulfur emissions can be controlled with the use of fluidized-bed combustion system. In this system, finely crushed limestone or dolomite is added to the coal to trap the sulfur oxides in the form of calcium or magnesium sulfides. One disadvantage of this system, however, is that it normally requires half again as much reactant (limestone or dolomite) as a good wet-scrubber system for a given sulfur removal.

Most of the sulfur-emission control systems in this country use some form of *flue-gas desulfurization* (FGD) system in which the sulfur dioxide in the flue

gas is removed by a wet-scrubbing process. There are two ways of classifying FGD systems—dry versus wet systems and regenerative versus nonregenerative systems. In the dry systems, the reactant (possibly lime or limestone) is mixed with only enough water so that it can be sprayed into the flue gas. When the solution hits the hot exhaust gas, the water evaporates and the reactant and the product is collected as a solid or "dry" compound.

In the recovery or regenerative FGD system, the reactant that is used to absorb the sulfur oxides from the flue gas is recovered and used again. The final product from these systems is normally either sulfuric acid (H_2SO_4) or elemental sulfur (S). In the nonregenerative or "throwaway" FGD system, the reactant is not regenerated and the final products are sulfur salts of calcium and magnesium ($CaSO_3$, $CaSO_4$, $MgSO_3$, $MgSO_4$) which are then stored in holding ponds or land fills.

There are many different proposed regenerative FGD systems. Among there are the Wellman-Lord process, the FW-Bergbau Forshung process, the wet-magnesium oxide process, the catalytic/IFP ammonia process, the aqueous-carbonate process, and the Foster-Wheeler dry adsorption process, among many others. The Wellman-Lord process and the FW-Bergbau Forshung processes are shown in Figs. 6.9 and 6.10.

Some of these processes, including the Wellman-Lord process, are fully commercial and have been used in Japan and other countries but are not widely used in the electrical power generation systems in the United States. In general, they remove the sulfur dioxide by absorbing it with an alkali (sodium, calcium, and/or magnesium) solution or by adsorbing it with char, charcoal, or alumina pellets. The resulting sulfur salt or saturated adsorber is then regenerated, producing the original reactant and a concentrated stream of sulfur dioxide. The original reactant is then reused and the concentrated SO_2 stream is then either oxidized to sulfur trioxide (SO_3) and then combined with water to produce sulfuric acid or it is passed over charcoal and reduced to elemental sulfur and carbon dioxide.

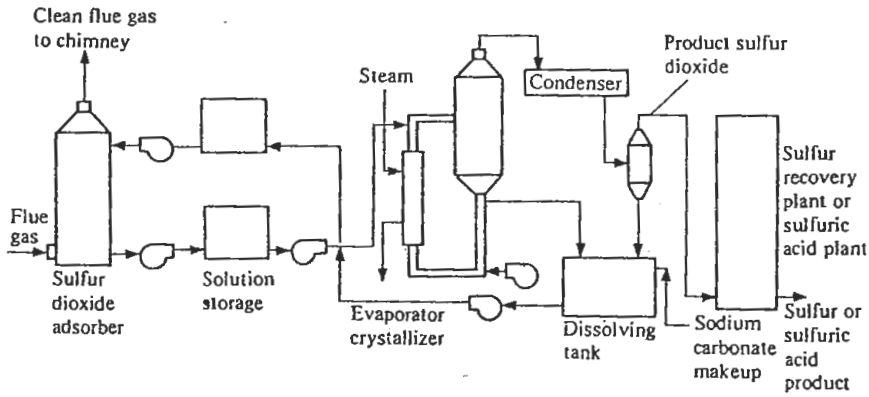


FIGURE 6.9
The Wellman-Lord absorption system. (*From Heeney, 1976.*)

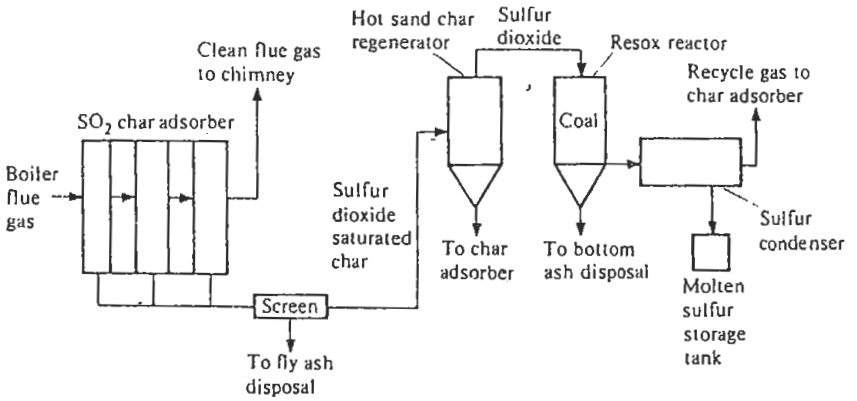


FIGURE 6.10
The FW-Bergbau Forshung adsorption FGD regenerative system. (*From Heeney, 1976.*)

The resulting product (either the H_2SO_4 or S) can usually be sold to fertilizer companies and the resulting income helps defray the operating cost of the sytem.

Most of the FGD systems in use in this country are the throwaway or nonregenerative systems using either lime or limestone as the principal reactant. A schematic diagram of a typical lime/limestone throwaway system is shown in Fig. 6.11. The lime or limestone can be used directly in the scrubber solution as

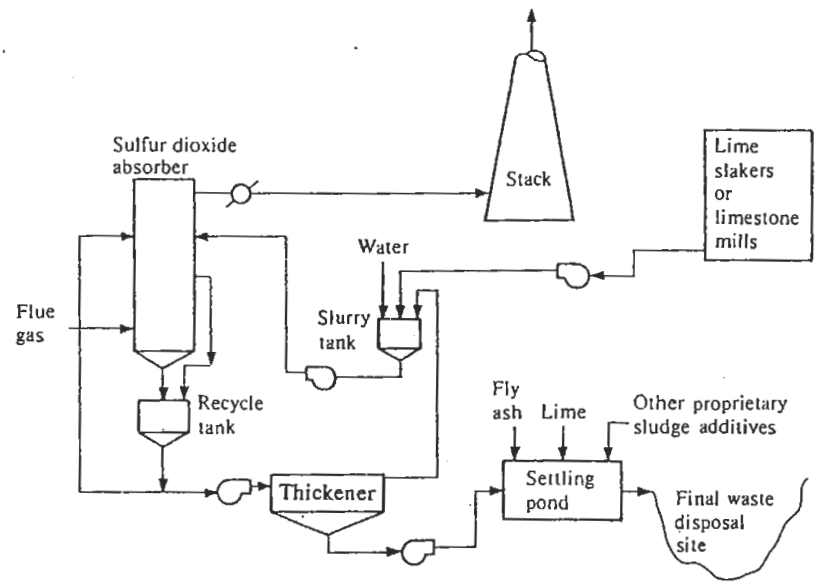


FIGURE 6.11
The lime-limestone FGD nonregenerative system. (*From Heeney, 1976.*)

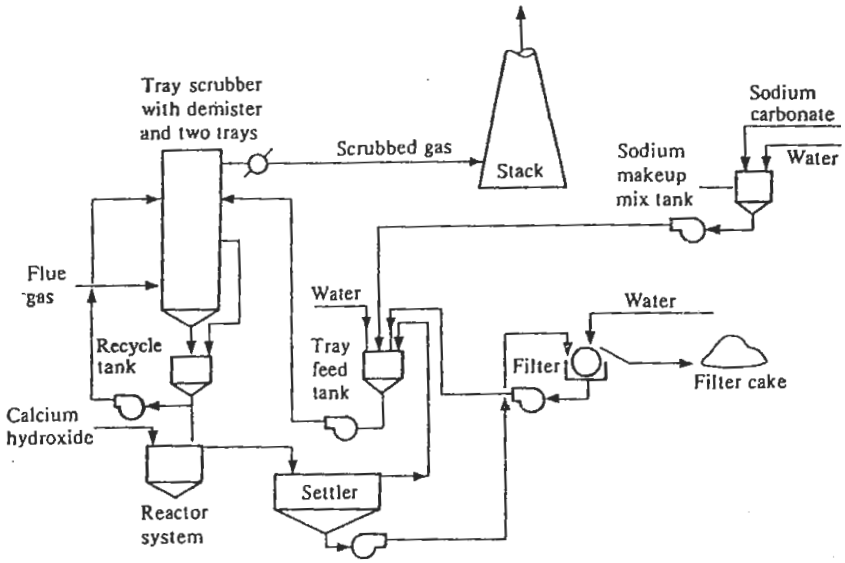


FIGURE 6.12
The double-alkali FGD nonregenerative system. (*From Heeney, 1976.*)

in the process shown in Fig. 6.11, or it can be used to regenerate sodium carbonate (Na_2CO_3) as in the double-alkaline process shown schematically in Fig. 6.12.

In the double-alkali process, the sodium carbonate solution is used to scrub the flue gas because it is more reactive than the calcium or magnesium solutions and it is relatively nonscaling. The final products of the throwaway systems are calcium and magnesium sulfites ($CaSO_3$ or $MgSO_3$) and calcium and magnesium sulfates ($CaSO_4$ or $MgSO_4$). Limestone is usually less expensive and more abundant than lime but the lime system requires less fan and/or pump power and, moreover, experience with these systems indicates that the lime systems have better performance records. During 1976, the estimated capital cost of these systems was about \$70 kW_e or around \$70 million for a 1000-MW_e power plant. In addition, there is the continuing added cost of the reactant (limestone).

At the present time, most of the sludge from the throwaway systems is discharged to holding ponds. This is considered to be a temporary solution. The EPA is concerned because it may cause groundwater pollution and also because it degrades large land areas. Some companies are working on the possibility of chemically stabilizing the sludge so that it can be used as land fill or a road-base material.

NITROGEN OXIDES (NO_x). The emission oxides of nitrogen (nitric oxide and nitrogen dioxide) are also limited by the Clean-Air Act of 1970. At the present time, the EPA is not actively enforcing the NO_x emission standards. The power

industry, however, is taking steps to produce combustion systems and methods that reduce the NO_x emissions.

Since the production of NO_x is an endothermic reaction, the concentration is very temperature-dependent. Consequently, the NO_x emissions can be reduced by lowering the combustion temperature and by eliminating hot spots in the furnace. The formation of nitrogen oxides can also be inhibited by lowering the actual air-fuel ratio and/or by employing exhaust gas recirculation. Lowering the air-fuel ratio restricts the amount of oxygen available for the reaction while exhaust gas recirculation reduces the combustion chamber temperature.

In the fluidized-bed combustion system, the boiler evaporator tubes are located directly in the burning bed in an effort to lower the combustion temperature and limit the formation of NO_x. While the average bed temperature is around 870°C (1600°F), the temperatures of the individual burning coal particles exceed this level. There are no new cyclone furnaces being built because of the very high combustion temperatures (1760°C or 3200°F) required in the combustion chamber and also because this system has difficulty burning low-sulfur coal. The new pulverized-coal furnaces are designed so that the combustion zone is spread over a large volume in order to keep the temperature low.

By the mid 1980s, the only NO_x scrubbers in use in the world were found in Japan. These systems are NO_x-reduction processes—such as the selective catalytic reduction (SCR) process or the selective noncatalytic reduction (SNR) processes. Both of these systems involve the injection of ammonia (NH_3) into the exhaust gas to reduce the NO_x to nitrogen and water. Many utilities in the United States are closely following the developments and techniques used in the removal of nitrogen oxides. Unlike sulfur, which can be removed before, during, or after the combustion process, nitrogen oxides can only be removed from the exhaust gas.

6.4. THERMAL POLLUTION

Another area of pollution associated with the generation of electrical energy is water pollution. The two general areas of water pollution associated with power generation are the chemical and solid waste pollution from mining, oil drilling, transportation, etc., and the thermal discharge from the power plant itself. Since this text deals primarily with power plant design and operation, the primary focus of water pollution here is on thermal discharges to the water, although the leaching of sulfuric acid from abandoned coal mines and slag piles is a major problem in some areas of the country. The pollution associated with the transportation of oil is also a major concern.

The discharge of thermal energy into natural waters is commonly called *thermal pollution* by environmentalists and antipower people. The addition of heat to the water reduces the water's ability to hold dissolved gases, including the dissolved oxygen vital to the aquatic life. If the water temperature exceeds 35°C (95°F), the dissolved oxygen content is to low to support life. At lower temperatures, however, the aquatic growth is usually enhanced by the warm water

and most of the plants and fish grow at a faster rate. In fact, the warm-water discharge from a power plant is usually an excellent place to fish, particularly during cold weather.

In an effort to compare power-generating systems with respect to the amount of thermal energy discharged to the environment, a term will be introduced here called the *thermal discharge index* or TDI. The thermal discharge index of any power system is the number of thermal energy units discharged to the environment for each unit of electrical energy produced by the plant. It may be expressed in terms of power units, as follows:

$$\text{TDI} = \frac{\text{thermal power to the environment, MW}_{\text{th}}}{\text{electrical power output, MW}_e} \tag{6.4}$$

Needless to say, a low value of thermal discharge index is desirable but it must be nonzero in order to satisfy the second law of thermodynamics.

The thermal discharge index is strongly dependent on the thermal efficiency of the power system, η_{th}. If P_{th} is the input thermal energy to the power system, in megawatts, $P_{\text{th}}\eta_{\text{th}}$ is the electrical power out of the system, and the difference, which is $P_{\text{th}}(1-\eta_{\text{th}})$, is the thermal power discharged from the plant. Thus, the thermal discharge index becomes

$$\text{TDI} = \frac{P_{\text{th}}(1-\eta_{\text{th}})}{P_{\text{th}}\eta_{\text{th}}} = \frac{1-\eta_{\text{th}}}{\eta_{\text{th}}} \tag{6.5}$$

The newer fossil-fired power systems have thermal efficiencies up to 40 percent, which means that they have a thermal discharge index of 1.5. Thus 1.5 MW of thermal energy is discharged to the environment at the plant for each MW of electrical energy produced. Light-water reactors, on the other hand, typically have thermal efficiencies of 32 to 33 percent, which yields a thermal discharge index around 2. Geothermal power systems usually have thermal efficiencies of less than 20 percent, which means the thermal discharge index of these systems is greater than 4.

In evaluating the thermal pollution from a power system, it is important to determine just how the thermal energy is disposed—whether it goes to the atmosphere or to lakes and streams. For the gas-turbine and internal-combustion engine power systems, essentially all of the waste energy is discharged to the atmosphere, primarily through the exhaust system. In the case of fossil-fueled power systems, some of the waste thermal energy (the boiler losses) is discharged to the atmosphere from the stack while most of the balance is removed in the condenser. In a nuclear reactor power system, on the other hand, essentially all of the waste heat is discharged through the condenser. Consequently, the nuclear unit requires considerably more condenser cooling water than a comparable fossil-fired unit even if the thermal discharge indices are the same.

The power discharge from a fossil-fueled power system can normally be divided into three groups—the electrical power output P_e, the stack power P_s, and the condenser power P_c. The sum of these three quantities must equal the total input thermal energy P_{th}. The stack power can be determined from the

following equation:

$$P_s = P_{th}(1 - \eta_b) \tag{6.6}$$

where η_b is the boiler efficiency. Since $P_e = \eta_{th} P_{th}$, the condenser power can be determined, as follows. From the first law of thermodynamics:

$$P_{th} = P_e + P_s + P_c = \eta_{th} P_{th} + (1 - \eta_b) P_{th} + P_c$$

Rearranging and solving for P_c gives:

$$P_c = P_{th}[1 - \eta_{th} - (1 - \eta_b)] = P_{th}[\eta_b - \eta_{th}] \tag{6.7}$$

There are several ways to supply the condenser cooling water. These include once-through cooling from natural lakes and streams, once-through cooling from artificial cooling ponds or lakes, and the use of wet and dry cooling towers. The once-through cooling-water system is one where the water from a river or lake is strained to remove the debris and aquatic life and is then pumped through the condenser of the power plant. This water normally undergoes a temperature rise of around 10C° (18F°) as it passes through the condenser. This method of waste-heat removal is the least expensive method of discharging the waste heat and probably gives the highest thermal efficiency for the plant because it produces the lowest average sink temperature for the power system.

While the above system is the most desirable from the standpoint of the power engineer, it has met a lot of opposition from political and environmental groups. Some states have enacted laws that prohibit the introduction of water into a natural lake or river that is more than 1F° above the ambient water temperature. As a consequence, it is becoming increasingly difficult to use this method of waste-heat removal.

Some utilities are still using once-through cooling in their new plants but they are constructing large company-owned lakes to supply the water. If the cooling lake is too small during the hottest period of the year, floating spray pumps are sometimes used to enhance the atmospheric cooling of the lake water. These lakes are commonly popular fishing spots because the fish grow very quickly and the water is usually free of ice the entire year. Some water makeup to the lake may be required during dry weather to replace the water lost by evaporation.

If it is not feasible to use cooling lakes, most power companies are opting for cooling towers to reject the waste heat from the condenser cooling water to the atmosphere. There are two basic types of cooling towers—dry and wet. Most power systems employ the wet cooling tower in which the hot condenser water is sprayed directly into the tower. The hot water makes direct contact with the air flowing up through the tower and heat transfer is accomplished as the result of sensible and latent (evaporative) heat transfer. The wet cooling tower requires continuous water makeup to compensate for the evaporative loss, and the addition of large quantities of water vapor to the atmosphere can adversely affect the weather downwind of the tower, causing higher than average precipitation.

The minimum sink temperature that can be achieved with a wet cooling tower approaches the atmospheric wet-bulb temperature. As a result, the overall

thermal efficiency of the plant is probably lower than that of a system using a once-through cooling system, particularly on a hot day when the demand is high.

Most of the high-capacity wet cooling towers are the natural-convection systems characterized by the large hyperbolic structures that run to 500 ft (150 m) in height and 500 ft in diameter at the base. A typical wet cooling tower is shown in Fig. 6.13. The air flow in a wet tower is established by the difference in density of the "cold" air entering the bottom of the tower and the density of the "warm" air and water vapor leaving the top of the tower. The estimated capital cost of these units is around \$20 to \$25/kW_e or up to \$25 million for a 1000-MW_e power system.

Smaller power systems may employ cooling towers with mechanical-draft systems using induced-draft or force-draft fans. The use of a mechanical-draft system eliminates the need for height. these towers are somewhat less expensive than the natural-draft systems, with an estimated cost of \$15 to \$20/kW_e. Although this system has somewhat lower capital costs, it does have higher maintenance and operating costs associated with it, and consequently, it is not widely used in large utility systems.

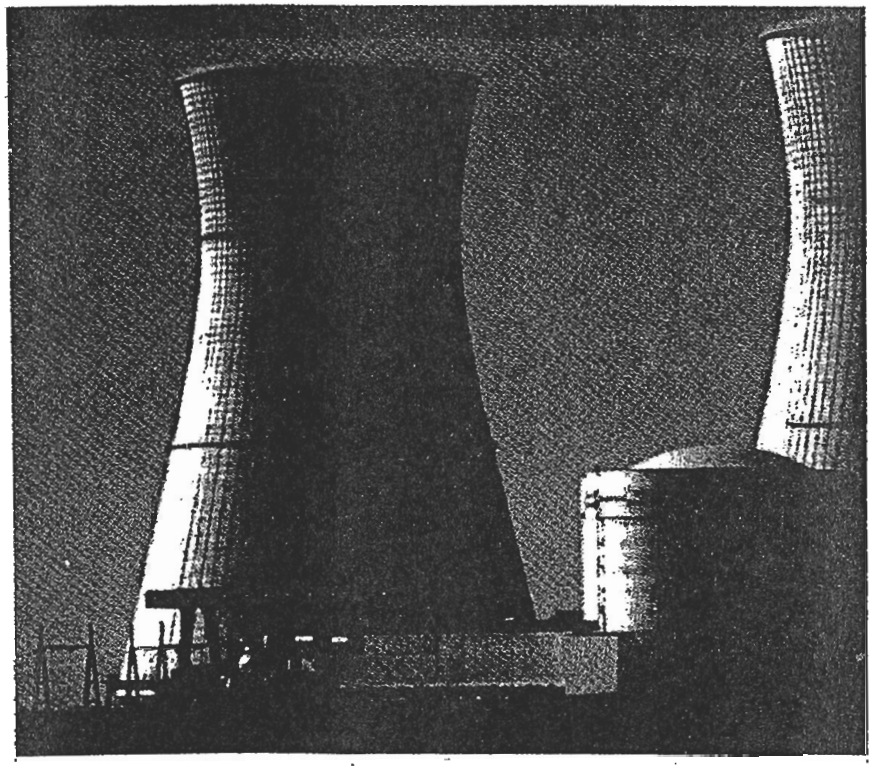


FIGURE 6.13
A nuclear power station with large natural-draft cooling towers. (*Courtesy of Babcock and Wilcox.*)

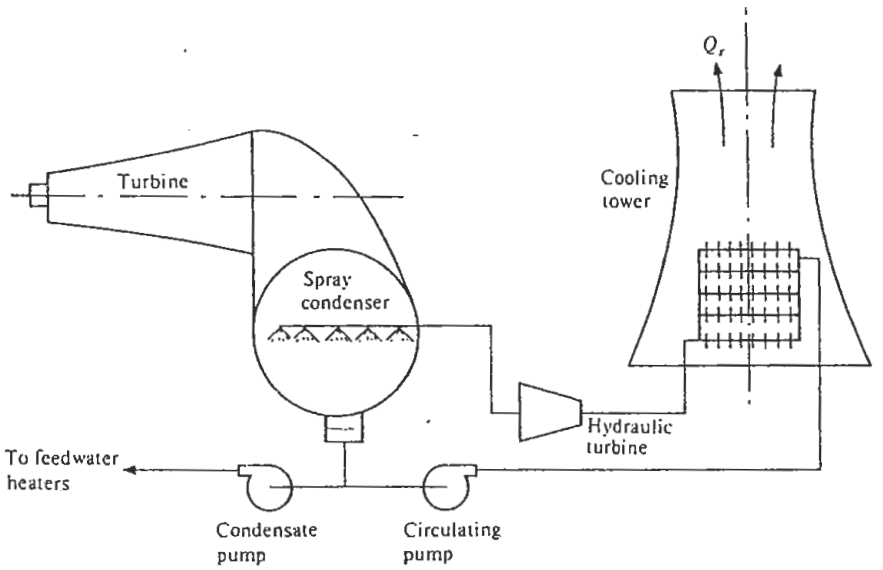


FIGURE 6.14
Schematic diagram of the Heller dry cooling tower system.

The dry cooling tower is a possible alternative to the wet cooling tower, particularly where makeup water is not available or where the large vapor plumes from the wet towers are not environmentally acceptable. In this system, the cooling fluid is contained in the tubes in the cooling tower so that all the heat transfer for this system is sensible heat transfer and the minimum sink temperature approaches the dry-bulb temperature.

The dry cooling tower eliminates the need for a surface condenser at the turbine exhaust as the steam could theoretically be condensed directly in the tower. However, the steam pressure and density at the turbine exhaust is so low and the pipes in the tower would have to be so large that the scheme is impractical. A possible dry cooling tower system is shown schematically in Fig. 6.14. In this system the turbine steam is condensed in a direct-contact, spray condenser using part of the condensate that has been subcooled in the dry tower. The dry tower is considerably more expensive than the wet tower. This system, like the wet tower, also affects the weather downwind, except that, by superheating the air, it probably produces less rain than normal.

6.5 SOLID-WASTE POLLUTION

In addition to the particulate and gaseous material discharged to the atmosphere, the average coal-fired power plant produces a considerable amount of solid waste in the form of ash. A 1000-MW_e coal-fired power plant burning coal with 10

percent ash will generate about 40 tons of ash per hour or around 333,000 tons of ash per year. Bottom ash or slag is relatively inert and normally can be used as landfill. The flyash collected at the electrostatic precipitator or baghouse filter is usually quite acidic, however, because of the sulfur dioxide in the flue gas. This flyash does find use in the making of cement and concrete blocks.

If a fossil-fuel system (either coal or oil) uses a throwaway sulfur-dioxide, wet-scrubber system, such as the lime/limestone scrubbers, massive amounts of calcium and magnesium salts will also be generated. The same 1000-MW_e coal-fired power system discussed in the preceding paragraph, with a sulfur content of approximately 2.5 percent, will generate about 30 tons of sulfur salts per hour or roughly 240,000 tons per year.

The solid-waste products from the nuclear power systems are the fission products and the transuranic isotopes from the fission reaction and low-level radioactive wastes generated during operation of the unit. The fission and transuranic products are highly radioactive and will be eventually separated from the unburned fuel in spent reactor fuel elements during chemical reprocessing. A 1000-MW_e power system will generate about 1.1 tons of fission and transuranic products each year along with approximately 10 tons of low-level waste. The low-level radioactive waste is currently being buried in licensed low-level radioactive land fills along with radioactive waste from hospitals, etc.

Because of the massive amounts of radiation emitted by the fission and transuranic products, it is imperative that they be isolated from the biosphere for a minimum of 600 years or longer. At 600 years, the activity of these products is equivalent to the activity of the uranium ore from which the fuel was originally obtained. After 600 years, the activity of the products decrease much faster than that of the uranium ore. It is interesting to note that the uranium-235 atom eventually undergoes 11 stages of radioactive decay while the average fission product undergoes three stages of radioactive decay or a total of six stages of radioactive decay per fission. Thus, fissioning the uranium atom actually decreases the total amount of radioactivity from the uranium atom.

There are several proposals for disposing of the fission products. Most of the storage schemes involve the fixation of the products in a borosilicate or phosphorous glass and then storing this glass in leaktight capsules. Since glass is actually a liquid, it is not permanently damaged by the beta and alpha particles and it is also relative impervious to water. The resulting capsules can then be stored in deep salt mines or in deep wells drilled in stable geological strata or drilled in a stable ocean floor. The use of salt deposits for storage was suggested because the presence of salt pockets indicates that there has been no active groundwater in the vicinity for thousands of years. The U.S. government began construction on a high-level waste depository in Nevada during the end of the 1980s.

Other possible solutions for the disposition of the fission products include chemically separating the long-lived products and putting them in a breeder or fusion reactor where they can be transmuted to either short-lived or stable products as the result of neutron absorption. Some thought has also been given to the

possibility of firing the long-lived products into the sun or into a long-term stable earth orbit.

It is interesting to compare the amount of solid waste generated in a nuclear power plant with that produced in a coal-fired unit. The average person in the United States consumes about 10 $MW_e \cdot h$/year or approximately 800 $MW_e \cdot h$ of energy during a lifetime. If this energy is produced in a coal-fired unit, it will lead to the production of about 27 tons of ash plus additional amounts of sulfur salts. If the same energy is produced from a light-water reactor, it will lead to the production of about 100 g or about 0.25 lbm of fission products. This is about 1 in^3 of products, although the total volume, including the glass matrix, will be somewhat greater.

Example 6.1. Estimate the condenser cooling water requirements for a 400-MW_e power plant if the water undergoes a 10C° (18F°) temperature rise and determine the solid waste generated in short tons per year of full-power operation, if:

(*a*) The system is a coal-fired system burning a coal with an HHV of 30,200 kJ/kg, an ash fraction of 8.3 percent, and a sulfur fraction of 5.1 percent. Assume that the system uses a throwaway FGD system using $CaCO_3$ (limestone) as the feed material. Assume the overall plant efficiency is 40 percent and the boiler efficiency is 82 percent.

(*b*) The system is a nuclear reactor with a thermal efficiency of 32 percent.

Since the EPA emission limits are expressed in English units, this problem will be worked in English units.

Solution

(*a*) For a coal-fired system,

$$(\text{HHV})_{\text{coal}} = (30{,}200 \text{ kJ/kg})(0.43 \text{ Btu} \cdot \text{kg/lbm} \cdot \text{kJ}) = 12{,}986 \text{ Btu/lbm}$$

$$\text{Input thermal power} = \frac{P_{\text{th}}}{\eta_{\text{th}}} = \frac{400}{0.4} = 1000 \text{ MW}_{\text{th}}$$

$$= 3.412 \times 10^9 \text{ Btu/h} = 3{,}412 \text{ MBtu/h}$$

$$\text{Coal rate} = \frac{(1{,}000{,}000 \text{ kW})(3412 \text{ Btu/kW} \cdot \text{h})}{(12{,}986 \text{ Btu/lbm})(2000 \text{ lbm/ton})} = 131.4 \text{ ton/h}$$

$$\text{Stack power} = P_s = P_{\text{th}}(1 - \eta_{\text{th}}) = 1000(1 - 0.82) = 180 \text{ MW}_{\text{th}}$$

$$\text{Condenser Power} = P_c = P_{\text{th}}(\eta_b - \eta_{\text{th}}) = 1000(0.82 - 0.4)$$

$$= 420 \text{ MW}_{\text{th}}$$

Condenser water rate:

$$P_c = \dot{m} c_p \Delta T = (420 \text{ MW})(3{,}412{,}000 \text{ Btu/MW} \cdot \text{h})$$

$$= (\dot{m} \text{ lbm/h})(1 \text{ Btu/lbm} \cdot \text{F°})(18\text{F°})$$

$$= 1.433 \times 10^9 \text{ Btu/h} = 18\dot{m} \text{ Btu/h}$$

$$\dot{m} = 1.433 \times 10^9/18 = 7.961 \times 10^7 \text{ lbm/h} = 1.327 \times 10^6 \text{ lbm/min}$$

$$\text{Water rate} = \frac{1.327 \times 10^6 \text{ lbm/min}}{8.33 \text{ lbm/gal}} = 159{,}300 \text{ gal/min}$$

$$\text{SO}_2 \text{ production rate} = \mathscr{P}_s = \frac{(2 \times 10^6)\text{S}}{(\text{HHV})_{\text{Btu}}}$$

$$\mathscr{P}_s = \frac{(2 \times 10^6)(0.051)}{12{,}986} = 7.855 \text{ lbm SO}_2\text{/MBtu}$$

$$\text{Allowable release rate (Eq. 6.2}c\text{)} = 0.1\mathscr{P}_s = 0.786 \text{ lbm SO}_2\text{/MBtu}$$

$$\text{Total SO}_2 \text{ release rate} = (0.786 \text{ lb/MBtu})(3412 \text{ MBtu/h})/(2000 \text{ lb/ton})$$

$$= 1.340 \text{ tons SO}_2\text{/h}$$

$$\text{Total SO}_2 \text{ collection rate} = (7.855 \text{ lb/MBtu})(0.9)(3.412 \text{ MBtu/h})/2000 \text{ lb/ton})$$

$$= 12.06 \text{ tons SO}_2\text{/h}$$

Chemical reaction:

$$\text{SO}_2 + \text{CaCO}_3 \rightarrow \text{CaSO}_3 + \text{CO}_2$$

$$\text{Mol wt of CaCO}_3 = 40.08 + 12.01 + 3(16) = 100.09 \text{ ton/ton} \cdot \text{mol}$$

$$\text{Mol wt of CaSO}_3 = 40.08 + 32.06 + 3(16) = 120.14 \text{ ton/ton} \cdot \text{mol}$$

$$\text{Mol wt of SO}_2 = 32.06 + 2(16) = 64.06 \text{ ton/ton} \cdot \text{mol}$$

$$\text{Mass of CaCO}_3 \text{ required} = 12.06 \frac{100.09}{64.06} = 18.84 \text{ tons CaCO}_3\text{/h}$$

$$\text{Mass of CaSO}_3 \text{ produced} = 12.06 \frac{120.14}{64.06} = 22.62 \text{ tons CaSO}_3\text{/h}$$

$$= (22.62 \text{ tons/h})(8766 \text{ h/y})$$

$$= 198{,}300 \text{ tons/year}$$

$$\text{Mass of ash produced} = (131.2 \text{ ton fuel/h})(0.083 \text{ ton ash/ton fuel})(8766 \text{ h/year})$$

$$= 95{,}580 \text{ ton ash/year}$$

(*b*) For the nuclear reactor,

$$\text{Input power} = \frac{P_{\text{th}}}{\eta_{\text{th}}} = \frac{400}{0.32} = 1250 \text{ MW}_{\text{th}}$$

$$\text{Condenser power} = P_c = 1250 - 400 = 850 \text{ MW}_{\text{th}} = mc_p\Delta T$$

$$= (850 \text{ MW})(3{,}412{,}000 \text{ Btu/MW} \cdot \text{h}) = 2.9 \times 10^9 \text{ Btu/h}$$

$$= 18\dot{m} \text{ Btu/h}$$

$$\dot{m} = 2.9 \times 10^9/18 = 1.611 \times 10^8 \text{ lbm water/h}$$

$$\text{Water rate} = \frac{1.611 \times 10^8 \text{ lb/h}}{(8.33 \text{ lb/gal})(60 \text{ m/h})} = 322{,}400 \text{ gal/min}$$

$$\text{Number of U-235 atoms fissioned per year} = (3.1 \times 10^{16} \text{ fissions/MW} \cdot \text{s})(1250 \text{ MW}) \times (3600 \text{ s/h})(8766 \text{ h/year}) \times (1 \text{ atom U-235/fission})$$

$$= 1.223 \times 10^{27} \text{ atoms/year}$$

$$\text{Mass of U-235 fissioned} = \frac{(1.223 \times 10^{27} \text{ atoms/year})(235 \text{ kg/mol})}{6.022 \times 10^{26} \text{ atoms/mol}}$$

$$= 477.1 \text{ kg/year} = 1052 \text{ lbm/year}$$

$$= 0.526 \text{ tons U-235/year}$$

Fission reaction:

$${}_{92}U^{235} + {}_{0}n^{1} \rightarrow {}_{96}U^{236*} \rightarrow 2.5\,{}_{0}n^{1} + \text{fission product 1} + \text{fission product 2} + 200 \text{ MeV}$$

Mass of compound nucleus = 236 amu

Mass of fission neutrons = 2.5 amu

$$\text{Equivalent mass of fission energy} = \frac{200}{931.5} = 0.215 \text{ amu}$$

$$\text{Mass of fission products/Mass of U-235 fissioned} = \frac{236 - 2.5 - 0.2}{235}$$

$$= 0.9928$$

$$\text{Mass of fission products produced per year} = 0.9928(0.526)$$

$$= 0.522 \text{ tons fission products/year}$$

LIST OF SYMBOLS

A	Ash mass fraction of the fuel, kg ash/kg fuel
c_p	Specific heat of cooling water = 1 Btu/lbm · F°(4.187 kJ/kg · C°)
$(HHV)_{kJ}$	Higher heating value of the fuel, kJ/kg fuel
$(HHV)_{Btu}$	Higher heating value of the fuel, Btu/lbm fuel
$\dot{m}$	Mass flow rate of cooling water, kg/s or lbm/h
P_c	Condenser power, MW_{th}
P_e	Electrical power output of the power plant, MW_e
P_s	Stack power, MW_{th}
P_{th}	Thermal power input to the power plant, MW_{th}
$\mathscr{P}_s$	Maximum possible SO_2 generation rate, lbm SO_2/MBtu
R	Allowable SO_2 release rate, lbm SO_2/MBtu
S	Sulfur mass fraction of the fuel, kg S/kg fuel
TDI	Thermal discharge index, MW_{th}/MW_e
η_b	Boiler efficiency, MW_{th}/MW_{th}
η_{th}	Overall thermal efficiency of the power plant, MW_e/MW_{th}

PROBLEMS

6.1. A given power plant with a 600-MW_e output and an overall heat rate of [9100; 9300; 9500; 9700; 9900] Btu/$kW_e \cdot h$ burns Sangamon County, Illinois, coal with moisture and ash fractions of 0.14 and 0.12, respectively. If the plant meets the 1983 EPA emission standards, find the tons of flyash discharged per year and the tons of SO_2 per year legally discharged from the unit, and also determine the collection efficiency required for the electrostatic precipitator. Assume that the plant has a capacity factor of [60; 65; 70; 75; 80] percent and that 70 percent of the ash is trapped in the cyclone burners. If the boiler efficiency is 83 percent and the temperature rise across the condenser is 10C°, find the design flow rate of river water through the condenser in gal/min.

6.2. A large fossil-fuel-fired power station has a total capacity of 3000 MW_e and an overall thermal efficiency of [32; 34; 36; 38; 40] percent. The station burns Hopkins County, Kentucky, coal with moisture and ash fractions of 0.07 and 0.08, respectively. [55; 60; 65; 70; 75] percent of the ash is trapped in the furnace and the balance enters the electrostatic precipitator. Using the 1983 EPA standards, calculate the tons of ash and SO_2 released to the environment per day of full-power operation and also determine the minimum collection efficiency of the electrostatic precipitator. If a tax of 10 cents is levied on each pound of sulfur discharged to the environment, calculate the annual tax for their facility.

6.3. A 2400-MW_e coal-fired power plant burns Belmont County, Ohio, coal ($M = 5$, $A = 12$) with an overall heat rate of [9000; 9200; 9400; 9600; 9800] Btu/kW · h. The plant utilizes dry-bottom, pulverized-coal furnaces in which [14; 16; 18; 20; 22] percent of the ash is trapped in the firebox. If the boilers have a boiler efficiency of 82 percent and the temperature rise of the cooling water through the condenser is [8; 9; 10; 11; 12]C°, find:

(*a*) The maximum flow rate of the condenser cooling water, in gal/min

(*b*) The mass rate of ash, in lb/h, legally discharged to the atmosphere

(*c*) The minimum collection efficiency of the electrostatic precipitator

(*d*) The generation rate of SO_2, in lb/h, in the combustion chamber

(*e*) The mass rate of lime (CaO), in lb/h, that must be added and the mass rate of $CaSO_3$ that must be collected to reduce the SO_2 discharge to the atmosphere to legal 1983 levels

(*f*) The mass rate of CO_2 discharged to the atmosphere, in ton/year

6.4. Find the mass rate, in lb/h, of fission products produced and the cooling-water flow rate, in gal/min, for a nuclear power plant producing [800; 900; 1000; 1100; 1200] MW_e at a thermal efficiency of [33; 34; 35; 36; 37] percent. Assume the cooling water temperature increases 22F° in the condenser.

6.5. A [100; 200; 300; 400; 500]-MW_e coal-fired power plant has a thermal efficiency of [33; 35; 37; 39; 41] percent. The plant burns Polk County, Iowa, coal with moisture and ash fractions of 14 percent and 8 percent, respectively, and 65 percent of the ash is trapped as molten slag at the bottom of the furnace. The plant uses a wet lime-limestone process and an electrostatic precipitator to reduce the sulfur dioxide and ash emissions to 1983 standards. For a 24-h period of full-power operation, determine: (*a*) the mass of ash, in lb/h, that can be discharged to the atmosphere; (*b*) the minimum efficiency of the electrostatic precipitator; (*c*) the mass of SO_2, in lb/h, that can be discharged to the atmosphere; (*d*) the minimum

mass of $CaSO_3$, in lb/h, generated; and (e) the total quantity of cooling water, in L/h required if the water enters at 16°C and leaves at 27°C and the boiler efficiency is 81 percent.

6.6. Consider two power plants, one coal and one nuclear, operating at a thermal power input of [2600; 2900; 3200; 3500; 3800] MW_{th} for 1 year. Assume that both plants have a heat rate of [8750; 9000; 9250; 9500; 9750] Btu/kW · h. The coal-fired plant burns Randolph County, Missouri, coal with $M = 12$ percent and $A = 12$ percent. This plant has a boiler efficiency of 82.5 percent and it employs a wet lime (CaO) process to reduce SO_x emissions to meet the 1983 EPA standards. Find the mass of solid waste generated in each plant, in ton/year, and find the cooling-water flow rate, in gal/min, to the condenser of each unit if the temperature rise of the water is 20°F. If the pressure rise across the pumps supplying the water is 35 ft of water, find the total pumping power for each unit.

6.7. Compare a 1200-MW_e nuclear power plant and a 1200-MW_e coal-fired power system that are designed to operate for 1 year at a capacity factor of [60; 65; 70; 75; 80] percent. Assume that the coal-fired plant has an overall thermal efficiency of [33; 35; 37; 39; 41] percent and burns Macoupin County, Illinois, coal with a moisture and ash content of 12 percent and 15 percent, respectively. The efficiency of the nuclear unit is [30; 31; 32; 33; 34] percent. Fifteen percent of the flyash is collected in the bottom of the boiler of the coal-fired system and the system uses a wet limestone ($CaCO_3$) scrubber to reduce SO_2 emission to the level required by the EPA.

For the coal-fired system, find:

(a) The mass of SO_2 discharged to the atmosphere, in ton/year.
(b) The minimum mass of ($CaCO_3$) required, in ton/year.
(c) The minimum mass of ($CaSO_3$) collected, in ton/year.
(d) The mass of ash discharged to the atmosphere, in ton/year.
(e) The mass of ash collected, in ton/year.
(f) The minimum collection efficiency of the baghouse filter.
(g) The mass of CO_2 (assuming perfect combustion and including that from the scrubber) discharged to the atmosphere, in ton/year.
(h) The design cooling-water flow rate through the condenser, in gal/min, if once-through cooling is used and the water temperature increases 10C°. Assume the boiler efficiency is 82 percent.

For the nuclear plant, find:

(i) The mass of U-235 consumed (in fission and radiative capture), in ton/year.
(j) The mass of fission products generated, in ton/year.
(k) The design condenser cooling-water flow rate, in gal/min, for a 10C° temperature rise across the condenser.

REFERENCES

Aimone, R. J., B. J. Bourke, and J. J. Stuparich: "Experience with Precipitators when Collecting Ash from Low-Sulfur Coals," *Proceedings of the American Power Conference*, vol. 36, pp. 615–620, Illinois Institute of Technology, Chicago, 1974.

Atkins, R. S., and D. H. Klipstein: "Improved Precipitator Performance by SO_3 Gas Conditioning," *Proceedings of the American Power Conference*, vol. 37, pp. 693–700, Illinois Institute of Technology, Chicago, 1975.

Baruch, S. B.: "Trends in Pollution Control at Coal-Burning Power Plants," *Proceedings of the American Power Conference*, vol. 38, pp. 817–824, Illinois Institute of Technology, Chicago, 1976.

Boexmann, J., and H. Heeren: "Surface Condensers for Dry Cooling?" *Power*, vol. 110, no. 4, pp. 80–81, April 1975.

Bond, R. G., and C. P. Straub: *Handbook of Environmental Control, Volume II, Solid Waste*, CRC Press, Boca Raton, Fla., 1973.

"Emissions Control," *Power*, vol. 132, no. 6, pp. B81–90, June 1988.

"EPA Picks Three Winners in SO_2 Removals Race," *Electric Light and Power* (Energy/Generation Edition), pp. 56–58, June 1972.

Faith, W. L.: *Air Pollution Control*, John Wiley and Sons, New York, 1959.

Foster, A. R., and R. L. Wright, Jr.: *Basic Nuclear Engineering*, Allyn and Bacon, Boston, 1973.

Heeney, J. M.: "State of the Art of Flue Gas Desulfurization," Paper FEC-P 143, Faculty Engineering Conference, Sargent and Lundy (Architect Engineering Firm), Mar. 12, 1976, Chicago, Ill.

Helfritch, D. J., and G. H. Beach: "Coal Fired Flyash Control by Fabric Filter Dust Collector," *Combustion*, vol. 48, no. 4, pp. 38–41, October 1976.

Kinch, A. H.: "Retrofitting Wet Scrubbing Systems to Industrial Boilers," *Proceedings of the American Power Conference*, vol. 36, pp. 636–640, Illinois Institute of Technology, Chicago, 1974.

McIlvaine, R. W.: "Flue Gas Desulfurization—Controversial Aspects Examined," *Combustion*, vol. 48, no. 4, pp. 33–37, October 1976.

Skrotski, B. J. A., and W. A. Vopat: *Power Station Engineering and Economy*, McGraw-Hill, New York, 1960.

Tieman, J. W.: "Available and Proposed Devices for the Control of Sulfur Oxide Emissions from Coal Burning Boilers," *Proceedings of the American Power Conference*, vol. 35, pp. 495–503, Illinois Institute of Technology, Chicago, 1973.

CHAPTER 7

PRODUCTION OF MECHANICAL ENERGY

7.1 INTRODUCTION

Mechanical energy is one of the more desirable energy forms in that it can be converted into thermal energy with an efficiency of 100 percent and it can also be converted into electrical energy with a very high conversion efficiency. Unfortunately, the production of mechanical energy from thermal energy is not as easy. There are no large-scale processes or systems for the direct production of mechanical energy from nuclear energy, electromagnetic energy, and chemical energy. It can be argued that muscular contraction is actually the direct conversion of chemical energy into mechanical energy but this is not a large-scale source of mechanical energy at this time.

Essentially all mechanical energy is produced as the result of thermal energy or from the direct conversion of electrical energy. The conversion of thermal energy into mechanical energy is normally accomplished in some sort of a heat engine operating on a thermodynamic heat-engine or power cycle with limited conversion efficiency. The conversion of electrical energy into mechanical energy is usually accomplished as the result of the interacting magnetic fields found in electric motors.

7.2 CONVERSION OF THERMAL ENERGY

7.2.1 Thermodynamic Power Cycles

Almost all of the mechanical energy produced today is produced from the conversion of thermal energy in some sort of a heat engine. The operation of all heat-engine cycles can usually be approximated by an ideal thermodynamic power cycle of some kind. A basic understanding of these cycles can often show the power engineer how to improve the operation and performance of the system. A brief review of the basic laws of thermodynamics, particularly as they apply to power cycles, will be presented in this section.

Any thermodynamic cycle is made up of a series of thermodynamic processes that returns the working fluid to its initial state. During many of these processes, one property is commonly held constant. These include isothermal (constant temperature), isobaric (constant pressure), isometric (constant volume), isentropic (constant entropy), adiabatic (no heat transfer), and throttling (constant enthalpy) processes. All reversible adiabatic processes are isentropic processes.

It is common practice to plot the processes composing the cycle on a graph of property coordinates—usually P-v or T-s plots. When plotting constant-property lines on any property graph, two of the lines, a horizontal line for the ordinate property and a vertical line for the abscissa property, are easily established. Starting with the constant-pressure line and going in a clockwise direction, the order of the other constant-property lines are temperature, enthalpy, entropy, and volume, or: p, T, h, s, v. For a phase change, the isobaric and the isothermal lines have the same slope, while for an ideal gas, the isothermal and the constant-enthalpy lines have the same slope. The various constant-property lines are plotted on the common property coordinates in Fig. 7.1.

For any thermodynamic cycle, the first law of thermodynamics states that the cyclic integral ($\oint$) of work is equal to the cyclic integral of heat, or

$$\oint \delta W = \oint \delta Q \tag{7.1}$$

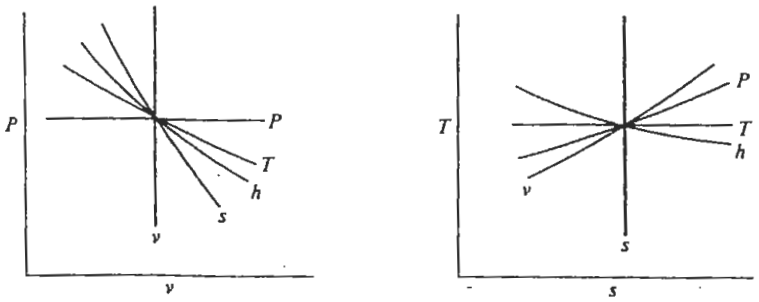


FIGURE 7.1
The relative slope of constant-property lines.

This means that the net work transferred from the cycle (designated as *positive work*) is equal to the net heat transferred to the cycle (designated as *positive heat flow*).

The figure of merit of any thermodynamic cycle is defined as the ratio of the desired energy output to the energy that costs. For a thermodynamic heat-engine cycle, the figure of merit is called the *thermal efficiency*, or η_{th}. The desired energy output is the net work output of the cycle and the energy that costs is the heat added from the high-temperature heat source. Since the net work output, according to the first law of thermodynamics, is equal to the net heat addition, the thermal efficiency becomes:

$$\text{Thermal efficiency} = \eta_{th} = \frac{\text{net work output}}{\text{heat added at high temperature}}$$

$$= \begin{cases} \oint \dfrac{\delta W}{Q_a} & (7.2) \\ \oint \dfrac{\delta Q}{Q_a} & (7.3) \end{cases}$$

The thermal efficiency of any heat-engine cycle should be as high as possible, but according to the second law of thermodynamics, it must be less than 100 percent.

Another important parameter of any heat-engine cycle is the specific work w, which is the net work output per pound of working fluid in the cycle. It is also equal to the areas enclosed by the cycle diagram when it is plotted on either a P–v or a T–s diagram, providing the mass flow of the working fluid is the same throughout the cycle and the processes are reversible. A high value of specific work is desirable because a high value means that a lower working fluid flow rate or a lower engine speed is required to produce a given power output. Thus, when evaluating a particular thermodynamic power cycle, a high value of thermal efficiency and a high value of specific work are desired.

7.2.2 Reversible Heat-Engine Cycles

One result of the second law of thermodynamics states that it is impossible to build a device whose sole effect is to produce work while exchanging heat with a single thermal reservoir at constant temperature. Effectively, this means that it is impossible to construct a heat engine or to develop a power cycle that has a thermal efficiency of 100 percent. This means that at least part of the thermal energy transferred to a power cycle must be transferred to a low-temperature sink.

In the search for the ideal or most efficient heat engine, it turns out that any power cycle that is completely reversible will give the maximum possible thermal efficiency when operating between the given conditions of heat source

and heat sink. There are four phenomena that render any thermodynamic process irreversible. They are:

1. Friction
2. Unrestrained expansion
3. Mixing of different substances
4. Transfer of heat across a finite temperature difference

If a power cycle is to be completely reversible, none of the cycle processes can experience any of these four phenomena.

Of the four phenomena listed above, the one that has the greatest implication for completely reversible power cycles is the stipulation that any reversible heat transfer *must* take place across an infinitesimal temperature difference. Because of the second law of thermodynamics, any heat-engine cycle must have two external heat-transfer processes—heat transfer to the working fluid from the high-temperature source and heat transfer from the working fluid to the low-temperature sink. Since it is illogical to expect that the source and sink temperatures will change at the same rate that the working fluid temperature changes, these two processes *must* be reversible isothermal processes in order for the cycle to be completely reversible. This isothermal restriction on the heat-transfer processes applies only to those processes in which heat is transferred to or from external systems. This limitation does not apply to any heat-transfer process within the engine providing the heat is transferred across an infinitesimal temperature difference in an internal cycle component.

Three ideal power cycles are completely reversible power cycles, called *externally reversible power cycles.* These three ideal cycles are the Carnot cycle, the Ericsson cycle, and the Stirling cycle. All of them are four-process cycles and have two reversible isothermal processes for heat addition and heat rejection to the environment. The ideal thermal efficiency for each of these systems is:

$$\eta_{th,max} = 1 - \frac{T_L}{T_H} \tag{7.4}$$

where T_H and T_L are the temperatures of the heat source and sink, respectively. The thermal efficiency for any heat-engine cycle, operating between the fixed temperature limits T_H and T_L cannot exceed that given by Eq. (7.4).

The Carnot cycle is an externally reversible power cycle and is sometimes referred to as the *optimum power cycle* in thermodynamic textbooks. Actually, it is not better and, in fact, it is not as good as the other two externally reversible power cycles. The Carnot cycle is composed of two reversible isothermal processes and two reversible adiabatic (isentropic) processes. This cycle is plotted on P–v and T–s coordinates in Fig. 7.2. The Carnot cycle is not a practical power cycle because it has so little specific work that any friction in the actual processes would probably "eat up" the net work output and drastically reduce the cycle efficiency.

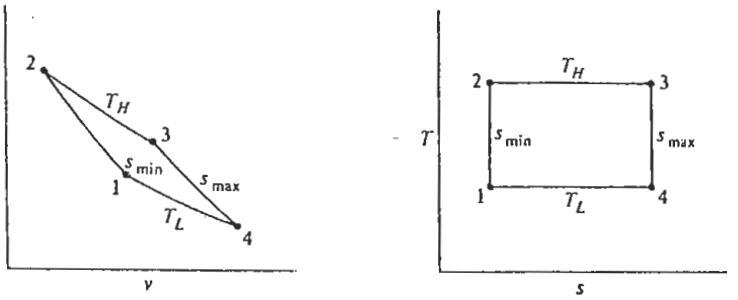


FIGURE 7.2
The Carnot heat-engine cycle.

The Ericsson power cycle is another heat-engine cycle that is completely reversible or "externally reversible." It is composed of two reversible isothermal processes and two reversible isobaric processes, as shown on the P-v and T-s coordinates in Fig. 7.3. Since there is heat transfer in all four processes, the heat transfer in the two isobaric processes must take place in an internal component, called a *regenerator.* A possible system, composed of a compressor, turbine, and

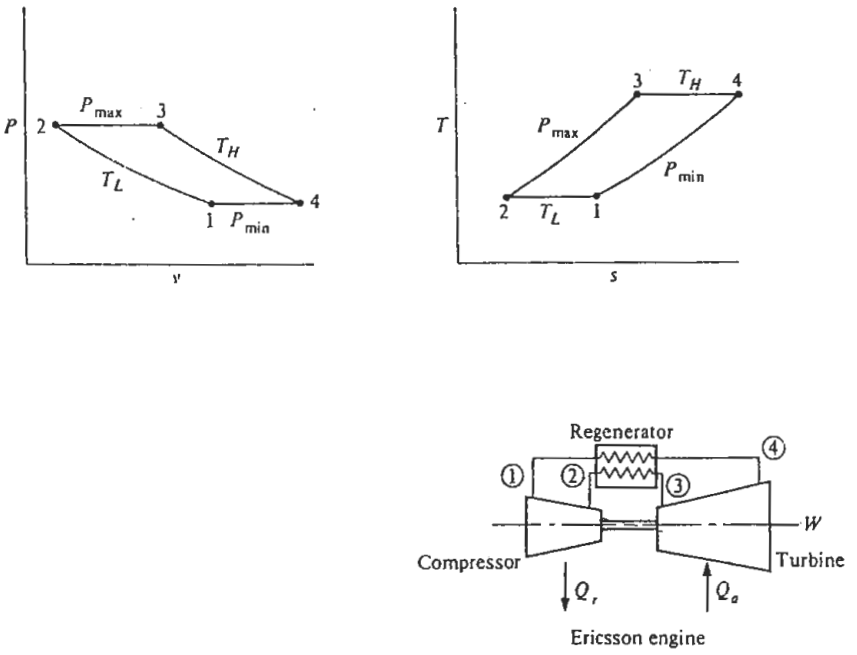


FIGURE 7.3
The Ericsson heat-engine cycle and engine.

counterflow heat exchanger, is also shown in Fig. 7.3. The counterflow heat exchanger serves as the regenerator in this system. The engine shown in Fig. 7.3 is not a practical engine because it is difficult to add and extract heat from the gas as it passes through a compressor and/or turbine. It might be possible to approximate the Ericsson cycle with a series of small compressors with intercoolers and a series of small turbines with reheaters. The ideal thermal efficiency of the reversible Ericsson cycle is the same as that given by Eq. (7.4).

The Stirling cycle is also an externally reversible heat-engine cycle and is the only one of the three ideal power cycles that has seen considerable practical application. It is composed of two reversible isothermal processes and two reversible isometric (constant volume) processes, as shown in Fig. 7.4. It also employs a regenerator for reversible heat transfer to and from the working fluid during the two isometric processes. As was the case for the Ericsson and the Carnot cycles, the thermal efficiency of the ideal Stirling cycle is equal to $1 - T_H/T_L$.

The N. V. Phillips Laboratory of the Netherlands has done a considerable amount of developmental research on Stirling-cycle engines. It has designed two basic Stirling engines—a single-acting, single-cylinder engine as shown in Fig. 7.5, and the double-acting, multiple-cylinder engine which is shown in Fig. 7.6. The earliest Stirling engine was the single-acting engine shown in Fig. 7.5. This engine is an external-combustion system that has two pistons driven by concentric piston rods that are connected to a rhombic drive system. The top piston is simply a displacer piston that drives the gas back and forth through the regenerator. The bottom piston is the power piston. This engine is perfectly balanced and is essentially vibrationless. In the early 1960s, General Motors Corporation, in cooperation with the Phillips Laboratory, conducted a considerable amount of research on this engine, but General Motors is no longer interested in it.

The Phillips Laboratory subsequently designed and developed a double-acting multiple-cylinder engine similar to that shown in Fig. 7.6. The Ford Motor Company tested an experimental engine of this type in a Ford Torino for possible adaptation to automobile propulsion. This engine is an external-combustion

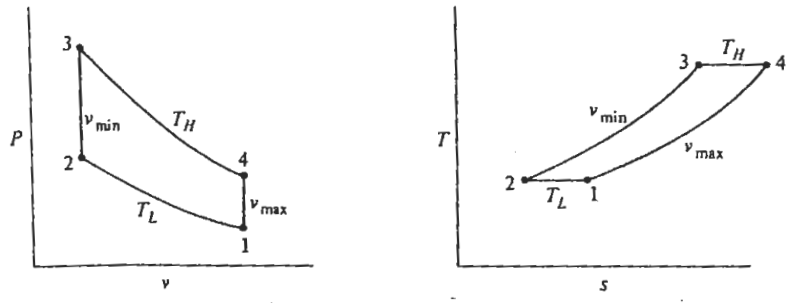


FIGURE 7.4
The Stirling heat-engine cycle.

The single-acting Stirling engine—and how it works

Power piston and displacer piston have coaxial rods connected to different points on the rhomic drive. Rhomic drive is what keeps pistons in proper relation to each other. Each cylinder has its own burner. "Crankcase" is pressurized. At left, all gas is in cool space between pistons. Then power piston moves up, compressing cool gas at constant temperature. Next, displacer comes down, forcing the gas up through regenerator to the hot end, where the heated gas expands, driving the power piston, and also derives some push from the expanding gas. After the power stroke, the displacer returns to top position, returning hot gases via regenerator to cool space.

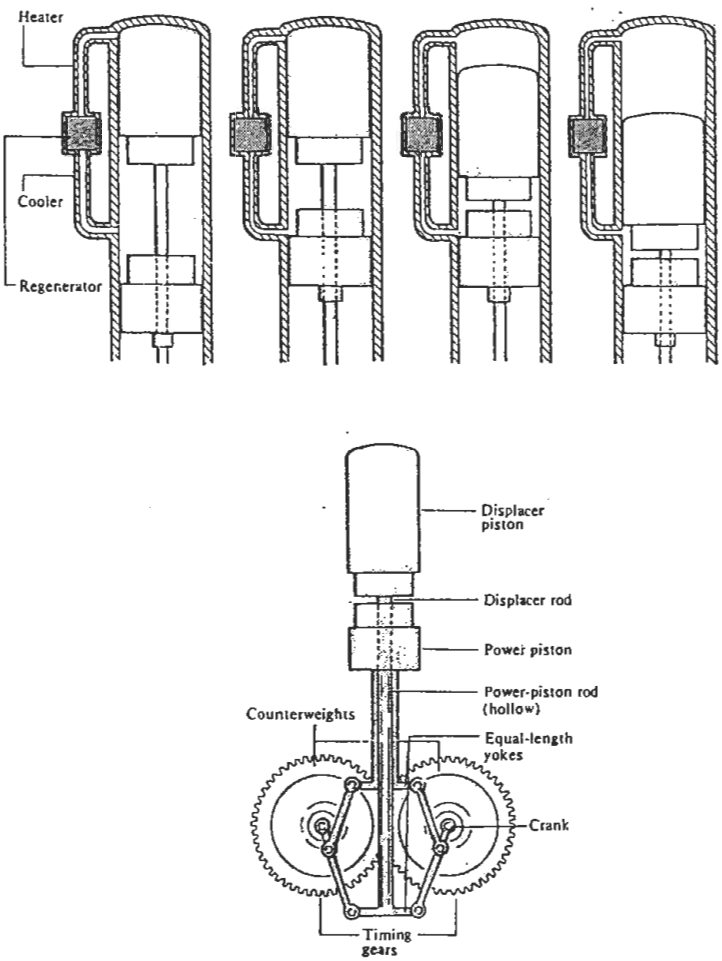
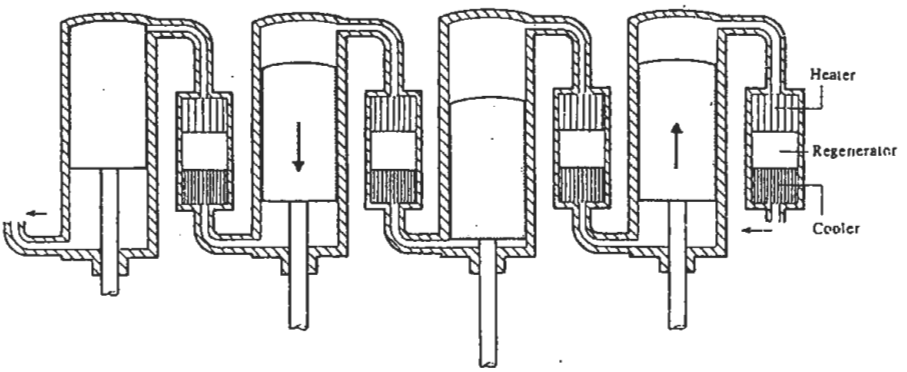


FIGURE 7.5
The single-acting, single-cylinder, Stirling-cycle engine. (*From Popular Science, vol. 202, no. 2, p. 74, February, 1973.*)

The new double-acting Stirling engine—and how it works

Single burner serves four cylinders grouped in a square. Hot end of one cylinder connects to cool end of neighbor via a regenerator that collects heat from hot gases on their way down, restores heat to cool gases on their way up. There's no displacer piston, and cool end is sealed off from crankcase, no longer pressurized. All four piston rods connect to a swashplate. Rods run in guides, do not bend or swing. They exert pressure against the angled plate, transmitting a wedging action causing swashplate to revolve and turn the output shaft. Four pistons, phased 90 degrees apart, deliver one power impulse for every quarter turn of the output shaft.



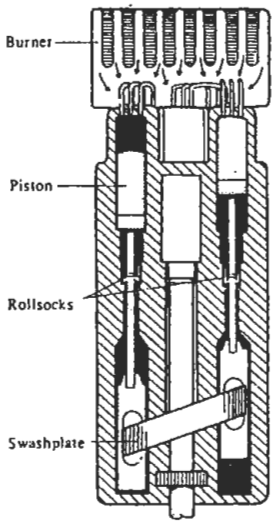


FIGURE 7.6
Double-acting, multiple-cylinder, Stirling-cycle engine. (*From Popular Science, vol. 202, no. 2, p. 75, February, 1973.*)

system that uses hydrogen as the working fluid. The engine power is varied by controlling the hydrogen pressure, which can run as high as 20.68 MPa (3000 psia). Power is transmitted from the pistons to the driveshaft through a swash-plate drive system. The principal reason for being interested in this engine is not because it is much more efficient than conventional engines but because of the promise of low pollution associated with external combustion and the possible utilization of low-grade fuels.

7.2.3 Internal-Combustion Engine Cycles

Internal-combustion (IC) engines cannot operate on an ideal externally reversible heat-engine cycle but they can be approximated by internally reversible cycles in which all the processes are reversible except the heat-addition and heat-rejection processes. In general, the internal-combustion engines are more polluting than external-combustion (EC) engines because of the formation of nitrogen oxides, carbon monoxide, and unburned hydrocarbons. Because of the cyclic nature of engine operation, reciprocating internal engines can operate at extremely high peak temperatures. Consequently, these systems can produce reasonably high values of thermal efficiency.

The Otto cycle is the basic thermodynamic power cycle for the spark-ignition (SI), internal-combustion (IC) engine. It is a four-process cycle and is plotted on P–v and T–s coordinates in Fig. 7.7. Theoretically, a air-fuel mixture is compressed (process 1-2) reversibly and adiabatically (isentropically, $s = s_{min}$) to minimum volume (piston at "top dead center"); the mixture is then ignited (by the spark plug) and the energy is added in a reversible isometric process (process 2-3, $v = v_{min}$); the combustion products then expand in a reversible adiabatic process (process 3-4, $s = s_{max}$); and the heat is rejected to the atmosphere (exhaust and intake strokes) in a reversible isometric process (process 4-1, $v = v_{max}$). This last process actually takes place in the atmosphere as the burned gases are expelled and are replaced by a fresh charge of fuel and air.

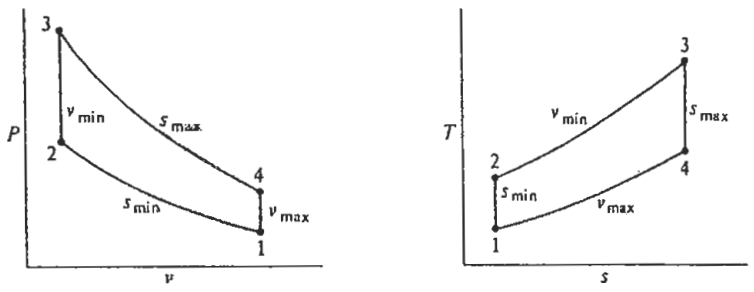


FIGURE 7.7
The Otto heat-engine cycle.

The important Otto-cycle engine parameter is the *compression ratio*, or r_v, which is the ratio of maximum to minimum volumes:

$$r_v = \frac{v_{max}}{v_{min}} = \frac{v_1}{v_2} = \frac{v_4}{v_3} \tag{7.5}$$

For the air-standard Otto cycle, which is an ideal Otto cycle that uses cold air as the working fluid, the thermal efficiency can be shown to be equal to:

$$\eta_{th} = 1 + \frac{\text{heat rejected } (-)}{\text{heat added}} = 1 + \frac{Q_r}{Q_a} = 1 + \frac{mc_v(T_1 - T_4)}{mc_v(T_3 - T_2)}$$

$$= 1 - \frac{T_1}{T_2} = 1 - r_v^{(1-k)} \tag{7.6}$$

where k is the ratio of specific heats, c_p/c_v.

If the Otto cycle was completely reversible, the thermal efficiency would be $1 - T_1/T_3$ instead of the lower value of $1 - T_1/T_2$. Since k is always greater than unity, the thermal efficiency can be improved by increasing the compression ratio and/or by using a working fluid with a high value of k. Since this is an internal-combustion system and an air-fuel mixture and/or combustion products must be used as the working fluid, k is essentially fixed at a value close to that for a diatomic gas ($k = 1.4$).

Effectively, the only way to increase the thermal efficiency of the ideal Otto cycle is to increase the compression ratio. There is a limit, however, to the maximum value of compression ratio that can be employed in an actual engine. This limit is caused by the premature ignition of the fuel-air mixture before the flame front, initiated by the spark plug, reaches the unburned charge. The premature ignition of the unburned fuel charge produces a pressure imbalance that causes detonation or "ping." Detonation in a reciprocating engine can be very destructive to the engine.

Prior to 1972, some stock automobile engines had compression ratios as high as 12.5, but these engines had to use "premium" or high-octane gasoline. Since 1972, the increased concern about automobile emissions and pollution has brought about the development of Otto-cycle engines with compression ratios around 9.

The other principal internal-combustion heat-engine cycle is the Diesel cycle, which is the ideal power cycle for the compression-ignition (CI), internal-combustion (IC) engine—commonly called the *diesel engine*. In this system, atmospheric air is compressed to a very small volume, generating high pressures and temperatures. At or near top dead center (minimum volume), diesel fuel is injected into the hot air and this fuel, unlike the spark-ignition fuel, is designed to burn within a short time after it is injected into the cylinder. The combined effect of burning fuel and increasing volume makes the process approach an isobaric process. At some point during the power stroke, called the *fuel cutoff*, the fuel addition (heat addition) is terminated and the piston continues the expansion process adiabatically until it reaches bottom dead center (maximum

volume). At this point, the exhaust and intake strokes essentially produce a constant-volume heat-rejection process that takes place in the atmosphere.

The ideal Diesel cycle is a four-process cycle that is composed of a reversible adiabatic ($s = s_{min}$) compression process (process 1-2); a reversible isobaric ($p = p_{max}$) heat-addition process (process 2-3); a reversible adiabatic ($s = s_{max}$) expansion process (process 3-4); and a reversible isometric ($v = v_{max}$) heat-rejection process (process 4-1). The Diesel cycle is plotted on P-v and T-s coordinates in Fig. 7.8.

The Diesel cycle has two important engine parameters. One of these is the compression ratio r_v, which was defined earlier as the ratio of maximum-to-minimum volumes. The other is the cutoff ratio r_{cf}, which is the ratio of the volume at the end of fuel addition (fuel cutoff, state 3) to the minimum volume (state 2):

$$r_{cf} = \frac{\text{volume at the end of fuel addition}}{\text{minimum volume}} \tag{7.7}$$

The thermal efficiency of the air-standard Diesel cycle is:

$$\eta_{th} = 1 + \frac{\text{heat rejected } (-)}{\text{heat added}} = 1 + \frac{Q_r}{Q_a} = 1 + \frac{mc_v(T_1 - T_4)}{mc_p(T_3 - T_2)}$$

$$= 1 - \frac{r_{cf}^k - 1}{kr_v^{(k-1)}(r_{cf} - 1)} \tag{7.8}$$

Although there are three cycle parameters in Eq. (7.8), that is, k, r_v, and r_{cf}, k is fixed at a value of about 1.4 as this system is only employed for internal-combustion systems. Effectively, only the compression ratio and the cutoff ratio can be altered in the engine design.

Since only air is compressed in the diesel engine (process 1-2), there is no problem with respect to detonation as in the Otto-cycle engine and these systems operate at much higher compression ratios than the spark-ignition engines. Where most spark-ignition engines have compression ratios of 6 to 12, the compression-ignition engines have compression ratios of 18 to 25. For the same compression

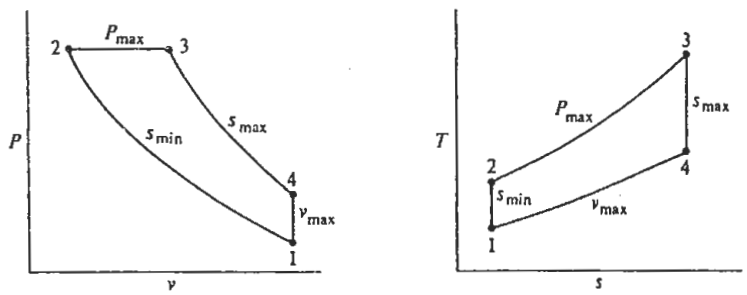


FIGURE 7.8
The Diesel heat-engine cycle.

ratio, the Otto cycle is more efficient than the Diesel cycle, but the diesel engine operates at much higher compression ratios.

The cutoff ratio of a Diesel cycle must be greater than unity but it should be as low as possible to attain a high value of thermal efficiency. Although a lower cutoff ratio does improve the thermal efficiency, which is desirable, it also lowers the value of the specific work, which is undesirable. Consequently, the value of the cutoff ratio must be optimized to give a high thermal efficiency but also to yield a reasonable value of specific work.

There are several other minor internal-combustion engine cycles, and some are shown in Fig. 7.9. The limited-pressure cycle, sometimes called the *combined cycle*, is a five-process cycle which is really a combination of the Otto and the Diesel cycles in that the heat-addition process is composed of an isometric and an isobaric process. If an actual Otto or Diesel cycle is to be approximated by an ideal thermodynamic power cycle, the limited-pressure cycle will probably give the best fit to the actual cycle.

The Atkinson cycle is an ideal internal-combustion engine cycle which is almost identical to the Otto cycle except that the heat-rejection process is a reversible isobaric process instead of an isometric process. This means that the hot exhaust gas must expand to atmospheric pressure in the prime mover before it is exhausted. Since the Atkinson cycle has a greater specific work (larger cycle diagram) than a comparable Otto-cycle engine with the same minimum volume and heat addition, it has a higher thermal efficiency. This cycle can be approximated by a combination of a free-piston compressors and a gas-turbine prime mover, as shown in Fig. 7.10.

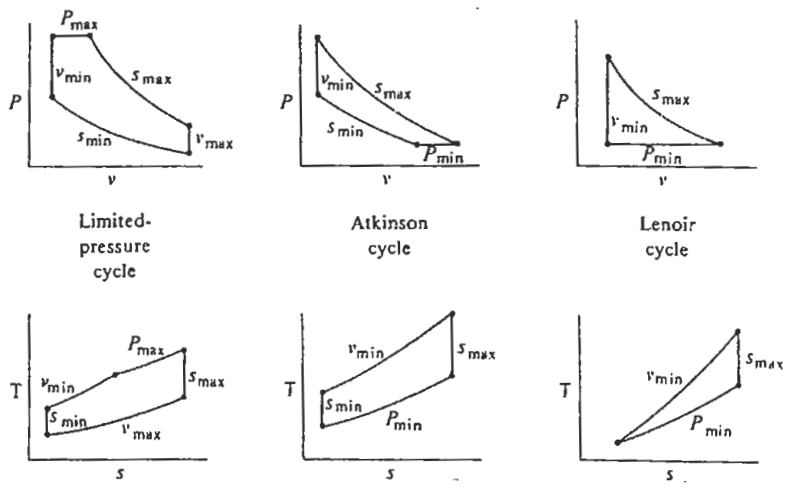


FIGURE 7.9
Secondary internal-combustion, thermodynamic, heat-engine cycles.

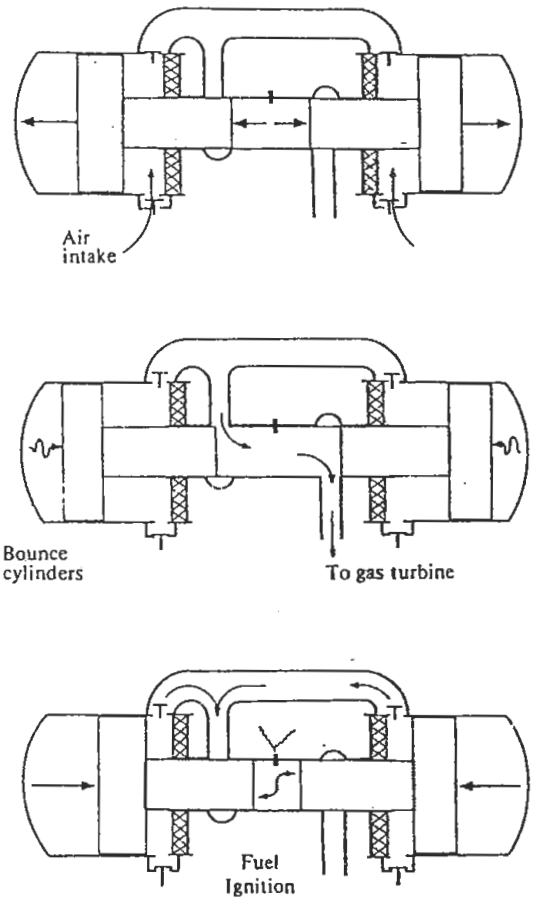


FIGURE 7.10
A free-piston compressor and gas-turbine, prime mover operating on the Atkinson power cycle. (*From Skrotzki and Vopat, 1960.*)

The Lenoir cycle is a three-process cycle that is the ideal thermodynamic power cycle for the oldest internal-combustion engine—the noncompression engine. In the noncompression engine, a charge of natural gas and air is drawn into the cylinder. Partway through the intake stroke, and intake valve is closed and the fuel-air mixture is ignited, producing essentially an isometric heat-addition process. The hot combustion products are then allowed to expand adiabatically to atmospheric pressure and the spent exhaust gases are then discharged to the atmosphere during the exhaust stroke. These engines were used to pump water out of the coal mines in the late nineteenth century.

The Lenoir cycle is also the ideal heat-engine cycle for the pulse-jet engine used by the Germans in the V-1 "buzz bomb" of World War II. This engine consists of a series of reed valves, a fuel-injection system, and igniter, and an expansion nozzle. This system is shown in Fig. 7.11. Although the Lenoir cycle

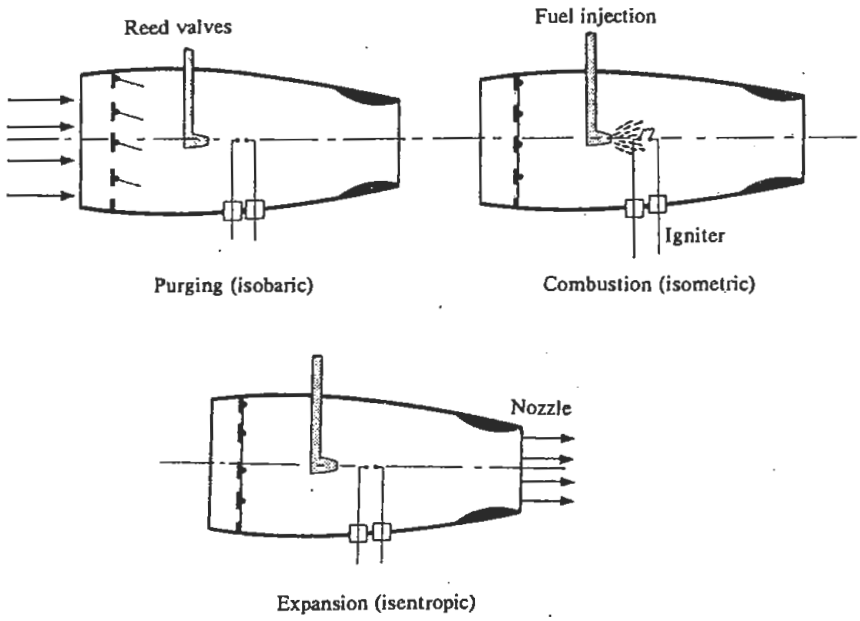


FIGURE 7.11
The pulse-jet engine, which was used to power the V-I "buzz bomb" of World War II.

is a very simple cycle, it does not find widespread application today because it has very low values of specific work and thermal efficiency.

7.2.4 Internal-Combustion Engines

Most of the internal-combustion engines are reciprocating engines with pistons and cylinders. There are several ways of classifying them but the two common systems are according to the order of firing and according to cylinder arrangement. The two basic types of ignition or firing systems are the four-stroke-cycle engines, commonly called *four-cycle engines*, and the two-stroke-cycle engines, commonly called *two-cycle engines*.

The four-stroke-cycle engine requires four full piston strokes to complete one cycle. The four strokes are shown in Fig. 7.12 and consist of the intake stroke (1) with the intake valve open, the compression stroke (2) with all valves closed, ane ignition and power stroke (3) with all valves closed, and the exhaust stroke (4) with the exhaust valve open.

The two-stroke-cycle engine combines the four strokes required to complete a cycle in a four-stroke-cycle engine into just two strokes. A typical two-stroke-cycle engine is shown in Fig. 7.13. As the piston moves down the cylinder on the power stroke, the exhaust port is uncovered first and the pressurized exhaust gas starts to escape to the atmosphere. While the piston moves down the cylinder, it

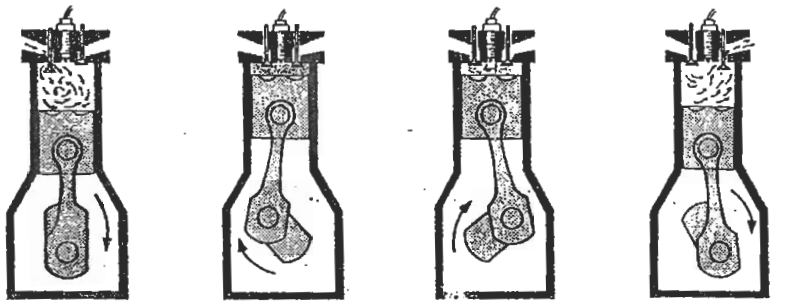


FIGURE 7.12
The four-stroke cycle, compression-ignition, internal-combustion engine.

also compresses the air-gas-oil mixture in the crankcase. As the piston continues downward, it uncovers the intake port, allowing the compressed fuel-air mixture to enter the cylinder from the crankcase. On the compression (upward) stroke, the piston covers the intake port, then the exhaust port, and compresses the remaining fuel charge until the spark plug ignites the mixture slightly before top dead center. The piston is then forced down by the expanding combustion products in another power stroke. When the piston is near top dead center, the carburetor intake port is uncovered and an additional charge of air, fuel, and oil is added to the crankcase. In this system, oil is mixed with the gasoline to provide

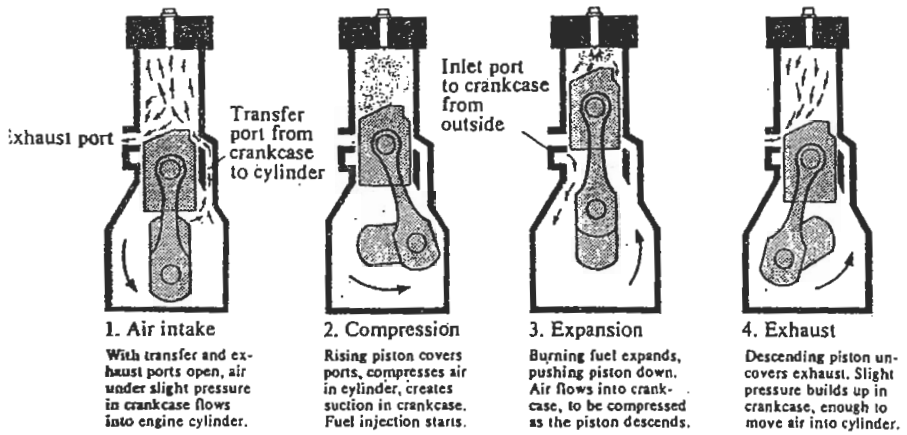


FIGURE 7.13
A typical two-stroke-cycle, compression-ignition, internal-combustion engine.

lubrication for the crankshaft and rod bearings. In this engine, every cylinder fires every revolution.

The four-stroke-cycle engine has a number of advantages over the usual two-stroke-cycle engine, including better fuel economy, better lubrication, and easier cooling. The two-stroke-cycle engine has a number of advantages, including fewer moving parts, lighter weight, and smoother operation. It should be pointed out, however, that there are some two-stroke-cycle engines that have valves and separate lubrication systems.

Figure 7.14 shows schematic diagrams of some of the different cylinder arrangements for reciprocating engines. The vertical in-line engine is commonly used today in four- and six-cylinder automobile engines. The V-engine is commonly employed in eight-cylinder and some six-cylinder automotive engines and these systems are commonly called *V-8* or *V-6 engines.* The horizontal engine is essentially a V-engine with 180° between the opposed cylinders. This system was used as the four-cylinder, air-cooled engine that powered the Volkswagon "bug."

The opposed-piston engine consists of two pistons, two crankshafts, and one cylinder. The two crankshafts are geared together to assure synchronization. These opposed-piston systems are often employed in large diesel engines. The

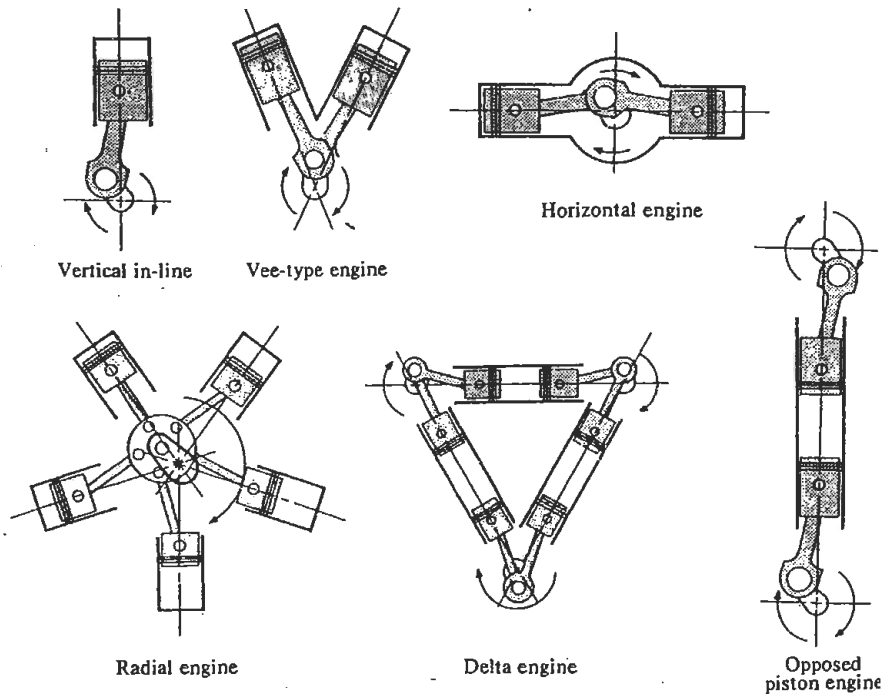


FIGURE 7.14
Various cylinder arrangements for reciprocating engines.

delta engine is composed of three opposed-piston cylinders connected in a delta arrangement. These systems have found application in the petroleum industry.

The radial engine is composed of a ring of cylinders in one plane. One piston rod, the "master" rod, is connected to the single crank on the crankshaft and all the other piston rods are connected to the master rod. If the engine is a four-stroke-cycle engine, each bank of cylinders must contain an odd number of cylinders to obtain balanced firing. These engines are commonly constructed with several banks of cylinders to increase the power output. Radial engines have a high power-to-weight ratio and were commonly employed in large aircraft before the advent of the turbojet engine.

In some of the early radial engines used to power World War I fighter planes, the crankshafts were fastened to the aircraft, and the cylinder bank, with the propellor attached, revolved. Such engines were commonly called *rotary engines.* These planes gave the pilots some interesting handling problems because of the gyroscopic effects.

When the term "rotary engine" is used today, it implies something other than a radial engine with a stationary crank. The term "rotary" is essentially applied to any internal-combustion system that is anything other than a reciprocating engine, except for the gas turbine.

The most famous rotary engine in use at this time is the Wankel engine. Shown in Fig. 7.15, it utilizes a triangular-shaped lobe as the rotating member. Power is transferred from the rotating lobe to the driveshaft, whose angular velocity is 3 times that of the rotating lobe. This system is inherently a high-speed engine with the driveshaft turning at 3000 to 8000 r/min. While this engine is lighter, has fewer moving parts, and is cheaper to build than a comparable reciprocating engine, the sealing problems, leading to poor fuel economy, have reduced interest in the Wankel engine.

A number of different rotary engines have been proposed and some of them, shown in Fig. 7.16, have been built and operated. The Tschudi engine has a torus-shaped cylinder with curved pistons. The Selwood engine is a rotary engine that also has curved cylinders and pistons in the plane of the crankshaft. The shaft of this engine is stationary and contains the carburetor while the outer housing rotates. The Mallory-vane engine operates like a reversed sliding-vane air compressor. The Bricklin rotary engine is a V-engine with fixed floating pistons. There are many other proposed rotary engines but, so far, none of them appear to be significantly better than the typical reciprocating engine.

7.2.5 Engine Performance

There are several performance factors that are common to all engines and prime movers. One of the main operating parameters of interest is the actual output of the engine. The brake horsepower (Bhp) is the power delivered to the driveshaft of the engine. This power is normally measured by means of some sort of dynamometer such as an electric dynamometer (generator or eddy-current), a water brake or a friction (prony) brake. The brake horsepower is usually measured

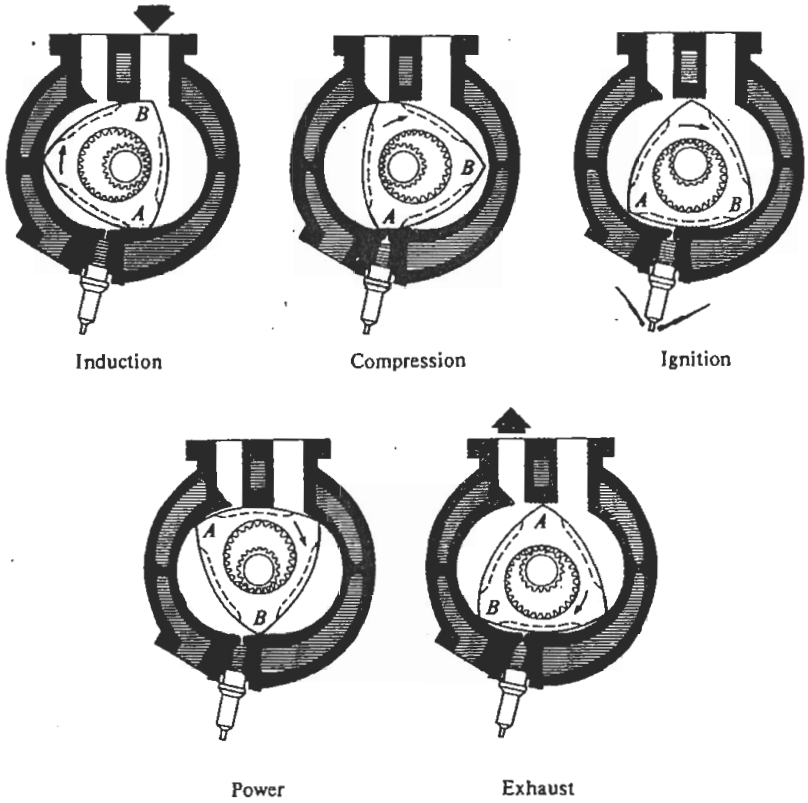


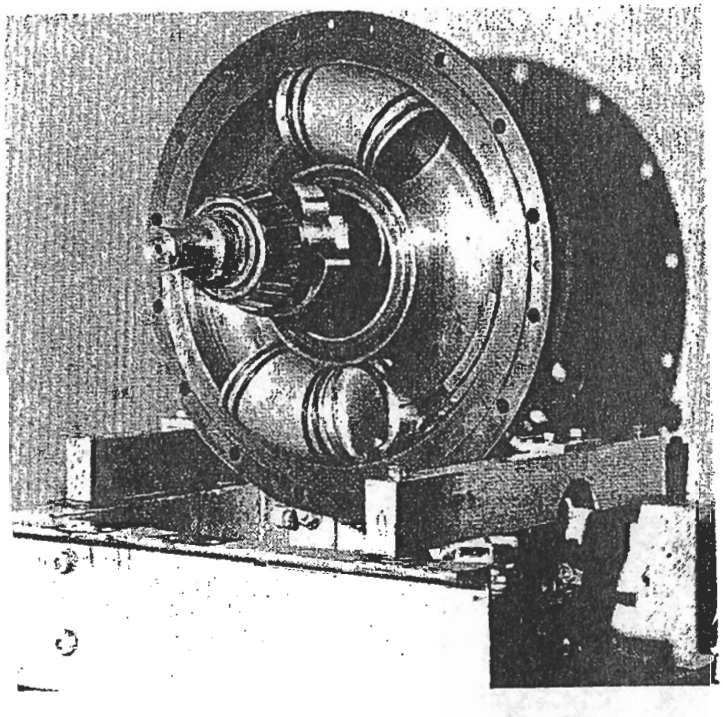
FIGURE 7.15
The Wankel rotary internal-combustion engine.

by determining the reaction force on the dynamometer and using the following equation:

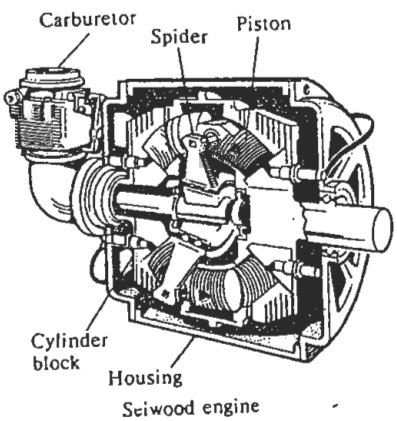
$$\text{Bhp} = \frac{2\pi FRN_d}{33{,}000} \tag{7.9}$$

where F is the net reaction force of the dynamometer, in pounds-force (lbf), R is the radius arm, in feet, and N_d is the angular velocity of the dynamometer, in revolutions per minute. For an energy-absorbing machine, like a pump or compressor, the brake horsepower is the power actually supplied to the shaft of the machine.

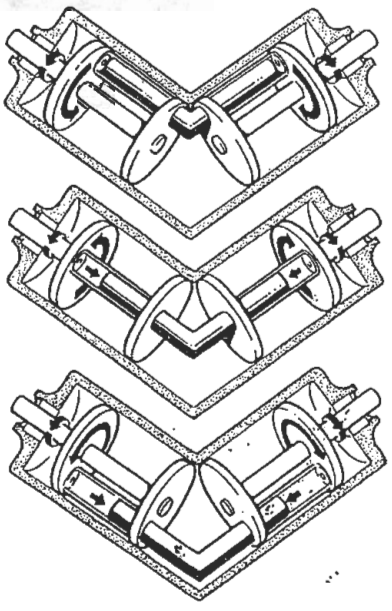
FIGURE 7.16
Some unusual rotary engines. (*From Walton, 1968.*)



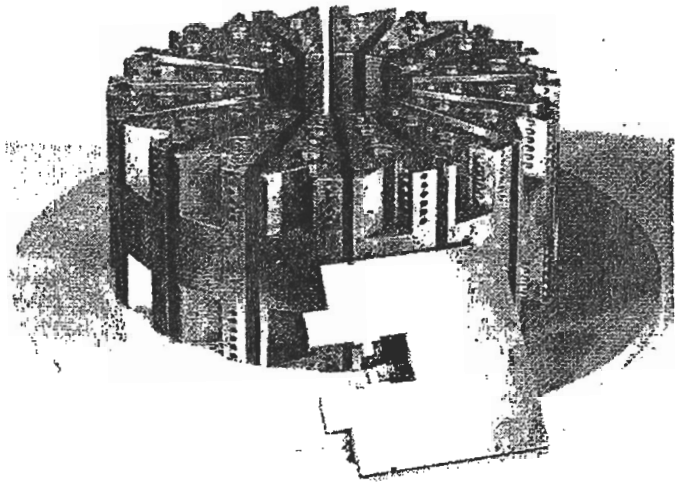
Tschudi engine

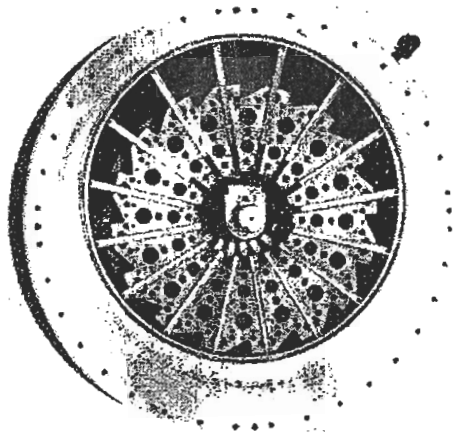


Selwood engine



Bricklin-Turner engine





Mallory engine

FIGURE 7.16 (*Continued*)

Another power term associated with any fluid machinery is the power delivered to or by the working fluid, called the *indicated power* because it used to be determined by the use of an indicator diagram. For a prime mover, the *indicated horsepower* (Ihp) is the power delivered to the piston or impeller by the working fluid. For a compressor or pump, the indicated horsepower is the power delivered to the working fluid by the piston or impeller. The difference

between the indicated and brake horsepowers is the power dissipated in the machine and is called the *friction horsepower* (Fhp). For the prime mover,

$$\text{Ihp} = \text{Bhp} + \text{Fhp} \tag{7.10}$$

For a pump or a compressor, on the other hand,

$$\text{Bhp} = \text{Ihp} + \text{Fhp} \tag{7.11}$$

The mechanical efficiency η_m of a machine is the measure of the machine's ability to transfer mechanical energy. As is the case for most efficiencies, the mechanical efficiency is the ratio of the output power to the input power. For a prime mover, such as an engine or a turbine,

$$\eta_m = \frac{\text{Bhp}}{\text{Ihp}} \tag{7.12}$$

For a pump or compressor,

$$\eta_m = \frac{\text{Ihp}}{\text{Bhp}} \tag{7.13}$$

The mean effective pressure (mep) is a parameter that is applied only to reciprocating engines and is effectively the average gage pressure acting on the piston during the power stroke. Perhaps a better definition of the mean effective pressure is to define it as the net work output, in inch · pounds-force per cubic inch of piston displacement. For a closed system, like a reciprocating engine during the power stroke, the reversible specific work is equal to $\int p\,dv$. If the effective average pressure or mean effective pressure is used, the work becomes equal to (mep) $\int dV$ or simply (mep)(V_{dis}), where V_{dis} is the piston displacement, or

$$V_{\text{dis}} = \frac{\pi(\text{bore})^2(\text{stroke})}{4} \tag{7.14}$$

Two mean effective pressures are commonly used—the brake mean effective pressure (Bmep), which is obtained from the brake horsepower, and the indicated mean effective pressure (Imep), which is obtained from the indicated horsepower. For a particular engine, the relationship between the mean effective pressures and the power is:

$$\text{Horsepower (Bhp or Ihp)} = \frac{(\text{Bmep or Imep})(V_{\text{dis}})(N_p)}{33{,}000} \tag{7.15}$$

where N_p is the number of power strokes per minute, or,

$$N_p = \frac{CN_e}{\zeta} \tag{7.16}$$

where C is the number of cylinders in the engine, N_e is the revolutions per minute of the engine, and ζ is the equal to 1 for a two-stroke-cycle engine and 2 for a four-stroke-cycle engine.

The brake specific fuel consumption (Bsfc) of an engine is a measure of the fuel economy and is normally expressed in units of mass of fuel consumed per unit energy output. In the United States, the common units of the brake specific fuel consumption are pounds-mass per Bhp · hour. The brake specific fuel consumption can be determined from the following equation:

$$\text{Bsfc} = \frac{(\text{fuel rate, lbm/h})}{\text{Bhp}} \tag{7.17}$$

The brake thermal efficiency of an engine, η_{th}, unlike power plants, is usually based on the lower heating value (LHV) of the fuel. The relationship between efficiency and the brake specific fuel consumption is

$$\eta_{th} = \frac{2545}{(\text{Bsfc})(\text{LHV})} \tag{7.18}$$

where the lower heating value is in Btu/lbm.

Another parameter associated with internal-combustion engines is the volumetric efficiency η_v of the engine. The volumetric efficiency is sometimes referred to as a measure of the ability of an engine to "breathe" and can be determined from the following equation:

$$\eta_v = \frac{\text{volume of air brought into the cylinder at ambient conditions}}{\text{piston displacement}} \tag{7.19}$$

The volumetric efficiency of an engine can exceed 100 percent if the system employs a supercharger or turbocharger. Use of these systems increases the engine output and performance.

7.2.6 External-Combustion Systems

External-combustion power systems have several advantages over internal-combustion systems. In general, they are less polluting. The primary pollutants from internal-combustion engines are unburned hydrocarbons, carbon monoxide, and oxides of nitrogen. In the external-combustion engines, the CH_x and CO can be drastically reduced by carrying out the combustion with excess air and the NO_x production can be markedly reduced by lowering the combustion temperature. By burning the fuel with excess air, more energy is released per pound of fuel.

Two other advantages of the external-combustion systems is that they can utilize less expensive fuels and different working fluids. All internal-combustion engines are limited to the use of air or air and fuel vapor and/or combustion products as the working fluid. While most internal-combustion engines are limited to the use of highly refined, expensive hydrocarbon fuels, the external-combustion systems can use coal, residual fuel oil, organic refuse (biomass), or any combustible fuel. These units can also utilize nuclear or solar energy as the energy source.

There are essentially three general ideal external-combustion engine cycles. The Stirling cycle and the Brayton cycle are two ideal gas-power cycles that can

operate with external combustion. All vapor power cycles are cycles that can operate only with external combustion. The Stirling cycle is also a cycle that can operate only with external combustion and this system was discussed earlier in the section on externally reversible power systems.

The Brayton power cycle is the ideal thermodynamic power cycle for the gas-turbine or turbojet engines. This is the only major power cycle that can operate as either an internal- or external-combustion engine. The Brayton cycle is a four-process cycle and is shown in Fig. 7.17. In the ideal Brayton cycle, the working fluid is compressed reversibly and adiabatically (isentropically, $s = s_{min}$) in the compressor (process 1-2); heat is added in a reversible isobaric ($p = p_{max}$) process (process 2-3) in a combustion chamber or heat exchanger; the hot gas expands reversibly and adiabatically (isentropically, $s = s_{max}$) in the turbine (process 3-4); and then the heat is rejected in a reversible isobaric ($p = p_{min}$) process in the atmosphere or in a heat exchanger (process 4-1).

The Brayton cycle may be classed as either open or closed. In the open cycle, the working fluid is atmospheric air and the heat-rejection process occurs in the atmosphere as the turbine exhaust is discharged into the atmosphere. In the closed cycle, any working fluid can be employed and the heat-rejection process

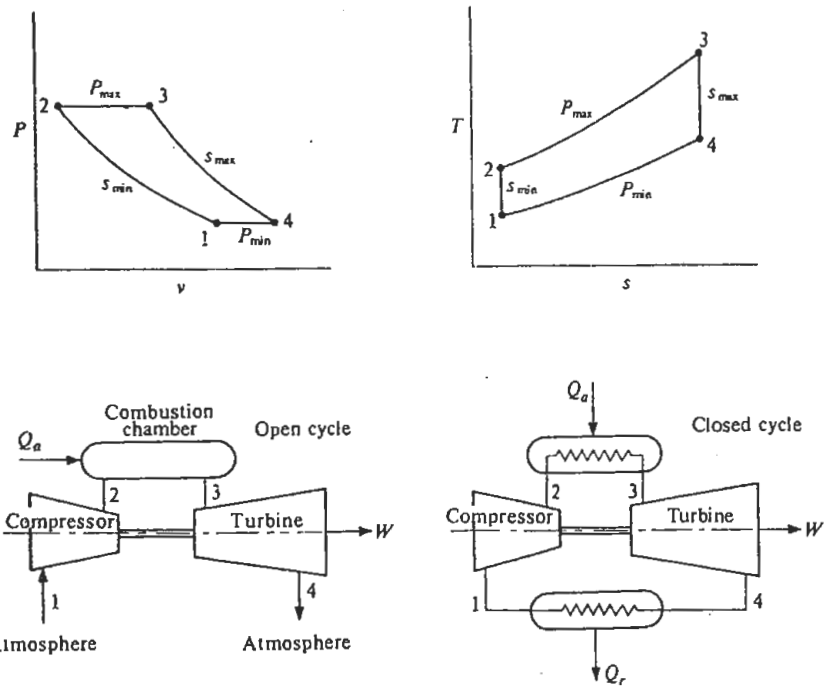


FIGURE 7.17
The Brayton power cycle and systems.

is accomplished in a heat exchanger. In this system, the same working fluid is cycled continuously.

The turbojet engine, in which part of the expansion process occurs in a nozzle that expands the hot gas into the atmosphere to produce thrust, must operate on the open cycle. All internal-combustion, Brayton-cycle engines must operate on the open cycle. It is also possible to use external-combustion systems using low-grade fuels or nuclear or solar heat that operate on the open cycle, but the working fluid must be atmospheric air.

Most external-combustion, Brayton-cycle systems are closed cycles in which the heat is added to the working fluid in a heat exchanger and the heat is rejected from the working fluid in another heat exchanger, as shown in Fig. 7.17. The closed cycle has the advantage that it can employ any gas as the working fluid.

The important cycle parameter for the simple Brayton-cycle engine is the compressor pressure ratio r_p, which is the ratio of maximum-to-minimum system pressures. The thermal efficiency of the simple Brayton cycle is

$$\eta_{th} = 1 + \frac{Q_r}{Q_a} = 1 + \frac{\dot{m}c_p(T_1 - T_4)}{\dot{m}c_p(T_3 - T_2)}$$

$$= 1 - \frac{T_1}{T_2} = 1 - r_p^{(1-k)/k} \tag{7.20}$$

There are two parameters in this equation, k and r_p, and an increase in either improves the efficiency of the simple Brayton cycle.

The so-called "noble" gases, such as helium, neon, argon, etc., are monatomic gases and consequently have the highest value of the ratio of specific heats, k, of any gaseous working fluid. The specific-heat ratio for these gases is $\frac{5}{3}$, while that for a diatomic gas, such as air, N_2, CO, etc., is $\frac{7}{5}$, and that for a triatomic gas such as H_2O, CO_2, etc., is $\frac{4}{3}$. The noble gases also make excellent working fluids because they produce no corrosion. Helium has the best thermal properties of any gas other than hydrogen.

Increasing the compressor pressure ratio r_p increases the thermal efficiency of the simple Brayton cycle and also increases the compressor discharge temperature. If the turbine inlet temperature is fixed because of turbine material limitations, an increase in the compressor pressure ratio may reduce the specific work of the cycle, requiring a higher gas-flow rate for the same power output. Forcing the compressor to operate over a wider range of pressures means that the mechanical efficiency of the compressor is probably reduced, and this can make the actual cycle less efficient.

There are several ways to improve the thermal efficiency of the simple Brayton cycle but they all involve the use of a heat-recovery device, called a *regenerator*. The regenerator is essentially a counterflow heat exchanger in which heat is transferred from the hot turbine exhaust gas to the compressor discharge gas. The regenerative Brayton cycle is shown schematically in Fig. 7.18 and is plotted on a T-s diagram in that figure. In the regenerator, the compressor gas can be heated to some temperature T_a, and the turbine discharge gas can be

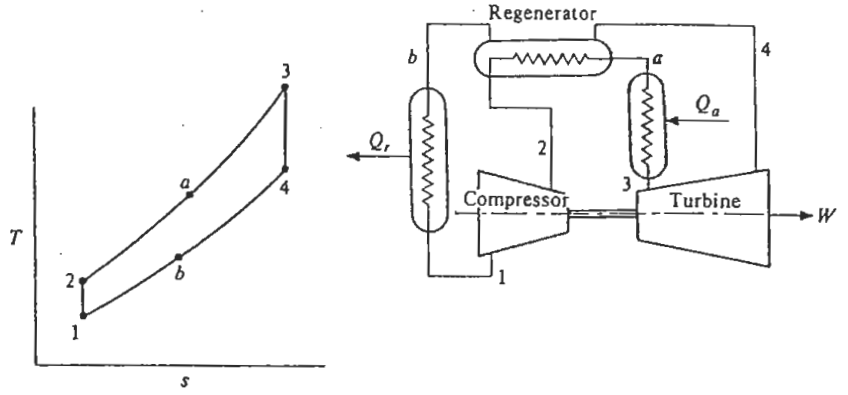


FIGURE 7.18
The regenerative Brayton power cycle and system.

cooled to temperature T_b. Theoretically, T_a can approach the turbine exhaust temperature T_4, and the value of T_b can approach the compressor discharge temperature T_2. The performance parameter of the regenerator is called the *regenerator effectiveness*, or ε_r, which is defined as the ratio of the actual heat transfer in the exchanger divided by the maximum possible heat transfer:

$$\varepsilon_r = \frac{T_4 - T_b}{T_4 - T_2} = \frac{T_a - T_2}{T_4 - T_2} \tag{7.21}$$

The thermal efficiency of the regenerative Brayton cycle is given by the following equation:

$$\eta_{th} = 1 - \frac{T_b - T_1}{T_3 - T_a} = 1 - \frac{T_b - T_{min}}{T_{max} - T_a} \tag{7.22}$$

If the regenerator effectiveness is 100 percent, T_a and T_b become equal to T_4 and T_2, respectively, and the above equation reduces to:

$$\eta_{th} = 1 - \frac{T_1}{T_3}(r_p)^{(k-1)/k} = 1 - \frac{T_{min}}{T_{max}}(r_p)^{(k-1)/k} \tag{7.23}$$

The efficiency of the regenerative Brayton cycle can be increased by increasing the maximum temperature and/or by decreasing the minimum temperature, by decreasing the compressor pressure ratio r_p, and/or by using a gas with a low value of k. These last two parameters, r_p and k, have the opposite effect on this cycle that they have on the simple Brayton cycle.

The Brayton-cycle efficiency can be increased by using multistage compression with intercooling, providing a regenerator is also used. The use of multistage compression with intercooling decreases the required compressor work and increases the specific work for this cycle. This system is shown schematically along with a plot on a T–s diagram in Fig. 7.19. The use of multistage compression

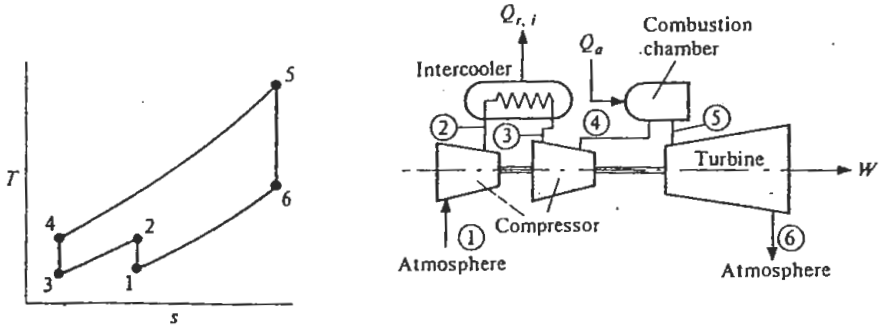


FIGURE 7.19
The Brayton power cycle and engine with multistage compression and intercooling.

with intercooling produces a lower compressor discharge temperature than that resulting from a single-state compressor. Consequently, more heat is required to heat the gas to the turbine-inlet temperature and, unless part of this energy is supplied by a regenerator, the ideal cycle efficiency will be lower than that of the comparable simple cycle. In the actual cycles, however, the use of multistage compression with intercooling may actually improve the efficiency of the simple cycle because of the improved compressor efficiency over the smaller pressure range.

For a two-stage compression process, there is some optimum interstage pressure that produces the minimum amount of compressor work. If the change in kinetic and potential energy is negligible, the ideal compressor work is equal to $-\int_1^2 V\,dp$. This means that an isothermal ($T = C$) compression process gives a lower value of compressor work than an isentropic compression process because of the less-negative slope of the isothermal line on the P–v diagram, as shown in Fig. 7.20. The actual ideal compression process approaches a polytropic process where pv^n is a constant and n ranges from a value of k for an isentropic process to 1.0 for an isothermal process. If the compression process is carried out in two stages with intercooling to the original temperature, as shown in Fig. 7.20, the

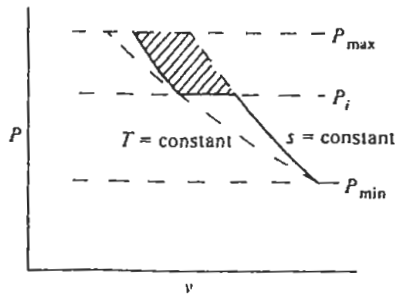


FIGURE 7.20
The effect of using multistage compression with intercooling.

compressor work is reduced by an amount indicated by the shaded area in the figure.

If j stages of compression are employed, with intercooling to the original temperature between compression stages, the minimum compression work is realized when the same compression work is performed in each stage. If the same compression work is performed in each stage, the temperature rise and the compressor pressure ratio are the same in each compressor. For j compression stages with intercooling to the initial temperature, the optimum pressure rise across each stage that minimizes the work should equal the jth root of the overall pressure ratio, or

$$\left(\frac{p_{out}}{p_{in}}\right)_{stage,opt} = \left(\frac{p_{max}}{p_{min}}\right)^{1/j} \tag{7.24}$$

In a two-stage compressor, with one intercooler, the optimum intercooler pressure is found from Eq. (7.24):

$$\frac{p_i}{p_{min}} = \frac{p_{max}}{p_i} \qquad \text{or} \qquad p_i = [(p_{min})(p_{max})]^{1/2} \tag{7.25}$$

As j approaches infinity, the compression process approaches an isothermal compression process. While additional stages of compression with intercooling reduces the compression work, a point of diminishing returns limits the number of practical stages that can be used.

The specific work of the Brayton cycle can also be increased by using the reheat Brayton cycle. The reheat Brayton-cycle engine is shown schematically in Fig. 7.21 along with a plot on the T-s diagram. Additional heat can be added to the gas by simply burning more fuel in the turbine gas before it expands to atmospheric pressure. The air-fuel ratio is so high in the typical gas turbine engine that there are no problems associated with the combustion of additional fuel. The efficiency of the reheat Brayton cycle can be greatly improved with the use of a regenerator and the higher turbine-exit temperature makes the regenerator more effective.

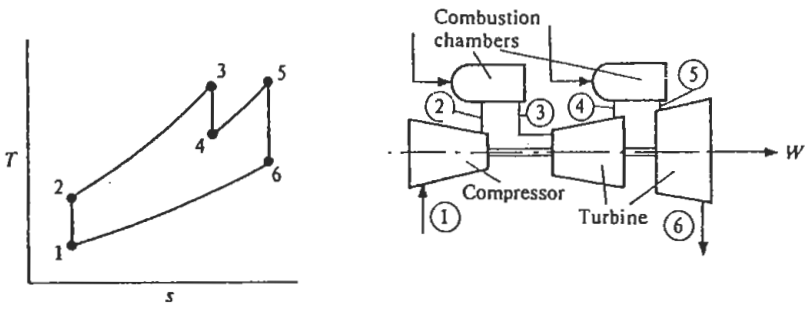


FIGURE 7.21
The reheat Brayton power cycle and system.

When the open-cycle, turbojet engine is employed in military aircraft, reheat is often utilized under certain conditions to provide additional thrust. This reheat device is called an *afterburner* and is essentially a device that injects fuel into the turbine exhaust gas before it goes through the engine nozzle. While this device produces significantly higher trust, it drastically reduces the engine efficiency and the range of the aircraft.

Example 7.1. The compression ratio of an Otto cycle is 8.8 : 1. The minimum pressure and temperature are 95 kPa and 25°C. The amount of heat added to the air per cycle is 1400 kJ/kg. On the basis of the air-standard cycle, determine (*a*) the pressures and temperatures at each point in the cycle, (*b*) the theoretical thermal efficiency, and (*c*) the specific work.

Solution

(*a*)
$$T_1 = 25 + 273 = 298 \text{ K} = 537°\text{R}$$

$$T_2 = T_1(r_v)^{(k-1)} = 298(8.8)^{0.4} = 711.2 \text{ K} = 1281°\text{R}$$

$$q = c_v(T_3 - T_2) = (0.7177 \text{ kJ/kg} \cdot \text{K})(T_3 - 711.2) \text{ K}$$

$$T_3 = T_2 + \frac{q}{c_v} = 711.2 + \frac{1400}{0.7177} = 2662 \text{ K} = 4791°\text{R}$$

$$T_4 = T_3(r_v)^{(1-k)} = 2661.9(8.8)^{-0.4} = 1115 \text{ K} = 2008°\text{R}$$

$$p_2 = p_1\left(\frac{v_1}{v_2}\right)^k = 95(8.8)^{1.4} = 1995 \text{ kPa} = 289.4 \text{ psia}$$

$$p_3 = p_2\frac{T_3}{T_2} = 1995\frac{2661.9}{711.2} = 7468 \text{ kPa} = 1083 \text{ psia}$$

$$p_4 = p_3(r_v)^{-k} = 7468(8.8)^{-1.4} = 356 \text{ kPa} = 51.7 \text{ psia}$$

(*b*)
$$\eta_{th} = 1 + \frac{q_r}{q_a} = 1 - \frac{T_4 - T_1}{T_3 - T_2}$$

$$= 1 - \frac{1115.3 - 298}{2661.9 - 711.2} = 58.10\%$$

Check:
$$\eta_{th} = 1 - (r_v)^{1-k} = 1 - 8.8^{-0.4} = 58.10\%$$

(*c*)
$$\text{Specific work} = w_{net} = q_r + q_a = c_v(T_1 - T_4) + c_v(T_3 - T_2)$$

$$= c_v(T_1 + T_3 - T_2 - T_4)$$

$$= 0.7177(298 + 2661.9 - 711.2 - 1115.3)$$

$$= 813.4 \text{ kJ/kg} = 349.7 \text{ Btu/lbm}$$

Example 7.2. A stationary gas-turbine power plant delivers 20,000 kW to an electric generator under the following conditions: air enters the compressor at 20°C and 98 kPa and leaves at 420 kPa; the gas enters the turbine at 850°C. If the mechanical efficiency of the turbine and compressor are 80 percent, find (*a*) the temperatures at each point in the cycle; (*b*) the specific work of the cycle; (*c*) the specific work

of the turbine and compressor; (d) the thermal efficiencies of the actual and ideal cycles; and (e) the required air-flow rate, in kg/min.

Solution

(a) $T_1 = 20 + 273 = 293\ \text{K} = 528°\text{R} \qquad r_p = \dfrac{420}{98} = 4.286$

$T_3 = 850 + 273 = 1123\ \text{K} = 2022°\text{R}$

$T_{2,s} = T_1(r_p)^{(k-1)/k} = 293(4.286)^{(1.4-1)/1.4} = 444.1\ \text{K} = 799.4°\text{R}$

$T_{4,s} = \dfrac{T_3}{(r_p)^{(k-1)/k}} = \dfrac{1123}{(4.286)^{0.4/1.4}} = 741.0\ \text{K} = 1334°\text{R}$

Actual temperatures:

$$T_{2,a} = T_1 + \frac{T_{2,s} - T_1}{\eta_c} = 293 + \frac{444.1 - 293}{0.8} = 481.8\ \text{K}$$
$$= 867.2°\text{R}$$

$$T_{4,a} = T_3 - (T_3 - T_{4,s})\eta_t = 1123 - (1123 - 741)(0.8) = 817.4\ \text{K}$$
$$= 1471°\text{R}$$

(b) $q_a = c_p(T_3 - T_{2,a}) = 1.0035(1123 - 481.8) = 643.4\ \text{kJ/kg}$
$= 276.7\ \text{Btu/lbm}$

$q_r = c_p(T_1 - T_{4,a}) = 1.0035(293 - 817.4) = -526.2\ \text{kJ/kg}$
$= -226.3\ \text{Btu/lbm}$

Net specific work $= w_{net} = q_a + q_r = 643.4 - 526.2 = 117.2\ \text{kJ/kg}$
$= 50.4\ \text{Btu/lbm}$

(c) Specific work of turbine $= w_t = h_3 - h_4 = c_p(T_3 - T_{4,a})$
$= 1.0035(1123 - 817.4) = 306.7\ \text{kJ/kg}$
$= 131.9\ \text{Btu/lbm}$

Specific work of compressor $= w_c = h_1 - h_2 = c_p(T_1 - T_{2,a})$
$= 1.0035(293 - 481.8)$
$= -189.5\ \text{kJ/kg}$
$= -81.5\ \text{Btu/lbm}$

Net specific work $= w_t + w_c = 306.7 - 189.5 = 117.2\ \text{kJ/kg}$
$= 50.4\ \text{Btu/lbm}$

(d) Actual thermal efficiency $= \dfrac{w_{net}}{q_a} = \dfrac{117.2}{643.4} = 18.22\%$

$$\text{Theoretical thermal efficiency} = 1 - \frac{T_{4,s} - T_1}{T_3 - T_{2,s}}$$

$$= 1 - \frac{741 - 293}{1123 - 444.1}$$

$$= 34.01\%$$

Check: $$\text{Theoretical thermal efficiency} = 1 - (r_p)^{(1-k)/k}$$

$$= 1 - 4.286^{-0.4/1.4} = 34.02\%$$

(e) $$\text{Air-flow rate} = \frac{P}{w_{net}} = (20{,}000\ \text{kW})(1\ \text{kJ/kW} \cdot \text{s})(60\ \text{s/m})$$

$$\times (1/117.2\ \text{kJ/kg}) = 10{,}240\ \text{kg/min}$$

$$= 22{,}570\ \text{lbm/min}$$

7.2.7 Vapor-Power Cycles

All vapor-power cycles must be classified as external-combustion systems and, unlike the Brayton cycle, they must employ a heat exchanger for the heat-addition process. Most of these systems also employ a heat exchanger (the condenser) for the heat-rejection process although it is possible to operate a water system by discharging the steam directly to the atmosphere and supply continuous water makeup, as in the old steam railroad engine. As was discussed earlier, the primary advantage of external-combustion systems is that they generally produce less pollution and permit the use of low-grade inexpensive fuels as well as the utilization of nuclear or solar energy.

The basic ideal thermodynamic vapor-power cycle is the Rankine cycle and the thermodynamic processes for this cycle are identical to the processes of the Brayton cycle—isentropic compression, isobaric heat addition, isentropic expansion, and isobaric heat rejection. The difference between these cycles is that the Rankine cycle employs a two-phase (liquid and vapor) working fluid, whereas the Brayton cycle is a gas-power cycle.

Water is the common working fluid used in the vapor-power cycles but a number of other fluids have been used or proposed for them. Mercury was actually employed along with water in two high-temperature binary power systems constructed in the 1950s and has been proposed for use as the working fluid for some high-temperature space power systems. The binary mercury-water Rankine cycle is composed of a high-temperature mercury Rankine cycle in which the heat-rejection process in the mercury condenser is the heat-addition process in a conventional water cycle. The use of two Rankine-cycle systems produces a higher overall thermal efficiency. Although mercury has been used as the high-temperature fluid in the past, it is very expensive, its vapor is chemically toxic, and it is very difficult to contain as it amalgamates most structural materials. Consequently, it is no longer commonly employed in vapor-power systems.

Other proposed Rankine-cycle working fluids are potassium, sodium, rubidium, ammonia, and a number of chain and aromatic hydrocarbon and

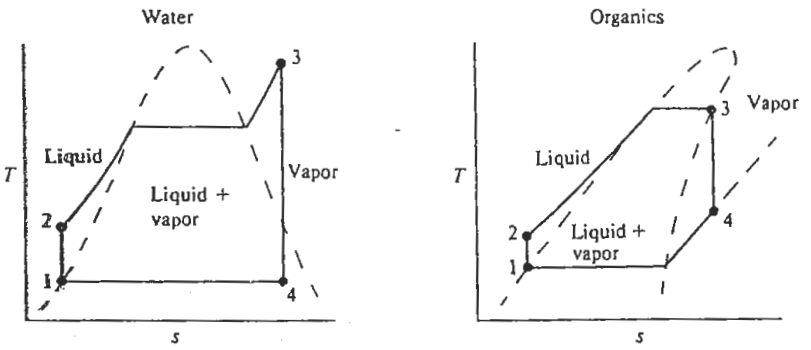


FIGURE 7.22
The Rankine heat-engine vapor cycle.

fluorocarbon compounds. There has been some interest in developing a potassium-water binary vapor-power system to achieve higher overall thermal efficiencies. Water is by far the most common fluid employed in these cycles and, in general, any further discussion of vapor-power systems will be limited to those systems using water as the working fluid, unless specifically designated otherwise. The Rankine cycle for a water system is shown on a T–s diagram in Fig. 7.22, and the same cycle is shown for an organic working fluid in the same figure. There is a considerable difference in the operation of these systems because of the different phase diagrams.

The simple steam-power cycle is composed of the four components shown in Fig. 7.23 and one of the four thermodynamic processes occurs in each com-

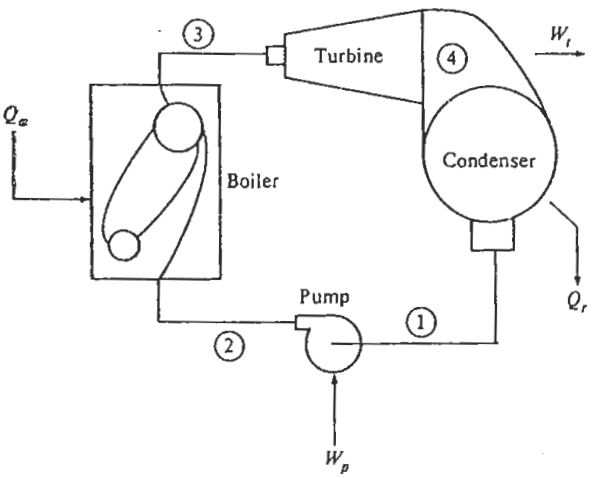


FIGURE 7.23
The Rankine-cycle components and system.

ponent. Process 1-2 is a reversible adiabatic (isentropic, $s = s_{min}$) compression process that takes place in the pump; process 2-3 is the reversible isobaric ($p = p_{max}$) heat-addition process that occurs in the boiler; process 3-4 is the reversible adiabatic (isentropic, $s = s_{max}$) expansion in the turbine or reciprocating steam engine; and, process 4-1 is the reversible isobaric ($p = p_{min}$) heat rejection in the condenser. If an energy balance is performed on each of these components, the steady-flow energy equation, neglecting the change in potential and kinetic energy is:

$$q = \Delta h + w \tag{7.26}$$

where q is the specific heat transfer in the component, Δh is the change in enthalpy across the component, and w is the thermal equivalent of the specific work done by the component, all in kilojoules per kilogram.

Since the processes in the boiler and condenser are isobaric, the ideal work in these components is zero and the energy equation in (7.26) reduces to:

$$q = \Delta h \tag{7.27}$$

Since the compression and expansion processes in the pump and turbine are adiabatic processes ($q = 0$), Eq. (7.26) reduces to:

$$w = -\Delta h \tag{7.28}$$

If the change in kinetic and potential energy in a steady-flow component is negligible, the reversible work produced by that component is equal to the integral of $-v\,dp$. Since the fluid in the pump is essentially incompressible, the ideal specific pump work is

$${}_1w_2 = -\Delta h = h_1 - h_2 = -\int_1^2 v\,dp \approx -v_1 \int_1^2 dp = -v_1(P_2 - P_1) \tag{7.29}$$

The negative value for this work term means that the work is done on the working fluid by the pump. Using the energy equation (7.28), the turbine work is:

$${}_3w_4 = -\Delta h = h_3 - h_4 \tag{7.30}$$

The specific work for the ideal cycle is the sum of the specific works of the pump and the turbine, or

$$w_{net} = {}_1w_2 + {}_3w_4 = h_1 - h_2 + h_3 - h_4 = h_3 - h_4 - v_1(P_2 - P_1) \tag{7.31}$$

The thermal efficiency of the simple cycle, η_{th}, becomes

$$\eta_{th} = \frac{w_{net}}{q_a} = \frac{h_1 - h_2 + h_3 - h_4}{h_3 - h_2}$$

$$= 1 - \frac{h_4 - h_1}{h_3 - h_2} = 1 + \frac{q_r}{q_a} \tag{7.32}$$

An important operating limitation for any vapor cycle using water as the working fluid is the moisture content of the steam at the turbine exhaust. The turbine-outlet steam is usually at a very, very low pressure, which means that the

density is also extremely low. This low steam density produces a very high velocity in the low-pressure part of the turbine. If there are any moisture droplets in this steam, they can actually erode the leading edge of the low-pressure turbine blades like raindrops erode the surface of the earth. This condition is likely to be severe if the moisture content of the steam at the turbine exhaust exceeds 10 percent.

The thermal efficiency of the simple steam or Rankine cycle can be improved by increasing the maximum steam temperature (the vapor superheat), by increasing the maximum system pressure p_{max}, and/or by increasing the condenser vacuum (decreasing the minimum system pressure p_{min}). Increasing the superheat of the steam also increases the specific work of the cycle and decreases the moisture content of the steam at the turbine exhaust. Increasing the maximum system pressure may increase the specific work if the same temperature is maintained, but it always increases the moisture content at the turbine exhaust. Lowering the minimum steam pressure increases the specific work of the cycle, which is desirable, but it also increases the moisture at the turbine exhaust, which is undesirable. The moisture, thermal efficiency, and the specific work of the basic Rankine cycle are plotted in Fig. 7.24 as a function of the maximum temperature and maximum and minimum pressures for the ideal cycle.

The maximum steam temperature is normally limited by the materials employed in the superheater section of the steam generator and particularly by the materials in the inlet of the high-pressure turbine. Most modern steam systems are limited to maximum operating temperatures of 540 to 600°C (1000 to 1100°F). The maximum steam pressure is limited by the operating conditions in the steam generator and particularly by the moisture content at the turbine exhaust. The minimum vapor pressure in the condenser is limited by the temperature of the heat sink. In modern steam power plants, the minimum pressure ranges from about 1 in Hg absolute (79°F) to around 2 psia (126°F).

The thermal efficiency of the ideal Rankine cycle is strongly affected by the compression and expansion efficiencies of the pump and turbine. The inefficiencies of these systems irreversibly converts some of the mechanical energy into thermal energy, thereby increasing the enthalpy of the fluid leaving the component. In a steam turbine, this effect is sometimes referred to as *stage reheat.* If the turbine efficiency is η_t, the actual enthalpy of the steam leaving the turbine, $h_{4,a}$, is:

$$h_{4,a} = h_3 - \eta_t(h_3 - h_{4,s}) = h_{4,s} + (1-\eta_t)(h_3 - h_{4,s}) \tag{7.33}$$

where h_3 is the enthalpy of the turbine inlet steam and $h_{4,s}$ is the enthalpy at the turbine outlet for an isentropic expansion. If the pump efficiency is η_p, the actual enthalpy of the water leaving the pump, $h_{2,a}$, is:

$$h_{2,a} = h_1 + \frac{h_{2,s} - h_1}{\eta_p} = h_1 + \frac{v_1(p_2 - p_1)}{\eta_p} \tag{7.34}$$

Since $h_{4,a}$ is increased by the inefficiencies in the turbine, this improves (decreases) the moisture content at the turbine exhaust. Although this last effect is desirable, the lower turbine efficiency adversely effects the overall cycle performance.

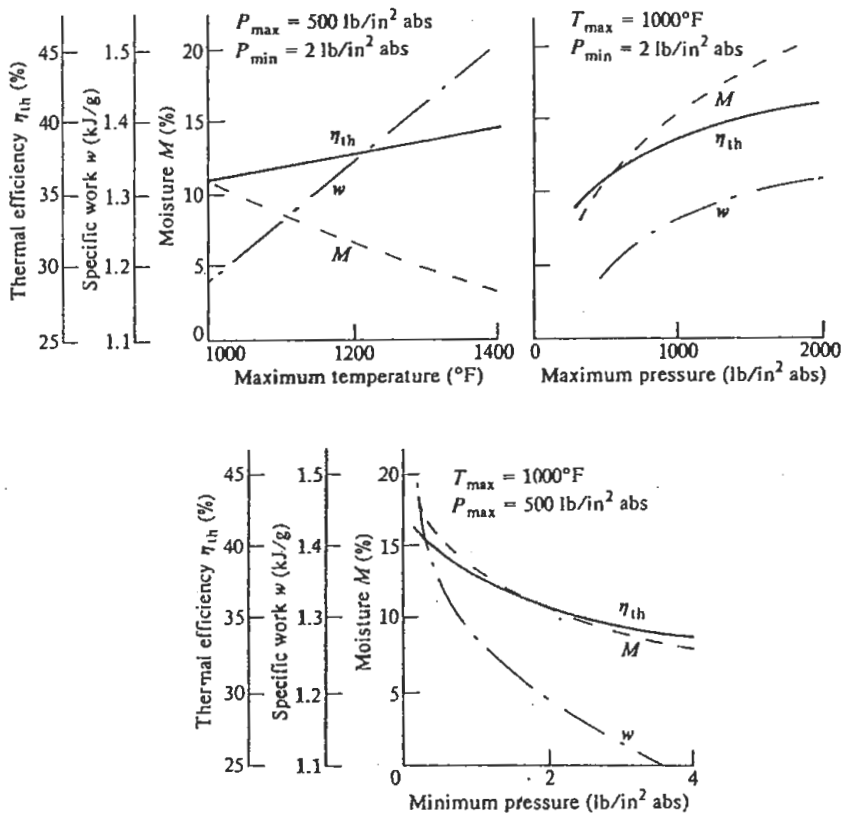
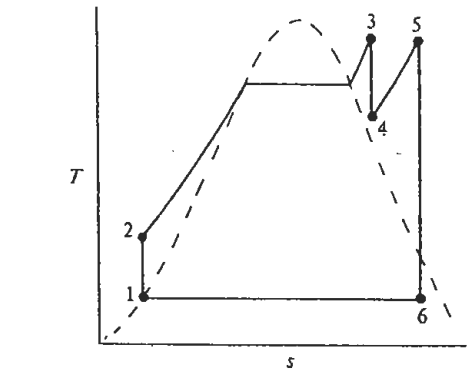


FIGURE 7.24
The variation of Rankine-cycle performance with cycle parameters.

The reheat Rankine cycle is a modification of the simple Rankine cycle in which all of the steam is removed from the turbine after partial expansion and returned to the boiler where additional heat is supplied to the steam at constant pressure in the reheat section of the boiler. The reheat vapor power cycle is shown plotted on a T-s diagram in Fig. 7.25 along with a schematic diagram of the system. This cycle permits the use of very high steam pressures without excessive moisture at the condenser inlet. The use of higher vapor pressure increases the thermal efficiency of the cycle, if the cycle is a simple cycle. The efficiency of the reheat cycle may or may not be as efficient as a simple Rankine cycle operating between the same pressures and maximum temperature depending on the reheat pressure.

For maximum thermal efficiency, the reheat pressure should be as high as possible. This pressure is obtained by starting at the desired turbine discharge condition, such as a moisture content of 10 percent at minimum pressure, then working backward (isentropically for a reversible adiabatic process) to the



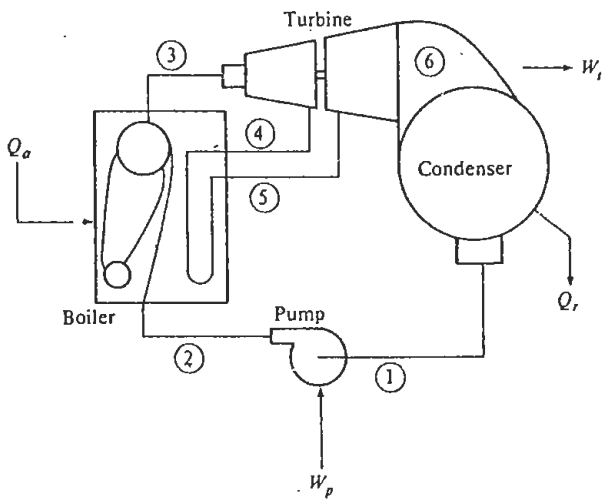


FIGURE 7.25
The reheat Rankine heat-engine vapor cycle and system.

maximum allowable reheat temperature to obtain the maximum reheat pressure. If the turbine efficiency is less than unity, an iterative calculation is required to determine the desired reheat pressure. The typical reheat pressure normally runs around one-quarter of the maximum system pressure.

Using the cycle notation, as given in Fig. 7.25, the specific work for the cycle, becomes

$$w_{net} = {}_1w_2 + {}_3w_4 + {}_5w_6 = h_1 + h_3 + h_5 - h_2 - h_4 - h_6$$

$$= h_3 + h_5 - h_4 - h_6 - \frac{v_1(p_2 - p_1)}{\eta_p} \tag{7.35}$$

and the thermal efficiency for the reheat cycle becomes

$$\eta_{th} = \frac{w_{net}}{q_a} = \frac{h_1 + h_3 + h_5 - h_2 - h_4 - h_6}{h_3 + h_5 - h_2 - h_4}$$

$$= 1 - \frac{h_6 - h_1}{h_3 + h_5 - h_2 - h_4} = 1 + \frac{q_r}{q_a} \tag{7.36}$$

The regenerative vapor-power cycle is a modification of the basic Rankine cycle that improves the thermal efficiency of the basic simple cycle. In the regenerative vapor cycle, some steam is bled from the turbine before it reaches the condenser and this steam is used to heat the liquid boiler feed before it reenters the steam generator. The low-efficiency part of the Rankine cycle is that part of the cycle where heat is added to the feedwater. Thus, the thermal efficiency of the basic cycle can be improved if some of this heat addition is accomplished with the use of internal energy from the cycle, particularly if most of that internal energy is latent heat which would eventually be rejected in the condenser.

Extraction of underexpanded turbine steam from the turbine for feedwater heating always reduces the specific work for the cycle. In this case, the area enclosed by the cycle processes on the p–v or T–s diagram overestimates the specific work. This reduction in the net specific work means that higher steam-flow rates are required for the same power output.

There are two basic types of feedwater heaters—open and closed (Fig. 7.26). In the open heater, the steam is mixed directly with the feedwater, whereas the closed heater is essentially a tube-and-shell heat exchanger with no direct contact between the fluids. The positioning of the heaters with respect to extraction pressures is important in order to obtain the maximum increase in the thermal efficiency for a given number of heaters.

If $T_{sat,H}$ is the saturation temperature at the maximum pressure and $T_{sat,L}$ is the saturation temperature at the minimum pressure, the increase in feedwater temperature, ΔT_{Htr}, across each of the n heaters for maximum thermal efficiency is:

$$\Delta T_{Htr} = \frac{T_{sat,H} - T_{sat,L}}{n+1} \tag{7.37}$$

The value of the saturation temperature for the extracted steam in the ith feedwater heater is:

$$T_{i,out} = T_{sat,L} + i(\Delta T_{Htr}) \tag{7.38}$$

where the first heater ($i = 1$) is the low-pressure heater. The optimum extraction pressure for the ith heater can then be found by determining the saturation pressure corresponding to a saturation temperature of $T_{i,out}$ from the steam tables.

The open feedwater heater has some advantages over the closed heater. The open heater is essentially a tank and consequently is less expensive than the closed heater. The heat transfer in the open heater is excellent since the water and steam can be mixed directly. However, this means that it is impossible to increase the temperature of the exit water above the saturation temperature of

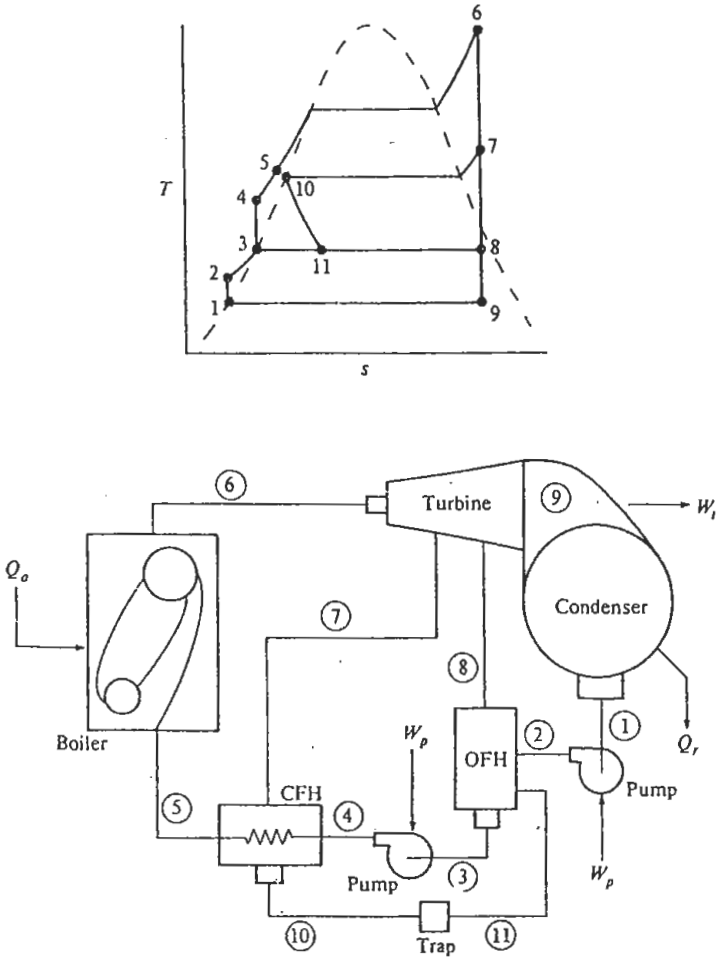


FIGURE 7.26
The regenerative vapor power cycle and system with open (OFH) and closed (CFH) feedwater heaters.

the extraction steam. In a properly designed closed heater, the feedwater exit temperature may exceed the saturation temperature of the extraction steam if the inlet steam is superheated.

Each open heater must be accompanied by a feedwater pump and care must be taken to assure that there is no way that feedwater can be pumped up the extraction line into the turbine. Every regenerative power cycle normally contains at least one open feedwater heater that operates at a pressure slightly higher than atmospheric pressure. This heater, commonly called the *deaerating heater*, is used to remove any dissolved gases, particularly oxygen, from the boiler feed. A typical deaerating heater is shown in Fig. 7.27.

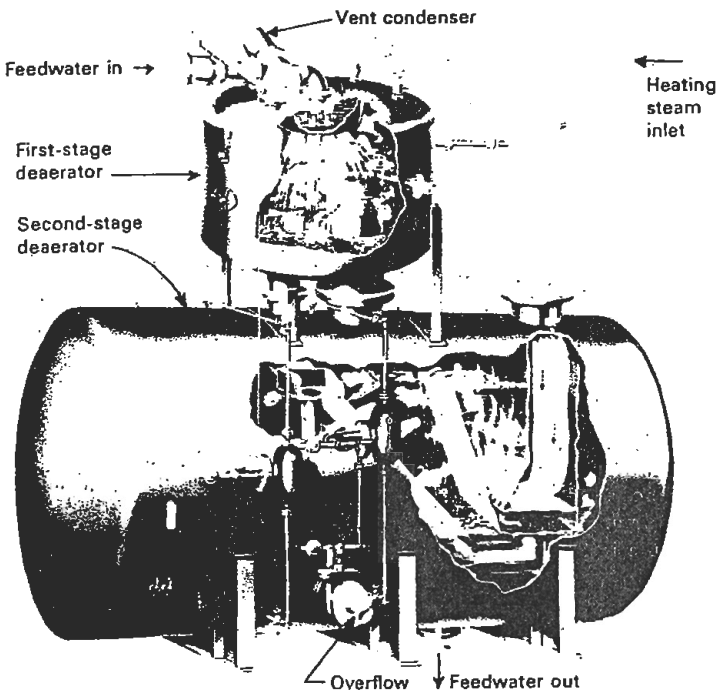


FIGURE 7.27
A spray-type deaerating heater. (*From Editors of Power Magazine, 1967.*)

The closed feedwater heater is essentially a tube-and-shell heat exchanger with the high-pressure water flowing in the tubes and the condensing steam in the shell. The condensate produced in the shell of the exchanger can either be pumped to higher pressure or it can be "trapped" to lower pressure. A "steam trap" is a float valve and when the water level reaches a given point, the float opens the valve and the condensate is throttled to the next lower heater or to the condenser. The use of a pump produces a slightly higher cycle efficiency, but pumps are more expensive and require more maintenance than steam traps. Consequently, most closed heaters use a steam trap to remove the condensate.

The important performance parameter for feedwater heaters is the terminal temperature difference (TTD). The terminal temperature difference is equal to the saturation temperature of the extracted steam, T_{sat}, minus the outlet feedwater temperature, $T_{w,out}$, or

$$\text{TTD} = T_{sat} - T_{w,out} \tag{7.39}$$

This quantity should be as low as possible, preferable negative, but the limiting value for an open heater is zero. If the extraction steam is superheated, proper design of a counterflow closed heater can produce a negative value of the terminal temperature difference.

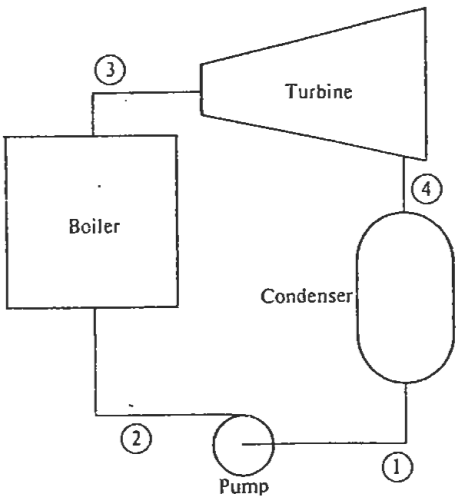
The required fractional steam flow rate m_j to a feedwater heater is determined by performing an energy balance on the heater. The feedwater heater is a steady-flow device in which there is no work ($w = 0$) and no external heat transfer ($q = 0$). This means that the total enthalpy entering the heater must equal the total enthalpy leaving the heater, or:

$$\dot{H}_{in} = \sum_j (\dot{m}_j h_j)_{in} = \dot{H}_{out} = \sum_j (\dot{m}_j h_j)_{out} \tag{7.40}$$

It is not possible to develop a more specific equation for a given heater because the enthalpy equation depends on the way that the system components are connected and the type of heaters and pumps or traps used in the cycle. If more than one feedwater heater is employed in the cycle, the analyst must start with the highest-pressure heater and work down through the lower-pressure heaters, sequentially.

Example 7.3. Find the thermal efficiency and the specific work of a simple Rankine cycle if the maximum temperature and pressure are 540°C and 7.0 MPa and the minimum pressure is 10 kPa. Assume that the turbine and pump efficiencies are both 85 percent.

Solution



All steam and water values are taken from steam tables by Keenan, Keys, Hill, and Moore and use metric units.

$$h_1 = h_f(\text{at } 10 \text{ kPa}) = 191.8 \text{ kJ/kg}$$

$$h_2 = h_1 + v_1(p_2 - p_1) = 191.8 \text{ kJ/kg} + \frac{(0.0010102 \text{ m}^3/\text{kg})(7000 - 10) \text{ kPa } (1 \text{ kJ/kPa} \cdot \text{m}^3)}{0.85}$$

$$= 200.1 \text{ kJ/kg}$$

$$h_3 = h(\text{at } 540°C,\ 7 \text{ MPa}) = 3506.9 \text{ kJ/kg}$$

$$s_3 = s_{4,s} = 6.9193 \text{ kJ/kg} \cdot \text{K}$$

$$M_{4,s} = \frac{s_g - s_{4,s}}{s_{fg}} = \frac{8.1502 - 6.9193}{7.5009} = 16.41\%$$

$$h_{4,s} = h_g - M_{4,s} h_{fg} = 2584.7 - 0.1641(2392.8) = 2192.0 \text{ kJ/kg}$$

$$h_{4,a} = h_{4,s} + (1 - \eta_t)(h_3 - h_{4,s}) = 2192 + (0.15)(3506.9 - 2192)$$

$$= 2389.2 \text{ kJ/kg}$$

$$\text{Actual moisture at turbine exhaust} = M_{4,a} = \frac{h_g - h_{4,a}}{h_{fg}}$$

$$= \frac{2584.7 - 2389.2}{2392.8} = 8.17\%$$

$$\text{Net specific work} = w_{net} = h_1 + h_3 - h_{2,a} - h_4$$

$$= 191.8 + 3506.9 - 200.1 - 2389.2$$

$$= 1109.4 \text{ kJ/kg}$$

$$\text{Thermal efficiency} = \eta_{th} = 1 + \frac{q_r}{q_a} = 1 + \frac{h_1 - h_{4,a}}{h_3 - h_{2,a}}$$

$$= 1 + \frac{191.8 - 2389.2}{3506.9 - 200.1}$$

$$= 33.55\%$$

Example 7.4. It is proposed to upgrade the system of Example 7.3 by increasing the maximum pressure to 16.5 MPa while holding the maximum inlet and reheat temperatures to 540°C and holding the minimum pressure to 10 kPa. Calculate the specific work and thermal efficiency of the system if the turbine and pump efficiencies are 85 percent and the maximum moisture at the turbine exhaust is kept at 10 percent by using one stage of reheat.

Solution

$$h_1 = h_f \text{ (at 10 kPa)} = 191.8 \text{ kJ/kg}$$

$$h_2 = h_1 + v_1(p_2 - p_1) = 191.8 + \frac{(0.0010102)(16{,}500 - 10)}{0.85}$$

$$= 211.4 \text{ kJ/kg}$$

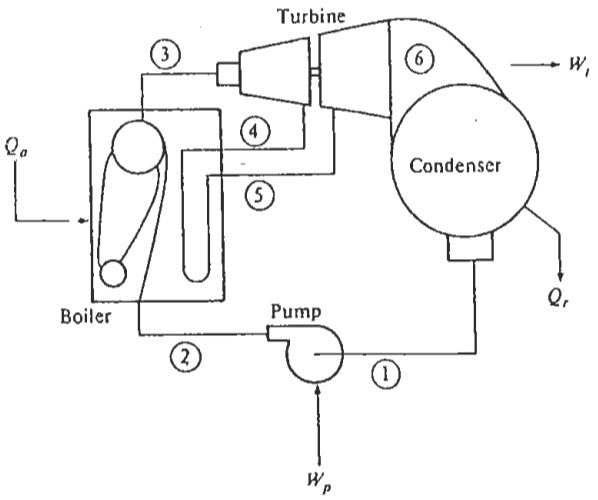
$$h_3 = h(\text{at } 16.5 \text{ MPa},\ 540°C) = 3404.3 \text{ kJ/kg}$$

$$s_3 = s_{4,s} = 6.4262 \text{ kJ/kg} \cdot \text{K}$$

At state point 6, the turbine exhaust, $M_{6,a} = 10\% = 0.1$ and

$$h_{6,a} = h_g - M_{6,a} h_{fg} = 2584.7 - 0.1(2392.8) = 2345.4 \text{ kJ/kg}$$

$$T_5 = 540°C$$



By trial and error and using the Mollier diagram, $P_5 = P_4 = 9.2$ MPa and

$$h_5 = h \text{ (at 9.2 MPa and 540°C)} = 3484.2 \text{ kJ/kg}$$

Check of reheat pressure:

$$s_5 = s_{6,s} = s \text{ (at 9.2 MPa and 540°C)} = 6.7718 \text{ kJ/kg} \cdot \text{K}$$

$$M_{6,s} = \frac{s_g - s_{6,s}}{s_{fg}} = \frac{8.1502 - 6.7718}{7.5009} = 0.1838$$

$$h_{6,s} = h_g - M_{6,s}(h_{fg}) = 2584.7 - 0.1838(2392.8)$$
$$= 2145.0 \text{ kJ/kg}$$

$$h_{6,a} = h_5 - \eta_t(h_5 - h_{6,s}) = 3484.2 - 0.85(3484.2 - 2145)$$
$$= 2345.9 \text{ kJ/kg}$$

$$M_{6,a} = \frac{h_g - h_{6,a}}{h_{fg}} = \frac{2584.7 - 2345.9}{2392.8} = 9.98\% \qquad \text{(Close enough!)}$$

$$h_5 = h \text{ (at 9.2 MPa, 540°C)} = 3484.2 \text{ kJ/kg}$$

$$h_{4,s} = h \text{ (at 9.2 MPa, } s = 6.4262) = 3221.5 \text{ (by interpolation)}$$

$$h_{4,a} = h_3 - \eta_t(h_3 - h_{4,s}) = 3404.3 - 0.85(3404.3 - 3221.5)$$
$$= 3248.9 \text{ kJ/kg}$$

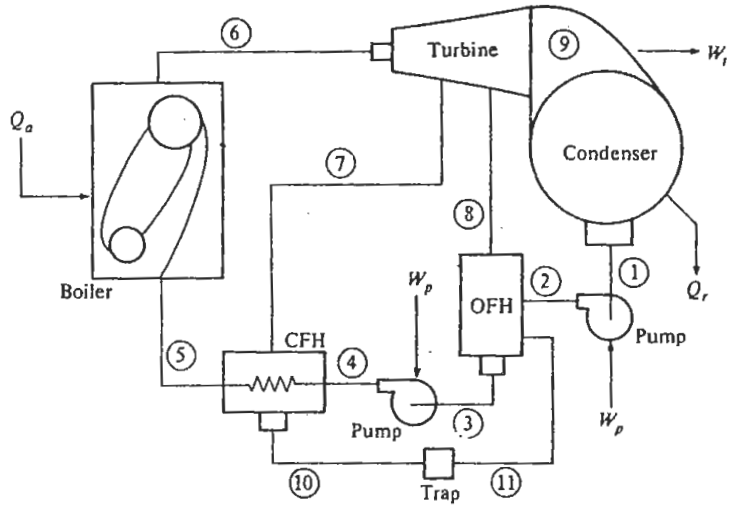
$$\text{Specific work} = w_{net} = h_1 + h_3 + h_5 - h_2 - h_{4,a} - h_{6,a}$$
$$= 191.8 + 3404.3 + 3484.2 - 211.4 - 3248.9 - 2345.9$$
$$= 1274.1 \text{ kJ/kg}$$

$$\text{Thermal efficiency} = \eta_{th} = \frac{w_{net}}{q_a} = \frac{w_{net}}{h_3 + h_5 - h_2 - h_{4,a}}$$

$$= \frac{1274.1}{3404.3 + 3484.2 - 211.4 - 3248.9}$$

$$= 37.17\%$$

Example 7.5. Suppose two feedwater heaters, one open and one closed, as in the figure below are added to the system of Example 7.3 to achieve a higher thermal efficiency. Assuming a TTD of zero and an optimum spacing of the heaters, calculate the maximum thermal efficiency and the specific work of the system. Assume the turbine and pump efficiencies both remain at 85 percent.



Solution. From Example 7.3,

$$p_{min} = p_9 = p_1 = 10 \text{ kPa};\ T_{max} = 540°\text{C};\ p_{max} = p_4 = p_5 = p_6 = 7 \text{ MPa}$$

Location of optimum heater extraction pressures for maximum thermal efficiency:

$$T_{sat,H} = T_{sat}(\text{at } 7 \text{ MPa}) \simeq 286°\text{C}$$

$$T_{sat,L} = T_{sat}(\text{at } 10 \text{ kPa}) \simeq 46°\text{C}$$

$$\Delta T_{Htr} = \frac{T_{sat,H} - T_{sat,L}}{n+1} = \frac{286 - 46}{2+1} = 80\ \text{C}°$$

$$T_3 \simeq T_1 + \Delta T_{Htr} = 46 + 80 = 126°\text{C}$$

$$p_3 = p_{sat}(\text{at } 126°\text{C}) \simeq 240 \text{ kPa} = p_2 = p_8 = p_{11}$$

$$T_5 \simeq T_1 + 2(\Delta T_{Htr}) = 46 + 2(80) = 206°\text{C}$$

$$p_7 \simeq p_{sat}(\text{at } 206°\text{C}) = 1.75 \text{ MPa} = p_{10}$$

Calculation of system enthalpies:

$$h_1 = h_f(\text{at } 10 \text{ kPa}) = 191.8 \text{ kJ/kg}$$

$$h_2 = h_1 + \frac{v_1(p_2 - p_1)}{\eta_p} = 191.8 + \frac{0.0010102(240 - 10)}{0.85}$$

$$= 192.1 \text{ kJ/kg}$$

$$h_3 = h_f(\text{at } 240 \text{ kPa}) = 529.7 \text{ kJ/kg}$$

$$h_4 = h_3 + \frac{v_3(p_4 - p_3)}{\eta_p} = 529.7 + \frac{0.001066(7{,}000 - 240)}{0.85}$$

$$= 538.1 \text{ kJ/kg}$$

$h_5 = h$ (at 205.76°C and 7.0 MPa)

= 880.6 kJ/kg (from compressed liquid tables by double interpolation)

$h_6 = h$ (at 540°C and 7.0 MPa) = 3506.9 kJ/kg

$s_6 = s$ (at 540°C and 7.0 MPa) = 6.9193 kJ/kg · K = $s_{7,s} = s_{8,s} = s_{9,s}$

$$h_{7,s} = 3075.7 + \frac{(3098.0 - 3075.7)(6.9193 - 6.9148)}{(6.9521 - 6.9148)} = 3078.4 \text{ kJ/kg}$$

$$h_{7,a} = h_6 - \eta_t(h_6 - h_{7,s}) = 3506.9 - 0.85(3506.9 - 3078.4)$$

$$= 3142.7 \text{ kJ/kg} = h_7$$

$$M_{8,s} = \frac{s_g - s_{8,s}}{s_{fg}} = \frac{7.0663 - 6.9193}{5.4733} = 0.02686$$

$$h_{8,s} = h_g - M_{8,s}h_{fg} = 2715.0 - 0.02686(2185.4) = 2656.3 \text{ kJ/kg}$$

$$h_{8,a} = h_6 - \eta_t(h_6 - h_{8,s}) = 3506.9 - 0.85(3506.9 - 2656.3)$$

$$= 2783.9 \text{ kJ/kg} = h_8$$

$$M_{9,s} = \frac{s_g - s_{9,s}}{s_{fg}} = \frac{8.1502 - 6.9193}{7.5009} = 0.1641$$

$$h_{9,s} = h_g - M_{9,s}h_{fg} = 2584.7 - 0.1641(2392.8) = 2192.0 \text{ kJ/kg}$$

$$h_{9,a} = h_6 - \eta_t(h_6 - h_{8,s}) = 3506.9 - 0.85(3506.9 - 2192.0)$$

$$= 2389.3 \text{ kJ/kg} = h_9$$

$$h_{10} = h_f \text{ (at 1.75 MPa)} = 878.5 \text{ kJ/kg}$$

$$h_{11} = h_{10} = 878.5 \text{ kJ/kg}$$

Summary:

State Pt.:	1	2	3	4	5	6
p, kPa	10	240	240	7000	7000	7000
h, kJ/kg	191.8	192.1	529.7	538.1	880.6	3506.9

State Pt.:	7	8	9	10	11
p, kPa	1750	240	10	1750	240
h, kJ/kg	3142.7	2783.9	2389.3	878.5	878.5

Extraction fractions for the heaters (m_1 and m_2):

m_1 = fraction of total turbine inlet flow extracted at point 7
m_2 = fraction of total turbine inlet flow extracted at point 8

For the high-pressure heater,

$$\sum h_{in} = m_1 h_7 + h_4 = \sum h_{out} = m_1 h_{10} + h_5$$

$$m_1 = \frac{h_5 - h_4}{h_7 - h_{10}} = \frac{880.6 - 538.1}{3142.7 - 878.5} = 0.1512 \text{ kg/kg}$$

For the low-pressure heater,

$$\sum h_{in} = m_1 h_{11} + (1 - m_1 - m_2) h_2 + m_2 h_8 = \sum h_{out} = h_3$$

$$m_2 = \frac{m_1(h_2 - h_{11}) + h_3 - h_2}{h_8 - h_2} = \frac{0.1512(192.1 - 878.5) + 529.7 - 192.1}{2783.9 - 192.1}$$

$$= 0.0902 \text{ kg/kg}$$

$$q_a = h_6 - h_5 = 3506.9 - 880.6 = 2626.3 \text{ kJ/kg}$$

$$q_r = (1 - m_1 - m_2)(h_1 - h_9) = (1 - 0.1512 - 0.0902)(191.8 - 2389.3)$$

$$= -1666.9 \text{ kJ/kg}$$

$$w_{net} = q_a + q_r = 2626.3 - 1666.9 = 959.4 \text{ kJ/kg}$$

$$\eta_{th} = \frac{w_{net}}{q_a} = \frac{959.4}{2626.3} = 36.53\%$$

Two engineers at DuPont have developed and tested a novel rotary engine that operates on the Rankine cycle. This system employs an organic working fluid and is novel in that it has both a rotating boiler and a condenser. A test engine has been built and operated at a rated power of 20 hp. The schematic diagram of this engine and a discussion of its operation are given in Fig. 7.28.

7.2.8 Combined Cycles

Earlier, it was pointed out the mercury and water have been employed in a binary vapor-power system. When two power cycles, A and B, with respective thermal efficiencies of η_A and η_B, are connected in series so that q_A is the specific heat transfer to cycle A and the heat rejection from cycle A plus some additional quantity of heat, q_B, is the heat added to cycle B, the overall thermal efficiency of the combination is

$$\eta_{th,tot} = \frac{q_A \eta_A + (1 - \eta_A) q_A \eta_B + q_B \eta_B}{q_A + q_B}$$

$$= \eta_B + \frac{q_A \eta_A (1 - \eta_B)}{q_A + q_B} \tag{7.41}$$

—Du Pont's 20 hp laboratory test engine. Boiler, nozzle ring, and condenser are an integral unit—rotated by external electric motor (not shown) at 2500 rev/min. The expanding gas rotates the turbine in the opposite direction at 27,500 rev/min

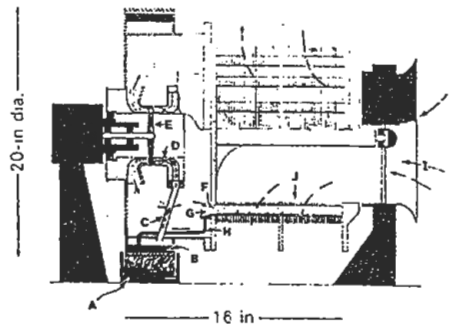


FIGURE 7.28
A rotary Rankine-cycle engine. External burner (A) boils fluid in annular chamber where liquid (B) is held on outer surface by centrifugal force. Hot vapor travels through tubes (C) to nozzle ring (D), expands through ring and drives turbine wheel (E). Engine power from turbine shaft drives external load (not shown). Vapor goes into condenser tubes (F). Condensed fluid flows back to channel (G). Centrifugal action forces liquid from channel through tubes (H) back to boiler (B). Cooling air is pulled into hollow center of condenser cylinder (I), then between condenser fins (J) by viscous drag of rotating fin assembly. (*From Doerner et al., 1972.*)

If there is no additional heat added to cycle B ($q_B = 0$), Eq. (7.41) reduces to:

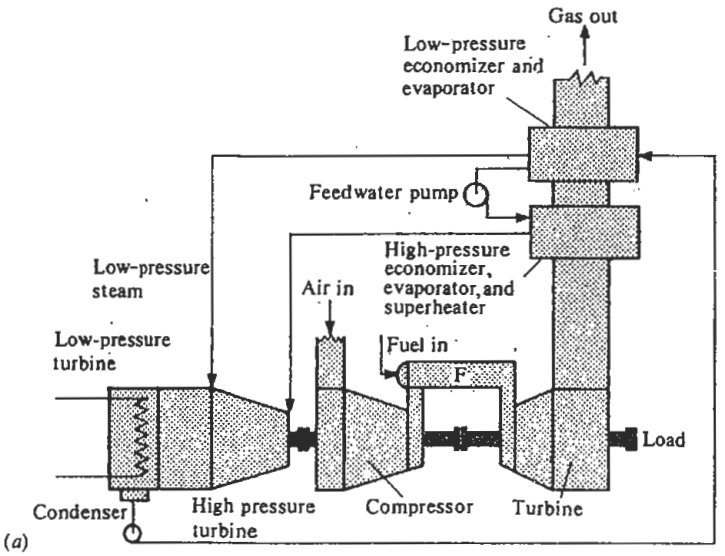
$$\eta_{th,tot} = \eta_A + \eta_B - \eta_A \eta_B \tag{7.42}$$

Thus, if $\eta_A = 30$ percent and $\eta_B = 20$ percent, the combined thermal efficiency would be: $0.30 + 0.20 - 0.06 = 44$ percent.

In recent years, considerable interest has been given to the possibility of combining the Brayton or gas-turbine cycle with the Rankine or vapor-power cycle in the so-called *combined-cycle* power system. In these systems, a heat-recovery steam generator (HRSG) is connected directly to the exhaust of a gas turbine. The steam generator may operate with the turbine exhaust alone ($q_B = 0$), or supplemental heat can be easily added to the turbine exhaust because the typical gas turbine operates with very high excess air. The schematic diagrams of the unfired combined cycle (a) and also for the supplementary fired combined cycle (b) are shown in Fig. 7.29. A more detailed diagram of the HRSG is shown in Fig. 7.30.

Since the early 1970s, a number of companies have developed combined-cycle power systems in package form. Westinghouse designed a unit, called PACE (an acronym for power at combined efficiencies). The General Electric system is called *STAG* (an acronym for steam and gas turbines) and the firm of Stone and Webster has developed a combined-cycle system called *FAST*.

The combined-cycle power systems appear to be very promising for the so-called *intermediate-load service* between the peaking units (gas turbines and



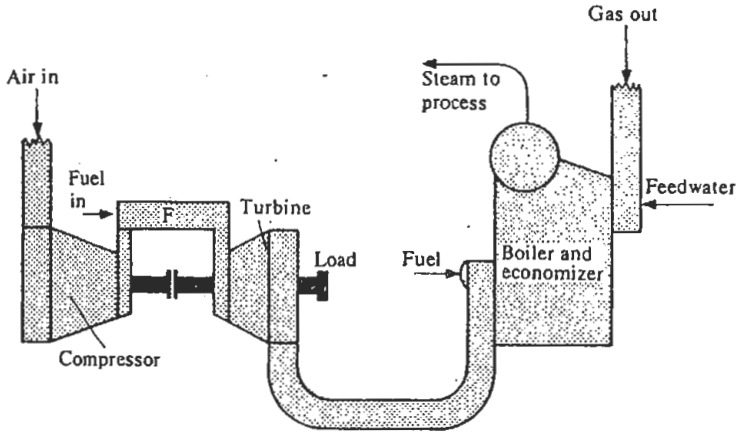


FIGURE 7.29
The combined (Brayton and Rankine)-cycle systems, (*a*) with no supplementary firing and (*b*) with supplementary firing. (*From Skrotzki, 1963.*)

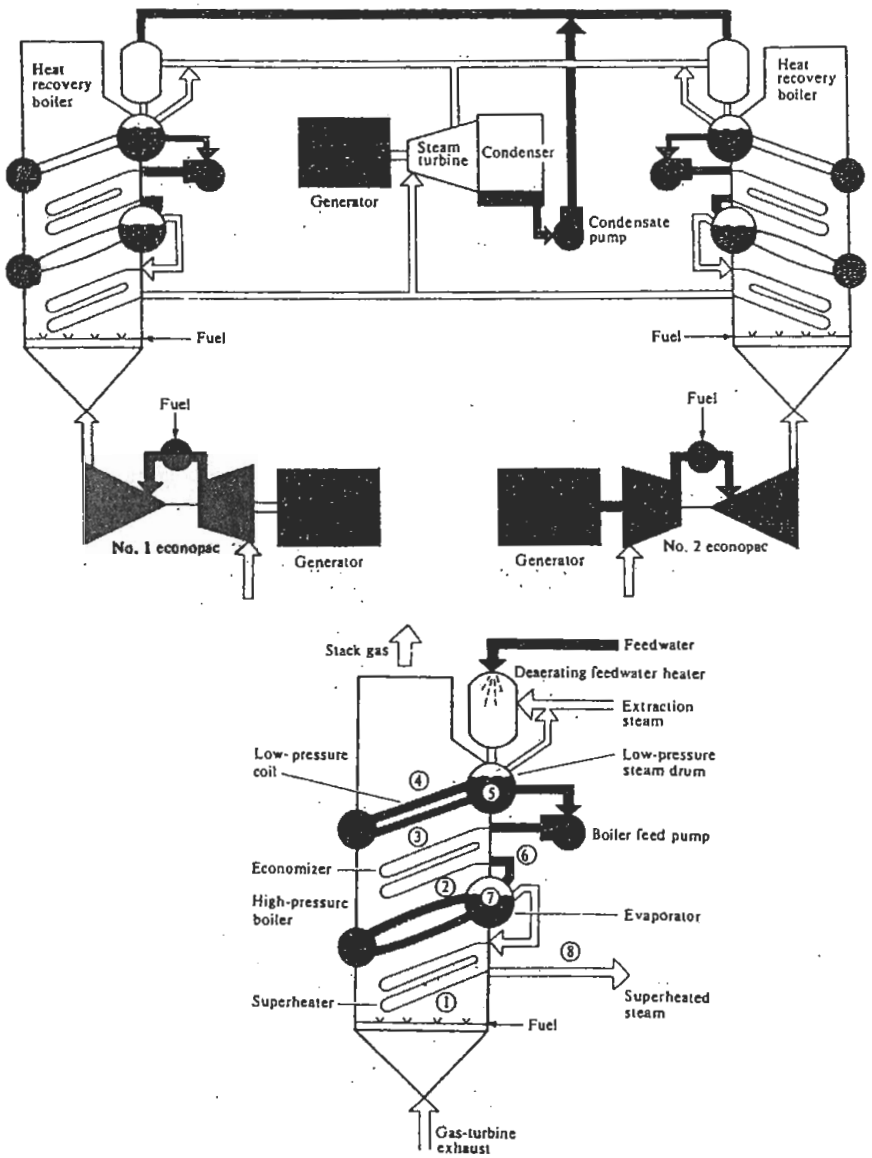


FIGURE 7.30
The combined cycle and the heat-recovery steam generator (HRSG). (*From Berman and Lebonette, 1971.*)

diesels) and the base-load units (large fossil-fuel or nuclear steam power plants). These units also offer the advantage of producing power very quickly. The turbine part of the units can normally be started and brought to full power in 20 min.

7.3 TURBINES

7.3.1 Steam Turbines

GENERAL. The turbine is a device that converts the stored mechanical energy in a fluid into rotational mechanical energy. There are several different types, including steam turbines, gas turbines, water turbines, and wind turbines or windmills. The material presented in this section is applicable to only steam or gas turbines, although some of the general principles are applicable to the other systems, as well.

There are several different ways to classify steam turbines. One is with respect to the purpose of the turbine. This system includes the central-station units which are used to drive electrical generators at synchronous speed (usually 3600 or 1800 r/min) with power ratings of 16 to 1500 MW_e.

Superposed or topping steam turbines are high-pressure turbines that are installed in older, low-pressure steam systems to improve the overall efficiency of the power plant. They are also being installed by industrial firms that have a use for the low-pressure turbine exhaust process steam, in a cogeneration power system. The relatively high-pressure turbine exhaust is fed directly to the low-pressure turbine or to a manufacturing process.

Mechanical-drive turbines are used to power large draft fans, pumps, compressors, and other large rotating equipment. These systems normally operate between 900 and 10,000 r/min and range in capacity from 0.5 to 10 MW. They have a number of advantages over electrical-drive systems, including better utilization of thermal energy, easy speed control, and fast startup. In addition, no sparks are generated during normal operation; they are amenable to hot, damp environments; and the low-pressure steam can be used for other purposes, such as process steam in a manufacturing process.

Steam turbines can also be classified according to the exhaust or back pressure of the unit. Under this system, turbines are classed as either condensing or noncondensing. In the noncondensing turbine, the turbine-exhaust pressure is above or equal to atmospheric pressure and the system can operate with or without a condenser. If there is no condenser, this system will require continuous water makeup. A condensing turbine normally discharges steam to a condenser at a very high vacuum to improve the thermal efficiency of the cycle. There is no need for continuous makeup to this system.

Steam turbines may be classified according to the method of steam injection or extraction from the turbine. Bleeder or extraction turbines are used where turbine steam is removed partway through the turbine for process use or for feedwater heating. Reheat turbines are used in the reheat vapor-power cycles. Extraction-induction turbines have ports for both the extraction and injection of steam at intermediate points in the turbine. The different types of steam turbines

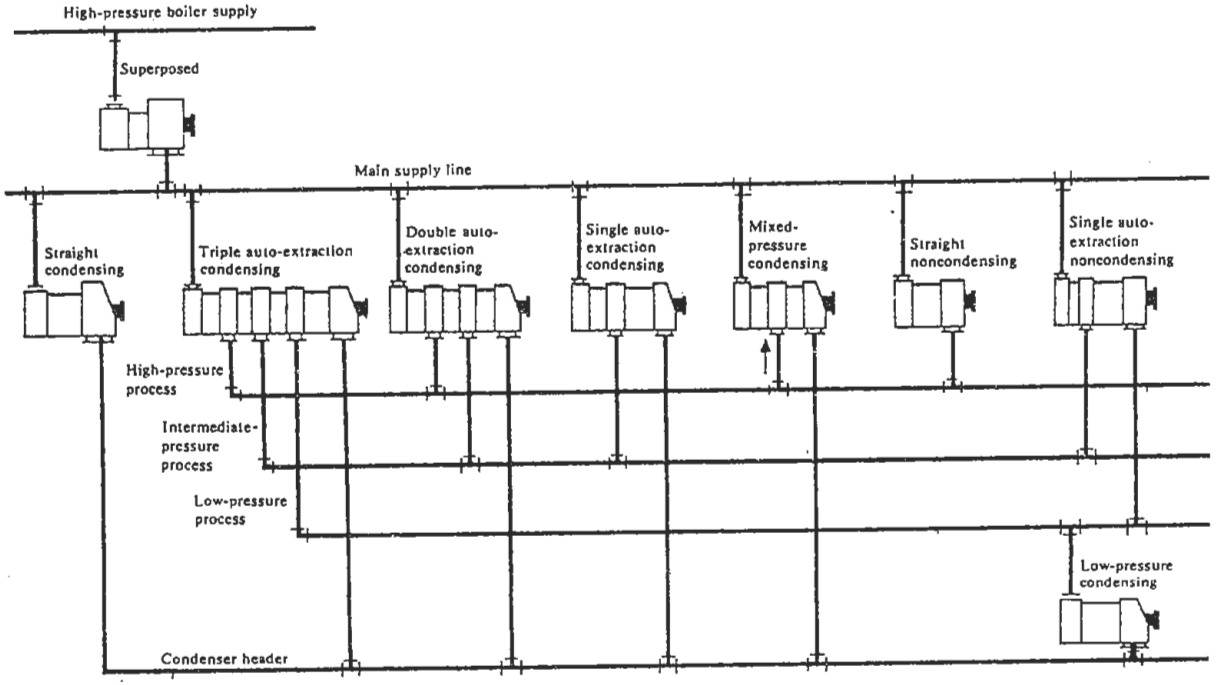


FIGURE 7.31
The different types of steam turbines and their connections. Heat-balance arrangements are almost endless. Turbines fit almost any heat balance as long as there is sufficient steam-pressure drop. Most efficient hookup occurs when process-steam flow and shaft-power demands coincide. Shaft power needs in excess of that generated by process steam call for condensing units. Throttling valves meet any steam needs over and above what is required for shaft power. (*From Skrotski, 1962.*)

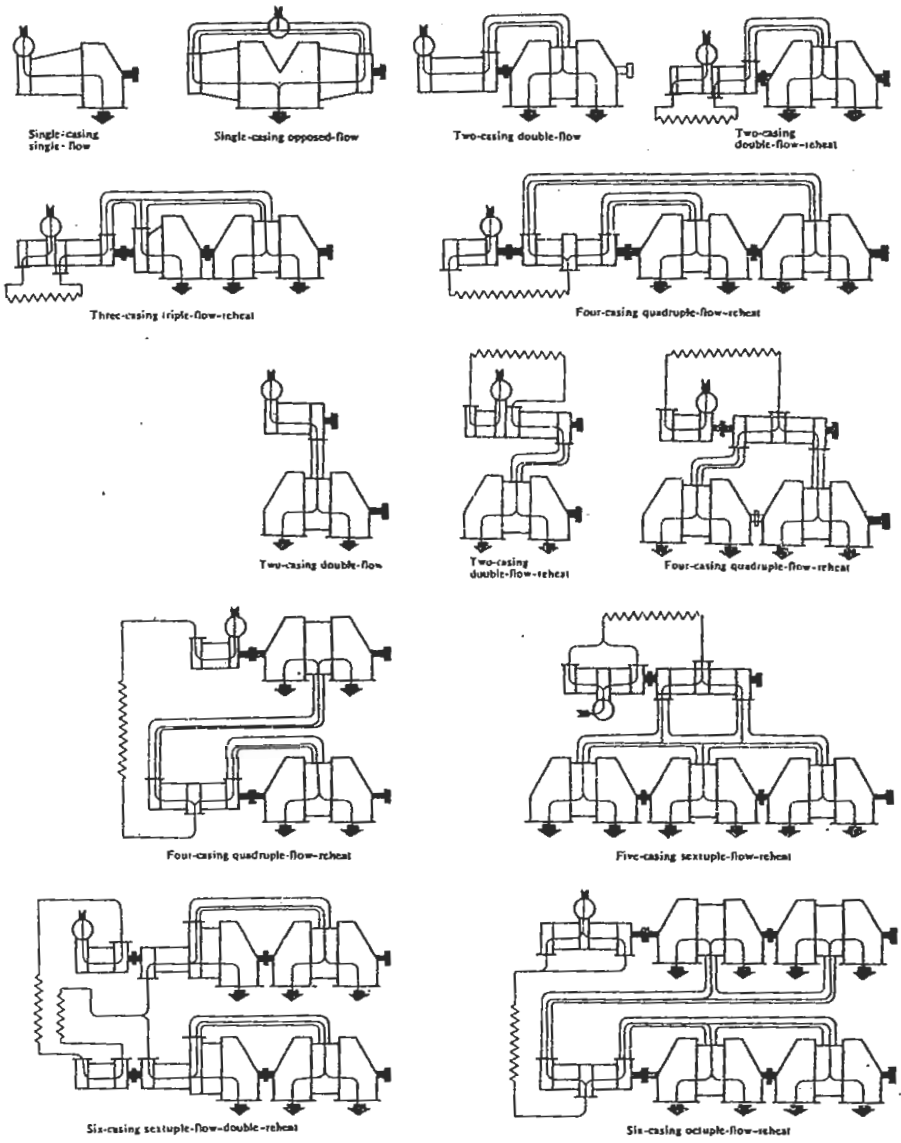


FIGURE 7.32
Casing and shaft arrangements for steam turbines, which depend on capacity and steam conditions. (*From Skrotski, 1962.*)

and their connections are given in Fig. 7.31. The various turbine arrangements, including tandem and cross-compounded units, are shown in Fig. 7.32.

TURBINE BLADING. Although there are a few radial-flow turbines, most of the steam and gas turbines are axial-flow machines, and a typical unit of this type is shown in Fig. 7.33. There are two basic types of turbine blading—impulse and reaction. Two different types of impulse staging and a typical reaction stage are shown in Fig. 7.34.

In the typical impulse stage, all of the steam first passes through a nozzle block where the compressed-fluid potential energy of the steam is converted into kinetic energy. Flow through these nozzles approaches a reversible adiabatic (isentropic) process. If the inlet velocity is negligible, the exit velocity $\bar{V}_1$ becomes

$$\bar{V}_1 = (-2\Delta h)^{1/2} = 223.73(-\Delta h_{\text{Btu}})^{1/2} \quad \text{ft/s} \qquad (7.43a)$$

$$= 44.721(-\Delta h_{kJ})^{1/2} \quad \text{m/s} \qquad (7.43b)$$

where Δh is the decrease in enthalpy across the nozzle, in USCS (7.43a) or SI (7.43b) units. The minimum-to-maximum pressure ratio across each nozzle block is around 0.53 for superheated and about 0.58 for saturated steam.

The high-velocity steam jet leaving the nozzle is then directed toward the moving blades where part of the kinetic energy of the steam is then transferred to the blades. The velocity vectors in the tangential and axial directions of the turbine rotor are shown in Fig. 7.35. The force on the moving blade, F_b, is equal to ma_t, which can be written as $m(d\bar{V}_t/dt)$, or, letting $\dot{m}$ represent the steam flow rate through the blades,

$$F_b = \dot{m}(\bar{V}_{1,t} - \bar{V}_{2,t}) \qquad (7.44)$$

The energy transferred to the moving blades is equal to the product of the force on the blade times the distance moved by the blade, while the power absorbed by the blade, P_b, is equal to the energy rate to the blade or the product of the blade force F_b and the blade velocity $\bar{V}_b$:

$$P_b = F_b\bar{V}_b = \dot{m}(\bar{V}_{1,t} - \bar{V}_{2,t})\bar{V}_b = \dot{m}(\bar{V}_1 \cos\alpha + \bar{V}_2 \cos\delta)\bar{V}_b \qquad (7.45)$$

Using geometry, it can be shown that Eq. (7.45) reduces to:

$$P_b = \frac{\dot{m}}{2}[(\bar{V}_1^2 - \bar{V}_2^2) - (\bar{V}_{1,r}^2 - \bar{V}_{2,r}^2)] \qquad (7.46)$$

If the steam flow through the blades is frictionless, the steam velocity, relative to the blade, is unchanged and $\bar{V}_{1,r} = \bar{V}_{2,r}$. In the actual case, however, there is friction and the relative steam velocity decreases as it flows through the blades, or $\bar{V}_{1,r} > \bar{V}_{2,r}$. For the case of frictionless flow, it can be seen from Eq. (7.46) that the effective rate of energy transfer to the blade is equal to the rate of change of the kinetic energy of the steam. For the case of flow with friction, the blade power is reduced by the second term of the equation, or $(m/2)(\bar{V}_{1,r}^2 - \bar{V}_{2,r}^2)$. This last term represents the mechanical power that is converted into thermal energy by friction.

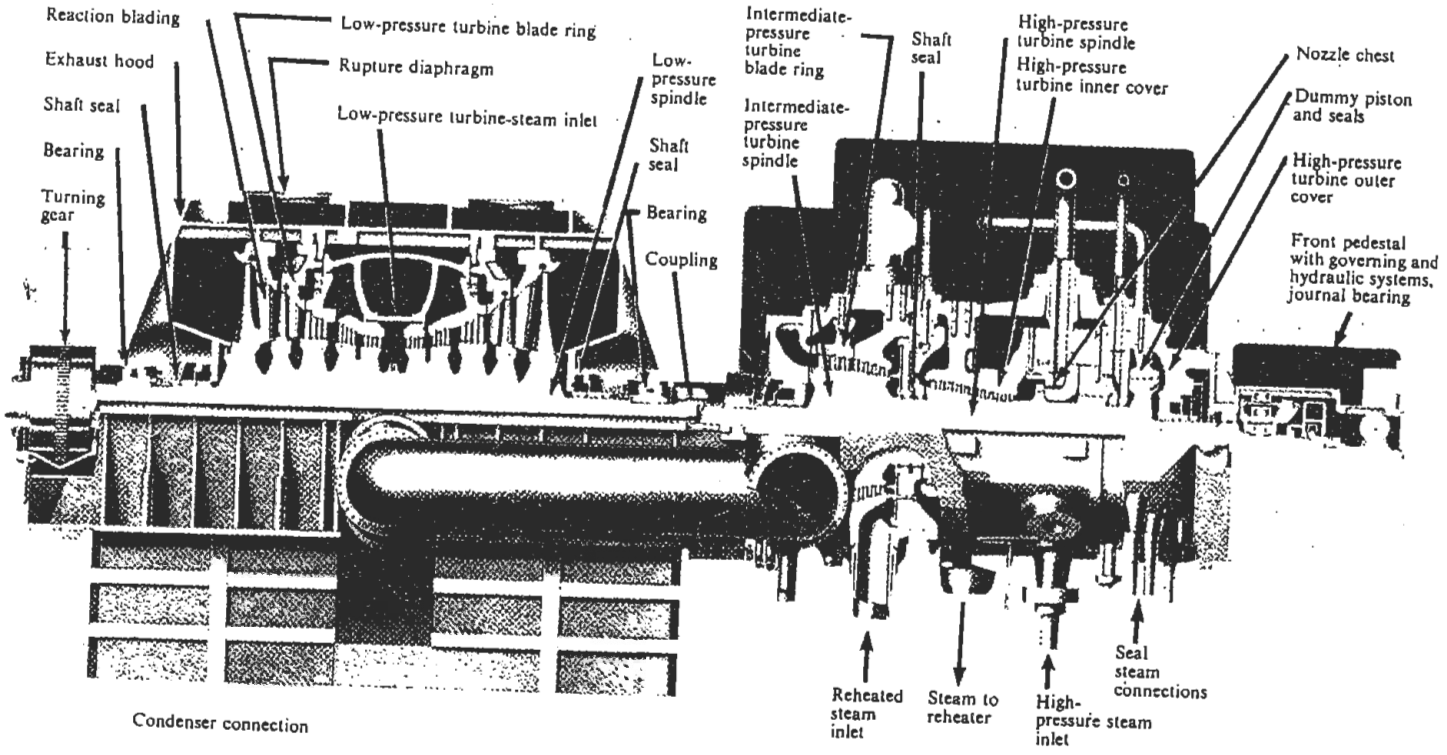


FIGURE 7.33
A typical steam-turbine installation. (*From Skrotzki, 1962.*)

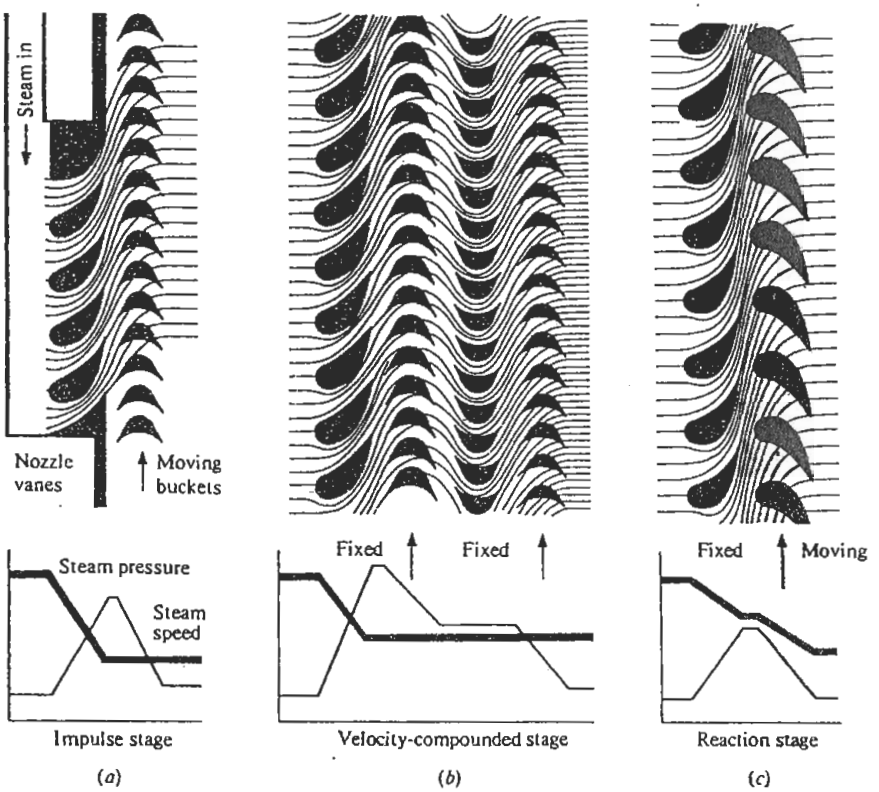


FIGURE 7.34
The various configurations, pressure distributions, velocity profiles, and specific-volume distributions for different types of turbine blading: (*a*) a Rateau impulse stage, (*b*) a Curtis impulse stage, and (*c*) two reaction stages. (*From Skrotski, 1962.*)

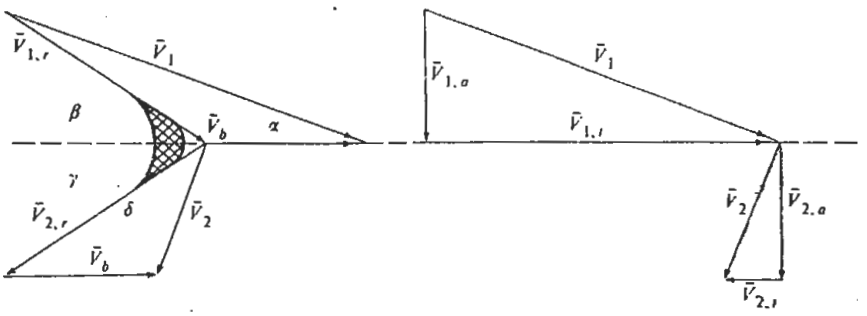


FIGURE 7.35
Steam velocity vectors for impulse turbine blading.

The performance of a given turbine blade is given by the blade efficiency, which is defined as the fraction of the kinetic power of the inlet steam that is transferred to the blade, or

$$\text{Blade efficiency} = \frac{2(\bar{V}_{1,t} - \bar{V}_{2,t})\bar{V}_b}{\bar{V}_1^2} = \frac{(\bar{V}_1^2 - \bar{V}_2^2) - (\bar{V}_{1,r}^2 - \bar{V}_{2,r}^2)}{\bar{V}_1^2} \tag{7.47}$$

For frictionless flow, the above equation reduces to:

$$\text{Blade efficiency} = 1 - \left(\frac{\bar{V}_2}{\bar{V}_1}\right)^2 \tag{7.48}$$

The blade efficiency and blade power are a maximum when $\bar{V}_2$ is a minimum and this occurs when $\bar{V}_{2,t}$ is zero and $\bar{V}_2$ is equal to $\bar{V}_{2,a}$. When there is no friction, this condition is attained when the tangential component of the steam velocity is equal to twice the blade velocity, or

$$\text{Optimum blade velocity} = \bar{V}_{b,\text{opt}} = \frac{\bar{V}_{1,t}}{2} = \frac{\bar{V}_1}{2}\cos\alpha \tag{7.49}$$

The actual steam flow through the turbine blades does occur with friction and, in this case, V_2 can be minimized by reducing the blade exit angle γ. This produces an asymmetric impulse turbine blade. Both the reduction in the blade exit angle and the presence of friction creates an axial load or thrust on the blade. Friction also increases the value of the exit steam enthalpy. This phenomenon is called *stage reheat.*

As indicated earlier, there are two kinds of impulse blading. A Rateau stage is composed of a nozzle block followed by a single set of moving blades, as shown in Fig. 7.34*a*. A Curtis stage is composed of the nozzle block followed by a set of moving blades, followed by a set of stationary turning blades, which are followed, in turn, by another set of moving blades, as shown in Fig. 7.34*b*. When two or more Rateau stages are put in series, they are said to be *pressure-compounded.* The Rateau stage normally has a higher blade efficiency than the Curtis stage. The Curtis stage is commonly used as the first high-pressure stage in the turbine because it can accommodate a large pressure and enthalpy drop across the stage. Only a small fraction of the total stage power is generated in the second set of moving blades.

The other basic type of steam and gas turbine blading is the reaction blading shown in Fig. 7.34*c*. Reaction blades are shaped like airfoils and this produces a steam flow passage that is shaped like a converging-diverging nozzle. The stationary and moving blades have approximately the same shape. Thus, there is a pressure drop across the moving blades. This is different from impulse blading which, barring friction, has no pressure drop across the moving blades. The

expansion through the moving blades gives an added thrust or reaction to those blades. If the enthalpy drop across both the stationary and the moving blades are the same, the reaction stage is said to be a *50 percent reaction stage.* This condition results in $\bar{V}_1 = \bar{V}_{2,r}$.

The Rateau impulse stage produces the maximum power per stage, and, while the reaction stage is more efficient, the Curtis staging can undergo a larger pressure drop. Impulse staging is commonly employed in the high-pressure part of the turbine because there is a very low pressure drop across the moving blades. It is important to keep the end leakage to a minimum in the high-pressure part of the turbine where the blades are very short.

Reaction blading is commonly used in the intermediate- and low-pressure part of the turbine. Although end leakage is greater with reaction blading because of the higher pressure drop across the moving blades, the fractional loss is less because of the longer blades.

7.3.2 Hydraulic Turbines

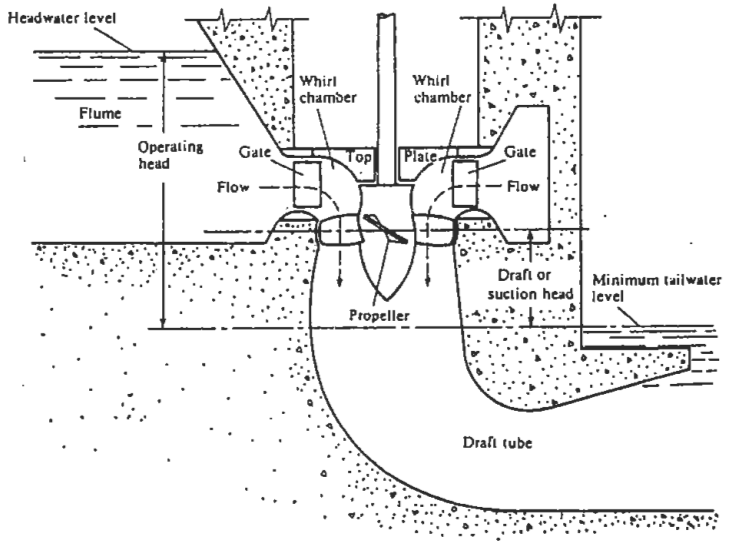
Hydraulic turbines convert the potential energy of the water into mechanical work. These systems provide approximately 14 percent of the electrical energy in the United States although this percentage is dropping as electrical generation capacity increases. Hydraulic turbines range in size from 2 to 615 MW for one of the units at the Grand Coulee power complex. The Grand Coulee hydroelectric system is designed to operate at 7000 MW.

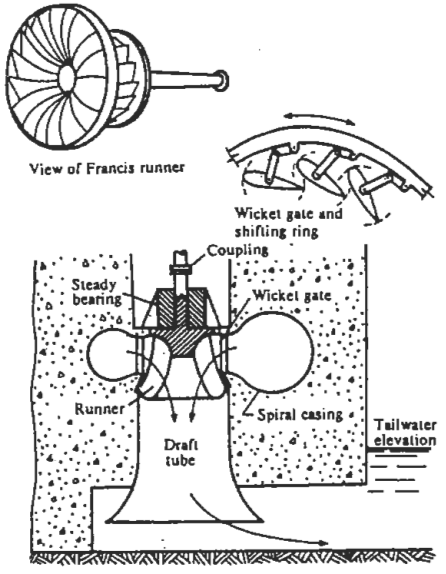
Hydraulic turbines may be classified as reaction, impulse, or mixed-flow, or as radial, axial, or combined-flow. There are three basic types of hydraulic turbines—propeller, Francis, and Pelton-wheel. These systems are shown in Fig. 7.36, along with a plot of their relative conversion efficiencies.

Propeller or axial-flow turbines are used for low heads (10 to 100 ft, or 3 to 30 m). Fixed-bladed propeller turbines are inexpensive and have a high conversion efficiency at the design conditions but relatively poor conversion efficiency at lower flow rates. The Kaplan turbine is a propeller turbine with variable-pitch blades and these blades can be adjusted to give high efficiency for off-load conditions. Blade pitch is not achieved automatically but must be adjusted manually while the turbine is shut down.

The Francis turbine is one of the more common hydraulic turbines and is a radial, mixed-flow turbine that is employed for intermediate heads (15 to 1500 ft, or 4.6 to 460 m). These units have an excellent conversion efficiency at their rated loads but a relatively poor efficiency at off-load conditions.

The Pelton wheel is an impulse hydraulic turbine which is normally employed at heads above 150 ft (46 m). These units require a relatively low water-flow rate and the water velocity is controlled by a nozzle. Each "bucket" on the wheel has a "splitter" that deflects half of the flow to each side of the wheel to reduce the axial thrust. The Pelton wheel has a high conversion efficiency over a wide range of water flow.


Headwater level
Flume
Operating head
Whirl chamber
Whirl chamber
Gate
Top
Plate
Gate
Flow
Flow
Draft or suction head
Minimum tailwater level
Propeller
Draft tube


View of Francis runner
Wicket gate and shifting ring
Coupling
Steady bearing
Wicket gate
Runner
Spiral casing
Draft tube
Tailwater elevation

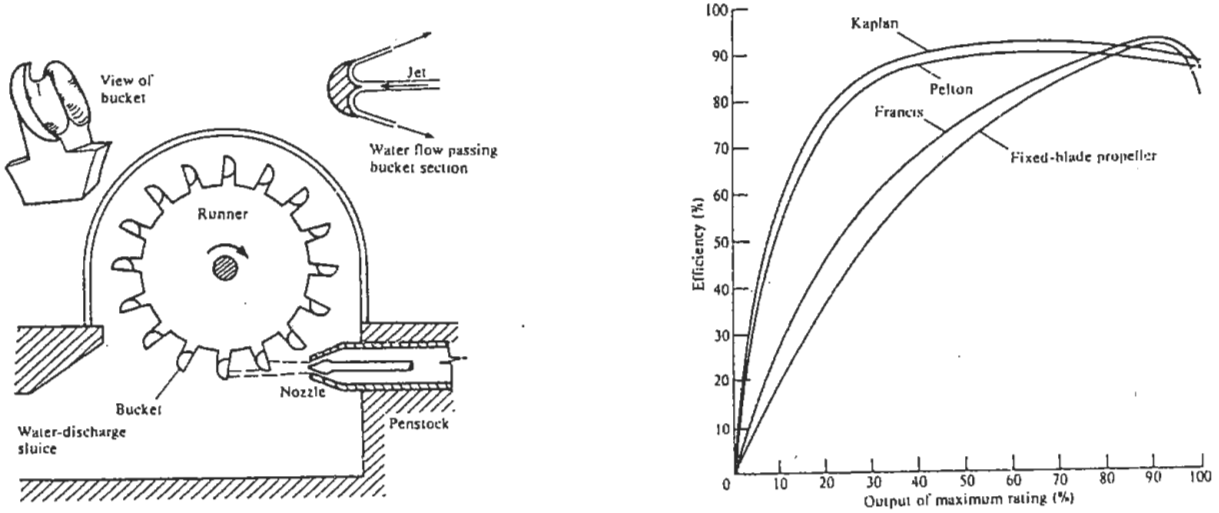
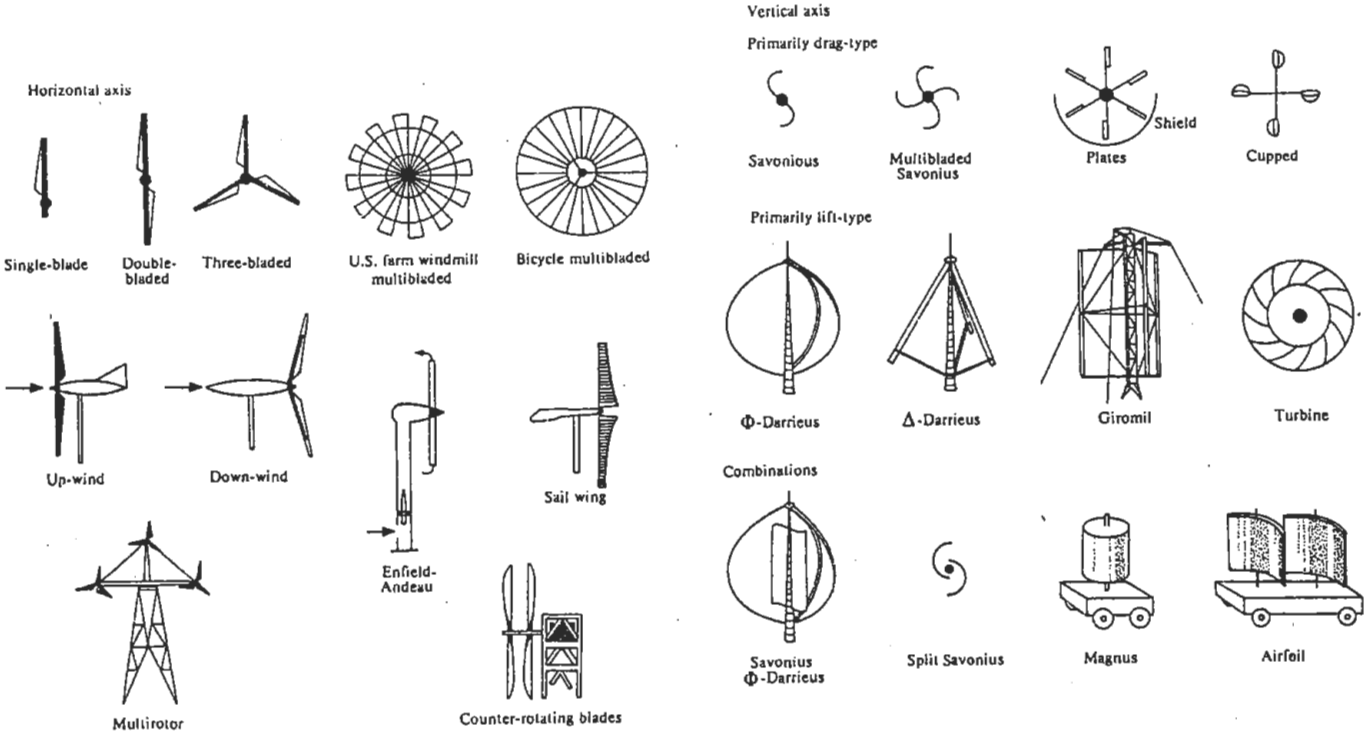


FIGURE 7.36
Hydraulic turbines and their performance. (*From Skrotzki and Vopat, 1960, and courtesy of V. A. Thiemann.*)


Horizontal axis
Single-blade
Double-bladed
Three-bladed
U.S. farm windmill multibladed
Bicycle multibladed
Up-wind
Down-wind
Sail wing
Enfield-Andeau
Multirotor
Counter-rotating blades
Vertical axis
Primarily drag-type
Savonious
Multibladed Savonius
Shield
Plates
Cupped
Primarily lift-type
Φ-Darrieus
Δ-Darrieus
Giromil
Turbine
Combinations
Savonius Φ-Darrieus
Split Savonius
Magnus
Airfoil

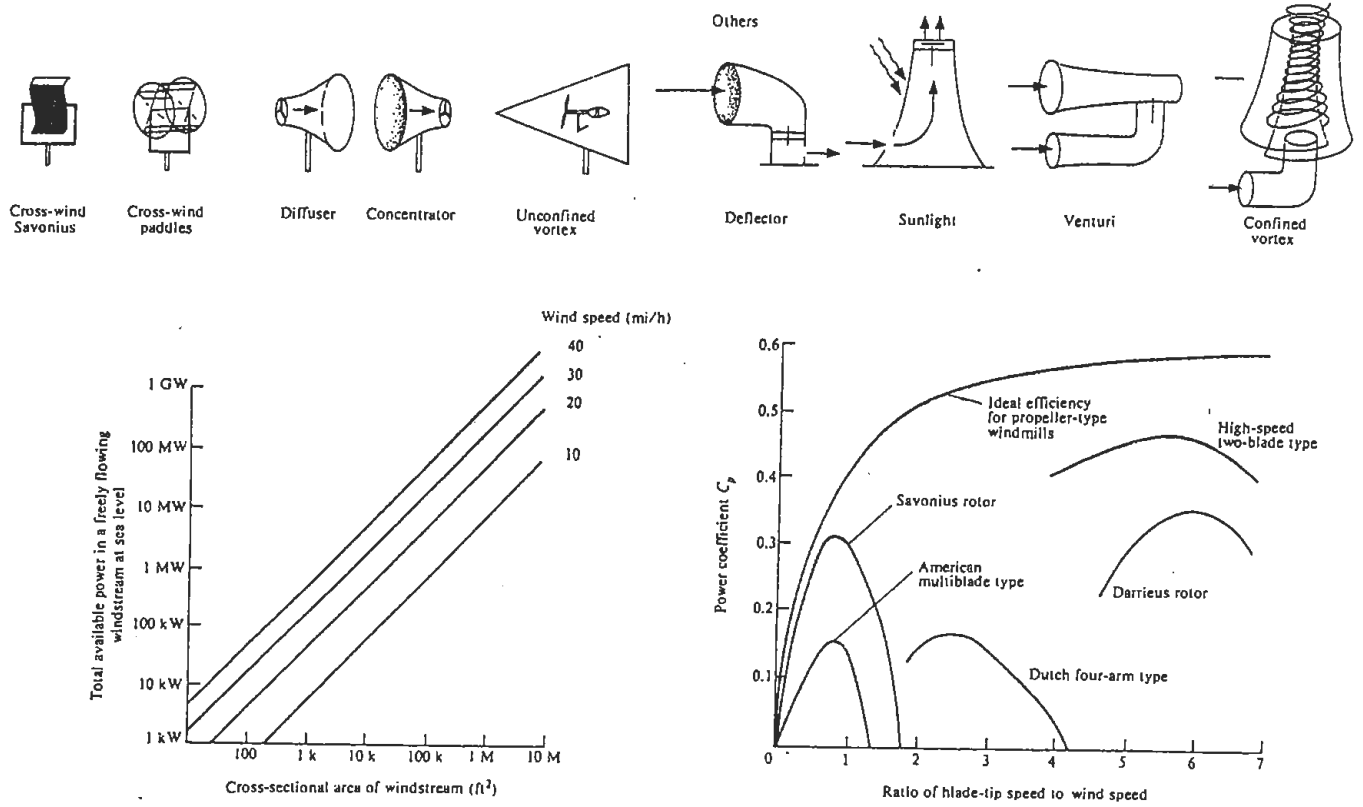
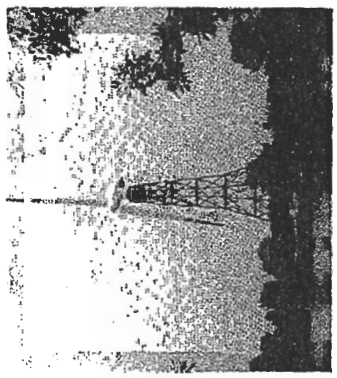
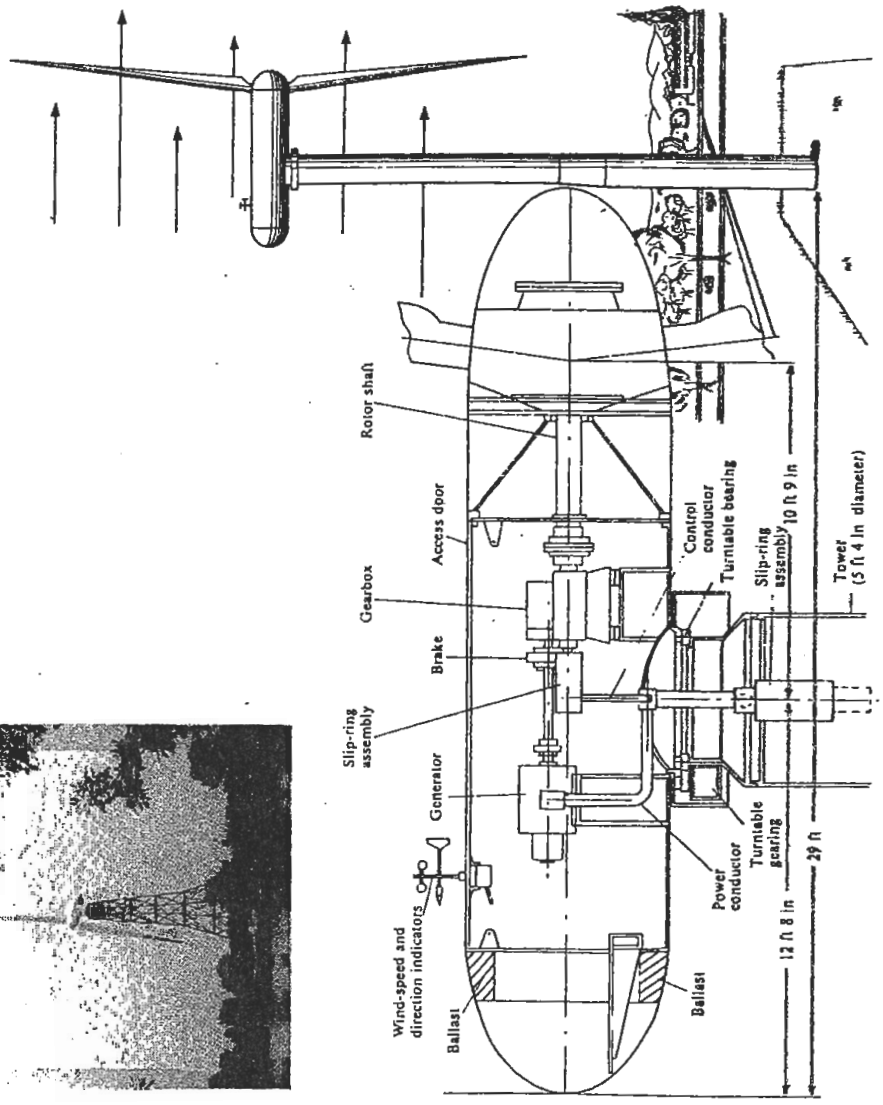


FIGURE 7.37
Basic wind-turbine systems and their performance. (*From Hirschfeld, 1977.*)




Rotor shaft
Access door
Gearbox
Brake
Slip-ring assembly
Generator
Wind-speed and direction indicators
Ballast
Ballast
Power conductor
Turntable gearing
Control conductor
Turntable bearing
Slip-ring assembly
Tower (5 ft 4 in diameter)
10 ft 9 in
12 ft 8 in
29 ft

7.3.3 Wind Turbines

Wind turbines or windmills convert the kinetic energy of the wind into mechanical work. For the production of alternating-current (ac) electricity, these systems must be designed to operate a constant angular velocity over a wide range of wind speeds in order to produce a constant frequency. There are many different kinds of windmills, including propeller and other axial-flow turbines, as well as radial systems mounted on vertical axes. Some of the various wind-powered systems are shown in Fig. 7.37.

Wind-powered systems have been widely used since the tenth century for pumping water, grinding grain, and other low-power applications. There were several early attempts to build large-scale wind-powered systems to generate electricity. In 1931, the Russians built a large windmill with a 100-ft (30.5-m)-diameter blade, but it had a very low conversion efficiency and was abandoned. In 1945, a Vermont utility built a large wind-powered generator to produce electricity. This system cost $1.25 million and had an electrical power output of 1250 kW_e. This unit operated for 23 days before one of the blades failed due to fatigue and the project was abandoned.

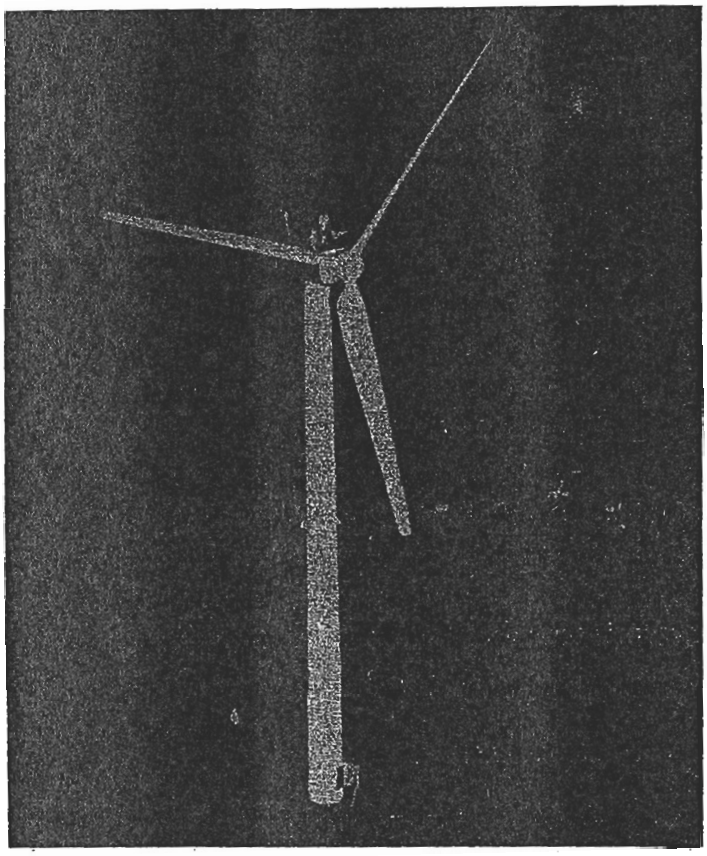
The National Aeronautics and Space Administration (NASA), in conjunction with the Energy Research and Development Agency (ERDA), has built and tested a number of large wind-powered generators. The first machine was a 100-kW_e unit built at Sandusky, Ohio, for around a million dollars. A diagram and picture of this downwind rotor machine is shown in Fig. 7.38. A number of other machines have been constructed with powers up to 2.5 MW_e and rotor diameters up to 350 ft (107 m). During the 1980s, it became popular to invest money in wind systems because of tax benefits. Consequently, a number of "wind farms" were built, particularly in the mountain passes of California. In 1985, about half of the world's wind-generated electricity was produced in the Altamont Pass area of California. This area has 6700 wind turbines with a total rated capacity of 630 MW_e. A typical wind farm is shown in Fig. 7.39.

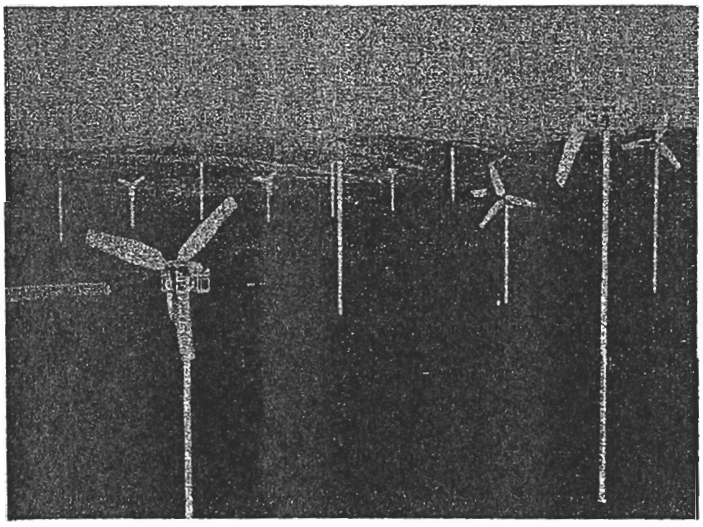
The total power that is available to a given wind turbine is equal to the product of the mass flow rate of the wind, $\dot{m}_w$, and its kinetic energy, $\bar{V}^2/2$. Assuming constant area or ducted flow, the continuity equation states that $\dot{m}_w = A\rho\bar{V}$, where A is the area normal to the wind, ρ is the air density, and $\bar{V}$ is the wind velocity. Thus, the total wind power becomes:

$$\text{Total wind power} = P_w = \frac{\dot{m}_w \bar{V}^2}{2} = \frac{A\rho\bar{V}^3}{2} \tag{7.50}$$

It will be noted from Eq. (7.50) that the wind power varies as the cube of the wind velocity.

FIGURE 7.38
The 100-kW_e, wind-powered, NASA-ERDA system constructed at Sandusky, Ohio. (*From Kidd and Garr, 1972, and Lindsley, 1974.*)





Unfortunately, the total wind energy cannot be recovered in a wind turbine because the outlet wind velocity cannot be reduced to zero, otherwise there would be no flow through the turbine. If the inlet wind velocity is $\bar{V}_i$ and the outlet velocity is $\bar{V}_o$, the mass flow rate through the system is approximately $A\rho\bar{V}_{ave}$ where the average velocity is $(\bar{V}_i+\bar{V}_o)/2$, and the power removed from the wind is equal to the mass rate times the change in kinetic energy, or:

$$P_{out}=\frac{\dot{m}_w}{2}(\bar{V}_i^2-\bar{V}_o^2)=\frac{A\rho}{4}(\bar{V}_i+\bar{V}_o)(\bar{V}_i^2-\bar{V}_o^2)$$

$$=\frac{A\rho\bar{V}_i^3}{4}(1+x)(1-x^2)$$

$$=\frac{P_w}{2}(1+x-x^2-x^3) \tag{7.51}$$

where $x=\bar{V}_o/\bar{V}_i$. Differentiating Eq. (7.51) with respect to x and setting the differential to zero gives the optimum value of x for the maximum power output:

$$\frac{d(P_{out})}{dx}=0=1-2x-3x^2$$

and, using the quadratic equation,

$$x_{maxP}=\frac{2-(4+12)^{1/2}}{-6}=\tfrac{1}{3} \tag{7.52}$$

Substituting this value into Eq. (7.51), the maximum power recovered is:

$$P_{out,max}=\frac{P_w}{2}(1+\tfrac{1}{3}-\tfrac{1}{9}-\tfrac{1}{27})=\tfrac{16}{27}P_w$$

$$=0.593P_w \tag{7.53}$$

Thus, the maximum power that can be realized from a wind system is 59.3 percent of the total wind power. This is the asymptotic value in the plot presented in Fig. 7.37.

One of the more unusual wind systems is the Flettner rotor. The Flettner rotor is composed of an externally powered rotating cylinder. As the cylinder spins, it establishes a high-pressure region on that part of the cylinder turning against the wind due to the stagnated flow in the boundary layer. This gives rise to a net force acting on the cylinder, as shown in Fig. 7.40. This effect is called the *Magnus effect* or *magnus force.*

A wind-powered sailing vessel sailed across the Atlantic in the early 1930s using the Magnus force as the mode of propulsion, and at about the same time a novel wind-powered electric generating system was proposed by J. D. Madaras. This system was to be composed of a circular train track with a continuous train

---

FIGURE 7.39
A typical "wind farm" and power windmill.

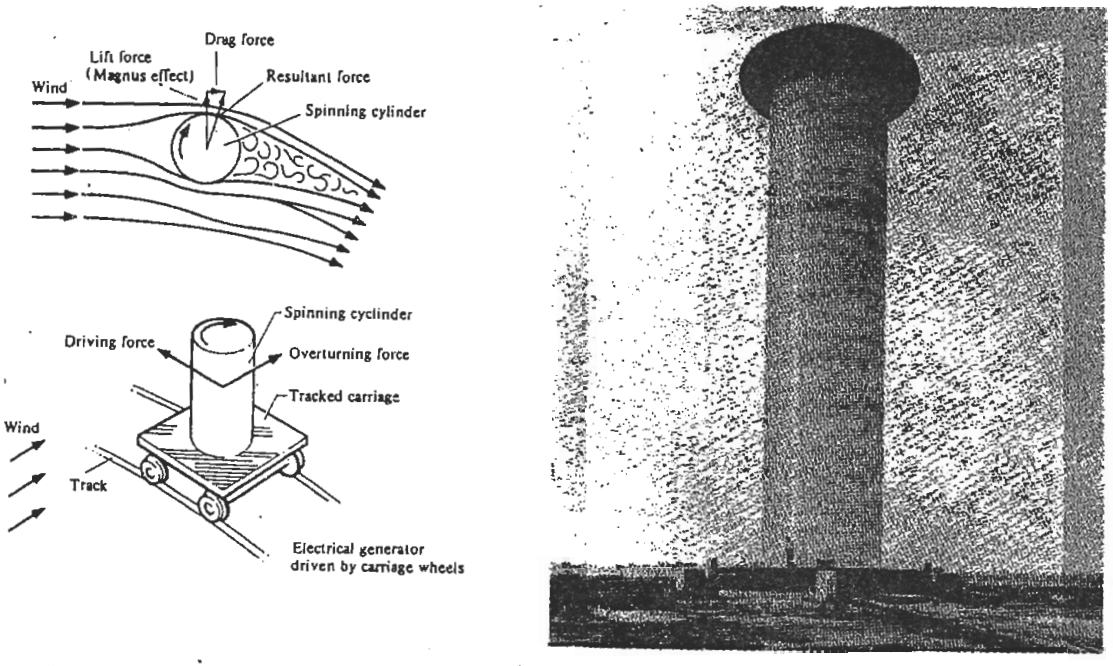


FIGURE 7.40
The proposed wind-powered Madaras electrical generating system and a picture of the pilot model of the Madaras plant that was erected in Burlington, New Jersey, in 1933; and that system subsequently blew down. (*From Hirschfeld, 1977.*)

of flatcars. A 90-ft-high cylinder was to be mounted on each flat car with an angular velocity of 120 r/min. As the wind drove the cars around the circular track, the angular velocity of the cylinders reversed every 180° of track rotation. Electrical energy was to be produced by generators driven by the wheels of the flatcars. This system is also depicted in Fig. 7.40.

The design and successful operation of large-scale wind-powered generators face a number of formidable problems. If the system is designed to produce ac power, a constant angular velocity and force is desirable. Unfortunately, the wind velocity is neither constant in magnitude or direction nor is it constant from the top to the bottom of a large rotor. This imposes severe cyclic loads on the turbine blades, creating fatigue problems. This problem is compounded if a downwind rotor system is used because the "shadow" of the support tower unloads the blade. This effect also produces a noticeable "popping" noise which can be objectionable.

There are also times when the wind velocity is too low to produce significant power. This means that some sort of energy-storage system or backup energy system must be utilized. The wind systems must also be shut down when the wind velocity is too high so as to prevent damage to the machine. More windmills are destroyed or damaged by high winds than by any other natural phenomena.

While these and other problems are difficult to overcome, the research and development of wind-powered systems continues because of the environmentally clean energy that is produced and the zero fuel costs.

7.4 ELECTROMECHANICAL CONVERSION

7.4.1 General

Most of the systems that convert electrical energy into mechanical energy depend on the interaction of magnetic fields established by the flow of electrons (electric current) through conductors. When a direct current is passed through a conductor, a magnetic field is produced around the conductor, as shown in Fig. 7.41*a*. The "right-hand rule" states that if the thumb of the right hand points in the direction of current flow, the fingers wind around the conductor in the direction of the magnetic field lines. The lines of force between the two poles of a magnet flow from the north pole to the south pole, by convention, as shown in Fig. 7.41*b*.

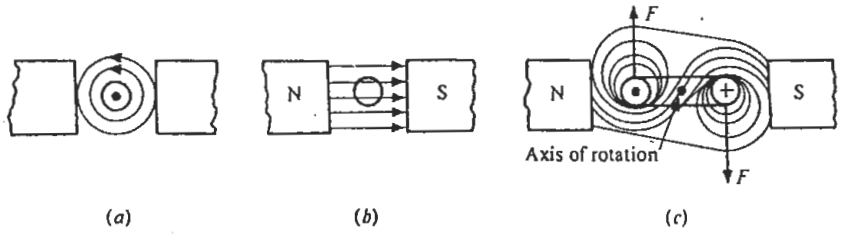


FIGURE 7.41
The interaction of magnetic fields around conductors.

If the conductor with the current flowing through it is placed between the two poles of the magnet, the magnetic field lines will have a high density on one side and low density on the other side. This produces a net force on the conductor in the direction of low magnetic flux density or perpendicular to the magnetic field. This phenomenon is depicted for a coil of wire in Fig. 7.41*c*. The force on the conductor is proportional to the cross-vector product of the electric current through the conductor and the magnetic field strength. The force on the conductor, in newtons, is equal to:

$$\text{Force} = l(\bar{i} \times \bar{B}) \tag{7.54}$$

where $\bar{i}$ is the current flowing in the conductor, in amperes, $\bar{B}$ is the magnetic flux density, in webers/m^2, and l is the length of the conductor, in meters.

7.4.2 Electric Motors

The operation of an electric motor depends upon the interaction between the magnetic field of the stator or field winding and the magnetic field established in the rotor or armature winding. The magnetic field of the stator is established by a series of stationary coils wound around the fields poles, as shown in Fig. 7.42. The stator magnetic field is stationary if direct current is used in the motor. If alternating current is passed through the field coils, however, the field-pole polarity reverses with current reversal. Relative to the armature, it appears that the magnetic field of the stator revolves at synchronous speed. If 60-Hz current is put through the stator windings, the synchronous speed of the field is:

$$\text{Synchronous speed} = \frac{7200}{\not p} \quad \text{r/min} \tag{7.55}$$

where $\not p$ is the number of poles in the field.

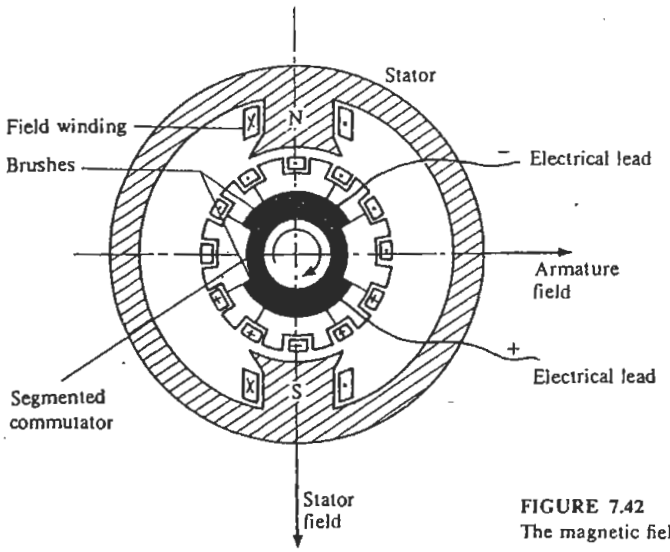


FIGURE 7.42
The magnetic fields in an electric motor.

In a direct-current (dc) motor, current is only supplied to those armature conductors that are directly opposite the stator poles, similar to that pictured in Fig. 7.42. This means that the magnetic field of the armature is 90° out of phase with the magnetic field of the stator, producing maximum torque. This condition is accomplished with the use of a segmented commutator and brushes.

In an ac motor, the magnetic field of the armature can be established by either introducing a direct durrent in the armature winding with a pair of slip rings and brushes or by inducing or generating a current in the rotor conductors as the lines of force of the rotating field pass through the armature conductors. When direct current is supplied to the armature of an ac motor, it effectively makes the rotor a permanent magnet and, if the system is not overloaded, the fixed armature field will "lock" into the rotating field of the stator and turn at a constant speed equal to the synchronous speed. These motors are called *synchronous.* They are constant-speed machines as long as the line frequency is constant and the system is not overloaded.

If the current flow through the armature conductors is produced by the "rotating" field, the motor is called an *induction motor.* The armature of an induction motor always runs at slower angular velocity than the synchronous speed of the field. The difference between the synchronous speed and the actual speed of the motor is called the *slip,* and is reported in units of revolutions per minute. The slip increases as the load is increased. The rotor of an induction motor requires no electrical connections (the "squirrel-cage" motor), although the wound-rotor motor commonly uses a rheostat (a variable resistor) connected to the rotor winding by slip rings and brushes. This is done to improve the starting torque.

Direct-current motors have a number of advantages over the ac systems. The dc motors are more efficient than the ac systems because they do not have the hysteresis and eddy-current losses associated with the ac windings. Consequently, it is common practice to employ dc motors for high-power applications if a source of direct current energy is available. Direct-current motors also used to be best for variable-speed applications but with the new solid-state frequency controllers, ac motors can also be used in variable-speed applications.

There are a number of problems associated with the use of dc motors: They have higher capital and maintenance costs than ac motors. The use of segmented commutators and brushes greatly increases the required maintenance. The low availability of large-capacity dc power also limits the application of these motors.

7.4.3 Types of Motors

DC MOTORS. There are three basic types of dc motors. They include the series-wound motor, the shunt-wound motor, and the compound-wound motor. The schematic diagrams for each of these motors are presented in Fig. 7.43, along with their speed-torque characteristics and their uses.

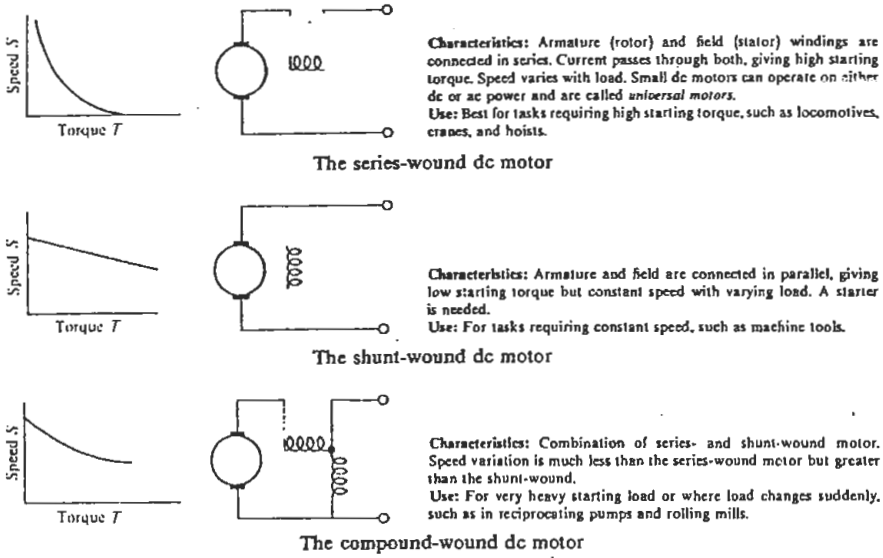


FIGURE 7.43
Schematics, characteristics, and uses of dc electrical motors. (*From Collins, 1969.*)

In the series-wound motor, the field and armature windings are connected in series. This system has excellent starting torque but the speed varies widely with the load. In fact, this motor "runs away" if it is unloaded under power.

In the shunt-wound motor, the stator and armature windings are connected in parallel. These motors run at fairly constant speed. This motor must have a rheostat (variable resistor), called a *starter* or *starting box*, in the armature circuit. This resistance is inserted in the armature circuit at startup and then removed as the machine attains operating speed. At rest, there is no back electromotive force (emf) in the armature circuit and the armature resistance is very low. Consequently, very high (short-circuit) currents will develop in the armature winding unless a resistance is inserted into the circuit to limit the starting current. As the angular velocity increases, the back emf increases to limit the armature current.

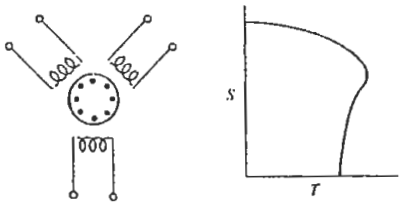
The compound-wound motor has part of the field winding connected in series and part of it connected in parallel with the armature circuit. Some compound-wound motors have a centrifugal switch in the parallel-field winding so that the motor starts as a series-wound motor and runs as a compound-wound motor.

AC MOTORS. The two basic types of ac motors are the synchronous and the induction motors. High-powered ac systems commonly require polyphase, usually three-phase, ac power. Large synchronous motors require a dc power supply to the motor armature and this is provided through brushes and slip rings. These motors are started like a large induction motor. The schematic diagram of this

system is shown in Fig. 7.44, along with the other polyphase ac motors. The speed-torque characteristics and uses of these ac systems are also given in Fig. 7.44.

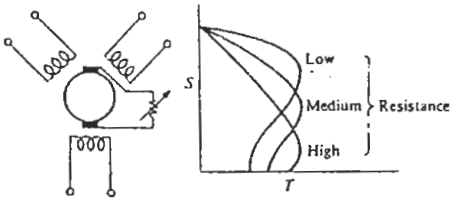
Polyphase induction motors can be divided into either squirrel-cage motors or the wound-rotor motors. Squirrel-cage motors have a rotor that literally looks like a cage and there are no electrical connections to the armature. The wound-rotor motor has no power to the armature but it does have a rheostat in the rotor circuit to produce better speed-torque characteristics. Although the induction motors are less expensive than synchronous motor, and they require no power to the armature, they do produce a low, lagging power factor. This means that there is poor utilization of the ac energy.

Almost all single-phase squirrel-cage motors are limited to a maximum power of $7\frac{1}{2}$ hp. These systems normally require some method of initial phase



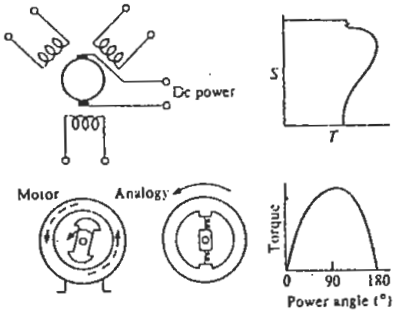
Characteristics: The rotor has copper conductor bars set into the periphery and connected to form a "squirrel cage." The simple design offers rugged service. Slip (difference between synchronous speed and actual speed of the rotor) and starting torque vary between the various types. Squirrel-cage motors are preferable to de motors for constant-speed work, because the initial cost is less and the absence of a commutator reduces maintenance. Speed is determined by the number of poles.
Use: General-purpose, heavy applications such as blowers and drill presses. Absence of electrical contacts makes these motors ideal for operation in inflammable atmospheres.

Polyphase, squirrel-cage induction motor



Characteristics: Wound-rotor induction motors are commutator machines very much like dc motors and have slip rings to provide external connections to the armature windings. Adjustable speeds are obtained through insertion of resistors in the armature circuit. The speed of maximum torque depends on the rotor resistance.
Use: Particularly adaptable wherever high starting torque and low starting current are required, where heavy or delicate loads must be accelerated gradually and smoothly, and where adjustable speed is desired.

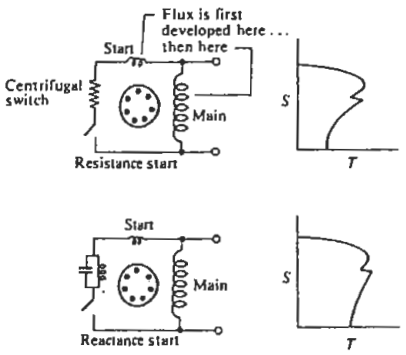
Polyphase, wound-rotor induction motor



Characteristics: In contrast to the induction motor, the rotor of the synchronous motor rotates in exact step with line frequency (thus the name). The rotor is connected to a de supply which provides a strong field in the rotor that locks in step with the stator's rotating ac field. However, small motors have what is effectively a permanently magnetized rotor. Speed is determined by the number of pole pairs and is always a ratio of line frequency. Since synchronous motors are not self-starting, a built-in squirrel cage in the large motors makes them start as an induction motor.
Use: Widely used to power electrical timing devices and machines which must operate in a synchronized manner with each other. Should not be used where torque fluctuations are violent. They are smaller in size than induction motors of the same horsepower and, therefore, cost less initially.

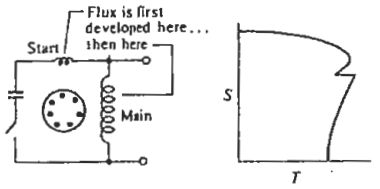
Polyphase, alternating-current, synchronous motor

FIGURE 7.44
Schematics, characteristics, and uses of large polyphase ac motors. (*From Collins, 1969.*)



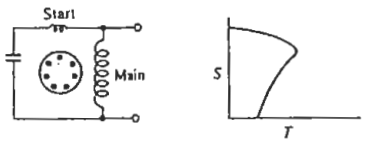
Characteristics: A split-phase motor has two windings—the main winding and start winding. Since the large main winding is highly inductive, its current lags applied voltage by nearly 90 degrees. All that remains is to provide a winding with no inductance, one in which the current and voltage are in phase, and a virtual two-phase motor is produced. This is done by a resistance circuit (called *resistance start*) or a reactance circuit (*reactance start*) which drops out after the motor reaches operating speed.
Use: These are low or moderate-starting-torque motors that are inexpensive. Since power is limited to about ½ hp, these motors are used mainly for small appliances and office machines.

Split-phase, single-phase, squirrel-cage ac motors



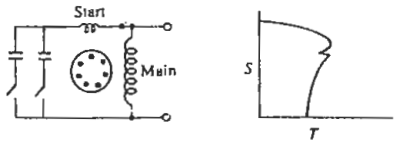
Characteristics: This motor has a capacitor connected to the stator to cause a momentary lead of current over voltage in that winding. The capacitor-start motor has fewer losses and a greater phase displacement than the split-phase motor, but is more expensive.
Use: Higher starting torque than the split-phase motor, hence useful for applications requiring more torque, such as household refrigerators. Available in up to 3 hp.

The capacitor-start, single-phase squirrel-cage ac motor



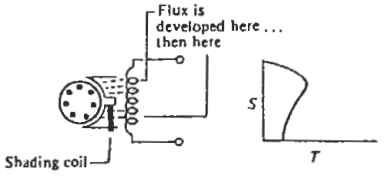
Characteristics: Also called capacitor split phase. A capacitor permanently connected in the start winding starts and runs the motor like a two-phase motor. This motor has the least starting torque of the three capacitor types, but it has a high maximum torque and requires the least maintenance of all single-phase motors.
Use: Due to high maximum torque, these motors are useful where momentary overloads are experienced, such as with grinders and sanders. Available in up to about ½ hp.

The permanent-split-capacitor, single-phase, squirrel-cage ac motor



Characteristics: Capacitance in the rotor auxiliary circuit remains connected, but it is reduced in value after starting. Larger sizes are more expensive than three-phase motors, but three-phase power is usually not available.
Use: Probably the best of the single-phase motors. Exceptionally quiet. Available in fractional horsepower to 20 hp.

The two-value-capacitor, single-phase, squirrel-cage ac motor



Characteristics: One pole piece in each pole is modified by placing a shorted copper turn or "shading coil" around it to split the component of the magnetic field. High slip, torque very slight.
Use: Low-torque applications, such as in small fans. Available in subfractional to fractional horsepower.

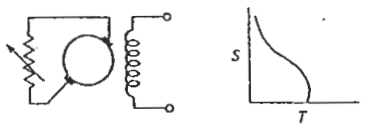
The shaded-pole, single-phase, squirrel-cage ac motor

FIGURE 7.45
Schematics, characteristics, and uses of single-phase, squirrel-cage, ac motors. (*From Collins, 1969.*)

displacement in the field windings, so that they actually start as two-phase motors, in order to produce sufficient starting torque. This is usually accomplished by using an auxilliary starting-field winding with some sort of a reactance in the circuit to change the phase of the starting-field current. This starting circuit commonly contains a centrifugal switch that opens slightly below the rated speed so that the motor starts as a two-phase motor but runs as a single-phase motor. The schematic diagrams for several of the single-phase squirrel-cage motors are presented in Fig. 7.45, along with their speed-torque characteristics and their applications.

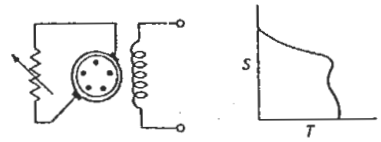
The single-phase wound-rotor motor has an independent rotor circuit connected, in series, to a rheostat through slip rings. This system has excellent starting torque but the speed varies widely with load. Squirrel-cage rotors are sometimes used in wound-rotor systems to produce a relatively constant angular velocity. The schematic diagrams for several of the single-phase wound-rotor induction motors along with their speed-torque characteristics and their applications are given in Fig. 7.46.

Single-phase synchronous motors are usually low-powered systems that depend upon reluctance and hysteresis effects to establish rotor polarity and there are no electrical connections to the armature. The reluctance motor has a "dumbbell-shaped" rotor that "locks" into the rotating magnetic field to give minimum magnetic reluctance. The schematic diagrams of some of the single-phase synchronous motors are shown in Fig. 7.47, along with the speed-torque characteristics and their applications.



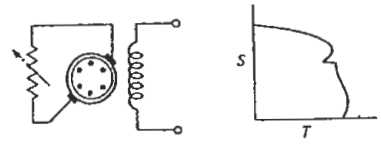
Characteristics: Like all wound-rotor motors, this type has an independent rotor circuit. However, unlike the polyphase motor, the commutator is placed so that the rotor's magnetic axis is offset from that of the stator to give the desired phase shift. Starting characteristics are very good, but the motor runs with varying speed.
Use: Like all repulsion types, this motor has good starting characteristics and is used for heavy loads.

Repulsion, single-phase, wound-rotor ac motor



Characteristics: This motor has two windings on the rotor—a repulsion winding for starting and an inner squirrel-cage winding for running smoothly. However, electrical and mechanical noise, and extra maintenance are disadvantages.
Use: Applications requiring starting under full load, such as in conveyors and stokers.

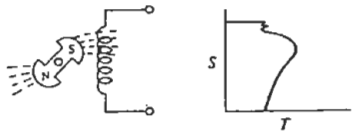
The repulsion-induction, single-phase, wound-rotor ac motor



Characteristics: This motor, also with two windings, starts as a repulsion motor with high torque and runs as a squirrel-cage motor with good constant-speed characteristics. Brush wear is minimized by using commutator circuit only at start.
Use: Most popular commutator, single-phase motor for industrial applications.

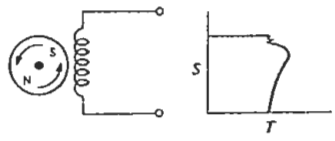
The repulsion-start, single-phase, wound-rotor ac motor

FIGURE 7.46
Schematics, characteristics, and uses of single-phase, induction, ac motors. (*From Collins, 1969.*)



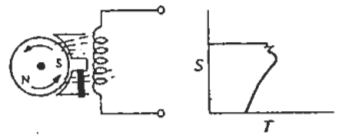
Characteristics: The reluctance (resistance to establishing a magnetic field) rotor tends to align itself in the magnetic field so that magnetic reluctance is minimum. Roughly dumbbell shaped, the poles tend to align themselves along the flux field. Current alternating off and on continually pulls the poles around in exact step. The motor starts as an induction motor with split-phase or capacitor windings.
Use: This motor is inexpensive, simple, and suitable for light loads.

The single-phase, reluctance, synchronous motor



Characteristics: If the discrete poles of a reluctance motor are eliminated, the rotor still becomes magnetized, but the flux is not channeled as in the reluctance motor, and thus it is not as efficient. The rotor's tendency to maintain its magnetized condition in one position is called *hysteresis*. The hysteresis rotor uses this principle to run as the induced rotor poles are pulled around by the alternating field. However, the poles can move over the rotor surface slowly, and thus the rotor can slip while still providing torque. The hysteresis motor starts the same as the reluctance type.
Uses: Very steady speed makes this motor desirable for applications such as record-player drives. Having less tendency to hum and vibrate around synchronous speed, this motor is used more widely than reluctance motors.

The single-phase, hysteresis, synchronous motor



Characteristics: A special type of hysteresis motor, this type operates the same as a squirrel-cage shaded-pole motor, but at synchronous speed.
Use: Of all hysteresis motors, this type has the widest use in applications such as clocks, timing mechanisms, and advertising displays.

The single-phase, shaded-pole, synchronous motor

FIGURE 7.47
Schematics, characteristics, and uses of single-phase, synchronous, ac motors. (*From Collins, 1969.*)

The National Electrical Manufacturers Association (NEMA) has specified normal service conditions for electric motors. These conditions are as follows:

1. The ambient air temperature should not exceed 40°C (104°F).
2. The input voltage should be held within ±10 percent of the nameplate rating.
3. The frequency variation must be within ±5 percent of the nameplate rating.
4. The combined voltage and frequency swings should be within ±10 percent of the rated values but the frequency must not vary more than ±5 percent.
5. The motor should not be used at elevations more than 3300 ft (1000 m) above sea level.
6. Dust, moisture, dirt and fumes must not seriously interfere with the motor ventilation.
7. All belt, chain, and gear drives must be solidly mounted.

It should be noted that if a standard motor is used in Denver, Colorado, it violates condition 5 because of the "mile-high" altitude.

7.4.4 Electromagnetic Pump

The electromagnetic pump converts electrical energy directly into kinetic energy of a conducting fluid. This system is sometimes used to pump liquid metals and

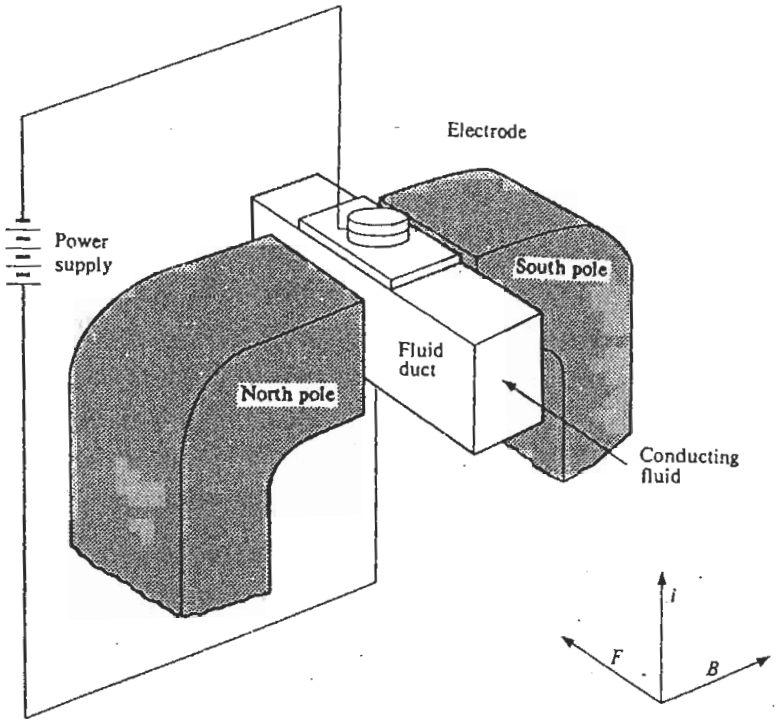


FIGURE 7.48
Schematic diagram of an electromagnetic pump.

other fluids with high electrical conductivities. In this pump, a low-voltage, high-amperage current is passed through the liquid metal by means of electrodes mounted on opposite sides of the rectangular duct. The high-flux magnetic field, perpendicular to the current flow, produces a force on the conductor, which, in this case, is the fluid.

The electromagnetic pump has no moving parts and this can be important in the operation of a leaktight liquid-metal system. Unfortunately, this system has a conversion efficiency of only 30 to 40 percent, which is approximately half that of a conventional centrifugal pump. Consequently, electromagnetic pumps are used only where the expected flow rates are low and where it is important to have a leaktight system. A schematic diagram of this pump is shown in Fig. 7.48.

LIST OF SYMBOLS

B or $\bar{B}$	The magnetic field strength, Wb/m^2
Bhp	Brake horsepower, hp
Bmep	Brake mean effective pressure, kPa (lb/in^2)
Bsfc	Brake specific fuel consumption, kg/kWh (lbm fuel/Bhp · h)

c_p	Specific heat at constant pressure, kJ/kg · K (Btu/lbm · R°)
c_v	Specific heat at constant volume, kJ/kg · K (Btu/lbm · R°)
D	Diameter or "bore" of a reciprocating engine, m (ft)
F	Force on engine dynamometer, N (lbf)
Fhp	Friction horsepower, hp
h	Specific enthalpy, kJ/kg (Btu/lbm)
$\dot{H}$	Total enthalpy "flow" rate, kJ/s (or Btu/h) = $\dot{m}h$
i or $\bar{i}$	Electric current, A
Ihp	Indicated horsepower, hp
Imep	Indicated mean effective pressure, kPa (lb/in^2)
Isfc	Indicated specific fuel consumption, kg/kWh (lbm fuel/Bhp · h)
j	Number of compressors in Brayton cycle
k	Ratio of specific heats, c_p/c_v
l	Length of electrical conductor, m (ft)
L	Length of piston stroke in a reciprocating engine, m (ft)
LHV	Lower heating value of the fuel, kJ/kg (Btu/lbm)
m	Mass, kg (lbm)
$\dot{m}$	Mass flow rate, kg/s (lbm/h)
$\dot{m}_w$	Mass rate of flow of wind, kg/s (lbm/h)
mep	Mean effective pressure, kPa (lb/in^2)
n	Number of feedwater heaters in regenerative vapor cycle
N_d	Angular velocity of dynamometer, r/min
N_e	Angular velocity of engine, r/min
N_p	Number of power strokes per minute
p	Absolute pressure, kPa (psia)
p_{max}	Maximum system pressure, kPa (psia)
p_{min}	Minimum system pressure, kPa (psia)
P	Power, MW
p	Number of poles in a motor
q	Specific heat transfer, kJ/kg (Btu/lbm)
q_a	Specific heat transfer to the cycle, kJ/kg (Btu/lbm)
q_r	Specific heat transfer from the cycle, kJ/kg (Btu/lbm)
Q	Total heat, kJ (Btu)
Q_a	Total heat transfer to the cycle, kJ (Btu)
Q_r	Total heat transfer from the cycle, kJ (Btu)
r_{cf}	Cutoff ratio for diesel cycle, v_{cutoff}/v_{min}
r_p	Compressor pressure ratio, p_{max}/p_{min}
r_v	Compression ratio, v_{max}/v_{min}
R	Radius arm of dynamometer, ft (m)
s	Specific entropy, kJ/kg · K (Btu/lbm · °R)
T_i	Temperature at state point i, K (°R)
T_H	Absolute temperature of heat source, K (°R)
T_L	Absolute temperature of heat sink, K (°R)
$T_{Sat.H}$	Saturation temperature at maximum water temperature, K (°R)
$T_{Sat.L}$	Saturation temperature at minimum water temperature, K (°R)

ΔT_{Htr}	Temperature difference of feedwater across feedwater heater, C° (F°)
TTD	Terminal temperature difference for a feedwater heater, K (R°)
v	Specific volume, m^3/kg (ft^3/lbm)
v_{max}	Maximum specific volume, m^3/kg (ft^3/lbm)
v_{min}	Minimum specific volume, m^3/kg (ft^3/lbm)
V_{dis}	Piston displacement volume in reciprocating engine, m^3 (ft^3)
$\bar{V}$	Velocity, m/s (ft/s)
$\bar{V}_i$	Steam velocity, m/s (ft/s)
$\bar{V}_a$	Axial component of steam velocity, m/s (ft/s)
$\bar{V}_b$	Tangential component of blade velocity, m/s (ft/s)
$\bar{V}_r$	Steam velocity relative to the blade, m/s (ft/s)
w	Specific work, kJ/kg (Btu/lbm)
w_{net}	Net specific work of cycle, kJ/kg (Btu/lbm)
W	Total work, kJ (Btu)
η_m	Mechanical efficiency of system
η_p	Mechanical efficiency of pump
η_t	Mechanical efficiency of turbine
η_{th}	Thermal efficiency of power system
η_v	Volumetric efficiency of an internal-combustion engine
ζ	An engine constant (1 for a two-stroke-cycle engines and 2 for four-stroke-cycle engines)

PROBLEMS

7.1. A four-stroke compression-ignition engine takes in ambient air at [10; 15; 20; 25; 30]°C and 100 kPa with a volumetric efficiency of 85 percent at [2000; 2500; 3000; 3500; 4000] r/min. The effective fuel-air ratio is 0.058 and the LHV of the fuel is 44,200 kJ/kg. The six cylinders each have a 0.15-m bore and a 0.18-m stroke. For an assumed thermal efficiency of 28 percent, estimate the brake power, in kW, the brake specific fuel consumption, in kg/kWh, and the brake mean effective pressure, in kPa.

7.2. A four-stroke compression-ignition engine takes in ambient air at [50; 60; 70; 80; 90]°F and 14.5 psia with a volumetric efficiency of 85 percent at [2000; 2500; 3000; 3500; 4000] r/min. The effective fuel-air ratio is 0.058 and the LHV of the fuel is 19,000 Btu/lbm. The six cylinders each have a 6-in bore and a 7-in stroke. For an assumed thermal efficiency of 28 percent, estimate the brake horsepower, the brake specific fuel consumption, and the brake mean effective pressure.

7.3. Determine the approximate cylinder dimensions of a four-cylinder four-stroke-cycle gasoline engine to deliver [50; 60; 70; 80; 90] Bhp at [2200; 2400; 2600; 2800; 3000] r/min if the diameter-stroke ratio (bore/stroke) is 0.8. From past experience, it is anticipated that the Bmep will be 120 psia, the mechanical efficiency is about 80 percent, the Bsfc is around 0.55 lbm/Bhp · h, and the LHV of the fuel is about 19,000 Btu/lbm. Assume the compression ratio is 7.0 and use an average value of k for the combustion products of 1.32. Calculate the expected and theoretical thermal efficiencies.

7.4. Determine the approximate cylinder dimensions of a four-cylinder four-stroke-cycle gasoline engine to deliver [40; 45; 50; 55; 60] kW at [2200; 2400; 2600; 2800;

3000] r/min if the diameter-stroke ratio (bore/stroke) is 0.8. From past experience, it is anticipated that the Bmep will be 830 kPa, the mechanical efficiency is about 80 percent, the Bsfc is around 0.34 kg/kWh, and the LHV of the fuel is about 44,200 kJ/kg. Assume the compression ratio is 7.0 and use an average value of k for the combustion products of 1.32. Calculate the expected and theoretical thermal efficiencies.

7.5. The air-standard Otto cycle has a compression ratio of [8.5; 9.0; 9.5; 10.0; 10.5]. At the start of the compression process, the temperature is 80°F and the pressure is [13; 13.5; 14; 14.5; 15] psia. If the maximum temperature is 3000°F, determine the specific work of the cycle, the specific heat transferred to and from the cycle, the maximum system pressure, and the thermal efficiency of the cycle.

7.6. The air-standard Otto cycle has a compression ratio of [8.5; 9.0; 9.5; 10.0; 10.5]. At the start of the compression process, the temperature is 27°C and the pressure is [90; 95; 100; 105; 110] kPa. If the maximum temperature is 1650°C, determine the specific work of the cycle, the specific heat transferred to and from the cycle, the maximum system pressure, and the thermal efficiency of the cycle.

7.7. A six-cylinder four-stroke-cycle automobile engine is required to develop [75; 80; 85; 90; 95] hp at 3500 r/min. The probable friction horsepower is [32; 34; 36; 38; 40] hp and the probable Bmep is 85 lb/in^2. For an L/D of 1.35, determine the bore and stroke for the engine. What are the probable brake torque, the mechanical efficiency, and the indicated mean effective pressure?

7.8. A six-cylinder four-stroke-cycle automobile engine is required to develop [40; 45; 50; 55; 60] kW at 3500 r/min. The probable friction power is [24; 25.5; 27; 28.5; 30] kW and the probable Bmep is 585 kPa. For an L/D of 1.35, determine the bore and stroke for the engine. What are the probable brake torque, the mechanical efficiency, and the indicated mean effective pressure?

7.9. A certain IC engine that is connected to an electric dynamometer and operated at full load gives these data: [1200; 1500; 1800; 2100; 2400] r/min, [63.0; 63.5; 64.0; 64.5; 65.0] lbf on the dynamometer scale at the end of a 1.5-ft brake arm. At the same angular velocity and no load on the dynamometer, the scale is adjusted to read zero, so there is no tare weight. The fuel has a LHV of 16,280 Btu/lb and is used by this engine at the rate of 0.27 lb/min. Friction and windage losses are 2.5 hp. Determine the horsepower delivered to the dynamometer, the mechanical efficiency of the engine, and the thermal efficiency of the engine.

7.10. A certain IC engine that is connected to an electric dynamometer and operated at full load gives these data: [1200; 1500; 1800; 2100; 2400] r/min, [280; 300; 320; 340; 360] N on the dynamometer scale at the end of a 0.5-m brake arm. At the same angular velocity and no load on the dynamometer, the scale is adjusted to read zero, so there is no tare weight. The fuel has a LHV of 38,000 kJ/kg and is used by this engine at the rate of 0.12 kg/min. Friction and windage losses are 1.9 kW. Determine the power delivered to the dynamometer, the mechanical efficiency of the engine, and the thermal efficiency of the engine.

7.11. A four-stroke-cycle engine operates on the air-standard Diesel cycle. The engine has eight cylinders each with a 0.105-m bore and a 0.124-m stroke. The engine speed is [1800; 2000; 2200; 2400; 2600] r/min. At the beginning of compression, the air is at 95 kPa, 24°C, and the maximum temperature is 1950°C. If the clearance volume (piston at top dead center) is [4.8; 5.1; 5.4; 5.7; 6.0] percent of the piston displacement, compute the compression ratio, the pressure and temperature at the end of

the compression process, the thermal efficiency, and the power output of the engine. Also, determine the efficiency and power output if the cutoff ratio is halved.

7.12. A four-stroke-cycle engine operates on the air-standard Diesel cycle. The engine has eight cylinders each with a 4-in bore and a 5-in stroke. The engine speed is [1800; 2000; 2200; 2400; 2600] r/min. At the beginning of compression, the air is at 14.0 psia, 75°F, and the maximum temperature is 3540°F. If the clearance volume (piston at top dead center) is [4.8; 5.1; 5.4; 5.7; 6.0] percent of the piston displacement, compute the compression ratio, the pressure and temperature at the end of the compression process, the thermal efficiency, and the horsepower output of the engine. Also, determine the efficiency and power output if the cutoff ratio is halved.

7.13. The inlet pressure and temperature before compression in an air-standard Diesel cycle are 94 kPa and [20; 22; 24; 26; 28]°C, respectively, and the conditions after the heat-addition process are 6400 kPa and [1750; 1800; 1850; 1900; 1950]°C. Compute the compression ratio, the cutoff ratio, and the thermal efficiency of the cycle.

7.14. The inlet pressure and temperature before compression in an air-standard Diesel cycle are 14 psia and [70; 75; 80; 85; 90]°F, respectively, and the conditions after the heat-addition process are 930 psia and [3180; 3270; 3360; 3450; 3540]°F. Compute the compression ratio, the cutoff ratio, and the thermal efficiency of the cycle.

7.15. An eight-cylinder four-stroke-cycle automobile engine is required to develop [130; 140; 150; 160; 170] Bhp at [2800; 3200; 3600; 4000; 4400] r/min. The friction torque is 30 ft · lbf at the same angular velocity and the probable Bmep is 95 lbf/in^2. For an L/D of 1.2, determine the bore, stroke, probable torque, and mechanical efficiency of the engine.

7.16. An eight-cylinder four-stroke-cycle automobile engine is required to develop [95; 105; 115; 125; 130] kW at [2800; 3200; 3600; 4000; 4400] r/min. The friction torque is 92 N · m at the same angular velocity and the probable Bmep is 655 kPa. For an L/D of 1.2, determine the bore, stroke, probable torque, and mechanical efficiency of the engine.

7.17. A certain generating plant requires [0.8; 1.0; 1.2; 1.4; 1.6] MW of output. Two types of diesel-engine installations are available. One is a low-speed unit that can operate on a low-grade fuel at 508 kPa Imep. The other two high-speed units can operate at 680 kPa Imep but require a higher-grade fuel. If the Isfc is 0.1015 kg/kWh, the cost of the low-speed engine fuel is [176; 242; 308; 374; 440] dollars/tonne, the cost of the high-speed engine fuel is 1.1 times the cost of the low-grade fuel, and the friction mep is 122 kPa in both cases, determine the fuel cost of the two installations, in cents/kWh and in dollars/h.

7.18. A certain generating plant requires [1650; 1700; 1750; 1800; 1850] hp of output. Two types of diesel-engine installations are available. One unit is a low-speed unit that can operate on a low-grade fuel at 74 lb/in^2 Imep. The other two high-speed units can operate at 99 lb/in^2 Imep but require a higher-grade fuel. If the Isfc is 0.167 lbm/hp · h, the cost of the low-speed engine fuel is [160; 220; 280; 320; 360] dollars/ton, the cost of the high-speed engine fuel is 1.1 times the cost of the low-grade fuel, and the friction mep is 17.7 lb/in^2 in both cases, determine the fuel cost of the two installations, in cents/hp · h and in dollars/h.

7.19. An air-standard Brayton cycle operates with a compressor pressure ratio of [4.0; 4.5; 5.0; 5.5; 6.0]. The actual expansion and compression efficiencies of the gas processes are 0.88 and 0.82, respectively, and the maximum and minimum temperatures are [700; 750; 800; 850; 900]°C and 16°C, respectively. Compute the compression work, the expansion work, the ratio of compression to expansion work (the back-work ratio), and the actual and theoretical thermal efficiencies. If the power output of the installation is 8 MW, determine the mass flow rate, kg/min.

7.20. An air-standard Brayton cycle operates with a compressor pressure ratio of [4.0; 4.5; 5.0; 5.5; 6.0]. The actual expansion and compression efficiencies of the gas processes are 0.88 and 0.82, respectively, and the maximum and minimum temperatures are [1290; 1380; 1470; 1560; 1650]°F and 60°F, respectively. Compute the compression work, the expansion work, the ratio of compression to expansion work (the back-work ratio), and the actual and theroretical thermal efficiencies. If the power output of the installation is 8 MW, determine the mass flow rate, lbm/min.

7.21. An open Brayton-cycle engine operates with a compressor-pressure ratio of [3.5; 4.0; 4.5; 5.0; 5.5], and inlet temperature of 70°F, and a turbine-inlet temperature of [1650; 1700; 1750; 1800; 1850]°F. The engine drives an electric generator that produces 25 MW_e with a generator efficiency of 90 percent. For the following system, find the thermal efficiency, the specific work, and the air-mass-flow rate, if the compressor and turbine efficiencies are 80 percent.

(*a*) A simple Brayton cycle
(*b*) A regenerative Brayton cycle with a regenerator effectiveness of 80 percent
(*c*) A Brayton cycle using two stages of compression with intercooling to 70°F
(*d*) A Brayton cycle that employs both the regenerator of (*b*) and the intercooler of (*c*)

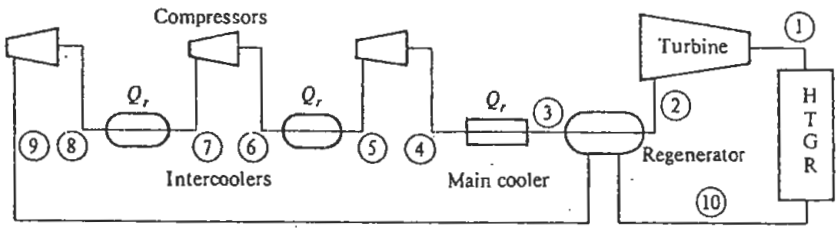
7.22. An open Brayton-cycle engine operates with a compressor-pressure ratio of [3.5; 4.0; 4.5; 5.0; 5.5], an inlet temperature of 20°C, and a turbine-inlet temperature of [900; 925; 950; 975; 1000]°C. The engine drives an electric generator that produces 25 MW_e with a generator efficiency of 90 percent. For the following system, find the thermal efficiency, the specific work, and the air-mass-flow rate, if the compressor and turbine efficiencies are 80 percent.

(*a*) A simple Brayton cycle
(*b*) A regenerative Brayton cycle with a regenerator effectiveness of 80 percent
(*c*) A Brayton cycle using two stages of compression with intercooling to 20°C
(*d*) A Brayton cycle that employs both the regenerator of (*b*) and the intercooler of (*c*)

7.23. An open-cycle regenerative gas-turbine power plant receives air at [90; 92; 94; 96; 98] kPa and 20°C. The air is compressed to [450; 500; 550; 600; 650] kPa, heated to 425°C in the regenerator, and then reaches a maximum temperature of 870°C in the combustion chamber. Assuming an air-standard cycle, compute the thermal efficiency and the regenerator effectiveness if the mechanical efficiency of the compressor and turbine are 82 and 87 percent, respectively.

7.24. An open-cycle regenerative gas-turbine power plant receives air at [13; 13.4; 13.8; 14.2; 14.6] psia and 70°F. The air is compressed to [65; 72.5; 80; 87.5; 95] psia, heated to 800°F in the rengenerator, and then reaches a maximum temperature of 1600°F in the combustion chamber. Assuming an air-standard cycle, compute the thermal efficiency and the regenerator effectiveness if the mechanical efficiency of the compressor and turbine are 82 and 87 percent, respectively.

7.25. A high-temperature gas-cooled reactor (HTGR) is to be coupled to a gas turbine in a direct cycle, as shown below. The helium flow rate is 145,000 kg/h. Gas enters the turbine at [710; 720; 730; 740; 750]°C and 2500 kPa and is discharged at 450°C and 980 kPa. The regenerator effectiveness is [82; 84; 86; 88; 90] percent. At the



inlet to the first stage of the three-stage compressor, the pressure is 952 kPa and the temperature at all three inlets is 16°C. The outlet temperatures are each 66°C and the discharge pressure from the third stage is 2550 kPa. Find:

(*a*) The pressure and temperature at each stage in the cycle
(*b*) The reactor power in thermal megawatts
(*c*) The fuel cost in cents/kW$_e$h, if the fuel cost is 75 cents/million Btu
(*d*) The thermal efficiency and the heat rate of the power cycle

7.26. A high-temperature gas-cooled reactor (HTGR) is to be coupled to a gas turbine in a direct cycle, as shown above. The helium flow rate is 195,000 lbm/h. Gas enters the turbine at [1310; 1330; 1350; 1370; 1390]°F and 365 psia and is discharged at 840°F and 142 psia. The regenerator effectiveness is [82; 84; 86; 88; 90] percent. At the inlet to the first stage of the three-stage compressor, the pressure is 138 psia and the temperature at all three inlets is 60°F. The outlet temperatures are each 151°F and the discharge pressure from the third stage is 370 psia. Find:

(*a*) The pressure and temperature at each stage in the cycle
(*b*) The reactor power in thermal megawatts
(*c*) The fuel cost in cents/kW$_e$h, if the fuel cost is 75 cents/million Btu
(*d*) The thermal efficiency and the heat rate of the power cycle

Refer to the figure in Prob. 7.25.

7.27. An open Brayton cycle operates with a compressor-pressure ratio of [4.0; 4.5; 5.0; 5.5; 6.0], an inlet temperature of 80°F, and a turbine-inlet temperature of 1800°F, and produces a total of 50 MW of mechanical power. For the following systems, find the thermal efficiency, the air-mass-flow rate, and the total compressor and turbine powers, in hp, assuming that the compressor and turbine efficiencies are [82; 84; 86; 88; 90] percent. Find:

(*a*) A simple Brayton cycle
(*b*) A regenerative Brayton cycle with a regenerator effectiveness of 80 percent
(*c*) A reheat Brayton cycle with a reheat at 45 psia to 1750°F
(*d*) A Brayton cycle with three stages of compression with two intercoolers that cool the gas back to 80°F
(*e*) A system that uses the regenerator of (*b*) and the reheater of (*c*)
(*f*) A system that uses the intercoolers of (*d*) and the regenerator of (*b*)

7.28. An open Brayton cycle operates with a compressor-pressure ratio of [4.0; 4.5; 5.0; 5.5; 6.0], an inlet temperature of 27°C, and a turbine-inlet temperature of 980°C, and produces a total of 50 MW of mechanical power. For the following systems,

find the thermal efficiency, the air mass flow rate, and the total compressor and turbine powers, in kW, assuming that the compressor and turbine efficiencies are [82; 84; 86; 88; 90] percent. Find:

(*a*) A simple Brayton cycle
(*b*) A regenerative Brayton cycle with a regenerator effectiveness of 80 percent
(*c*) A reheat Brayton cycle with a reheat at 310 kPa to 955°C
(*d*) A Brayton cycle with three stages of compression with two intercoolers that cool the gas back to 27°C
(*e*) A system that uses the regenerator of (*b*) and the reheater of (*c*)
(*f*) A system that uses the intercoolers of (*d*) and the regenerator of (*b*)

7.29. It is desired to use a reheat vapor-power cycle operating at a maximum system pressure of 16.5 MPa. If the turbine inlet temperature is [450; 475; 500; 525; 550]°C and the minimum system pressure is [5; 10; 15; 20; 25] kPa, find the maximum reheat pressure if the turbine efficiency is 100 percent. Assume the moisture at the low-pressure turbine exhaust is 10 percent and the reheat temperature is 500°C.

7.30. Repeat Prob. 7.29 for a turbine efficiency of 86 percent.

7.31. It is desired to use a reheat vapor-power cycle operating at a maximum system pressure of 2400 psia. If the turbine inlet temperature is [850; 900; 950; 1000; 1050]°F and the minimum system pressure is [1; 1.5; 2; 2.5; 3] psia, find the maximum reheat pressure if the turbine efficiency is 100 percent. Assume the moisture at the low-pressure turbine exhaust is 10 percent and that the reheat temperature is 900°F.

7.32. Repeat Prob. 7.31 for a turbine efficiency of 86 percent.

7.33. A steam power system operates with turbine throttle conditions of [13; 14; 15; 16; 17] MPa, 550°C, and turbine outlet conditions of 10 percent moisture and [5; 10; 15; 20; 25] kPa. If four feedwater heaters are used, find the extraction pressures for each heater that will give the maximum thermal efficiency.

7.34. A steam power system operates with turbine throttle conditions of [1900; 2050; 2200; 2350; 2500] psia, 1000°F, and turbine outlet conditions of 10 percent moisture and [1; 1.5; 2; 2.5; 3] psia. If four feedwater heaters are used, find the extraction pressures for each heater that will give the maximum thermal efficiency.

7.35. Determine the thermal efficiency, the required steam-flow rate, and the moisture at the turbine exhaust for a reheat-regenerative cycle which is to produce 200 MW at the turbine coupling if the throttle conditions are [14.5; 15.0; 15.5; 16.0; 16.5] MPa and 540°C; reheat is at 8.0 MPa and 590°C; one closed heater is at 3.4 MPa; an open feedwater heater is at 170 kPa; and the condenser pressure is 13 kPa. The turbine and pump efficiencies are [80; 82; 84; 86; 88] percent. The terminal temperature difference from both heaters is 3C° and the drain from the closed heater is trapped to the open heater. Also sketch the cycle on a T–s diagram.

7.36. Repeat Prob. 7.35 for the condition when the condensate from the closed heater is pumped into the boiler, instead of being trapped to the open heater.

7.37. Determine the thermal efficiency, the required steam flow rate, and the moisture at the turbine exhaust for a reheat-regenerative cycle which is to produce 200 MW at the turbine coupling if the throttle conditions are [2000; 2100; 2200; 2300; 2400] psia and 1000°F; reheat is at 1150 psia and 1000°F; one closed heater is at 500 psia; an open feedwater heater is at 25 psia; and the condenser pressure is 2 psia. The turbine and pump efficiencies are [80; 82; 84; 86; 88] percent. The terminal temperature

difference from both heaters is 5F° and the drain from the closed heater is trapped to the open heater. Also sketch the cycle on a T–s diagram.

7.38. Repeat Prob. 7.37 for the condition when the condensate from the closed heater is pumped into the boiler, instead of being trapped to the open heater.

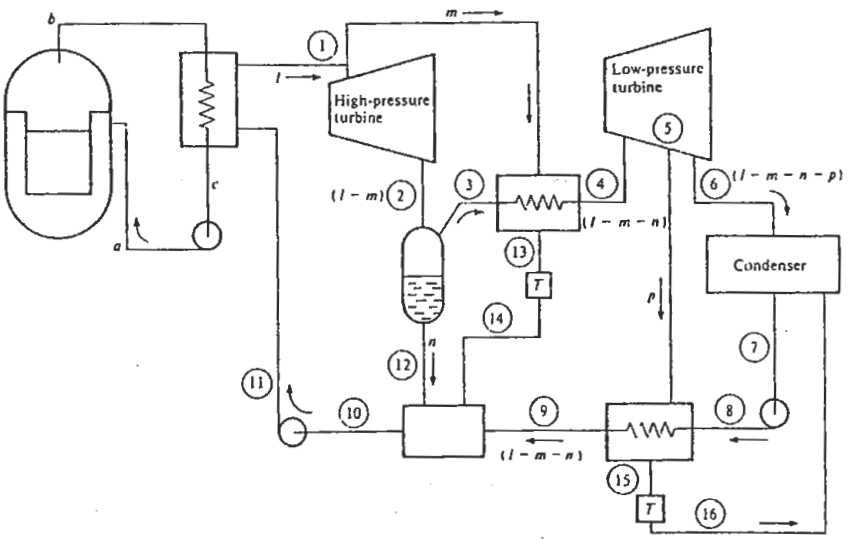
7.39. Calculate the optimum heater pressures for Prob. 7.35 and recalculate the thermal efficiency for this cycle.

7.40. Calculate the optimum heater pressures for Prob. 7.37 and recalculate the thermal efficiency for this cycle.

7.41. Determine the thermal efficiency, the required steam-flow rate, and the moisture at the turbine exhaust for a reheat-regenerative cycle which is to produce 325 MW at the turbine coupling if the throttle conditions are 8.2 MPa and [545; 550; 555; 560; 565]°C; reheat is at 2.1 MPa and [520; 525; 530; 535; 540]°C; one closed heater is at 2.1 MPa (before reheat); an open feedwater heater is at 140 kPa; and the condenser pressure is 7 kPa. The turbine and pump efficiencies are 88 and 82 percent, respectively. The terminal temperature difference from both heaters is 2 C° and the drain from the closed heater is trapped to the open heater. Also sketch the cycle on a T–s diagram.

7.42. Determine the thermal efficiency, the required steam-flow rate, and the moisture at the turbine exhaust for a reheat-regenerative cycle which is to produce 325 MW at the turbine coupling if the throttle conditions are 1200 psia and [1000; 1010; 1020; 1030; 1040]°F; reheat is at 300 psia and [960; 970; 980; 990; 1000]°F; one closed heater is at 300 psia (before reheat); an open feedwater heater is at 20 psia; and the condenser pressure is 1 psia. The turbine and pump efficiencies are 88 and 82 percent, respectively. The terminal temperature difference from both heaters is 4 F° and the drain from the closed heater is trapped to the open heater. Also sketch the cycle on a T–s diagram.

7.43. A 3800-MW_{th} PWR is cooled with 15.3-MPa water that enters the core at 300°C and leaves at 332°C. In the once-through steam generator (see illustration below), the



high-pressure water is used to produce steam at [7.2; 7.4; 7.6; 7.8; 8.0] MPa and 315°C (1). This steam expands to 0.68 MPa (2) in the high-pressure turbine. Moisture (12) is separated and the saturated steam (3) is reheated with live steam (1) to 288°C (4). Before it enters the low-pressure turbine, the steam expands to 110 kPa (5), where a fraction is bled to a closed feedwater heater. Expansion continues to the condenser pressure of [10; 12.5; 15; 17.5; 20] kPa (6). The separated moisture (12) is drained to an open feedwater heater and the reheater condensate (13) is "trapped" (14) to the same heater. The closed feedwater heater has a terminal temperature difference of 3 C°. Each segment of the turbine expansion is 85 percent efficient and the pumps are 75 percent efficient.

(*a*) Sketch the cycle on the T–s plane.
(*b*) Find the cooling-water flow rate in the core, in L/min.
(*c*) Find the steam generation rate, in kg/h.
(*d*) Determine the power output of the system, MW_e, if the turbines drive a generator with an efficiency of 94 percent.
(*e*) What is the thermal efficiency of the cycle?

7.44. A 3800-MW_{th} PWR is cooled with 2250-psia water that enters the core at 572°F and leaves at 630°F. In the once-through steam generator, the high-pressure water is used to produce steam at [1050; 1075; 1100; 1125; 1150] psia and 600°F (1). This steam expands to 100 psia (2) in the high-pressure turbine. Moisture (12) is separated and the saturated steam (3) is reheated with live steam (1) to 550°F (4). Before it enters the low-pressure turbine, the steam expands to 16 psia (5), where a fraction is bled to a closed feedwater heater. Expansion continues to the condenser pressure of [1; 1.5; 2; 2.5; 3] psia (6). The separated moisture (12) is drained to an open feedwater heater and the reheater condensate (13) is "trapped" (14) to the same heater. The closed feedwater heater has a terminal temperature difference of 5 F°. Each segment of the turbine expansion is 85 percent efficient and the pumps are 75 percent efficient.

(*a*) Sketch the cycle on the T–s plane.
(*b*) Find the cooling-water flow rate in the core, in gal/min.
(*c*) Find the steam generation rate, in lbm/h.
(*d*) Determine the power output of the system, MW_e, if the turbines drive a generator with an efficiency of 94 percent.
(*e*) What is the thermal efficiency of the cycle?

Refer to the figure in Prob. 7.43.

7.45. A reaction stage receives steam at [3.4; 3.6; 3.8; 4.0; 4.2] MPa and 305°C and expands the steam through a pressure range of [300; 320; 340; 360; 400] kPa. A flow of 13,600 kg/h occurs, and at this rate the stage has an efficiency of 78 percent. Compute the blade power.

7.46. A reaction stage receives steam at [500; 525; 550; 575; 600] psia and 580°F and expands the steam through a pressure range of [44; 48; 52; 56; 60] lb/in^2. A flow of 30,000 lbm/h occurs, and at this rate the stage has an efficiency of 78 percent. Compute the blade power.

7.47. Steam at [8.0; 10.0; 12.0; 14.0; 16.0] MPa and 510°C undergoes a pressure drop to 55 percent of the inlet pressure as it passes through the nozzle of an impulse stage. The nozzle makes an angle of 15° with the blade entrance and the nozzle efficiency is [88; 90; 92; 94; 96] percent. Determine the maximum steam work against the blade face per kilogram of steam flowing through the nozzle. The ratio of

7.48. Steam at [1200; 1500; 1800; 2100; 2400] psia and 950°F undergoes a pressure drop to 55 percent of the inlet pressure as it passes through the nozzle of an impulse stage. The nozzle makes an angle of 15° with the blade entrance and the nozzle efficiency is [88; 90; 92; 94; 96] percent. Determine the maximum steam work against the blade face per pound of steam flowing through the nozzle.

7.49. It is desired to build an upwind windmill that will produce [0.5; 1.0; 1.5; 2.0; 2.5] MW of mechanical energy in a [22; 24; 26; 28; 30]-mi/h wind. If the efficiency of the windmill is 75 percent the theoretical efficiency, find the blade diameter of the windmill, in ft, if the air is at 14.7 psia and 80°F.

7.50. A combined-cycle power plant uses a gas-turbine system with a thermal efficiency of [34; 36; 38; 40; 42] and the turbine discharge is put into a HRSG with no additional heat. The steam-power system has a thermal efficiency of [16; 18; 20; 22; 24] percent. Find the combined thermal efficiency of the power system.

7.51. If 20 MW of heat is added to the gas-turbine system of Prob. 7.50, and 5 MW of heat is added to the gas-turbine exhaust which raises the efficiency of the steam system to [25; 27; 29; 31; 33] percent, determine the combined thermal efficiency of the power system.

REFERENCES

Berman, P. A., and F. A. Lebonette: "Combined-Cycle Plant Serves Intermediate System Loads Economically," *Combustion*, vol. 42, no. 9, pp. 19-23, March 1971.

Collins, G. W.: "The Family Tree of Electric Motors," *Machine Design*, vol. 41, no. 1, pp. 152-156, January 9, 1969.

Dillio, C. C., and E. P. Nye: *Thermal Engineering*, International Textbook Company, Scranton, Pa., 1963.

Doerner, W. A., R. J. Dietz, O. R. Van Buskirk, S. B. Levy, R. J. Rennolds, and M. F. Bechtold: *A Rankine Cycle Engine with Rotary Heat Exchangers*, SAE publication 7200d53, 1972.

Editors of *Power Magazine: Power Generation Systems*, McGraw-Hill, New York, 1967.

Hirschfeld, F.: "Wind Power: Pipe Dream or Reality?" *Mechanical Engineering*, vol. 99, no. 9, pp. 20-28, September 1977.

Keenan, J. H., F. G. Keyes, P. G. Hill, and J. G. Moore: *Steam Tables* (International Edition—Metric Units), Wiley, New York, 1969.

Kidd, S., and D. Garr: "Electric Power from Windmills," *Popular Science*, vol. 201, no. 5, pp. 70-72, November 1972.

Lindsley, E. P.: "Wind Power: How New Technology is Harnessing an Age-Old Energy Source," *Popular Science*, vol. 205, no. 1, pp. 54-59, July 1974.

Schefter, J.: "Energy from Wind Farms," *Popular Science*, vol. 222, no. 1, January 1983.

Skrotzki, B. G. A. (associate ed.): "Steam Turbine," a *Power Magazine* special report, McGraw-Hill, New York, June 1962.

Skrotzki, B. G. A.: "Gas Turbines," a *Power Magazine* special report, McGraw-Hill, New York, 1963.

Skrotzki, B. G. A., and W. A. Vopat: *Power Station Engineering and Economy*, McGraw-Hill, New York, 1960.

Walton, H.: *The How and Why of Mechanical Movements*, Popular Science Publishing Company, E. P. Dutton & Co., New York, 1968.

Wark, K.: *Thermodynamics*, fifth edition, McGraw-Hill, New York, 1988.

Wood, B. D.: *Applications of Thermodynamics*, Addison-Wesley Publishing Company, Reading, Mass., 1969.

CHAPTER 8

PRODUCTION OF ELECTRICAL ENERGY

8.1 INTRODUCTION

Electrical energy is the energy associated with the flow or accumulation of electric charge. It is a very useful form of energy as it can be easily converted into almost every other energy form with a high conversion efficiency. Moreover, electrical energy can be produced directly from the other energy forms without going through an intermediate form such as thermal or mechanical energy.

Some of the conversion systems used to produce electricity are often called *direct-energy converters.* Thermal energy can be converted directly to electrical energy in the thermoelectric converter and the thermionic converter, among others. These systems, however, are saddled with the maximum possible thermal efficiency of an externally reversible heat-engine cycle, or $1 - T_L/T_H$. Chemical energy can be converted directly into electricity in the fuel cell and the battery. Electromagnetic energy can be converted into electricity in the photovoltaic or solar cell. Nuclear energy can be converted into electricity in the nuclear battery. Mechanical energy can be converted into electricity in the conventional generator or alternator or in a fluiddynamic conversion system, like the magnetohydrodynamic or electrogasdynamic system.

In all these conversion systems, except the ones involving the conversion of thermal energy, the conversion efficiency is not limited to the efficiency of an externally reversible heat-engine cycle. As a result, there is considerable interest and research in some of these direct-energy conversion systems, in order to produce a more efficient electrical generation system.

8.2 CONVERSION OF THERMAL ENERGY INTO ELECTRICITY

8.2.1 Thermoelectric Converters

As was indicated earlier, there are a number of different systems that can be used to convert thermal energy into electricity but only the thermoelectric generator and the thermionic generator have found widespread application. All of these systems have a maximum thermal efficiency which is less than $1 - T_L/T_H$.

The operation of thermoelectric generator or converter depends on the Seebeck effect, the Peltier effect, and the Thomson effect. The Seebeck effect was discovered in 1822 by the German physicist Thomas J. Seebeck. According to the Seebeck effect, a voltage is produced in a circuit of two dissimilar materials if the two junctions are maintained at different temperatures. The Seebeck coefficient S is a material property and gives the rate of change of thermoelectric potential v_s with temperature T, or:

$$S \equiv \frac{dv_s}{dT} \tag{8.1}$$

The Seebeck coefficients are strong functions of temperature.

The induced thermoelectric potential v_s produced in a circuit composed of two materials is obtained from the following equation:

$$v_s = \int_{T_L}^{T_H} (S_a - S_b)\, dT = \int_{T_L}^{T_H} S_{ab}\, dT \tag{8.2}$$

The combined Seebeck coefficient S_{ab} is defined as positive if the electric current (the flow of positive charge) flows from material A to material B at the cold junction where the heat of recombination is released.

Some typical values of Seebeck coefficients are listed in Table 8.1. It will be noted that the Seebeck coefficients for metals and alloys are very low compared to those for semiconducting materials. The combined Seebeck coefficient for an iron-constantan circuit is 60.6 μV/K, while that for a combination germanium and silicon is 830 μV/K. The Seebeck coefficients for metals and alloys are too

TABLE 8.1
Seebeck coefficients (at 100°C)

Material	S, V/K
Aluminum	-0.2×10^{-6}
Constantan	-47.0×10^{-6}
Copper	$+3.5 \times 10^{-6}$
Iron	$+13.6 \times 10^{-6}$
Platinum	-5.2×10^{-6}
Germanium	$+375.0 \times 10^{-6}$
Silicon	-455.0×10^{-6}

low for the efficient generation of electricity, although the dissimilar metal junctions are commonly used in thermocouple circuits to monitor system temperatures.

The Seebeck coefficients of *n-p* semiconductors are also high and these are the materials that are commonly used in thermoelectric generators. Two common thermoelectric materials that are used are lead telluride or bismuth telluride. An *n*-type semiconductor is one is which impurity atoms are added to the lattice that have one more electron than is needed to satisfy the valence-bond requirements. Thus, the material has extra negative electrons in the lattice although the material has no net charge associated with these electrons. A *p*-type semiconductor is one in which impurity atoms are added to the lattice which have one less electron than is needed to satisfy the valance-bond requirements. This introduces positive "holes" into the lattice although this material is also neutrally charged.

In a thermoelectric converter constructed of semiconductors, both the holes and the electrons migrate toward the cold junction where they "pile up" and combine. The combined Seebeck coefficient for these lattices is $S_{ab} = S_{pn} = -S_{np}$, and the thermoelectric potential becomes

$$v_s = \int_{T_L}^{T_H} (S_p - S_n)\, dT = \int_{T_L}^{T_H} S_{pn}\, dT \tag{8.3}$$

The Peltier effect was discovered in 1844 by the French physicist J. C. A. Peltier. It states essentially that if a direct current is passed through a circuit of dissimilar materials, one of the junctions will be heated and the other cooled. This is the reversed Seebeck effect, and it is also reversible, in that if the direction of current flow is reduced, the junction that was formerly heated will be cooled and the formerly cooled junction will be heated.

The Peltier coefficient for a circuit composed of material *A* and material *B* is designated, π_{ab}, and is defined as

$$\pi_{ab} \equiv \frac{-Q}{i_{ab}} \tag{8.4}$$

where $-Q$ is the heat-transfer rate from the junction, in watts, and i_{ab} is the direct current flowing in the generator, in amperes. Thus, π_{ab} has units of volts.

Like the Seebeck coefficient, the Peltier coefficient is a strong function of temperature and is related to the Seebeck coefficient by the following relationship:

$$\pi_{ab} = T_{(L \text{ or } H)} S_{ab} = T_{(L \text{ or } H)} (S_a - S_b) = -\pi_{ba} \tag{8.5}$$

where $T_{(L \text{ or } H)}$ is either the absolute temperature of the cold junction, T_L, or the absolute temperature of the hot junction, T_H. The Peltier coefficient π_{ab} is positive if heat is generated in the junction (the hot junction) when the direct current flows from material *A* to material *B*.

The Thomson effect was discovered in 1854 by the English physicist William Thomson (Lord Kelvin). This effect says that there is reversible absorption or liberation of heat in a homogeneous conductor exposed to simultaneous tem-

is defined by the following equation:

$$\tau \equiv \frac{Q/\Delta T}{i} \tag{8.6}$$

where Q is the heat-transfer rate, in watts, absorbed by the conductor when the current flows toward the higher temperature. The Thomson coefficient is related to the Seebeck coefficient by the following relationship:

$$\tau = T\frac{dS}{dT} \tag{8.7}$$

This coefficient is positive for p-type materials and negative for n-type materials. The Thomson effect is only of secondary importance in the operation of thermoelectric generators.

A typical p-n thermoelectric generator is shown in Fig. 8.1. As can be seen in the figure, the legs or elements of the generator are connected in series for the flow of electricity and connected in parallel for the flow of heat. The total electrical resistance of the generator is R_g, and for a series connection it is equal to the sum of the resistances of each of the legs:

$$R_g = m(R_p + R_n) \tag{8.8}$$

where m is the number of pairs of p-n legs of the generator and R_p and R_n are the electrical resistances of the p leg and n leg, respectively:

$$R_p = \frac{\rho_p L_p}{A_p} \qquad \text{and} \qquad R_n = \frac{\rho_n L_n}{A_n} \tag{8.9}$$

In the previous equations, ρ is the electrical resistivity of the materials, in ohm-meters, L is the length of the semiconductor legs, in meters, and A is the cross-sectional area of the legs, in square meters. It is normally assumed that the metallic connections between the semiconductor legs have negligible resistance.

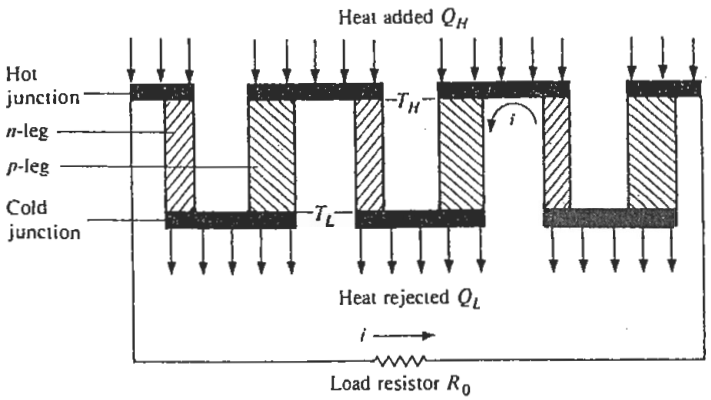


FIGURE 8.1
Schematic of the typical n-p thermoelectric generator.

The thermal conductance K_g of the generator is equal to the sum of the thermal conductances (the reciprocal of the thermal resistance) of the semiconductor legs, or

$$K_g = m(K_p + K_n) \tag{8.10}$$

where

$$K_p = \frac{k_p A_p}{L_p} \tag{8.11}$$

$$K_n = \frac{k_n A_n}{L_n} \tag{8.12}$$

and k is the thermal conductivity of the semiconductor materials, in watts per meter per degree Celsius.

An energy balance on either the hot or cold node is composed of four energy terms. First, there is the heat-transfer rate to or from the junction from the environment, $\pm Q$. Second, there is the heat-transfer rate through the generator from the hot to the cold junction, $\pm K_g \Delta T$. Third, there is heat transfer due to the Peltier effect, $\pm \pi_{pn} i = \pm T_{(L \text{ or } H)} i\overline{S_{pn}}$. Fourth, there is the power dissipated in the device due to Joule heating and it can be shown that effectively half of the resistance heating is deposited in each junction, $i^2 R_g/2$.

At the hot junction, the Peltier heat-transfer rate is $m\overline{\pi_{pn}} i$ or $m\overline{S_{pn}} T_H i$, in watts, where

$$\overline{S_{pn}} = \int_{T_L}^{T_H} \frac{S_p - S_n}{T_H - T_L}\, dT \tag{8.13}$$

The energy or power entering the hot junction is equal to $i^2 R_g/2$ plus Q_a, while the power leaving the hot junction is equal to the sum of $K_g \Delta T$ and $m\overline{S_{np}} T_H i$. Combining these terms gives

$$Q_a = m\overline{S_{pn}} T_H i + K_g (T_H - T_L) - \frac{i^2 R_g}{2} \tag{8.14}$$

The useful power produced by the device is equal to the power dissipated in the external load. Since this system generates direct current, the useful power generation is $i^2 R_L$, where R_L is the resistance of the external load. The thermal efficiency of the thermoelectric generator is

$$\eta_{th} = \frac{i^2 R_L}{Q_a} = \frac{i^2 R_L}{m\overline{S_{pn}} T_H i + K_g \Delta T - i^2 R_g/2} \tag{8.15}$$

Multiplying the numerator and the denominator by $\Delta T / R_g i^2$ and letting M equal the ratio of the external load resistance to the generator resistance, R_L / R_g,

$$\eta_{th} = \frac{M \Delta T}{m\overline{S_{pn}} T_H \Delta T / i R_g + K_g \Delta T^2 / i^2 R_g - \Delta T/2} \tag{8.16}$$

The current in the converter is equal to the total generated voltage divided by

the total resistance of the circuit, or

$$i = \frac{v_t}{R_t} = \frac{m\overline{S_{pn}}\Delta T}{R_g + R_L} = \frac{m\overline{S_{pn}}(T_H - T_L)}{R_g(1+M)} \tag{8.17}$$

Substituting this equation into Eq. (8.16), gives

$$\eta_{th} = \frac{M\Delta T}{(1+M)T_H + (1+M)^2/Z - \Delta T/2} \tag{8.18}$$

where Z is defined as the *figure of merit* of the generator and is equal to

$$Z \equiv \frac{m^2\overline{S_{pn}^2}}{K_g R_g} \tag{8.19}$$

The figure of merit of a generator is a function of the properties of the generator material (S, k, and ρ) and the dimensions of the generator legs (A and L). To improve the thermal efficiency of the generator, the figure of merit Z should be as large as possible. Once the generator materials have been picked, the minimum product of $K_g R_g$ gives the maximum figure of merit, Z_{max}:

$$\begin{aligned} K_g R_g &= \left(\frac{k_p A_p}{L_p} + \frac{k_n A_n}{L_n}\right)\left(\frac{\rho_p L_p}{A_p} + \frac{\rho_n L_n}{A_n}\right) m^2 \\ &= m^2\left(k_p\rho_p + k_p\rho_n x + \frac{k_n\rho_p}{x} + k_n\rho_n\right) \end{aligned} \tag{8.20}$$

where $x = A_p L_n / A_n L_p$. The optimum value of x that gives the minimum value of $K_g R_g$ or Z_{max} can be found by setting $d(K_g R_g)/dx$ equal to zero and solving for x. This gives the optimum value of x, or

$$x_{opt} = \frac{A_p L_n}{A_n L_p} = \left(\frac{\rho_p k_n}{\rho_n k_p}\right)^{1/2} \tag{8.21}$$

and this gives

$$Z_{max} = \frac{\overline{S_{pn}^2}}{[(k_p\rho_p)^{1/2} + (k_n\rho_n)^{1/2}]^2} \tag{8.22}$$

The above equation is independent of the system geometry as long as the area and length of the generator elements are proportioned according to the resistivity and the thermal conductivity of the materials, as given in Eq. (8.21).

Once the thermoelectric generator has been built, the only variable in Eq. (8.18) that can be easily adjusted to improve the generator efficiency is the ratio of the external load resistance to the generator resistance, M. The optimum value of M that gives the maximum thermal efficiency can be determined by setting $(d\eta_{th}/dM)$ equal to zero and solving for M. This gives

$$M_{opt} = \left(\frac{R_L}{R_g}\right)_{opt} = (1 + Z_{max} T_{ave})^{1/2} \tag{8.23}$$

where T_{ave} is the average absolute temperature in the generator, $(T_H + T_L)/2$.

Substituting this equation into the thermal efficiency equation yields

$$\eta_{\text{th,max}} = \frac{M_{\text{opt}} \Delta T}{T_H(1+M_{\text{opt}}) + (1+M_{\text{opt}})^2 / Z_{\text{max}} - \Delta T/2} \tag{8.24}$$

While the above equation gives the condition for maximum thermal efficiency, there may be some times when the system will be operated at the condition for maximum power output rather than maximum efficiency. The output voltage of the generator is equal to the total generated voltage minus the internal voltage drop in the generator:

$$v_{\text{out}} = m\overline{S_{pn}}\Delta T - iR_g \tag{8.25}$$

and the output power is

$$P_{\text{out}} = iv_{\text{out}} = m\overline{S_{pn}}\Delta Ti - i^2 R_g \tag{8.26}$$

Differentiating Eq. (8.26) with respect to i and setting (dP_{out}/di) equal to zero gives the current required for maximum power, $i_{\text{max}P}$:

$$i_{\text{max}P} = \frac{m\overline{S_{pn}}\Delta T}{2R_g} \tag{8.27}$$

This current value gives a maximum power output for the generator equal to

$$P_{\text{out,max}} = \frac{m^2\overline{S_{pn}^2}\Delta T^2}{4R_g} \tag{8.28}$$

The output voltage for the condition maximum power is found by substituting Eq. (8.27) into Eq. (8.25):

$$\begin{aligned} v_{\text{out,max}P} &= i_{\text{max}P} R_L = m\overline{S_{pn}}\Delta T - i_{\text{max}P} R_g = 2i_{\text{max}P} R_g - i_{\text{max}P} R_g \\ &= i_{\text{max}P} R_g \end{aligned} \tag{8.29}$$

Equation (8.29) shows that for the condition of maximum power, $R_L = R_g$, or

$$M_{\text{max}P} = \left(\frac{R_L}{R_g}\right)_{\text{max}P} = 1.0 \tag{8.30}$$

Comparing Eq. (8.23) with Eq. (8.30) indicates that for the condition of maximum thermal efficiency, the load resistance R_L should exceed the generator resistance R_g, while, for the condition of maximum power, the two resistances must be equal (matched impedances).

8.2.2 Thermoelectric Refrigerators

Thermoelectric systems can also be used as heat-pump or refrigeration systems as well as electric generators. When used as a thermoelectric refrigerator, a direct current is passed through the unit and one junction is heated and the other is cooled. Reversing the flow of direct current reverses the mode of operation of the system. The energy relationships for the thermoelectric generator are essen-

The performance factor of any refrigeration system is the coefficient of performance, β, which is defined as

$$\beta = \frac{\text{heat added at low temperature}}{\text{input energy}} = \frac{Q_a}{P_{in}} \tag{8.31}$$

The coefficient of performance should be as high as possible and may be greater or less than unity. An energy balance on the cold junction shows that the input power terms are the heat-transfer rate to the junction, Q_a, the conduction heat transfer rate from the hot junction, $K_g \Delta T$, and the Joule heating in the junction $i^2 R_g/2$. The removal rate from the cold junction is equal to the Peltier heat flow rate, $m\overline{S_{pn}} T_L i$. This gives the following equation for Q_a:

$$Q_a = m\overline{S_{pn}} T_L i - \frac{i^2 R_g}{2} - K_g \Delta T \tag{8.32}$$

The power input to the thermoelectric cooler is equal to iv_{in}, where the voltage v_{in} is the sum of the Peltier voltage drop in each junction and the drop due to the internal resistance:

$$v_{in} = m\overline{\pi_{pn}} + iR_g = m\overline{S_{pn}} \Delta T + iR_g \tag{8.33}$$

and

$$P_{in} = m\overline{S_{pn}} \Delta T i + i^2 R_g \tag{8.34}$$

Substituting Eqs. (8.32) and (8.34) into Eq. (8.31) gives the following equation for the coefficient of performance:

$$\begin{aligned} \beta &= \frac{m\overline{S_{pn}} T_L i - i^2 R_g/2 - K_g \Delta T}{m\overline{S_{pn}} \Delta T i + i^2 R_g} \\ &= \frac{NT_L - N^2/2 - \Delta T/Z}{N\Delta T + N^2} \end{aligned} \tag{8.35}$$

where N is equal to $R_g i / m\overline{S_{pn}}$ and Z is the figure of merit for the generator, $m^2 S_{pn}^2 / K_g R_g$.

In order to achieve as high a value of the coefficient of performance as possible, the figure of merit Z should be a maximum, as given by Eq. (8.22). The optimum value of N for maximum β can be found by taking the derivative of Eq. (8.35) with respect to N and setting $d\beta/dN$ to zero and solving for N. The optimum value of N is

$$N_{opt} = \frac{R_g i_{opt}}{m\overline{S_{pn}}} = \frac{\Delta T}{(1 + T_{ave} Z_{max})^{1/2} - 1} \tag{8.36}$$

The optimum input current for the maximum coefficient of performance is

$$i_{opt} = \frac{m\overline{S_{pn}} N_{opt}}{R_g} \tag{8.37}$$

If the temperatures T_L and T_H are fixed across a given thermoelectric refrigerator, the heat-pumping rate from T_L to T_H is

$$Q_a = m\overline{S_{pn}}T_L i - \frac{i^2 R_g}{2} - K_g \Delta T \tag{8.38}$$

The maximum heat-transfer rate $Q_{a,\max}$ can be found as a function of the input current. If the current is too high, the Joule heating term predominates, but if it is too low, the Peltier pumping rate is too low, also. The value of the current that gives the maximum pumping rate is

$$i_{\max Q} = \frac{m\overline{S_{pn}}T_L}{R_g} \tag{8.39}$$

If this current is maintained to a thermoelectric refrigerator and the heat-pumping rate is decreased, the temperature of the cold junction approaches some minimum value as Q_a approaches zero. This minimum temperature T'_L is

$$T'_L = \frac{T_H + Z_{\max} T_L^2/2}{1 + Z_{\max} T_L} \tag{8.40}$$

An even lower temperature can be achieved in this device if the current is lowered as the heat flow from the cold junction is decreased. According to Eqs. (8.38) and (8.39), the lowest possible temperature that can be reached is

$$T_{L,\min} = \frac{(1 + Z_{\max} T_H)^{1/2} - 1}{Z_{\max}} \tag{8.41}$$

Example 8.1. A thermoelectric generator that will operate between 30 and 500°C is to be constructed of *n-p* semiconductors with the following properties:

	Material	
Properties	*n*-type	*p*-type
S, μV/K	−170	210
ρ, μΩ · m	14	18
k, W/m · K	1.5	1.1

If this system is designed to produce 500 W_e at the highest possible thermal efficiency, find the number of element pairs, the maximum possible thermal efficiency, and the maximum possible power output. Assume that the cross-sectional area and the length of the *n*-leg are 1 cm^2 and 1 cm, respectively, and that the length of the *p*-leg is 1 cm.

Solution. $T_H = 273 + 500 = 773$ K; $T_L = 273 + 30 = 303$ K.

$$\text{Average Seebeck coefficient} = \overline{S_{pn}} = \overline{S_p} - \overline{S_n} = 210 - (-170)$$

$$= 380 \text{ μV/K}$$

Maximum figure of merit = $Z_{max} = \overline{S_{pn}^2}/[(\rho_p k_p)^{1/2} + (\rho_n k_n)^{1/2}]^2$. Thus

$$Z_{max} = \frac{(0.00038\ \text{V/K})^2}{[(14\times10^{-6}\times1.5)^{1/2} + (18\times10^{-6}\times1.1)^{1/2}]^2\ \Omega\cdot\text{W/K}} = 0.00177/\text{K}$$

For minimum value of $K_g R_g$,

$$\frac{A_n L_p}{A_p L_n} = \left(\frac{\rho_n k_p}{\rho_p p_n}\right)^{1/2} = \left(\frac{14\times10^{-6}\times1.1}{18\times10^{-6}\times1.5}\right)^{1/2} = 0.7552$$

$$A_p = \frac{A_n L_p}{(0.7552)L_n} = \frac{(1)(1)}{(0.7552)(1)} = 1.324\ \text{cm}^2 = 0.0001324\ \text{m}^2$$

$$K_g = m\left(\frac{k_p A_p}{L_p} + \frac{k_n A_n}{L_n}\right) = m\left[\frac{1.1(0.0001324)}{0.01} + \frac{1.5(0.0001)}{0.01}\right]$$

$$= 0.02957m \quad \text{W/K}$$

$$R_g = m\left(\frac{\rho_p L_p}{A_p} + \frac{\rho_n L_n}{A_n}\right) = m\left(\frac{18\times10^{-6}}{0.01324} + \frac{14\times10^{-6}}{0.01}\right)$$

$$= 0.002759m \quad \Omega$$

$$M_{opt} = (1 + Z_{max} T_{ave})^{1/2} = \left[1 + \frac{(0.00177)(303+773)}{2}\right]^{1/2} = 1.3972$$

$$R_L = M_{opt} R_g = 1.3972(0.002759m) = 0.003855m \quad \Omega$$

$$\text{Total circuit resistance} = R_L + R_g = 0.002759m + 0.003855m$$

$$= 0.006614m \quad \Omega$$

$$\text{Current} = i_{opt} = \frac{v_t}{R_t} = \frac{S_{pn}\Delta T}{R_t} = \frac{0.00038(500-30)}{0.006614} = 27\ \text{A}$$

$$\text{Power output} = P_{out} = i^2 R_L = 500 = (27)^2(0.003855m)$$

$$m = \text{number of pairs of elements} = \frac{500}{(27^2)(0.003855)} = 177.9\ \text{pairs}$$

Use 178 pairs.

Maximum thermal efficiency = $\eta_{th,max}$. Thus

$$\eta_{th,max} = \frac{M_{opt}\Delta T}{T_H(1+M_{opt}) + (1+M_{opt})^2/Z_{max} - \Delta T/2}$$

$$= \frac{1.3972(470)}{773(2.3972) + (2.3972)^2/0.00177 - 470/2}$$

$$= 13.50\%$$

$$\text{Maximum output power} = \frac{(mS_{pn}\Delta T)^2}{4R_g}$$

$$= \frac{[178(0.00038)(470)]^2}{4(0.002759)(178)}$$

$$= 514.5\ \text{W}$$

8.2.3 Thermoelectric Systems

As indicated earlier, *n-p* semiconductors are commonly used in thermoelectric systems. Since a low thermal conductivity or thermal conductance is desired, materials with high atomic or molecular weights are commonly employed because they have lower values of thermal conductivity. The thermal conductivity can be reduced further by using materials in the form of solid solutions. The product ZT of some of the proposed thermoelectric materials is shown in Fig. 8.2

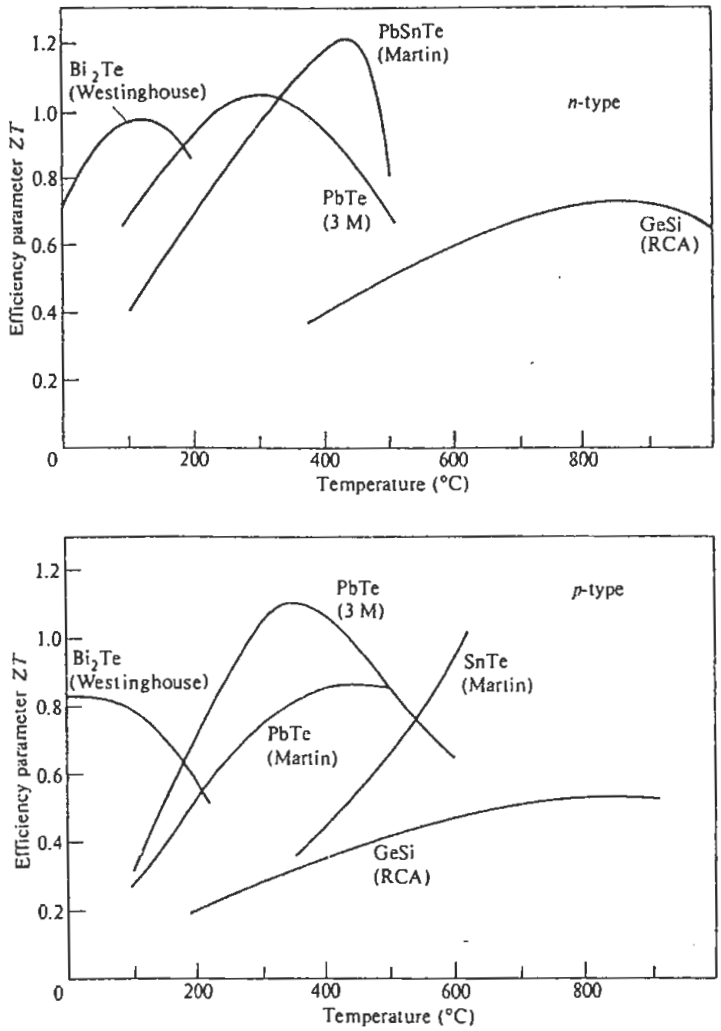


FIGURE 8.2
Properties of some typical thermoelectric materials.

for both n and p materials. Lead telluride (PbTe) is commonly employed in thermoelectric generators while bismuth telluride (Bi_2Te) is commonly employed in thermoelectric refrigerators.

The thermoelectric generator can use almost any source of thermal energy to produce electricity. Figure 8.3 depicts a kerosene-powered thermoelectric generator and Fig. 8.4 shows a radioisotope-powered thermoelectric SNAP system similar to that used to power the experimental laboratories on the moon.

Thermoelectric generators have a number of advantages over the conventional thermodynamic heat-engine systems. The thermoelectric systems are compact, rugged, and reliable and have no moving parts. Unfortunately, the thermal efficiency of these systems is very low, normally 5 to 10 percent, and the components are quite expensive. Consequently, the thermoelectric generating systems are usually employed for relatively low-power systems.

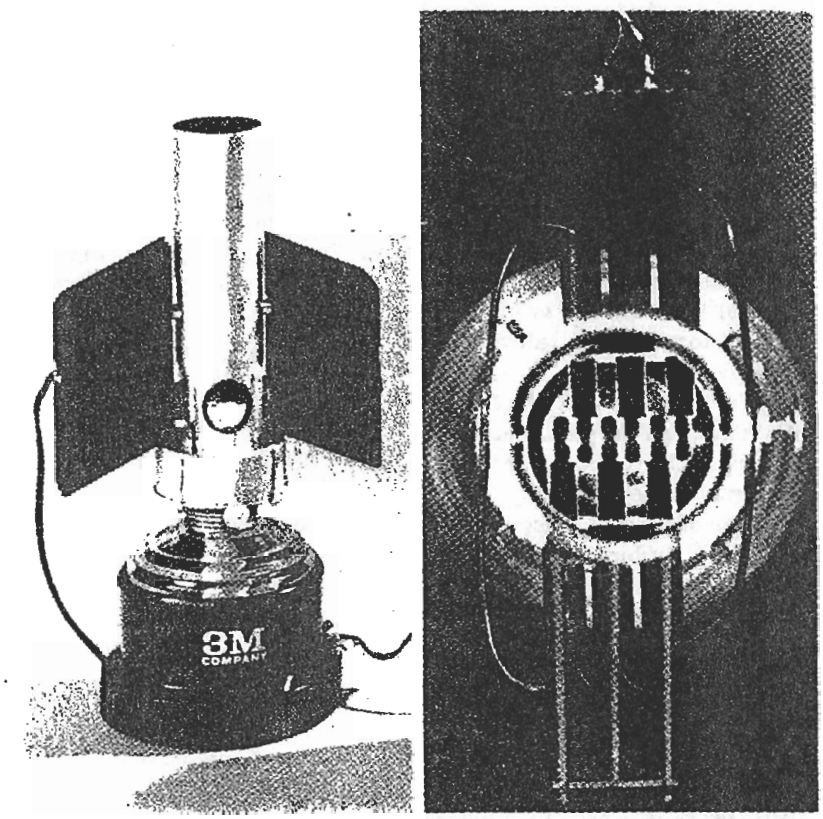


FIGURE 8.3
A kerosene-powered thermoelectric generator. (*Courtesy of Global Thermoelectric Power Systems, Ltd.*)

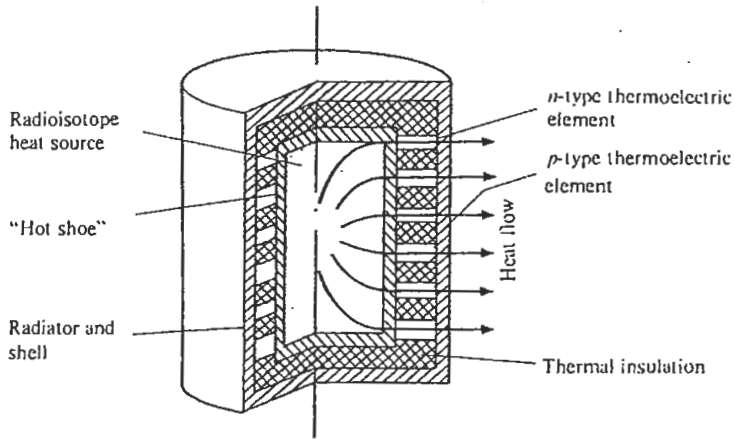


FIGURE 8.4
A radioisotope-powered thermoelectric generator.

8.2.4 Thermionic Converters

In the operation of a thermionic generator, the electrons are effectively "boiled off" the hot cathode and "condensed" on the cold anode. These electrons then flow back to the cathode through the external load resistor, producing useful energy. Thermionic emission was discovered in 1883 by Thomas A. Edison.

The valence electrons in orbit around a nucleus have an average kinetic energy equal to a quantity called the *Fermi-level energy*. The electrons vibrate about this Fermi level with an amplitude that is proportional to the absolute temperature. The work-function energy ϕ is the amount of energy required to strip the valence electron from an atom. This energy must be overcome before the electron can leave the surface. The work-function and Fermi-level energies vary from material to material.

The rate of thermal emission of electrons from a given surface is given by the Richardson-Dushman equation. According to this relationship, the current density J_0, in amperes per square meter, is

$$J_0 = \xi T^2 \exp\left(\frac{-e\phi}{kT}\right) \qquad (8.42)$$

where e is the charge of an electron, k is the Boltzmann constant (0.0001551 eV/K), T is the absolute temperature of the surface in kelvin, ϕ is the work function of the surface in electronvolts, and ξ is a constant with units of amperes per square meter per kelvin squared. ξ was supposed to be a universal constant with a value of 1.2×10^8 A/m$^2 \cdot$ K^2. However, it has been found that ξ varies from material to material. The thermionic emission properties of some

TABLE 8.2
Thermionic-emission properties of some materials

Material	ϕ, eV	ξ, A/m^2 · K^2
Cs	1.89	0.50×10^6
Mo	4.2	0.55×10^6
Ni	4.61	0.30×10^6
Pt	5.32	0.32×10^6
Ta	4.19	0.55×10^6
W	4.52	0.60×10^6
W+Cs	1.5	0.03×10^6
W+Ba	1.6	0.015×10^6
W+Th	2.7	0.04×10^6
BaO	1.5	0.001×10^6
SrO	2.2	1.00×10^6

A schematic diagram of a typical vacuum thermionic diode is shown in Fig. 8.5, along with the electron energies. The vacuum thermionic converter or generator is composed of the hot emitter or cathode and a cold collector, the anode, separated by a vacuum gap. When electrons leave the cathode, the cathode is left with a positive charge and the free electrons are attracted back to the cathode surface as well as being repelled by the negatively charged anode surface. Other emitted electrons already in the interelectrode gap also tend to drive the emitted electrons back to the cathode surface. As a result, electrons emitted from the hot

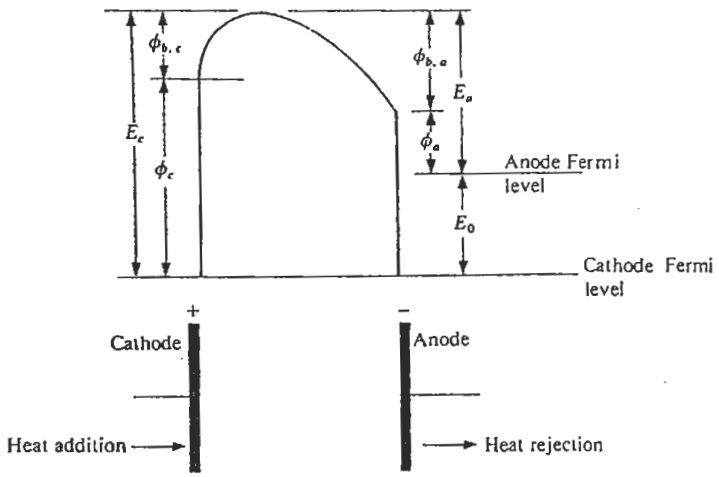


FIGURE 8.5
The vacuum, thermionic-diode generator.

cathode tend to "pile up" in the interelectrode gap, creating an additional energy barrier to the flow of electrons. This additional energy barrier is called the *space-charge-barrier energy* and is designated by ϕ_b.

In order for an electron to reach the anode, it must have a total energy E_c equal to the sum of the cathode work function and the space-charge-barrier energy, or $E_c = \phi_c + \phi_b$. With the existence of the space-charge-barrier energy, the net current density from the cathode is

$$J_0 = \xi T^2 \exp\left(\frac{-eE_c}{kT}\right) \tag{8.43}$$

Using the energy diagram in Fig. 8.5, it can be seen that the output voltage E_o, from the generator, is equal to the sum of the Fermi-level energy and the work function of the cathode plus the space-charge-barrier energy minus the sum of the Fermi-level energy, the work-function energy, and the space-charge-barrier energy of the anode, or

$$E_o = E_c - E_a \tag{8.44}$$

For a high output voltage, the cathode should have a low Fermi level and a high work function. It should also have a high value of ξ because the high work function inhibits the flow of electrons. The anode should have a high Fermi level, a low value of ϕ, and a low work function, even though this does increase the emission of electrons from the anode, thereby reducing the net flow of electron emission from the cathode. For optimum performance, the approximate temperature-work function relationship is

$$\frac{\phi_a}{T_a} = \frac{\phi_c}{T_c} \tag{8.45}$$

In order to keep the space-charge-barrier energy within reason for a vacuum converter, the interelectrode gap must be kept very small. In fact, for optimum thermal efficiency, this gap is only several microinches in width. It is extremely difficult to fabricate such a system and maintain the small gap spacing.

The space charge barrier is a difficult problem to overcome in a vacuum converter and, for that reason, the vacuum thermionic converter is seldom used. One solution to the barrier problem is to use a low-pressure ionized gas or plasma in the interelectrode gap. The use of an ionized gas or vapor at an absolute pressure of around 5 kPa significantly reduces the charge barrier, permitting the use of a wider electrode gap in the generator. The principal disadvantage of using an interelectrode gas is that it increases the convection heat transfer across the gap.

Most of the developmental work in the area of thermionic conversion has been centered on those systems employing cesium vapor between the two thermionic electrodes. Cesium has two major advantages over other gases. First, since it is a metallic vapor that ionizes easily, it effectively reduces the space-charge-barrier energy. Second, cesium has a low work function (1.89 eV), and, if the cesium condenses on the cold anode, it effectively lowers the anode work function. To achieve appreciable ionization of the cesium, the cathode or emitter

temperature must exceed 1800 K (3240°R). This system may be operated in either the ignited (continuous discharge) mode or in the unignited mode.

Other research has been directed toward systems using an ionized inert gas, such as helium or argon. The use of an inert gas minimizes the corrosion problems in the converter. In these systems, the inert gas is ionized by supplying a high voltage to a third (corona discharge) electrode. This permits operation as relatively low temperatures with the cathode operating in the neighborhood of 1500 K (2700°R).

The thermal efficiency of the thermionic conversion system is difficult to analyze explicitly because the losses are strongly dependent on the system geometry and the mode of operation. Since this system produces dc electricity, the output power of the system is simply equal to the product of the current i and the external load voltage v_L, or

$$P_{out} = iv_L = J_0 A_c v_L \tag{8.46}$$

A_c is the surface area of the cathode, in square meters, and v_L is the voltage drop across the external load resistor. This voltage drop is equal to the output voltage of the converter, E_a, as given by Eq. (8.44) minus the voltage drop in the electrical leads connecting the cathode and the anode to the load resistor.

There are three major losses in the operation of the thermionic converter. One of these is the heat transferred between the cathode and the anode, either by radiation for the vacuum converter or by combined radiation and convection for the gas or vapor-filled converters. Another thermal loss is the conduction heat transfer along the electrical leads connected to the cathode and anode. The last major system loss in the device occurs in the anode as the work-function and space-charge-barrier energies of the "condensing" electrons are converted into thermal energy.

The radiation heat-transfer rate or power P_r between the cathode and the anode can be estimated by using the conventional radiation heat-transfer equations. The spacing between the two electrodes is small enough that they may be approximated by infinite plane surfaces. The resulting equation is

$$P_r = \frac{\sigma A_c (T_c^4 - T_a^4)}{1/\varepsilon_c + 1/\varepsilon_a - 1} \tag{8.47}$$

where σ is the Stefan-Boltzmann constant, 5.67×10^{-8} W/m$^2 \cdot$ K^4, and ε_c and ε_a are the emissivities of the cathode and anode, respectively, If there is a low-pressure vapor between the electrodes, the heat-transfer rate will be increased because of convective heat transfer.

The biggest single power loss from the cathode is the energy carried away by the electrons, P_{el}. The potential energy of an electron leaving the cathode must exceed the work function energy plus the space-charge-barrier energy for the electrode ($\phi_c + \phi_{b,c}$). In addition, each electron has an average total kinetic energy of $2kT_c$. For a net emitter current density of J_0, the energy rate from the

emitter is

$$P_{el} = J_0 A_c \left(\phi_c + \phi_{b,c} + \frac{2kT_c}{e} \right) \tag{8.48}$$

If the input lead wire, connected to the cathode has an electrical resistivity ρ_w, a length L_w, a thermal conductivity k_w, and a cross-sectional area A_w, the conduction heat-transfer rate from the cathode combined with the Joule heating rate to the cathode is

$$P_w = \frac{k_w A_w}{L_w}(T_c - T_0) - (J_0 A_c)^2 \frac{\rho_w L_w}{2A_w} \tag{8.49}$$

where $T_c - T_0$ is the linear temperature drop over the conductor length L_w.

Since the sum of these three energy rates is the power loss from the cathode and must be made up by heat addition to the converter, the thermal efficiency of a thermionic converter can be estimated from the following equation:

$$\eta_{th} = \frac{P_{out}}{P_r + P_{el} + P_w} \tag{8.50}$$

Example 8.2. A thermionic converter is operating with a thoriated-tungsten (W + Th) emitter at 1900 K with a space-charge-barrier energy of 0.3 eV and a collector-barrier energy of 0.5 eV. Find the emitter area needed to produce 100 W if the collector (anode) is constructed of barium oxide (BaO).

Solution. From Table 8.2: $\xi_c = 0.04 \times 10^6$ A/m$^2 \cdot$ K^2, $\phi_c = 2.7$ eV, and $\xi_a = 0.001 \times 10^6$ A/m$^2 \cdot$ K^2, $\phi_a = 1.5$ eV.

Emitter current density $= J_c = \xi_c T_c^2 \exp[-e(\phi_c + \phi_{b,a})/kT_c]$. Thus

$$J_c = 0.04 \times 10^6 (1900)^2 \exp\left[\frac{-11{,}600(2.7+0.3)}{1900}\right]$$

$$= 1603.7 \text{ A/m}^2$$

$$\text{Output voltage} = v_L = \phi_c + \phi_{b,c} - \phi_a - \phi_{b,a}$$

$$= 2.7 + 0.3 - 0.5 - 1.5 = 1.0 \text{ V}$$

$$\text{Optimum anode temperature} = T_a = \frac{\phi_a T_c}{\phi_c} = \frac{1.5(1900)}{2.7} = 1056 \text{ K}$$

Anode current density $= J_a = \phi_a T_a^2 \exp[-e(\phi_a + \phi_{b,a})/kT_a]$. Thus

$$J_a = 0.001 \times 10^6 (1056)^2 \exp\left[\frac{-11{,}600(1.5+0.5)}{1056}\right] = 0.3 \text{ A/m}^2$$

Converter area:

$$\text{Output power} = P_{out} = 100 \text{ W}_e = A(J_c - J_a)v_L$$

$$= A(1603.7 - 0.3)(1.0) = 1603.4 \text{ A}$$

$$\text{Converter area} = A = \frac{100}{1603.4} = 0.06237 \text{ m}^2 = 623.7 \text{ cm}^2$$

Neglecting the radiation and conduction losses from the system, calculate the thermal efficiency, η_{th}:

$$\eta_{th} = \frac{v_{out}}{\phi_c + \phi_{b,c} + 2kT_e/e}$$

$$= \left[\frac{1.00}{2.7+0.3+2(1900)/11{,}600}\right](100) = 30.05\%$$

The maximum possible thermal efficiency for a system operating between the same temperature differences is:

$$\eta_{max} = 1 - \frac{T_L}{T_H} = 1 - \frac{1056}{1900} = 44.42\%$$

If one uses an environmental temperature of 298 K, the maximum possible conversion efficiency will be $= 1 - 298/1900 = 84.32\%$.

The thermionic conversion systems require a high-temperature, high heat-flux, thermal energy source. Possible energy sources include radioisotopes, nuclear fuel elements, concentrated solar energy, and combustion systems using heat pipes. The heat pipe is a device that permits the transfer of thermal energy fluxes across a relatively large distance with a very small temperature drop. In this system, the heat boils a working fluid at one end of the heat pipe and then this heat is removed by condensation at the other end of the pipe. The resulting condensate in the pipe is returned to the hot end of the pipe by either gravity or the capillary action of a wick.

A typical thermionic converter, using cesium vapor to reduce the space charge barrier, is shown in Fig. 8.6. Like the thermoelectric conversion systems, these converters have no moving parts; but they commonly have thermal efficien-

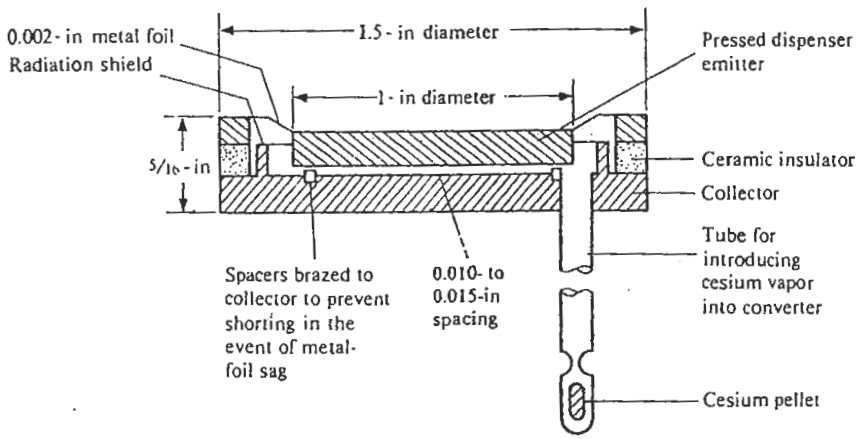


FIGURE 8.6
A cesium thermionic converter. (*From Angrist, 1976.*)

cies that range from 15 to 20 percent, considerably above that for the thermoelectric systems. Unfortunately, these systems are not as rugged as the thermoelectric systems, they are complicated to build because of the very small gap spacing, and they are very expensive. Thermionic converters also experience a problem due to the deterioration of the electrodes, particularly the hot cathode.

8.2.5 Other Thermal-Electric Conversion Systems

A number of minor systems convert thermal energy directly into electricity, including the ferroelectric converter, the Nernst-effect generator, and the thermomagnetic converter. Some present interesting concepts for the production of electricity.

One of the more unusual methods of thermal energy conversion takes place in the ferroelectric system shown in Fig. 8.7. This system essentially consists of a capacitor that uses barium titanate as the dielectric material. At low temperatures, barium titanate has a very high dielectric constant, which means the capacitor has a very high value of electrical capacitance. This system is charged at low voltage through a zenor diode labelled number 1 in Fig. 8.7. Once the capacitor is charged, heat is applied to it. When barium titanate is heated above 49°C (120°F), its Curie point, the value of the dielectric constant drops significantly, and, for the same charge on the plates, the voltage increases markedly. The high voltage current then flows through a second zenor diode (labeled number 2 in Fig. 8.7), through the external load resistor, and back to the battery. The capacitor is then cooled and the cycle is repeated.

The thermomagnetic converter operates in somewhat the same manner as the ferroelectric converter except that it operates with inductive-field energy instead of electrostatic-field energy. In the thermomagnetic generator, a ferromagnetic material is placed in the core of an induction coil, increasing its reactance and the strength of the stored magnetic field. The core is then heated above the Curie point, which makes it paramagnetic. This results in a marked decrease in the inductance of the coil and the collapsing magnetic field produces a high-voltage pulse.

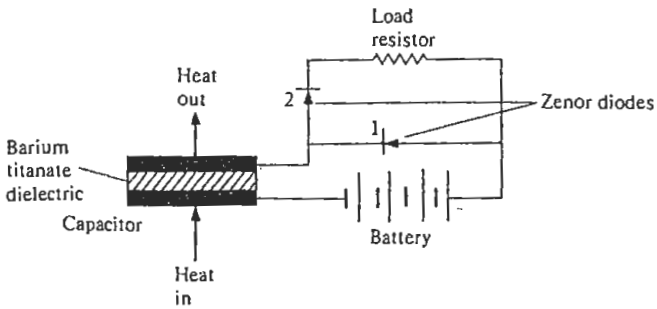


FIGURE 8.7
A schematic of the ferroelectric conversion system

The Nernst-effect generator operates by passing a thermal heat flux through a semimetal or a semiconductor in the presence of a perpendicular magnetic field. This system, as well as the other systems discussed in this section, are not practical modes for the production of electrical energy at this time.

8.3 CONVERSION OF CHEMICAL ENERGY INTO ELECTRICITY

8.3.1 General Systems

The battery and the fuel cell are systems in which stored chemical energy is converted directly into electrical energy. Since they do not go through the thermal energy regime, they are not limited by the efficiency of an externally reversible heat-engine cycle, or $1 - T_L/T_H$. For this reason, considerable interest in and research into these systems have been generated.

Batteries and fuel cells are very similar in operation, the major difference being that batteries contain a fixed quantity of fuel or chemical energy whereas fuel cells operate with a continuous supply of fuel. Some batteries are reversible devices in that the products of the chemical reactions are separated back into the original reactants by supplying reversed direct current to the battery during recharging. Fuel cells cannot be recharged, as the products of the chemical reactions are thrown away.

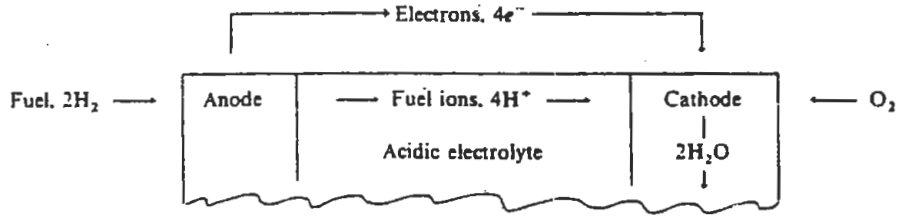
Batteries are employed as energy-storage systems and can be divided into two major categories—primary and secondary. A primary battery, like the conventional C and D cells, cannot normally be recharged, while the secondary battery, like the lead-acid automobile battery, can be recharged many times.

Fuel cells and batteries are similar in composition in that both normally contain two electrodes separated by an electrolyte solution or matrix. In the fuel cell, the fuel reactant, usually hydrogen or carbon monoxide, is fed into one porous electrode and oxygen or air is fed into the other porous electrode.

The fuel-cell electrodes must accomplish three things. The electrode must be porous so that both the fuel and electrolyte can penetrate it to achieve proper contact. The pore size of the electrodes is very critical. If the pores are too large, the fuel gas will "bubble through" and be wasted. If the pores are too small, there will not be sufficient contact between the reactant and the electrolyte and the capacity of the cell will be reduced. The electrode must contain a chemical catalyst that breaks the fuel compound into atoms that are more reactive. Both platinum and sintered nickel have been used as catalysts in these systems. Finally the electrodes must be able to conduct the electrons to the terminal.

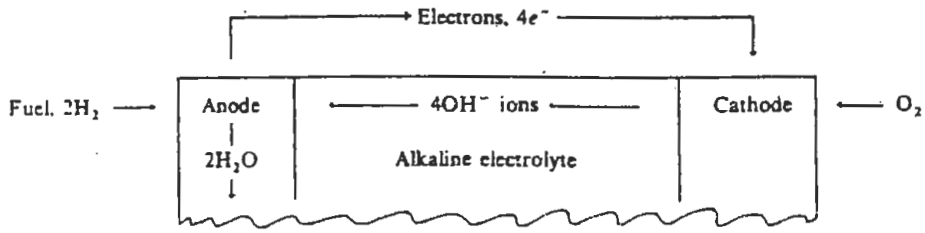
The electrolyte solution must be highly permeable to either a H^+ or OH^- ion which is produced as an intermediate product at one of the electrodes. This same ion is transferred through the electrolyte to the other electrode where it combines with the other reactant. The electrons travel through the external circuit to the other electrode where the oxidation product is formed.

If the cell "burns" oxygen and hydrogen and has an acidic electrolyte, the intermediate ion is H^+ and the general reactions are



Anode reaction: $2H_2 \longrightarrow 4e^- + 4H^+$
Cathode reaction: $4e^- + 4H^+ + O_2 \longrightarrow 2H_2O$

In an oxygen-hydrogen fuel cell with an alkaline electrolyte (such as potassium hydroxide), the intermediate ion is OH^- and the general reactions are



Anode reaction: $2H_2 + 4OH^- \longrightarrow 4H_2O + 4e^-$
Cathode reaction: $2H_2 + O_2 + 4e^- \longrightarrow 4OH^-$

Some fuel cells employ a solid electrolyte that is actually an ion-exchange membrane. One such membrane was composed of finely powdered sulfenated polystyrene held in an inert polymer. This membrane is flexible, has good mechanical strength, is chemically inert, and is impervious to the reactant gases. While the membrane does permit the passage of ions, it has a relatively high electrical resistance even though the total thickness is about 3 mm (0.188 in). This type of converter was used as an auxiliary power source on some of the early Gemini two-person orbital space missions. A schematic diagram of fuel cell of this type along with a typical fuel cell is shown in Fig. 8.8.

8.3.2 Fuel-Cell Performance

The total energy released in any chemical reaction is equal to the change in the enthalpy of formation, ΔH. The change in the enthalpy of formation is equal to the sum of the enthalpy of formation for the products minus the sum of the

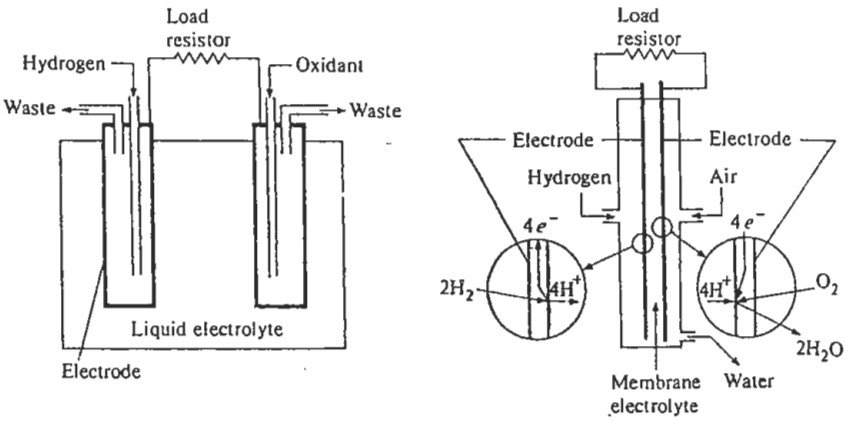


FIGURE 8.8
Schematic diagrams of some typical fuel cells.

enthalpy of formation of the reactants:

$$\Delta H = \sum (\Delta H)_{\text{products}} - \sum (\Delta H)_{\text{reactants}} \tag{8.51}$$

The change in the enthalpy of formation is equivalent to the higher heating value (HHV) of the fuels, discussed in Chap. 2.

Values of ΔH are given in Table 8.3 for the oxidation of various fuels at 25°C and 1 atm. Normally, all naturally-occurring elements have a ΔH of zero. Consider the following combustion reaction:

$$C + O_2 \rightarrow CO_2$$

TABLE 8.3
Enthalpy of formation ΔH^0 and Gibbs free energy ΔG^0 of compounds and ions (at 1 atm and 298 K)

Compound or ion	Enthalpy of formation ΔH^0, J/kg · mol	Gibbs free energy ΔG^0, J/kg · mol
CO	-110.0×10^6	-137.5×10^6
CO_2	-394.0×10^6	-395.0×10^6
CH_4	-74.9×10^6	-50.8×10^6
Water	-286.0×10^6	-237.0×10^6
Steam	-241.0×10^6	-228.0×10^6
LiH	$+128.0\times10^6$	$+105.0\times10^6$
$NaCO_2$	-1122.0×10^6	-1042.0×10^6
CO_3^{-2}	-675.0×10^6	-529.0×10^6
H^+	0.0	0.0
Li^+	-277.0×10^6	-293.0×10^6
OH^-	-230.0×10^6	-157.0×10^6

The change in the enthalpy of formation, ΔH, for this reaction is

$$\Delta H = \Delta H_{CO_2} - \Delta H_C - \Delta H_{O_2} = (-394 \times 10^6) - 0 - 0$$
$$= -394 \times 10^6 \text{ J/kg} \cdot \text{mol } CO_2 = -394 \times 10^6 \text{ J/kg} \cdot \text{mol C}$$

Dividing by the appropriate molecular/atomic weights gives

$$\Delta H = -8{,}953 \text{ kJ/kg } CO_2 = -32{,}810 \text{ kJ/kg C} = -14{,}110 \text{ Btu/lbm C}$$

The minus sign indicates that this is energy lost from the reaction and would represent energy added to the combustion process (positive in this case), or $HHV = -\Delta H$. Consequently, ΔH is negative for any exothermic reaction and positive for any endothermic reaction.

Theoretically, all of the energy in the enthalpy of formation could be converted into electrical energy if none of it were converted into any other energy form. Unfortunately, in an oxidation reaction, some of the chemical energy is converted into thermal energy and only the balance of the energy can be theoretically converted into electricity. The minimum amount of thermal energy generated is the reversible heat transfer which is equal to $\int T\,dS$. Since the fuel cell is essentially an isothermal device, $\int T\,dS = T \int dS = T\,\Delta S$. This means that the amount of electrical energy W_e produced in a fuel cell is

$$W_e \leq \Delta H - T\,\Delta S \tag{8.52}$$

Thus, the electrical generation per kg-mole of fuel is equal to $(\Delta H - T\,\Delta S)$ for a reversible reaction but is less than this quantity if there are any irreversibilities in the cell.

Gibbs free energy G is a thermodynamic function that is defined as the enthalpy H minus the product of temperature and entropy, TS:

$$G \equiv H - TS \tag{8.53}$$

The derivative of this equation for an isothermal process ($dT = 0$) is

$$dG = dH - T\,dS \quad \text{or} \quad \Delta G = \Delta H - T\,\Delta S \tag{8.54}$$

Thus, Eq. (8.52) reduces to

$$W_e \leq \Delta G \tag{8.55}$$

where the change in Gibbs free energy for a given reaction is

$$\Delta G = \sum (\Delta G)_{\text{products}} - \sum (\Delta G)_{\text{reactants}} \tag{8.56}$$

Gibbs free energy is a function of the pressure and temperature at which the reaction takes place. The general thermodynamic property relationship is

$$T\,dS = dH - V\,dp \quad \text{or} \quad V\,dp = dH - T\,dS \tag{8.57}$$

Substituting Eq. (8.57) into Eq. (8.54) gives

$$dG = V\,dp \tag{8.58}$$

For each mole of gaseous constituent, $V = R_u T/p$, so that for an isothermal

process,

$$\int_{G^0}^{G} dG = \int_{p^0}^{p} \frac{R_u T}{p}\, dp = R_u T \int_{p^0}^{p} \frac{dp}{p} = G - G^0 = R_u T \ln \frac{p}{p^0} \tag{8.59}$$

G^0 is the value of Gibbs free energy for 1 atm, $p^0 = 1.0$ if p is the constituent pressure in atmospheres, and Eq. (8.59) reduces to

$$G = G^0 + R_u T \ln P \tag{8.60}$$

Consider the following general chemical reaction for a fuel cell:

$$aA + bB \rightarrow cC + dD$$

Assume that the reactants (A and B) and the products (C and D) are all ideal gases with partial pressures p_A, p_B, p_C, and p_D. The change in Gibbs free energy with constituent pressure for this reaction becomes

$$\Delta G = \Delta G^0 + R_u T \ln \frac{p_A^a p_B^b}{p_C^c p_D^d} \tag{8.61}$$

In some instances, the reaction products may appear in the liquid phase, and in that case Eq. (8.61) can be used providing the partial pressure of component x, p_x, is replaced by a quantity θ_x, where θ_x is called the *activity of component x* and has a value equal to the partial pressure of component x only when the component obeys the ideal-gas law.

Since both ΔG and ΔH are expressed in units of energy (joules) per kg-mole, this means W_e is the electrical energy associated with the passage of 1 kg · mol of electrons through the electrical circuit. One kg · mol of electrons is equal to Avagadro's number (6.022×10^{26}) and the charge of one electron is 1.602×10^{-19} C. This means that the charge associated with 1 kg · mol of electrons is 9.65×10^7 C, and this quantity of charge is defined as the Faraday F_y. If n mol of electrons are released in the reaction and the internal cell voltage is E_g, the value of electrical power W_e is

$$W_e = nF_y E_g \simeq \Delta G \tag{8.62}$$

The maximum value of the internal cell voltage is

$$E_g = E_g^0 - \frac{R_u T}{nF_y} \ln \frac{\theta_C^c \theta_D^d}{\theta_A^a \theta_B^b} \tag{8.63}$$

This is called the *Nernst equation.* It will be noted that increasing the fuel-cell temperature T decreases the value of the output voltage and hence the value of the electrical energy output.

As was discussed earlier, the fuel cell is not limited by the efficiency of an externally reversible heat-engine cycle, but there is an upper limit to the conversion efficiency. This maximum conversion efficiency is equal to

$$\eta_{max} = \frac{W_{e,max}}{\Delta H} = \frac{\Delta G}{\Delta H} = 1 - \frac{T \Delta S}{\Delta H} \tag{8.64}$$

The actual conversion efficiency of the fuel cell is lower than that given by Eq. (8.64) and may be calculated from

$$\eta_{act} = \frac{W_{e,act}}{\Delta H} = \frac{nF_v v_L}{\Delta H} \tag{8.65}$$

where v_L is the output voltage of the cell. Efficiencies as high as 60 to 70 percent may be realized with most fuel cells without resorting to the high temperatures required for the heat-engine cycles. In fact, as mentioned earlier, an increase in the operating temperature decreases the actual output and hence the conversion efficiency.

Example 8.3. Find the output voltage and theoretical conversion efficiency of an oxygen-hydrogen fuel cell operating at 600°C. Assume that the hydrogen is supplied at 1.1 atm and the oxygen is supplied from air at 1.2 atm, and assume that the steam product is at 1 atm.

Solution. From Table 8.3:

$$\Delta G^0 \text{ (for steam)} = 228{,}000 \text{ kJ/kg} \cdot \text{mol } H_2O$$

$$\Delta H^0 \text{ (for steam)} = 241{,}000 \text{ kJ/kg} \cdot \text{mol } H_2O$$

$$\Delta H^0 \text{ (for water)} = 286{,}000 \text{ kJ/kg} \cdot \text{mol } H_2O$$

$$\Delta G^0 = nF_v E_R^0 \qquad F_v = 9.65 \times 10^7 \text{ C/kg} \cdot \text{mol electrons}$$

Combustion equation:

$$H_2 + \tfrac{1}{2}O_2 \rightarrow 2e^- + 2H^+ + O \rightarrow H_2O$$

For this reaction, $n = 2$ kg · mol electrons/kg · mol H_2O.

$$E_R^0 = \frac{\Delta G^0}{nF_v} = \frac{(228{,}000 \text{ kW} \cdot \text{s/kg} \cdot \text{mol } H_2O)}{(2 \text{ mol electrons/mol } H_2O)(9.65 \times 10^7 \text{ C/mol electrons})} = 0.001181 \text{ kV}$$

$$= 1.181 \text{ V}$$

Partial pressure of the O_2 in the reactants = $1.2(0.21) = 0.252$ atm

Partial pressure of the H_2 in the reactants = 1.1 atm

Partial pressure of the H_2O in the products = 1.0 atm

$$E_R = E_R^0 + \frac{R_u T}{nF_v} \ln \frac{p_{H_2} p_{O_2}^{1/2}}{p_{H_2O}}$$

$$= 1.181 + \frac{8314(873)}{2(9.65 \times 10^7)} \ln \frac{1.1(0.252)^{1/2}}{1.0}$$

$$= 1.181 - 0.022 = 1.159 \text{ V}$$

Maximum conversion efficiency $= \eta = \Delta G/\Delta H$.

$$\Delta G = \Delta G^0 + R_u T \ln \frac{p_{H_2} p_{O_2}^{1/2}}{p_{H_2O}}$$

$$= 228 \times 10^6 + (8314)(873) \ln \frac{1.1(0.252)^{1/2}}{1.0}$$

$$= 223.7 \times 10^6 \text{ J/kg} \cdot \text{mol } H_2O$$

$$\text{Conversion efficiency} = \eta = \frac{223.7 \times 10^6}{286 \times 10^6} = 0.7821 = 78.21\%$$

The performance of a fuel cell is a function of the operating characteristics of the cell. Like a battery, the output voltage of a fuel cell decreases as the electrical output of the cell increases. There are three major voltage losses associated with operation of the cell. The chemical-polarization or activation-polarization loss v_c is essentially the voltage required to cause the ions to break away from the electrode where they are formed. The internal-resistance loss is equal to the product of iR_i, where i is the current flow and R_i is the internal cell resistance. At very high loads, there is an additional loss called the *concentration-polarization loss* which is associated with electrostatic effects and concentration gradients caused by the localized depletion of the ions in the vicinity of the electrodes at high power output. The typical voltage-current characteristics of a fuel cell are shown in Fig. 8.9.

8.3.3 Types of Fuel Cells

Any successful fuel cell should satisfy two major requirements—invariance and reactivity. The invariance requirement specifies that the system must be designed to operate reliably for long periods of time. There must be no poisoning of the

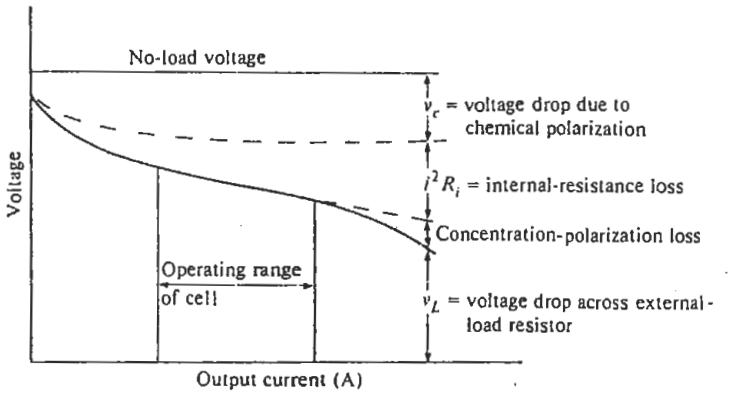


FIGURE 8.9
The voltage-current characteristics of fuel cells.

catalysts by impurities in the reactants, no clogging of the electrode pores, no "bubbling through" of the reactants, and no interdiffusion of the reactants.

The reactivity requirement is concerned with obtaining the maximum possible energy from the chemical reactions at relatively high reaction rates. Thus it is important that all fuel atoms are completely oxidized during operation of the cell. The reaction rate can be increased by using porous electrodes that are very large to produce a large interaction interface between the gas and the electrolyte. The reaction rate can also be increased by increasing the operating pressure and/or temperature of the cell. Unfortunately, the steps that are taken to increase the reaction rate are usually in conflict with the invariance requirement.

Most of the early operational fuel cells were low-temperature systems "burning" hydrogen and oxygen as the reactants. Most of them operated at temperatures below 500 K (900°R), and, while lowering the operating temperature improves the conversion efficiency, the oxidation rate or power output of the cell is decreased when the system pressure and/or temperature is decreased.

The membrane fuel cell (discussed earlier) and the redox fuel cell were among the unusual early fuel cells. The redox fuel cell is a hydrogen-oxygen system that differs from the normal fuel cell in that the chemical reactions do not occur at the electrodes. A schematic diagram of the redox fuel cell is shown in Fig. 8.10. The redox cell has two electrolyte solutions separated by an ion-exchange membrane, and the reactant gases are bubbled through each electrolyte. This cell is inherently less efficient than the conventional cell but it has lower resistance and polarization losses and potentially higher current densities. A primary advantage of this cell is that it can operate on relatively impure reactants.

A number of fuel cells have been used successfully for special applications. These systems have been used extensively in the space program for relatively short-term applications such as the piloted orbital space flights and the Apollo missions to the moon. Unfortunately, these were not long-term power systems but were just designed to provide power and potable water during the life of the mission.

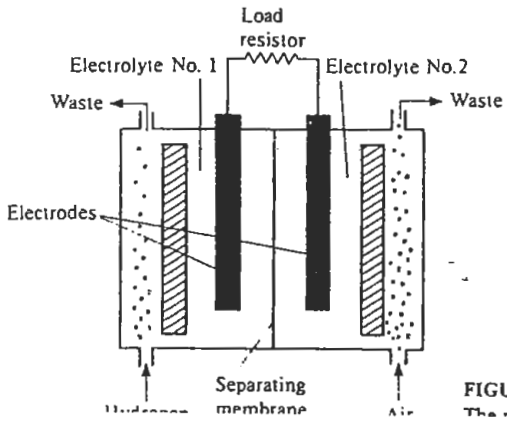


FIGURE 8.10
The redox fuel cell

A lot of research has been expended on the development of high-temperature fuel cells that can be used to operate with impure and inexpensive fuels, like natural gas. In order to utilize a hydrocarbon fuel, it must first be "cracked" into hydrogen and carbon monoxide. The use of two fuel gases (CO and H_2) in a fuel cell complicates the choice of electrolyte. These systems operate at temperatures up to 1200 K (2160°R). One of the more promising systems is the phosphoric acid fuel cell developed in early 1980s. It is supposed to supply electricity from natural gas and a number of them were put in use in the mid-1980s to determine their actual performance in the field.

A schematic diagram of a proposed 100-kW_e phosphoric-acid fuel cell is shown in Fig. 8.11. The heat rate for this unit is estimated to be 8300 Btu/kWh. Its capital costs are projected to be \$2500/kW, with operating costs of 0.8 cents/kWh. This unit is powered by natural gas, but it contains a reformer that converts the natural gas into a hydrogen-rich fuel. In the mid-1980s, a prototype of this system operated in Chicago for several thousand hours. Research is continuing on this type of fuel cell aimed at eventual application to the commercial production of electricity.

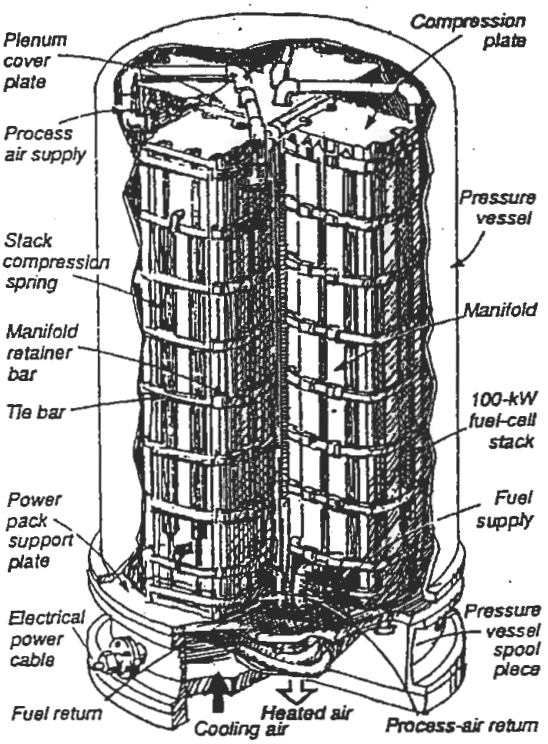


FIGURE 8.11
Schematic of a proposed 100-kW_e, phosphoric-acid, fuel cell. (*From Makansi, 1989.*)

8.4 CONVERSION OF ELECTROMAGNETIC ENERGY INTO ELECTRICITY

8.4.1 Operational Characteristics of Solar Cells

Electromagnetic energy can be converted directly to electrical energy in the photoelectric cell, commonly called the *solar cell.* Like the fuel cell, the maximum conversion efficiency of this system is not limited by the efficiency of an externally reversible heat-engine cycle. Despite this, however, the conversion of solar energy into electrical energy is limited to relatively low conversion efficiencies.

The principle of operation of the photovoltaic cell was discovered by Adams and Day in 1876, using selenium. In 1919, Coblenz discovered that a voltage is induced between the illuminated and dark regions of semiconducting crystals. However, photoelectric conversion was essentially a laboratory phenomenon until 1941, when Ohl discovered the photoelectric effect at a *p-n* junction of two semiconductors.

Primary interest in these systems concerns the possible conversion of the electromagnetic energy from the sun directly into electricity. Using the solar constant of 1395 W/m^2, it can be shown that the effective radiating temperature at the surface of the sun is around 6000 K (10,800°R). According to the Wiens displacement law for thermal radiation, the most probable energy of the solar radiation is about 2.8 eV. While this value is very small compared to the electromagnetic radiation produced in nuclear reactions, it is more than sufficient to strip the valence electrons from many materials.

The successful operation of a solar cell relies on the action of the *p-n* junction. When a *p-n* junction is first formed, there is an initial transient charging processes that establishes an electric field in the vicinity of the junction. Although both the *n*-type and the *p*-type materials are neutrally charged by themselves, the electron concentration in the *n*-type material is so high that when it is connected to the *p*-type semiconductor, some of the electrons in the *n* material "spill over" into the holes of the *p* material. This essentially makes the *n* material positively charged and the *p* material negatively charged in the vicinity of the junction. This charging process continues until the electric field or junction potential inhibits the further net flow and the electron and hole flow is the same in both directions, as indicated in Fig. 8.12*a.*

If a forward-bias voltage v_L is applied across the junction, the junction potential is reduced by the amount of the bias voltage. The forward-bias voltage increases the flow of majority carriers (electrons to the *p* material and holes to the *n* material) across the junction, as indicated in Fig. 8.12*b.* The net current density J across the junction is

$$J = J_0 \exp\left(\frac{ev_L}{kT} - 1\right) \tag{8.66}$$

where J_0 is the reverse-saturation current density. The reverse-saturation current density is the current that flows when a large reverse-bias voltage is applied across

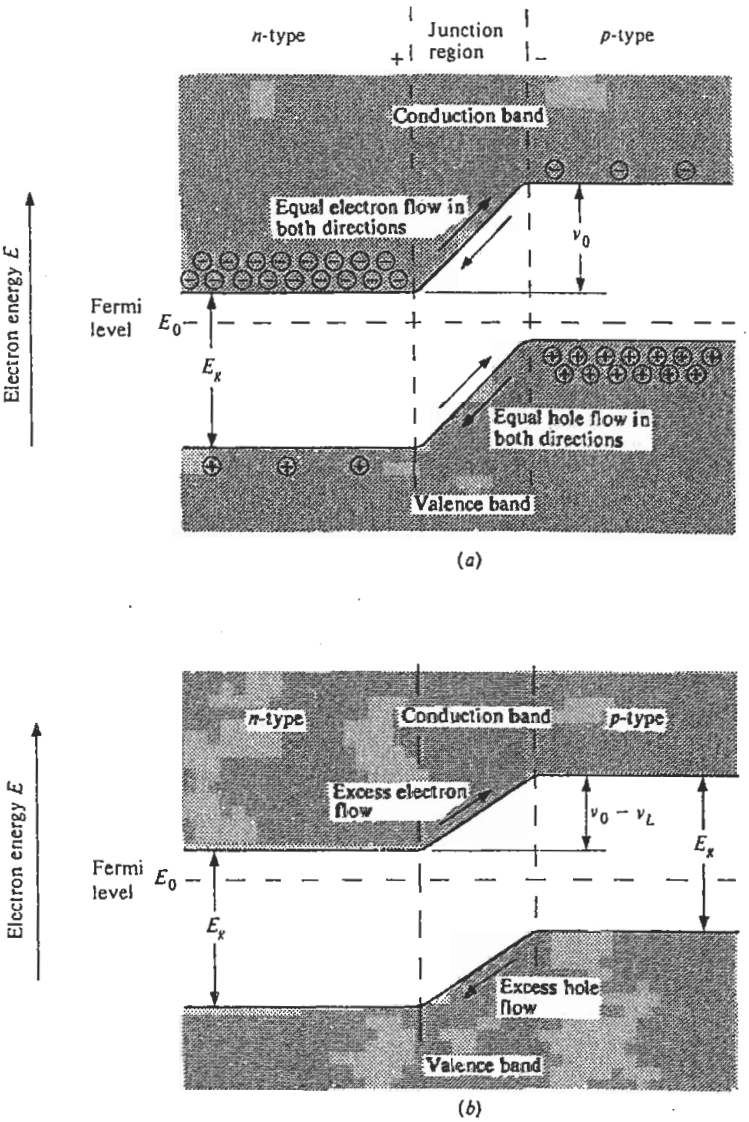


FIGURE 8.12
The charge distribution at an *n-p* junction of semiconductors (*a*) without and (*b*) with an applied voltage v_L. (*From Walsh, 1967.*)

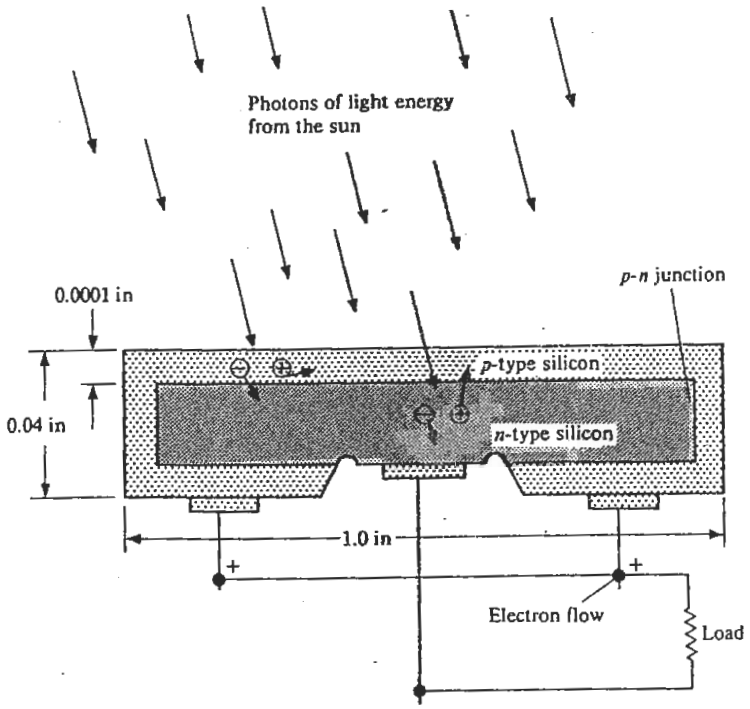


FIGURE 8.13
Schematic diagram of a typical solar cell. (*From Encyclopedia of Energy, 1976.*)

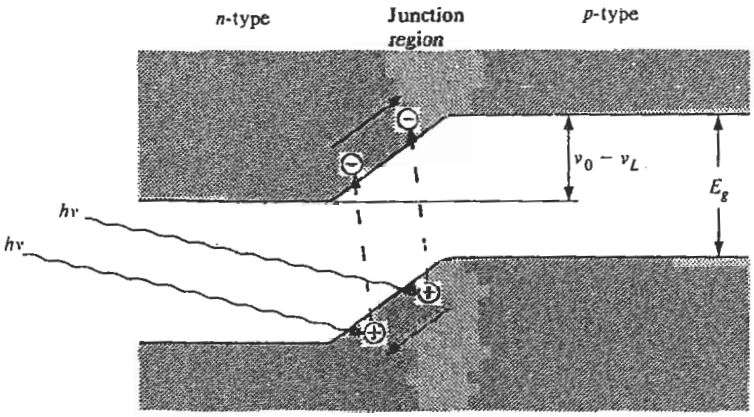


FIGURE 8.14
The charge-carrier flow due to irradiation of the solar cell. (*From Walsh, 1967.*)

the junction and current flow is due to only the minority carriers (electrons to the n material and holes to the p material).

The photons react with the valence electrons near a p-n junction to produce an effect similar to that produced by the forward-bias voltage. In this case, v_L is the external voltage that is generated by the photons. A typical solar-cell schematic is shown in Fig. 8.13. The nonreflected photons incident on the surface of the cell enter the thin outer layer of the semiconducting material and are either converted into heat or produce ion-pairs by stripping the valence electrons from the semiconductor atoms. In order to produce an ion pair, the incoming photon must have an energy in excess of E_G, which is called the *excitation energy* of the semiconductor material. Some of these ions will be separated by the electric field of the junction. These ions reduce the electric field at the junction and this increases the flow of the majority carriers producing a current flow, as shown in Fig. 8.14. The typical current-voltage characteristics of a solar cell are shown in Fig. 8.15.

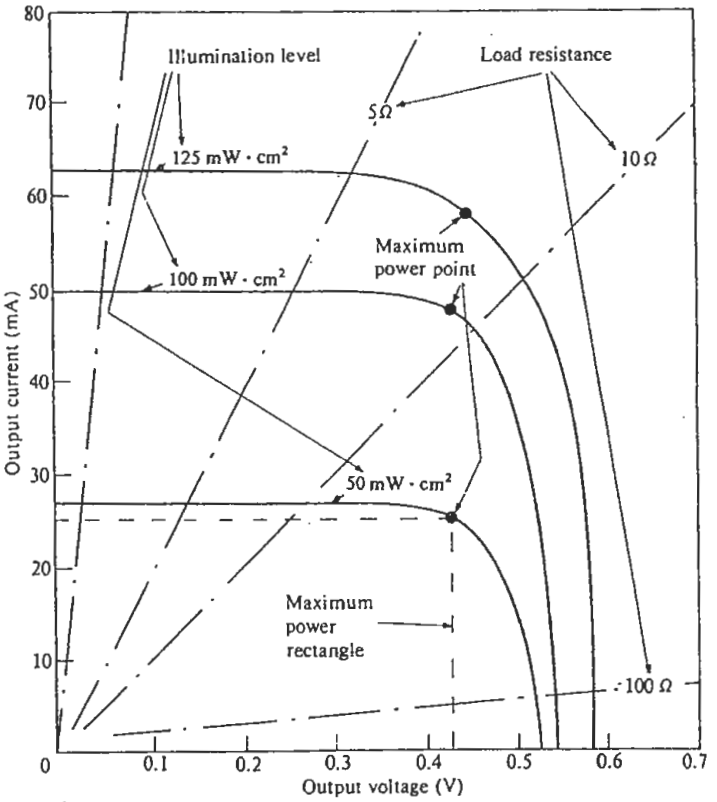


FIGURE 8.15
The current-voltage characteristics of a typical solar cell. (*From Angrist, 1976.*)

The conversion efficiency of a solar cell is not limited by the thermal efficiency of a heat-engine cycle, but there are some inherent losses that severely limit the performance of the cell. The two major ones are the junction loss and the spectrum loss. The junction loss is that loss associated with the flow of minority carriers in the junction [the (-1) in Eq. (8.66)]. Although this flow is usually small compared to the flow of majority carriers, it is not negligible. For silicon solar cells exposed to solar radiation, the junction loss reduces the conversion efficiency to about 50 percent. The junction loss decreases as the radiation intensity is increased as this effectively increases v_L in the current equation. Care must be taken in increasing the radiation intensity because, if the temperature T increases very much, it can negate the increase in v_L.

Another major solar-cell loss is the energy-spectrum loss. This is associated with the energy spectrum of the incident photons and the excitation energy of the semiconductor material. Any photon with an incident energy less than the excitation energy of the material cannot produce an ion pair and the photon energy is converted into thermal energy and lost. Those photons that have an energy in excess of the excitation energy will normally produce one ion pair and the excess energy will be converted into thermal energy, although the excess energy may help prevent some recombination of the ion pairs. For silicon solar cells, the excitation energy is 1.1 eV and the spectrum loss for solar radiation is about 50 percent.

There are a number of minor losses associated with operational solar cells, including the reflection of the photons, recombination of the ion pairs before they reach the junction, and also the loss due to Joule heating, particularly in the thin outer semiconductor layer. Taking into consideration all the losses, the maximum conversion efficiency of any solar cell is about 25 percent while the actual efficiency ranges between 15 and 20 percent.

Silicon is one material that is commonly used as the base material in solar cells because it gives one of the highest conversion efficiencies. The silicon is doped with phosphorus to produce the n-type semiconductor and it is doped with boron to produce the p-type semiconductor. A considerable amount of research has also been carried out on cadmium sulfide (CdS) cells, but while these systems are less expensive than the silicon cells, they have lower conversion efficiencies. Research has been carried out and is continuing on the following semiconductor materials: InP, GaAs, CdTe, AlSb, and CdSe.

Solar cells have a number of advantages over the other solar-energy conversion systems. They are simple and compact, and have a very high power-to-weight ratio. This makes them very attractive for space applications. Solar cells have no moving parts and probably yield the highest overall conversion of solar energy into electricity. Theoretically, solar cells have unlimited lives although, in practice, it is found that they actually suffer from radiation damage, particularly by the bombardment of high-energy charged particles such as electrons and protons in the Van Allen radiation belts surrounding the earth. The radiation damage in a silicon solar cell can be reduced by using n-on-n configuration

The major problem associated with solar cells is the high cost associated with the system fabrication. Actually, the principle of fabrication is relatively simple and the raw materials are inexpensive, but the actual production techniques are quite expensive. Recently, there have been some breakthroughs in fabrication methods that have reduced the costs. But the costs must be lowered much more if these systems are to become economically competitive with the other solar conversion systems.

A problem associated with any terrestrial solar conversion system is that it must be integrated with either an energy-storage system or with another type of conversion system to supply energy at night and on cloudy days. Earth-orbiting spacecraft also normally require an energy-storage system to supply energy when the spacecraft passes through the shadow of the earth. Storage batteries are commonly employed with low-powered solar-cell systems.

8.4.2 Solar-Cell Performance

The operation of the photoelectric cell is such that part of the current generated by the photoelectric effect, J_s, is shunted through the internal cell resistance if there is any load on the cell at all. That portion of the current density in the cell that goes through the external load is J_L, and is given by the following equation:

$$J_L = J_s - J \tag{8.67}$$

Substituting Eq. (8.66) into Eq. (8.67) for J gives

$$J_L = J_s - J_0\left[\exp\left(\frac{ev_L}{kT}\right) - 1\right] \tag{8.68}$$

If v_L is zero, the short-circuit condition, the exponential term in the last quantity approaches unity and $J_L = J_s$, the short-circuit current density.

The output power from the photovoltaic cell is

$$P = v_L J_L A \tag{8.69}$$

where A is the surface area of the cell. Substituting Eq. (8.68) into Eq. (8.69) gives

$$P = Av_L J_s - Av_L J_0\left[\exp\left(\frac{ev_L}{kT}\right) - 1\right] \tag{8.70}$$

Differentiating the above equation with respect to v_L and setting the derivative equal to zero gives the value of the external load voltage $v_{L,\max P}$, which gives the maximum cell output power. This gives the following relationship:

$$\exp\left(\frac{ev_{L,\max P}}{kT}\right) = \frac{1 + J_s/J_0}{1 + ev_{L,\max P}/kT} \tag{8.71}$$

If the short-circuit current density J_s and the reverse-saturation current density J_0 are known, the value of $v_{L,\max P}$ can be evaluated from Eq. (8.71) by trial and

error. The maximum power output of the cell is then equal to

$$P_{max} = \frac{A v_{L,max\,P}(J_0 + J_s)}{1 + kT/ev_{L,max\,P}} \tag{8.72}$$

If the energy flux incident on the cell is known, P_{in}/A, the conversion efficiency for the maximum power becomes

$$\eta_{max\,P} = \frac{P_{max}}{P_{in}} = \frac{A v_{L,max\,P}(J_0 + J_s)}{P_{in}(1 + kT/ev_{L,max\,P})} = \eta_{max} \tag{8.73}$$

Since the input energy flux to the cell is normally constant, the efficiency given by Eq. (8.73) is also the maximum possible conversion efficiency, as indicated. The value of J_s is a function of the incident photon flux.

Example 8.4. At a given intensity on a solar cell, the short-circuit current density is 180 A/m^2 and the reverse-saturation current density is 8×10^{-9} A/m^2. At a temperature of 27°C and the condition of maximum power, find the effective surface area needed for an output of 1000 W and also estimate the conversion efficiency if the radiation intensity is 930 W/m^2.

Solution. For the condition of maximum power output,

$$\exp\left(\frac{ev_{L,max\,P}}{kT}\right) = \frac{1 + J_s/J_0}{1 + ev_{L,max\,P}/kT}$$

$$= \exp\left(\frac{11{,}600\, v_{L,max\,P}}{300}\right) = \exp\,(38.67 v_{L,max\,P})$$

$$= \frac{1 + 180/8 \times 10^{-9}}{1 + 38.67 v_{L,max\,P}} = \frac{22.5 \times 10^9}{1 + 38.67 v_{L,max\,P}}$$

Solving for $v_{L,max\,P}$,

$$v_{L,max\,P} = \frac{1}{38.67} \ln\left(\frac{22.5 \times 10^9}{1 + 38.67 v_{L,max\,P}}\right)$$

$$v_{L,max\,P} \Rightarrow 0.3 \Rightarrow 0.5509 \Rightarrow 0.5361 \Rightarrow 0.5368 \Rightarrow 0.5368 \text{ V}$$

$$\frac{P_{max}}{A} = \frac{v_{L,max\,P}(J_0 + J_s)}{1 + kT/ev_{L,max\,P}}$$

$$= \frac{0.5368(180)}{1 + 300/(11{,}600)(0.5368)} = 92.177 \text{ W/m}^2$$

$$\text{Area of cell} = \frac{P_{out}}{P_{max}/A} = \frac{1000}{92.177} = 10.85 \text{ m}^2$$

$$\text{Conversion efficiency} = \frac{P_{max}/A}{P_{in}/A} = \frac{92.177}{930} = 0.097 = 9.7\%$$

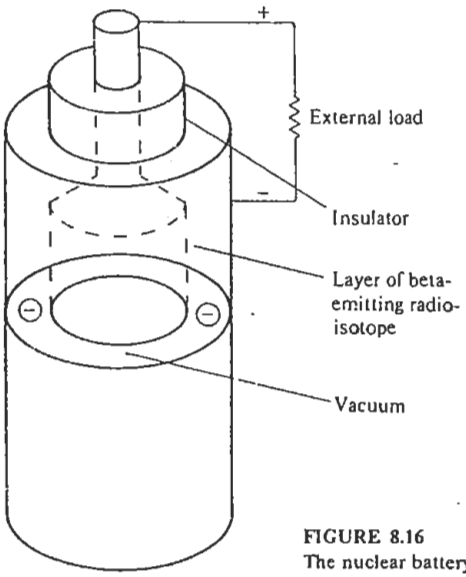


FIGURE 8.16
The nuclear battery.

8.5 CONVERSION OF NUCLEAR ENERGY INTO ELECTRICITY

There are no large-scale converters that transform nuclear energy directly into electrical energy. The nuclear battery, which is shown schematically in Fig. 8.16, consists of an inner electrode that is coated with a thin layer of an alpha- or beta-emitting radioisotope. Over half of the alpha particles or electrons emitted by the radioisotope travel across the vacuum gap and are absorbed by the outer case which serves as the other electrode. This system produces very high voltages (in the kilovolt range) but the current is normally in the micro-microampere range so that the system has very low power. The power output, like the radio-isotope, decays exponentially with time unless the resultant product is also radioactive.

It may be possible to produce electrical energy directly from the fusion reaction by using the interaction between the plasma and the magnetic-field containment system. This is particularly true for the mirror machines.

8.6 CONVERSION OF MECHANICAL ENERGY INTO ELECTRICITY

8.6.1 Electric Generators and Alternators

Almost all of the devices that convert mechanical energy into electrical energy depend on the Faraday effect for their principle of operation. According to the Faraday effect, a voltage gradient is produced in an electrical conductor that is

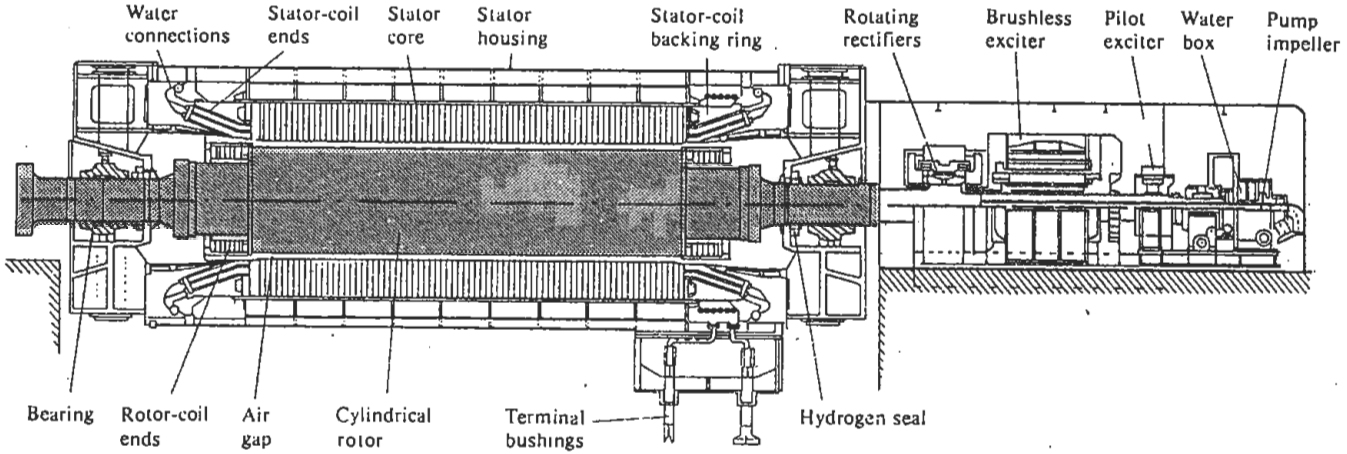


FIGURE 8.17
A conventional, large, a.c. generator (alternator). (*Courtesy of Allis-Chalmers Power Systems.*)

forced perpendicularly through a magnetic field. The induced voltage gradient dv/dx in the conductor is equal to the cross-vector product of the conductor velocity $\bar{V}_c$ and the magnetic field strength $\bar{B}$:

$$\frac{dv}{dx} = \bar{V}_c \times \bar{B} \tag{8.74}$$

where $\bar{V}_c$ is the conductor velocity, in meters per second, and $\bar{B}$ is the magnetic flux density, in webers/per square meter. If $\bar{V}_c$ is perpendicular to B, dv/dx is equal to the product $\bar{V}_c B$, but if $\bar{V}_c$ is parallel to $\bar{B}$, dv/dx is equal to zero.

Almost all of the electrical energy produced in the world comes from electrical generators or alternators. These systems obey the same basic laws as the electric motors. They normally have a conversion efficiency ranging from 50 percent for small generators to more than 90 percent for some of large commercial alternators. If a coil is rotated between the poles of an electromagnet or a permanent magnet, the output from the rotating coil will be either alternating current or direct current, depending on whether a slip ring (ac) or segmented (dc) commutator is employed. The ac output of an alternator can be converted into direct current with the use of rectifiers, as in the conventional automobile alternator.

The field windings of a conventional dc generator require a dc power supply and the generator can be "excited" in several ways. Some machines are separately excited from an external power source, such as a battery. Other dc generators are either shunt-excited, series-excited, or compound-excited. These machines are started from the small amount of residual magnetic flux present in them. The output voltage of these machines depends on the rotor speed and the number of field poles in the generator. There must be a set of brushes for each pair of field poles.

Alternating-current generators or alternators also require a dc power supply for the field winding. The dc power can be supplied from an external source but in most of the systems the dc supply is produced by a small dc generator connected to the alternator shaft. This small dc generator is called the *exciter*. In a large conventional alternator, the field winding is mounted on the rotor and the power is generated in the stator winding. This arrangement precludes the necessity of having to transfer the high-voltage output through brushes and slip ring commutators. A typical large alternator is shown in Fig. 8.17.

Almost all commercial power generated in the United States is 60-Hz, three-phase current and the angular velocity of the rotor field is

$$N_a = \frac{7200}{\not p} \tag{8.75}$$

where N_a is the angular velocity of the alternator, in revolutions per minute, and $\not p$ is the number of poles on the alternator rotor. Some other countries use systems that generate 50-Hz current. Care must be taken when connecting an alternator to an ac power grid to be sure that the alternator is in phase with the alternating

current in the grid at the instant of connection. If the alternator is not "synchronized" with the grid at the instant of connection, the grid will cause immediate acceleration or deceleration of the rotor and *severe* damage can result.

Almost all large alternators are cooled with hydrogen at pressures somewhat above atmospheric pressure. The use of hydrogen reduces the windage losses without losing cooling ability. In large machines, the hydrogen is pumped through the hollow conductors in the stator and armature. Some of the newer systems employ a water coolant in the stator windings. At high powers, the hydrogen pressure may be increased to facilitate the cooling process.

8.6.2 Fluiddynamic Converters

GENERAL. The fluiddynamic conversion systems transform the kinetic energy or the compressed fluid potential energy directly into electrical energy. There are two principal fluiddynamic generators—magnetohydrodynamic (MHD) and electrogasdynamic (EGD) converters. There are some other minor mechanical-electrical conversion systems such as the electrokinetic generator, the piezoelectric converter, and the fluid-drop electrostatic generator. The balance of this chapter deals with the MHD and the EGD conversion systems.

MAGNETOHYDRODYNAMIC GENERATORS. The magnetohydrodynamic generator depends on the Faraday effect for its principle of operation, just like the conventional mechanical-electrical generators. In MHD generators, an electrically conducting fluid is forced through a perpendicular magnetic field at high velocity, as shown in Fig. 8.18. In most MHD generators, the working fluid is an ionized gas, but liquid metals can also be employed. The MHD converter is usually proposed as a topping cycle or system for a conventional steam-power system

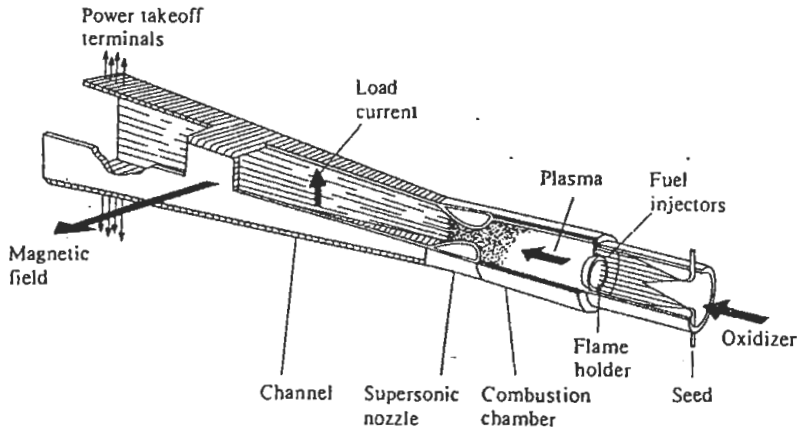


FIGURE 8.18
The magnetohydrodynamic (MHD) generator. (*From Proceedings of the American Power Conference, vol. 36, p. 585, Illinois Institute of Technology, Chicago, 1974.*)

to improve the overall thermal efficiency of the system. From Eq. (7.42), it can be shown that the combined conversion efficiency of such a system, $\eta_{overall}$, is

$$\eta_{overall} = \eta_{MHD} + \eta_{steam} - \eta_{MHD}\eta_{steam} \tag{8.76}$$

where η_{MHD} and η_{steam} are the individual conversion efficiencies of the MHD and the steam systems, respectively.

If the fluid velocity $\bar{V}_c$, and the magnetic-field strength $\bar{B}$ are constant in the interelectrode gap, Eq. (8.74) gives a generated voltage v_G of

$$v_G = \bar{V}_c B d \tag{8.77}$$

where d is the interelectrode gap width, in meters. If J is the current density, in amperes per square meter, the internal voltage drop is $iR_g = i\rho d/A = J\rho d$ and the external voltage drop from the unit is

$$v_L = v_G - J\rho d \tag{8.78}$$

where ρ is the average electrical resistivity of the MHD fluid, in ohmmeters. The ratio of the external load voltage to the generated voltage is defined as the loading factor K of the unit, or

$$K = \frac{v_L}{v_G} = \frac{v_L}{B\bar{V}_c d} \tag{8.79}$$

The generator current density is equal to the internal cell-voltage drop divided by the product of the interelectrode resistance and the electrode area:

$$J = \frac{i}{A} = \frac{(1/A)(v_G - v_L)}{\rho d/A} = \frac{(v_G - v_L)}{\rho d}$$

$$= \left(\frac{\bar{V}_c B}{\rho}\right)(1 - K) \tag{8.80}$$

The output power density, P/V, is the output electrical power of the MHD generator per unit volume of the generator. Thus, the power density is

$$\left(\frac{P}{V}\right)_{out} = \frac{v_L i}{Ad} = \frac{K v_G J}{d} = K\bar{V}_c B J = \frac{\bar{V}_c^2 B^2}{\rho}(K - K^2) \tag{8.81}$$

The maximum power density as a function of the loading factor K can be found by setting $d(P/V)_{out}/dK = 0$ and then solving for K. This gives an optimum value of K of $\frac{1}{2}$, which, in turn, gives a maximum power density of

$$\left(\frac{P}{V}\right)_{out,max} = \frac{\bar{V}_c^2 B^2}{4\rho} \tag{8.82}$$

The maximum conversion efficiency of an MHD converter is found by assuming that the only loss in the unit is the joule-heating power loss P_j. The loss per unit volume of converter is P_j/V, or

$$\frac{P_j}{V} = \frac{i^2 R_g}{Ad} = \frac{J^2 A^2 (d\rho/A)}{Ad} = J^2\rho = \frac{V_c^2 B^2}{\rho}(1 - K)^2 \tag{8.83}$$

and the conversion efficiency for maximum power density becomes

$$\eta = \frac{P_0}{P_0 + P_j} = \frac{1}{1 + P_j/P_0} = \frac{1}{1 + (1-K)/K} = K \tag{8.84}$$

and

$$\eta_{max} = K_{max} \tag{8.85}$$

For the maximum power density, $K_{max} = \frac{1}{2}$, and, for this condition, the maximum possible conversion efficiency is 50 percent.

Example 8.5. An MHD converter uses a combustion gas that is seeded with 1 percent potassium to decrease its electrical resistivity to $0.03\ \Omega \cdot \text{m}$. The magnetic field is uniform and perpendicular to the gas velocity and has a magnetic flux of $1.5\ \text{Wb/m}^2$. The system is designed for a gas velocity of 900 m/s and a loading factor of 0.55. If the width of the duct, d, is 0.25 m and the electrode area is $1.2\ \text{m}^2$, determine the output current, voltage, and power. Neglect the Hall effect and the other losses.

Solution

Total generated voltage $= v_G = \bar{V}_t Bd = 900(1.5)(0.25) = 337.5$ V

Voltage drop across load resistor $= v_L = Kv_G = 0.55(337.5) = 185.6$ V

$$\text{Current density} = J = \frac{v_g - v_L}{\rho d} = \frac{337.5 - 185.6}{(0.03)(0.25)}$$

$$= 20{,}250\ \text{A/m}^2$$

Output current $= i = AJ = 1.2(20{,}250) = 24{,}300$ A

Output power $= iv_L = 24{,}300(185.6) = 4.51 \times 10^6\ \text{W}_e = 4.51\ \text{MW}_e$

The MHD generator has a number of other losses besides the joule-heating loss. The Hall-effect loss is the loss caused by the Lorentz force acting on the electrons in the interelectrode gap. When any charged particle passes through a perpendicular magnetic field, it is acted on by a force called the *Lorentz force*, F_L. For an electron, this force makes the electron travel in a circular arc and its magnitude is

$$F_L = e\bar{V} \times \bar{B} \tag{8.86}$$

This means that all the electrons try to travel to one end of the collecting electrode, which produces very large currents in the collecting electrode with the accompanying resistance loss. One possible solution to this problem is to use an insulated, segmented, collecting electrode, similar to that shown schematically in Fig. 8.19. The problem with the segmented electrode is that each segment must be isolated and loaded independently, as shown in the figure.

The end loss in an MHD generator is associated with the reverse flow (short circuit) of electrons through the conducting fluid around the ends of the magnetic field. It can be reduced by increasing the aspect ratio (L/d) of the generator, by permitting the magnetic field poles to extend beyond the end of the electrodes,

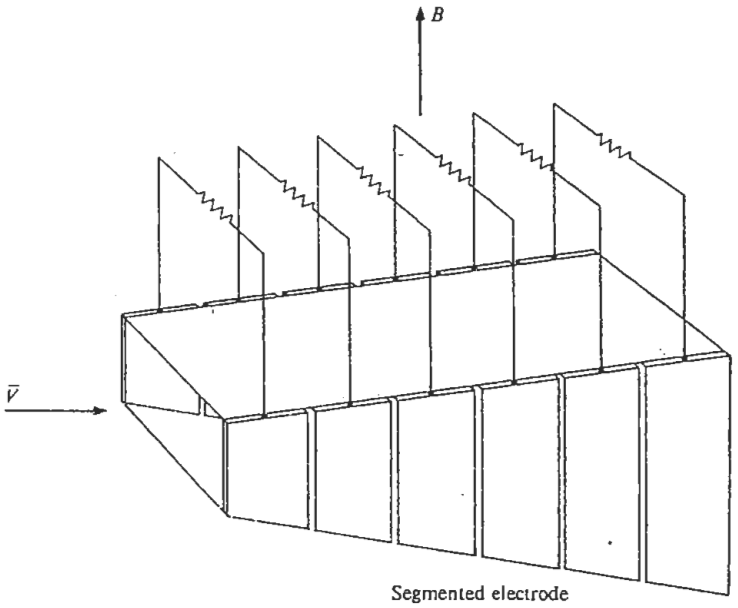


FIGURE 8.19
A MHD generator with segmented electrodes. (*From Walsh, 1967.*)

and/or by using insulated vanes in the fluid duct in the inlet and outlet of the generator.

The MHD system also experiences high friction and heat-transfer losses. The fluid flow is highly turbulent through the device and the friction loss may be as high as 12 percent of the input. The high fluid turbulence also increases the convection heat-transfer rate from the gas or liquid metal to the containment walls.

Another loss that can be very important in an ionized-gas or plasma converter is the electrode loss. These systems must operate at extremely high temperatures in order to obtain a high electrical conductivity. Since the electrodes must be relatively cool, the gas in the vicinity of the electrodes must be much cooler than the average gas. This significantly increases the fluid resistivity next to the electrodes, resulting in a very large voltage drop across the gas film.

TYPES OF MHD CONVERTERS. The plasma converter employs an ionized gas as the working fluid. The major problem associated with this system is that it is difficult to find a working fluid that can be ionized at a reasonable temperature. Gases at 2000 K (4060°F) have too high a value of electrical resistivity ρ to serve as a satisfactory working fluid in an MHD converter. Even at the maximum adiabatic flame temperature from combustion of 3000 K (5860°F), the normal combustion products still have too high an electrical resistivity for MHD operation.

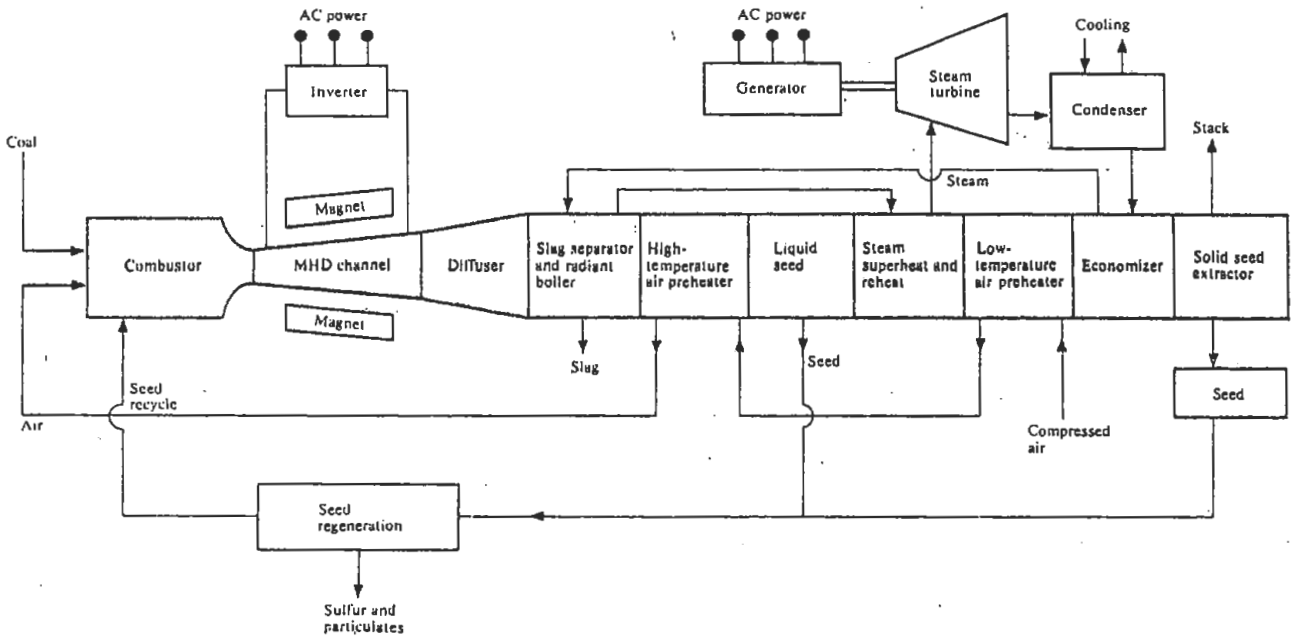


FIGURE 8.20
A proposed open-cycle MHD-steam binary power system. (*From Angrist, 1976.*)

Most of the research on the plasma converter has been concerned with the use of an additive or "seed" material to the combustion products which will ionize easily. The seed material should have a low ionization potential and should be easily recovered from the exhaust gases. The addition of 1% potassium by volume decreases the resistivity of the gas from $5\,\Omega \cdot m$ at 2200 K (3960°R) to about $1\,\Omega \cdot m$ and the resistivity decreases further to $0.11\,\Omega \cdot m$ at 3000°K (5400°R).

It may also be possible to decrease the gas resistivity by using a glow discharge or by subjecting the gas to ionizing radiation. Research has been conducted into the possibility of passing a hypersonic gas stream through a series of shock waves in the converter to increase the conductivity of the gas. A highly conducting region of ionized gas normally occurs in the region immediately behind a shock wave.

A schematic diagram of a possible power system employing a plasma converter is shown in Fig. 8.20. As mentioned earlier, the MHD converter is normally designed to be a topping power system to a conventional steam power plant. It has been estimated that such a topping system could increase the overall conversion efficiency from around 40 to about 55 percent. The system shown in Fig. 8.20 is classed as open because the main MHD working fluid is not recirculated. If coal is used as the source of thermal energy in this device, the electrodes may be short-circuited by the molten ash. Consequently, oil and natural gas are considered to be much better fuels.

Liquid-metal MHD converters are closed systems that must operate at much lower temperatures than plasma converters. High temperatures are not required in them to achieve a low value of electrical resistivity, and they are normally designed to operate at temperatures below 1400 K. This temperature is low enough that the energy can be supplied by a nuclear reactor as well as a fossil-fueled system. A possible liquid-metal system, using either potassium or cesium as the working fluid, as shown in Fig. 8.21.

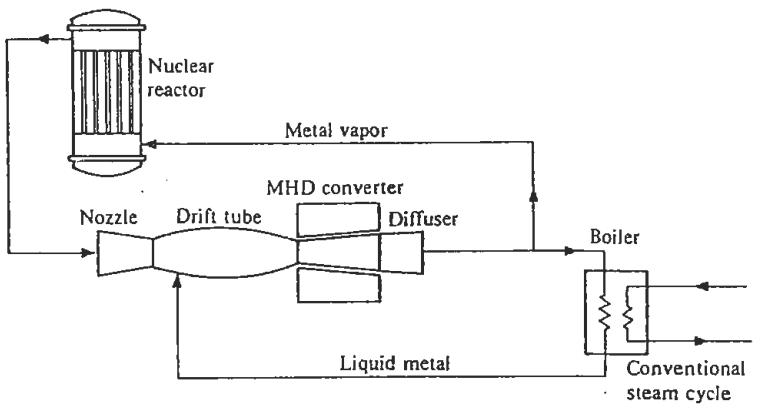


FIGURE 8.21
The proposed liquid-metal MHD-steam binary power system. (*From Walsh, 1967.*)

The main problem associated with liquid MHD conversion systems is that it is much more difficult to achieve a high fluid velocity in the converter. In the system shown in Fig. 8.20, superheated metallic vapor is expanded through a supersonic nozzle into the drift tube or mixer. Atomized subcooled liquid droplets are injected in the high-velocity vapor and are accelerated by the vapor. The vapor also condenses on the liquid droplets so that the fluid entering the generator is essentially a liquid. The resulting fluid velocity is in excess of 150 m/s.

At temperatures below 1400 K (2520°R), it is anticipated that this system could increase the thermal efficiency of a steam-power system by 6 percent. The maximum overall thermal efficiencies are expected to be around 55 percent.

The liquid-metal MHD converter has several advantages over the gas-plasma MHD system. It can utilize nuclear energy since it does not require the high temperatures of the plasma system. The liquid-metal MHD converter can easily produce ac power directly, while this is almost impossible to do in a plasma system. The power density of the liquid-metal system is around an order of magnitude higher than that of a plasma generator and this significantly reduces the size of the system, including that of the magnets. The magnet cost is a major expense associated with these systems.

The primary advantage of the plasma converter is that it is much easier to achieve a high fluid velocity using a gas and a nozzle. Because of the high gas resistivity, the plasma converter can produce relatively high dc voltages, which is difficult to do in the liquid system. It is generally agreed that the plasma generator can produce higher overall conversion efficiencies than the liquid-metal system.

ELECTROSTATIC MECHANICAL GENERATORS. The electrostatic mechanical generators convert gravitational and compressed-fluid mechanical energy of a fluid directly into electrical energy. This is done by transferring electrons from one electrode to another as in the Van de Graff accelerator. In this device, electrons are transferred from one electrode to another by means of an insulated belt. The operation of some of the fluiddynamic machines is the same except that the electrons are transferred by means of a fluid driven by gravity or compressed fluid energy. All of these devices are characterized by low currents and high voltages.

The liquid-drop electrostatic generator converts the gravitational potential energy of water droplets directly into electrical energy. A schematic diagram of this system is presented in Fig. 8.22. While this device makes an interesting laboratory demonstration, it is not used for the large-scale production of electricity as it cannot compete with the conventional hydroelectric generator.

The electrogasdynamic (EGD) converter is the only converter of this general type that shows possible promise for the large-scale production of electricity. The EGD generator uses the potential energy of a compressed gas to carry electrons from a low-potential electrode to a high-potential electrode, thereby doing work against an electric field. Thus, the potential energy is converted

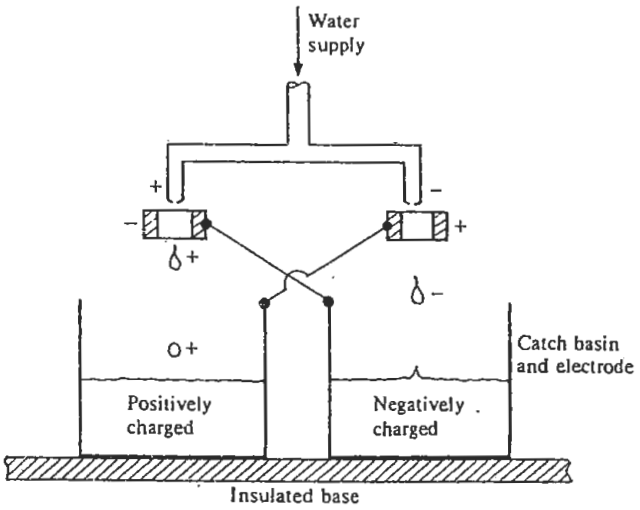


FIGURE 8.22
The liquid-drop electrostatic generator.

In the EGD converter, electrons are generated at the entrance of the EGD duct by some means such as a corona electrode. The ionized-gas particles are carried down the duct along with the neutral atoms. The ionized particles are neutralized by a collector electrode at the end of the insulated duct. The working fluid for these systems is commonly either combustion gases produced by burning fuel at high pressure or a pressurized reactor gas coolant.

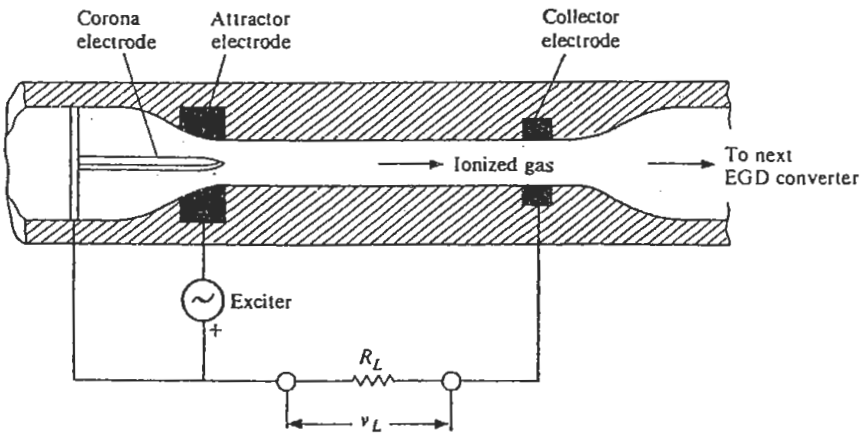


FIGURE 8.23
A typical gas duct in an electrogasdynamic (EGD) converter. (*From Walsh, 1967.*)

EGD PERFORMANCE. In the ideal EGD generator, the only major pressure loss is the friction pressure drop Δp_f, in kPa:

$$\Delta p_f = \frac{C_f \bar{V}^2 L \rho}{2D} \tag{8.87}$$

where $\bar{V}$ is the gas velocity, in meters per second, L is the duct length, in meters, D is the duct diameter, in meters, ρ is the gas density, in kilograms per cubic meter, and C_f is the friction factor. The pressure drop due to the voltage gradient, Δp_e, in kPa, is

$$\Delta p_e = E_x n_p e L \tag{8.88}$$

where e is the charge of an electron in coulombs, n_p is the average ion density in the duct, in ions per cubic meter, and E_x is the constant electric field in the axial direction, in volts per meter. The product $n_p e$ is equal to $4E_r\varepsilon_0/d$, where E_r is the radial electric field in volts per meter, and ε_0 is the permitivity of free space, or a constant of 8.85×10^{-12} C/N. The maximum value of Δp_e occurs when $E_x = E_r = E_b$, where E_b is the limiting or breakdown voltage gradient of the gas:

$$\Delta p_{e,\max} = \frac{4\varepsilon_0 E_b^2 L}{D} \tag{8.89}$$

The conversion efficiency of the EGD converter is approximately equal to the ratio of the pressure drops. The output power is proportional to Δp_e, while the total input power is proportional to the total pressure drop $\Delta p_e + \Delta p_f$. Thus, the maximum conversion efficiency is

$$\eta_{\max} = \frac{\Delta p_{e,\max}}{\Delta p_{e,\max} + \Delta p_f} = \frac{1}{1 + \Delta p_f / \Delta p_{e,\max}}$$

$$= \frac{1}{1 + C_f V^2 \rho / 8\varepsilon_0 E_b^2} \tag{8.90}$$

The maximum power density in the gas volume $(P/V)_{\max}$ in the EGD generator is

$$\left(\frac{P}{V}\right)_{\max} = \frac{i_{\max} v_{L,\max}}{AL} \tag{8.91}$$

where A is the cross-sectional area of the gas duct. The current flow i in the system is equal to the rate of charge flow in the system:

$$i = n_{p,\max} e \bar{V} A = \pi \varepsilon_0 E_{r,\max} \bar{V} d = \pi \varepsilon_0 E_b \bar{V} d \tag{8.92}$$

The maximum external load voltage is

$$v_{L,\max} = E_{x,\max} L = E_b L \tag{8.93}$$

Most EGD converters have relatively low maximum power outputs of 10 to 30 W per channel. They usually have several hundred channels connected in series and parallel combinations. These systems are normally very-high-voltage

systems with output voltages of 10,000 to 200,000 V. Because of the high voltages generated, these machines need reliable high-voltage insulation for both the ducts and the electrode leads. The material commonly proposed is beryllium oxide (BeO).

COMPARISON OF FLUIDDYNAMIC CONVERTERS. The EGD systems potentially offer a number of advantages over MHD systems. EGD converters operates at relatively low temperatures and there is no need to inject seed material into the working fluid. They are also self-contained in that they do not require a bottoming steam system or any condenser cooling water. Although the EGD systems are still under development, it is anticipated that the overall conversion efficiency of an EGD combined system could approach that of a MHD-steam system.

EGD systems also have a number of difficult problems that must be solved before they can be used as large-scale generators of electricity. It is difficult to find a constant source of high-pressure nonconducting gas using thermal energy. There is also a major problem associated with finding structural material for these systems. Because of these problems the systems have not seen large-scale utilization.

Of all the so-called direct-energy converters, including thermoelectrics, thermionics, solar cells, fuel cells, and the MHD and EGD converters, the MHD converter and possibly the fuel or solar cell offer the best hope for a solution to the search for a high-efficiency, large-capacity system for the production of low-cost electricity.

LIST OF SYMBOLS

A	Cross-sectional area of EGD duct, m^2 (ft^2)
A	Cross-sectional area of MHD electrode, m^2 (ft^2)
A_c	Cathode or conductor cross-sectional area, m^2 (ft^2)
A_n	Cross-sectional area of n leg of n-p semiconductor, m^2 (ft^2)
A_p	Cross-sectional area of p leg of n-p semiconductor, m^2 (ft^2)
B or $\bar{B}$	Magnetic field strength, Wb/m^2
C_f	Friction factor for fluid pressure drop
d	Width of MHD duct, m (ft)
D	Equivalent diameter of EGD duct, m (ft)
e	Charge of an electron = 1.602×10^{-19} C
E_a	Sum of anode work function and charge barrier energy, eV
E_b	Breakdown voltage gradient of a material, V/m (v/ft)
E_c	Sum of cathode work function and charge barrier energy, eV
E_g	Internal voltage of a fuel cell, V
E_G	Excitation energy of solar cell material, eV
E_o	Open-circuit output voltage of thermionic converter, V
E_r	Radial voltage gradient, V/m (v/ft)
E_x	Voltage gradient in an electrostatic field, V/m

F_y	Charge per kg-mole of electrons ≡ 1 F = 9.649×10^7 C/kg · mol of electrons
G	Gibbs free energy, J
ΔG	Change in Gibbs free energy for a chemical reaction, J/kg · mole
H	Enthalpy or enthalpy of formation, J
ΔH	Change in the enthalpy of formation for a chemical reaction, J/kg · mole
HHV	Higher heating value of a fuel, kJ/kg (Btu/16m)
i	Electric current, A
J	Current density, A/m^2
J_L	Current density to the external load, A/m^2
J_0	Net current density, A/m^2
J_s	Current density through the solar cell, A/m^2
k	Boltzmann's constant, = 0.0001551 eV/K
k	Thermal conductivity of a material, W/m · C° (Btu/h · ft · F°)
k_n	Thermal conductivity of n-semiconductor material, W/m · C° (Btu/h · ft · F°)
k_p	Thermal conductivity of p-semiconductor material, W/m · C° (Btu/h · ft · F°)
K	Loading factor for MHD generator ≡ v_L/v_g
K_g	Thermal conductance of thermoelectric generator, W/C° (Btu/h · F°)
K_n	Thermal conductance of n-leg of generator, W/C° (Btu/h · F°)
K_p	Thermal conductance of p-leg of generator, W/C° (Btu/h · F°)
L	Length, m
L_n	Length of n-semiconductor leg, m (ft)
L_p	Length of p-semiconductor leg, m (ft)
L_w	Length of connecting wire, m (ft)
m	Number of pairs of n-p semiconductors in generator
M	Ratio of load to generator resistance ≡ R_L/R_g
n_p	Ion density, ions/m^3
N	Parameter used in thermoelectric generator equations
N_a	Angular velocity of alternator rotor, r/min
p	Absolute pressure, kPa (psi)
p^0	Absolute reference pressure of one atmosphere = 101.3 kPa (14.7 psi)
Δp	Pressure difference, kPa (psi)
Δp_{el}	Pressure drop caused by the transfer of ions, kPa (psi)
Δp_f	Pressure drop caused by fluid friction, kPa (psi)
P	Power, W
P_{in}	Input power, W
P_{max}	Maximum output power of system, W
P_{out}	Output power, W
P_r	Power radiated from thermionic cathode to anode, W
P_w	Power loss due to lead-in wire resistance, W
Q	Heat-transfer rate, W (Btu/h)
Q_s	Heat-transfer rate to the system, W (Btu/h)

R_g	Total generator resistance, Ω
R_i	Internal resistance of fuel cell, Ω
R_L	Resistance of external load resistor, Ω
R_n	Resistance of n leg of n-p generator, Ω
R_p	Resistance of p leg of n-p generator, Ω
R_t	Total resistance of circuit, Ω
S	Total entropy, J/K (Btu/°R)
ΔS	Change in total entropy, J/K (Btu/°R)
S	Seebeck coefficient, V/K
S_n	Seebeck coefficient for n-type semiconductor, V/K
S_{np}	Combined Seebeck coefficient for n-p semiconductor junction, V/K
S_p	Seebeck coefficient for p-type semiconductor, V/K
T	Absolute temperature, K (°R)
T_H	Maximum absolute temperature of system, K (°R)
T_L	Minimum absolute temperature of system, K (°R)
ΔT	Temperature difference, K or C° (F° or R°)
v	Electrical potential, V
v_g	Voltage drop across generator, V
v_G	Voltage generated in MHD generator, V
v_L	Voltage drop across external load resistor, V
v_t	Total voltage drop in circuit, V
$\bar{V}$	Velocity of fluid, m/s (ft/s)
$\bar{V}_c$	Velocity of electrical conductor, m/s (ft/s)
W_e	Electrical work (energy), J
Z	Figure of merit of thermoelectric (TE) generator, 1/K
Z_{max}	Maximum figure of merit of TE generator, 1/K
β	Coefficient of performance of TE refrigerator
ε_0	Permitivity of free space = 8.854×10^{-12} F/m
ε_a	Emissivity of anode surface
ε_c	Emissivity of cathode surface
η	Conversion efficiency of system
η_{th}	Thermal efficiency of system
θ	Activity of a component in a chemical reaction
ξ	Thermionic emission constant, $A/m^2 \cdot K^2$
π	Peltier coefficient, W/A
ρ	Electrical resistivity of a material, Ω · m
ρ_n	Electrical resistivity of n-semiconductor material, Ω · m
ρ_n	Electrical resistivity of p-semiconductor material, Ω · m
σ	Stefan-Boltzmann's constant = 5.670×10^{-8} W/m^2 · K^4 = 0.1714×10^{8} Btu/h · ft^2 − °R^4
τ	Thomson coefficient, V/K
ϕ	Work function or space-charge-barrier energy, eV
ϕ_a	Work function energy of anode, eV
ϕ_c	Work function energy of cathode, eV
$\phi_{b,c}$	Space-charge-barrier energy of the cathode, eV

PROBLEMS

8.1. The properties for an *n-p* semiconductor thermoelectric generator are as follows:

Properties	Material	
	n type	*p* type
Seebeck coefficient, S, μV/K	$S_n = -104 - 0.35T$	$S_p = 440 - 0.55T$
Electrical resistivity, $\Omega \cdot$ m	$\rho_n = 8 \times 10^{-6}$	$\rho_p = 3.5 \times 10^{-5}$
Thermal conductivity, W/m · K	$k_n = 1.32$	$k_p = 1.55$

where T is the temperature in K. If the converter operates between [100; 110; 120; 130; 140]°C and [400; 420; 440; 460; 480]°C, find the average Seebeck coefficient, the average Peltier coefficient, and the average Thomson coefficient. Also, find the maximum figure of merit for the converter.

8.2. For the system described in Prob. 8.1, find:
- (*a*) The value of the resistance ratio M_{opt} that give the maximum thermal efficiency
- (*b*) The optimum value of the ratio of A/L for the *n* material if the A/L ratio for the *p* material is 1.2 cm
- (*c*) The value of the electrical resistance R_g/m and the thermal conductance K_g/m for the generator
- (*d*) The number of element pairs needed to produce 100 W of dc power at the maximum thermal efficiency
- (*e*) The maximum power output of the converter from part (*d*)
- (*f*) The thermal efficiencies for parts (*d*) and (*e*)

8.3. A thermoelectric generator operates between [200; 215; 230; 245; 260]°C and 550°C. The average value of the Seebeck coefficient is [400; 425; 450; 475; 500] $\times 10^{-6}$ V/K, the generator resistance is 0.004 Ω, and the thermal conductance is 0.035 W/K for each *n-p* junction. Find the open-circuit voltage, the maximum power output, and the thermal efficiency for maximum power output if there are 100 *n-p* junctions.

8.4. Using the Richardson-Dushman equation, determine the current from a 2-cm^2 electrode in a vacuum at [1800; 1900; 2000; 2100; 2200] K if the electrode is constructed of strontium oxide (SrO) and the space-charge-barrier potential is zero. Also evaluate the current if there is a space-charge-barrier potential of [0.1; 0.2; 0.3; 0.4; 0.5] eV.

8.5. A thoriated-tungsten emitter is supposed to supply [4; 6; 8; 10; 12] A/cm^2 when the space-charge-barrier energy is [0.08; 0.10; 0.12; 0.14; 0.16] eV. Determine the emitter temperature, in °C.

8.6. Consider a thermionic vacuum diode with a cathode and anode having a surface area of 10 cm^2. The emitter is constructed of strontium oxide (SrO) and the collector is constructed of barium oxide. The space-charge-barrier energy for the emitter is [0.15; 0.16; 0.17; 0.18; 0.19] eV and the collector (anode) barrier energy is 0.11 eV. The emitter is maintained at a temperature of [1800; 1900; 2000; 2100; 2200] K. Find the output current and power of the device and estimate the thermal efficiency if the emissivities of all surfaces are 0.15. Neglect the conduction loss through the lead-in wire.

8.7. Calculate the higher and lower heating values (HHV and LHV), in Btu/lbm, for the combustion of [hydrogen; carbon monoxide] at [1.0; 1.2; 1.4; 1.6; 1.8] atm and [25; 50; 75; 100; 125]°C, using the enthalpies of formation from Table 8.3. Assume that oxygen is supplied by air at 1 atm and that the reaction products are also at 1 atm.

8.8. Calculate the maximum possible conversion efficiency of the system selected in Prob. 8.7.

8.9. Determine the maximum internal cell voltage of a hydrogen-oxygen fuel cell and of a carbon monoxide-oxygen fuel cell operating at [100; 200; 300; 400; 500]°C. Assume that the oxygen is supplied at 2 atm, the reactant gases supplied at [1.2; 1.4; 1.6; 1.8; 2.0] atm, and the products are at 1.1 atm.

8.10. A 2-cm^2 solar cell at 30°C has an output voltage of [0.3; 0.4; 0.5; 0.6; 0.7] V at maximum power. If the reverse-saturation current density is [0.2; 0.4; 0.6; 0.8; 1.0] $\times 10^{-7}$ A/m^2, find the output power of the cell.

8.11. The reverse-saturation current i_0 of a solar cell at 35°C is [1.0; 1.2; 1.4; 1.6; 1.8] $\times 10^{-7}$ A and the short-circuit current is [4; 5; 6; 7; 8] A when it is exposed to sunlight. Calculate the power output of the cell.

8.12. If the conversion efficiency of a topping MHD converter is [18; 20; 22; 24; 26] percent and the thermal efficiency of the bottoming steam plant is [32; 34; 36; 38; 40] percent, find the overall conversion efficiency of the binary system.

8.13. If the combined thermal efficiency of an MHD steam-power system is [50; 52; 54; 56; 58] percent and that of the steam cycle is [36; 37; 38; 39; 40] percent, find the conversion efficiency of the MHD system.

8.14. An MHD converter uses a seeded combustion gas with an electrical resistivity of [0.024; 0.026; 0.028; 0.030; 0.032] $\Omega \cdot$ m and a velocity of [800; 900; 1000; 1100; 1200] m/s. The spacing between two 0.75-m^2 electrodes is 0.35 m and the magnetic field density is 2.2 Wb/m^2. If the external load has a resistance of 0.015 Ω, find the output voltage, current, and power.

8.15. The following parameters are picked for a MHD plasma converter:

$$\bar{B} = [1.4;\ 1.6;\ 1.8;\ 2.0;\ 2.2]\ \text{Wb/m}^2$$

$$\bar{V} = [900;\ 1000;\ 1100;\ 1200;\ 1300]\ \text{m/s}$$

$$A = 0.6\ \text{m}^2 \qquad d = 0.25\ \text{m} \qquad \rho = 0.028\ \Omega \cdot \text{m}$$

For an output voltage of 250 V, find the output current and power, the external load resistance, and the conversion efficiency.

REFERENCES

Angrist, S. W.: *Direct Energy Conversion*, 3d ed., Allyn and Bacon, Boston, 1976.

Berger, C. (ed.): *Handbook of Fuel Cell Technology*, Prentice-Hall, Englewood Cliffs, N.J., 1968.

Cowan, P. L., M. C. Gourdine, and D. H. Malcolm: *EGD Power Generation*, Institute of Electrical and Electronics, Power Group, February 1968.

Currin, C. G., et al.: "Feasibility of Low-Cost Silicon Solar Cells," *Conference Record of the Ninth IEEE Photovoltaic Specialists Conference*, pp. 363–369, IEEE, New York, 1972. *Encyclopedia of Energy*, McGraw-Hill, New York, 1976.

Gietzen, A. J., and W. G. Hohmeyer: "Thermionic Reactor Power Systems," *Proceedings Seventh Intersociety Energy Conversion Engineering Conference*, American Chemical Society, Washington, D.C., 1972.

Harris, C. J.: "MHD Augmented Shock Tunnel Experiments with Unseeded High Density Air Flows," *AIAA J.* vol. 13, no. 2, pp. 229–231, February 1975.

Harris, L. P., and G. E. Moore: "Combustion-MHD Power Generation for Central Stations," General Electric Report No. 70-C-388, November 1970.

Kettani, M. A.: *Direct Energy Conversion*, Addison-Wesley Publishing Company, Reading, Mass., 1970.

Makansi, J.: "Several Developments in Fuel-Cell Technology," *Power*, vol. 133, no. 5, pp. 86–87, May 1989.

Needrach, L. W., W. T. Grubb, and A. Fickett: "The Current Status of Ion Exchange Membrane Fuel Cells," General Electric Report No. 71-C-303, October 1971.

Russell, C. R.: *Elements of Energy Conversion*, Pergamon Press, Long Island City, N.Y., 1967.

Smith, A.: "Status of Photovoltaic Power Technology," *J. Eng. Power, Trans. Amer. Soc. Mech. Eng.*, series A, vol. 91, pp. 1–12, 1969.

Soo, S. L.: *Direct Energy Conversion*, Prentice-Hall, Englewood Cliffs, N.J., 1968.

Walsh, E. M.: *Energy Conversion*, The Ronald Press, New York, 1967.

Weller, A. E., and W. T. Reid: "The Economic Position of MHD for Central Power," ASME Paper 64 WA/ENER-1, September 1964.

Westinghouse Electric Corporation: *1970 Final Report Project Fuel Cell: Research and Development Report 57*, U.S. Government Printing Office, Washington, DC., 1970.

Wood, B. D.: *Applications of Thermodynamics*, Addison-Wesley Publishing Company, Reading, Mass., 1969.

CHAPTER 9

ENERGY STORAGE

9.1 INTRODUCTION

All six of the major energy classifications can be stored in some form of that general energy classification except electromagnetic energy, which is purely a transitional energy form. Mechanical energy can be stored as some form of potential energy—kinetic, gravitational-potential, elastic-strain, compressed-fluid, and/or magnetic-field energy. Electrical energy can be stored as either inductive-field or as electrostatic-field energy. Chemical energy and nuclear energy, two of the six major energy classifications, are actually pure forms of stored energy. Thermal energy can be stored as either latent heat and/or sensible heat addition.

Energy storage is very important and even essential in many power-generating systems. Terrestrial-solar-energy power systems require either an energy-storage system or an alternative source of energy to supply energy when there is insufficient sunlight. Energy-storage systems are also very useful to companies that generate electricity, providing the stored energy can be easily and efficiently converted back to electrical energy. With such a storage system, it becomes feasible to produce and store electrical energy during times of low power demand, such as late at night and on weekends. The stored energy is then recovered during times of peak power demand. This stored energy can be produced from the coal-fired and nuclear-powered base-loaded units with their low fuel costs. This not only increases the average-to-maximum power ratio (the capacity factor) for the base-loaded systems, reducing their capital costs, but it also reduces the need for the peaking units with their correspondingly high fuel costs.

TABLE 9.1
Specific energy storage of various materials (all values in kJ/kg)†

Deuterium (D-D fusion reaction)	3.3×10^{11}	Silver oxide-zinc battery	437
Uranium-235 (fission reaction)	7.0×10^{10}	Lead-acid battery	119
Heavy water (fusion reaction)	3.5×10^{10}	Flywheel (uniformly stressed disc)	79
Reactor fuel (2.5% enriched UO_2)	1.5×10^{9}		
Natural uranium	5.0×10^{8}	Compressed gas (spherical container)	71
95% Po-210 (radioactive decay)	2.5×10^{6}		
80% Pu-238 (radioactive decay)	1.8×10^{6}	Flywheel (cylindrical)	56
Hydrogen (LHV)	1.2×10^{5}	Organic elastomer	20
Methane (LHV)	5.0×10^{4}	Flywheel (rim-arm)	7
Gasoline (LHV)	4.4×10^{4}	Torsion spring	0.24
Lithium hydride (at 700°C)	3.8×10^{3}	Coil spring	0.16
Falling water ($\Delta z = 100$ m)	9.8×10^{2}	Capacitor	0.016

† 1 kJ/kg = 0.43 Btu/lbm.

Several things must be considered in the selection, design, and operation of any energy-storage system. First, what is its overall efficiency? This includes the charging process, the storage loss, and the recovery process. Second, what is the energy-storage density, in kilojoules per cubic meter or Btu per cubic foot, and/or the specific energy storage, in kilojoules per kilogram or Btu per pound-mass? Third, what are the maximum allowable charge and discharge rates in the storage medium and how do they affect the efficiencies? Fourth, what are the economics of the storage system, including capital and operating costs? Fifth, what are the environmental and political problems associated with the energy units? Finally, how many times can the system be cycled and how does that affect the system's efficiency?

The specific energy storage in kilojoules per kilogram for a number of different materials and systems is given in Table 9.1.

9.2 STORAGE OF MECHANICAL ENERGY

9.2.1 Kinetic Energy Storage

Mechanical energy storage is associated with a substance's position in a force field. There are at least five possible force fields—inertial (kinetic energy), gravitational, elastic-strain, compressed-fluid, and magnetic field. Kinetic energy is mechanical energy that is associated with the movement of one mass relative to another. For a linear velocity, the kinetic energy (KE) of a given body, in joules, is

$$\mathrm{KE} = \frac{m\bar{V}^2}{2} \tag{9.1}$$

where m is the mass, in kilograms, and $\bar{V}$ is the linear velocity, in meters per second. Kinetic energy can also be stored in a rotating wheel, commonly called

a *flywheel.* The kinetic energy associated with a wheel rim of mass m kg, rotating at an angular velocity of ω rad/s at a radius of R meters, is

$$\text{KE} = \frac{mR^2\omega^2}{2} = 2\pi^2 mR^2 N^2 \tag{9.2}$$

where N is the angular velocity of the flywheel, in revolutions per second. For a given flywheel, $\int_0^R r^2\,dm$ is called the *moment of inertia* I, and Eq. (9.2) reduces to the more general form of

$$\text{KE} = \frac{I\omega^2}{2} = 2\pi^2 N^2 I \tag{9.3}$$

For a thin-rimmed flywheel with all the mass in the rim, the relationship between the trangential stress σ in the wheel, the angular velocity ω, and the radius R is

$$\sigma = \omega^2 R^2 \rho \tag{9.4}$$

where ρ is the density of the material in kilograms per cubic meter. Substituting this into Eq. (9.2) gives

$$\text{KE} = \frac{m\sigma}{2\rho} \tag{9.5}$$

The specific energy storage in the flywheel is the energy per unit mass. For a thin-rimmed flywheel, the specific energy is

$$\text{Specific energy} = \frac{\text{KE}}{m} = \frac{\sigma}{2\rho} \tag{9.6}$$

This equation is commonly written as

$$\text{Specific energy} = K_w \frac{\sigma}{\rho} \tag{9.7}$$

where K_w is the flywheel weight factor and ranges from approximately 1.0 for constant-stress discs to 0.5 for a thin-rimmed flywheel.

In order to compare flywheels, it is common practice to evaluate the maximum stored kinetic energy in the wheel per unit volume of a uniform disc having axial and radial dimensions equal to the maximum width and radius of the given wheel. This energy ratio is usually expressed as

$$\left(\frac{\text{KE}}{V}\right)_{\text{max}} = K_v \sigma \tag{9.8}$$

where K_v is equal to the product of K_w and the fraction of the uniform disc occupied by the given flywheel. The values of K_w and K_v for some high-performance flywheels are shown in Fig. 9.1.

It can be seen from Eq. (9.5) that in order to achieve high energy storage in a flywheel, the materials should have a high mechanical strength and a low

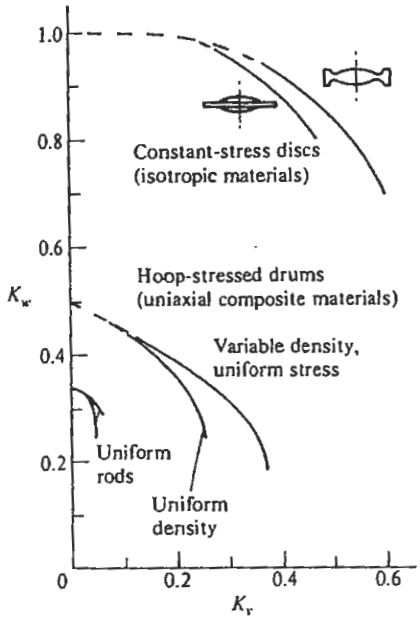


FIGURE 9.1
The relationship between K_w and K_v for some high-performance flywheels. (*From Fullman, 1975.*)

density. The low density permits operation at high angular velocities or with a larger radius before the centrifugal force tears the wheel apart. Fiber composites, which were developed originally for the aerospace program, appear to have much higher storage capability than the conventional steel systems. Moreover, these materials are less expensive than steel. Some possible materials for flywheels are listed in Table 9.2.

Flywheels have been proposed as alternative energy systems for the mechanical-energy storage systems for the production of electricity and also as possible propulsion systems for automobiles and buses. The flywheel systems can normally accept and give up power at much higher rates than some of the more conventional energy-storage systems, such as the storage battery.

9.2.2 Elastic-Strain Energy Storage

The elastic-strain energy-storage systems are among the oldest forms of energy storage. These systems include the compression of springs and the twisting of torsion bars, etc. Most of these systems have relatively low storage capability and are used to power clocks, watches, toys, and other systems where small, compact storage systems are required.

One of the common elastic-strain-energy methods is achieved in the compression of springs. The energy stored in a spring is equal to $\int_0^x K_s x'\,dx'$, where K_s is the spring constant. If the spring is a "linear spring," the spring constant

TABLE 9.2
Properties of flywheel materials

Materials	Density, kg/m³	Relative cost, $/kg	Cycles	Working stress, 10^6 Pa	Stress density, m²/s²	Stress density ÷ cost, m² · kg/$ · s²
Maraging steel (18 Ni-No. 250)	8000	6.60	10^4	7.00	875	132
			10^5	3.38	423	64
4340 steel	7833	1.30	10^4	4.34	554	426
			10^5	2.83	361	278
Ti-6-4	4429	6.60	10^4	6.27	1416	214
			10^5	2.76	623	94
Al 2024-T3	2768	1.10	10^4	2.27	820	745
			10^5	1.17	423	384
60 v/o S-glass/epoxy	1965	1.80	10^4	10.00	5089	2827
			10^5	7.58	3858	2143
60 v/o E-glass/epoxy	1993	1.10	10^4	8.27	4150	3772
			10^5	6.21	3116	2833
62 v/o graphite/epoxy	1689	33.00	$\leq 10^6$	8.27	4896	148
63 v/o Kevlar/epoxy	1356	7.70	$\leq 10^6$	10.00	7375	958

is indeed a constant and the stored potential energy, in joules, is

$$\mathrm{PE} = \frac{K_s x^2}{2} \tag{9.9}$$

Springs can also be wound in a spiral and loaded with a torsional force.

For a bar loaded elastically in tension, compression, and/or bending, the potential energy stored in the bar, in joules, is

$$\mathrm{PE} = \frac{\sigma A \Delta x}{\zeta} \tag{9.10}$$

where σ is the actual stress, in pascals, A is the cross-sectional area, in square meters, and Δx is the deformation, in meters. The denominator ζ has a value of 2 for pure tension or compression but has a value greater than 2 for bending modes.

For a bar in elastic torsion, the stored elastic-strain potential energy, in joules, is

$$\mathrm{PE} = \frac{T^2 L}{2JG} \tag{9.11}$$

where L is the length of the bar, in meters, T is the torque at the end of the bar, in newton-meters, J is the polar moment of inertia of the bar, in m⁴, and G is the torsional modulus of elasticity, in pascals. This equation is valid only for systems with circular cross sections and is only approximate for other geometries because the angular distortion of a noncircular cross section by the torque changes the value of J.

9.2.3 Gravitational Energy Storage

Mass-weight energy-storage systems are relatively simple and consist of raising a weight against a gravitational force field. The amount of gravitational potential energy that can be stored in a uniform gravitational force field is

$$PE = mg\Delta z \tag{9.12}$$

where m is the mass, in kilograms, g is the acceleration of gravity, 9.81 m/s^2, and Δz is the change in elevation, in meters. In order to store 1 kWh of energy with a weight system, a 1000-kg (1.1-ton) mass would have to be raised 367 m ($\approx$0.5 mi) or a mass of 100 lbm would have to be raised approximately 5 mi into the air. These systems are commonly used to supply small amounts of energy to certain systems such as cuckoo clocks, etc.

Despite the small amount of energy that can be obtained from a unit mass, this system is used to store large amounts of energy by moving large quantities of water through reasonable distances in the so-called *pump-storage* energy system. In this system, a reversible hydroelectric generator-pump system is used to pump water from a river or lake into a reservoir at higher elevation during periods of low power demand on the utilities. During times of peak power demand, the system is reversed to recover most of the stored energy. This scheme effectively raises the capacity factor for the utility and permits the utilization of the low-cost base-load energy sources instead of the high-cost peaking units.

There are a number of pumped-storage systems in use today by various utilities. Approximately 27,000 MW$_e$ of electrical capacity had been installed by 1980. The storage efficiency of these systems includes the pumping efficiency, the evaporative and leakage losses from the upper reservoir (offset to some extent

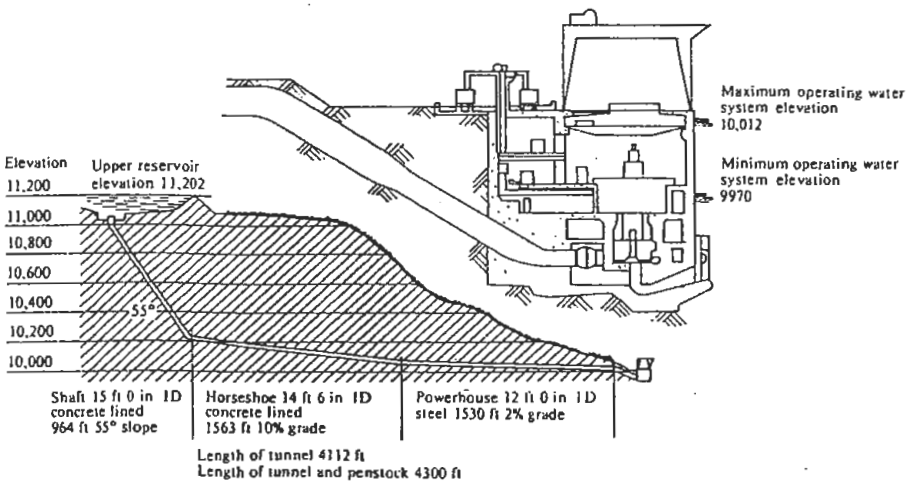


FIGURE 9.2
Layout of a typical pumped-storage facility—the Cabin Creek Project.

by rainfall), and the efficiency of the hydraulic turbine and generator, when the flow is reversed. An overall pumped-storage system is shown in Fig. 9.2.

Unfortunately, the pumped-storage system requires a specific type of topography that severely limits its application. In addition to the water system described earlier and shown in Fig. 9.2, some studies have also considered underground water systems that use abandoned mines or natural caverns.

9.2.4 Compressed-Fluid Energy Storage

One of the possible sources of stored mechanical energy is compressed-fluid energy. Although it takes energy to compress any fluid, the relative incompressibility of liquids means that large quantities of energy cannot be stored in these systems. Consequently, all compressed fluid energy storage systems employ gases or vapors. Stored compressed air tanks are commonly used to supply air to drive pneumatic tools, etc.

Recently, a different kind of pumped-storage system has been proposed for use by utilities. This system uses compressed air instead of water. The compressed-air energy-storage (CAES) system uses an underground cavity, an abandoned mine, abandoned oil and gas fields, a sealed aquifer, a natural cavern, an excavated cavity, or a leached salt deposit to contain the compressed air. Air is pumped into the chamber by using a motor-generator to drive the compressor part of a gas turbine during times of low power demand on the power grid. At time of peak power demand, the compressed air is taken from the storage vault, heated, and expanded through a gas turbine. Since approximately half of the output of a conventional gas turbine is required to drive the compressor, this system significantly increases the available power from the unit. A schematic diagram of a typical CAES system is shown in Fig. 9.3.

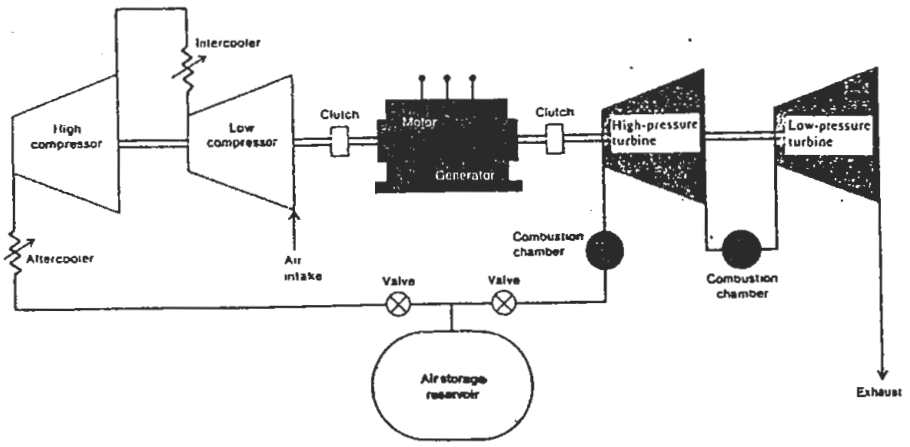


FIGURE 9.3
Schematic diagram of a CAES system.

The air storage volume required for this system is directly proportional to the amount of energy to be stored and is inversely proportional to the air pressure to be maintained in the cavern. It is desirable to keep the compressed air pressure in the storage chamber as constant as possible in order to achieve high compressor and turbine efficiencies. This can be accomplished by using water from a lake or reservoir to flood the cavern. The compressed air is then pumped into the cavern, which forces the water back up the water supply line into the lake. The resulting hydraulic pressure keeps the air pressure in the top of the cavern essentially constant as air is added or extracted from the storage volume.

The first compressed-air energy-storage system was built in Huntorf, West Germany, and went into operation in 1978. This system has a 2-h output of 290 MW, and the air is stored at a pressure of 6890 kPa (1000 psia). The compressed air is extracted, heated from the combustion of jet fuel, and injected into a gas turbine at 4460 kPa (650 psia). The Huntorf system has both a high pressure turbine and a low-pressure turbine with reheat between the two turbines. The plant charges for 8 h and can deliver full power within 11 min after notification.

9.2.5 Magnetic-Field Energy Storage

Mechanical energy can be stored and removed by changing the position of a ferromagnetic substance's position in a magnetic field. It takes energy to move a piece of iron away from the face to a magnet and energy can be released by letting the iron piece move closer to the face of the magnet by the magnetic attraction. This storage system has not seen much application in the past. However, with the recent developments in the area of superconducting magnets, it may see much wider application.

9.3 STORAGE OF ELECTRICAL ENERGY

9.3.1 Introduction

Electrical energy can be stored as electrical energy in either electrostatic-energy fields or inductive-energy fields. The battery is commonly considered to be a device that stores electrical energy, and, while it does receive and deliver electrical energy, it actually converts the input electrical energy into chemical energy in an endothermic reaction that is reversible. When the battery is discharged, the reactants in the battery combine in an exothermic chemical reaction that directly produces electricity.

9.3.2 Electrostatic-Field Energy Storage

The storage of electrical energy in the form of electrical energy can be achieved by the accumulation of charge on the plates of an electric capacitor—electrostatic-field energy. Capacitors are commonly used as storage devices in electric circuits and large banks of capacitors have been used for the storage of energy to improve

the lagging power factor of an ac power system. Capacitors have also been used to provide large bursts of dc power such as in some of the fusion experiments.

The amount of electrical energy E that is stored in a capacitor is equal to

$$E = \frac{Cv^2}{2} \tag{9.13}$$

where C is the capacitance of the unit, in farads, and v is the final voltage across the capacitor. Capacitor storage systems have the advantage of rapid charge and discharge without affecting their efficiency or the operation.

9.3.3 Inductive-Field Energy Storage

The storage of electrical energy in the form of electrical energy can also be accomplished in the magnetic field established by the flow of electrons (current) through an induction coil—inductive-field energy. This form of energy storage has not seen widespread application because it requires continuous current flow through the coil to maintain the field. In fact, it has been considered a liability because it commonly occurs in ac systems with induction motors and produces a power loss unless a bank of capacitors is used in series with the motors to balance the inductive reactance.

The amount of energy that is stored in the magnetic field of an electromagnet is

$$E = \frac{Li^2}{2} \tag{9.14}$$

where L is the inductance of the coil, in henrys, and i is the current in the coil, in amperes.

There is some interest in using this method of energy storage with the recent developments in superconductor materials. In the proposed storage system, a magnetic field would be established in a superconducting coil and associated circuit. Then the coil would short-circuited, producing an all superconducting circuit. Since a superconductor has absolutely no electrical resistance, the current and the magnetic field would continue until the energy was needed.

9.3.4 Batteries

Electrochemical batteries are commonly used to store electrical energy although, in reality, the energy is stored in the form of chemical energy. Batteries are normally divided into two general categories—primary and secondary. Primary batteries are systems which normally cannot be recharged; consequently only the secondary batteries can be employed for the cyclic storage of electrical energy. The performance of most secondary cells is strongly dependent on the rate that the battery is charged and discharged.

The common battery is composed of two electrodes separated by an electrolyte material, similar to fuel cells. Unlike fuel cells, however, one or all of the

chemical reactants are contained within the battery. During the charging process, an endothermic chemical reaction converts the electrical energy into chemical energy. During discharge, an exothermic chemical reaction converts the chemical energy into electricity.

Secondary batteries usually employ an aqueous electrolyte. Lead-acid batteries are commonly used in automobiles and, while they can withstand many shallow charge-discharge cycles, they cannot take many deep discharges. Nickel-iron batteries can withstand many deep discharges and are used in battery-powered forklifts and other low-powered vehicles. A number of other promising aqueous electrolyte systems include the nickel-zinc battery, the zinc-bromine battery, the nickel-hydrogen battery, and the zinc-chlorine battery.

Organic electrolyte batteries, such as the sodium-bromine, the lithium-sulfur dioxide, and the lithium-bromine batteries are under investigation because of the relatively low cost of these systems. These systems have high specific energy but low specific power because of the low conductivity of the organic electrolyte, such as propylene carbonate. The low electrolyte conductivity and the accompanying joule-heating loss yields a low charge-discharge efficiency for these systems.

The metal-air batteries include zinc-air, aluminum-air, and iron-air, although almost any metal can be employed. In these systems, a metal is used to form the negative electrode and gas electrode, using air as the oxidant, forms the positive electrode. These batteries have very high theoretical specific energies with values ranging from 64,620 kJ/kg for beryllium to 873 kJ/kg for lead. Most of the research on metal-air systems has centered on the zinc-air battery.

Considerable attention and research has also been focused on high-temperature batteries using fused-salt or solid electrolytes. The high electrical conductivity of the fused-salt electrolyte means that high power capability is possible. The lithium-sulfur battery employs a eutectic salt of lithium chloride-potassium chloride as an electrolyte. These systems have a high theoretical specific energy and they normally operate between 375 and 425°C.

The most popular high-temperature battery is the sodium-sulfur cell. This system operates between 300 and 350°C and employs a solid electrolyte, called *beta-alumina*, which has very high conductivity. Another promising battery system that operates at high temperature is the lithium-tellurium tetrachloride battery.

The performance characteristics of some of commonly used secondary batteries are listed in Table 9.3.

9.4 STORAGE OF CHEMICAL ENERGY

Chemical energy is actually a stored energy form and is one of the more compact forms of stored energy, as can be seen from the values in Table 9.1. Except for batteries, about the only major form of sorted chemical energy that is expected to see considerable application in the future is the production of elemental or molecular hydrogen. Many energy experts believe that with the demise of low-cost fossil fuels, the human race will shift to a hydrogen or a hydrogen-electric powered economy. Hydrogen makes an excellent fuel as the major combustion product

TABLE 9.3
Characteristics of common secondary batteries

Type	Average voltage	Open-circuit voltage	Charge loss per month, %	Charge-discharge cycles	Specific power, Wh/kg	Power density, kWh/m³
Nickel-iron	1.2	1.34	30	2000	24	54.9
Lead-acid	2.0	2.14	25	300	33	79.3
Nickel-cadmium	1.2	1.34	2	2000	26	54.9
Silver oxide-cadmium	1.1	1.34	3	2000	53	146.4
Silver oxide-zinc sealed	1.45	1.86	3	100	444–110	79–189
Silver oxide-zinc primary	1.45	1.86	...	...	121	220.0

is water and it can then be extracted again from water using solar energy, nuclear energy, or some other energy source.

Hydrogen can be stored in several ways and the systems used for its production and storage are well developed. It can be stored as a high-pressure gas, as a liquid at cryogenic temperatures, or in metal hydrides. Hydrogen gas has a very low density and consequently either very high pressures or very large volumes are required to contain a reasonable supply of energy. Liquifaction of hydrogen requires more energy and adds about 30 percent to the cost of the hydrogen fuel. Storage of hydrogen in metal hydrides results in severe weight and heat-loss penalties as well as the problem of oxygen and/or water contamination of the hydrides that result in significantly reduced energy-storage capacity.

Hydrogen can be produced from a large number of reactions. The most familiar is probably that of electrolysis where direct current is passed through a conducting aqueous solution producing hydrogen at one electrode and oxygen at the other. The electrolysis process has an actual conversion efficiency of about 85 percent, but since the input energy for this process is electricity, the overall yield of the process is going from thermal to mechanical to electrical to chemical energy is a maximum of about 35 percent. Since hydrogen can be produced more easily and more efficiently from fossil fuels, electrolysis production processes are used only when very pure hydrogen is desired or where inexpensive non-fossil-fuel energy can be employed.

Most of the hydrogen produced today is made from methane in the *steam-reforming process*, which takes place at 900°C. This system uses methane gas in the following reaction:

$$CH_4 + H_2O \rightarrow 3H_2 + CO$$

This reaction is endothermic, requiring about 230 kJ/kg · mol of CH_4. The carbon monoxide formed is subsequently used to produce additional hydrogen in the following reaction at 400°C:

$$CO + H_2O \rightarrow H_2 + CO_2$$

The carbon dioxide is then stripped from the fuel gas employing alkalies or amines and discarded.

Other methods of producing hydrogen include the reacting of steam with hot naphtha, a heavy fuel oil, or even coke, coal, and/or coal char. In an oil refinery, large amounts of hydrogen are generated by converting the common feedstock naphtha (C_8H_{16}) into aromatic compounds. Consider the production of hydrogen during the formation of xylene (C_8H_{10}):

$$C_8H_{16} \rightarrow C_8H_{10} + 3H_2$$

Hydrogen can also be produced in the *steam-iron process* where steam is reacted with a hot (900°C) bed of ferrous oxide (FeO). Magnetic iron oxide and hydrogen are produced in this reaction along with about 71 kJ/mol of H_2:

$$H_2O + 3FeO \rightarrow Fe_3O_4 + H_2$$

The bed is regenerated by passing the exhaust gas obtained by burning carbon with insufficient air. The carbon monoxide in the exhaust reduces the Fe_3O_4 to FeO.

A considerable amount of research has been carried out on the possibility of generating hydrogen in the so-called *thermochemical water-splitting process.* In this process, the water is split into hydrogen and oxygen in a series of closed-cycle chemical reactions operating at different temperatures. Unless there is a major breakthrough, however, it is unlikely that this method will become competitive from an economical standpoint until the carbonaceous fossil fuels become scarce and expensive.

Water is dissociated into hydrogen and oxygen by ionizing radiation such as that found in the core of a nuclear reactor. This method is not used in the generation of hydrogen, however, as it is very inefficient. In fact, this reaction presents a problem in the operation of light-water reactors and is discouraged as much as possible with the addition of various inhibitors.

9.5 STORAGE OF NUCLEAR ENERGY

Nuclear energy, like chemical energy, exists only as a stored form of energy and has the highest value of specific energy storage of any form of stored energy. One kg of uranium-235 has a theoretical specific of 7×10^{10} kJ/kg in the fission process and 0.6 kg of H-3 reacting with 0.4 kg of H-2 yields a theoretical specific energy storage of of 3×10^{11} kJ/kg in the fusion reaction. Radioisotopes are also sources of stored nuclear energy, but they have much lower values of specific energy, as noted in Table 9.1.

Stored nuclear energy can be produced by generating radioisotopes, like polonium-210 or cobalt-60, from the stable isotopes bismuth-209 and cobalt-59, respectively, using particles produced in a nuclear reactor or a particle accelerator. The manufactured fissionable isotopes uranium-233 and plutonium-239 are also normally generated in a nuclear reactor from the fertile isotopes thorium-232

and uranium-238, respectively. Breeder reactors are systems that produce more fuel atoms than they "burn," as they consume fertile atoms.

Another proposed nuclear-energy-storage system actually stores the energy produced in either the fission or fusion reaction in the earth in the form of thermal energy. In this scheme, small thermonuclear (fusion) bombs would be detonated within large salt deposits in the earth's crust. The resulting thermal energy would then be used to generate high-pressure steam to drive a conventional turbine-generator system.

A private organization, working closely with the Los Alamos Scientific Laboratory, in New Mexico, tried to develop such a system. This project was called *PACER* and tried to take advantage of the research carried out in the government's underground testing of nuclear weapons.

9.6 STORAGE OF THERMAL ENERGY

Thermal-energy storage (TES) systems utilize three basic modes of thermal-energy storage. These include sensible-heat, latent-heat, and quasi-latent-heat storage. The last system is actually not purely thermal energy, since it undergoes a chemical reaction.

In the sensible-heat-storage systems, the heat is simply stored by increasing the temperature of a solid or liquid. If the specific heat is constant, the amount of energy stored in the system is directly proportional to the temperature rise of the substance.

The storage of thermal energy as latent heat occurs in isothermal processes as the material undergoes a phase change, usually from a solid to a liquid. Such a phase change is accompanied by the absorption (charging) or the release (discharging) of relatively large amounts of thermal energy. The latent-heat TES systems have much higher energy-storage densities, on the average, than the sensible-heat TES systems.

The quasi-latent-heat TES system operates in essentially the same manner and is essentially indistinguishable from the latent-heat TES system. In it, thermal energy is converted into chemical energy in a reversible endothermic reaction that takes place at constant temperature. In order to reverse the process, the equilibrium constant is changed by changing the concentration or the pressure of the reactants and/or by changing the temperature. In this last case, the system acts like a sensible-heat TES system with a high specific heat.

Thermal-energy-storage systems range from the relatively simple, where water or air is pumped through the storage system, to the very complex, where thermal energy is converted into chemical energy in a reversible endothermic reaction that occurs at constant temperature. In order to achieve the maximum rate of energy addition or removal, the operating temperature range, corrosion and materials compatibility, environmental risks, and system economics must be considered. In a two-phase latent-heat system, additional consideration must be given to the problems of melting, expansion, solidification, thermal stability, and containment of the storage media.

TABLE 9.4
Materials for thermal-energy storage

(*a*) Sensible heat storage

Material	Formula	Specific heat, kJ/kg · °C	Volumetric heat capacity, kJ/m³ · °C
Water	H_2O	4.18	4191
Isobutyl alcohol	C_4H_9OH	3.01	2381
Ethyl alcohol	C_2H_5OH	2.85	2226
Beryllium	Be	2.81	5231
Limestone	$CaCO_3$	0.91	2548
Sand	SiO_2	0.80	1341
Iron	Fe	0.47	3688

(*b*) Latent heat storage (solid to liquid)

Material	Formula	Melting point, °C	Heat of fusion	
			kJ/kg	kJ/m³
Ethylene glycol	$C_2H_6O_2$	−13	146.5	162,800
Water	H_2O	0	334.9	305,500
Eastman 1-decanol	$C_{10}H_{22}O$	6	206.1	171,000
Sodium hydroxide $3\frac{1}{2}$ hydrate	$2NaOH \cdot 7H_2O$	15	223.5	364,000
Glycerol	$C_3H_8O_3$	18	200.5	250,000
Sodium sulfate decahydrate	$Na_2SO_4 \cdot 10H_2O$	32	152.8	350,200
Calcium nitrate tetrahydrate	$Ca(NO_3)_2 \cdot 4H_2O$	42	152.8	288,700
Sodium hydroxide octahydrate	$NaOH \cdot 8H_2O$	64	272.1	472,000
Barium hydroxide octahydrate	$Ba(OH)_2 \cdot 8H_2O$	78	300.0	655,700
Sodium	Na	98	116.3	117,400
Benzoic acid	$C_2H_6O_2$	122	141.6	179,300
Ammonium thiocyanate	NH_4CNS	146	260.5	337,200
Lithium nitrate	$LiNO_3$	252	367.5	875,500
Sodium hydroxide	NaOH	300	225.6	465,700
Potassium perchlorate	$KClO_4$	527	1251.3	3,148,000
Magnesium	Mg	651	293.1	499,200
Aluminum	Al	660	395.4	1,655,000
Lithium hydride	LiH	685	3780.0	3,100,000
Sodium chloride	NaCl	810	493.1	763,800
Sodium sulfate	Na_2SO_4	884	162.8	439,600
Magnesium fluoride	MgF_2	1266	930.3	2,273,000
Iron	Fe	1533	151.2	1,192,000

(*c*) Latent heat storage (solid to solid transition)

Material	Formula	Transition temperature, °C	Heat of transition, kJ/m³
Vanadium tetraoxide	V_2O_4	72	208,600
Silver selenide	Ag_2Se	133	193,700
Ferrous sulfide	FeS	138	231,000

The two most important conditions that affect the design of TES systems are the lost thermal power and the integrated energy storage density. The lost thermal power depends on the surface area of the storage system and the effectiveness of the thermal insulation employed around the containment system. The integrated energy density is the energy stored per unit volume and is commonly expressed in units of kilojoules per cubic meter or Btu per cubic foot in terms of the integrated intrinsic energy-storage density. The latter value is lower because it includes the volume for heat transfer, controls, etc. In general, the large-capacity TES systems usually have the lowest area-to-volume ratio and some may not require any insulation at all.

TES systems are commonly classed as either low-temperature or high-temperature. The low-temperature TES systems normally operate at temperatures below 150°C (300°F) and are commonly composed of either sensible heat storage in water, rocks, and scrap iron or latent heat storage in ice, glauber's salt ($Na_2SO_4 \cdot 10H_2O$), disodium hydrogen phosphate dodecahydrate ($Na_2HPO_4 \cdot 12H_2O$), paraffin waxes, and fatty acids. Some of these latent-heat substances experience deterioration as they are cycled and require further developmental work before they find widespread application.

One application of such a system for home heating and cooling is called *ACES* (an acronym for annual cyclic energy storage). This system uses a water-to-water heat pump, extracting heat from water storage in the winter, freezing it, and melting it during the summer for cooling. Some possible TES materials for low-temperature thermal storage are listed in Table 9.4.

Medium- and high-temperature TES systems have been used extensively in homes and industry. They include the heating of rocks, brick, bulk iron, and other ceramics. In general, these systems have not received as much attention as may be warranted because of their relatively high cost and operational difficulties and the current low cost of primary energy supplies. Some of the materials that may be used for the high-temperature TES systems are also listed in Table 9.4. The complexity, expense, and operational problems will probably limit the application of these systems to large industrial power consumers.

LIST OF SYMBOLS

A	Cross-sectional area, m^2
C	Capacitance of a capacitor, F
E	Energy J
g	Acceleration of gravity, m/s^2; standard gravity is 9.81 m/s^2
G	Torsional modulus of elasticity, kPa
i	Electric current, amperes
I	Moment of inertia, $kg \cdot m^2$
J	Polar moment of inertia, m^4
K_v	Flywheel volumetric factor
K_w	Flywheel weight factor
KE	Kinetic energy, J

L	Electrical inductance of a coil, H
L	Length, m
m	Mass, kg (lbm)
N	Angular velocity, r/min
PE	Potential energy, J
R	Radius of flywheel, m
T	Temperature, K
v	Electrical potential, V
V	Volume, m^3
$\bar{V}$	Linear velocity, m/s
x	Linear distance, m
Δx	Change in x dimension, m
Δz	Change in elevation, m
ω	Angular velocity, rad/s
ρ	Material density, kg/m^3
σ	Stress, kPa
ζ	Constant for bending of bars

REFERENCES

Angrist, S. W.: *Direct Energy Conversion*, 3d ed., Allyn and Bacon, Boston, 1976.

Brown, J. T., and J. H. Cronin: "Battery Systems for Peaking Power Generation," *Ninth Intersociety Energy Conversion Engineering Conference*, American Society of Mechanical Engineers, New York, 1974.

Bundy, F. P., C. S. Herris, and P. G. Kosky: "The Status of Thermal Energy Storage," General Electric Report No. 75CRD051, April 1975.

"CAES—It's More than Hot Air," *Mechanical Engineering*, vol. 104, no. 1, January 1982.

Fullman, R. L.: "Energy Storage by Flywheels," General Electric Report No. 75CRD051, April 1975.

Hamlen, R. P., and H. A. Christopher: "Battery Power and Energy Density Requirements for Vehicle Propulsion," General Electric Report No. 71-C-306, October 1971.

Housz, W.: "Hydrogen Energy and the Environment," General Electric Report No. P-681, February 1975.

Russell, C. R.: *Elements of Energy Conversion*, Pergamon Press, Long Island City, N.Y., 1967.

Wentorf, R. H., Jr.: "Hydrogen Generation," General Electric Report No. 75CRD119, May 1975.

APPENDIXES

A	Physical Constants
B	Conversion Factors and Standards
C	Ultimate Analysis of Biomass Fuels
D	ASTM Coal Classification System (Summary of ASTM D 388)
E	Typical Coal Analyses
F	Converting Proximate to Ultimate Analyses
G	Liquid Fuels
H	Fuel-Gas Analyses
I	Reactant Properties
J	List of Chemical Elements
K	Partial List of Isotopes
L	Radioisotope Fuels
M	Solar Constants (for Northern Latitudes)
N	Solar Position and Irradiation Values
O	Variation of Solar Radiation with Latitude (for Northern Latitudes)

APPENDIX A

PHYSICAL CONSTANTS

Avogadro's number = Av = 6.022×10^{26} molecules (or atoms)/(kg · mol)
= 2.732×10^{26} molecules (or atoms)/(lbm · mol)

Boltzmann's constant = $k = 1.381 \times 10^{-23}$ J/K
= 8.618×10^{-11} MeV/K
= 4.788×10^{-11} MeV/°R

Electron charge = $e = 1.602 \times 10^{-19}$ C
= 1.602×10^{-19} J/V

Faraday's constant = $F_y = 9.649 \times 10^{7}$ C/(kg · mol of electron)

Mass-energy conversion: 1 atomic mass unit (amu) = 1.661×10^{-27} kg
= 1.492×10^{-10} J
= 931.5 MeV

Mass of the earth = $m_E = 5.979 \times 10^{24}$ kg
= 1.318×10^{25} lbm

Newton's gravitational constant = $G = 6.672 \times 10^{-11}$ N · m^2/kg^2

Permittivity of free space = $\varepsilon_0 = 8.854 \times 10^{-12}$ F/m

Planck's constant = $h = 6.626 \times 10^{-34}$ J · s
= 4.136×10^{-21} MeV · s

Radius (average) of the earth = $r_E = 6.371 \times 10^{6}$ m
= 2.090×10^{7} ft
= 3959 mi

Rest masses:
Electron: $m_e = 0.0005486$ amu = 9.110×10^{-31} kg
Neutron: $m_n = 1.0086654$ amu = 1.675×10^{-27} kg
Proton: $m_p = 1.0072766$ amu = 1.673×10^{-27} kg

Solar constant (average) $= 1.353\ \text{kW/m}^2$
$= 4871\ \text{kJ/(h} \cdot \text{m}^2\text{)}$
$= 428.9\ \text{Btu/(h} \cdot \text{ft}^2\text{)}$

Standard atmospheric pressure $= 1.013 \times 10^5\ \text{Pa} = 0.1013\ \text{MPa}$
$= 14.696\ \text{lbf/in}^2$

Standard gravitational constant $= g = \dfrac{Gm_E}{r_E^2} = 9.807\ \text{m/s}^2$
$= 32.17\ \text{ft/s}^2$

Stefan-Boltzmann constant $= \sigma = 5.670 \times 10^{-8}\ \text{W/(m}^2 \cdot \text{K}^4\text{)}$
$= 0.1714 \times 10^{-8}\ \text{Btu/(h} \cdot \text{ft}^2 \cdot {}^\circ\text{R}^4\text{)}$

Universal (molar) gas constant $= R_u = 8.314\ \text{kJ/(kg} \cdot \text{mol} \cdot \text{K)}$
$= 1.986\ \text{Btu/(lbm} \cdot \text{mol} \cdot {}^\circ\text{R)}$
$= 1545\ \text{ft} \cdot \text{lbf/(lbm} \cdot \text{mol} \cdot {}^\circ\text{R)}$

Velocity of light $= c = 2.998 \times 10^8\ \text{m/s}$
$= 9.836 \times 10^8\ \text{ft/s}$
$= 186{,}300\ \text{mi/s}$

APPENDIX B

CONVERSION FACTORS AND STANDARDS

FUNDAMENTAL UNITS

Length

1 meter = 1 m = 10^{10} ångströms = 10^{10} Å
= 10^{6} micrometers = 10^{6} μm
= 1000 millimeters = 1000 mm
= 100 centimeters = 100 cm
= 39.37 inches = 39.37 in
= 3.281 feet = 3.281 ft

Mass

1 kilogram = 1 kg = 1000 grams = 1000 g
= 0.001 metric ton = 0.001 tonne
= 2.205 pounds mass = 2.205 lbm
= 0.001102 short ton = 0.001102 ton
= 6.022×10^{26} atomic mass units (amu)

Temperature

Normal scales: Degrees Celsius = °C = (°F − 32)/1.8
Degrees Fahrenheit = °F = 1.8°C + 32

Absolute scales: Degrees Kelvin = °C + 273.16 = 1.8°R
Degrees Rankine = °F + 459.67 = K/1.8

Temperature difference = ΔT:
1 Celsius degree = 1 C°
= 1 Kelvin degree = 1 K
= 1.8 Rankine degrees = 1.8 R°
= 1.8 Fahrenheit degrees = 1.8 F°

Time

1 second = 1 s = (1/3600) hour = 2.778×10^{-4} h
= (1/86,400) day = 1.157×10^{-5} day
= (1/31,536,000) year = 3.171×10^{-8} year

SECONDARY UNITS

Area

1 square meter = 1 m^2 = 10^{28} barns = 10^{28} b
= 10^4 square centimeters = 10^4 cm^2
= 1550 square inches = 1550 in^2
= 10.76 square feet = 10.76 ft^2
= 2.471×10^{-4} acres
= 3.861×10^{-7} square miles (mi^2)

Density

1 kilogram/cubic meter = 1 kg/m^3 = 10^{-3} g/cm^3
= 0.008345 lbm/U.S. gallon (gal)
= 0.06243 lbm/ft^3

Electrical and Magnetic Units

1 ampere = A = 1 watt/volt = 1 W/V
= 1 coulomb/second = 1 C/s
1 volt = V = 1 watt/ampere = 1 joule/coulomb = 1 ampere · ohm
= 1 A · Ω
1 ohm = Ω = 1 volt/ampere
1 farad = F = 1 coulomb/volt = 1 ampere · second/volt = 1 A · s/V
1 henry = H = 1 volt · second/ampere = 1 V · s/A
1 weber = 1 volt · second = 1 V · s
1 weber/m^2 = 1 tesla = 1 newton/ampere · meter = 10^4 gauss = 1N/A · m

Energy

$$
\begin{aligned}
1 \text{ joule} = 1\ \text{J} &= 1\ \text{W} \cdot \text{s} = 1\ \text{N} \cdot \text{m} = 1\ \text{kg} \cdot \text{m}^2/\text{s}^2 \\
&= 6.242 \times 10^{18} \text{ electron volts (eV)} \\
&= 6.242 \times 10^{12} \text{ million eV (MeV)} \\
&= 10^7 \text{ ergs} \\
&= 200 \text{ fissions/s} \\
&= 0.2388 \text{ calorie (cal)} \\
&= 9.478 \times 10^{-4} \text{ British thermal unit (Btu)} \\
&= 3.725 \times 10^{-7} \text{ horsepower-hour (hph)} \\
&= 2.778 \times 10^{-7} \text{ kilowatt-hour (kWh)} \\
&= 2.381 \times 10^{-10} \text{ ton of TNT}
\end{aligned}
$$

1 Therm = 100,000 Btu
1 quad = 10^9 Joul
1 Btu = 1.055 kJ

Force

$$
\begin{aligned}
1 \text{ newton} = 1\ \text{N} &= 1\ \text{kg} \cdot \text{m/s}^2 \\
&= 7.233\ \text{lbm} \cdot \text{ft/s}^2 \\
&= 0.2248\ \text{lbf}
\end{aligned}
$$

Gravimetric (Mass) Heating Value

$$
\begin{aligned}
1 \text{ joule/gram} = 1\ \text{J/g} &= 1\ \text{kJ/kg} = 1000\ \text{m}^2/\text{s}^2 \\
&= 0.430\ \text{Btu/lbm}
\end{aligned}
$$

Heat Flux

$$
\begin{aligned}
1\ \text{W/m}^2 &= 1\ \text{J/(s} \cdot \text{m}^2) = 1\ \text{N/(s} \cdot \text{m}) = 1\ \text{kg/s}^3 \\
&= 0.3170\ \text{Btu/(h} \cdot \text{ft}^2)
\end{aligned}
$$

Power

$$
\begin{aligned}
1 \text{ watt} = 1\ \text{W} &= 1\ \text{J/s} = 1\ \text{N} \cdot \text{m/s} = 1\ \text{kg} \cdot \text{m}^2/\text{s}^3 \\
&= 0.001\ \text{kW} \\
&= 3.412\ \text{Btu/h} \\
&= 0.001341\ \text{hp} \\
&= 6.242 \times 10^{12}\ \text{MeV/s}
\end{aligned}
$$

= 0.86 K cal/h

Power Density and Volumetric Heat Generation Rate

$$
\begin{aligned}
1 \text{ watt/cubic meter} = 1\ \text{W/m}^3 &= 1\ \text{J/(s} \cdot \text{m}^3) = 1\ \text{kg/(m} \cdot \text{s}^3) \\
&= 0.0966\ \text{Btu/(h} \cdot \text{ft}^3)
\end{aligned}
$$

Pressure

$$\begin{aligned}1 \text{ pascal} = 1 \text{ Pa} &= 1 \text{ N/m}^2 = 1 \text{ kg/(m} \cdot \text{s}^2) \\ &= 9.869 \times 10^{-6} \text{ atmosphere (atm)} \\ &= 10^{-5} \text{ bar} \\ &= 1.45 \times 10^{-4} \text{ pound force/square inch (psi)} \\ &= 2.953 \times 10^{-4} \text{ inch Hg (inHg)} \\ &= 0.004018 \text{ inch } H_2O \text{ (in}H_2O\text{)} \\ &= 0.007502 \text{ torr} = 0.007502 \text{ mmHg}\end{aligned}$$

$$\begin{aligned}\text{Absolute pressure} &= \text{gage pressure} + \text{atmospheric pressure} \\ &= \text{atmospheric pressure} - \text{vacuum pressure}\end{aligned}$$

Specific Heat (c)

$$\begin{aligned}1 \text{ joule/kilogram} \cdot \text{C}^\circ &= 1 \text{ J/(kg} \cdot \text{C}^\circ\text{)} \\ &= 1 \text{ m}^2/(\text{s}^2 \cdot \text{C}^\circ) \\ &= 0.2388 \text{ cal/(kg} \cdot \text{C}^\circ\text{)} \\ &= 2.388 \times 10^{-4} \text{ Btu/(lbm} \cdot \text{F}^\circ\text{)}\end{aligned}$$

Heating Value: 1 Btu/Lb = 2.326 KJ/Kg
1 KJ/Kg = 0.43 Btu/Lbm

Specific Power

$$\begin{aligned}1 \text{ kilowatt/kilogram} = 1 \text{ kW/kg} &= 1000 \text{ m}^2/\text{s}^3 \\ &= 1548 \text{ Btu/h} \cdot \text{lbm} \\ &= 0.6081 \text{ hp/lbm}\end{aligned}$$

Surface Conductance (h)

$$\begin{aligned}1 \text{ W/(m}^2 \cdot \text{C}^\circ\text{)} &= 1 \text{ J/(s} \cdot \text{m}^2 \cdot \text{C}^\circ\text{)} \\ &= 1 \text{ kg/(s}^3 \cdot \text{C}^\circ\text{)} \\ &= 0.1761 \text{ Btu/h} \cdot \text{ft}^2 \cdot \text{F}^\circ\end{aligned}$$

Thermal Conductivity (k)

$$\begin{aligned}1 \text{ watt/meter} \cdot \text{Celsius degree} &= 1 \text{ W/m} \cdot \text{C}^\circ = 1 \text{ J/(s} \cdot \text{m} \cdot \text{C}^\circ\text{)} \\ &= 1 \text{ N/(s} \cdot \text{C}^\circ\text{)} = 1 \text{ kg} \cdot \text{m/(s}^3 \cdot \text{C}^\circ\text{)} \\ &= 0.2388 \text{ cal/(s} \cdot \text{m} \cdot \text{C}^\circ\text{)} \\ &= 0.5778 \text{ Btu/(h} \cdot \text{ft}^2 \cdot \text{F}^\circ\text{/ft)}\end{aligned}$$

Velocity

$$\begin{aligned}1 \text{ meter/second} &= 1 \text{ m/s} \\ &= 3.281 \text{ ft/s}\end{aligned}$$

Viscosity

1 poise = 1 P = 100 centipoise = 100 cP
= 0.1 kg/(s · m)
= 241.9 lbm/(ft · h)
= 0.002089 lbf · s/ft^2

Volume

1 cubic meter = 1 m^3 = 10^6 cm^3
= 10^3 liters (L)
= 264.2 U.S. gal
= 35.31 ft^3
= 1.308 cubic yards

1 U.S. gal = 3.785 liter

STANDARD U.S. FUEL ENERGY VALUES

Coal

Anthracite: HHV = 12,700 Btu/lbm = 29,540 kJ/kg
= 25.4 × 10^6 Btu/short ton

Bituminous: HHV = 11,750 Btu/lbm = 27,330 kJ/kg
= 23.5 × 10^6 Btu/short ton

Lignite: HHV = 11,400 Btu/lbm = 26,515 kJ/kg
= 22.8 × 10^6 Btu/short ton

Crude Oil

HHV = 18,100 Btu/lbm = 42,100 kJ/kg
= 138,100 Btu/U.S. gal
= 5,800,000 Btu/barrel (bbl)

Natural Gas (Dry)

HHV = 24,700 Btu/lbm = 57,450 kJ/kg
= 1021 Btu/standard cubic foot (scf)

FUEL-ENERGY EQUIVALENTS

One barrel (42 U.S. gal) of oil = 460 lbm of coal
= 5680 scf of natural gas
= 612 kWh of electricity (assumes a conversion efficiency of 36 percent)

One short ton of coal = 4345 bbl of crude oil
= 24,682 scf of natural gas
= 2660 kWh of electricity (assumes a conversion efficiency of 36 percent)

1000 scf of natural gas = 0.176 bbl of crude oil
= 81.0 lbm of coal
= 189 kWh of electricity (assumes a conversion efficiency of 36 percent)

DECIMAL MULTIPLES AND SUBMULTIPLES

Number	Power of 10	Prefix	Symbol
0.000 000 000 000 000 001	10^{-18}	atto	a
0.000 000 000 000 001	10^{-15}	femto	f
0.000 000 000 001	10^{-12}	pico	p
0.000 000 001	10^{-9}	nano	n
0.000 001	10^{-6}	micro	μ
0.001	10^{-3}	milli	m
1	10^{0}	—	—
1,000	10^{3}	kilo	k
1,000,000	10^{6}	mega	M
1,000,000,000	10^{9}	giga	G
1,000,000,000,000	10^{12}	tera	T
1,000,000,000,000,000	10^{15}	peta	P
1,000,000,000,000,000,000	10^{18}	exa	E

APPENDIX C

ULTIMATE ANALYSIS OF BIOMASS FUELS

Material	C,†%	H_2,†%	O_2,†%	N_2,†%	S,†%	A,†%	HHV, kJ/kg‡
Agricultural wastes							
Bagasse (sugar cane refuse)	47.3	6.1	35.3	0.0	0.0	11.3	21,255
Feedlot manure	42.7	5.5	31.3	2.4	0.3	17.8	17,160
Rice hulls	38.5	5.7	39.8	0.5	0.0	15.5	15,370
Rice straw	39.2	5.1	35.8	0.6	0.1	19.2	15,210
Municipal solid waste							
General	33.9	4.6	22.4	0.7	0.4	38.0	13,130
Brown paper	44.9	6.1	47.8	0.0	0.1	1.1	17,920
Cardboard	45.5	6.1	44.5	0.2	0.1	3.6	18,235
Corrugated boxes	43.8	5.7	45.1	0.1	0.2	5.1	16,430
Food fats	76.7	12.1	11.2	0.0	0.0	0.0	38,835
Garbage	45.0	6.4	28.8	3.3	0.5	16.0	19,730
Glass bottles (labels)	0.5	0.1	0.4	0.0	0.0	99.0	195
Magazine paper	33.2	5.0	38.9	0.1	0.1	22.7	12,650

Material	C,†%	H_2,†%	O_2,†%	N_2,†%	S,†%	A,†%	HHV, kJ/kg‡
Municipal solid waste							
Metal cans (labels, etc.)	4.5	0.6	4.3	0.1	0.0	90.5	1,725
Newspapers	49.1	6.1	43.0	0.1	0.2	1.5	19,720
Oils, paints	66.9	9.6	5.2	2.0	0.0	16.3	31,165
Paper food cartons	44.7	6.1	41.9	0.2	0.2	6.9	17,975
Plastics							
General	60.0	7.2	22.6	0.0	0.0	10.2	33,415
Polyethylene	85.6	14.4	0.0	0.0	0.0	0.0	46,395
Vinyl chloride	47.1	5.9	18.6	(chlorine = 28.4%)			20,535
Rags	55.0	6.6	31.2	4.6	0.1	2.5	13,955
Rubber	77.7	10.3	0.0	0.0	2.0	10.0	26,350
Sewage							
Raw sewage	45.5	6.8	25.8	3.3	2.5	16.1	16,465
Sewage sludge	14.2	2.1	10.5	1.1	0.7	71.4	4,745
Wood and wood products							
Hardwoods							
Beech	51.6	6.3	41.5	0.0	0.0	0.6	20,370
Hickory	49.7	6.5	43.1	0.0	0.0	0.7	20,165
Maple	50.6	6.0	41.7	0.3	0.0	1.4	19,955
Poplar	51.6	6.3	41.5	0.0	0.0	0.6	20,745
Oak	49.5	6.6	43.4	0.3	0.0	0.2	20,185
Softwoods							
Douglas fir	52.3	6.3	40.5	0.1	0.0	0.8	21,045
Pine	52.6	6.1	40.9	0.2	0.0	0.2	21,280
Redwood	53.5	5.9	40.3	0.1	0.0	0.2	21,025
Western hemlock	50.4	5.8	41.4	0.1	0.1	2.2	20,045
Wood products							
Charcoal (made at 400°C)	76.5	3.9	15.4	0.8	0.0	3.4	28,560
Charcoal (made at 500°C)	81.7	3.2	11.5	0.2	0.0	3.4	31,630
Douglas fir bark	56.2	5.9	36.7	0.0	0.0	1.2	22,095
Pine bark	52.3	5.8	38.8	0.2	0.0	2.9	20,420
Dry sawdust pellets	47.2	5.5	46.3	0.0	0.0	1.0	20,500
Ripe leaves	40.5	6.0	45.1	0.2	0.1	8.1	16,400
Plant wastes							
Brush	42.5	5.9	41.2	2.0	0.1	8.3	18,370
Evergreen trimmings	49.5	6.6	41.2	1.7	0.2	0.8	6,425
Garden plants	48.0	6.8	41.3	1.2	0.3	2.4	8,835
Grass	48.4	6.8	41.6	1.2	0.3	1.7	18,520

† All percentages on moisture-free basis.
‡ 1 kJ/kg = 0.43 Btu/lbm.

MUNICIPAL SOLID WASTE

Municipal solid waste is commonly divided into seven different classes:

TYPE 0 WASTE. Trash is a mixture of highly combustible waste such as paper, cardboard, cartons, wood boxes, and combustible floor sweepings, from commercial and industrial activities. The mixtures contain up to 10 percent by weight of catalogs, magazines, or packaged paper, treated corrugated cardboard, oily rags, and plastic or rubber scraps. This type of waste contains 10 percent moisture and 5 percent incombustible solids, and has a heating value of 8500 Btu/lb, (19,770 kJ/kg) as fired.

TYPE 1 WASTE. Rubbish is a mixture of combustible waste such as paper, cardboard cartons, wood scrap, foliage, and combustible floor sweepings, from domestic, commercial, and industrial activities. This mixture contains up to 20 percent by weight of restaurant or cafeteria waste, but contains little or no treated papers, plastic, or rubber wastes. This type of waste contains 25 percent moisture and 10 percent incombustible solids, and has a heating value of 6500 Btu/lb (15,120 kJ/kg), as fired.

TYPE 2 WASTE. Refuse consists of an approximately even mixture of rubbish and garbage by weight. This type of waste is common to apartment and residential occupancy, consisting of up to 50 percent moisture and 7 percent incombustible solids, and has a heating value of 4300 Btu/lb (10,000 kJ/kg), as fired.

TYPE 3 WASTE. Garbage consists of animal and vegetable wastes from restaurants, cafeterias, hotels, hospitals, markets, and like installations. This type of waste contains up to 70 percent moisture and up to 5 percent incombustible solids, and has a heating value of 2500 Btu/lb (5815 kJ/kg), as fired.

TYPE 4 WASTE. Human and animal remains consisting of carcasses, organs, and solid organic wastes from hospitals, laboratories, slaughterhouses, animal pounds, and similar sources. This type of waste contains up to 85 percent moisture and 5 percent incombustible solids, and has a heating value of 1000 Btu/lb (2326 kJ/kg), as fired.

TYPE 5 WASTE. Byproduct wastes, gaseous, liquid, or semiliquid, are composed of tar, paints solvents, sludge, fumes, etc., from industrial operations. The energy content must be determined by the individual materials to be destroyed.

TYPE 6 WASTE. Solid byproduct waste is composed of rubber, plastics, wood waste, etc., from industrial operations. The energy content must be determined by the individual materials to be destroyed.

APPENDIX D

ASTM COAL CLASSIFICATION SYSTEM (SUMMARY OF ASTM D 388)

DEFINITIONS

Percent, dry, mineral-matter-free fixed carbon = % dry, mm-free FC:

$$\%\ \text{dry, mm-free FC} = \frac{(\text{FC} - 0.15\text{S})(100)}{1 - \text{M} - 1.08\text{A} - 0.55\text{S}} = \text{D, mm} - \text{f FC}$$

Moist, mineral-matter-free Btu content of coal, Btu/lbm = moist, mm-free Btu:

$$\text{Moist, mm-free Btu} = \frac{\text{Btu} - 0.55\text{S}}{1 - 1.08\text{A} - 0.55\text{S}} = \text{M, mm} - \text{f Btu}$$

COAL CLASSIFICATIONS

Class Group	Ranking parameter	Agglomerating character
Class I: Anthracitic coals		
Group 1. Metaanthracite	Dry, mm-free FC > 98%	Nonagg.
Group 2. Anthracite	98% > D, mm-f FC > 92%	Nonagg.
Group 3. Semianthracite	92% > D, mm-f FC > 86%	Nonagg.
Class II: Bituminous coals		
Group 1. Low-volatile bituminous	86% > D, mm-f FC > 78%	Usually agg.
Group 2. Medium-volatile bituminous	78% > D, mm-f FC > 69%	Usually agg.
	If dry, mm-free FC is less than 69%, rank coal according to the moist, mm-free Btu value	
Group 3. High-volatile A bituminous	M, mm-f Btu > 14,000	Usually agg.
Group 4. High-volatile B bituminous	13,000 < M, mm-f Btu < 14,000	Usually agg.
Group 5. High-volatile C bituminous	11,500 < M, mm-f Btu < 13,000	Usually agg.
	10,500 < M, mm-f Btu < 11,500	Agg.
Class III: Subbituminous coals		
Group 1. Subbituminous A	10,500 < M, mm-f Btu < 11,500	Nonagg.
Group 2. Subbituminous B	9,500 < M, mm-f Btu < 10,500	Nonagg.
Group 3. Subbituminous C	8,300 < M, mm-f Btu < 9,500	Nonagg.
Class IV: Lignitic coals		
Group 1. Lignite A	6300 < M, mm-f Btu < 8300	Nonagg.
Group 2. Lignite B	M, mm-f Btu < 6300 Btu/lbm	Nonagg.

Notes:

An agglomerating coal is one that has a caking characteristic which, during the volatile-matter determination, produces a coke residue in the form of an agglomerating button.

This classification system does not include a few coals, all of which contain less than 48% mm-free FC or have more than 15,500 Btu/lbm for moist, mm-free coal.

"Moist" refers to coal containing its inherent moisture, not liquid moisture on the coal surface.

If a Class I, Group 3 coal is agglomerating, classify it as a Class II, Group 1 coal.

APPENDIX E

TYPICAL COAL ANALYSES

States and counties	Moisture and ash-free values								As received	
	VM	FC	C	H_2	O_2	N_2	S	kJ/kg†	*M*	*A*
ALABAMA										
Jefferson, Tuscaloosa	27.7	72.3	88.1	5.2	4.2	1.7	0.8	36,340	2-5	3-10
Jefferson, Tuscaloosa	32.9	67.1	86.7	5.3	5.0	1.8	1.2	35,875	2-5	2-10
Jefferson, St. Clair	35.4	64.6	85.2	5.4	5.8	1.8	1.8	35,470	2-5	4-12
Walker, Bibb, Shelby	38.0	62.0	84.3	5.4	7.6	1.7	1.0	35,120	1-5	2-14
ARKANSAS										
Sebastian, Logan	19.0	81.0	89.3	4.4	2.0	1.8	2.5	36,040	2-4	6-12
Franklin, Johnson	16.1	83.9	89.4	4.2	2.1	1.8	2.5	35,935	2-4	6-12
COLORADO										
Las Animas	36.5	63.5	84.9	5.5	7.4	1.5	0.7	35,525	1-7	6-20
Huerfano, Gunnison, Garfield	40.7	59.3	80.6	5.5	11.6	1.6	0.7	35,575	3-10	3-12
Weld, Boulder	42.5	57.5	75.0	5.1	17.9	1.5	0.5	30,085	17-30	3-6
Routt, Fremont	43.0	57.0	76.6	5.2	16.0	1.3	0.9	31,515	10-18	3-10
El Paso	46.4	53.6	71.5	5.0	21.8	1.1	0.6	28,095	20-35	5-14
ILLINOIS										
Franklin, Williamson	39.1	60.9	81.3	5.3	9.8	1.7	1.9	33,725	8-12	8-12
Saline, Perry	39.6	60.4	80.6	5.4	10.3	1.7	2.0	33,770	6-11	7-12
Macoupin, Sangamon	46.3	53.7	77.5	5.4	10.2	1.4	5.5	32,970	12-16	8-16
Madison, St. Clair	46.7	53.3	77.0	5.4	10.6	1.3	5.7	32,865	9-16	11-20
INDIANA										
Sullivan, Greene	45.2	54.8	80.9	5.6	9.7	1.8	2.0	33,725	10-14	6-12
Vigo, Vermillion, Knox	48.0	52.0	79.6	5.6	8.8	1.5	4.5	33,750	6-12	7-12

States and counties	Moisture and ash-free values								As received	
	VM	FC	C	H_2	O_2	N_2	S	kJ/kg†	*M*	*A*
IOWA										
Appanoose, Polk, Lucas	47.9	52.1	77.0	5.5	9.7	1.5	6.3	33,155	13–19	7–15
KANSAS										
Cherokee, Crawford	39.5	60.5	83.0	5.4	6.1	1.5	4.0	34,955	2–8	9–12
Leavenworth	47.2	52.8	79.6	5.4	7.8	1.5	5.7	33,560	10–12	12–16
KENTUCKY										
Letcher, Pike	37.8	62.2	85.2	5.4	7.0	1.6	0.8	35,320	1–4	2–7
Harlan, Perry, Bell, Knox	40.2	59.8	83.5	5.6	7.9	1.9	1.1	34,785	2–6	2–8
Muhlenburg, Hopkins	44.7	55.3	80.3	5.4	8.6	1.7	4.0	33,595	4–10	5–12
Webster, Union, Butler	45.0	55.0	81.0	5.5	7.7	1.7	4.1	33,945	4–10	5–12
MARYLAND										
Alegheny, Garrett	18.2	81.8	89.3	4.7	2.7	1.7	1.6	33,400	2–4	6–14
MISSOURI										
Barton	38.0	62.0	83.0	5.5	5.1	1.4	5.0	35,165	5–7	8–13
Bates	42.3	57.7	81.0	5.5	7.5	1.5	4.5	34,190	7–12	11–15
Ray, Lafayette, Linn, Adair	46.3	53.7	78.6	5.6	9.3	1.3	5.2	33,315	11–16	7–15
Henry, Macon, Clay, Randolph	45.4	54.6	79.2	5.5	8.4	1.3	5.6	33,420	9–16	8–16
MONTANA										
Rosebud, Custer	44.4	55.6	71.7	4.4	22.0	1.1	0.8	27,980	27–30	3–15
Musselshell, Gallatin	42.8	57.2	78.5	5.4	13.6	1.4	1.1	32,365	4–14	6–30
Carbon, Fergus	40.6	59.4	76.0	5.1	14.2	1.4	3.3	31,025	8–24	8–18
Cascade	35.0	65.0	77.8	4.8	12.6	1.0	3.8	31,445	3–12	14–25
Valley	47.4	52.6	69.0	4.6	24.1	1.2	1.1	26,490	32–45	4–9
NEW MEXICO										
Colfax, Lincoln	43.1	56.9	82.6	5.7	9.3	1.5	0.9	34,560	2–5	9–17
McKinley	47.2	52.8	79.2	5.5	13.0	1.4	0.9	32,420	10–16	3–10
NORTH DAKOTA										
McLean, Morton, Stark	54.0	46.0	72.4	4.7	18.6	1.5	2.8	28,920	35–43	5–12
Williams, Ward	47.6	52.4	72.1	4.9	21.0	1.1	0.9	27,910	35–43	5–12
OHIO										
Belmont, Guernsey	46.0	54.0	80.3	5.6	8.0	1.5	4.6	34,120	3–6	9–16
Tuscarawas, Noble, Jackson	46.2	53.8	79.2	5.6	9.2	1.5	4.5	33,680	3–9	7–15
Athens, Perry, Meigs, Hocking	41.8	58.2	79.7	5.5	10.8	1.4	2.6	33,455	6–10	4–12
Jefferson, Guernsey	41.5	58.5	82.2	5.5	7.7	1.7	2.9	34,560	3–7	5–12
OKLAHOMA										
Pittsburgh, Latimer	40.0	60.0	84.0	5.5	7.4	2.0	1.1	34,990	2–10	4–8
Okmulgee, Tulsa	41.9	58.1	82.4	5.5	7.0	2.0	3.1	34,655	2–8	4–10
Coal	46.6	53.4	77.8	5.2	10.4	1.8	4.8	32,420	5–7	9–12
Haskell	23.6	76.4	89.1	4.8	3.2	1.9	1.0	36,165	2–4	3–8
LeFlore	18.2	81.8	90.4	4.6	2.2	1.9	0.9	36,190	1–3	6–12
PENNSYLVANIA										
Fayette	31.4	68.6	86.0	5.2	6.3	1.5	1.0	36,095	3–5	7–9
Fayette, Washington, Elk	37.8	62.2	84.8	5.5	5.7	1.6	2.4	35,525	2–4	6–13
Allegheny, Butler	39.6	60.4	83.7	5.5	7.1	1.7	2.0	35,050	2–5	4–13
Cambria, Center,	24.6	75.4	88.2	5.1	3.4	1.4	1.9	36,320	1–5	5–12

States and counties	Moisture and ash-free values								As received	
	VM	FC	C	H_2	O_2	N_2	S	kJ/kg†	*M*	*A*
Somerset, Tioga	23.5	76.5	88.6	4.8	3.1	1.6	1.9	36,145	1–5	5–12
Westmoreland, Indiana	26.5	73.5	87.6	5.2	3.3	1.4	2.5	36,355	1–5	5–12
Westmoreland, Jefferson	35.4	64.6	85.0	5.4	5.8	1.7	2.1	35,550	2–4	7–15
Cambria, Bedford	19.8	80.2	89.4	4.8	2.4	1.5	1.9	36,435	1–6	5–12
Huntingdon, Somerset	17.1	82.9	90.3	4.6	2.3	1.4	1.4	36,715	1–6	5–12
Sullivan	10.6	89.4	91.6	3.8	2.5	1.2	0.9	35,925	3–4	10–15
Lackawanna, Luzerne	7.3	92.7	93.5	2.6	2.3	0.9	0.7	35,120	2–6	6–16
Schuylkill	2.0	98.0	93.9	2.1	2.3	0.8	0.9	34,585	2–3	8–13
TENNESSEE										
Campbell, Anderson	40.3	59.7	83.1	5.5	7.4	2.1	1.9	34,610	2–6	2–8
Claiborne, Overton, Scott	40.5	59.5	83.5	5.6	6.5	2.0	2.4	34,770	2–6	2–11
Morgan, Fentress, White	41.6	58.4	83.0	5.7	6.1	1.7	3.5	35,095	2–5	4–12
Marion, Hamilton	31.1	68.9	87.3	5.4	4.2	1.6	1.5	35,875	3–5	3–11
Rhea, Roane, Grundy	34.5	65.5	85.7	5.3	6.1	1.6	1.3	35,260	2–4	9–15
TEXAS										
Houston, Milam, Wood	53.3	46.7	72.8	5.3	19.3	1.4	1.2	29,550	29–37	6–13
UTAH										
Carbon, Emery, Grand	45.8	54.2	80.3	5.7	11.7	1.6	0.7	33,420	3–10	4–20
Summit, Uintah, Iron	45.3	54.7	76.2	5.4	13.7	1.2	3.5	31,490	5–17	3–13
VIRGINIA										
Wise, Russell	36.9	63.1	86.3	5.5	5.7	1.6	0.9	35,840	2–5	4–9
Tazewill	17.8	82.2	90.4	4.8	2.9	1.2	0.7	36,960	2–6	2–6
Lee, Scott	37.8	62.2	83.6	5.4	8.3	1.6	1.1	35,085	3–6	3–9
Dickenson, Buchanan, Henico	31.2	68.8	87.3	5.2	4.3	1.8	1.4	35,855	2–4	3–18
Montgomery	13.6	86.4	90.7	4.2	3.3	1.0	0.8	35,715	1–5	16–25
WASHINGTON										
Kittitas, King	43.3	56.7	80.5	6.0	10.8	1.9	0.8	34,005	3–9	10–20
King, Pierce	39.4	60.6	82.5	5.9	8.6	2.0	1.0	34,655	2–6	8–20
Lewis, Thurston	49.3	50.7	71.7	5.8	19.5	1.3	1.7	29,305	16–30	6–23
King	44.8	55.2	76.6	5.7	15.1	1.8	0.8	31,865	7–18	5–16
Pierce	25.4	74.6	87.5	5.4	4.0	2.5	0.6	36,120	2–5	9–15
WEST VIRGINIA										
Logan, Fayette	36.2	63.8	86.3	5.5	5.4	1.7	1.1	35,680	1–3	4–8
McDowell, Fayette, Wyoming	17.7	82.3	90.4	4.8	2.7	1.3	0.8	36,540	2–4	3–6
Raleigh, Mercer, Fayette	18.5	81.5	90.1	4.8	3.0	1.4	0.7	36,560	2–4	3–6
Monongalia, Greenbriar	30.2	69.8	87.2	5.2	5.1	1.6	0.9	35,910	2–4	4–12
Preston, Fayette, Randolph	31.0	69.0	87.5	5.3	4.2	1.5	1.5	36,050	2–4	4–12
Marion, Kanawha, Harrison	40.9	59.1	83.9	5.6	7.4	1.6	1.5	35,075	2–4	4–10
WYOMING										
Sweetwater, Hot Springs	41.8	58.2	77.3	5.3	14.8	1.5	1.1	31,920	8–16	3–8
Sweetwater, Carbon	39.5	60.5	76.2	5.1	16.3	1.6	0.8	30,840	15–25	4–7
Lincoln, Uinta, Sweetwater	43.4	56.6	79.8	5.4	12.2	1.5	1.1	33,075	6–18	4–12
Sheridan, Campbell, Carbon	45.3	54.7	74.1	5.1	18.7	1.3	0.8	29,795	18–30	5–15
Albany, Converse, Freemont	45.1	54.9	73.6	5.2	18.8	1.3	1.1	29,610	17–27	4–15

† 1 kJ/kg = 0.43 Btu/lbm.

APPENDIX F

CONVERTING PROXIMATE TO ULTIMATE ANALYSES

This method gives good results for the great bulk of coals used in steam generation. It is less accurate with anthracite, cannel, and coals with unusual amounts of resins and waxes. The calculational procedure is as follows:

Start with the as-received proximate analysis:

Volatile matter	= 38.0%	Sulfur	= 2.4%
Fixed carbon	= 52.3%	HHV	= 13,770 Btu/lbm
Moisture	= 1.8%		
Ash	= 7.9%		
	100.0%		

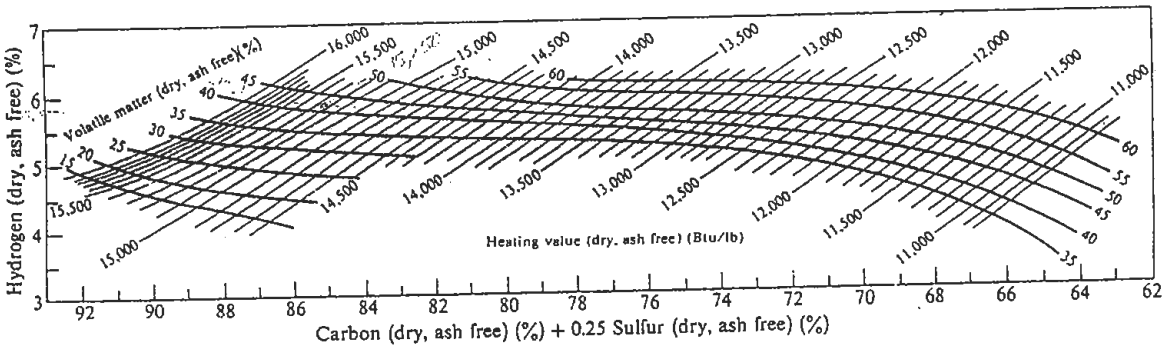
Convert the as-received proximate analysis to a dry, ash-free basis by dividing the above values by $(1 - M - A)$ or $(1 - 0.018 - 0.079)$ or (0.903):

$$\text{Volatile matter} = \frac{38.0}{0.903} = 42.1\% \qquad \text{Sulfur} = \frac{2.4}{0.903} = 2.7\%$$

$$\text{Fixed carbon} = \frac{52.3}{0.903} = 57.9\% \qquad \text{HHV} = \frac{13,770}{0.903} = 15,250 \text{ Btu/lbm}$$

$$100.0\%$$

Locate the intersection of the dry, ash-free volatile matter (42.1 percent) and the British thermal unit (15,250) lines on the graph. This corresponds to a hydrogen reading of 5.9% H_2 and a (carbon+sulfur/4) reading of 84.9 percent. Assuming a nitrogen value of 1.5 percent (used for all coals) for the dry, ash-free condition, build up the following ultimate analysis for the dry, ash-free basis.


Hydrogen (dry, ash free) (%)
Volatile matter (dry, ash free) (%)
Heating value (dry, ash free) (Btu/lb)
Carbon (dry, ash free) (%) + 0.25 Sulfur (dry, ash free) (%)

Dry, ash-free ultimate analysis (estimated):

$\%C = [(\%C + \%S/4)$ from graph$] - \%S/4 = 84.9 - 2.7/4 =$		84.2%
$\%H_2 = \%H_2$ (from graph)	=	5.9%
$\%N_2 = 1.5\%$ (assumed to be the same for all coals)	=	1.5%
$\%S = \%S$ (from the proximate analysis)	=	2.7%
$\%O_2 = 100 -$ (sum of other values)	=	5.7%
		100.0%

These dry, ash-free analyses can be converted into an as-received ultimate analysis by multiplying the values by $(1 - M - A)$, or 0.903. This gives:

C = 76.0%	or, if the moisture is distributed to H_2 and O_2,	C = 76.0%	
H_2 = 5.3%		H_2 = 5.5%	
N_2 = 1.4%		N_2 = 1.4%	
S = 2.4%		S = 2.4%	
O_2 = 5.1%		O_2 = 6.7%	
M = 1.8%		A = 7.9%	
A = 7.9%			99.9%
99.9%			

This method has been checked against laboratory analyses for many coals and here are some of the results (from E. O. Smith, Asst. Manager, Inspection Dept., Eastern Gas and Fuel Associates):

Producing area	Proximate analysis, as-received						Ultimate analysis, as-received				
	Moist	VM	FC	Ash	Sulfur	Btu		C	H_2	O_2	N_2
Penn. (1)	2.2	16.2	72.1	9.5	2.1	13,710	Actual	79.2	4.4	3.4	1.4
							Calculated	79.4	4.5	3.2	1.3
Penn. (2)	3.3	34.4	54.1	8.2	1.1	13,380	Actual	74.5	5.3	9.4	1.5
							Calculated	75.0	5.3	9.0	1.4
W. Va. (1)	3.3	16.0	76.1	4.6	0.6	14,450	Actual	83.9	4.6	5.2	1.1
							Calculated	83.7	4.7	4.9	1.5
W. Va. (2)	1.8	38.0	52.3	7.9	2.4	13,770	Actual	76.0	5.2	7.1	1.4
							Calculated	76.0	5.4	6.9	1.4
Ky. (1)	3.6	37.2	56.5	2.7	0.7	14,220	Actual	79.6	5.5	9.9	1.6
							Calculated	79.6	5.7	9.8	1.5
Ky. (2)	3.4	37.4	54.8	4.4	1.0	13,800	Actual	77.4	5.5	10.2	1.5
							Calculated	77.6	5.6	9.9	1.5
Ill.	9.2	33.8	48.6	8.4	0.9	11,930	Actual	67.3	5.5	16.3	1.5
							Calculated	67.1	5.6	16.7	1.3
Colo.	14.4	38.4	41.2	6.0	0.8	10,600	Actual	60.6	5.8	25.6	1.2
							Calculated	60.2	6.1	25.6	1.3
Tenn.	5.1	36.3	55.8	2.8	1.0	13,570	Actual	76.5	5.6	12.2	1.9
							Calculated	76.4	5.6	12.7	1.5
Iowa	16.6	36.5	37.4	9.5	4.3	10,480	Actual	57.4	6.0	21.8	1.0
							Calculated	57.6	6.1	21.3	1.2
Alaska	10.7	30.4	44.0	14.9	0.7	9,640	Actual	55.3	5.0	23.6	0.6
							Calculated	55.5	5.2	22.5	1.2

APPENDIX G

LIQUID FUELS

Commercial fuels	Molecular weight	Specific gravity, °API	Flash point, °F	Higher heating value, kJ/kg†	Relative cost, per energy unit
Propane (LPG)‡	44	112.5	···	50,400	122
Butane (LPG)‡	58	103.1	···	49,590	118
Gasolene	113	70.0	0	47,590	167
Gasolene	126	60.0	0	47,120	144
Methanol	32	47.3	60	22,675	
Ethanol (denatured)	46	48.0	170	29,770	
Aviation jet fuel	···	45.0	110	46,050	
Aviation jet fuel	···	50.0	···	46,010	
Kerosene	154	40.0	130	45,940	116
Diesel oil (1-D)	170	30.2	100	44,750	
Diesel oil (2-D)	184	22.2	125	44,450	
Diesel oil (4-D)	198	15.8	130	43,800	
Available fuel oils:					
No. 1 fuel oil	···	42.0	100	46,070	118
No. 2 fuel oil	···	34.0	100	45,260	100
No. 4 fuel oil	···	22.5	130	43,820	76
No. 5 fuel oil	···	18.0	130	43,170	60
No. 6 fuel oil	···	14.5	150	42,330	51

† 1 kJ/kg = 0.43 Btu/lbm.
‡ Stored as liquid under pressure.

Composition of typical American crude oils

Crude Oils	Mass fractions				Specific gravity, °API	HHV, kJ/kg†
	C	H_2	O_2+N_2	S		
Texas No. 1	84.60	10.90	2.87	1.63	21.68	44,140
Texas No. 2	83.26	12.41	3.83	0.50	21.37	45,710
Pennsylvania	84.90	13.70	1.40	0.00	28.20	44,680
California	81.52	11.51	6.42	0.55	14.98	43,420

† 1 kJ/kg = 0.43 Btu/lbm.

APPENDIX H

FUEL-GAS ANALYSES

Fuel gases	Higher heating value,† kJ/m³‡	Composition, in percentage by volume or mole								
		CH_4	C_2H_4	C_2H_6sp	H_2	CO	O_2	N_2	CO_2	H_2O
Natural gases:										
Alabama	36,140	97.6						2.1	0.3	
Arkansas	36,730	99.2						0.6	0.2	
California-A	39,080	77.5		16.0					6.5	
California-B	40,880	83.4		15.4				0.5	0.7	
Illinois	35,400	95.6						3.9	0.5	
Indiana	43,110	75.4		23.4				1.2		
Kansas	36,290	98.0						0.8	1.2	
Kentucky	43,350	75.0		24.0				1.0		
Louisiana-A	34,760	78.8	9.5				0.3	11.3	0.1	
Louisiana-B	36,570	90.0		5.0				5.0		
Missouri	35,490	84.1		6.7				8.4	0.8	
New York	40,840	84.0		15.0				1.0		
Ohio-A	35,000	93.3	0.3		1.8	0.5	0.3	3.4	0.2	0.2
Ohio-B	35,060	93.4	0.4		1.6	0.4	0.4	3.4	0.4	
Oklahoma-A	39,160	73.5		18.4				8.1		
Oklahoma-B	35,490	84.1		6.7				8.4	0.8	
Pennsylvania-A	39,170	90.0		9.0				0.8	0.2	
Pennsylvania-B	41,140	83.4		15.8				0.8		
West Virginia	43,040	76.8		22.5				0.7		

Fuel gases	Higher heating value,† kJ/m³‡	Composition, in percentage by volume or mole								
		CH_4	C_2H_4	C_2H_6	H_2	CO	O_2	N_2	CO_2	C_6H_6
Artificial gases:										
Producer gas										
Anthracite	4,520				15.5	22.7	0.3	56.0	5.5	
Bituminous	5,690	3.7		0.1	11.6	24.4	0.6	54.8	4.8	
Blast-furnace (BF) gas	3,620	0.2			3.6	26.5		57.0	12.7	
B-F gas (lean)	3,170	0.1			2.5	24.1		58.4	14.9	
Coke-oven gas	22,030	33.9	5.2		47.9	6.1	0.6	3.7	2.6	
Illuminating gas	18,560	23.6		10.5	11.7	13.7	0.7	32.6	7.2	
Water gas (carb.)	19,470	15.5	4.7		34.0	32.0	0.7	6.5	4.3	2.3
Landfill gas	22,220	60.0			(Balance is normally CO_2)					

† All gas values are corrected to 1 atm and 20°C (68°F).
‡ 1 kJ/m³ = 0.02684 Btu/ft³.

APPENDIX I

REACTANT PROPERTIES

Substance	Chemical formula	Molecular weight	Density,† kg/m³	Higher heating value		Lower heating value	
				kJ/m³‡	kJ/kg‡	kJ/m³‡	kJ/kg‡
Fuels:							
Hydrogen	H_2	2.016	0.0838	11,910	142,097	10,060	120,067
Carbon	C	12.011	···	···	32,778	···	32,778
Sulfur	S	32.064	···	···	9,257	···	9,257
Hydrogen sulfide	H_2S	34.080	1.4168	23,390	16,506	21,540	15,204
Carbon monoxide	CO	28.006	1.1643	11,770	10,110	11,770	10,110
Methane	CH_4	16.043	0.6669	37,030	55,529	33,340	49,994
Methyl alcohol	CH_3OH	32.043	1.3321	31,780	23,858	28,090	21,086
Ethane	C_2H_6	30.071	1.2501	64,910	51,920	59,370	47,489
Ethylene	C_2H_4	28.055	1.1663	58,690	50,322	55,000	47,156
Acetylene	C_2H_2	26.039	1.0825	54,140	50,010	52,290	48,305
Ethyl alcohol	C_2H_5OH	46.071	1.9153	58,630	30,610	53,090	27,717
Propane	C_3H_8	44.099	1.8333	92,390	50,399	85,010	46,370
Propylene	C_3H_6	42.083	1.7495	85,640	48,954	80,110	45,789
n-Butane	C_4H_{10}	58.126	2.4164	119,820	49,589	110,590	45,768
Isobutane	C_4H_{10}	58.126	2.4164	119,540	49,472	110,310	45,652
n-Butene	C_4H_8	56.110	2.3326	113,130	48,503	105,750	45,338
Isobutene	C_4H_8	56.110	2.3326	112,500	48,231	105,110	45,065
n-Pentane	C_5H_{12}	72.153	2.9996	147,170	49,064	136,090	45,370
Isopentane	C_5H_{12}	72.153	2.9996	146,830	48,952	135,750	45,258
Neopentane	C_5H_{12}	72.153	2.9996	146,350	48,791	135,270	45,098
n-Pentene	C_5H_{10}	70.137	2.9157	140,510	48,191	131,280	45,026
n-Hexane	C_6H_{14}	86.181	3.5827	174,710	48,764	161,780	45,156
Benzene	C_6H_6	78.117	3.2475	137,350	42,293	131,810	40,588
Toluene	C_7H_8	92.141	3.8305	164,830	43,030	157,440	41,102
Xylene	C_8H_{10}	106.172	4.4138	191,460	43,377	182,320	41,307
Naphthalene	$C_{10}H_8$	128.179	5.3287	214,450	40,244	207,070	38,860
Ammonia	NH_3	17.031	0.7080	15,920	22,484	13,150	18,572

Substance	Chemical formula	Molecular weight	Density,† kg/m³	Higher heating value		Lower heating value	
				kJ/m³‡	kJ/kg‡	kJ/m³‡	kJ/kg‡
Nonfuels:							
Oxygen	O_2	31.999	1.3303				
Nitrogen	N_2	28.013	1.1646				
Air	···	28.970	1.2043				
Carbon dioxide	CO_2	44.010	1.8296				
Sulfur dioxide	SO_2	64.063	2.6632				

† All gas values corrected to one atmosphere and 20°C (68°F), $\rho = 0.04157$ (M.W.).
‡ 1 kJ/m³ = 0.02684 Btu/ft³; 1 kJ/kg = 0.43 Btu/lbm; 1 kg/m³ = 0.0624 lbm/ft³.

APPENDIX J

LIST OF CHEMICAL ELEMENTS

Chemical element	Symbol	Atomic number (Z)	Chemical element	Symbol	Atomic Number (Z)
Actinium	Ac	89	Curium	Cm	96
Aluminum	Al	13	Dysprosium	Dy	66
Americium	Am	95	Einsteinium	Es	99
Antimony	Sb	51	Erbium	Er	68
Argon	A	18	Europium	Eu	63
Arsenic	As	33	Fermium	Fm	100
Astatine	At	85	Fluorine	F	9
Barium	Ba	56	Francium	Fr	87
Berkelium	Bk	97	Gadolinium	Gd	64
Beryllium	Be	4	Gallium	Ga	31
Bismuth	Bi	83	Germanium	Ge	32
Boron	B	5	Gold	Au	79
Bromine	Br	35	Hafnium	Hf	72
Cadmium	Cd	48	Hahnium†	...	105
Calcium	Ca	20	Helium	He	2
Californium	Cf	98	Holmium	Ho	67
Carbon	C	6	Hydrogen	H	1
Cerium	Ce	58	Indium	In	49
Cesium	Cs	55	Iodine	I	53
Chlorine	Cl	17	Iridium	Ir	77
Chromium	Cr	24	Iron	Fe	26
Cobalt	Co	27	Krypton	Kr	36
Copper	Cu	29	Lanthanum	La	57

Chemical element	Symbol	Atomic number (Z)	Chemical element	Symbol	Atomic Number (Z)
Lawrencium	Lw	103	Rhodium	Rh	45
Lead	Pb	82	Rubidium	Rb	37
Lithium	Li	3	Ruthenium	Ru	44
Lutecium	Lu	71	Rutherfordium†	...	104
Magnesium	Mg	12	Samarium	Sm	62
Manganese	Mn	25	Scandium	Sc	21
Mendelevium	Md	101	Selenium	Se	34
Mercury	Hg	80	Silicon	Si	14
Molybdenum	Mo	42	Silver	Ag	47
Neodymium	Nd	60	Sodium	Na	11
Neon	Ne	10	Strontium	Sr	38
Neptunium	Np	93	Sulfur	S	16
Nickel	Ni	28	Tantalum	Ta	73
Niobium	Nb	41	Technetium	Tc	43
Nitrogen	N	7	Tellurium	Te	52
Nobelium	No	102	Terbium	Tb	65
Osmium	Os	76	Thallium	Tl	81
Oxygen	O	8	Thorium	Th	90
Palladium	Pd	46	Thulium	Tm	69
Phosphorus	P	15	Tin	Sn	50
Platinum	Pt	78	Titanium	Ti	22
Plutonium	Pu	94	Tungsten (Wolfram)	W	74
Polonium	Po	84	Uranium	U	92
Potassium	K	19	Vanadium	V	23
Praseodymium	Pr	59	Xenon	Xe	54
Promethium	Pm	61	Ytterbium	Yb	70
Protactinium	Pa	91	Yttrium	Y	39
Radium	Ra	88	Zinc	Zn	30
Radon	Rn	86	Zirconium	Zr	40
Rhenium	Re	75			

† There is currently a disagreement as to who first discovered elements 104 and 105—the Americans or the Russians. The Americans have proposed the name "Rutherfordium" for element 104 and the name "Hahnium" for element 105. The Russians have proposed the Name "Kurchatovium" for element 104 and the name "Neilsbohrium" for element 105. An international body will decide who gets to name these elements.

APPENDIX K

PARTIAL LIST OF ISOTOPES

Element Chemical symbol Atomic weight	Atomic number Z	Atomic mass number A	Isotopic mass, amu	Natural abundance, %	Half-life†	Type of decay†
Electron	−1	0	0.000549			
Neutron	0	1	1.008665		11.7 m	β^-
Hydrogen	1	1	1.007825	99.985		
H	1	2	2.01410	0.015		
1.00797	1	3	3.01605		12.26 y	β^-
Helium	2	3	3.01603	0.00013		
He	2	4	4.00260	99.99987		
4.0026	2	5	5.01230		2×10^{-21} s	α
	2	6	6.01888		0.8 s	β^-
	2	8	8.03750		0.122 s	β^-
Lithium	3	5	5.01250		10^{-21} s	α
Li	3	6	6.01512	7.42		
6.939	3	7	7.01600	92.58		
	3	8	8.02247		0.85 s	β^-
Beryllium	4	6	6.01970		4.0×10^{-21} s	β^+
Be	4	7	7.01690		53.6 d	K
9.0122	4	8	8.00530		10^{-16} s	2α
	4	9	9.01218	100.00		
	4	10	10.01350		2.0×10^{6} y	β^-
	4	11	11.02160		13.6 s	β^-

Element Chemical symbol Atomic weight	Atomic number Z	Atomic mass number A	Isotopic mass, amu	Natural abundance, %	Half-life†	Type of decay†
Boron	5	8	8.02460		0.77 s	β^+
B	5	9	9.01333		8.0×10^{-19} s	$p/2\alpha$
10.811	5	10	10.01294	19.78		
	5	11	11.00931	80.22		
	5	12	12.01430		0.02 s	β^-
	5	13	13.01780		0.019 s	β^-
Carbon	6	10			19.0 s	β^+
C	6	11	11.01141		20.3 m	β^+
12.011	6	12	12.00000	98.89		
	6	13	13.00335	1.11		
	6	14	14.00323		5730.0 y	β^-
	6	15	15.00939		2.40 s	β^-
Nitrogen	7	12	12.01895		0.011 s	β^+
N	7	13	13.00572		9.96 m	β^+
14.0067	7	14	14.00307	99.63		
	7	15	15.00011	0.37		
	7	16	16.00656		7.20 s	β^-
	7	17	17.00862		4.16 s	β^-
Oxygen	8	14	14.00856		73.0 s	β^+
O	8	15	15.00300		0.122 s	β^+
15.9994	8	16	15.99491	99.759		
	8	17	16.99914	0.037		
	8	18	17.99915	0.204		
	8	19	19.00344		29.0 s	β^-
Fluorine	9	16	16.01148		10^{-19} s	β^+
F	9	17	17.00210		66.0 s	β^+
18.9984	9	18	18.00094		109.7 s	β^+
	9	19	18.99841	100.00		
	9	20	19.99999		11.4 s	β^-
Neon	10	18	18.00546		1.67 s	β^+
Ne	10	19	19.00187		17.5 s	β^+
20.179	10	20	19.99244	90.52		
	10	21	20.99395	0.26		
	10	22	21.99138	9.22		
	10	23	22.99437		37.6 s	β^-
Sodium	11	20	20.00887		0.4 s	β^+
Na	11	21	20.99760		23.0 s	β^+
22.9898	11	22	21.99432		2.62 y	β^+
	11	23	22.98977	100.0		
	11	24	23.99102		15.0 h	β^-
	11	25	24.98984		60.0 s	β^-
Magnesium	12	23	22.99380		11.3 s	β^+
Mg	12	24	23.98504	78.99		
24.305	12	25	24.98584	10.00		
	12	26	25.98259	11.01		

Element Chemical symbol Atomic weight	Atomic number Z	Atomic mass number A	Isotopic mass, amu	Natural abundance, %	Half-life†	Type of decay†
	12	27	26.98436		9.50 m	β^-
	12	28	27.98381		21.3 h	β^-
Aluminum	13	24	24.00006		2.10 s	β^+
Al	13	25	24.99036		7.20 s	β^+
26.98153	13	26	25.98793		7.4×10^5 y	β^+
	13	27	26.98153	100.00		
	13	28	27.98193		2.31 m	β^-
	13	29	28.98053		6.60 s	β^-
Silicon	14	27	26.98667		4.20 s	β^+
Si	14	28	27.97693	92.21		
28.086	14	29	28.97649	4.70		
	14	30	29.97376	3.09		
	14	31	30.97536		2.62 h	β^-
	14	32	31.97396		280 y	β^-
Phosphorus	15	28	27.99168		0.28 s	β^+
P	15	29	28.98178		4.40 s	β^+
30.9738	15	30	29.97863		2.50 m	β^+
	15	31	30.97376	100.00		
	15	32	31.97392		14.3 d	β^-
	15	33	32.97168		25.0 d	β^-
	15	34	33.97331		12.4 s	β^-
Sulfur	16	31	30.97901		2.60 s	β^+
S	16	32	31.97207	95.01		
32.064	16	33	32.97146	0.75		
	16	34	33.96786	4.21		
	16	35	34.96923		86.7 d	β^-
	16	36	35.96709	0.013		
	16	37	36.97029		5.10 m	β^-
Chlorine	17	32	31.98601		0.31 s	β^+
Cl	17	33	32.99725		2.50 s	β^+
35.453	17	34	33.97376		1.56 s	β^+
	17	35	34.96885	75.77		
	17	36	35.96852		3.1×10^5 y	β^-
	17	37	36.96590	24.23		
	17	38	37.96797		37.3 m	β^-
	17	39	38.96742		55.5 m	β^-
Argon	18	35	34.97459		1.83 s	β^+
A	18	36	35.96755	0.337		
39.948	18	37	36.96674		35.0 d	K
	18	38	37.96272	0.063		
	18	39	38.96428		265.0 y	β^-
	18	40	39.96238	99.60		
	18	41	40.96454		1.83 h	β^-
Potassium	19	37	36.97324		1.20 s	β^+
K	19	38	37.96905		7.70 m	β^+
39.0983	19	39	38.96371	93.26		

Element Chemical symbol Atomic weight	Atomic number Z	Atomic mass number A	Isotopic mass, amu	Natural abundance, %	Half-life†	Type of decay†
	19	40	39.97400	0.012	1.28×10^9 y	K/β^-
	19	41	40.96184	6.73		
	19	42	41.96352		12.4 h	β^-
	19	43	42.96066		22.4 h	β^-
	19	44	43.96192		22.0 m	β^-
Calcium	20	39	38.97100		0.87 s	β^+
Ca	20	40	39.96259	96.94		
40.080	20	41	40.96228		1.3×10^5 y	K
	20	42	41.95863	0.6445		
	20	43	42.95878	0.135		
	20	44	43.95549	2.09		
	20	45			165 d	β^-
	20	46	45.95367	0.0035		
	20	48	47.95253	0.187		
	20	49	48.95559		8.80 m	β^-
Scandium	21	40	39.97753		0.18 s	β^+
Sc	21	41	40.96860		0.87 s	β^+
44.956	21	43	42.96106		3.89 h	β^+
	21	44	43.95928		3.92 h	β^+
	21	45	44.95592	100.00		
	21	46	45.95487		83.8 d	β^-
	21	47	46.95230		3.40 d	β^-
	21	48	47.95216		44.0 h	β^-
	21	49	48.94997		57.5 m	β^-
Titanium	22	45	44.95797		3.08 h	β^+
Ti	22	46	45.95263	8.25		
47.900	22	47	46.95177	7.45		
	22	48	47.94795	73.70		
	22	49	48.94787	5.40		
	22	50	49.94479	5.20		
	22	51	50.94645		5.80 m	β^-
Vanadium	23	46	45.96028		0.40 s	β^+
V	23	47	46.95469		32.0 m	β^+
50.942	23	48	47.95220		16.1 d	β^+
	23	49	48.94847		330.0 d	K
	23	50	49.94716	0.24	6.0×10^{15} y	K
	23	51	50.94396	99.76		
	23	52	51.94418		3.76 m	β^-
Chromium	24	49	48.95122		42.0 m	β^+
Cr	24	50	49.94605	4.31		
51.996	24	51	50.94418		27.8 d	K
	24	52	51.94050	83.76		
	24	53	52.94065	9.55		
	24	54	53.93890	2.38		
	24	55	54.94095		3.50 m	β^-

Element Chemical symbol Atomic weight	Atomic number Z	Atomic mass number A	Isotopic mass, amu	Natural abundance, %	Half-life†	Type of decay†
Manganese	25	50	49.95411		0.29 s	β^+
Mn	25	51	50.94809		45.0 m	β^+
54.938	25	52	51.94618		5.60 d	β^+
	25	53	52.94126		3.8×10^6 y	K
	25	54	53.94040		303.0 d	K
	25	55	54.93805	100.00		
	25	56	55.93904		2.58 h	β^-
Iron	26	52	51.94769		8.00 h	K
Fe	26	53	52.94541		9.00 m	β^+
55.847	26	54	53.93960	5.82		
	26	55	54.93856		2.60 y	K
	26	56	55.93490	91.66		
	26	57	56.93540	2.19		
	26	58	57.93330	0.33		
	26	59	58.93490		45.1 d	β^-
Cobalt	27	54	53.94904		0.18 s	β^+
Co	27	55	54.94188		18.0 h	β^+
68.933	27	56	55.93982		77.3 d	K/β^+
	27	57	56.93587		270.0 d	K
	27	58	57.93520		71.3 d	K
	27	59	58.93320	100.00		
	27	60	59.93344		5.26 y	β^-
	27	61	60.93199		99.0 m	β^-
	27	62	61.93324		13.9 m	β^-
Nickel	28	57	56.9394		36.1 h	K
Ni	28	58	57.9353	68.30		
58.710	28	59	58.9342		8.0×10^4 y	K
	28	60	59.9308	26.13		
	28	61	60.9310	1.09		
	28	62	61.9283	3.56		
	28	63	62.9286		100.0 y	β^-
	28	64	63.9280	0.92		
	28	65	64.9291		2.56 h	β^-
Copper	29	58	57.9456		3.30 s	β^+
Cu	29	60	59.9375		24.0 m	β^+
63.546	29	61	60.9327		3.30 h	β^+
	29	62	61.9316		9.80 m	β^+
	29	63	62.9298	69.20		
	29	64	63.9288		12.9 h	$\beta^+/K/\beta^-$
	29	65	64.9278	30.80		
	29	66	65.9288		5.10 m	β^-
	29	67	66.9278		61.0 h	β^-
Zinc	30	62	61.9339		9.30 h	β^+
Zn	30	63	62.9330		38.8 m	β^+
65.370	30	64	63.9291	48.60		
	30	65	64.9283		243.6 d	K/β^+

Element Chemical symbol Atomic weight	Atomic number Z	Atomic mass number A	Isotopic mass, amu	Natural abundance, %	Half-life†	Type of decay†
	30	66	65.9260	27.90		
	30	67	66.9271	4.10		
	30	68	67.9249	18.80		
	30	69	68.9257		58.0 m	β^-
	30	70	69.9253	0.60		
	30	71	70.9273		2.20 m	β^-
Gallium	31	64	63.9368		2.60 m	β^+
Ga	31	65	64.9325		15.0 m	β^+
69.720	31	66	65.9315		9.50 h	β^+
	31	67	66.9283		78.0 h	K
	31	68	67.9270		68.3 m	β^+
	31	69	68.9257	60.10		
	31	70	69.9259		21.0 m	β^-
	31	71	70.9249	39.90		
	31	72	71.9245		14.1 h	β^-
	31	73	72.9248		4.80 h	β^-
Germanium	32	67	66.9330		19.0 m	β^+
Ge	32	69	68.9280		40.0 h	K
72.590	32	70	69.9243	20.52		
	32	71	70.9251		11.0 d	K
	32	72	71.9221	27.43		
	32	73	72.9234	7.76		
	32	74	73.9212	36.53		
	32	75	74.9228		82.8 m	β^-
	32	76	75.9214	7.76		
	32	77	76.9215		11.3 h	β^-
Arsenic	33	71	70.9271		62.0 h	K/β^+
As	33	72	71.9264		26.0 h	β^+
74.9216	33	73	72.9237		80.3 d	K
	33	74	73.9217		17.9 d	K
	33	75	74.9216	100.00		
	33	76	75.9201		26.5 h	β^-
	33	77	76.9206		39.0 h	β^-
	33	78	77.9217		91.0 m	β^-
	33	79	78.9209		9.00 m	β^-
Selenium	34	73	72.9266		7.10 h	β^+
Se	34	74	73.9225	0.87		
78.960	34	75	74.9225		120.4 d	K
	34	76	75.9192	9.02		
	34	77	76.9199	7.58		
	34	78	77.9173	23.52		
	34	79	78.9185		6.5×10^4 y	β^-
	34	80	79.9165	49.82		
	34	81	80.9185		18.6 m	β^-
	34	82	81.9167	9.19		

Element Chemical symbol Atomic weight	Atomic number Z	Atomic mass number A	Isotopic mass, amu	Natural abundance, %	Half-life†	Type of decay†
Bromine	35	78	77.9211		6.40 m	β^+
Br	35	79	78.9183	50.69		
79.904	35	80	79.9172		17.6 m	β^-
	35	81	80.9163	49.31		
	35	82	81.9158		35.5 h	β^-
Krypton	36	78	77.9204	0.35		
Kr	36	79	78.9200		34.9 h	K
83.800	36	80	79.9164	2.27		
	36	81	80.9165		2.1×10^5 y	K
	36	82	81.9135	11.56		
	36	83	82.9141	11.55		
	36	84	83.9116	56.90		
	36	85	84.9126		10.76 y	β^-
	36	86	85.9109	17.37		
	36	87	86.9136		76.0 m	β^-
Rubidium	37	84	83.9142		33.0 d	K
Ru	37	85	84.9117	72.15		
85.470	37	86	85.9100		18.66 d	β^-
	37	87	86.9092	27.85	5.0×10^{10} y	β^-
	37	88	87.9113		17.7 m	β^-
Strontium	38	84	83.9142	0.56		
Sr	38	85	84.9095		64.0 d	K
87.620	38	86	85.9094	9.86		
	38	87	86.9089	7.02		
	38	88	87.9056	82.56		
	38	89	88.9057		52.0 d	β^-
	38	90	89.9072		28.1 y	β^-
	38	91	90.9097		9.67 h	β^-
Yttrium	39	88	87.9096		106.6 d	K
Y	39	89	88.9059	100.00		
88.906	39	90	89.9066		64.0 h	β^-
	39	91	90.9069		58.8 d	β^-
	39	92	91.9083		3.54 h	β^-
Zirconium	40	89	88.9086		78.4 h	K
Zr	40	90	89.9047	51.46		
91.220	40	91	90.9056	11.23		
	40	92	91.9050	17.11		
	40	93	92.9063		1.5×10^{-6} y	β^-
	40	94	93.9061	17.40		
	40	95	94.9072		65.0 d	β^-
	40	96	95.9082	2.80	3.6×10^{17}	β^-
	40	97	96.91104		17.0 h	β^-
Niobium	41	92	91.9062		10.13 d	K/β^-
Nb	41	93	92.9064	100.00		
92.906	41	94	93.9063		2.0×10^4 y	β^-
	41	95	94.9060		3.50 d	β^-

Element Chemical symbol Atomic weight	Atomic number Z	Atomic mass number A	Isotopic mass, amu	Natural abundance, %	Half-life†	Type of decay†
Molybdenum	42	92	91.9068	14.80		
Mo	42	93	92.9057		3,500 y	K
95.940	42	94	93.9051	9.30		
	42	95	94.9058	15.90		
	42	96	95.9046	16.70		
	42	97	96.9058	9.60		
	42	98	97.9055	24.10		
	42	99	98.9069		66.7 h	β^-
	42	100	99.9076	9.60		
Technetium	43	95	94.9073		20.0 h	K
Tc	43	97	96.9068		2.6×10^6 y	K
———	43	98			4.2×10^6 y	β^-
	43	99	98.9054		2.12×10^5 y	β^-
Ruthenium	44	95	94.9095		1.70 h	K
Ru	44	96	95.9076	5.51		
101.07	44	97			2.90 d	K
	44	98	97.9055	1.87		
	44	99	98.9061	12.72		
	44	100	98.9042	12.62		
	44	101	100.9056	17.07		
	44	102	101.9043	31.63		
	44	103	102.9058		39.6 d	β^-
	44	104	103.9055	18.58		
	44	105	104.9075		4.44 h	β^-
	44	106	105.9073		367.0 d	β^-
Rhodium	45	102	101.9064		206.0 d	$K/\beta^+/\beta^-$
Rh	45	103	102.9055	100.00		
102.905	45	104	103.9064		43.0 s	β^-
Palladium	46	102	101.9056	0.96		
Pd	46	103	102.9058		17.0 d	K
106.400	46	104	103.9040	10.97		
	46	105	104.9051	22.23		
	46	106	105.9032	27.32		
	46	107	106.9049		7.0×10^6 y	β^-
	46	108	107.9039	26.71		
	46	109	108.9059		13.47 h	β^-
	46	110	109.9052	11.81		
	46	111	110.9076		22.0 m	β^-
Silver	47	106	105.9061		8.40 d	K
Ag	47	107	106.9051	51.82		
107.87	47	108	107.9059		2.20 m	β^-
	47	109	108.9047	48.18		
	47	110	109.9072		24.4 s	β^-
Cadmium	48	106	105.9065	1.22		
Cd	48	107	106.9064		6.50 h	K
112.40	48	108	107.9060	0.88		

Element Chemical symbol Atomic weight	Atomic number Z	Atomic mass number A	Isotopic mass, amu	Natural abundance, %	Half-life†	Type of decay†
	48	109	108.9048		450.0 d	K
	48	110	109.9030	12.39		
	48	111	110.9042	12.75		
	48	112	111.9028	24.07		
	48	113	112.9046	12.26		
	48	114	113.9036	28.85		
	48	115	114.9070		53.5 h	β^-
	48	116	115.9050	7.58		
	48	117	116.9076		2.40 h	β^-
Indium	49	113	112.9043	4.28		
In	49	114	113.9070		72.0 s	β^-
114.82	49	115	114.9041	95.72	6.0×10^{14} y	β^-
	49	116	115.9071		14.0 s	β^-
Tin	50	112	111.9048	1.01		
Sn	50	113			115.0 d	K
118.69	50	114	113.9030	0.67		
	50	115	114.9035	0.38		
	50	116	115.9017	14.70		
	50	117	116.9031	7.73		
	50	118	117.9018	24.30		
	50	119	118.9034	8.58		
	50	120	119.9022	32.40		
	50	121	120.9025		27.0 h	β^-
	50	122	121.9034	4.62		
	50	123	122.9037		42.0 m	β^-
	50	124	123.9052	5.61		
Antimony	51	120	119.9040		15.9 m	K
Sb	51	121	120.9038	57.25		
121.75	51	122	121.9035		2.80 d	β^-
	51	123	122.9041	42.75		
Tellurium	52	120	119.9040	0.089		
Te	52	122	121.9030	2.46		
127.60	52	123	122.9042	0.87		
	52	124	123.9028	4.61		
	52	125	124.9044	6.99		
	52	126	125.9032	18.71		
	52	127	126.9053		9.40 h	β^-
	52	128	127.9047	31.79		
	52	129	128.9066		69.0 m	β^-
	52	130	129.9062	34.48		
	52	131	130.9084		25.0 m	β^-
Iodine	53	126	125.9053		13.0 d	$K/\beta^+/\beta^-$
I	53	127	126.9044	100.00		
126.9044	53	128	127.9060		25.08 m	β^-
	53	129	128.9047		1.7×10^7 y	β^-
	53	130	129.9065		12.3 h	β^-
	53	131	130.9060		8.07 d	β^-

Element Chemical symbol Atomic weight	Atomic number Z	Atomic mass number A	Isotopic mass, amu	Natural abundance, %	Half-life†	Type of decay†
Xenon	54	124	123.9061	0.096		
Xe	54	125			17.0 h	K
131.30	54	126	125.9042	0.09		
	54	127	126.9055		36.41 d	K
	54	128	127.9035	1.92		
	54	129	128.9048	26.44		
	54	130	129.9035	4.08		
	54	131	130.9051	21.18		
	54	132	132.9042	26.89		
	54	133	132.9054		5.27 d	β^-
	54	134	133.9054	10.44		
	54	135			9.20 h	β^-
	54	136	135.9072	8.87		
Cesium	55	132	131.9060		6.50 d	K
Cs	55	133	132.9051	100.00		
132.905	55	134	133.9064		2.05 y	β^-
	55	137	136.9073		33.0 y	β^-
Barium	56	130	129.9062	0.101		
Ba	56	132	131.9050	0.097		
137.34	56	134	133.9043	2.42		
	56	135	134.9056	6.59		
	56	136	135.9044	7.81		
	56	137	136.9058	11.32		
	56	138	137.9050	71.66		
	56	139	138.9079		82.9 m	β^-
	56	140	139.9099		12.8 d	β^-
Lanthanum	57	138	137.9071	0.089	1.1×10^{11}	$K/\beta^+/\beta^-$
La	57	139	138.9064	99.911		
138.91	57	140	139.9085		40.22 h	β^-
	57	141	140.9095		3.90 h	β^-
Cerium	58	136	135.9071	0.19		
Ce	58	137			9.00 h	K
140.12	58	138	137.9060	0.25		
	58	139	138.9054		140.0 d	K
	58	140	139.9053	88.48		
	58	141	140.9069		33.0 d	β^-
	58	142	141.9093	11.08	5.0×10^{16} y	β^-
	58	143	142.9111		33.0 h	β^-
	58	144	143.9127		285.0 d	β^-
Praseodymium	59	140	139.9079		3.39 m	K
Pr	59	141	140.9077	100.00		
140.907	59	142	141.9087		19.2 h	β^-
	59	143	142.9096		13.7 d	β^-
Neodymium	60	142	141.9075	27.11		
Ne	60	143	142.9096	12.17		
144.24	60	144	143.9099	23.85		

Element Chemical symbol Atomic weight	Atomic number Z	Atomic mass number A	Isotopic mass, amu	Natural abundance, %	Half-life†	Type of decay†
	60	145	144.9122	8.30		
	60	146	145.9131	17.22		
	60	147			11.1 d	β^-
	60	148	147.9169	5.73		
	60	149	148.9169		1.73 h	β^-
	60	150	149.9207	5.62		
Promethium	61	146	145.9125		5.52 y	K/β^-
Pm	61	147	146.9152		2.50 y	β^-
———	61	148	147.9171		5.39 d	β^-
	61	149	148.9175		53.1 h	β^-
Samarium	62	144	143.9120	3.09		
Sm	62	145			340.0 d	K
150.35	62	146	145.9129		1.03×10^8 y	α
	62	147	146.9149	14.97	1.06×10^{11} y	α
	62	148	147.9146	11.24	8.0×10^{15} y	α
	62	149	148.9171	13.83	10^{16} y	α
	62	150	149.9173	7.44		
	62	151			93.0 y	β^-
	62	152	151.9195	26.72		
	62	153			46.8 h	β^-
	62	154	153.9220	22.71		
	62	155	154.9242		22.0 m	β^-
Europium	63	148	147.9182		54.5 d	K
Eu	63	151	150.9199	47.82		
151.96	63	153	152.9212	52.18		
	63	154	153.9240		8.20 y	β^-
	63	155	154.9219		4.76 y	β^-
Gadolinium	64	148	147.9181		93.0 y	α
Gd	64	149	148.9193		9.00 d	K
157.24	64	150	149.9185		1.8×10^6 y	α
	64	152	151.9198	0.20	1.1×10^{14} y	α
	64	154	153.9207	2.15		
	64	155	154.9226	14.73		
	64	156	155.9221	20.47		
	64	157	156.9239	15.68		
	64	158	157.9241	24.87		
	64	159			18.0 h	β^-
	64	160	159.9271	21.90		
	64	161			3.70 m	β^-
Terbium	65	158			150.0 y	K
Tb	65	159	158.9253	100.00		
158.925	65	160	159.9269		73.0 d	β^-
Dysprosium	66	156	155.9243	0.052		
Dy	66	157			8.10 h	K
162.50	66	158	157.9243	0.09		
	66	160	159.9252	2.29		

Element Chemical symbol Atomic weight	Atomic number Z	Atomic mass number A	Isotopic mass, amu	Natural abundance, %	Half-life†	Type of decay†
	66	161	160.9269	18.88		
	66	162	161.9268	25.53		
	66	163	162.9287	24.97		
	66	164	163.9291	28.18		
	66	165	164.9303		2.30 h	β^-
Holmium	67	164	163.9306		37.0 m	β^-/K
Ho	67	165	164.9303	100.00		
164.93	67	166			26.9 h	β^-
Erbium	68	162	161.9288	0.136		
Er	68	164	163.9293	1.56		
167.26	68	165			10.3 h	K
	68	166	165.9304	33.41		
	68	167	166.9320	22.94		
	68	168	167.9324	27.07		
	68	170	169.9355	14.88		
	68	171			7.50 h	β^-
Thulium	69	168			93.1 d	K
Tm	69	169	168.9344	100.00		
168.93	69	170			128.0 d	β^-
Ytterbium	70	168	167.9339	0.135		
Yb	70	170	169.9349	3.03		
173.04	70	171	170.9365	14.31		
	70	172	171.9366	21.82		
	70	173	172.9383	16.13		
	70	174	173.9390	31.84		
	70	175			101.0 h	β^-
	70	176	175.9427	12.73		
Lutecium	71	173			1.37 y	K
Lu	71	175	174.9409	97.41		
174.97	71	176	175.9427	2.59	3.0×10^{10} y	β^-
	71	177			6.70 d	β^-
Hafnium	72	174	173.9400	0.18	2.0×10^{15} y	α
Hf	72	175			70.0 d	K
178.49	72	176	175.9414	5.20		
	72	177	176.9435	18.50		
	72	178	177.9439	27.14		
	72	179	178.9460	13.75		
	72	180	179.9468	35.23		
	72	181			42.5 d	β^-
Tantalum	73	180	179.9475	0.0123		
Ta	73	181	180.9480	99.9877		
180.948	73	182	181.9475		115.0 d	β^-
Tungsten	74	180	179.9467	0.14		
W	74	181			121.0 d	K
183.85	74	182	181.9483	26.41		

Element Chemical symbol Atomic weight	Atomic number Z	Atomic mass number A	Isotopic mass, amu	Natural abundance, %	Half-life†	Type of decay†
	74	183	182.9503	14.40		
	74	184	183.9510	30.64		
	74	185			75.8 d	β^-
	74	186	185.9543	28.41		
	74	187	186.9530		24.0 h	β^-
Rhenium	75	185	184.9530	37.07		
Re	75	186	185.9515		90.0 h	β^-/K
186.207	75	187	186.9560	62.93	5.0×10^{10} y	β^-
	75	188	187.9565		16.7 h	β^-
Osmium	76	184	183.9526	0.018		
Os	76	185			94.0 d	K
190.20	76	186	185.9539	1.59	2.0×10^{15}	α
	76	187	186.9560	1.60		
	76	188	187.9560	13.30		
	76	189	188.9582	16.10		
	76	190	189.9586	26.40		
	76	191	190.8607		15.0 d	β^-
	76	192	191.9615	41.00		
	76	193	192.9650		31.0 h	β^-
Iridium	77	191	190.9606	37.30		
Ir	77	192	191.9636		74.0 d	β^-
192.22	77	193	192.9629	62.70		
	77	194	193.9647		19.2 h	β^-
Platinum	78	190	189.9600	0.0127	6.0×10^{11} y	α
Pt	78	191			3.0 d	K
195.09	78	192	191.9611	0.786	10^{15} y	α
	78	193	192.9640		50.0 y	K
	78	194	193.9628	32.90		
	78	195	194.9648	33.80		
	78	196	195.9650	25.30		
	78	197	196.9666		18.0 h	β^-
	78	198	197.9679	7.21		
Gold	79	196	195.9658		6.18 d	K/β^-
Au	79	197	196.9666	100.00		
196.967	79	198	197.9675		2.693 d	β^-
	79	199	198.9677		3.15 d	β^-
Mercury	80	196	195.9658	0.146		
Hg	80	197			65.0 h	K
200.59	80	198	197.9668	10.01		
	80	199	198.9683	16.84		
	80	200	199.9683	23.13		
	80	201	200.9703	13.22		
	80	202	201.9706	29.80		
	80	203	202.9719		46.57 d	β^-
	80	204	203.9735	6.85		
	80	205	204.9751		5.50 m	β^-

Element Chemical symbol Atomic weight	Atomic number Z	Atomic mass number A	Isotopic mass, amu	Natural abundance, %	Half-life†	Type of decay†
Thallium	81	203	202.9723	29.50		
Tl	81	204	203.9721		3.80 y	β^-
204.37	81	205	204.9745	70.50		
	81	206	205.9747		4.19 m	β^-
Lead	82	204	203.9730	1.48		
Pb	82	205	204.9731		1.4×10^7 y	K
207.18	82	206	205.9745	24.10		
	82	207	206.9759	22.10		
	82	208	207.9766	52.30		
	82	209	208.9798		3.30 h	β^-
	82	210	209.9842		21.0 y	β^-
Bismuth	83	208	207.9784		3.7×10^5 y	K
Bi	83	209	208.9804	100.00	2.0×10^{18} y	α
208.98	83	210	209.9841		5.01 d	β^-/α
	83	211	210.9873		2.15 m	α/β^-
Polonium	84	206	205.9805		8.80 d	K/α
Po	84	207	206.9816		5.70 h	K/α
———	84	208	207.9813		2.93 y	α/K
	84	209	208.9825		103.0 y	α/K
	84	210	209.9829		138.4 d	α
	84	211	210.9866		0.52 s	α
	84	212	211.9889		0.304 μs	α
	84	213	212.9928		4.120 μs	α
	84	214	213.9952		0.162 ms	α
	84	215	214.9995		1.780 ms	α
	84	216	216.0019		0.150 s	α
	84	218	218.0089		3.05 m	α
Astatine	85	210	209.9871		8.30 h	K/α
At	85	211	210.9875		7.20 h	K/α
———	85	212	211.9907		0.30 s	α
	85	213	212.9929		0.10 μs	α
	85	214	213.9963		2.00 μs	α
	85	215	214.9987		0.10 ms	α
	85	216	216.0024		0.30 ms	α
	85	217	217.0046		0.032 s	α
	85	218	218.0086		2.00 s	α
	85	219	219.0114		0.90 m	α
Radon	86	219	219.0095		4.00 s	α
Rn	86	220	220.0114		55.0 s	α
———	86	221	221.0154		25.0 m	β^-/α
	86	222	222.0175		3.823 d	α
Francium	87	220	220.0123		27.55 s	α
Fr	87	221	221.0142		4.80 m	α
———	87	222	222.0161		14.8 m	β^-
	87	223	223.0198		22.0 m	β^-

Element Chemical symbol Atomic weight	Atomic number Z	Atomic mass number A	Isotopic mass, amu	Natural abundance, %	Half-life†	Type of decay†
Radium	88	220	220.0110		0.023 s	α
Ra	88	221	221.0139		30.0 s	α
———	88	222	222.0154		38.0 s	α
	88	223	223.0186		11.43 s	α
	88	224	224.0202		3.65 d	α
	88	225	225.0219		14.8 d	β^-
	88	226	226.0254		1600.0 y	α
	88	227	227.0276		41.2 m	β^-
	88	228	228.0296		5.75 y	β^-
Actinium	89	225	225.0231		10.0 d	α
Ac	89	226	226.0261		29.0 h	β^-/α
———	89	227	227.0278		21.6 y	β^-
	89	228	228.0295		6.13 h	β^-
	89	229	229.0308		66.0 m	β^-
Thorium	90	227	227.0277		18.7 d	α
Th	90	228	228.0287		1.91 y	α
232.038	90	229	229.0316		7340 y	α
	90	230	230.0331		80,000 y	α
	90	231	231.0347		25.5 h	β^-
	90	232	232.0382	100.00	1.41×10^{10} y	α
	90	233	233.0387		22.2 m	β^-
	90	234			24.2 d	β^-
Protactinium	91	226	226.0278		1.80 m	α
Pa	91	227	227.0289		38.3 m	α/K
———	91	228	228.0310		22.0 h	K
	91	229	229.0321		1.50 d	K
	91	230	230.0345		17.4 d	K/β^-
	91	231	231.0359		33,500 y	α
	91	232	232.0371		1.31 d	β^-
	91	233	233.0384		27.0 d	β^-
	91	234	234.0414		6.75 h	β^-
	91	235	235.0438		23.7 m	β^-
Uranium	92	227	227.0309		1.30 m	α
U	92	228	228.0313		9.30 m	α/K
238.03	92	229	229.0335		58.0 m	K/α
	92	230	230.0339		20.8 d	α
	92	231	231.0363		4.30 d	K
	92	232	232.0372		73.6 y	α
	92	233	233.0395		1.65×10^5 y	α
	92	234	234.0409	0.006	2.4×10^5 y	α
	92	235	235.0439	0.720	7.1×10^8 y	α
	92	236	236.0457		2.39×10^7 y	α
	92	237	237.0469		6.75 d	β^-
	92	238	238.0508	99.274	4.51×10^9	α
	92	239	239.0526		23.5 m	β^-
	92	240	240.0546		14.1 h	β^-

Element Chemical symbol Atomic weight	Atomic number Z	Atomic mass number A	Isotopic mass, amu	Natural abundance, %	Half-life†	Type of decay†
Neptunium	93	231	231.0383		50.0 m	α
Np	93	233	233.0406		35.0 m	K
———	93	234	234.0419		4.40 d	K
	93	235	235.0441		410.0 d	K
	93	236	236.0466		22.0 h	β^-/K
	93	237	237.0480		2.14×10^6 y	α
	93	238	238.0494		2.10 d	β^-
	93	239	239.0513		2.35 d	β^-
	93	240	240.0537		63.0 m	β^-
	93	241	241.0558		16.0 m	β^-
Plutonium	94	232	232.0411		36.0 m	K/α
Pu	94	234	234.0433		9.00 h	K
———	94	235	235.0453		26.0 m	K
	94	236	236.0461		2.85 y	α
	94	237	237.0483		45.6 d	K
	94	238	238.0495		86.0 y	α
	94	239	239.0522		24,400 y	α
	94	240	240.0540		6580 y	α
	94	241	241.0568		14.7 y	β^-
	94	242	242.0587		3.79×10^5 y	α
	94	243	243.0601		5.0 h	β^-
	94	244	244,0642		8.0×10^7 y	α
Americium	95	240	240.0552		51.0 h	K
Am	95	241	241.0567		458.0 y	α
———	95	242	242.0574		16.0 h	β^-/K
	95	243	243.0614		7370 y	α
	95	244	244.0625		10.1 h	β^-
	95	245	245.0648		2.10 h	β^-
Curium	96	238	238.0530		2.50 h	K/α
Cm	96	240	240.0555		26.8 d	α
———	96	241	241.0577		32.8 d	K
	96	242	242.0588		163.0 d	α
	96	243	243.0614		28.5 y	α
	96	244	244.0629		17.6 y	α
	96	245	245.0653		8500 y	α
	96	246	246.0674		4730 y	α
Berkelium	97	245	245.0664		4.98 d	K
Bk	97	246	246.0672		1.80 d	K
———	97	247	247.0702		1400 y	α
	97	248	248.0730		9.0 y	β^-/K
	97	249	249.0750		314.0 d	β^-
Californium	98	244	244.0659		20.0 m	α
Cf	98	245	245.0680		44.0 m	K/α
———	98	246	246.0688		36.0 h	α
	98	247	247.0690		3.2 h	K
	98	248	248.0724		350.0 d	α

Element Chemical symbol Atomic weight	Atomic number Z	Atomic mass number A	Isotopic mass, amu	Natural abundance, %	Half-life†	Type of decay†
	98	249	249.0748		360.0 y	α
	98	250	250.0766		13.0 y	α
Einsteinium	99	251	251.0800		1.50 d	K
Es	99	252	252.0829		471.0 y	α
———	99	253	253.0847		20.47 d	α
	99	254	254.0881		276.0 d	α/β^-
	99	255	255.0900		38.4 d	β^-
Fermium	100	250	250.0795		30.0 m	α
Fm	100	252	252.0827		23.0 h	α
———	100	253	253.0852		3.00 d	K/α
	100	254	254.0870		3.20 h	α
	100	255	255.0899		20.1 h	α
Mendelevium	101	255	255.0911		27.0 m	K/α
Mv	101	256	256.0939		76.0 m	K
———	101	257	257.0956		5.20 h	K/α
	101	258	258.0986		55.0 d	α
Nobelium	102	255	255.0933		3.10 m	α
No	102	256	256.0943		3.20 s	α
———	102	257	257.0969		26.0 s	α
Lawrencium	103	255	255.0969		22.0 s	α
Lr	103	256	256.0986		31.0 s	α
———	103	258	258.1018		5.40 s	α
Rutherfordium	104	257	257.1030		4.80 s	α
‡	104	259	259.1057		3.20 s	α
———	104	261	261.1087		65.0 s	α
Hahnium	105	260	260.1213		1.50 s	α/SF
‡	105	261	261.1121		1.80 s	α/SF
———	105	262	262.1138		40.0 s	α

† Abbreviations used in this table. For half-lives; s = seconds, m = minutes; h = hours; d = days; y = years. For types, of radioactive decay: α = alpha decay; β^- = beta decay; β^+ = positron decay; p = proton decay; K = K-capture decay; SF = spontaneous fission.

‡ See footnote at end of App. J.

APPENDIX L

RADIOISOTOPE FUELS

Radioisotope and half-life†	Active material	Mass fraction of radioisotope in material	Melting point, °C‡	Specific power, kW/kg‡	Power density, kW/L‡
$^{90}_{38}Sr$	Metal	55.0% Sr-90	772	0.50	1.28
$t_{1/2} = 28.1$ y	$SrTiO_3$	24.5% Sr-90	1910	0.23	1.17
	SrO	44.0% Sr-90	2457	0.42	1.94
	SrF_2	36.0% Sr-90	1463	0.34	1.44
	$SrTiO_4$	31.5% Sr-90	1860	0.30	1.48
$^{137}_{55}Cs$	CsCl	28.9% Cs-137	645	0.12	0.37
$t_{1/2} = 33.0$ y	$CsSO_4$	26.9% Cs-137	1019	0.11	0.46
$^{144}_{58}Ce$	Ce_2O_3	10.8% Ce-144	2190	2.76	19.0
$t_{1/2} = 285.0$ d	Ce_2O_2S	10.3% Ce-144	1890	2.64	15.8
	Ce_2S_3	9.0% Ce-144	1437	2.31	14.3
$^{147}_{61}Pm$	Metal	95.0% Pm-147	865	0.31	2.30
$t_{1/2} = 2.50$ y	Pm_2O_3	78.0% Pm-147	2130	0.27	1.87
$^{210}_{84}Po$	Metal	95.0% Po-210	254	144.00	1324.0
$t_{1/2} = 138.4$ d	GdPo-Ta (98%)	1.06% Po-210	1675	1.60	16.6
	GdPo-Ta (91%)	4.95% Po-210	1675	7.50	77.2
$^{238}_{94}Pu$	Metal	80.0% Pu-238	600	0.45	6.80
$t_{1/2} = 86.0$ y	PuO_2	71.0% Pu-238	2150	0.40	2.70
	PuC	74.6% Pu-238	1654	0.42	5.70
	PuN	74.6% Pu-238	2570	0.42	6.20
	PuZr	73.0% Pu-238	730	0.41	5.60
	PuZr	77.0% Pu-238	615	0.44	6.50

APPENDIX M

SOLAR CONSTANTS (FOR NORTHERN LATITUDES)

Date	Angle of declination δ	Equation of time, min	A_S,† W/m²‡	B_S,† am§	C_S†	Day of year
January						
1	−23.0	−3.6	1231	0.142	0.057	1
11	−21.7	−8.0	1230	0.142	0.058	11
21	−19.6	−11.4	1229	0.142	0.058	21
31	−17.3	−13.5	1224	0.142	0.058	31
February						
1	−17.0	−13.6	1223	0.143	0.059	32
11	−13.9	−14.4	1218	0.143	0.059	42
21	−10.4	−13.8	1213	0.144	0.060	52
28	−7.6	−12.6	1206	0.147	0.063	59
March						
1	−7.4	−12.5	1205	0.148	0.063	60
11	−3.5	−10.2	1195	0.152	0.067	70
21	0.0	−7.4	1185	0.156	0.071	80
31	4.3	−4.3	1169	0.164	0.079	90
April						
1	4.7	−4.0	1167	0.165	0.080	91
11	8.5	−1.1	1151	0.172	0.088	101
21	12.0	1.2	1135	0.180	0.096	111
30	14.9	2.8	1126	0.185	0.104	120

Radioisotope and half-life†	Active material	Mass fraction of radioisotope in material	Melting point, °C‡	Specific power, kW/kg‡	Power density, kW/L‡
$^{242}_{96}Cm$ $t_{1/2} = 163.0$ d	Cm_2O_3-AmO_2	35.7% Cm-242	2000	42.80	500.00
$^{244}_{96}Cm$ $t_{1/2} = 17.6$ y	Metal	95.5% Cm-244	1340	2.67	36.00
	Cm_2O_3	86.9% Cm-244	1950	2.42	26.10
	Cm_2O_2S	84.4% Cm-244	2000	2.35	23.30
	CmF_3	77.5% Cm-244	1406	2.15	21.10

† y = years; d = days.
‡ 1 kW/kg = 0.4536 W/lbm; 1 kW/L = 28.31 kW/ft^3; °F = 1.8°C + 32.
Source: From G. L. Tuve and R. E. Bole, *Handbook of Tables for Applied Engineering Science*, The Chemical Rubber Company, Cleveland, Ohio, 1970, p. 348.

Date	Angle of declination δ	Equation of time, min	A_S,† W/m²‡	B_S,† am§	C_S†	Day of year
May						
1	15.2	2.9	1125	0.186	0.105	121
11	17.9	3.7	1114	0.191	0.113	131
21	20.3	3.6	1103	0.196	0.121	141
31	22.0	2.5	1098	0.199	0.125	151
June						
1	22.1	2.4	1097	0.199	0.126	152
11	23.1	0.6	1092	0.202	0.130	162
21	23.45	−1.5	1087	0.205	0.134	172
30	23.1	−3.4	1086	0.206	0.135	181
July						
1	23.1	−3.4	1086	0.206	0.135	182
11	22.1	−5.6	1085	0.206	0.135	192
21	20.6	−6.2	1084	0.207	0.136	202
31	18.1	−6.2	1091	0.205	0.132	212
August						
1	17.9	−6.2	1092	0.205	0.132	213
11	15.2	−5.1	1099	0.203	0.126	223
21	12.0	−3.1	1106	0.201	0.122	233
31	8.7	−1.5	1120	0.193	0.113	243
September						
1	8.2	0.0	1122	0.192	0.112	244
11	4.4	3.3	1136	0.185	0.097	254
21	0.0	6.8	1150	0.177	0.092	264
30	−2.9	9.9	1162	0.172	0.086	273
October						
1	−3.3	10.2	1164	0.171	0.086	274
11	−7.2	13.1	1177	0.166	0.079	284
21	−10.8	15.3	1191	0.160	0.073	294
31	−14.3	16.2	1200	0.157	0.070	304
November						
1	−14.6	16.3	1201	0.156	0.069	305
11	−17.5	15.9	1211	0.153	0.066	315
21	−20.0	15.1	1220	0.149	0.063	325
30	−21.7	11.3	1224	0.147	0.061	334
December						
1	−21.9	11.0	1224	0.147	0.061	335
11	−23.0	6.8	1228	0.144	0.059	345
21	−23.45	2.0	1232	0.142	0.057	355
31	−23.1	−3.1	1231	0.142	0.057	365

† A is the apparent solar irradiation at air mass zero (outside the earth's atmosphere).
B is the atmospheric extinction coefficient, in units of (standard atmosphere)$^{-1}$.
C is the ratio of the diffuse to direct normal irradiation on a horizontal surface.
‡ 1 W/m² = 0.3173 Btu/h · ft².
§ am = units of standard air mass.
Source: Reprinted, with permission, from the *Handbook and Product Directory, Applications Volume*, ASHRAE, New York, 1974.

APPENDIX N

SOLAR POSITION AND IRRADIATION VALUES

(For 40° N. Lat.; 1.0 clearness factor; 0 percent ground reflectance)

			Solar position angles		Total solar insolation, W/m²†		
	Solar time						
Date	a.m.	p.m.	Altitude $\lvert\beta_1\rvert$	Azimuth $\lvert\alpha_1\rvert$	Direct normal	Horizontal	South-facing vertical
Jan. 21	8	4	8.1	55.3	448	88	265
	9	3	16.9	44.0	753	262	539
	10	2	23.9	30.9	864	400	703
	11	1	28.5	16.1	911	485	797
	12		30.1	0.0	927	517	829
	Surface daily totals, Wh/m²†				6878	2988	5440
Feb. 21	7	5	4.4	72.2	217	32	69
	8	4	15.0	61.8	706	230	337
	9	3	24.5	49.8	863	416	526
	10	2	32.3	35.5	930	561	662
	11	1	37.5	18.7	961	649	744
	12		39.4	0.0	971	681	772
	Surface daily totals, Wh/m²†				8321	4457	5453

Date	Solar time a.m.	Solar time p.m.	Solar position angles: Altitude $\lvert\beta_1\rvert$	Solar position angles: Azimuth $\lvert\alpha_1\rvert$	Total solar insolation, W/m²†: Direct normal	Total solar insolation, W/m²†: Horizontal	Total solar insolation, W/m²†: South-facing vertical
Mar. 21	7	5	11.4	80.2	539	145	110
	8	4	22.5	69.6	788	359	281
	9	3	32.8	57.3	889	545	435
	10	2	41.6	41.9	936	687	555
	11	1	47.7	22.6	961	779	630
	12		50.0	0.0	968	810	656
	Surface daily totals, Wh/m²†				9191	5838	4678
Apr. 21	6	6	7.6	99.2	281	63	13
	7	5	19.1	89.7	649	274	38
	8	4	30.5	79.5	794	479	167
	9	3	41.5	67.5	864	652	293
	10	2	51.4	51.7	901	788	397
	11	1	58.9	29.4	920	873	463
	12		61.9	0.0	924	905	485
	Surface daily totals, Wh/m²†				9746	7168	3221
May 21	5	7	2.1	115.0	3	0	0
	6	5	12.9	105.8	454	154	28
	7	6	24.1	96.9	681	359	41
	8	4	35.6	87.5	788	552	79
	9	3	47.0	76.4	842	716	189
	10	2	57.7	61.3	873	842	280
	11	1	66.5	37.5	892	924	340
	12		70.3	0.0	895	949	359
	Surface daily totals, Wh/m²†				9960	8044	2282
June 21	5	7	4.2	117.3	69	13	3
	6	6	14.8	108.4	489	189	32
	7	5	26.0	99.7	681	388	44
	8	4	37.4	90.7	775	574	50
	9	3	48.8	80.2	829	734	148
	10	2	59.8	65.8	857	857	233
	11	1	69.2	41.9	873	933	290
	12		73.5	0.0	879	958	309
	Surface daily totals, Wh/m²†				10023	8346	1923
July 21	5	7	2.3	115.1	6	0	0
	6	6	13.0	106.0	435	158	28
	7	5	24.3	97.1	656	359	44
	8	4	35.7	87.7	760	548	76
	9	3	47.1	76.6	816	709	183
	10	2	57.8	61.6	848	835	271
	11	1	66.7	37.7	867	914	328
	12		70.5	0.0	870	939	350
	Surface daily totals, Wh/m²†				9651	7987	2213

Date	Solar time a.m.	Solar time p.m.	Solar position angles: Altitude $\lvert\beta_s\rvert$	Solar position angles: Azimuth $\lvert\alpha_s\rvert$	Total solar insolation, W/m²†: Direct normal	Total solar insolation, W/m²†: Horizontal	Total solar insolation, W/m²†: South-facing vertical
Aug. 21	6	6	7.7	99.3	255	66	16
	7	5	19.2	90.1	602	274	38
	8	4	30.6	79.7	747	473	158
	9	3	41.6	67.7	820	646	281
	10	2	51.6	51.9	857	775	378
	11	1	59.1	29.5	876	860	441
	12		62.1	0.0	883	889	463
	Surface daily totals, Wh/m²†				9191	7073	3083
Sept. 21	7	5	11.4	80.2	469	136	101
	8	4	22.5	69.5	725	344	265
	9	3	32.8	57.3	829	526	416
	10	2	41.6	41.6	883	665	530
	11	1	47.7	22.6	905	753	605
	12		50.0	0.0	914	785	630
	Surface daily totals, Wh/m²†				8536	5636	4463
Oct. 21	7	5	4.3	72.1	151	22	50
	8	4	14.9	61.7	643	214	315
	9	3	24.4	49.7	810	397	504
	10	2	32.4	35.5	882	536	640
	11	1	37.4	18.7	917	627	722
	12		39.3	0.0	927	656	750
	Surface daily totals, Wh/m²†				7735	4249	5213
Nov. 21	8	4	8.1	55.3	429	88	255
	9	3	16.9	44.0	731	258	526
	10	2	23.9	30.9	845	397	690
	11	1	28.5	16.1	892	482	782
	12		30.1	0.0	908	514	813
	Surface daily totals, Wh/m²†				6707	2969	5314
Dec. 21	8	4	5.5	53.0	281	44	177
	9	3	14.0	41.9	684	205	514
	10	2	20.7	29.4	823	337	697
	11	1	25.0	15.2	883	422	794
	12		26.6	0.0	898	451	829
	Surface daily totals, Wh/m²†				6235	2465	5188

† 1 W/m² = 0.3173 Btu/h · ft²; 1 Wh/m² = 0.09289 Wh/ft² = 0.3173 Btu/ft².

Source: Reprinted, with permission, from the *Handbook and Product Directory, Applications Volume*, ASHRAE, New York, 1974.

APPENDIX O

VARIATION OF SOLAR RADIATION WITH LATITUDE

(For northern latitudes)

Date	Latitude, degrees	Direct normal irradiation, Wh/m²†	Total horizontal irradiation, Wh/m²†	Date	Latitude, degrees	Direct normal irradiation, Wh/m²†	Total horizontal irradiation, Wh/m²†
Jan. 21	24	8,718	5,113	Apr. 21	24	9,569	7,735
$\delta = -19.6°$	32	7,748	4,060	$\delta = +12.0°$	32	9,696	7,533
	40	6,878	2,988		40	9,746	7,168
	48	5,390	1,879		48	9,696	6,638
	56	3,549	889		56	9,532	5,954
	64	965	142		64	9,399	5,182
Feb. 21	24	9,569	6,298	May 21	24	9,557	8,057
$\delta = -10.4°$	32	9,053	5,434	$\delta = +20.3°$	32	9,809	8,138
	40	8,321	4,457		40	9,960	8,044
	48	7,344	3,404		48	10,257	7,823
	56	6,260	2,332		56	10,528	7,483
	64	4,514	1,261		64	10,937	7,048
Mar. 21	24	9,702	7,155	June 21	24	9,437	8,113
$\delta = 0.0°$	32	9,494	6,569	$\delta = +23.45°$	32	9,721	8,302
	40	9,191	5,838		40	10,023	8,346
	48	8,763	4,974		48	10,439	8,277
	56	8,151	3,997		56	10,837	8,075
	64	7,237	2,938		64	11,505	7,842

Date	Latitude, degrees	Direct normal irradiation, Wh/m²†	Total horizontal irradiation, Wh/m²†	Date	Latitude, degrees	Direct normal irradiation, Wh/m²†	Total horizontal irradiation, Wh/m²†
July 21	24	9,242	7,962	Oct. 21	24	9,040	6,077
$\delta = +20.6°$	32	9,494	8,063	$\delta = -10.8°$	32	8,498	5,213
	40	9,651	7,987		40	7,735	4,249
	48	9,954	7,798		48	6,789	3,221
	56	10,212	7,477		56	5,686	2,169
	64	10,628	7,086		64	3,902	1,128
Aug. 21	24	9,027	7,590	Nov. 21	24	8,529	5,075
$\delta = +12.0°$	32	9,147	7,414	$\delta = -20.0°$	32	7,584	4,035
	40	9,191	7,073		40	6,707	2,969
	48	9,134	6,575		48	5,257	1,879
	56	8,983	5,938		56	3,448	895
	64	8,851	5,188		64	952	145
Sept. 21	24	9,071	6,915	Dec. 21	24	8,271	4,646
$\delta = 0.0°$	32	8,851	6,348	$\delta = -23.45°$	32	7,401	3,581
	40	8,536	5,636		40	6,235	2,465
	48	8,094	4,797		48	4,551	1,406
	56	7,464	3,845		56	2,357	492
	64	6,537	2,811		64	76	6

† $Wh/m^2 = 0.09289\ Wh/ft^2 = 0.3173\ Btu/ft^2$.

Source: Reprinted, with permission, from the *Handbook and Product Directory, Applications Volume*, ASHRAE, New York, 1974.

INDEX

Absorber control, 176, 177, 261
Absorption, electromagnetic, 123
Absorption cross sections and reactions, 147–149, 151, 165, 166, 286, 299, 305
Absorptivity (emissivity), 106, 443
Abundances, 75, 525–541
Ac motors:
  induction motors, 411–415
  synchronous motors, 411, 415–416
ACES (annual cyclic energy storage), 495
Activation, 86–88, 91
Activation products, 73, 91
Activity, 74
Actual air-fuel ratio, 126–140
Afterburner, 472
Air:
  combustion, 126–129
  composition, 126
Air compressors, 189, 193
  dynamic, 193–195
  free-piston, 356–357
  positive-displacement, 193
Air-fuel ratios:
  actual, 126–140
  theoretical, 126–129
Air mass, 104, 545
Air-pollution control:
  gaseous control, 319, 321, 329–333
  legislative requirements, 319, 321
  particulate removal, 319, 321–329
Air preheaters, 221, 228–234
  recuperative, 229–232
  regenerative, 229–233
Alicyclic hydrocarbons, 48–50
Aliphatic hydrocarbons, 48–49
Alkane hydrocarbons, 48–49
Alkene hydrocarbons, 48, 49
Alkyne hydrocarbons, 48, 49
Alpha decay and emitters, 71, 463
Alpha-neutron source, 173
Alpha power sources, 77, 542–543
Alternators, 428, 464–466
Altitude angle, 103, 104, 544–545
Angles, solar, 99–103
Annihilation, 7, 72
Annual cyclic energy storage (ACES), 495
Annuity equation, 22
Apparent sun time, 98, 99
Aqueous electrolyte batteries, 492
Aromatic hydrocarbons, 48–50
Ash, 52–54, 60, 511–513
  deposition, 60, 229

Ash (*Cont.*):
disposal, 209, 212, 217, 338
removal, 230, 232
softening temperature, 54–55
Atkinson power cycle, 356
Atmospheric extinction coefficient, 104, 544–545
Atom:
mass, 67, 525–541
nucleus, 67
number of, 75
Atomic energy (*see* Nuclear energy)
Atomic Energy Commission, 251
Atomic mass, 67, 525–541
Atomic mass number, 66
Atomic mass unit, 67
Atomic number, 66
Atomization, 204–205
Attemperator, 228
Availability factor, 31
Average-neutron lifetime, 286
Avogadro's number, 75, 451, 498
Axial-flow fans, 194
Azimuth angle:
of sun, 101, 544–545
of surface, 103

Babcock and Wilcox pressurized-water reactor, 252, 253
Baghouse filters, 217, 326–329
Barium titanate, 446
Batteries, 447, 461, 463, 465, 489–490
primary, 447, 489
secondary, 447, 489
Becker-nozzle process, 85
Becquerel, 15
Benson boiler, 223, 225–226
Beryllium, 172
Beryllium oxide, 172, 475
Beta decay and emitters, 71–72, 463
Beta power sources, 77, 542
Binary Rankine power cycle, 374
Binding energy, 68, 82, 89
Binding energy per nucleon, 68
Biological shielding, 179–180
Biomass fuel, 8, 43–47, 366, 506–507
Bismuth telluride, 430, 439
Blast-furnace gas, 65, 134, 520
Blowdown, 223
Blue-flame combustion, 140
Boilers:
classification, 221–226
definition of, 219–220
efficiency, 234–235, 335
feed pumps, 189–192
fire-tube, 221–222
forced-circulation, 223, 225–226
horsepower, 234
losses, 235–239, 334
natural-circulation, 222–224
nuclear, 160, 252, 255, 257
packaged, 222
primary heat-transfer surfaces, 221, 226–228
rating, 234–239
secondary heat-transfer surfaces, 221, 228–234
testing, 239
water-tube, 221–226
Boiling heat transfer, 260
Boiling-water reactors (BWRs), 160, 162, 177, 251, 256–262, 295
comparison, 256
control, 258
dual cycle, 256–257
fuel elements, 261
pressure vessel, 258–259
operation parameters, 258
single-cycle, 162, 258
Boltzmann's constant, 440, 498
Boron:
absorber control rods, 177, 308
burnable poison, 308
fusion fuel, 90
Boron trifluoride, 176
Brake horsepower, 361–362, 364–365
Brake specific fuel consumption, 366
Brayton power cycle, 164, 226, 264, 366–374, 389
closed cycle, 367, 368
engines, 368
multistage compression, 369–371
open cycle, 367–368
regenerative, 368–369
reheat, 371–372
simple, 368
Breakdown voltage, 474
Breeder reactors, 88, 155, 338, 493

Breeding, 88, 153
Breeding ratio, 88, 153, 154
Buckling, reactor, 169
Burnable poison, 308
Burners, fossil fuel:
  coal, 206–219
  gas, 202–204
  oil, 204–206
Burning-bed combustion, 141, 206–213, 217–219
Burnout heat flux, 260, 267
Burnup, reactor fuel, 158, 304–306
Burnup rate by neutrons, 299
"Buzz" bomb, 358–359
Byproduct fuel gases, 64, 520

Cadmium-sulfide solar cells, 460
CANDU reactors, 161, 165, 172
Capacitors, 5, 488, 489.
Capacity factor, 31
Capital costs, 21–24
Capital energy, 7, 11
Capital recovery factor, 29, 30
Capture-gamma radiation, 80
Capture reactions, 73, 79, 80, 85, 88, 147, 173
Carbohydrate compounds, 14, 47
Carbon:
  as fuel, 48, 53, 125, 237
  as moderator, 160, 164, 171, 262
  in refuse, 54, 131–132, 237
Carbon dioxide, 124–126, 130, 133, 318, 368, 449, 450
Carbon monoxide, 125, 130, 133, 353, 368, 455
Carnot power cycle, 348–349
Catalyst, 442
Cavitation, 191
Centrifugal fans, 193–194
Ceramic reactor fuel, 171, 278
Cesium thermionic converter, 445
Cetane rating, 50, 51
Chain hydrocarbon compounds, 48–49
Chain reaction, 80
Charge carriers, 456
Charge conservation, 66
Chemical element, 66
Chemical energy, 5–7, 124–141, 219, 234, 481, 490–492
Chemical energy (*Cont.*):
  conversion of:
    into electrical energy, 428, 447–455
    into mechanical energy, 345
    into thermal energy, 124–141
  reactions, 6, 124–126, 449–450, 491
  storage, 490–492
Chernobyl nuclear accident, 19, 160, 249
Chimney, 195
Cinder catchers, 323
Cladding, 159, 171, 178, 276–279
Clean-Air Act of 1970, 319
Clearness number, 104, 105
Closed feedwater heaters, 380, 381
Coal, 16, 17, 51–58, 60, 65, 319, 366
Coal analyses, 52–53, 511–513
  as-burned, 52
  as-received, 52
  ASTM classification, 51–53
  bed-moisture basis, 52
  dry:
    ash-free, 52, 511–513
    Mm-free, 53, 509, 510
  proximate, 53, 511–513
  ultimate, 52, 133, 511–513
Coal formation, 51
Coal furnaces (*see* Furnaces, coal-fired)
Coal-oil mixtures (COM), 60
Coal properties:
  ash-softening temperature, 54, 55
  caking properties, 54
  grindability index, 54
  higher heating value (HHV), 53, 56, 59, 61, 62, 511–513
  lower heating value (LHV), 56
  weatherability, 54
Coal pulverizers:
  actions, 213
  types, 213–214
Coal rate, 3
Coal reserves, 14
Coefficient of performance, 435
Coefficients of reactivity (*see* Reactivity coefficients)
Cogeneration, 30
Coke-oven gas, 65, 520
Cold fusion:
  hydride fusion, 96–97
  muon fusion, 96

Collection efficiency, 322
Collection systems, solar, 108–113
Combination firing, 213
Combined-cycle power plants, 226, 374, 388–392
Combustion, 7, 124–125
Combustion-air requirements, 129–134
Combustion Engineering, 252, 253
Combustion mechanics, 140–141
Combustion methods, 141
Combustion reactions, 124–126
Combustion systems:
  biomass-fired, 43–47
  coal-fired, 206–219
  gas-fired, 202–204
  oil-fired, 204–206
Commercial power reactors, 158
Compact-power reactors, 157
Compensated-ion chamber, 176
Compound excited nucleus, 79, 80
Compound-interest formula, 22
Compressed-air energy storage (CAES), 487, 488
Compressed-fluid energy, 481, 487–488
Compression ratio, 354, 355
Compressor (*see* Air compressors)
Compressor pressure ratio, 368
Concentration polarization loss, 453
Condenser, 334, 335, 374–376
Condenser power, 334, 335
Conductivity, 277, 432
Conservation:
  of charge, 66
  of momentum, 66, 70, 96
  of nucleons, 66
  of sum of mass and energy, 3, 66, 70
Constants, physical, 498–499
Construction costs, 21, 27
Construction work in progress (CWIP), 29, 32
Containment:
  primary, 177
  secondary, 180–182
Control reactor, 158, 176–177, 253, 257, 258, 308
Control systems, 176–177, 253, 258, 308
Conversion:
  of fertile material, 88–89
  limiting value, 89
Conversion factors, 500–505
Conversion ratio, 88, 167, 305
Converter reactors, 88, 167
Coolant, alternator, 466
Coolants, reactor, 160–165, 173
Cooling lakes and ponds, 335
Cooling towers, 335–337
Cooling water requirements, 335, 339–340
Core, reactor, 170–177
Core power distributions, 267–274
Corona discharge, 473
Cosmic radiation, 72, 73
Cost evaluation:
  capital costs, 21–24
  operating costs, 21, 24–25
  power costs, 25–30
Cracking, 141, 455
Crey's-Malville fast-breeder reactor, 265, 266
Critical equation, 169, 295, 296, 308
Critical heat flux, 260, 267
Critical mass, 142
Critical point, 223
Critical reactor, 142, 167, 284
Cross section, nuclear:
  absorption, 147–149
  average, 148–149
  capture, 144, 147
  dependence on energy, 148–149
  elastic scattering, 148
  fission, 144, 147
  inelastic scattering, 148
  macroscopic, 146
  microscopic, 144–146
  (n,α) reaction, 147
  (n,p) reaction, 147
  $(n,2n)$ reaction, 147
  radiative capture, 144, 147
  resonance, 149–150
  scattering, 147, 148, 171
  threshold, 148
  total, 148, 153
  values, 151
Crude oil (*see* Petroleum)
Curie, 75
Curie point, 446
Current density, 440, 456, 461, 467

Curtis staging, 397, 398
Cutoff ratio, 355, 356
Cycle, heat-engine:
  Atkinson, 357
  binary, 374
  Brayton (*see* Brayton power cycle)
  Carnot, 348–349
  closed, 367, 368
  combined, 226, 374, 388–392
  Diesel, 354–356
  Ericcson, 348–350
  external combustion, 350, 366–388
  externally reversible, 347–353
  figure of merit, 347
  gas power, 366
  internal combustion, 353–366
  internally reversible, 353
  Lenoir, 356–358
  limited-pressure, 356
  open, 367–368
  Otto, 353–356
  Rankine, 226, 374–378
  regenerative, 368–369, 380–383
  reheat, 371–372, 378–380
  reversible, 347–353
  Stirling, 348, 350–353, 366, 367
  vapor power, 367, 374–388
Cyclone furnace, 141, 209, 212–213, 324
Cyclone scrubber, 323–325
Cylindrical fuel elements, 171, 251, 278–281

Damage, radiation, 91, 154, 162, 170
Daylight savings time, 99
Dc generators, 465
Dc motors, 411–412
Deaerating feedwater heater, 381–382
Decay (*see* Radioactive decay)
Decay constant, 74, 299
Decay-heat removal, 81
Decay rate, 73–76, 299
Declination angle, 99–100, 546–548
Delayed-neutron precursors, 286, 287, 290
Delayed neutrons, 286, 287, 289
Delayed temperature coefficient, 295
Departure from nucleate boiling (DNB), 260, 267
Depleted uranium, 82, 85
Depreciation, 32
Desuperheater, 228
Detectors, neutron, 174, 176
Detonation, 51, 354
Deuterium:
  as fusion fuel, 90–91
  as neutron moderator, 172
Dew-point temperature, 202, 228
Dielectric constant, 446
Diesel power cycle, 354–356
Diffusion length, 169, 295
Dilution coefficient, 130
Direct energy conversion, 428, 475
Dissociation, 126
Dollar as unit of reactivity, 292
Doppler broadening, 150, 294
Double-alkali FGD (flue-gas desulfurization) system, 332
Doubling time:
  breeder reactors, 88
  growth rates, 19
Downcomers, 223, 224
Draft systems, 195–202
Dry-bottom furnaces, 217
Dry cooling towers, 337
Dry-gas loss, boiler, 235
Dual-cycle BWR (boiling-water reactor), 256–257
Dulong's formula, 56
DuPont laboratory tests, 388, 389
Dynamic compressors, 193–195
Dynamometer, 361–362

Earth's orbital motion, 99–100
Ecliptic plane, 99
Ecology problems, 3, 47, 54, 129–130, 317–318
Economics, energy, 21–30
Economizer, 221, 228–229
Effectiveness, regenerator, 369
Efficiency:
  boiler, 235, 239, 335
  brake thermal, 366
  combined cycle, 388–389, 467
  compressor, 189, 365
  conversion, 13
    EGD, 474
    fuel cell, 452
    MHD, 468
    solar cell, 462

Efficiency (*Cont.*):
mechanical, 189, 365
pump, 189, 365, 377
thermal (*see* Thermal efficiency)
turbine, 190, 365, 377
volumetric, 366
Einstein's mass-energy relationship, 3
Elastic scattering, 148
Elastic-strain energy, 5, 481, 484–485
Electric field, 5, 488–489
Electric generators, 463–466
Electric motors, 410–416
Electrical energy, 5, 16, 17, 19, 123, 345, 428–475, 481, 488–490
conversion of:
into mechanical energy, 345, 409–417
into thermal energy, 123
generation and consumption, 17–19
production of, 428–475
stored forms, 5, 481, 488–490
Electrical resistance, 123, 431
Electrical resistivity, 431, 469, 471
Electrodes, 447
Electrogasdynamic (EGD) converter, 466, 472–475
Electrolytes, 447, 490
Electromagnetic energy, 5–6, 96, 345, 428
conversion of:
into electrical energy, 428, 456–462
into mechanical energy, 345
into thermal energy, 123–124
energy relationships, 6
solar, 99–114, 456
spectrum, 6
Electromagnetic isotope separation, 82
Electromagnetic pump, 416–417
Electron, 66, 71, 72
Electron emission, 440
Electron flow, 5, 409
Electrostatic converters, 472–475
Electrostatic field energy, 5, 472, 481, 488–489
Electrostatic precipitator, 217, 324–326
Element, 66, 523–524
Emergency core cooling system (ECCS), 81
Emissivity, 105, 106, 443
Endothermic reactions, 7, 126, 490, 491, 493
Energy:
annihilation, 7, 72
atomic (*see* Nuclear energy)
binding, 68, 73, 79, 80, 89, 90
capital, 7
chemical (*see* Chemical energy)
classification, 4–7
compressed fluid, 5, 481, 487–488
conservation of, 3, 66, 70
consumption, 1, 2, 14–19
decay, 71
economics, 21–30
electrical (*see* Electrical energy)
electromagnetic (*see* Electromagnetic energy)
electrostatic field, 5, 472, 481, 488–489
fission, 7, 79–89, 142
geothermal, 8, 11–13
gravitational, 5, 8, 481, 486–487
growth rates, 19–21
heat, 7
hydro, 8, 14, 17, 399–401
hydrothermal, 11
income, 7
inductive field, 5, 481, 489
inertial field, 5, 70, 416, 481–484
kinetic, 5, 70, 416, 481–484
latent heat, 7, 56, 481, 493, 494
lunar, 8
mass dependence, 3
mechanical (*see* Mechanical energy)
nuclear (*see* Nuclear energy)
ocean thermal gradient, 8, 9
petrothermal, 11
potential, 5, 392, 466–475
radioactive decay, 7, 16, 69–79, 142, 492, 542–543
requirements in the future, 16–17
reserves, 13–14
sensible heat, 7, 481, 493, 494
solar (*see* Solar energy)
stored, 4, 5, 481–495
thermal (*see* Thermal energy)
tidal, 8, 14
transitional, 4
utilization, 14–17
wave, 8

Energy (*Cont.*):
wind, 8, 405–409
work, 5
Energy classification, 4–7
Energy consumption for constant growth, 19–21
Energy conversion efficiencies, 33
Energy conversion matrix, 34–35
Energy distribution from fission, 81
Energy economics, 21–30
Energy generation, 16
Energy Research and Development Administration (ERDA), 404, 405
Energy reserves, 13–14
Energy scales, 18
Energy sources, 7–13
Energy spectrum loss, 460
Energy storage, 97, 481
batteries, 447, 461, 463, 481, 489–490
chemical, 5, 6, 481, 490–492
compressed fluid, 5, 481, 487–488
density, 482
elastic-strain energy, 5, 481
electrical, 5, 481, 484–485
electrostatic field, 5, 472, 481, 488–489
flywheels, 5, 483–484
gravitational field, 5, 481, 486–487
inductive-field, 5, 481–484
kinetic, 5, 70, 416, 481–484
latent heat, 7, 56, 481, 493, 494
mechanical, 5, 481–488
nuclear, 5, 7, 481, 492–493
pumped, 486–487
sensible heat, 7, 481, 493, 494
specific energy, 482
thermal, 5, 7, 481, 493–495
Energy units, 4
Energy utilization, 14–17
Engines:
compression-ignition, 354
cycles, 346–358, 366–392
external-combustion, 350, 366–388
gas turbine, 226, 264, 366–374, 389
internal-combustion, 353–366
noncompression, 357
performance, 361–366
reciprocating, 358–361
rotary, 361–364
spark-ignition, 353
Enriched uranium, 82–85, 154, 160, 251
Enthalpy of formation, 448–452
Environment:
concern for, 3, 317
pollution of, 3, 54, 130, 317–341
Environmental Protection Agency (EPA), 319, 321, 329, 332
Equation of time, 98, 544–545
Equilibrium fission-product poisoning:
samarium-149, 303–304
xenon-135, 299–301
Equinox, 100, 112
Ericsson power cycle, 348–350
Erosion:
ash, 213, 219
steam-water, 376–377
Evaporator, 221, 226–227
Excess air, 130
Excitation energy, 459
Exciter, 464, 465
Exothermic reactions, 6, 124–126
Experimental reactors, 157, 159
External-combustion engines, 350, 366–388
Externally reversible power cycles, 347–353
Extrapolated core boundary, 269, 270
Extrapolation distance, 269, 270

Fan laws, 190
Fans, 189, 193–202
Faraday effect, 463
Faraday F_{y}, 451
FAST, Stone and Webster system, 389
Fast fission factor, 169
Fast fissions, 154
Fast neutrons, 143, 153, 154, 167
Fast nonleakage probability, 169
Fast reactors, 154–155, 165, 264–267, 286, 291, 294, 305
Feedwater heaters, 380–383
Fermi age, 169
Fermi level, 440, 441
Ferroelectric converter, 446
Fertile blanket, 177
Fertile isotopes, 80, 85, 88, 96, 153, 170, 177
Figure of merit, 347, 433
Fire-tube boiler, 221–222

First law of thermodynamics, 3, 346–347
Fission, 7, 68, 79–89, 142
  cross sections, 144, 146, 147, 151, 153
  energy distribution, 81
  energy release, 81
  fuels, 81–88
  neutrons, 142, 153, 167, 286
  parameters, 151, 153
  products of, 68, 73, 79–80, 142, 157, 159, 171, 286, 295, 298, 338–339
  rate, 146, 153
  reactions, 79–80, 146, 153
  reactors (*see* Nuclear reactors)
  thermonuclear, 90
  yield, 297, 298
Fission chamber, 176
Fission-fusion hybrid reactor, 96
Fission-product decay chain, 299
Fission-product disposal, 338
Fission-product poisoning, 295–304, 307
Fission products (*see* Fission, products of)
Fission yield constant, 297, 298
Fissionable isotopes, 81–88
Fixed carbon, 52, 509, 511–513
Flames, types of, 140–141
Flash point, 60, 517
Flettner rotor, 407
Flue-gas desulfurization (FGD) systems, 329–332
Fluid drop converter, 472, 473
Fluiddynamic converters, 428, 466–475
Fluidized-bed furnace, 141, 217–219, 329
Flux:
  distributions, 269–271
  heat, 260–261, 275–281
  neutron, 143, 144, 146, 262, 269–271, 300–302
Flyash, 213, 322, 326
Flywheels, 5
Forced-circulation boilers, 223, 225–226
Forced-draft fans and systems, 195, 196
Ford Motor Company, 350
Fossil fuels, 8, 11, 14, 16, 47–66
Four-stroke cycle engines, 358, 359
Francis hydraulic turbine, 399, 400
Free energy, Gibbs, 449–451
Frequency, 6
Friction, 122–123, 348
Friction horsepower, 365
Friction loss, 469, 474
Fuel cells, 428, 447–455
Fuel elements:
  cladding, 159, 171, 178, 276, 278
  cylindrical, 171, 278–280
  plate-type, 276–278
Fuel gases, 61–66, 519–520
Fuel loading, 153, 304–310
Fuel oil, 58, 366, 517
  advantages over coal, 59
  burners, 204–206
  grades, 58–59
  properties, 59–61, 517
Fuel requirements, reactor, 153, 304–310
Fuels:
  fossil, 8, 11, 14, 16, 47–66
  gaseous (*see* Gaseous fuels)
  nuclear (*see* Nuclear fuels)
Fumes, 322
Furnaces:
  coal-fired:
    cyclone, 141, 209, 212–213, 324
    fluidized bed, 141, 217–219, 329
    pulverized coal, 141, 213–217, 324
    stoker, 141, 205, 207–208, 210–211, 232
  gas-fired, 202–204
  oil-fired, 204–206
  packaged, 222
  refuse-fired, 46–47
  wall construction, 227
Fusion, 7, 68, 89–97, 144
  advantages, 91
  cold fusion, 96
  fusion-fission hybrid, 96
  inertial containment systems, 94–95
  Lawson's criteria, 92
  magnetic containment systems, 92–93
  problems, 91, 94
  reactions, 89–91, 96
  requirements, 92
  research, 92–97
  threshold energy, 92
FW-Bergbau Forshung FGD (flue-gas desulfurization), 331

Gamma-neutron source, 173
Gamma radiation, 6, 69–73, 77, 79, 80, 123, 173, 175, 177

Gas burners, 202–204
Gas centrifuge process, 85
Gas constant, universal, 62, 499
Gas-cooled reactors, 162–165, 262–264
Gas recirculation fan, 195–196
Gas turbine, 164, 226, 264, 366–374, 389, 392
Gas-turbine power cycles, 366–374
Gaseous diffusion process, 82–85
Gaseous fuels, 47, 61–68, 519–520
  analyses, 61, 519–520
  byproduct gases, 64, 520
  manufactured fuel gas, 64–65, 520
  natural gas, 63–64, 519
Gaseous pollution (*see* Pollution, gaseous)
Gaseous-torch combustion, 141
Gasification of coal, 64–65
Geiger-Muller region, 175
General Electric Company, 256, 389
General Motors Corporation, 350
Generators, electrical, 428, 463–466
Geothermal energy, 8, 11–13
Gibbs free energy, 449–451
Graphite, 160, 164, 172–73, 262
Gravitational field energy, 5, 8, 481–484
Grindability index, 54
Gross national product, 1, 2
Growth rates, 19–21
Gulf General Atomics, 164, 165, 265

Half-life, 71, 74, 173, 287, 525–543
Hall-effect loss, 468
Heat, 7
  of combustion (*see* Heating values)
Heat engines (*see* Cycle, heat-engine; Engines)
Heat flux, 260–261, 275–281
Heat-generation rate, volumetric, 275
Heat losses, boiler, 235–243
  dry-gas loss, 235
  incomplete-combustion loss, 237
  moisture in combustion air loss, 236
  moisture loss, 236
  radiation and accounted losses, 239
  unburned carbon loss, 237
Heat pipes, 445
Heat pumping rate, 436
Heat rate, 31
Heat recovery steam generator, 389, 391
Heat transfer:
  boiling, 260
  conduction, 276, 278
  convection, 277, 279
  from fuel elements, 275–285
  radiation, 6, 124, 443
  reversible, 122, 348, 450
Heating values:
  higher, 53, 56, 59, 61, 62, 506–507, 509, 511–513, 517–518, 521
  lower, 56, 521
Heavy water, 161–162, 172
Heavy-water reactors, 162, 172
Helium, 78, 164–165, 262, 368
Heller cooling system, 337
Heterogeneous reactors, 158–160, 170, 292, 294
High-energy reactions:
  fusion, 90
  neutron, 148–150, 153
High-temperature, gas-cooled reactor (HTGR), 164, 179, 262–265
  advantages, 262
  concrete pressure vessel, 179, 262
  cooling system, 262
  operational parameters, 264
  steam conditions, 262
High-temperature batteries, 491
High-temperature fuel cells, 455
High-temperature thermal energy storage, 495
Higher heating value (*see* Heating values, higher)
Holes, 430, 456
Homogeneous reactors, 158–159, 170, 292, 294
Horsepower, 361–365
  boiler, 234
Hour angle, 99, 102
Humidity ratio, 133, 134, 236, 237
Hydraulic turbines, 392, 399–401
Hydrides, 96, 171, 491
Hydrocarbon compounds, 47–51
Hydroelectric energy, 8, 14, 17, 399–401
Hydrogen, 47
  as chemical fuel, 48, 64, 65, 124, 448, 454, 455, 490
  as coolant, 466

Hydrogen (*Cont.*):
as fusion fuel, 90, 91
as moderator, 160, 171–172
production of, 455, 490–492
storage, 491
Hydroxylation, 140

Ignition temperatures, 91, 124, 125
Impulse turbine blading, 395, 397–399
Impurity atoms, 430, 460
Incident angle, 102
Income energy, 7
Incomplete combustion, 129
Incomplete combustion loss, 235, 237, 242
In-core instrumentation, 174–176
Indicated horsepower, 365
Induced-draft fan and system, 195–197
Induction ac motors, 412–415
Inductive field energy, 5, 481–484
Inelastic scattering, 148
Inertial containment, 94, 95
Inertial field energy, 5, 70, 481–484
Infinite cylindrical fuel element, 278–280
Infinite cylindrical reactor, 272
Infinite slab fuel element, 276–278
Infinite slab reactor, 271, 272
Infrared radiation, 6, 124
In-hour of reactivity, 292
In-line reciprocating engines, 360
Insolation, solar, 98, 103–107, 546–548
Instrumentation, reactor, 174–176
Insulators, 475
Intercooler, 369–371
Interest, compound, 22
Intermediate-load power plants, 31, 389
Intermediate neutrons, 143, 149, 154
Intermediate reactors, 154, 157
Internal-combustion engines, 353–361
Investment costs, 22–25
Ion-beam fusion, 94
Ion-exchange membrane fuel cell, 448, 454
Ion pairs, 174, 175, 459
Ionization chambers, 174–176
Irradiation, 104, 545–550
Irreversible processes, 348
Isopleths, 104
Isotopes, 66, 525–543
Isotopic abundance, 75, 525–541
Isotopic separation, 82–85

Jet pumps, 257, 258
Joule heating, 123, 432, 435, 436, 444, 460

K-capture decay process, 72
Kaplan hydraulic turbine, 399
Kerogen, 58
Kinetic energy, 5, 70, 416, 481–484

Lamont boiler, 226
LaRance tidal power plant, 9, 10
Laser beam fusion, 94
Laster isotope separation, 85, 87
Latent heat storage, 7
Latitude, 98, 549–550
Lawson's criteria, 92
Lead telluride, 430, 439
Leakage, neutron, 166
Lenoir power cycle, 356–358
Lifetime:
of neutrons, 154, 166–167, 284, 286–288
of radioisotopes, 75, 287
Light water:
as coolant, 160, 251, 466
as moderator, 160, 171, 251
Light-water reactors, 160, 251–262
Lime/limestone throwaway FGD (flue-gas desulfurization) system, 331
Limited-pressure power cycle, 356
Liquid-drop generator, 472, 473
Liquid fuels, 58–61, 517–518
Liquid-metal coolants, 165, 264–267, 417
Liquid-metal fast breeder reactor, 165, 264–267
Liquid-metal MHD (magnetohydrodynamic) generators, 471
Liquified petroleum gas, 64, 517
Load factor, 31
Loading factor (MHD), 467–468
Longitude, 98–99
Lorentz force, 468
Lower heating value, 56, 521
Lunar energy, 8

Macroscopic cross sections, 146–148, 286

Magnetic-field energy, 5
Magnetic-field interactions, 92, 345, 409–410
Magnetic force, 410
Magnetohydrodynamic (MHD) generator, 428, 466–472, 475
Magnets, 93, 409–410, 465, 466
Magnus effect, 407
Maintenance costs, 21, 24
Majority carriers, 456
Mass defect, 67
Mass-energy equivalence, 3, 68
Mass number, 66, 525–541
Mass units, 4
Maximum thermal efficiency, 348, 428, 434
Maximum-to-average power ratios, 177, 267–274
Maxwell-Boltzmann distribution, 148–149
Mean effective pressure, 365
Mean free path, 146
Mean lifetime:
  of neutrons, 154, 166–167, 284, 286–288
  of radioisotopes, 75, 287
Mean sun time, 98, 99
Mechanical dust collectors, 322–324
Mechanical efficiency, 189–190, 365
Mechanical energy, 5
  conversion of:
    into electrical energy, 428, 463–475
    into rotational mechanical energy, 392–409
    into thermal energy, 122–123
  production of, 345–417
  storage, 5, 481–488
Membrane fuel cell, 448, 454
Mercury, 374
Metal-air batteries, 490
Microscopic cross sections, 144–153
Microwave radiation, 6, 112
Minority carriers, 460
Mirror fusion reactors, 92, 93
Moderator, neutron, 155, 160, 171–173, 251, 262
Modified one-group critical equation, 169, 295, 296, 308
Moisture, 52, 53, 56, 236
  in combustion air loss, 236, 242
Moisture loss, boiler, 236, 242
Molecular weight, 62, 75, 521–522
Molten salt reactor, 159
Momentum, conservation of, 66, 70, 96
Mud drum, 223, 224
Multiplication factor, 142, 167, 169, 295, 296
Multistage compression with intercooling, 369–371
Muon, 96

n-type semiconductor, 430, 456
NASA (National Aeronautics and Space Administration), 404, 405
National Electric Manufacturers Association, 416
Natural-circulation boiler, 223, 224
Natural-convection air flow, 195
Natural gas, 47, 48, 63–64
  analyses, 519–520
  burning equipment, 202–204
  geology, 63
  heating vaues, 64, 519–520
  reserves, 14
  storage, 64
Natural uranium, 82, 162, 173, 539
Nerst-effect generator, 446
Neutrino, 71, 80
Neutron(s), 66
  absorbers, 176–177
  absorption, 167
  activation, 73, 91
  burnup, 159
  cross sections, 144–153
  damage, 91, 154
  decay, 166–167
  delayed, 286–289
  detection, 174–176
  energy distribution, 149, 169
  fast, 143, 153, 154, 167
  fission rate, 80, 146, 153
  flux, 143, 144, 146
  intermediate, 143, 149, 154
  leakage, 166, 274
  lifetime, 154, 166–167, 284, 286–288
  poisons, 159, 295–304, 307
  prompt, 286, 289
  reaction rate, 144, 299
  reactions (*see specific reactions*)

Neutron(s) (*Cont.*):
scattering, 147, 148
slowing down, 157, 160, 171
source, 173–174
thermal, 143, 148, 153, 171
Neutron balance, 167–168
Neutron source, 173–174
Nitrogen, 53, 58, 66, 126, 130, 131, 133
Nitrogen oxides, 196, 213, 217, 319, 332–333, 353
Noncompression engine, 357
Nozzle, 174, 229, 368, 395
Nuclear batter, 428, 463
Nuclear cross section (*see* Cross section)
Nuclear energy, 5, 7, 66–97, 249–310
conversion of:
into electrical energy, 428, 463
into mechanical energy, 345
into thermal energy, 141–183, 267–285
reserves, 14
source, 67–68
storage, 481, 492–493
Nuclear fission (*see* Fission)
Nuclear fuels, 66–97, 170–171
fission, 79–89
fusion, 89–97
Nuclear fusion (*see* Fusion)
Nuclear reactions, 7, 66–67, 147–154
Nuclear reactors:
breeders, 88, 153–155, 338
classification, 154–165
commercial power, 158, 251–267
compact-power, 157–158
control, 167, 176–177
converters, 88, 167
coolants, 160–165
critical mass, 142
definition of, 142
experimental, 157, 159
fast, 154–155, 165, 264–267, 291, 294, 305
fuel elements, 159, 171, 178
fuel requirements, 153, 304–310
heterogeneous, 158–160, 170, 292, 294
homogeneous, 158–159, 170, 292, 294
instrumentation, 174–176
intermediate, 154, 157
[illegible] 284, 295
Nuclear reactors (*Cont.*):
multiplication factor, 142, 167, 169, 295, 296
period, 143, 284, 288–293
physics, 165, 170
poisoning, 295–304, 307
production, 157
research, 157
shutdown power, 81, 163
terminology, 142–144
thermal, 153–157
types of, 154
Nuclear Regulatory Commission (NRC), 251
Nucleons, 66, 67
conservation of, 66
Nucleus (nuclei):
compound, 79
fertile, conversion of, 89
number of, 75

Oak Ridge National Laboratory (ORNL), 159, 304
Ocean currents and thermal gradients, 8
Ocean thermal energy conversion (OTEC), 8, 9, 109
Octane rating, 51, 52, 354
Oil (*see* Fuel oil; Petroleum)
Oil burners, 204–206
Oil shale, 58
Once-through cooling, 335
Open feedwater heaters, 380–382
Operating costs, 21, 24–25
Optimum interstage pressures, 371
Optimum steam extraction pressures, 380
Optimum steam reheat pressures, 378–379
Organic coolants, 162
Organic electrolyte batteries, 490
Orsat analysis, 130–131
Orsat apparatus, 131
Otto power cycle, 353–356
Overfire air, 206
Oxygen:
in air for combustion, 126
in boiler feedwater, 381
in flue gas, 130
in fuel, 53, 58, 448

p-n junction:
use in solar cells, 446
use in thermoelectric converters, 430, 438
p-type semiconductor, 430, 456
PACE, Westinghouse, 389, 391
PACER project, 493
Packaged boilers, 222
Palladium electrode fusion, 96
Particles (unusual):
alpha, 71
beta, 71
electron, 66, 71
muon, 96
neutrino, 71
neutron, 66
positron, 72
proton, 66
Particulate pollution, 319, 321–329
Peaking power plants, 32
Peltier coefficient, 430
Peltier effect, 430
Pelton hydraulic turbine, 399, 401
Percent excess air, 130
Performance number, 51
Permittivity of free space, 474, 498
Petroleum, 14, 47, 58
composition, 58, 518
formation, 48
properties, 59–60, 518
reserves, 14
types of, 58
Phillips Laboratory, 350
Phosphoric-acid fuel cell, 455
Photoneutron source, 173
Photosynthesis, 7, 47
Photovoltaic generator (*see* Solar cell)
Planck's constant, 6, 498
Plasma, 92, 442, 469
MHD generator, 469
Plutonium-239, 81, 82, 85, 88, 96, 167, 170, 287, 288, 298, 305, 492, 540
Poisoning:
fission product, 295–304, 307
samarium-149, 297, 303–304, 307
xenon-135, 297, 299–303, 307
Polarization, chemical, 453
Pollution, 317–318, 374
gaseous, 54, 129–130, 213, 217, 219, 318–321, 329–333, 353
particulate, 319, 329
solid-waste, 337–341
thermal, 11, 333–337
water, 333–337
Polyphase ac motors, 412–413
Positive displacement compressors, 193
Positron, 72
Potassium:
as seed material, 471
as working fluid, 374
Potential barrier, 442
Potential energy, 5, 481–488
Pour point, 60
Power, 4
coefficient of reactivity, 293, 307
costs, 27
distribution, 177, 267–274
maximum-to-average, 177, 271–274
radiosiotopes, 77, 141, 173, 463, 542–543
Power density, 30, 155, 267, 274, 275, 482, 542–543
Power distribution, reactor, 267–274
Power factor, 123
Power generation terminology, 30–32
Power reactors, 158, 160–161, 177, 251–267
boiling water (*see* Boiling-water reactors)
CANDU, 161, 163
gas-cooled, 163–165, 262–265
high-temperature, 164, 262–265
heavy water, 161–163
liquid-metal, fast-breeder, 165, 264–267
pressurized water, 160, 161, 177, 251–256
Superphoenix, 165, 265–267
Power units, 4
Preheaters, air, 221, 228–234
Pressure drop:
EGD converter, 474
MHD converter, 469
Pressure vessels, 177–179
concrete, 179, 262
LWR, 160, 178, 253, 254, 256, 258, 259
Pressurized-water reactors, 160, 161, 177, 251–256

Pressurized-water reactors (*Cont.*):
control rods, 177, 178, 253, 308
description, 251–252
operation, 251–252
operational parameters, 253
steam generators, 255–257
Pressurizer, nuclear, 254
Prestressed-concrete pressure vessel, 179, 262
Primary air, 203, 206, 212
Primary containment system, 177–178
Primary cooling system, 160, 252
Primary fission product, 297, 299
Primary heat-transfer surface, boiler, 221, 226–228
Producer gas, 65, 520
Production reactors, 157
Production time, neutron, 286
Prompt-critical condition, 291
Prompt neutrons, 286, 289
Prompt temperature coefficient, 294–295
Protons, 66
Proximate coal analysis, 52–53, 511–516
Pulse-jet engine, 357–358
Pulverized-coal furnace, 141, 213–217, 324
Pulverizers, 213–215
Pump efficiency, 189, 365, 377
Pump laws, 190
Pumped storage:
air (CAES), 487–488
water, 486–487
Pumps:
boiler feed, 189–192
centrifugal, 190–192
jet, 257, 258
specific speed, 190, 191

Quasi-latent-heat storage, 493

Radial engines, 361–364
Radiation:
damage, 91, 154, 162
detection, 174–176
gamma (*see* Gamma radiation)
infrared, 6, 124
microwave, 6, 112
radio, 6
solar, 8, 97–112, 456
Radiation (*Cont.*):
thermal, 5, 7, 123–124, 443
ultraviolet, 6, 123
visible, 6, 124
x-rays, 6, 72, 123
Radiation loss, boiler, 235, 238–239, 242
Radiative-capture reaction, 73, 79, 80, 85, 88, 147, 173, 305
Radio waves, 6
Radioactive decay, 7, 16, 69–79, 141
alpha decay, 71, 77, 173, 463, 542–543
application, 77, 173
beta decay, 71–72, 77, 463, 542
decay constant, 74, 75, 299
decay rates, 74–76, 299
energy distribution, 71
half-life, 71, 74, 299
K-capture decay, 72
mechanics, 69–71
neutron decay, 166–167
positron decay, 72
power from, 76–77, 542–543
problems with, 77–78
sources, 72–73, 141, 542–543
types of, 71–73
units, 75
Radioactive isotopes:
activation products, 73, 91, 542–543
applications, 77, 173, 463
choice as power sources, 76–77
cosmic-ray induced, 72, 73
fission products, 68, 73, 79–80, 142, 157, 159, 171, 286, 295, 338–339, 542
lifetime, 75, 287
long-lived, 72, 73
manufactured, 73
naturally-occurring, 72, 73
problems, 77
sources, 77
Radioactive waste, 318, 338–339
Radioactivity (*see* Radioactive decay)
Radioisotope fuels, 76–77, 542–543
Radioisotopes (*see* Radioactive isotopes)
Rankine vapor cycle, 226, 374–388
Rate base, 32
Rateau turbine stage, 397, 398
Reactants, chemical, 449, 521–522
Reaction rates, neutrons, 144–146, 299
Reaction turbine staging, 395, 397–399

Reactions, neutron (*see specific reaction*)
Reactivity, 142
  burnable poisons, 308
  coefficient, 293–295, 307, 308
  control, 158, 176–177, 253, 293–295, 307, 308
  definition of, 141
  fission-product poisoning, 295–304, 308
  fuel burnup, 158, 304–310
  temperature effect, 294–295, 306
  void, 295, 307
Reactivity coefficients:
  power, 293, 307
  temperature, 294–295, 307
  void, 295, 307
Reactor buckling, 169
Reactor control, 158, 176–177, 253, 257, 258, 308
Reactor coolants, 160–165, 173
Reactor core composition, 170–177
Reactor flux distributions, 267, 269–273
Reactor kinetics, 284, 286–292
Reactor period, 143, 284, 288–292
Reactor physics, 165–170
Reactor power distributions, 179, 270–274
Reactor pressure vessels, 177–179, 253, 254, 256, 258, 259
Reactor shutdown power, 81, 163
Reactors:
  chemical, 130
  nuclear (*see* Nuclear reactors)
  power (*see* Power reactors)
Reciprocating-piston engines, 358–361
Redox fuel cell, 454
Reflected reactor cores, 179, 274, 275
Reflector, neutron, 166, 177, 274, 275
Refueling, 158, 159, 308
Refuse analysis:
  coal, 131–132
  biomass, 506–508
Refuse utilization, biomass, 43–47
Regenerative Brayton cycle, 368–369
Regenerative vapor cycle, 380–383
Regenerator, 349–350, 368–369
Regenerator effectiveness, 369
Reheat Brayton cycle, 371–372
Reheat vapor cycle, 378–380
Reheater, 221, 228
Reprocessing, fuel, 171
Research reactors, 157
Reserve capacity, 31
Resistance, electrical, 123, 431
Resistance ratio, *M*:
  for maximum efficiency, 433
  for maximum power, 434
Resistivity, electrical, 431, 469, 471
Resonance cross sections, 149–150
Resonance escape probability, 169
Reverse-saturation current density, 456
Reversible heat-engine cycles, 347–353
Reversible thermodynamic processes, 347
Richardson-Dushman equation, 440
Ringelmann charts, 320
Risers, 223, 224
Rotary compressors, 193
Rotary engines, 361–364
Rotary vapor-cycle engine, 388–389

Salt pond, solar, 109, 111
Samarium-149 poisoning, 297, 303–304, 307
  equilibrium, 304
  maximum shutdown, 304
Satellite, solar, 111–113
Scattering cross sections and reactions, 147, 148, 171
Scram, 158, 177, 253, 260, 290
Scrubbers, 325, 330–331
Seasonal heat storage (ACES), 495
Second law of thermodynamics, 7, 347
Secondary air, 206, 212
Secondary containment:
  large volumes, 180
  vapor suppression, 180–182
Seebeck coefficient, 429–430
Seebeck effect, 429
Selective catalytic reduction (SCR), 333
Selective noncatalytic reduction (SNR), 333
Semiconductors, 429–431, 456–457, 460
Sensible heat storage, 7, 481, 493, 494
Separative work unit, 84
Series-wound dc motor, 411–412
Sewage gas, 66
Shale oil, 14, 47, 58

Shielding:
biological, 179–180
thermal, 177
Shot-cleaning system, 230, 232
Shunt-wound dc motor, 411, 412
Shutdown power, reactor, 81, 163
Silicon solar cell, 460
Slag, 212, 217
Slowing down of neutrons, 157, 160, 171
Slowing down time, neutron, 286
SNAP (systems for nuclear auxiliary power), 78, 440
Sodium, 165, 374
Softening temperature, ash, 54–55
Solar cell, 97, 428, 456–462
current-voltage characteristics, 459
efficiency, 460, 462
materials, 460
performance, 461–462
Solar collection systems, 108–113
Solar energy, 8, 97–113, 366, 445, 456
absorptivities (emissivities), 105, 106
advantages, 97
angles, 99–103
calculations, 98–107
clearness number, 104, 105
concentration factors, 108
direct, 8
disadvantages, 97
equation of time, 98, 544–545
indirect, 8
insolation, 98, 103–107, 546–548
reactions, 97
temperatures, 108
times, 98–99
Solar fusion, 92
Solar power satellite system (SPSS), 111–113
Solar-power-tower system, 109, 110
Solar salt ponds, 109, 111
Solid-waste disposal:
ash and sulfur salts, 318, 337–338
general biomass, 46–47
nuclear, 318, 338–339
Soluble poisons, 308
Soot blowers, 229, 230
Sources, neutron, 173
Space charge barrier energy, 442
Space charge control, 442–443
Specific energy, 472
Specific fuel consumption, 366
Specific gravity, 59–60
Specific heat ratio, 354, 355, 368, 369
Specific heat transfer, 376
Specific power, 30
Specific speed, 190, 191
Specific work, 347, 358, 369, 376, 379
Spectrum:
electromagnetic energy, 6
fission, 169
thermal neutron, 148–149
Spherical reactor core, 273
Spinning reserve, 31
Spreader stoker, 209, 211
Squirrel-cage ac motors, 413–415
Stable reactor period, 143, 288–291
Stack, draft, 195
Stack power, 334, 335
STAG, General Electric system, 389
Stage reheat, 377
Standard hydrocarbon fuels, 50–51
Standard meridian, 98–99
Steam drum, 223, 224
Steam generator efficiency, 235, 239, 335
Steam generators:
fossil fuel (*see* Boilers)
nuclear, 161, 251, 252, 255, 256
Steam trap, 382
Steam turbines, 377, 392–399
Stefan-Boltzmann's constant, 443, 499
Stirling power cycle, 348, 350–353, 366, 367
Stoker furnaces, 141, 205, 207–208, 210–211, 232
Stone and Webster FAST system, 389
Storage, energy, 4, 97
batteries, 447, 463, 465, 489–490
compressed air, 5, 487–488
flywheels, 5, 483–484
pumped hydro, 486–487
thermal, 7, 481, 493–495
Studded-tube walls, boiler, 227
Subcritical reactors, 142, 158, 167, 284
Substitute natural gas (SNG), 64–65
Sulfur, 53, 54, 125, 319
Sulfur compounds, 54, 319, 329–332
Sum of mass and energy (conservation), 3, 66, 70

Sun times, 98–99
Supercritical reactors, 142, 167, 284
Superheat, 227, 252, 377
Superheater, 221, 227, 377
Superphoenix reactor, 165, 265–267
Synchronous ac motors, 412–413, 415–416
  large polyphase, 412–413
  small single-phase, 415–416
Synchronous speed, 410, 465
Synthetic natural gas, 64–65
Systems for nuclear auxilliary power (SNAP), 78, 440

Temperature coefficient of reactivity, 294, 307
Temperature distributions in reactor fuel:
  axial distribution, 281–285
  cylindrical fuel elements, 278–281
  plate-type fuel elements, 276–278
Temperature measurement, 430
Temperatures in reactor core, 275–285
Terminal temperature difference, 382
Terminology:
  power generation, 30–32
  reactor, 142–144
Theoretical air-fuel ratio, 126–129
Thermal conductance, 432
Thermal conductivity, 277
Thermal diffusion length, 169, 296
Thermal diffusion time, neutron, 286
Thermal diffusivity, 276
Thermal discharge index, 334
Thermal efficiency, 31, 262, 334–336, 347, 348, 350, 354, 355, 366, 368, 369, 376, 380, 388, 389, 434, 445
Thermal energy, 5, 333–337, 428
  conversion of:
    into electrical energy, 429–447
    into mechanical energy, 345–392
  neutron, 143
  production of, 122–183
  storage, 7, 481, 493–495
Thermal fissions, 153
Thermal gradients in the ocean, 8, 9
Thermal-neutron distribution, 148–149
Thermal-neutron poisons, 295–304, 307
  samarium-149, 297, 303–304, 307
  xenon-135, 297–303, 307
Thermal neutrons, 143, 148, 153, 171, 286, 295
Thermal nonleakage probability, 169, 296
Thermal pollution, 11, 333–337
Thermal radiation, 6, 124, 443
Thermal reactors, 153–157, 297, 303, 307
Thermal shield, 177
Thermal utilization factor, 169, 196
Thermionic conversion, 428, 440–446
Thermionic generator, 440, 445
Thermocouples, 174, 430
Thermodynamic cycles, 346–358, 366–382
Thermodynamics:
  applied to power cycles, 346–358, 366–392
  first law of, 3, 346
  processes, 346–348
  second law, 7, 347
Thermoelectric generator (TEG), 78, 428–434
Thermoelectric refrigerators, 434–437
Thermomagnetic energy converter, 446
Thermonuclear fission reaction, 90
Thermonuclear fusion (*see* Fusion)
Theta-pinch fusion reactor, 92–93
Thomson coefficient, 431
Thomson effect, 430–431
Thorium, 14, 73, 85, 86, 96, 492
Three-Mile Island nuclear accident, 17, 19, 249
Tidal-power systems, 8–10, 14
Tilt angle, solar, 103
Tokamak fusion reactor, 92–94
Transitional energy, 4, 5
Trap, steam, 382
Traveling-flame-front combustion, 141
Tritium (H-3):
  fusion fuel, 90, 91
  production of, 94
  radioisotope, 73
Turbine blading, steam, 395–399
Turbine efficiency, 190, 365, 377
Turbines:
  gas (*see* Gas turbine)
  hydraulic, 392, 399–401
  steam, 377, 392–399
  wind, 392, 402–409
Turbojet engine, 368

Two-stroke-cycle engines, 358–360

Ultimate coal analysis, 52, 53, 132, 511–516
Ultraviolet radiation, 6, 123
Unburned carbon, 132, 236–237
Unburned carbon loss, boiler, 236–237, 242
Uncompensated ion chamber, 176
Underfeed stoker furnace, 209, 210
Units, 4
Universal gas constant, 62, 499
Universal-pressure (UP) boiler, 223, 225–226
Uranium:
  depleted, 82, 85
  enriched, 82–85, 154, 160, 251
  isotopic separation, 82–85
  natural, 82, 162, 173, 539
  reserves, 14
Uranium-233, 14, 81, 85, 86, 96, 153, 168, 287, 298, 492, 539
Uranium-235, 14, 81, 82, 85, 88, 167, 168, 287, 288, 290, 297, 298, 300, 305, 308, 539
Uranium-238, 14, 82, 85, 88, 168, 493, 539
Uranium hexafluoride, 82
Uranium oxides, 170

V-engines, 360
Vanadium in fuel oil, 60
Van Allen radiation belt, 92
Van de Graff generator, 472
Vapor-power cycles, 367, 374–388
Vapor-suppression containment system, 181–183
Velox boiler, 226
Vessels, pressure (*see* Pressure vessels)
Visible radiation, 6, 124
Void coefficient of reactivity, 295, 307
Volatile matter, 52, 53, 511–516
Volumetric efficiency, 366
Volumetric heat generation rate, 275
Volumetric heating value, 59, 62–63

Wankel engine, 362
Waste heat removal, 333–337
Water:
  heavy, 161–162, 172
  light, 160, 171, 251, 466
Water-cooled reactors, 160, 171, 252–262
Water gas, 64, 520
Water power, 8, 14, 399–401
Water purity in boilers, 226
Water-tube boilers, 221–226
Water walls, 226–227
Wave power, 8
Wavelength, 6
Wellman-Lord FGD (flue-gas desulfurization) process, 330
Westinghouse, 178, 252, 253
Wet-bottom furnace, 217
Wet cooling tower, 335–336
Wind power, 8, 405
Wind turbines (windmills), 392, 402–409
Work, 5
  specific, 347, 358, 369, 376, 379
Work function energy, 440
Wound-rotor ac motors, 413, 415

X-radiation, 6, 72, 123
Xenon-135 poisoning, 297–303, 307
  equilibrium operating, 301
  instability, 303
  override capability, 302–303
  shutdown values, 302

Yellow-flame combustion, 141
Yield constant, fission, 297, 298

Zirconium alloys, 171